πN NEWSLETTER

No. 15, December 1999 ISSN 0942-4148

EDITORS:

D. Drechsel G. Höhler W. Kluge H. Leutwyler

B. M. K. Nefkens H.-M. Staudenmaier

PROCEEDINGS

of the

Eighth International Symposium on Meson-Nucleon Physics and the Structure of the Nucleon

Zuoz, Switzerland

August 15 - 21, 1999

Impressum

Production and distribution:

for Europa, Africa, Western Asia by
W. Kluge
Institut für Experimentelle Kernphysik (IEKP)
Universität Karlsruhe
Postfach 3640
D-76021 Karlsruhe
Germany

for the Americas, Australia, and Eastern Asia by
B. M. K. Nefkens
Department of Physics
University of California, Los Angeles
Los Angeles, CA 90024-1547
USA

Editors: D. Drechsel, G. Höhler, W. Kluge, B. M. K. Nefkens,
H. Leutwyler, and H.-M. Staudenmaier

Printing Department: PSI, CH-5232Villigen, Switzerland

ISSN 0942-4148

πN NEWSLETTER

No. 15, December 1999 ISSN 0942-4148

EDITORS:

D. Drechsel G. Höhler W. Kluge H. Leutwyler
B. M. K. Nefkens H.-M. Staudenmaier

PROCEEDINGS

of the

Eighth International Symposium on Meson-Nucleon Physics and the Structure of the Nucleon

Zuoz, Switzerland
August 15 - 21, 1999

Note from the Editors

The purpose of the πN Newsletter is to improve the exchange of information between physicists working in πN scattering and related fields such as nucleon structure, $\pi N \to \pi\pi N$, $\pi^- p \to \eta n$, $\gamma N \to \pi N$, $\pi\pi \to \pi\pi$, and electromagnetic form factors of pions and nucleons. The Newsletters will give results of new experiments, plans for experiments in the near future, analyses of experimental data, and related theoretical developments.

Since our first Newsletter appeared, subjects that have come under the limelight are for instance: the 'experimental' value of the πN σ-term and other quantities related to the strange quark content of the nucleon, the origin of the spin of the nucleon, applications of the Skyrme model and the pole structure of πN and $\pi\pi$ resonances in different sheets. There continues to be an interest in various quark and bag models of nucleon resonances, the existence of clusters of nucleon resonances, and so forth.

Copies can be obtained from the editors W. K. and B. M. K. N. at the addresses below.

D. Drechsel
Universität Mainz
Institut für Kernphysik
Postfach 3980

D 55099 Mainz
Germany

Drechsel@kph.uni-mainz.de
FAX: (+49) 6131-395474

G. Höhler
Universität Karlsruhe
Institut für Theoret. Teilchenphysik

Postfach 6980
D 76128 Karlsruhe
Germany

Gerhard.Hoehler@phys.uni-karlsruhe.de
FAX: (+49) 721-370726

W. Kluge
Universität Karlsruhe
Institut für Exp. Kernphysik

Postfach 3640
D 76021 Karlsruhe
Germany

Wolfgang.Kluge@phys.uni-karlsruhe.de
FAX: (+49) 7247-823414

B. M. K. Nefkens
UC Los Angeles
Department of Physics
405 Hilgard Ave.

Los Angeles CA 90024
USA

BNefkens@uclapp.physics.ucla.edu
FAX: 310-206-4397

H. Leutwyler
Universität Bern
Institut für Theoretische Physik
Sidlerstr.. 5
CH-3012 Bern
Switzerland

leutwyle@butp.unibe.ch

H.- M. Staudenmaier
Universität Karlsruhe
Institut für Anwendungen der Informatik
Postfach 6980
D 76128 Karlsruhe
Germany

Hans.Staudenmaier@phys.uni-karlsruhe.de
FAX: (+49) 721-370726

Preface

The *Eighth International Symposium on Meson-Nucleon Physics and the Structure of the Nucleon* (MENU99) was held at the Lyceum Alpinum in Zuoz in the Engadin, Switzerland, August 15-21, 1999.
The very intense program consisted of seven plenary sessions with 21 invited talks, four working group sessions with a total of 21 presentations and four parallel sessions (a and b) with 31 talks. The working groups were focussing on hot topics of πN physics discussed extensively in recent years: the πN sigma term, isospin violation, the πNN coupling constant and electromagnetic corrections. The program of the conference followed the tradition of this series of symposia: As before, the largest part of the program was devoted to πN physics, especially to πN scattering, but the electromagnetic meson production, with new data coming from CEBAF and MAMI and soon also from DAΦNE, is growing in importance. The new developments in chiral perturbation theory, dealing with meson-meson and meson-nucleon interactions at low energy, were drawing much attention. Hadronic atoms were covered experimentally and theoretically; meson production by nucleons and some recent results on the nucleon structure from deep inelastic scattering experiments were also presented.

I would like to thank PSI for sponsoring this symposium. I also thank the Swiss Federal Government for the financial support of our colleagues from Eastern Europe. It is a pleasure to thank the staff of the Lyceum Alpinum, especially Mrs. Ch. Hübner, for their great effort to make our stay in Zuoz so pleasant. I would like to thank V. Markushin and T. Jensen from PSI for helping to make the meeting run smoothly. I got a lot of help and advice before and during the conference from Milan Locher, which I would like to acknowledge here. Special thanks go to Christine Kunz, the conference secretary, for the tremendous work she did for the organization of this conference. Her kind way of dealing with all kinds of problems during the week in Zuoz contributed a lot to the success of the meeting. Last, but not least, I would like to thank all participants, especially the speakers, who created a scientifically stimulating atmosphere during this whole week.

Res Badertscher, ETH Zurich
Organizer of MENU99

CNS
Center for Nuclear Studies

The George Washington University
WASHINGTON DC

MENU2001

9th International Symposium on Meson-Nucleon Physics and the Structure of the Nucleon

Washington, D. C., U. S. A.

26–31 July, 2001

First Announcement

The Symposium will cover experimental and theoretical developments in the following areas:

- **πN Physics**
- **KN Physics**
- **ηN Physics**
- **Photo- and Electroproduction of Mesons**
- **Structure of the Nucleon**
- **Chiral Symmetry-based Effective Field Theories**
- **QCD-inspired Quark Models of Hadrons**

There will be five full days of invited and contributed talks (no talks on Sunday, July 29th). The First Circular with more details will be sent out in the Fall of 2000.

Proceedings will be published in the πN NEWSLETTER.

The meeting will be held at the downtown campus of The George Washington University, located in northwest Washington, D.C., about four blocks from the White House along Pennsylvania Avenue. Inexpensive accommodation will be available in University Residence Halls. The attractions of the nation's capital are all within walking distance or easily accessible via the DC Metro system.

Contact:

William J. Briscoe — Email: briscoe@gwu.edu
Helmut Haberzettl — Email: helmut@gwu.edu
Fax: +202-994-3001

Department of Physics
The George Washington University
Washington, D. C. 20052, U. S. A.

Conference Web Site: http://www.gwu.edu/~cns/menu2001/menu2001.htm

MENU99 Program

Sunday **August 15, 1999**

16:00 Registration

17:30 Apero

18:30 Dinner

Monday **August 16, 1999**

08:30 Welcome M.P. Locher

Plenary Session I Chairman: M.P. Locher

08:45 H. Leutwyler Institut für theoretische Physik, Univ. Bern
"Effective Field Theory of the πN-Interaction"

09:15 G. Höhler Institut für theoretische Teilchenphysik, Univ. Karlsruhe
"New Results on πN Phenomenology"

09:45 J. Stahov Faculty of Chemical Engineering, Univ. Tuzla
"The Subthreshold Expansion of the πN Invariant Amplitude in Dispersion Theory"

10:15 Coffee Break

Plenary Session II Chairman: H.-M. Staudenmaier

10:45 G. Smith TRIUMF
"CNI Experiments with CHAOS"

11:15 M.E. Sadler Abilene Christian University, Texas
"Pion-Nucleon Charge Exchange Experiments"

11:45 S.P. Kruglov Petersburg Nuclear Physics Institute, Gatchina
"The Results from PNPI on πp Reactions"

12:15 Lunch Break

Plenary Session III Chairman: G.J. Wagner

13:30 E. Friedman Racah Inst. of Physics, The Hebrew Univ., Jerusalem
"Partial Total πN Cross Sections"

14:00 R. Meier Physikalisches Inst., Univ. Tübingen
"Measurement of π^+ p Analyzing Powers at Low Energy at PSI"

14:30 M. Pavan M.I.T., Cambridge, MA
"Updated Results from the VPI πN Partial-Wave and Dispersion Relation Analysis"

15:00 Coffee Break

Parallel Session 1a: Nucleon Structure / Electromagnetic Interactions with the Nucleon
Chairman: M. Sevior

15:30 D. Isenhower Abilene Christian Univ., Abilene, Texas
"Asymmetry in the Anti-Quark Sea of the Proton and Comparison to Meson Models of the Nucleon - Final Results of Fermilab E866"

15:50 P. Kroll Fachbereich Physik, Univ. Wuppertal
"Linking Parton Distributions to Form Factors and Compton Scattering"

16:10 W. Lorenzon Physics Dept., Univ. of Michigan
"Recent Results from HERMES"

16:30 A. Bamberger Univ. Freiburg
"Recent Results on the Nucleon Structure at HERA"

16:50 M.O. Distler Inst. für Kernphysik, Univ. Mainz
"Recent Measurements of the $\gamma^* p \rightarrow \Delta$ Response Functions at Bates"

Parallel Session 1b: Charge Symmetry Breaking/ Pion Absorption and Production/ Pionic Form Factors
Chairman: V. Markushin

15:30 A. Gridnev St. Petersburg Nuclear Physics Inst., Gatchina
"The Delta Resonance Mass Splitting in the K-Matrix Approach"

15:50 D. Kotlinski PSI
"Pion Absorption, a Summary of LADS Results"

16:10 J. Niskanen Dept. of Physics, Univ. of Helsinki
Some Topic on $NN \rightarrow NN\pi$.

16:30 T. Ueda Faculty of Science, Ehime Univ., Japan
"Pionic Form Factors of Baryons and Threshold Structure in πNN Amplitude"

18:30 Dinner

Tueday **August 17, 1999**

Plenary Session IV Chairman: G. Smith

08:30 M.E. Sevior School of Physics, Univ. of Melbourne
"Nuclear (π,2π) Results. A Smoking Gun for Medium Modifications?"

09:00 J. Gasser Institut für theoretische Physik, Univ. of Bern
"Low-Energy $\pi\pi$ Scattering in QCD"

09:30 M. Zeller Physics Dept., Yale Univ., New Haven CT
"Studies of Rare But Allowed K^+ Decays"

10:00 Coffee Break

Parallel Session 2a: Electro- and Photoproduction of Mesons
Chairman: R. Beck

10:30 H.Haberzettl Dept. of Physics, George Washington Univ.
"Gauge-invariant Electroproduction of Mesons".

10:50 O. Hanstein Inst. für Kernphysik, Univ. of Mainz
"Unsolved Problems in the Analysis of Pion Photoproduction Around the $\Delta(1232)$"

11:10 R. Alkofer Inst. für theoretische Physik, Univ. Tübingen
"Kaon Photoproduction in a Confining Covariant Diquark Model"

11:30 L. Tiator Inst. für Kernphysik, Univ. Mainz
"A Multipole Analysis for Eta Photoproduction"

Parallel Session 2b: Resonances and Baryon Spectroscopy
Chairman: D. Kotlinski

10:30 P.B. Siegel California State Polytechnic Univ., Pomona
"Dynamical Formation of S-Wave Baryon-Resonances: How Many Could There Be?"

10:50 F. Kleefeld Inst. für theoretische Physik III, Univ. Erlangen-Nürnberg
"Threshold Behaviour of Meson-Nucleon $S_{11}(1535)$ Vertexfunctions and Determination of the $S_{11}(1535)$ Mixing Angle"

11:10 A. Prokofiev PNPI, Gatchina
"Status of the SPES4 - π Experiment at Saclay (The Exclusive Investigation of the Roper Resonance)"

12:30 Lunch

13:30 *Working Group Session on πN Sigma Term*

Convener: M. Knecht, Centre de Physique Theorique, CNRS-Luminy, Marseille

P. Büttiker Institut für Kernphysik (Theorie), FZ Jülich
"πN Scattering Inside the Mandelstam Triangle and the Sigma Term "

M. Pavan MIT, Cambridge, MA
"Details of the VPI Extraction of the πN Sigma Term from $\pi^+ p$ Scattering Data"

G. Höhler Institut für theoretische Teilchenphysik, Univ. Karlsruhe
"Status of the π N Sigma-Term"

Discussion

15:30 Coffee Break

16:00 *Working Group Session on Isospin Violation*

Convener: U.-G. Meissner IKP (Th), FZ Jülich

G. Müller Inst. für theoretische Physik, Univ. of Vienna
"Isospin Violation to Fourth Order in Baryon Chiral Perturbation Theory"

N. Fettes Inst. für Kernphysik (Theory), FZ Jülich
"Isospin Violation in Pion-Nucleon Scattering"

A.M. Bernstein Laboratory for Nuclear Science, MIT
"πN Scattering and Isospin Violation in Electromagnetic Pion Production"

R. Lewis Dept. of Physics, Univ. of Regina
"Isospin Violation and the Proton's Strange Form Factors"

W. Gibbs Univ. of New Mexico
"Isospin Breaking in Pion-Nucleon Scattering: Where is it?"

H. Machner Inst. für Kernphysik, FZ Jülich
"Isospin Breaking in NN and pd Reactions"

18:30 Dinner

Wednesday, August 18, 1999

Plenary Session V Chairman: A. Bernstein

08:30 R. Beck Institut für Kernphysik, Univ. Mainz
"Photo- and Electroproduction of Pions at MAMI"

09:00 S. Dytman Physics Dept., Univ. of Pittsburgh
"New Results for Meson Production with Electromagnetic Beams using CLAS"

09:30 U.-G. Meissner IKP (Th), FZ Jülich
"Recent Developments in Chiral Effective Field Theories"

10:00 Coffee Break

Parallel Sessions 3a: Experiments with Exotic Atoms Chairman: J.-P. Egger

10:30 H.J. Leisi Inst. for Particle Physics, ETH Zurich
"Results from Pionic Hydrogen"

10:50 M. Daum PSI
"Kinetic Energy Distribution of πp Atoms in Hydrogen"

11:10 C.O. Petrascu LNF - INFN, Frascati
"The DEAR Experiment at *DAΦNE* "

11:30 A. Lanaro
"Lifetime Measurement of Dimeson Atoms with the DIRAC Experiment"

11:50 D. Gotta Inst. für Kernphysik, FZ Jülich
"Measurement of the Ground-State Shift and Width in Pionic Hydrogen to the 1% Level: A New Proposal at PSI"

Parallel Session 3b: Theory Chairman: P. Kroll

10:30 M. Birse Dept. of Physics, Univ. of Manchester
"A Renormalization-Group Treatment of Two-Body Scattering"

10:50 J. McGovern Dept. of Physics, Univ. of Manchester
"On the Absence of Fifth Order Contributions to the Nucleon Mass in HBCHPT"

11:10 V. Vereshagin Dept. for Theoretical Physics, St. Petersburg State Univ.
"Quark-Hadron Duality, Analyticity and the Structure of Chiral Coefficients"

12:30 Lunch

14:00 Excursion to Muotas Muragl (was cancelled due to bad weather)

19:30 Conference Dinner at the Hotel Engiadina

Thursday August 19, 1999

Plenary Session VI Chairman: W. Kluge

08:30 N. Kaiser Physik Dept. T39, Tech. Univ. München
"Eta and Kaon Production"

09:00 B.M.K. Nefkens Dept. of Physics and Astronomy, UCLA
"Hadron Physics with the Crystal Ball Multiphoton Spectrometer"

09:30 G. Pancheri INFN - Laboratori Nazionali di Frascati
"Meson Physics at *DAΦNE* "

10:00 Coffee Break

Parallel Session 4a: πN Chairman: R. Meier

10:30 D. Isenhower Abilene Christian Univ., Abilene, Texas
"Final Results on Low Energy CEX at 10, 20 and 40 MeV"

10:50 G. Oades Inst. of Physics and Astronomy, Aarhus Univ.
"πN Phases Below 100 MeV"

11:10 J. Patterson Univ. of Colorado
"πp Elastic Analyzing Powers Below 140 MeV"

11:30 W. Briscoe The George Washington Univ.
"Recent Results from the VPI (now GW) Group"

11:50 G. Oades Inst. of Physics and Astronomy, Aarhus Univ.
"Expansion of πN Invariant Amplitude About $t = 0$, $\nu = 0$ and Comparison with Heavy Baryon ChPT"

Parallel Session 4b: Few Body and Nuclear Reactions
Chairman: M. Daum

10:30 H. Machner Inst. für Kernphysik, FZ Jülich
"Study of the pd → 3He π^0 and 3H π^+ Reactions at COSY"

10:50 A. Gårdestig Div. of Nuclear Physics, Uppsala Univ.
"The ABC Effect, the dd → α Reaction and Charge Symmetry Breaking"

12:30 Lunch

13:30 *Working Group Session on the πNN Coupling Constant*

Convener: M. Sainio Dept. of Physics, Univ. of Helsinki

B. Loiseau Univ. P. & M. Curie, Paris
"How Precisely Can We Determine the πNN Coupling Constant from the Isovector GMO Sumrule?"

G. Höhler Institut für theoretische Teilchenphysik, Univ. Karlsruhe
"Some Remarks on the πNN Coupling Constant"

M. Pavan M.I.T., Cambridge, MA
"Details of VPI Determination of f^2 from πp Scattering Data"

Discussion

15:30 Coffee Break

16:00 *Working Group Session on Electromagnetic Corrections*

Convener: A. Rusetsky present address: Inst. für theoretische Physik, Univ. Bern

J. Soto Dept. d'ECM, Univ. of Barcelona
"Effective Field Theory Approach to Pionium"

V. Lyubovtiskij Bogoliubov Lab. of Theor. Physics, JINR, Dubna
"Hadronic Atoms in QCD"

H. Neufeld Inst. für Theoretische Physik, Univ. Wien
"Chiral Perturbation Theory with Photons and Leptons"

M. Knecht Centre de Physique Theorique, CNRS-Luminy, Marseille
"Electromagnetic Corrections in Low-Energy $\pi\pi$ Scattering"

A. Rusetsky present address: Inst. für theoretische Physik, Univ. of Bern
"Spectrum and Decays of Hadronic Atoms"

18:30 Dinner

Friday **August 20, 1999**

Plenary Session VII Chairman: E. Friedman

08:30 R. Bilger Pysikalisches Institut, Univ. Tübingen
"Search for a Narrow Resonance in the πNN System"

09:00 R. Tacik Univ. of Regina, Canada / TRIUMF
"DCX Experiments and the Search for the d' with the CHAOS Detector at TRIUMF"

09:30	T. Johansson	Dept. of Radiation Sciences, Uppsala Univ.
	"Meson Production Near Threshold in Nucleon-Nucleon Collisions"	
10:00	Coffee Break	
Summaries		Chairman: H.J. Leisi
10:30	M. Knecht	Centre de Physique Theorique, CNRS-Luminy, Marseille
	Summary of the Working Group Session on the πN Sigma Term	
11:15	U.-G. Meissner	IKP (Th), FZ Jülich
	Summary of the Working Group Session on Isospin Violation	
12:30	Lunch	
Summaries		Chairman: B.M. Nefkens
13:30	M. Sainio	Dept. of Physics, Univ. of Helsinki
	Summary of the Working Group Session on the πNN Coupling Constant	
14:15	A. Rusetsky	present address: Inst. für theoretische Physik, Univ. Bern
	Summary of the Working Group Session on Elmag. Corrections	
15:00	Coffee Break	
15:30	D. Bugg	RAL, Chilton, England
	Conference Summary	
18:30	Dinner	

Saturday August 21, 1999

Departure after breakfast

Contents

Effective Field Theory of the Pion-Nucleon-Interaction*

H. Leutwyler
Institute for Theoretical Physics, University of Bern, Sidlerstr. 5, CH-3012 Bern, Switzerland

Abstract

In the first part of the talk, I discussed the nature of the effective theory that describes the properties of the pion-nucleon-interaction at low energies, using the static model as a starting point. In the second part, I then pointed out that the infrared singularities occurring in the πN scattering amplitude are stronger and of a more complex structure than those encountered in $\pi\pi$ scattering. A formulation of the effective theory that properly accounts for these was described and the results obtained thereby were illustrated with a few examples. In the following, I restrict myself to a discussion of some qualitative aspects of this work.

INTRODUCTION

The static model represents a forerunner of the effective theories of the pion-nucleon interaction used today. In this model, the kinetic energy of the nucleon is neglected: The nucleon is described as a fixed source that only carries spin and isospin degrees of freedom. For an excellent review of the model and its application to several processes of interest, I refer to the book of Henley and Thirring[1].

The systematic formulation of the effective theory relies on an expansion of the effective Lagrangian in powers of derivatives and quark masses. Chiral symmetry implies that the leading term of this expansion is fully determined by the pion decay constant F_π and by the nucleon matrix element of the axial charge, g_A. Disregarding vertices with three or more pions, the explicit expression for the leading term reads

$$\mathcal{L}_{eff} = -\frac{g_A}{2F_\pi}\bar{\psi}\,\gamma^\mu\gamma_5\,\partial_\mu\pi\psi + \frac{1}{8F_\pi^2}\bar{\psi}\,\gamma^\mu i[\pi,\partial_\mu\pi]\psi + \ldots \qquad (1)$$

The success of the static model derives from the fact that it properly accounts for the first term on the right hand side – in the nonrelativistic limit, where the momentum of the nucleons is neglected compared to the nucleon mass.

The static model is only a model. In order for the effective theory to correctly describe the properties of QCD at low energies, that framework must be extended, accounting for the second term in the above expression for the effective Lagrangian, for the vertices that contain three or more pion fields, for the contributions arising at higher orders of the derivative expansion, as well as for the chiral symmetry breaking terms generated by the quark masses m_u, m_d. This can be done in a systematic manner, using a nonrelativistic expansion for the nucleon kinematics. The resulting framework is called "Heavy Baryon Chiral Perturbation Theory" (HBCHPT). It represents an extension of the static model that correctly accounts for nucleon recoil, order by order in the nonrelativistic expansion (for reviews of this approach, see for instance ref.[2]).

As pointed out in ref.[3], the nonrelativistic expansion of the infrared singularities generated by pion exchange is a subtle matter. The HBCHPT representations of the scattering amplitude or of the scalar nucleon form factor, for example, diverge in the vicinity of the point $t = 4M_\pi^2$. The problem does not arise in the Lorentz invariant approach proposed earlier[4]. It originates in the fact that for some of the graphs, the loop integration cannot be interchanged with the nonrelativistic expansion.

The reformulation of the effective theory given in ref.[3] exploits the fact that the infrared singular part of the one loop integrals can unambiguously be separated from the remainder. To any finite order of the nonrelativistic expansion, the regular part represents a polynomial in the momenta. Moreover, the singular and regular pieces separately obey the Ward identities of chiral symmetry. This ensures that a suitable renormalization of

*Work supported in part by Schweizerischer Nationalfonds

the effective coupling constants removes the regular part altogether. The resulting representation for the various quantities of interest combines the virtues of the Heavy Baryon approach with those of the relativistic formulation of ref.[4]: The perturbation series can be ordered with the standard chiral power counting and manifest Lorentz invariance is preserved at every stage of the calculation.

GOLDBERGER-TREIMAN RELATION

As a first illustration of the method, I briefly discuss the relation between the pion-nucleon coupling constant and the axial charge of the nucleon, obtained on the basis of a calculation of the πN scattering amplitude to order q^4. A detailed account of this work is in preparation[5]. Throughout the following, I consider the isospin limit, $m_u = m_d$, and replace the quark masses by the leading term in the expansion of M_π^2,

$$M^2 \equiv (m_u + m_d)B \; .$$

The Goldberger-Treiman relation may be written in the form

$$g_{\pi N} = \frac{g_A m_N}{F_\pi}\{1 + \Delta_{GT}\} \; . \tag{2}$$

If the quark masses m_u, m_d are turned off, the strength of the πN interaction is fully determined by g_A and F_π: $\Delta_{GT} = 0$. The effective theory allows us to analyze the correction that arises for nonzero quark masses. The quantities $g_{\pi N}$, g_A, m_N and F_π may be calculated in terms of the effective coupling constants. The result takes the form of an expansion in powers of M, i.e. in powers of the quark masses.

Some of the graphs occurring within the effective theory develop infrared singularities when the pion mass is sent to zero. These manifest themselves through odd powers of M and through logarithms thereof. The expansion of the nucleon mass, for instance, is of the form

$$m_N = m + k_1 M^2 + k_2 M^3 + k_3 M^4 \ln\frac{M^2}{m^2} + k_4 M^4 + O(M^5) \; . \tag{3}$$

The first term, m, is the value of the nucleon mass in the chiral limit. The coefficients $k_1, k_2, \ldots$ represent combinations of effective coupling constants that remain finite when the quark masses are turned off. In particular, the coefficient of the term proportional to M^3 is given by

$$k_2 = -\frac{3g^2}{32\pi F^2} \; , \tag{4}$$

where g and F represent the values of g_A and F_π in the chiral limit, respectively. The term is correctly described by the static model, where it arises from the self energy of the pion cloud that surrounds the nucleon. Numerically, this contribution lowers the nucleon mass by about 15 MeV.

Similar terms also occur in the chiral expansion of g_A – Kambor and Mojžiš[6] have worked out this quantity to order q^3. The expansion of F_π is known since a long time – it only contains even powers of M, accompanied by logarithms. The coupling constant $g_{\pi N}$ is obtained by evaluating the residue of the pole terms occurring in the scattering amplitude at $s = m_N^2$ and $u = m_N^2$. The representation of the amplitude to order q^4 yields an expression for $g_{\pi N}$ in terms of the effective coupling constants and of the quark masses, valid up to and including order q^3.

Using these results, we may evaluate the chiral expansion of Δ_{GT} to order q^3. Remarkably, the contributions of order $M^2 \ln M^2/m^2$ as well as those of order M^3 cancel – the Goldberger-Treiman relation is free of infrared singularities, up to and including order M^3:

$$\Delta_{GT} = k_{GT}\, M^2 + O(M^4) \; . \tag{5}$$

The coefficient k_{GT} represents a combination of effective coupling constants – chiral symmetry does not determine its magnitude. The result shows that in the case of the Goldberger-Treiman relation, the breaking of chiral symmetry generated by the quark masses does not get enhanced by small energy denominators. Assuming that the scale of the symmetry breaking is the same as in the case of F_K/F_π, where it is set by the massive scalar states, $M_S \simeq 1\,\mathrm{GeV}$, we obtain the crude estimate $\Delta_{GT} \simeq M_\pi^2/M_S^2 \simeq 0.02$. The detailed analysis based on models and on the SU(3) breaking effects seen in the meson-baryon coupling constants[7] confirms the expectation that Δ_{GT} must be very small – a discrepancy of order 4% or more would be very difficult to understand.

Since the days when the Goldberger-Treiman relation was discovered, the value of g_A has increased considerably. Also, F_π decreased a little, on account of radiative corrections. The main source of uncertainty is $g_{\pi N}$. The comprehensive analysis of πN scattering published by Höhler in 1983[8] led to $f^2 = g_{\pi N}^2 M_\pi^2/(16\pi m_N^2) = 0.079$. With $g_A = 1.267$ and $F_\pi = 92.4\,\mathrm{MeV}$, this value yields $\Delta_{GT} = 0.041$. As stressed by Pavan at this meeting, the data accumulated since then indicate that f^2 is somewhat smaller, numbers in the range from 0.076 to 0.077 looking more likely. This range corresponds to $0.021 < \Delta_{GT} < 0.028$.

I conclude that, within the current experimental uncertainties to be attached to the pion-nucleon coupling constant, the Goldberger-Treiman relation does hold to the expected accuracy. Note that at the level of 1 or 2 %, isospin breaking cannot be ignored. In particular, radiative corrections need to be analyzed carefully. Also, the coupling constant relevant for the neutral pion picks up a significant contribution from $\pi^0 - \eta$ interference. A precise determination of the pion-nucleon coupling constant is essential to arrive at reliable results for small quantities such as the σ-term. The various discussions at this meeting show that the issue is under close scrutiny by several groups and I am confident that the uncertainties will soon be reduced.

LOW ENERGY THEOREM FOR D^+

As a second example, I consider the low energy theorem for the value of the scattering amplitude $D^+(s,t,u)$ at the Cheng-Dashen point: $s = u = m_N^2$, $t = 2M_\pi^2$. The theorem relates this amplitude to the scalar form factor of the nucleon,

$$\langle N' |\, m_u\, \bar{u}u + m_d\, \bar{d}d \,| N\rangle = \sigma(t)\bar{u}'u\ . \tag{6}$$

The relation may be written in the form

$$F_\pi^2 D^+(m_N^2, 2M_\pi^2, m_N^2) = \sigma(2M_\pi^2) + \Delta_{CD}\ . \tag{7}$$

The theorem states that the term Δ_{CD} vanishes up to and including contributions of order M^2. The explicit expression obtained for $F_\pi^2 D^+(m_N^2, 2M_\pi^2, m_N^2)$ when evaluating the scattering amplitude to order q^4 again contains infrared singularities proportional to M^3 and $M^4 \ln M^2/m^2$. Precisely the same singularities, however, also show up in the scalar form factor at $t = 2M_\pi^2$, so that the result for Δ_{CD} is free of such singularities*

$$\Delta_{CD} = k_{CD} M^4 + O(M^5)\ . \tag{8}$$

Crude estimates like those used in the case of the Goldberger-Treiman relation indicate that the term Δ_{CD} must be very small, of order 1 MeV.

The value of the scalar form factor at $t = 0$ is referred to as the σ-term,

$$\sigma = \sigma(0)\ .$$

This quantity is of particular interest, because it represents the response of the nucleon mass to a change in the quark masses:

$$\sigma = m_u \frac{\partial m_N}{\partial m_u} + m_d \frac{\partial m_N}{\partial m_d}\ . \tag{9}$$

*The cancellation of the terms of order M^3 was pointed out in ref.[4,9] and the absence of logarithmic contributions of order M^4 was shown in ref.[10].

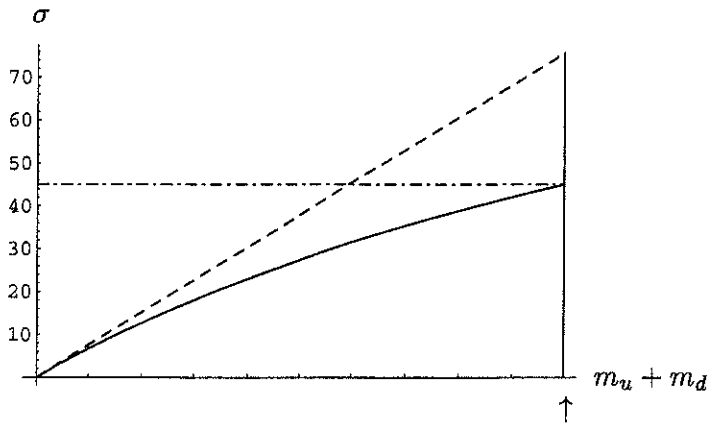

Figure. 1. σ-term (in MeV) as a function of the quark masses. It is assumed that the physical value of σ is 45 MeV (dash-dotted line). The arrow corresponds to the physical value of $m_u + m_d$. The dashed line depicts the linear dependence that results if the infrared singular contributions proportional to M_π^3 and to $M_\pi^4 \ln M_\pi^2/m_N^2$ are dropped.

The difference $\sigma(2M_\pi^2) - \sigma(0)$ is well understood: The results found on the basis of a dispersive analysis[11] are confirmed by the evaluation of the scalar form factor within the effective theory[12,3]. The net result is that an accurate determination of the scattering amplitude at the Cheng-Dashen point amounts to an accurate determination of the σ-term.

Unfortunately, the experimental situation concerning the magnitude of D^+ at the Cheng-Dashen point leaves much to be desired (for a recent review, see ref.[13]). The low energy theorem makes it evident that we are dealing with a small quantity here – the object vanishes in the chiral limit. The inconcistencies among the various data sets available at low energies need to be clarified to arrive at a reliable value for $g_{\pi N}$. Only then will it become possible to accurately measure small quantities such as the σ-term.

DEPENDENCE OF THE σ-TERM ON THE QUARK MASSES

In the following, I do not discuss the magnitude of σ as such, but instead consider the dependence of this quantity on the quark masses, which is quite remarkable. In this discussion, the precise value of σ is not of crucial importance. For definiteness, I use the value $\sigma = 45\,\mathrm{MeV}$[11]. The chiral expansion of the σ-term is readily obtained by applying the Feynman-Hellman theorem (9) to the formula (3), with the result

$$\sigma = k_1 M^2 + \frac{3}{2}\, k_2 M^3 + k_3 M^4 \left\{ 2 \ln \frac{M^2}{m^2} + 1 \right\} + 2\, k_4 M^4 + O(M^5)\,, \tag{10}$$

As discussed above, the term proportional to M^3 arises from an infrared singularity in the self energy of the pion cloud. It lowers the magnitude of the σ-term by $3/2 \times 15\,\mathrm{MeV} \simeq 23\,\mathrm{MeV}$. The coefficient k_3 can also be expressed in terms of measurable quantities[3]. Numerically the contribution from this term amounts to $-7\,\mathrm{MeV}$, thus amplifying the effect seen at $O(M^3)$. Chiral symmetry does not determine all of the effective coupling constants entering the regular contribution $k_4 M^4$, which is of the same type as the correction $\Delta_{CD} = k_{CD} M^4$ to the low energy theorem (7). As discussed above, corrections of this type are expected to be very small – I simply drop the term $k_4 M^4$. The value of k_1 is then fixed by the input $\sigma = 45\,\mathrm{MeV}$ for the total, so that we can now discuss the manner in which σ changes when the quark masses are varied.

At leading order, σ is given by $k_1 M^2$. In figure 1 this contribution is shown as a dashed straight line. The full curve includes the contributions generated by the infrared singularities, $k_2 M^3$ and $k_3 M^4 \{2 \ln M^2/m^2 + 1\}$. The figure shows that the expansion of the σ-term in powers of the quark masses contains large contributions from infrared singularities. These must show up in evaluations of the σ-term on a lattice: The ratio

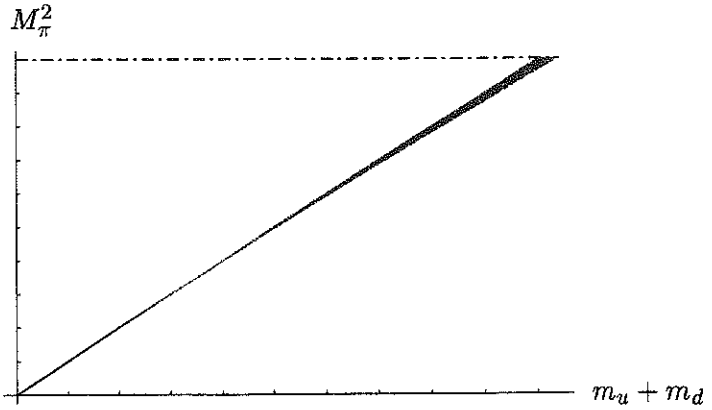

Figure. 2. Square of the pion mass as a function of the quark masses. The dash-dotted line indicates the physical value of M_π^2.

$\sigma/(m_u+m_d)$ must change significantly if the quark masses are varied from the chiral limit to their physical values. Note that in this discussion, the mass of the strange quark is kept fixed at its physical value – the curvature seen in the figure exclusively arises from the perturbations generated by the two lightest quark masses.

It is instructive to compare this result with the dependence of M_π^2 on the quark masses. In that case, the expansion only contains even powers of M:

$$M_\pi^2 = M^2 + \frac{M^4}{32\pi^2 F^2} \ln \frac{M^2}{\Lambda_3^2} + O(M^6) \,. \tag{11}$$

The quantity Λ_3 stands for the renormalization group invariant scale of the effective coupling constant l_3. The SU(3) estimate for this coupling constant given in ref.[14] reads $\bar{l}_3 \equiv -\ln M_\pi^2/\Lambda_3^2 = 2.9 \pm 2.4$. The error bar is so large that the estimate barely determines the order of magnitude of the scale Λ_3. Figure 2 shows, however, that this uncertainty does not significantly affect the dependence of M_π^2 on the quark masses, because the logarithmic contribution is tiny: the range of $\bar{l}_3$ just quoted corresponds to the shaded region shown in the figure.

The logarithmic term occurring in the chiral expansion of M_π^2 gets enhanced by about a factor of two if we consider the pion σ-term,

$$\sigma_\pi = \langle \pi | \, m_u \bar{u}u + m_d \bar{d}d \, | \pi \rangle = m_u \frac{\partial M_\pi^2}{\partial m_u} + m_d \frac{\partial M_\pi^2}{\partial m_d} \,. \tag{12}$$

I do not show the corresponding curve, because it is also nearly a straight line.

The main point here is that the infrared singularities encountered in the self energy of the nucleon are much stronger than those occurring in the self energy of the pion. A detailed account of the work on the low energy structure of the πN scattering amplitude done in collaboration with Thomas Becher is in preparation.

REFERENCES

1. E.M. Henley and W. Thirring, *Elementary Quantum Field Theory*, (McGraw-Hill, New York 1962), Part III. Pion Physics.
2. G. Ecker, Czech. J. Phys. **44**, 505 (1994).
   V. Bernard, N. Kaiser and U.-G. Meissner, Int. J. Mod. Phys. **E4**, 193 (1995).
3. T. Becher and H. Leutwyler, Eur. Phys. J. **C9** 643 (1999). For earlier work in this direction see P. J. Ellis and H.-B. Tang, Phys. Rev. **C57** 3356 (1998).
4. J. Gasser, M. E. Sainio and A. Svarc, Nucl. Phys. **B307** 779 (1988).
5. T. Becher and H. Leutwyler, to be published.
6. J. Kambor and M. Mojžiš, "Field redefinitions and wave function renormalization to $O(q^4)$ in HBCHPT", J. High Energy Physics **9904**, 031(1999)

7. C.A. Dominguez, Phys.Rev. **D27** 1572 (1983); Nuovo Cim. **8**, 1 (1985).
P.A.M. Guichon, G.A. Miller and A.W. Thomas, Phys.Lett. **124B** 109 (1983).
P.M. Gensini, Nuovo Cim. **102A**, 75 (1989), E: ibid. **102A** 1181 (1989).
8. G. Höhler, in Landolt-Börnstein, **9b2**, ed. H. Schopper (Springer, Berlin, 1983).
9. H. Pagels and W.J. Pardee, Phys.Rev. **D4**, 3335 (1971).
10. V. Bernard, N. Kaiser and U. Meissner, Phys.Lett. **B389**, 144 (1996).
11. J. Gasser, H. Leutwyler and M. E. Sainio, Phys. Lett. **B253**, 252, 260 (1991).
12. V. Bernard, N. Kaiser and U. Meissner, Z.Phys. **C60**, 111 (1993).
13. M.E. Sainio, "Low-energy pion-nucleon interaction and the sigma term", πN Newslett. **13** 144 (1997).
14. J. Gasser and H. Leutwyler, Ann. Phys. **158** 142 (1984).

Some Results on πN Phenomenology

G. Höhler
Institut für Theoretische Teilchenphysik der Universität
Postfach 6980 D-76128 Karlsruhe, Germany

Abstract

The first part deals with the relation between dispersion theory and chiral perturbation theory. In the second part, attention is called to ambiguities and uniqueness in πN partial wave analysis.

Δ-Exchange and t-Channel Exchange from fixed-t Dispersion Relations

Introduction

Fixed-t dispersion relations can be proved within the framework of QCD[1]. The reactions $\pi^{\pm}p \to \pi^{\pm}p$ can be described by 4 invariant amplitudes, e. g. $C^{\pm}(\nu,t), B^{\pm}(\nu,t)$, where the upper index indicates if the amplitude is even or odd under the crossing operation $\nu \to -\nu$, ($\nu = (s-u)/4m$, m=proton mass). It is assumed that electromagnetic contributions are subtracted as described by Tromborg et al.[2]. We subtract from all amplitudes the PV Born term and denote this by a bar. Then, the *subthreshold expansion* (sect. 2.4.7.1 in Ref.[3]) reads

$$X(\nu,t) = \sum_{m,n} x_{mn}\, \nu^{2m}\, t^n, \qquad m,n = 0,1,2\ldots \tag{1}$$

where X is a crossing even amplitude, or a crossing odd amplitude divided by ν. The coefficients are denoted by $b^+_{00}, b^+_{10}, \cdots$ for $\bar{B}^+/\nu$, etc. In the following we shall discuss only $t = 0$. Then ν is the total pion energy in the lab. ω and $C^{\pm} = D^{\pm}$.

For a comparison with predictions from chiral perturbation theory (CHPT), we have calculated the coefficients of all amplitudes from the fixed-t dispersion relation with the VPI solution SP98 which ends at $2.2\,GeV/c$ and with KA84 up to the same momentum and also up to $6\,GeV/c$[25]. There are no significant differences between the two results up to $2.2\,GeV/c$. The contribution from higher momenta was calculated for ImC^- from total cross section data up to $340\,GeV/c$ and estimated for ImB^- from the reggeized ρ-exchange model (sect.2.6.5 in Ref.[3]).

The situation of A^+ is still the same as in 1970[4]. $C^+ = A^+ + \omega B^+$ can be decomposed into contributions of A^+ and ωB^+ only if data for spin-rotation and polarization parameters are available, which do not exist at high energies. If $A^+/(\omega B^+) \to 0$ for $\omega \to \infty$, *asymptotic s-channel helicity conservation* is a consequence[4]. According to KH80, the contribution of ImA^+ to ImC^+ is much smaller than that of $\omega\, ImB^+$ in the range from 2 to 10 GeV/c.

Δ-exchange from fixed-t dispersion relations

Plots of the integrands of *all* fixed-t dispersion relations show a pronounced peak or dip at or near the range where the imaginary part of the partial wave $T(P33)$ has its peak. In order to get a numerical value for a $P33$ dominance, we have calculated all integrals also with the P33-contribution to the imaginary part of the amplitude up to $0.6\,GeV/c$[25]. It is well known from the partial wave dispersion relation that P33 includes not only the effect of the $\Delta(1232)$-pole but also a fairly large background from the nucleon Born term and t-channel exchanges[6,5]. (The Chew-Low plot is an approximation[6]). About 2/3 of the scattering volume a_{33} comes from the l.h. cut[5].

In the lowest order of an effective Lagrangian, Δ-exchange is treated in a way which corresponds to a narrow width approximation, where the dispersion integral leads to pole terms. In sect. 8.1.2 of Ref.[3], the two parameters of an effective Δ-pole term were determined by a best fit to both invariant amplitudes in the subthreshold region and over a small range of t. In the new calculation[25], the location of the pole on the real axis

is assumed to be $W = \sqrt{s} = 1232\,MeV$. The residue follows from the condition that for each amplitude the pole term gives at $\nu = 0$, $t = 0$ the same result as the evaluation of the dispersion integral with the P33 contribution of the numerator in the integrand. The non-Δ part of P33 was neglected (this should be improved).

As an example we consider the amplitude B^+. Our Δ-pole term reads

$$\hat{B}^+_\Delta(\omega) = \frac{\bar{B}^+_\Delta(\omega)}{\omega} = -\frac{5.88\,G^2_\Delta}{5.59 - \omega^2}, \qquad G^2_\Delta = 3.8, \qquad \hat{B}^+_\Delta(0) = -4.0\,m_\pi^{-3}. \tag{2}$$

The dispersion integral up to $6\,GeV/c$ gives practically the same value as at $2.2\,GeV/c$ with both solutions (–3.55), i.e. a correction of about +10% to the value –4.0 from Δ-dominance. A plot of the integrand shows that the correction comes from the mass range $1400 \ldots 1550\,MeV$.

If the lower index of a coefficient is $m0$, the integrand of the dispersion integral has an additional term ω^{2m} in the denominator. Therefore *the input from high momenta is strongly suppressed if* $m > 0$. This suppression also occurs *for coefficients which belong to the dependence on t*. For $m > 0$, the dip or peak is shifted to smaller momenta and its shape is distorted[25]: for b^+_{20} the P33 phase at the dip amounts to about 30°.

The large discrepancies of one-loop results of Bernard et al.[26] from the dispersion calculation, e. g. for b^+_{10} and b^+_{20}, follow from the fact that in the order of their calculation the large Δ contributions do not yet occur. It is not clear to me why their prediction for b^-_{10} agrees very well with my table.

An expansion in powers of ν^2 also follows from the t-channel partial wave expansion. This leads to a test of the internal consistency , e. g. with Table 2.4.6.1 in Ref.[3]

$$\frac{1}{4\pi}\tilde{B}^-(\nu,t) = \frac{3}{\sqrt{2}}\,\tilde{f}^1_-(t) - \frac{7\sqrt{3}}{4}\,[(p_-q_-)^2 - 5m^2\nu^2]\,\tilde{f}^3_-(t) + \ldots. \tag{3}$$

The tilde indicates that the contribution from the PS Born term has been subtracted. $p^2_- = m^2 - t/4$, $q^2_- = m^2_\pi - t/4$.

t-channel exchange from fixed-t dispersion relations

The dispersion integrals for c^-_{00} and b^-_{00} have a very slow convergence. We consider as an example $C^-(\omega)$ $(k = plab = \sqrt{\omega^2 - m^2_\pi})$

$$ImC^-(\omega) = k\,\sigma^-_{tot} \qquad \sigma^-_{tot} = \frac{1}{2}\left[\sigma_{tot}(\pi^- p) - \sigma_{tot}(\pi^+ p)\right]. \tag{4}$$

For k=10 to 340 GeV/c, $\sigma^-_{tot} \approx const/\sqrt{k}$. This is expected from the reggeized ρ-exchange model with $\alpha(t = 0) \approx 0.50$ (see e. g. sects.2.6.5 and A.9.1 in Ref.[3]).

We define

$$G(\omega) = \frac{\tilde{C}^-(\omega)}{\omega} = \frac{2}{\pi}\int_{m_\pi}^{\infty} \frac{ImC^-(\omega')}{\omega'^2 - \omega^2}\,d\omega', \tag{5}$$

where the tilde indicates that the nucleon pole term (=PS Born term) has been subtracted. Table 1 shows that $G(0)$ *is half as large as the P33 contribution.*

Subtraction of $\tilde{f}^1_+(0)$

The t-channel partial wave can be expressed by the Froissart-Gribov representation (sect.A.7 in Ref.[3]) (which can easily be extended to the t-dependence. The P33 contribution to the partial wave follows if the P33 contribution to ImC^- is inserted).

$$\tilde{f}^1_+(0) = \frac{m}{8\pi\,m^2_\pi}\int_{m\pi}^{\infty} ImC^-(\omega)Q_1(Z)\,d\omega \cdot m_\pi^{-1}, \qquad Z = \frac{\omega}{m_\pi}. \tag{6}$$

The integral up to 6 GeV/c gives $-0.121\,m_\pi^{-1}$ and the tail above 6 GeV adds $+0.015\,m_\pi^{-1}$.

Table 1. Dispersion integral for different upper limts and P33 contribution

$G(0)\, m_\pi^{-2}$	$pLab_{max}\, GeV/c$	
-0.46	∞	
-0.56	6.0	KA84
-0.62	2.2	KA84, SP98
-0.90	0.6	KA84, SP98; only P33
		Next lines: to be used later
-0.77	6.0	elastic
$+0.31$	∞	inelastic
$+0.21$	6.0	inelastic

This expression is multiplied by a factor chosen in such a way that the subtraction cancels the leading terms in the integrand at high energies. This idea was proposed by Mandelstam, used by Frazer and treated in detail in Ref.[7].

$$G(0) = \frac{12\,\pi}{m}\tilde{f}_+^1(0) + \frac{2}{\pi}\int_{m\pi}^{\infty} ImC^-(\omega)\left[\frac{1}{\omega^2} - \frac{3}{m_\pi^2}Q_1(Z)\right] d\omega. \tag{7}$$

$Q_1(Z)$ is the Legendre function of the 2nd kind:

$$Q_1(Z) = \frac{1}{3Z^2} + \frac{1}{5Z^4} + \ldots \tag{8}$$

The integrand of the subtracted integral has a serious shortcoming: the P33 contribution leads to a *peak instead of the dip* of the unsubtracted integral. Furthermore, the cut of $\tilde{f}_+^1(t)$ at $t < 0$ has a *large* contribution from P33.

Therefore, we apply a decomposition of the imaginary parts which was proposed in Ref.[8]. For the dimensionless s-channel partial waves (as used in Argand plots), unitarity leads to a decomposition of $ImT_{\ell\pm}$ into elastic and inelastic parts:

$$ImT_{\ell\pm} = |T_{\ell\pm}|^2 + ImT_{\ell\pm}^{in}; \qquad ImT_{\ell\pm}^{in} = (1 - \eta_{\ell\pm}^2)/4. \tag{9}$$

$\eta_{\ell\pm}$ is the absorption parameter. This decomposition leads to *elastic and inelastic parts* of the imaginary parts of invariant amplitudes and of t-channel partial waves.

The important point is now to consider *unitarity in the t-channel.* Because of G-parity conservation a 3-pion vertex is forbidden. We consider the two simplest unitarity graphs. The above defined inelastic s-channel amplitude belongs to 2-pion intermediate states in the t-channel. Since a 4-pion decay of the ρ has not been observed, *we carry out the subtraction only for the inelastic part.* The other simple t-channel unitarity graph belongs to 4-pion intermediate states and is of interest only if higher t-channel resonances are considered.

$$G(0) = G_{el}(0) + \frac{12\,\pi}{m}\tilde{f}_{+,inel}^1(0) + \frac{2}{\pi}\int_{m_\pi}^{\infty} ImC_{inel}^-\left[\frac{1}{\omega^2} - \frac{3}{m_\pi^2}Q_1(Z)\right] d\omega. \tag{10}$$

An evaluation with KA84 shows that *the subtracted integral is negligible.*

According to Table 1 the elastic (–0.77) and inelastic (+0.31) contributions give the total value (–0.46). P33 alone (–0.90) is *not dominant.* The other elastic contributions come from the mass range $1400 \ldots 1800\, MeV$. Above $6\, GeV/c$, the elastic part is comparable with its error.

Since our result was derived from the dispersion relation, *contributions from all 3 channels have been superimposed without double counting.* Empirical superpositions of contributions from all three channels are not allowed.

A t-channel contribution also occurs in the low-energy theorem of Brown et al.[27] from the ETC term of the Ward-Takahashi identity:

$$F_{1v}(t) \cdot \frac{1}{2F_\pi^2}, \qquad F_{1v}(0) = 1, \qquad F_\pi = 92.4\, MeV. \tag{11}$$

At $t = 0$ this is part of the tree graphs of the Chiral Effective Lagrangian. $F_{1v}(t)$ is the isovector Dirac nucleon form factor and F_π the pion decay constant.

Gasser et al.[27] pointed out that their low-energy constant b_9 occurs in their result for F_{1v} but not in the πN amplitudes. They found a logarithmic singularity in the second sheet at $t = 4m_\pi^2[1 - m_\pi^2/(4\,m^2)] \approx 3.98\, m_\pi^2$, which we had studied in detail with dispersive methods[28]. Further work on the relation between the result of Brown et al.[29] and our subtraction is necessary.

Ambiguities in πN Partial Wave Analysis

πN scattering can be described by four complex-valued invariant amplitudes, e. g. $C^\pm(s,t)$ and $B^\pm(s,t)$. If all measurable quantities are known with high precision, *one can determine only 7 real numbers at each (s,t)*, since a common phase $\Phi(s,t)$ of all amplitudes does not follow from πN scattering data. An exception are the amplitudes $C^\pm(s, t = 0)$. $ImC^\pm$ follows from total cross section data and the optical theorem and $ReC^\pm$ can be determined from data in the Coulomb interference region, so the phase follows from data.

Except for a small kinematical range, spin-rotation data have not been measured. Then *a second phase $\Psi(s,t)$ is not known.* Furthermore, there are discrete ambiguities, e. g. Barrelet[9] noticed that reflections of zeros of transversity amplitudes in the complex plane lead to new amplitudes, which *give the same $d\sigma/d\Omega$ and analyzing power P.*

One could think that *unitarity* strongly reduces the ambiguities. But the work of D. Atkinson et al.[10] has shown that, in the inelastic region, unitarity is a rather weak constraint. Instead of the discrete ambiguities there exist *islands of ambiguity* in the Argand diagrams of the partial waves. The pioneers used truncations of the partial wave series and the 'shortest path method', but it was shown that both methods are not satisfactory. Further details and references are given in the excellent review by Bowcock and Burkhardt[11] and in Refs.[3,13,14].

In order to get *unique πN amplitudes*, it is necessary to impose in addition to Lorentz invariance, unitarity and isospin invariance (except for small corrections) *further theoretical constraints.*

The only available general principle is analyticity of the invariant amplitudes. Since fixed-t analyticity can be applied only in a limited range of t and therefore of the angular region (except for low energies), one has to assume the Mandelstam hypothesis[12], which includes analyticity in two complex variables s and t. Of course, one cannot use the double dispersion relations in a πN partial wave analysis. However, there exists a number of quite different single-variable dispersion relations which have been derived from the hypothesis. One can use one of them in addition to fixed-t analyticity as a constraint in order to cover the whole angular region. Then, one can check, if the new partial wave solution is compatible with the other single-variable dispersion relations and with the predicted properties of the zero trajectories of the amplitudes[9,3].

Mathematical problems related to the application of analyticity constraints in πN partial wave analyses and to the uniqueness and stability of the solution have been treated in many papers, e. g. Refs.[13,14], where further references can be found.

Mandelstam analyticity plays also an important role in studies of the relation of dispersion theory to chiral effective theories[15].

The Methods of Pietarinen and of Cutkosky

In the early 70's, the use of dispersion relations as constraints in partial wave analyses on computers was difficult as long as principal value integrals had to be calculated. It was a crucial progress that E. Pietarinen[16,11] developed an expansion method combined with a conformal mapping. *A cut-off of the partial wave expansion was avoided by using*

a convergence test function method, which also allowed *to choose the degree of smoothing.* The fit to the data and to the constraint were applied alternatively, the last step was a fit to the data. In order to have constraints in the whole of the angular region at all energies, the method was extended to include analyticity along 20 fixed values of $\cos\theta$. The Karlsruhe-Helsinki solution KH80 is described in Refs.[17,18]. It is based on isospin invariance and uses only data for the reactions $\pi + N \to \pi + N$. Each partial wave is described by a real phase and an absorption parameter. Partial waves were given up to $10\,GeV/c$ and fixed-t analyticity was applied to data up to $200\,GeV/c$.

R.E. Cutkosky[19] had worked on expansion methods already in 1968, but he started to apply them to πN scattering data only after Refs.[16] had been published. The methods in the first paper[19] were different from those of Pietarinen, but the basic ideas were the same. The solution CMB80 also gives phases and absorption parameters in the smaller range $0.427 \ldots 2.5\,GeV/c$.

In the second paper the partial wave amplitudes have been analyzed, using a modified Breit-Wigner, coupled-channel parametrization. Data for inelastic final states were used as additional input. However, there were problems to fit the inelastic data in conjunction with the elastic amplitudes. The final results give resonance parameters for all resonances but no branching ratios for the inelastic channels.

A comparison of the speed plots for resonances found in KH80 and CMB80 shows a reasonable agreement, if one remembers that the data base contains many cases of contradictions between data sets[30].

Compatibility of KH80 with relations derived from the Mandelstam hypothesis

1) 50 hyperbolas through the Cheng-Dashen point[20].
2) s-channel partial wave projections of fixed-t dispersion relations[21].
3) Dispersion relations for s-channel partial wave amplitudes[5,22].
4) Interior dispersion relations (fixed lab. angle)[23,31].
5) Fixed-ν dispersion relations (p.291 in Ref.[3]).
6) Dispersion relations for t-channel partial waves (sect.2.4.6 in Ref.[3]).
7) Fixed-s dispersion relation at threshold[22].
8) Zero trajectories: test of analyticity in two variables.

For invariant amplitudes: sect. 2.4.3.3 in Ref.[3]. Barrelet zeros of transversity amplitudes are much more sensitive. The result for KH80 is not satisfactory, but up to 1 GeV/c Koch's solution KA84[22] is much better. It includes constraints from partial wave dispersion relations.

Remarks on the VPI solutions

In 1980 R.A. Arndt started with the aim to give *'the most economic description of the πN scattering data'*. He used *an empirical ansatz* with a large number of adjustable coefficients for the parametrization of the partial waves. *He ignored the well-known nearby l.h. cut singularities, even those from the nucleon Born term.* Since KH80 and CMB80 were available as start solutions, he could easily include new data and produce four new solutions per year.

In 1989 I pointed out in a talk that his solution is at variance with fixed-t analyticity. The group introduced constraints for the invariant amplitudes at a few t-values from 0 to $-0.3\,GeV^2$, but this was possible only in about 1/3 of the range of the analysis (2.2 GeV/c). For the dispersion integrals above 2.2 GeV/c, they took results from KH80, which do not include new data and do not join smoothly to their solution at 2.2 GeV/c.

The VPI solutions are a fit to the data, which can be used for continuations into other sheets. The uncertainties which follow from the ambiguities *are mainly resolved by the empirical ansatz and not by the theoretical constraints, which are very weak.* The information from the large amount of data above 2.2 GeV/c is not used. There is no good argument to expect *uniqueness* for the solution.

Conclusions

A first step should be *to determine unique invariant amplitudes from data.* The available results suggest that this can be done by applying constraints and tests from consequences of the Mandelstam hypothesis. An important further test is to check the compatibility with predictions from chiral perturbation theory. Therefore it is necessary to prepare an updated version of the solution KH80. This agrees with the first steps of Pietarinen and Cutkosky.

A second step should be to treat problems related to inelastic final states, e. g. to find out which resonances exist because of the opening of a threshold, how this can be understood in quark models, how branching ratios can be predicted etc. This can be done only by developing models, which should be compatible with the framework derived in the first step.

Thanks

I would like to thank A. Badertscher and the other organizers for the invitation to this very interesting Symposium and for hospitality. For discussions I am grateful to T. Becher, P. Büttiker, J. Gasser, H. Leutwyler, U.- G. Meißner and the VPI group, in particular R.A. Arndt and M.M. Pavan.

REFERENCES

1. R. Oehme, πN Newsletter 7,1 (1992)
2. B. Tromborg et al., Phys. Rev. **D15**, 725 (1977)
3. G. Höhler, *Pion-Nucleon Scattering, Landolt-Börnstein Vol.I/9b2*, ed. H. Schopper, Springer (1983)
4. G. Höhler et al., Z. Physik **232**, 205 (1970)
5. R. Koch and M. Hutt, Z. Physik **C19**, 119 (1983)
6. J. Hamilton, Pion-Nucleon Interactions in High Energy Physics, Vol.I, ed. E.H.S. Burhop, Academic Press (1967)
7. K. Dietz, *Z. Phys.* **170**, 212 (1962)
8. M. Cini and B. Vitale, *Lectures on High Energy Physics*, Hercegnovi 1961, Vol. II, ed. B. Jakšić, p.323ff
9. E. Barrelet, Nuovo Cim. **8A**, 331 (1972)
10. D. Atkinson et al., Phys. Lett. **148B**, 361 (1984)
11. E. Pietarinen, Nucl. Phys. **B107**, 21 (1976)
12. S. Mandelstam, Phys. Rev. **112**, 1344 (1958); **115**, 1741 (1959)
13. E. Pietarinen, Phys. Scripta **14**, 11 (1976)
14. I. Sabba Stefanescu, Fortschritte der Physik **35**, 573 (1987); Z. Phys. **C41**, 453 (1988)
15. T. Becher and H. Leutwyler, Eur. Phys. J. **C9**, 643,(1999) and contribution to this Symposium
16. E. Pietarinen, Nuovo Cim. **12A**, 522 (1972); Nucl. Phys. **B49**, 315 (1972); **B55**, 541 (1973)
17. G. Höhler, F.Kaiser, R. Koch, E. Pietarinen, *Handbook of Pion-Nucleon Scattering* Physics Data **12-1** (1979)
18. R. Koch and E. Pietarinen, Nucl. Phys. **A336**, 331 (1980)
19. R.E. Cutkosky et al., Phys. Rev. **D20**, 2804,2839 (1979); Proc. Baryon 1980 Conference, p.19, ed. N. Isgur, Toronto
20. R. Koch, Z. Phys. **C15**, 161 (1982)
21. R. Koch, Nucl. Phys. **A448**, 707 (1986)
22. R. Koch, Z. Phys. **C29**, 597 (1985)
23. E. Borie and F. Kaiser, Nucl. Phys. **B126**, 173 (1977)
24. R.A. Arndt et al., Phys. Rev. C49, 2729 (1994). Contributions to this Symposium by M.M. Pavan.
25. G. Höhler, in preparation
26. V. Bernard et al., Nucl. Phys. **A615**, 483 (1997)
27. J. Gasser et al., Nucl. Phys. **B307**, 779 (1988)
28. G. Höhler and E. Pietarinen, Nucl. Phys. **B95**, 210 (1975)
29. L.S. Brown, W.J. Pardee and R.D. Peccei, Phys. Rev. **D4**, 2801 (1971)
30. G. Höhler et al., πN Newsletter **7**, 94 (1992), *ibid* **9**, 1 (1993)
31. J. Stahov, πN Newsletter **13**, 174 (1997) and contribution to this Symposium

The Subthreshold Expansion of the πN Invariant Amplitudes in Dispersion Theory

J. Stahov
University Tuzla, Faculty of Chemical Engineering
Univerzitetska 8
75000 Tuzla, Bosnia and Herzegovina

Abstract:

The interior dispersion relations and the fixed-t dispersion relations are used to continue πN scattering amplitudes to the subthreshold region. Coefficients in the subthreshold expansion of the invariant amplitudes are derived. The result for the πN sigma term is $\sigma_{\pi N}$=(70±8) MeV.

Introduction and notation

In the last three decades there have been many published papers and many discussions about the πN invariant amplitudes in the unphysical regions. The most efforts have been concentrated mainly to the determination of the invariant amplitudes by means of the expansion near the point ν=0, t=0, and the subsequent determination of the πN σ term. The Karlsruhe group [1] proposed to perform an analytic continuation of the invariant amplitudes to subthreshold region by using the dispersion theory technique.

In this report we combine the fixed-t dispersion relations (FTDR) method and the interior dispersion relations (IDR) method to determine invariant amplitudes in the subthreshold region, and also corresponding coefficients in the subthreshold expansions.

We consider the isospin even and isospin odd combinations of the invariant amplitudes $B^{\pm}$, $A^{\pm}$ that are related to the $\pi^{\pm}$N amplitude $A_{\pm}, B_{\pm}$: $A^{\pm}=(A_{-}\pm A_{+})/2$, $B^{\pm}=(B_{-}\pm B_{+})/2$.

According to Mandelstam hypothesis, invariant scattering amplitudes are real analytic functions of three complex variables s, t, and u. Variables s and t are defined in terms of the total energy w and from the scattering angle θ in the c.m. frame

$$s=w^2, \qquad t=-2q^2(1-\cos\theta), \qquad s+t+u=\Sigma, \qquad \Sigma=2m^2+2m_\pi^2,$$

where q is momentum in c.m. frame, m = proton mass, m_π = mass of charged pion. For more details on πN kinematics we refer to ref. [2] which will be subsequently denoted by LB. Although four amplitudes defined above fully describe the πN scattering if the isospin invariance is assumed (we do so in our application), we introduce the additional amplitudes $D^{\pm}=A^{\pm}+\nu B^{\pm}$, $\nu=(s-u)/4m$ which are frequently used in the chiral perturbation theory.

In order to obtain invariant amplitudes having a smooth behavior in the subthreshold region, we introduce amplitudes from which the pseudo vector (PV) Born term is subtracted. We denote these amplitudes by a bar. Born term appearing in dispersion relations is pseudo scalar one. Due to the crossing symmetry, invariant amplitudes either remain unchanged after transformation ν→ -ν (crossing even amplitudes) or change a sign (crossing odd amplitudes). In our applications only crossing even amplitudes are considered. Crossing even amplitudes could be considered as being functions of variables ν^2 and t, X(ν^2,t), where X(ν^2,t) stands for $\overline{A}^{+}, A^{-}/\nu, \overline{B}^{-}/\nu, \overline{B}^{+}, \overline{D}^{+}, \overline{D}^{-}/\nu$.

In the region limited by the lines $s=(m+m_\pi)^2, u=(m+m_\pi)^2, t=4m_\pi^2$, (Mandelstam triangle), amplitudes are real. Each crossing even amplitude can be expanded near the point ν=0, t=0 using so called subthreshold expansion:

$$X(\nu^2,t)=\sum_{m,n} x_{mn}\nu^{2m}t^n,$$

where x_{mn} stands for $\overline{a}^{\pm}_{mn}, \overline{b}^{\pm}_{mn}, \overline{d}^{\pm}_{mn}$.

Interior dispersion relations

Studying various kinds of dispersion relations used in the early eighties, Hite and Steiner investigated more generalized dispersion relations on parameterized curves in the Mandelstam plane. In ref. [3] they proposed dispersion relations for crossing even amplitudes on hyperbolas $(s-a)(u-a)=b$, in the Mandelstam plane, where a is an asymptote and b is hyperbolae parameter. Dispersion relations obtained in such a way receive contributions from all three channels. Knowledge of absorptive parts is required only in the regions where corresponding partial wave expansions converge. Hite et al. [4] proposed one parameter family of hyperbolas passing through the s-channel threshold with $b=(m^2-m_\pi^2-a)^2-4m_\pi^2 a$. For $a \le 0$, the integration paths lie in the interior of the physical regions of the s and t-channels - interior dispersion relations (IDR). The backward dispersion relations follow from the IDR as a special case when $a=0$. If variable t is taken as an independent variable, other variables could be obtained by some algebra:

$$\nu=\frac{1}{4m}\sqrt{(t-t_0)^2-4b}, \quad t_0=\Sigma-2a,$$

$$s=\frac{\Sigma-t}{2}+\frac{1}{2}\sqrt{(t-t_0)^2-4b}, \quad u=\frac{\Sigma-t}{2}-\frac{1}{2}\sqrt{(t-t_0)^2-4b}.$$

Hyperbolas cross the ν=0 line at points: $t_\pm=t(\nu=0,a)=\Sigma-2a\pm\sqrt{b}$, $0\le t_-\le 4m_\pi^2, t_+\ge 4m^2$. The crossing even amplitudes have the cuts for $t\le 0$ (the s-channel cut), and for $t\ge 4m_\pi^2$ (the t-channel cut). In addition, amplitudes $B^\pm$ have a pole (the Nucleon pole) at $t=t_N$, where $t_N=m_\pi^2(4m^2-m_\pi^2)/(m^2-a)$.

Knowing analytic structure of invariant amplitudes along hyperbolas, it is easy to write the corresponding interior dispersion relations. In practical evaluation, imaginary part of amplitudes is known in the restricted region $t_L\le t\le 0$, where t_L corresponds to the highest momentum in the s-channel where results from PWA exist. The input from the t-channel exists for $4m_\pi^2\le t\le t_R$. Unknown contributions can be described using the method of discrepancy function pioneered by Hamilton and his coworkers in sixties :

$$\mathrm{Re}\,X(t,a)=X_N(t,a)+\frac{1}{\pi}\left\{P\int_{t_L}^{+0}+\int_{4m_\pi^2}^{t_R}\right\}\mathrm{Im}\,X(t',a)\frac{dt'}{t'-t}+\Delta(t),$$

where $X_N(t,a)=X_{Nps}-X_{Npv}$. X_{Nps} and X_{Npv} stand for pseudo scalar and pseudo vector Born terms, and $\Delta(t)$ is discrepancy function. In the subtracted form (subtraction point $t=t_0$), IDR read:

$$\mathrm{Re}\,X(t,a)=\Delta(X_N)+\frac{t-t_0}{\pi}\left\{P\int_{t_L}^{+0}+\int_{4m_\pi^2}^{t_R}\right\}\mathrm{Im}\,X(t',a)\frac{dt'}{(t'-t_0)(t'-t)}+\Delta(t),$$

where $\Delta(X_N)=X_N(t,a)-X_N(t_0,a)$.

The discrepancy function Δ(t) can be calculated at t-values where the input from the PWA exists. The obtained results are fitted to smooth, well behaved functions, usually polynomials of the low order in variable t. Having parameterized discrepancy function, the real part can be calculated at the points outside of the region where input exists-usually outside of the physical region.

The fixed-t dispersion relations

Among all dispersion relations, the fixed-t dispersion relations–FTDR are the most frequently used, especially the forward dispersion relations-FDR for which the input exists up to

k=300 GeV/c. We apply the FTDR method for crossing even amplitudes appearing also in the IDR method. The FTDR for crossing even amplitudes read :

$$\mathrm{Re}\,X(\nu,t)=X_N(\nu,t)+\frac{1}{\pi}\int_{m_\pi^2}^{\nu_{\max}^2}\mathrm{Im}\,X(\nu'^2,t)\frac{d\nu'^2}{\nu'^2-\nu^2}+\Delta(\nu)\,.$$

Once subtracted FTDR read:

$$\mathrm{Re}\,X(\nu,t)=\mathrm{Re}\,X(\nu_0,t)+\Delta(X_N)+\frac{\nu^2-\nu_0^2}{\pi}\int_{\nu_{th}^2}^{\nu_{\max}^2}\mathrm{Im}\,X(\nu^2,t')\frac{d\nu'^2}{(\nu'^2-\nu_0^2)(\nu'^2-\nu^2)}+\Delta(\nu),$$

where ν_0 is a subtraction point, $\nu_{\max}$ corresponds to the highest energy where the input from PWA exists, and $\Delta(X_N)=X_N(\nu,t)-X_N(\nu_0,t)$. The discrepancy function $\Delta(\nu)$ can be fitted to the low order polynomial in ν. In our method, applying the FTDR together with the IDR, we choice ν=0 as a subtraction point. It is pointed out in ref. [1], that the FDR, subtracted at ν=0, and calculated at the s-channel threshold, give a valuable quantity, the difference between the real parts of amplitude at the threshold and at the center of the Mandelstam triangle ν=0, t=0:

$$Diff\overset{def}{=}X(m_\pi,0)-X(0,0)=X_N(m_\pi,0)-X_N(0,0)+\frac{m_\pi^2}{\pi}\int_{\nu_{th}^2}^{+\infty}\mathrm{Im}\,X(\nu^2,t')\frac{d\nu'^2}{\nu'^2(\nu'^2-m_\pi^2)}.$$

The integral on the right hand side converges very fast, what make it possible to obtain reliable results using the input from existing PWA only.

Determination of Coefficients in the Subthreshold Expansion.

Using the FTDR and the IDR methods, determination of coefficients in the subthreshold expansion could be performed in the few steps:

- Construct 40 interior hyperbolas crossing the ν=0 line at equidistant points $t_-\in[m_\pi^2,3m_\pi^2]$. For values $t_-<m_\pi^2$ only a small part of the t-channel cut contribution can be described by the t - channel partial wave expansion because corresponding hyperbolas enter the double spectral region. From other side, for $t_->3m_\pi^2$ amplitudes show a cusp like behavior which can not be described by the first terms in the subthreshold expansion.
- Choice 40 t values $-3m_\pi^2\le t\le m_\pi^2$ to perform the FTDR at 20 equidistant values $\nu^2\in[0,\nu_{\max}^2,\nu_{\max}^2=0.3,\ 0.4,\ 0.5]$.
- Write the subthreshold expansion in the form

$$X(\nu^2,t)=a(\nu^2)+b(\nu^2)t+c(\nu^2)t^2+d(\nu^2)t^3,$$

where:

$$a(\nu^2)=x_{00}+x_{10}\nu^2+x_{20}\nu^4+x_{30}\nu^6+\ldots$$
$$b(\nu^2)=x_{01}+x_{11}\nu^2+x_{21}\nu^4+x_{31}\nu^6+\ldots$$
$$c(\nu^2)=x_{02}+x_{12}\nu^2+x_{22}\nu^4+x_{33}\nu^6+\ldots$$
$$d(\nu^2)=x_{03}+x_{13}\nu^2+x_{23}\nu^4+x_{33}\nu^6+\ldots$$

- For each of 20 values of ν^2, fit obtained values of invariant amplitudes in the subthreshold region to the polynomial of third order in terms of variable t.
- From the ν^2 dependence of coefficients a, b, c, and d calculate corresponding values of x_{mn} in previous step.
- In order to demonstrate cusp like behavior of invariant amplitudes near the t-channel branch point, we perform calculations at many points in the interval $t\in[3m_\pi^2,4m_\pi^2]$.

The Input

The *s*-channel part of the input consists of the results of the existing PWA. We used the Karlsruhe Ka84 solution [5] and the VPI Sp98 solution [6]. The Ka84 solution is essentially KH80 solution smoothed by use of the partial wave dispersion relations. As in the KH80 solution, results are available up to lab. momentum k_{max} = 6 GeV/c. Compared with the KH80 solution, Ka84 gives more reliable values of the higher partial waves which are " too small to be determined, and too large to be neglected ". The VPI group produces new partial wave analysis at least once a year including the newest available scattering data. Their solution Sp98, used in our calculation, is constrained to the FTDR for a few values of *t*, and for lab. momenta up to 700 MeV/c, although the PWA extends up to k_{max}= 2.2 GeV/c. The πN coupling constant f^2 is treated as a free parameter in this analysis. Results are available up to 2.2 GeV/c. In our applications we added Ka84 solution from 2.2 GeV/c to 6 GeV/c in the Sp98 data file, as it had already been done by the VPI group. In our calculations we use values of • N coupling constant as obtained in particular PWA; f^2=0.079 (Ka84), and f^2=0.076 (Sp98). In addition, for the FDR, applied to $D^{\pm}$ amplitudes, the input is available up to 300 GeV/c. The Tables of the • $^{\pm}$N total cross sections [7] or the parameterization from ref. [8] can be used equally well.

Input from the *t*-channel consists from the $\pi\pi N\overline{N}$ helicity amplitudes $f_{\pm}^{J}$. The input exists for $4m_\pi^2 \le t \le 50m_\pi^2$, and for *J*=0,1,2,3. We used results obtained by the Karlsruhe group, given in [9] and LB. The *s*-wave f_+^0 was calculated by Bonnier and Gauron [10] also, and more recently by Gasser et al. [11] who used values of scattering length and effective range obtained from the chiral perturbation theory. Gasser et al. used also their own parameterization of the • • phase shift δ_0^0 needed for calculation of f_+^0. Karlsruhe solution is based on δ_0^0 values from Frogatt and Petersen [12]. We adjusted Karlsruhe solution for f_+^0 to results of Gasser et al. in domain where the scattering length approximation is valid, taking their values for the *s*- wave scattering length and the effective range: $a_0^0 = 0.20 \pm 0.01$, $b_0^0 = 0.24 \pm 0.01$ (all in n.u.).

Results and discussion

It is important to point out that our results are obtained by applying the dispersion relations along 80 different curves passing through different kinematical regions in the *s*- channel and also in the *t*-channel, covering a broad angular domain from forward to backward angles. Values of corresponding coefficients in the subthreshold expansions are summarized in Table 1 and in Table 2. To our knowledge, none of papers based on the IDR method [13] include the existing information on the *t*-channel discontinuity although the extrapolation is made towards the *t*-channel branch point. That is the reason why we expect our results to be more reliable then those obtained before. Details of our calculations are given in the ref. [14]. The obtained results for the $\overline{D}^+$ amplitude are of special interest for the reason of its close connection with the πN sigma term: $\sigma_{\pi N} = F_\pi^2 \overline{D}^+(\nu = 0, t = 2m_\pi^2)$, where F_π=92.4 MeV is the pion decay constant. Using the values for $\overline{d}_{0n}^+$ from our tables, we obtain $\sigma_{\pi N} = (70 \pm 8)$ MeV. The error is estimated taking into account the error estimation of $\overline{d}_{00}^+$ from the FDR also [14]. Our result is somewhat higher then $\sigma_{\pi N}$=(64±8) MeV obtained by Koch [15] 17 years ago, but there is still no serious reason to reject Koch's value completely. As has been pointed out several times by the Karlsruhe group [2,15], the amplitude $\overline{D}^+(0,t)$ has a turning point at $t \approx -4m_\pi^2$, and it is linear for $-4m_\pi^2 \le t \le 0$. From the other side, the calculations, performed using the fixed-ν dispersion relations, show that $\overline{D}^+(0,t)$ has upward curvature for *t>0*. This is explanation for a slow convergence of the corresponding subthreshold expansion. A simple extrapolation to *t>0*, using only values of $\overline{D}^+(0,t)$ for *t<0* leads to misleading results. We mention this well-known

fact because several authors in the past, ignoring it, draw wrong conclusions concerning value of the πN σ term. It is also a wrong strategy to derive the linear part (i.e. coefficients $\overline{d}^+_{00}, \overline{d}^+_{01}$) of $\overline{D}^+$ using only its values for $t<0$, obtained from the FTDR method, and take the curvature terms (coefficients $\overline{d}^+_{02}, \overline{d}^+_{03}, \ldots$) from other determinations.

The only way to perform a reliable continuation to $t>0$ is to apply dispersion relations that use information from the t-channel as a part of the input. Presently, the IDR method seems to be the most reliable one.

Conclusions

- Obtained values of coefficients in the subthreshold expansions of invariant amplitudes are consistent with the values obtained using another methods. We conclude that the input from the t- channel, which we applied, is consistent with the input from the s-channel.
- The only way to perform reliable continuation of invariant scattering amplitudes to the subthreshold region in dispersion theory is to apply dispersion relations that use information from the t-channel as part of the input. Presently, the interior dispersion relations seem to be the most reliable one.
- Our result for the πN σ term $\sigma_{\pi N}$=(70±8) MeV is somewhat higher than the Karlsruhe value $\sigma_{\pi N}$=(64±8) MeV obtained by Koch, but there is still no serious reason to reject Koch's value.

Acknowledgments

I wish to thank Prof. G. Höhler for his encouragement and support and for many valuable discussions. I would like also to thank WUS Austria and Organizing Committee of the ***MENU99*** *for making my attendance at the Conference possible.*

References

1 G. Höhler, H. P. Jacob, R. Strauss, Nucl. Phys. **B39** (1972) 237
2. G. Höhler, Landolt-Börnstein vol. **I/9b2**, Pion-Nucleon Scattering, Springer, Berlin,1983
3. G. E. Hite, F. Steiner, Nuovo Cimento **18A** (1973) 237
4. G. E. Hite, R. J. Jacob, F. Steiner, Phys. Rev. **D6** (1973) 3333
5. R. Koch, E. Pietarinen, Nucl. Phys. **A336** (1980) 331
   R. Koch, Z. Physik **C29** (1985) 597
6. The unpublished PWA of the VPI group, see also :
   M. M. Pavan, R. Arndt, πN Newsletter **13** (1997) 165, and ref. therein
7. G. Hoehler, F. Kaiser, Review and Tables of Pion-Nucleon Forward Amplitudes, Kernforschungzentrum Karlsruhe, 1980
8. A. Donnachie, P. V. Landshoff, Phys. Lett. **B296** (1992) 227
9. E. Pietarinen, Helsinki Preprint, HU-TFT-17-77
10. B. Bonnier, P. Gauron, Nuovo Cimento, **57A** (1980) 261
11. J. Gasser, H. Leutwyler, M. Sainio, Phys. Lett. **B253** (1991) 260
12. C. D. Frogatt, J. L. Petersen, Nucl. Phys. **B91** (1977) 89
13. W. B. Kaufmann, G. E. Hite, R. J. Jacob, πN Newsletters **13** (1997) 16, and ref. therein
14. J. Stahov, In preparation
15. R. Koch, Z. Phys. **C15** (1982) 161

Table 1. The coefficients in the subthreshold expansion. Input Ka84

x_{mn}	$\overline{A}^+$	A^-/ν	$\overline{B}^+/\nu$	B^-	$\overline{D}^+$	$\overline{D}^-/\nu$
x_{00}	-1.386±0.018	-8.820±0.040	-3.490±0.028	10.354±0.020	-1.386±0.018	1.510±0.001
x_{01}	1.143±0.014	-0.378±0.010	0.198±0.005	0.220±0.003	1.143±0.014	-0.136±0.003
x_{02}	0.040±0.005	-0.016±0.004	-0.012±0.004	0.022±0.002	0.040±0.005	0.011±0.001
x_{10}	4.630±0.030	-1.242±0.040	-1.018±0.036	1.052±0.008	1.144±0.014	-0.166±0.002
x_{11}	0.068±0.007	0.013±0.003	0.094±0.006	-0.053±0.002	0.230±0.007	-0.036±0.001
x_{20}	1.190±0.130	-0.344±0.050	-0.327±0.050	0.305±0.050	0.189±0.043	-0.042±0.003
x_{03}	0.010±0.002	-	-		0.010±0.002	-

Table 2. The coefficients in the subthreshold expansion. Input Sp98

x_{mn}	$\overline{A}^+$	A^-/ν	$\overline{B}^+/\nu$	B^-	$\overline{D}^+$	$\overline{D}^-/\nu$
x_{00}	-1.317±0.016	-8.967±0.002	-3.480±0.020	10.448±0.006	-1.317±0.016	1.468±0.004
x_{01}	1.150±0.019	-0.379±0.002	0.194±0.002	0.235±0.006	1.150±0.019	-0.138±0.003
x_{02}	0.028±0.002	-0.014±0.001	-0.014±0.001	0.008±0.001	0.028±0.002	0.008±0.001
x_{10}	4.566±0.030	-1.180±0.008	-0.959±0.015	1.007±0.009	1.133±0.013	-0.166±0.002
x_{11}	0.031±0.001	-0.006±0.007	0.095±0.007	-0.030±0.006	0.202±0.005	-0.037±0.002
x_{20}	1.200±0.200	-0.374±0.055	-0.311±0.070	0.330±0.050	0.176±0.038	-0.038±0.002
x_{03}	0.006±0.002	-	-	-	0.006±0.002	-

CNI Experiments with CHAOS

G.R. Smith
on behalf of the CHAOS collaboration
TRIUMF, 4004 Wesbrook Mall, Vancouver, B.C. Canada V6T 2A3

Abstract

A brief introduction to the issues surrounding the πN Σ term and a discussion of the parameters it depends on will be given. Current constraints on these parameters and on $\Sigma_{\pi N}$ and the strange sea quark content of the proton will be reviewed. A strategy for measurements of $\pi^{\pm}$p scattering in the Coulomb-nuclear interference region will be presented, and an explanation of how these measurements can be used to extract the amplitude $\mathrm{Re}(D^+)|_{t\to 0}$, the πN S- and P-wave scattering lengths, and $\Sigma_{\pi N}$ will be given. A brief description of the experimental method and some preliminary results are also shown.

THE πN SIGMA TERM

The physics issues in low energy πN scattering are to test the predictions and measure the parameters of chiral perturbation theory (χPT). The foremost of these is the pion-nucleon sigma term, which is equal to the product of the pion decay constant squared and the isospin even, Born subtracted pion-nucleon scattering amplitude D at a point below threshold known as the Cheng-Dashen point,

$$\Sigma_{\pi N} = F_\pi^2 \bar{D}^+(\nu = 0, t = 2\mu^2). \tag{1}$$

$\Sigma_{\pi N}$ is interesting because it provides an explicit measure of chiral symmetry breaking, and can be related to the strange quark content of the proton through the σ commutator,

$$\sigma = -i < N|[\dot{Q}_5, Q_5]|N >^+ = \frac{\hat{m}}{2m} \frac{< p|\bar{u}u + \bar{d}d - 2\bar{s}s|p >}{1-y}. \tag{2}$$

The latest evaluation[1] of the sigma commutator is

$$\sigma = \Sigma_{\pi N} - 15\ MeV\ = \frac{36 \pm 7}{1-y}, \quad \text{where } y = \frac{2 < p|s\bar{s}|p >}{< p|u\bar{u} + d\bar{d}|p >} \tag{3}$$

accounts for the strange sea quark content of the proton.

Since $\Sigma_{\pi N}$ is below threshold, it cannot be directly measured. Instead, we have to rely on measurements made at threshold, or in the near-threshold regime, and extrapolate below threshold with dispersion constrained partial wave analysis (PWA)[2]. It's informative to have a look at the dispersion relation for the relevant isospin even amplitude $\bar{D}^+$:

$$Re\ \bar{D}^+(\omega) = \bar{D}^+(\mu) + \frac{2(\omega^2 - \mu^2)}{\pi} \int_\mu^\infty \frac{d\omega' \omega'}{\omega'^2 - \omega^2} \frac{Im D^+(\omega')}{\omega'^2 - \mu^2} \tag{4}$$

where ω is the total pion lab energy, and $\mu = m_\pi$. The relevant subtraction constants are

$$\bar{D}^+(\mu) = 4\pi(1+x)a_{0+}^+ + \frac{g^2 x^3}{\mu(4-x^2)}, \quad \text{and} \quad \bar{E}^+(\mu) = 6\pi(1+x)a_{1+}^+ - \frac{g^2 x^2}{\mu^3(2-x)^2}. \tag{5}$$

Here x denotes μ/M, $M = M_p$, a_{0+}^+ the isospin even, S-wave πN scattering length,and g^2 is the πN coupling constant. So clearly, the dispersion relations are characterized by the body of πN data (through ImD^+ in the integrand), the coupling constant, and the scattering length a_{0+}^+ (the P-wave scattering length a_{1+}^+ is also crucial, it enters through the dispersion relation for the E amplitude). If the coupling constant and the dispersion integral are held fixed, then $\Sigma_{\pi N}$ is characterized by the S- and P-wave scattering lengths.

For many years, the only available determination of $\Sigma_{\pi N}$ was derived from KH80, which was based exclusively on pre-meson factory data[3]. It yielded a value of $\Sigma = 64 \pm 8$ MeV,

which implies y= 0.2 ± 0.2, ie an $s\bar{s}$ content of 10%±10%. The whole community was turned upside down at the last MENU meeting when new determinations were announced based on analyses of modern data, which yielded results[4] up to $\Sigma = 92$ MeV, which implies y$\sim$ 0.44. The main reason for this discrepancy also became clear at MENU97, namely that at the time of the KH80 analysis the only available low energy πN data were those of Bertin, et al.[5]. Every modern analysis of low energy data clearly shows that the Bertin data are wrong since they are completely at odds with all other measurements in the low energy regime[6–8]. In spite of this, many researchers have a hard time accepting a value for $\Sigma_{\pi N}$ as large as 92 MeV, and as a result it has become more important than ever to obtain more accurate and more sensitive experimental information to bring to bear on this problem.

In order to pin down the information most needed to get to the bottom of this puzzle, it is instructive to expand $\Sigma_{\pi N}$ in a Taylor's series in ν^2 and t about the Cheng-Dashen point:

$$\bar{D}^+ = d^+_{00} + d^+_{10}\nu^2 + d^+_{01}t + d^+_{20}\nu^4 + d^+_{02}t^2 + \cdots|_{\nu=0,\ t=2\mu^2} \quad (6)$$

$$\Sigma(\nu=0,\ t=2\mu^2) = F_\pi^2(d^+_{00} + 2\mu^2 d^+_{01}) + \Sigma_1 \quad (7)$$

$$\equiv \Sigma_d + \Sigma_1 \quad (8)$$

where the so-called curvature term $\Sigma_1 = 12$ MeV represents the higher order terms in t, and is sensitive to $\pi\pi$ parameters like the $\pi\pi$ scattering lengths. The d coefficients depend on the πN scattering lengths, the coupling constant, and the dispersion integrals, as noted earlier. To see where the sensitivity is, we recall a table presented at the last meeting which separates these three inputs for each of the two coefficients, and compares the results with KH80 and the more modern VPI analysis[4]:

Soln	Σ_d (MeV)	$\approx a^+_{0+}$ C^+ S.C.	$\approx g^2$ Born	DI $\int D^+$	$\approx a^+_{1+}$ E^+ S.C.	$\approx g^2$ Born	DI $\int E^+$
VPI	75=	0.5	+9	−88	+359	−136	−69
KA84	50=	−7	+9	−91	+352	−142	−72
diff	25=	+7	0	+3	+7	+6	+3

Table 1. Comparison of KH80 and VPI solutions, showing the terms proportional to the scattering length, coupling constant, and dispersion integral for d^+_{00} (middle 3 columns), and d^+_{01} (right 3 columns).

The table shows that the scattering lengths are most responsible for the differences in the two determinations of $\Sigma_{\pi N}$. The coupling constant also influences the P-wave term d^+_{01}, but surprisingly the dispersion integral terms are not that different. It would appear that better experimental information on the scattering lengths would be a major step forward in resolving this discrepancy.

At present there is no direct measure of either a^+_{0+} or a^+_{1+}, which are determined in the context of partial wave analyses of πN data. The remarkable work of the ETH/PSI pionic atom group does provide important constraints. However they do not provide a measure of the required *isospin even* S-wave scattering length. Their precise determination of the strong interaction shift in pionic hydrogen[9] could be combined with their width measurement to obtain a^+_{0+}, however, that would require the assumption that there is no isospin breaking. In fact, such a comparison is one of the best pieces of evidence we have that isospin is violated. They could also combine the shift measurements in pionic hydrogen and deuterium[10] to determine a^+_{0+}. Unfortunately, the pionic deuterium result is dependent on large model-dependent corrections for absorption and multiple scattering which render such a result of questionable value.

The constraints on the scattering lengths provided by the pionic atom measurements[9,10] as well as by elastic data in the near threshold region[7] are shown in Fig. 1. The $\pi^\pm$p

elastic data and the strong interaction shift (ϵ_{1S}) results overlap reasonably well. The fact that the π^-H width measurement (Γ_{1S}) and SCX data[12] prefer a smaller b_1 is a reflection of the isospin violation noted earlier. The fact that the other bands indicate substantially different values for b_0 and b_1 than predicted by KH80 is significant. If we were to use the value of a^+_{0+} implied by the intersection of the $\pi^{\pm}$p elastic and ϵ_{1S} bands in Fig. 1, then the value of $\Sigma_{\pi N}$ would rise 10 MeV (keeping a^+_{1+} fixed at the KH80 value, since we have no new information on a^+_{1+} as yet). This extra 10 MeV in $\Sigma_{\pi N}$ would imply that the $s\bar{s}$ content of the proton rises from 10±10% to over 18%.

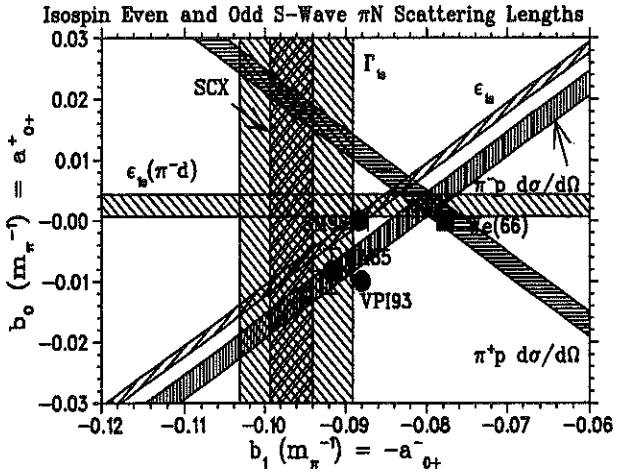

Figure. 1. Constraints on the isospin even and odd S-wave πN scattering lengths from various experiments, analyses, and predictions. For details, see text.

As a result, the TRIUMF CHAOS group has embarked on an experimental program which has as its goal the first direct measurement of both a^+_{0+} and a^+_{1+}, the quantities most crucial for a more reliable determination of $\Sigma_{\pi N}$ and therefore the $s\bar{s}$ content of the proton.

THE EXPERIMENT

The experiment consists of precise measurements of absolute differential cross sections for $\pi^{\pm}$p elastic scattering at far forward angles, deep into the Coulomb-Nuclear Interference (CNI) region[13]. Such cross sections provide a measure of the πN amplitude Re(D^+) at t=0, a crucial (and at present missing) piece of information in πN partial wave analyses (PWA). The Re(D^+) is precisely the amplitude which is connected to $\Sigma_{\pi N}$. ¿From measurements of $\mathrm{Re}(D^+)|_{t=0}$ at several energies, direct determinations of the S- and P-wave πN scattering lengths can be made, and from them, $\Sigma_{\pi N}$.

The $\mathrm{Re}(D^+)|_{t=0}$ can be obtained from either the difference in $\pi^{\pm}$p cross sections, the sum, or a ratio[14]. With G_C denoting the (calculable) Coulomb amplitude, we have

$$\begin{aligned} ReD^+(t=0) &= \frac{4\pi\sqrt{s}}{M}\lim_{\theta\to 0}\frac{\frac{d\sigma}{d\Omega}(\pi^+p)-\frac{d\sigma}{d\Omega}(\pi^-p)}{4Re(G_C)} \equiv \frac{4\pi\sqrt{s}}{M}\lim_{\theta\to 0}\Delta(t) \\ &= \frac{4\pi\sqrt{s}}{M}\lim_{\theta\to 0}\frac{\frac{d\sigma}{d\Omega}(\pi^+p)-\frac{d\sigma}{d\Omega}(\pi^-p)}{\frac{d\sigma}{d\Omega}(\pi^+p)+\frac{d\sigma}{d\Omega}(\pi^-p)}\cdot\frac{|G_C|^2}{2Re(G_C)} \equiv \frac{4\pi\sqrt{s}}{M}\lim_{\theta\to 0}A(t) \end{aligned} \qquad (9)$$

The expression for $\Delta(t)$ has the advantage that the t-dependence is linear in the small-t region, which simplifies the extrapolation to t=0. The expression for A(t) is non-linear, but since it is a ratio of cross sections, many experimental parameters cancel out.

These expressions show how the amplitude $\mathrm{Re}(D^+)|_{t=0}$ is derived from the cross sections measured in the experiment. The scattering lengths are obtained by extrapolating $\mathrm{Re}(D^+)|_{t=0}$ to T_π=0 using the relations for the subtraction constants noted earlier in Eq. 5. Note that the expressions for a^+_{0+} and a^+_{1+} in Eq. 5 *do not* depend on any PWA, dispersion relations, etc. They are direct relations. In a plot of $\mathrm{Re}(D^+)|_{t=0}$ vs T_π, the intercept ($\mathrm{Re}(D^+)|_{t=0}$ at T_π=0) is $\bar{D}^+(\mu)$, from which a^+_{0+} can be determined. The slope (of

$\mathrm{Re}(D^+)|_{t=0}$ at T_π=0) is $\bar{E}^+(\mu)$, from which a^+_{1+} can be obtained. Note that in terms of the more familiar Lorentz invariant A and B amplitudes, $D = A+\nu B$, and $E = \partial/\partial t(A+\omega B)$. At threshold, $\nu = \omega$.

The parameterization of $\Sigma(0, 2\mu^2)$ in terms of the scattering lengths is made explicit[2] via

$$\Sigma = \pi F_\pi^2[(4 + 2x + x^2)a^+_{0+} - 4\mu^2 b^+_{0+} + 12x\mu^2 a^+_{1+}] + \Sigma_0, \tag{10}$$

where $\Sigma_0 = -12.6$ MeV to one loop in chiral perturbation theory (χPT), and F_π is the pion decay constant. The effective range b^+_{0+} is connected[2] to a^+_{0+} and a^+_{1+} via dispersion relations (Geffen's sum rule). This Σ is in turn related to the $s\bar{s}$ content of the proton within the framework of χPT through Eq. 3.

In order to test the validity of this method in advance of the experiment, differential cross sections predicted by KH80 were used as input to the procedure and the resulting determinations of $\mathrm{Re}(D^+)$, a^+_{0+}, and a^+_{1+} were compared to the predicted ones from KH80. If the method proposed above is a viable one, consistent results should be obtained.

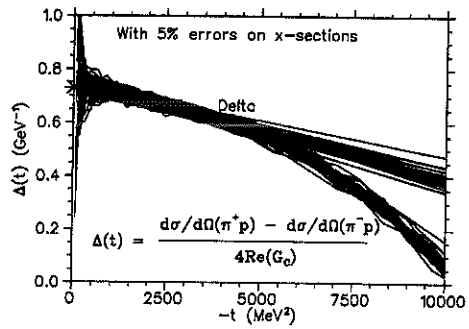

Figure. 2. A plot of $\Delta(t)$ as given by Eq. 9 for 44.6 MeV cross sections obtained from KH80, randomly varied to simulate experimental errors, and fit with straight lines in the small t region.

The expression for $\Delta(t)$ given in Eq. 9 is plotted in Fig. 2 for KH80 pseudo-cross sections at 44.6 MeV. Many sets of pseudo-data are plotted with random 5% shifts in absolute normalization and on an angle-by-angle basis to simulate statistical and systematic errors. Each result for $\Delta(t)$ is accompanied by a corresponding linear fit to the small t region, from which the slope and intercept at t=0 are determined. The mean value and standard deviation of these fits at 44.6 MeV are combined with similar analyses at other energies in Fig. 3. The results are also extrapolated to $T_\pi = 0$ in this figure, and related at that point to a^+_{0+} and a^+_{1+} using Eq. 5. The values deduced in this way from the extrapolation are consistent within the errors with those from KH80, indicating the method does indeed work.

CHAOS

The Canadian High Acceptance Orbit Spectrometer (CHAOS)[15] is a unique magnetic spectrometer for pion physics experiments at TRIUMF. CHAOS consists of a cylindrical dipole magnet which produces vertical magnetic fields up to 1.6T; fields of 0.9T are more typical in this experiment. Four concentric cylindrical wire chambers surround a liquid hydrogen scattering target located at the center of the magnet. The wire chambers are nominally enclosed by a concentric cylindrical array of scintillation counters and lead–glass Cerenkov detectors. A sophisticated, multi–tiered trigger system permits beam intensities up to 5 MHz to be utilized, although in this experiment intensities are limited to approximately 250 kHz. The spectrometer subtends 10% of 4π steradians and can detect charged particles scattered into all angles between 0° and 360° simultaneously, within ±7° of the horizontal plane. In this experiment the angular acceptance in the horizontal plane is limited to $6° < \theta <\sim 250°$. The momentum resolution of the device is approximately 1%. About 5,000 channels of information are available from the detector.

The most demanding experimental challenge in this type of measurement is the huge rate of muons which arise from the decay of pions along their trajectories, and which fall within the acceptance of the spectrometer trigger. In principle, roughly 20-30% of

the incident pion rate can produce muons in this category. Most of these muons fall into the low-momentum side of the beam where the experimental trigger is deadened. The remainder still pose a serious challenge both in terms of the trigger rate and in terms of distinguishing these events from real πp scattering events.

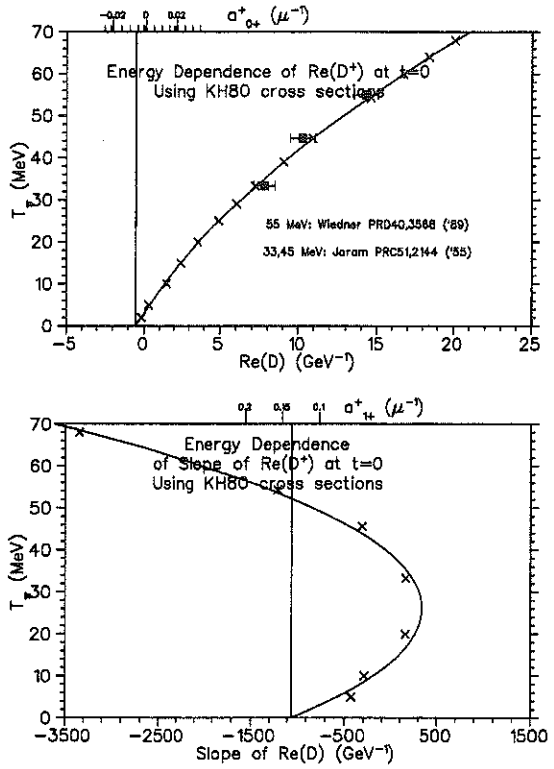

Figure. 3. Applying the analysis shown in the previous figure at many energies, the $Re(D^+)|_{t\to 0}$ is plotted as a function of pion bombarding energy in the upper figure. The lower figure shows the results for the slope of $Re(D^+)|_{t\to 0}$. The upper axis in both figures shows the relation to the scattering lengths as given by Eq. 5.

To reduce the remaining rate from these decay muons to a manageable level, conditions are established in the second level trigger which mitigate muon sources outside the target region. To help establish whether the detected particle was a pion or a muon, the detector has been modified from its standard configuration. The scintillation/lead-glass counters usually used with CHAOS were designed to provide π/e PID, not π/μ. So those counters subtending the first 30° were removed, and replaced by a scintillation counter stack interleaved with aluminum absorbers. The digitized time and pulse height from the scintillators in this stack are input to a neural net which provides the required π/μ identification. The neural net was trained using the RF-referenced TOF of particles from the pion production target to a beam defining scintillator just upstream of the spectrometer.

PRELIMINARY RESULTS

The experiment began collecting data with an LH2 target in the spring of 1999, shortly before this meeting took place, so we are not yet able to provide any final results. We anticipate that data collection will be finished early in 2001 and that final results will be available by the end of that year.

In the meantime, in Fig. 4 a plot of the interaction vertex is shown for events scattered outside 25°, determined by intersecting the incoming beam trajectory with the outgoing track, for both full and empty LH2 targets. The 125μ thick target windows, which are situated as far from the target cell as possible, are clearly visible. The 8μ thick windows of the target cell itself are hardly visible. They contain a 2 cm thick LH2 planar target.

Since the experiment relies on μH scattering for normalization, prior to the arrival of our LH2 target we studied μC scattering as a test. The (relative) angular distribution resulting from this test measurement is compared to a prediction in Fig. 5. In the angular range $7° < \theta < 25°$ covered by the π/μ stack (required in this analysis), the agreement

between the shape of the measured and predicted angular distributions is very good.

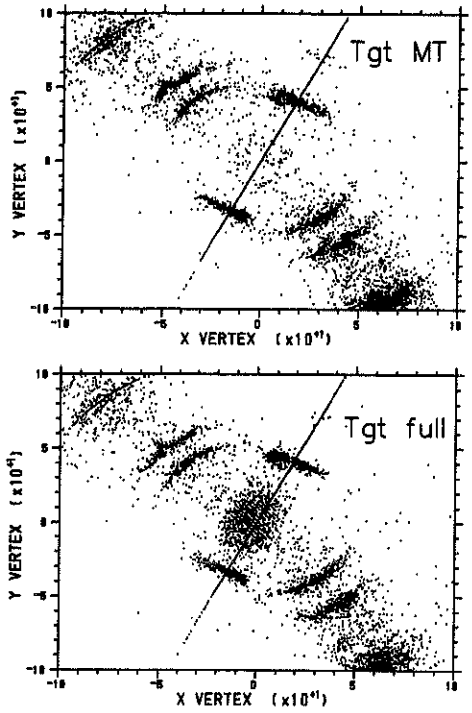

Figure. 4. The horizontal interaction vertex of events in CHAOS reconstructed with the LH2 target empty (upper) and full (lower).

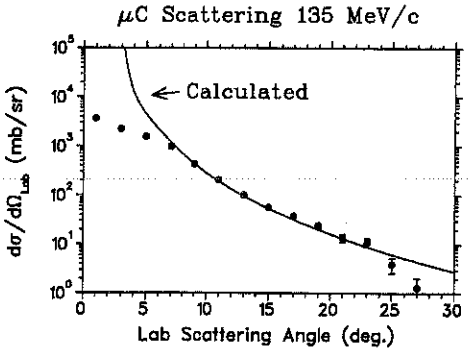

Figure. 5. A plot of the (relative) μC cross sections measured in CHAOS compared to prediction. Note that inside the acceptance of the π/μ stack the agreement in shape is excellent.

REFERENCES

1. U. Meissner, Ann. Phys. **254**, 192 (1997).
2. J. Gasser, H. Leutwyler, M.P. Locher and M.E. Sainio, Phys. Lett. **B213**, 85 (1988).
3. R. Koch and E. Pietarinen, Nucl. Phys. **A336**, 331 (1980); R. Koch, Z. Phys. **C15**, 161 (1982).
4. M.M. Pavan and R.A. Arndt, "Results for $\Sigma_{\pi N}$ and f^2 from a new VPI PW and DR Analysis", in *Proceedings of MENU97 (πN Newsletter #13)*, Vancouver, 1997.
5. P.Y. Bertin, *et al.*, Nucl. Phys. **B106**, 341 (1976).
6. R.A. Arndt, *et al.*, Phys. Rev. **C49**, 2729 (1994).
7. N. Fettes and E. Matsinos, Phys. Rev. **C55**, 464 (1997).
8. W.R. Gibbs, L. Ai, W.B. Kaufmann, Phys. Rev. Lett. **74**, 3740 (1995).
9. D. Sigg, *et al.*, Phys. Rev. Lett. **75**, 3245 (1995).
10. D. Chatellard, *et al.*, Phys. Rev. Lett. **74**, 4157 (1995).
11. A. Thomas and M. Landau, Phys. Rep. **C58**, 122 (1980).
12. P.B. Siegel, W.R. Gibbs, Phys. Rev. **C33**, 1407 (1986).
13. G.R. Smith, TRIUMF proposal E778, 1996.
14. C. Joram, et al., Phys. Rev. **C51**, 2144 (1995).
15. G.R. Smith *et al.*, Nucl. Instr. & Meth. **A362**, 349 (1995).

Pion-Nucleon Charge Exchange Experiments

M. E. Sadler for the Crystal Ball Collaboration*†
Abilene Christian University, Box 27963, Abilene, TX 79699

Abstract

An update of recent measurements of pion-nucleon charge-exchange scattering is presented. These data consist primarily of cross sections at 150–660 MeV/c obtained with the Crystal Ball detector. They are the first results of a rich and diverse new experimental program in baryon spectroscopy at the Alternating Gradient Synchrotron at Brookhaven National Laboratory. The physics motives for making more accurate measurements of $\pi^- p \to \pi^0 n$ in this region are to determine better the isospin-odd s-wave scattering length, to extrapolate scattering amplitudes to the non-physical region (e.g., for determinations of the πN σ term), to evaluate the πNN coupling constant and the mass splitting of the Δ resonance, to improve the determination of the mass, width and decay of the $P_{11}(1440)$ resonance and to investigate isospin invariance and charge splitting of the P_{33} scattering amplitude.

INTRODUCTION

Two measurements of pion-nucleon charge exchange scattering that have been presented at previous MENU conferences have been published since MENU97. These are a cross section measurement at 27.5 MeV by Frlez *et al.*[1] and analyzing powers at 98.1, 138.8, 165.9 and 214.4 MeV by Gaulard *et al.*[2]. The reader is referred to these publications for descriptions of these experiments, the final results, and comparison with partial-wave analyses.

The new data reported here, differential cross sections for $\pi^- p \to \pi^0 n$ at 150–660 MeV/c, were taken with the Crystal Ball (CB) multiphoton spectrometer during Fall, 1998, in the C6 line at the Alternating Gradient Synchrotron at Brookhaven National Laboratory. The CB detector, designed and built at SLAC, is a highly segmented, total-energy electromagnetic calorimeter and spectrometer that covers over 94% of 4π steradians. A description and schematic of the detector as well as some samples of our 1997 raw data are shown in a contribution by our collaboration[3] in the MENU97 Proceedings.

OVERVIEW OF THE 1998 RUN

The 1998 data run with the Crystal Ball at BNL was an incredible success. Completed measurements include 20 momenta for $\pi^- p \to$ neutrals, eight momenta for $K^- p \to$ neutrals, two momenta with π^- on nuclear targets, production of more than $2 \times 10^7 \eta$'s to search for rare neutral decay modes, and a test run with an antiproton beam. Preliminary results for $\pi^- p \to \pi^0 n$ at 147, 176, 189, 213, 239, 271, 301, 326, 359, 378, 408, 471, 547, 645 and 660 MeV/c are reported here, part of the first phase of E913 at the AGS. Other measurements obtained during our 1998 CB run are reported elsewhere in these proceedings[4].

The CB proper is a sphere with an entrance and exit opening for the beam and an inside cavity with radius of 25 cm for the target. It is constructed of 672 optically isolated NaI(Tl) crystals that detect individual γ's. Electromagnetic showers in the CB are measured with an energy resolution of $3\%/E^{1/4}$, where E is in GeV. Directions of the γ rays are measured

*The new Crystal Ball Collaboration consists of B. Draper, S. Hayden, J. Huddleston, D. Isenhower, C. Robinson and M. Sadler,*Abilene Christian University*, C. Allgower and H. Spinka, *Argonne National Laboratory*, J. Comfort, K. Craig and A. Ramirez, *Arizona State University*, T. Kycia, *Brookhaven National Laboratory*, M. Clajus, A. Marusic, S. McDonald, B. M. K. Nefkens, N. Phaisangittisakul and W. B. Tippens, *University of California at Los Angeles*, J. Peterson, *University of Colorado*, W. Briscoe, A. Shafi and I. Strakovsky *George Washington University*, H. Staudenmaier, *Universität Karlsruhe*, D. M. Manley and J. Olmsted, *Kent State University*, D. Peaslee, *University of Maryland*, V. Abaev, V. Bekrenev, N. Kozlenko, S. Kruglov, A. Kulbardis, I. Lopatin and A. Starostin, *Petersburg Nuclear Physics Institute*, N. Knecht, G. Lolos and Z. Papandreou, *University of Regina*, I. Supek, *Rudjer Boskovic Institute* and A. Gibson, D. Grosnick, D. D. Koetke, R. Manweiler and S. Stanislaus, *Valparaiso University*.

†Supported in part by US DOE, NSF, NSERC, Russian Ministry of Sciences and Volkswagen Stiftung.

with a resolution of 2-3 degrees in the polar angle. An electromagnetic shower from a single γ ray deposits energy in several crystals, called a cluster. The present cluster algorithm sums the energy from the crystal with the highest energy with that from the twelve nearest neighbors.

A 10 cm long liquid hydrogen target was installed inside the CB at the C6 beam line at the AGS. The beam phase space was measured by one drift chamber upstream and six drift chambers downstream of the last bending magnet. A data acquisition system was designed that utilizes the CEBAF Online Data Acquisition software (CODA)[5]. The trigger consisted of a disappearing beam requirement, determined by three scintillation counters upstream and veto counters downstream of the target, and a minimum energy in the CB. A veto barrel consisting of four plastic scintillation counters surrounding the hydrogen target was used to identify neutral (no signal in the veto barrel) and charged (at least one veto barrel signal) triggers. The charged triggers were prescaled by a factor of 10. Only the neutral triggers have received significant attention in the analysis thus far. An interface with the CERN Physics Analysis Workstation (PAW) software was implemented for on-line monitoring of the beam, detector and physics events.

The detector acceptance as a function of scattering angle was determined by using a GEANT Monte Carlo (MC) simulation. The measured beam phase space was used as input. An angular distribution of the outgoing π^0's at a given momentum was obtained from the VPI (now GW) SP99 partial-wave analysis (PWA).

The MC program propagated the electromagnetic processes from the $\pi^0 \rightarrow \gamma\gamma$ decay through the hydrogen target and container, the beam pipe, veto barrel scintillator and the CB elements. Surprisingly, on the order of 25% of the events produced a charged particle in the veto system according to the MC. The acceptance was corrected for this factor, which is one of the significant sources of systematic error at this point in the analysis.

In the present analysis the NaI crystals that border the entrance and exit tunnels for the beam were used as guard crystals, meaning that events were rejected if the highest energy in a cluster of crystals occurred in one of these crystals. Two-cluster events consistent with a single π^0 and three-cluster events consistent with a π^0 and a neutron were used in the present analysis.

The electron and muon contamination of the pion beam was measured from time-of-flight (TOF) at low momenta (below 300 MeV/c). The electron measurements were used to determine the efficiency of a differential gas Čerenkov counter in the beam downstream of the target. This efficiency (92.3%) was used to determine the electron contamination from the Čerenkov counter up to the highest momenta in the experiment. The on-momentum muon contamination was extrapolated from the measurements at low momentum. (On-momentum muons originate from pion decay near the production target.) The decay muons (muons that are registered in the beam counters which come from pion decay toward the end of the beam channel) must be calculated by Monte Carlo simulation and have only been estimated. As an example, the μ/π fraction was evaluated to be 3.5% and e/π was 5.9% at 301 MeV/c from these techniques.

Beam momentum calibrations for the C6 beam line were performed utilizing time-of-flight and stopping-range techniques. The ADC's for each crystal were calibrated by a combination of data from a ^{137}Cs source and monochromatic 129.4 MeV photons from the $\pi^-_{\text{stopped}}p \rightarrow \gamma n$ reaction. Cross comparisons between the calibrations for the beam momenta and the ADC's can also be made from kinematic relationships. For example, at a given beam momentum the energy of the π^0 from $\pi^-p \rightarrow \pi^0 n$ (or an η from $\pi^-p \rightarrow \eta n$) is determined by the scattering angle. This self-consistency check between the momentum calibration of the beam and the energy response of the detector is a feature that has been lacking in previous measurements of neutral-particle final states.

EXAMPLES OF THE CHARGE-EXCHANGE DATA

Shown in Fig. 1 are preliminary differential cross sections for $\pi^-p \rightarrow \pi^0 n$ at 301 MeV/c from E913 at the AGS. The data have been binned in intervals of 0.1 in cosθ. The predictions of the three PWA's, Karlsruhe (1984)[6], GW (SP99)[7] and Abaev/PNPI (1992)[8], are essentially indistinguishable at this momentum and agree very well with our data. The

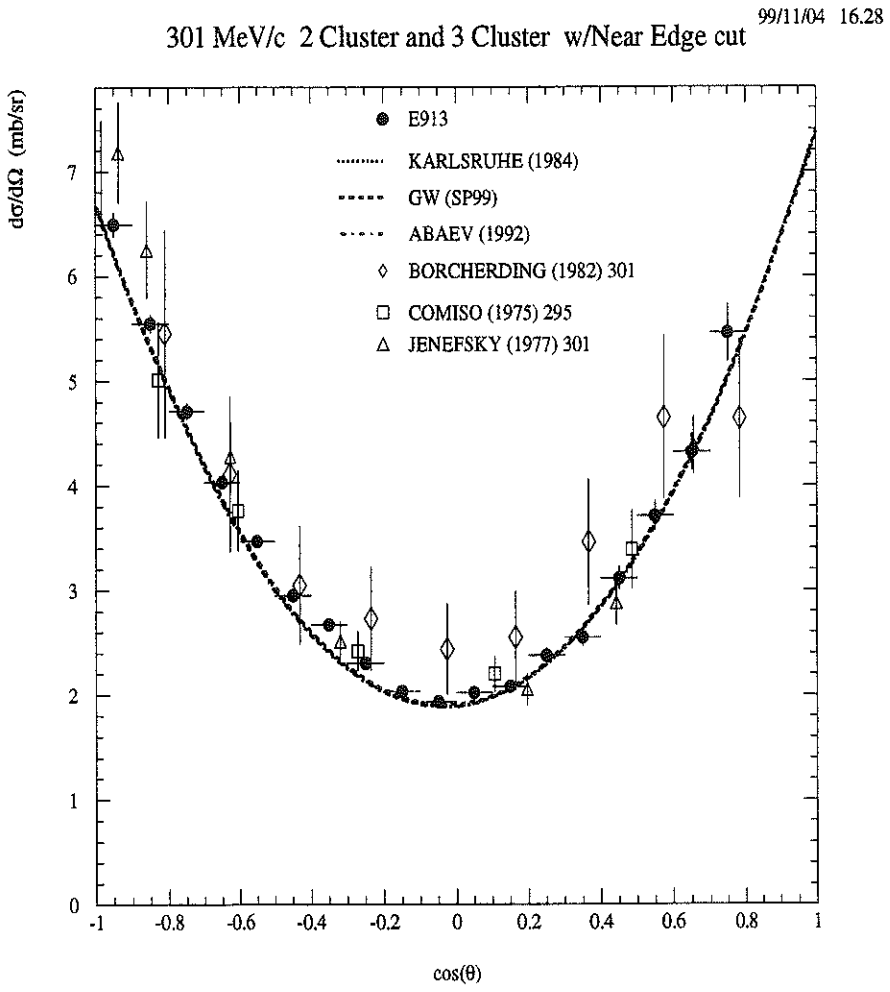

Fig. 1. Preliminary differential cross sections for $\pi^- p \to \pi^0 n$ at 301 MeV/c. The number following the previous measurements indicates the momentum. References for these measurements can be found in the SAID database[7].

data and analyses show the expected $(1 + 3\cos^2\theta)$ behavior at the Δ (P_{33}) resonance. Note that the (statistical) error bars are significantly smaller and the angular coverage is significantly larger than the previously available data. These data were obtained with the CB in about four hours of beam time, including the run with an empty target. The CB measures a complete angular distribution simultaneously with only one normalization for the beam and target. The lack of results shown at the forward angles is due to the near-edge cut which excludes events if the crystal with the highest energy in a cluster is one of the edge (or guard) crystals. The angular acceptance can be extended to more forward angles if this cut is relaxed, but this requires a more detailed dependence on the Monte Carlo. We are optimistic of eventually reporting results to at least $\cos\theta = 0.9$ at this momentum.

Figure 2 shows results at 147, 176, 213 and 271 MeV/c. The shapes of the angular distributions change gradually from a forward dip at 147 MeV/c, caused by the destructive interference between the s- and p-partial waves, toward the parabolic shape (as in Fig. 1) as the P_{33} resonance is approached. The GW (SP99) and Karlsruhe (1984) PWA's become distinct at the lower momenta, with the SP99 solution more closely resembling the data. Note that at the two lowest momenta there is no gap near $\cos\theta = 1$, even though the same

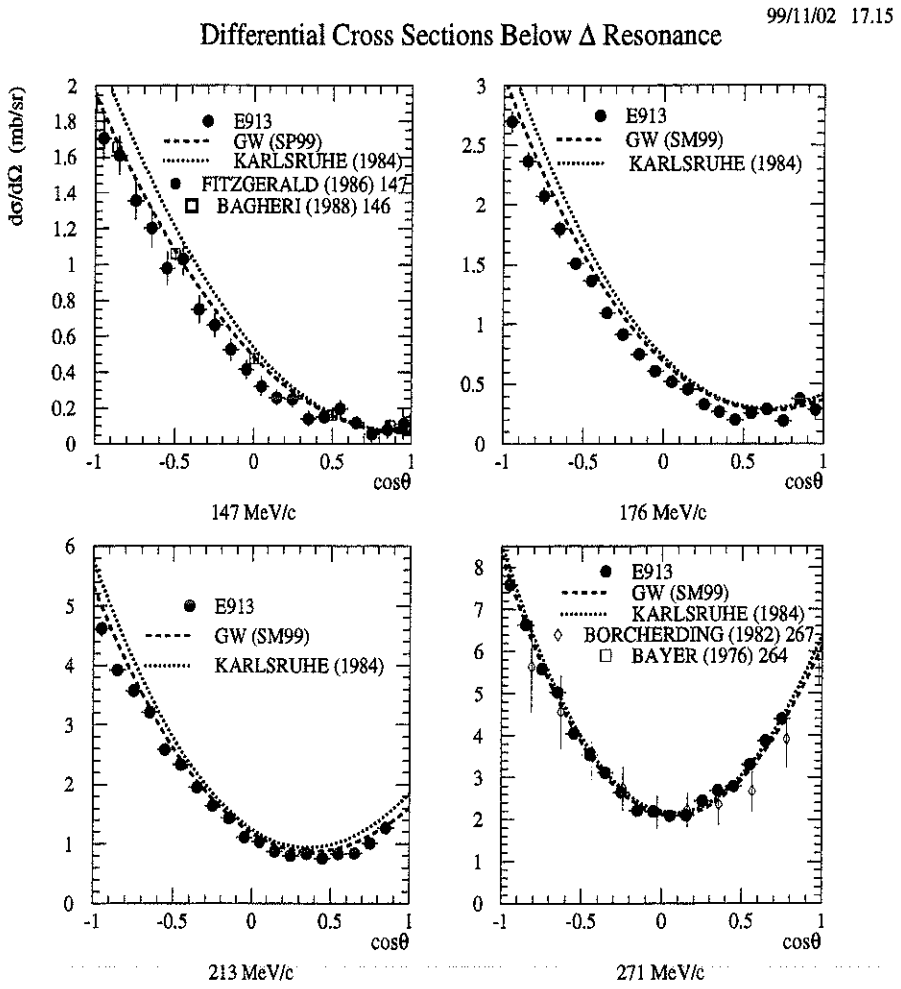

Fig. 2. Preliminary differential cross sections at four momenta below the Δ resonance.

near-edge cut was applied as above, since the opening angle between the γ's is large for the low-energy π^0's.

Figure 3 shows our results just above the P_{33}. The PWA's do a reasonable job of reproducing the data but some improvement is expected if the present data were included. Finally, results at four momenta in the vicinity of the $P_{11}(1440)$ resonance are shown in Fig. 4. Once again, note the interference dip at 547 MeV/c, this time at the back angles.

THE OVERALL PROGRAM AND FUTURE PLANS

E913 at the AGS is an experiment designed to study the formation of baryon resonances from $\pi^- p$ interactions and their decay into neutral final states, e.g. $\pi^- p \to \gamma n, \pi^0 n, \eta n, \pi^0\pi^0 n$... E914 is a similar experiment for $K^- p$ interactions. Shown in Fig. 1–4 is only a fraction of the results that we will eventually have from our 1998 run. The CB measures all final states simultaneously, requiring only one overall beam/target normalization.

The ability to make simultaneous measurements of all the reaction channels for $\pi^- p \to$ neutrals and $K^- p \to$ neutrals at finely-spaced momenta promises significant improvements in the data available for future partial-wave analyses. The data for $\pi^- p \to \pi^0 n$ and $\pi^- p \to \eta n$ are particularly incomplete and ambiguous (as compared to elastic πp scattering) in the present πN databases at beam momenta up to 750 MeV/c.

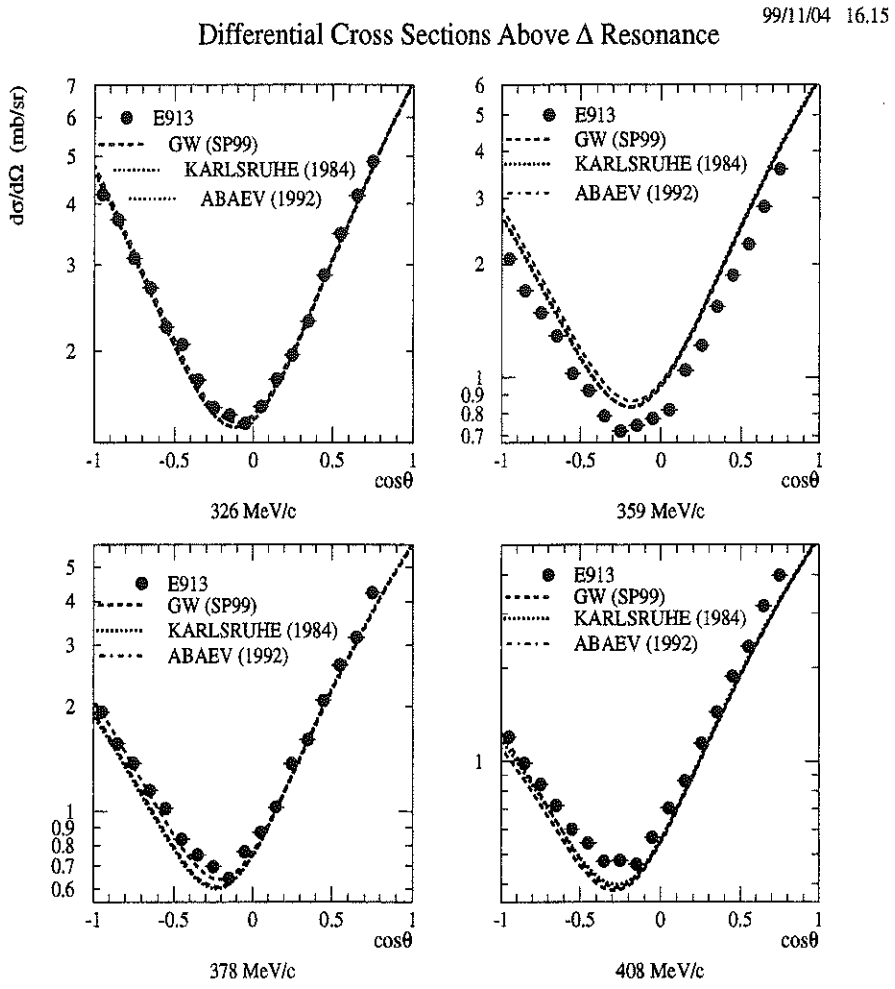

Fig. 3. Preliminary differential cross sections at four momenta above the Δ resonance.

The next running period for the Crystal Ball in the C6 beam line is not known due to the uncertainty surrounding fixed-target physics at the AGS in the RHIC era. It is hoped to resume experimental activity in 2001 after we have finished the analysis of the data in hand. Depending on the available beam time, we plan to measure the decay rate and spectrum for K_{e3} ($K^+ \to \pi^0 e^+ \nu$) and K_{e4} ($K^+ \to \pi^0 \pi^0 e^+ \nu$), η production from complex nuclei, and perhaps $\pi^- p \to$ neutrals at even lower energies.

Future plans are to move the CB to the D6 beam line that goes up to 1.9 GeV/c. If these plans are realized, πN resonances up to 2.1 GeV and $\bar{K}N$ resonances up to 2.2 GeV can be studied. In addition to the channels listed above, the CB will be able to measure angular distributions for reactions such as $\pi^- p \to \pi^0 \eta n$, $\pi^- p \to \omega n$, $\pi^- p \to K^0 \Lambda$, $\pi^- p \to K^0 \Sigma^0$, or $K^- p \to \eta \Sigma^0$.

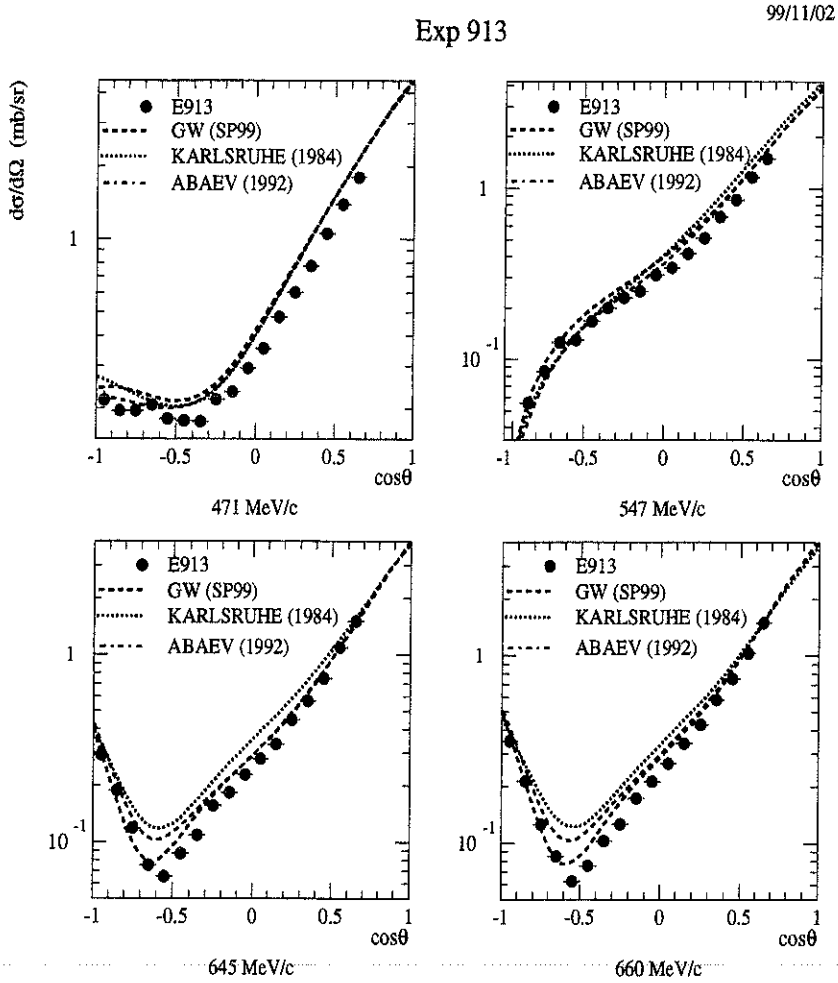

Fig. 4. Preliminary differential cross sections at four momenta in the vicinity of the $P_{11}(1440)$ resonance.

REFERENCES

1. E. Frlez *et al.*, "Differential cross sections for pion charge exchange on the proton at 27.5 MeV," Phys. Rev. **C57**, 3144 (1998).
2. C.V. Gaulard *et al.*, "Analyzing powers for the $\pi^- p \to \pi^0 n$ reaction across the $\Delta(1232)$ resonance," Phys. Rev. **C60**, 024604 (1999).
3. M.E. Sadler, "The Crystal Ball Multi-Photon Spectrometer: A New Facility for Baryon Spectroscopy," in *Proceedings of MENU97, The Seventh International Symposium on Meson-Nucleon Physics and the Structure of the Nucleon* TRIUMF TRI-97-1, Vancouver, British Columbia, Canada, 1997 pp. 123–126.
4. B.M.K. Nefkens and A.B. Starostin, "Hadronic Physics with the Crystal Ball," elsewhere in these Proceedings.
5. G. Heyes *et al.*, "The CEBAF on-line data acquisition system", Proc. CHEP Conf. (April 1994), 122-124.
6. R. Koch and E. Pietarinen, Nucl. Phys. **A448**, 707 (1986).
7. R. A. Arndt, *etal.*, Phys. Rev. **C52**, 2120 (1985). All PWA solutions presented were obtained from http://said.phys.vt.edu/analysis/go3pin.html.
8. V.V. Abaev and S.P. Kruglov, Z. Phys. **A352**, 85 (1995).

The Results from PNPI on πp Reactions

S.P. Kruglov *
Petersburg Nuclear Physics Institute,
Gatchina, Leningrad district, 188350 Russia

Abstract

A new phase shift analysis was performed at PNPI. The charge splitting in the P_{33} phase shift was obtained in the region $T_\pi = 200$–450 MeV. The differential cross sections (DCS) of $\pi^- p$ charge exchange scattering to backward angles were measured by means of a new method. Cusp effects in the momentum dependence of DCS in the region around $p_\pi = 685$ MeV/c were discovered. Yields of the process $\pi^- p \to \eta n$ were measured at nine angles of neutron emission in the near-threshold region. The value of the the η mass $M_\eta = 547.45$ MeV/c^2 was confirmed.

The program "Baryon spectroscopy with π-mesons in the energy range from 300 to 2000 MeV" is under way at PNPI. In the period after 1989 investigations are carried out in collaboration with the University of California at Los Angeles (USA) - Prof. B.M.K.Nefkens et al. and Abilene Christian University (USA) - Prof. M.E.Sadler et al.

Strong-interaction physics at intermediate energies has a great need for detailed and complete baryon spectroscopy. There exist various theoretical models which predict rather differing spectra and characteristics of the baryons, and unambiguous determination of such spectra from experimental data is required to choose the most adequate theoretical model.

For nonstrange excited baryons (pion-nucleon resonances), almost all information on the N^* and Δ resonances comes from πp-reactions, mainly elastic scattering, consisting of cross sections and polarization measurements. The data are synthesized by a phase shift analysis (PSA). The baryon spectrum can be extracted from the PSA's results using Breit–Wigner fit or speed plots.

The main aim of the pion-nucleon research program is to solve existing problems by obtaining new, precise experimental data, and by performing a new phase shift analysis.

The pion channel of the PNPI synchrocyclotron can produce intense pion beams in the energy region from 300 MeV up to 650 MeV with $\Delta p/p \simeq 0.015$ (FWHM). During the last decade, the differential cross sections (DCS) and the polarization parameters P, A, R for $\pi^\pm p$ elastic scattering were measured at PNPI at 20 energies in the region of 300–640 MeV. The total number of new experimental points amounts to 440.

Experimental data obtained at PNPI [1] were used together with the results of LAMPF [2] for performing a new phase shift analysis PNPI–94 [3]. The PNPI PSA resulted in the most precise amplitudes for incident pion energies ranging from 160 to 600 MeV (corresponding values of c.m.s. energies $\sqrt{s} = 1210$–1510 MeV).

One of the most interesting results obtained in PNPI PSA is the observation of charge splitting in the P_{33} wave; quantitatively this effect can be characterized by the difference of phase shifts $\delta_{33}^{++} - \delta_{33}^{0}$ (where δ_{33}^{++} and δ_{33}^{0} are the phase shifts extracted from $\pi^+ p$ elastic scattering and from $\pi^- p$ elastic and charge exchange scattering data). This difference depends on energy and varies from +2 degrees at $T_\pi = 200$ MeV to –2 degrees at $T_\pi = 450$ MeV, changing sign at $T_\pi = 350$ MeV (see Fig. 1). Shown by the curve in Fig. 1 are the results of a fitting which takes into account the Breit–Wigner resonance term and a nonresonance background [3]. The following values for the masses (M) and widths (Γ) of the P_{33}-resonances were obtained after the parametrization

$$M^0 = 1233.1 \pm 0.3 \text{ MeV}, \quad M^{++} = 1230.5 \pm 0.2 \text{ MeV},$$
$$M^0 - M^{++} = 2.6 \pm 0.4 \text{ MeV}, \quad \Gamma^0 - \Gamma^{++} = 5.1 \pm 1.0 \text{ MeV}.$$

*e-mail: kruglov@lnpi.spb.su

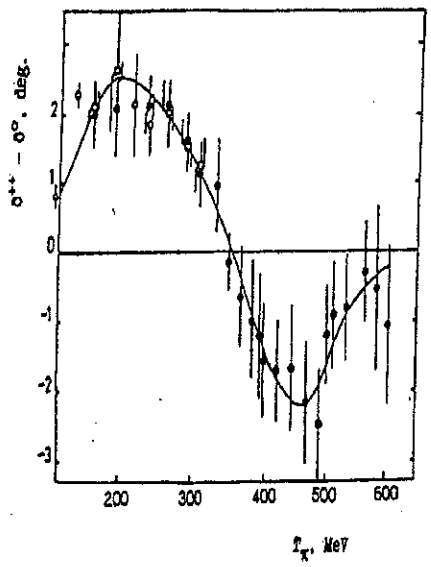

Fig. 1. Energy dependence of the phase shift difference $\delta_{33}^{++} - \delta_{33}^{0}$ obtained as a result of PNPI–94 PSA (•) and by D.Bugg [4] (○).

At present, the accuracy in determining the characteristics of πN resonances is limited mostly by a lack of high-quality experimental data on $\pi^- p$ charge exchange scattering. To improve the situation and fill the gap in the data-base, measurements of DCS for the reaction $\pi^- p \to \pi^0 n$ are now under way at PNPI in the energy range from 300 to 600 MeV (corresponding values of momenta are 417 to 725 MeV/c).

The experiment is carried out by detecting the recoil neutron in coincidence with one gamma from the decay $\pi^0 \to 2\gamma$. A schematic view of the experimental setup is shown in Fig. 2.

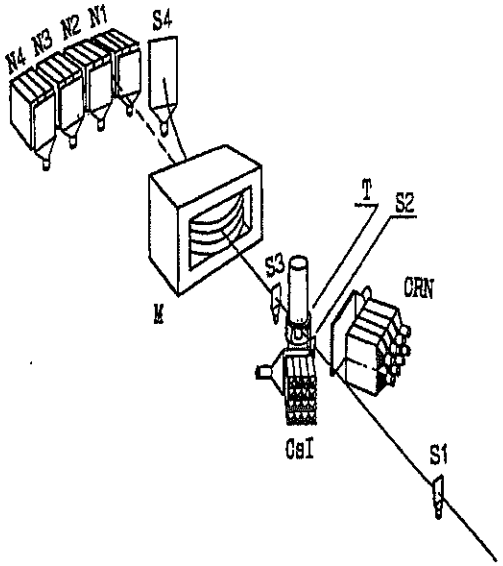

Fig. 2. Schematic drawing of the setup for measuring cross sections of $\pi^- p$ charge exchange scattering. S1, S2 – monitor counters; S3, S4 – beam veto counters; N1–N4 – neutron detectors; M – magnet deflecting incident pion beam; T – liquid hydrogen target; CsI – gamma-detector consisting of 16 crystals CsI(Na); CRN – gamma-detector consisting of 8 Čerenkov lead glass blocks.

Neutron detectors were designed and manufactured at UCLA. The detector consists of three contiguous scintillator blocks each having size of $25.4 \times 25.4 \times 8.9$ cm^3 (the last number indicating the width). Each block is viewed by two photomultiplier tubes connected

in coincidence. The energy of the neutrons is measured using the time-of-flight technique, with a 5 m base. Gamma detectors were placed at angles kinematically conjugated with the neutron detectors. Two different types of total absorption electromagnetic calorimeters are used in the experiment. The first detector is the Čerenkov spectrometer made of eight lead glass SF-5 blocks (with individual size $15 \times 15 \times 35$ cm^3) arranged in a 4×2 array, and the second consists of sixteen (4×4 array) CsI(Na) crystals each having a size of $6 \times 6 \times 30$ cm^3. A special hodoscope of beam counters (not shown in Figure 2), which was placed in the dispersive part of the pion channel, provides the possibility of dividing the total momentum acceptance (6% FWHM) into several narrower momentum bins.

At the first stage, measurements were performed for backward scattering angles. To eliminate the contribution due to charge exchange scattering of the incident pions on the scintillator of the monitor counter S2 and on elements of the target construction, at every energy setting measurements were made using both a hydrogen-filled and an empty target. Then a channel-by-channel subtraction of corresponding time-of-flight spectra is performed subsequently after a normalization to one incident pion.

The preliminary results are presented in Fig. 3. Only statistical uncertainties are shown. The statistical errors are equal to 2–3% for the momentum of 700 MeV/c and 10% in the region of 573 MeV/c (in the minimum of cross sections). We can evaluate the systematic uncertainties by means of comparison results measured with two different types of

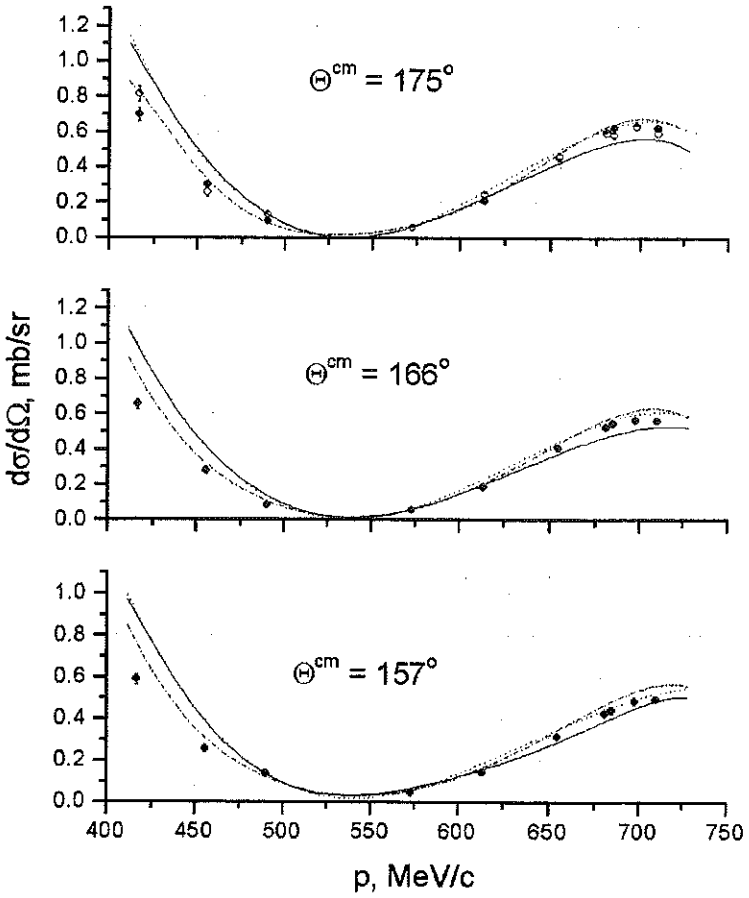

Fig. 3. Preliminary results of measuring differential cross sections of $\pi^- p$ charge exchange scattering to backward angles. Results obtained with Čerenkov spectrometers are shown by solid circles, those obtained with CsI(Na) crystals – by open circles. Shown by curves are the predictions of phase shift analyses KH–80 (solid lines), PNPI–94 (dashed lines) and VPI (dash-dotted lines).

total absorption electromagnetic calorimeters (Čerenkov spectrometer and CsI(Na) crystals) for $\theta^{cm} = 175°$. The difference between results is equal to 5–7% in the momentum range of 600–700 MeV/c and less than 14% in the range of 400–600 MeV/c. Therefore the systematic uncertanties in these momentum regions are less than 7% and 14%, corre-

spondingly. A more detailed analysis of systematic errors is in progress.

Shown by curves in Fig. 3 are the predictions of PSAs KH–80, PNPI–94 and VPI (SM–95). New PNPI results in the region of 700 MeV/c are between PSAs PNPI–94 and VPI (SM–95), on the one hand, and PSA KH-80, on the other hand. In the region of 400–450 MeV/c results are lower than the predictions of all PSAs. As one can see, DCS are near zero between 520 and 550 MeV/c. In this region predictions of PSAs KH–80, PNPI–94 and VPI (SM–95) are differing by a factor of two or three. The reason of this difference is a lack of good experimental data on DCS for $\pi^- p \to \pi^0 n$ in the data-base.

In the region of the η production threshold ($p_\pi = 685$ MeV/c) the measurements were made with a smaller momentum step in order to study cusps in the momentum dependence of the DCS, which arise as a result of the opening of the new inelastic channel $\pi^- p \to \eta n$. The use of the hodoscope of beam counters enabled us to make measurements simultaneously for several neighbouring momentum bins – the firing of a particular counter was used as a signal that the momentum of the incident pion belongs to the corresponding momentum bin. Two examples of obtained results are presented in Fig. 4. Solid curves

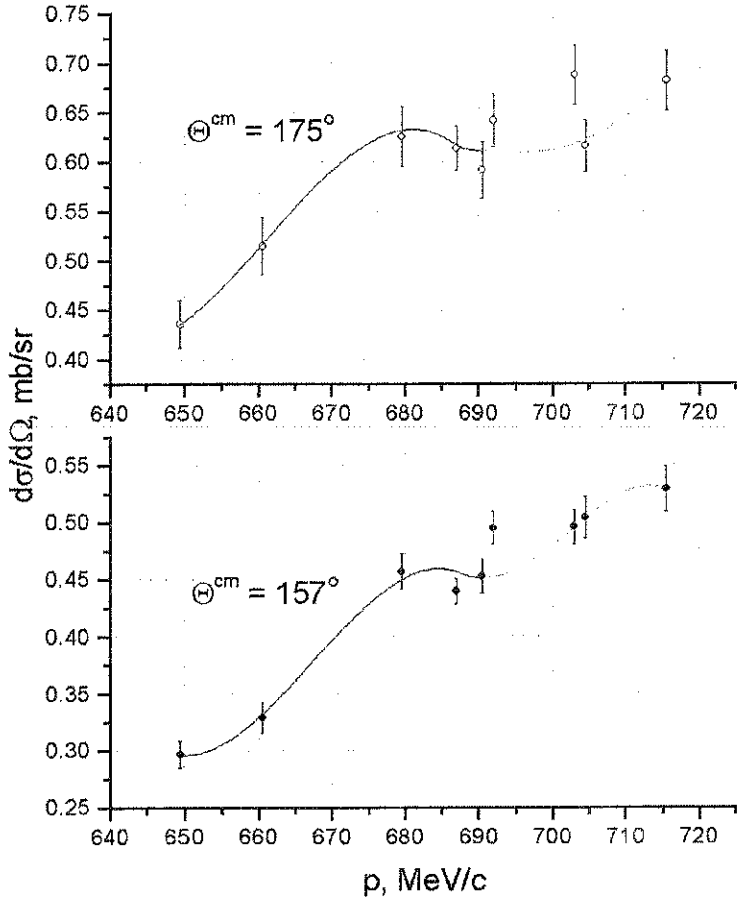

Fig. 4. Momentum dependences of differential cross sections of $\pi^- p$ charge exchange scattering in the region of η production threshold. Results obtained with Čerenkov spectrometers are shown by solid circles, those obtained with CsI(Na) crystals – by open circles. are drawn to guide the eye.

Irregularities in the momentum dependence of the DCS in the region around $p_\pi = 685$ MeV/c may be treated as a manifestation of the cusp effects.

PNPI has good prospects for studying the pion-induced processes of η production. For the elementary process $\pi^- p \to \eta n$ the threshold is 685 MeV/c, and the total cross section rises sharply from the threshold reaching the maximum value of $\sigma_{tot} \simeq 2.5$ mb at $p_\pi = 760$ MeV/c. The pion channel of the PNPI synchrocyclotron can produce intense pion beams in the momentum region from the threshold up to the maximum of the cross section.

Measurements of yields of the process $\pi^- p \to \eta n$ were carried out by detecting the emitted recoil neutrons and determining their energies by means of the time-of-flight technique.

The kinematics of the process $\pi^- p \to \eta n$ in the near-threshold region is such that all the neutrons are emitted in a relatively small cone in the forward direction in the laboratory system. The maximum angle of their emission increases with the momentum of the incident pions and with the most neutrons being emitted at angles close to the maximum angle. Another feature of this process is that at a given angle in the laboratory system, θ_n^{lab}, two groups of neutrons with different energies are detected (corresponding to neutron emission to the forward and to the backward hemispheres in the center-of-mass system).

In the near-threshold region, η production occurs only in the S-state. Under this constraint the number of detected neutrons is defined by the equation:

$$N = N_\pi N_p \varepsilon_n \sigma_{tot} A_n \quad , \tag{1}$$

where N_π is the number of the incident pions; N_p is the number of protons in a target ($1/\mathrm{cm}^2$); ε_n is the efficiency of the neutron detectors; σ_{tot} is the total cross section of the investigated process; and A_n is the angular acceptance (*e.g.* the fraction of the total solid angle in the c.m.s. subtended by the neutron detector). Evidently, the product of the two functions, σ_{tot}, which rises steeply, and A_n, which falls with the momentum of the incident pions, gives a dependence characterized by a peak. For real experimental conditions this dependence has to be averaged over the momentum spread of the beam.

The experimental layout is similar to that shown in Figure 2. The used neutron detectors are the same as in the $\pi^- p$ charge exchange scattering experiment. To lower the level of the background due to neutrons from reactions with more than two particles in the final state (such as $\pi^- p \to \pi^+ \pi^- n$ or $\pi^- p \to \pi^+ \pi^- \pi^0 n$), the target was surrounded with scintillation veto counters covering a solid angle of approximately 1.5 sr. The firing of any veto counter caused by a charge particle crossing the scintillator produced a veto-signal and prevented triggering.

In this experiment, the momentum acceptance of the pion channel was reduced by placing a 4-cm momentum slit just upstream of the hodoscope of beam counters. In another words, only two counters H4 and H5 of the beam hodoscope, which are nearest to the beam axis, were used.

Measurements were made at central momenta of the pion beam 670, 680, 690, 695, 700, and 710 MeV/c [5]. At each central momentum, data taking was performed simultaneously for the two momentum bins corresponding to the beam counters H4 and H5.

The yields of the η production process were determined by detecting the recoil neutrons. The selection of neutrons produced uniquely in the reaction $\pi^- p \to \eta n$ was made by measuring their time of flight on the base of 5 m between the monitor counter (located just upstream of the hydrogen target) and the corresponding neutron detector. After subtracting the background we have obtained the momentum dependences of the η yield presented in Fig. 5.

The error bars are the quadrature sums of the statistical uncertainties and systematic ones due to the procedure of the background subtraction. Maxima of the measured dependences shift to higher momentum when the angle of the neutron emission increases – this maximum is located at $p_\pi \simeq 690$ MeV/c for $\theta_n^{lab} = 0.9°$ and at $p_\pi \simeq 710$ MeV/c for $\theta_n^{lab} = 11.5°$.

Shown by the curves in Fig. 5 are the results of calculations performed using expression (1). The value of the angular acceptance, A_n, was obtained by a Monte Carlo simulation (GEANT code) taking into account the real geometry of the experiment, the measured spatial characteristics of the pion beam and the momentum distribution of particles in the beam. The value of the η mass, $M_\eta = 547.45$ MeV/c^2, was obtained from the most recent Listings of the Review of Particle Properties [6]. In the calculation we used, as a first approximation, the momentum dependence of the total cross section, $\sigma_{tot}(p)$, obtained by fitting published experimental data using the assumption that the process $\pi^- p \to \eta n$

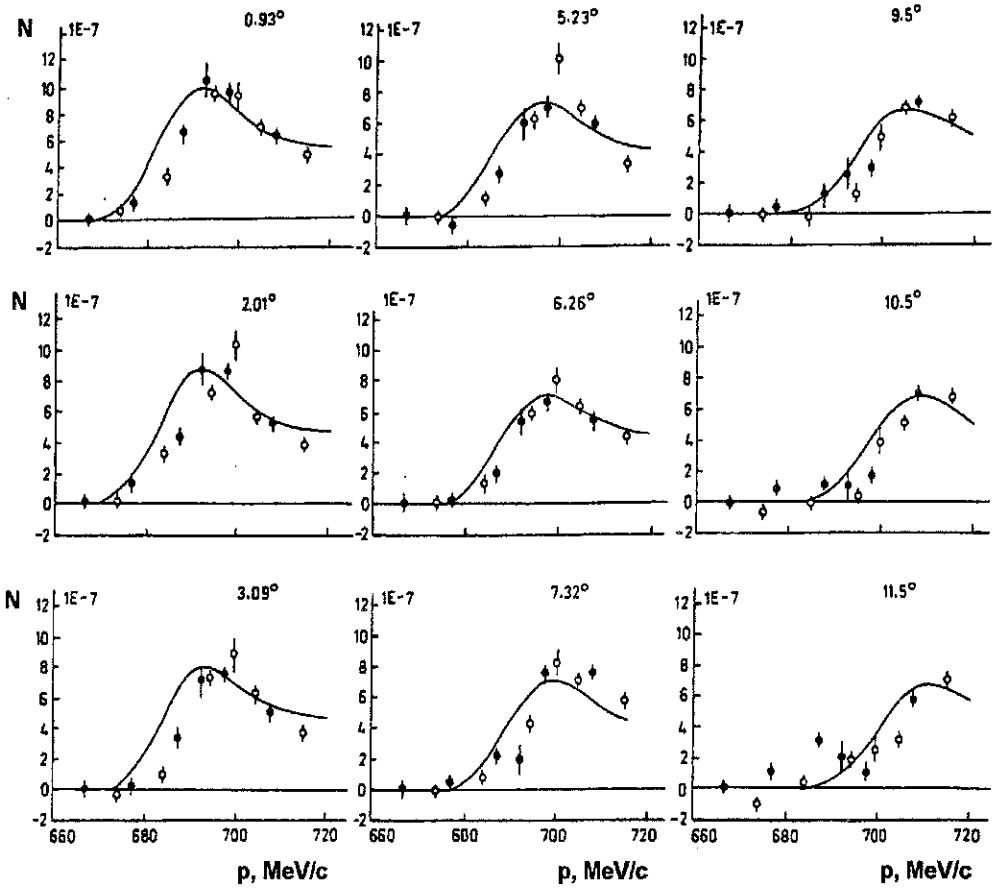

Fig. 5. Yields of the reaction $\pi^- p \to \eta n$ for different angles of neutron emission. Experimental points shown by open and solid circles correspond to the beam counters H4 and H5, respectively.

occurs through an excitation of the $S_{11}(1535)$ resonance. It can be seen that the calculations reproduce the shape of the momentum dependences rather well for all nine angles. This may be considered as an indication that the PNPI experimental data agree with the above-mentioned value of the η mass, and that the fitting $\sigma_{tot}(p)$ adequately reflects the real momentum dependence of the cross section.

This work was supported by the Russian Foundation for Basic Research (Grant No 99–02–17500) and the Russian State Scientific-Technical Program "Fundamental Nuclear Physics".

REFERENCES

1. S.P. Kruglov, "Investigation of πN scattering at LNPI", πN Newsletter **No 4**, 14 (1991).
2. M.E. Sadler, "Pion-nucleon experimental program at LAMPF (recent results and future experiments)", in *Proceedings of the International Conference on Mesons and Nuclei at Intermediate Energies, Dubna, Russia, 3 - 7 May 1994* (World Scientific Publishing Co., Singapore, 1994) pp. 3-10.
3. V.V. Abaev and S.P. Kruglov, "Phase shift analysis of πp scattering in the energy region from 160 to 600 MeV", Z. Phys. **A 352**, 85 (1995).
4. D.D. Bugg, "πN phase shifts, 0 – 310 MeV", πN Newsletter **No 6**, 7 (1992).
5. I.V. Lopatin, V.V. Abaev et al., Preprint PNPI–2244, Gatchina, 1998.
6. Particle Data Group, "Baryon particle listings", Europ. Phys. J. **3**, 653 (1998).

Partial-total πN cross sections

E. Friedman
Racah Institute of Physics, The Hebrew University, Jerusalem 91904, Israel

Abstract

Recent results from the LAMPF measurements of partial total cross sections for $\pi^{\pm}$ p interactions are compared with earlier results from TRIUMF and excellent agreement is found between the two sets of measurements. A systematic shift of +1.35% is made to the TRIUMF results for the total cross section for π^- p single charge exchange and good agreement is found with the older results of Bugg et al. Experimental results are compared with predictions of the KH80 and SP99 phase shifts.

INTRODUCTION

'Partial total' cross sections refer to integral cross sections obtained by integrating differential cross sections over angular ranges smaller than 4π, such as is encountered in a 'poor geometry' transmission experiment i.e. with a non-negligible solid angle of the detector. The concept was initially introduced[1] in order to check, in an independent experiment, the absolute normalization of π^+p differential cross sections near 70 MeV. It is essentially a partial result usually obtained in the measurement of total cross sections, except that we treat it as a well defined (experimental and theoretical) quantity in its own right, thus avoiding the need to extrapolate to zero solid angle with its associated Coulomb corrections. It is particularly simple in the case of π^+p interaction below the pion production threshold because then it is the integral of the elastic scattering differential cross section between the detector solid angle Ω and 4π.

Final results of the TRIUMF series of experiments[2–4] were presented at the MENU95 meeting[5]. These differ slightly from the originally published results because of a correction made in 1994 to the energy calibration of the M11 channel at TRIUMF which applied to some of the measurements. A follow-up experiment at LAMPF differed from the TRIUMF experiments in many technical details but otherwise was based on the same method. It also covered a broader energy range. The two experiments differed in almost all the major technical points; the TRIUMF experiments used solid CH_2 and graphite targets whereas the LAMPF experiment used liquid hydrogen target. In the TRIUMF experiments discriminators and scalers were used and protons recoiling from the target were stopped in absorbers. At LAMPF time and pulse height information from all the detectors were recorded event by event and the recoiling protons were excluded by software cuts. It is therefore of interest to compare results from the two very different experiments, that obviously had totally independent calibrations of beam energy.

Very recently the final results of the LAMPF experiment have been published[6]. The present talk compares the results of the two experiments both for π^+p and π^-p interactions. In the latter case the total cross section for the single charge exchange (SCX) reaction forms a part of the measured cross sections and we therefore discuss also the total cross section for the SCX reaction.

π^+p CROSS SECTIONS

Figure 1 shows partial total cross sections for 30° laboratory angle for π^+p interaction from the two experiments over the energy range where they can be compared. It is clearly seen that the two sets of results are in full agreement with each other without any indication of systematic differences. Also shown in the figure are the predictions of the SP99 solution obtained from the SAID analysis[7] and it is evident that both experiments are in good agreement with the predictions and in particular the shape of the resonance is very well reproduced. Note, however, that the TRIUMF data were included in the data base behind the SP99 phase shifts.

Figure 2 shows ratios of the experimental cross sections to calculated values based on the SP99 and on the Karlsruhe-Helsinki KH80 phases[8], the latter obtained long before any of the present experiments were performed. On such a curve it is easier to see trends,

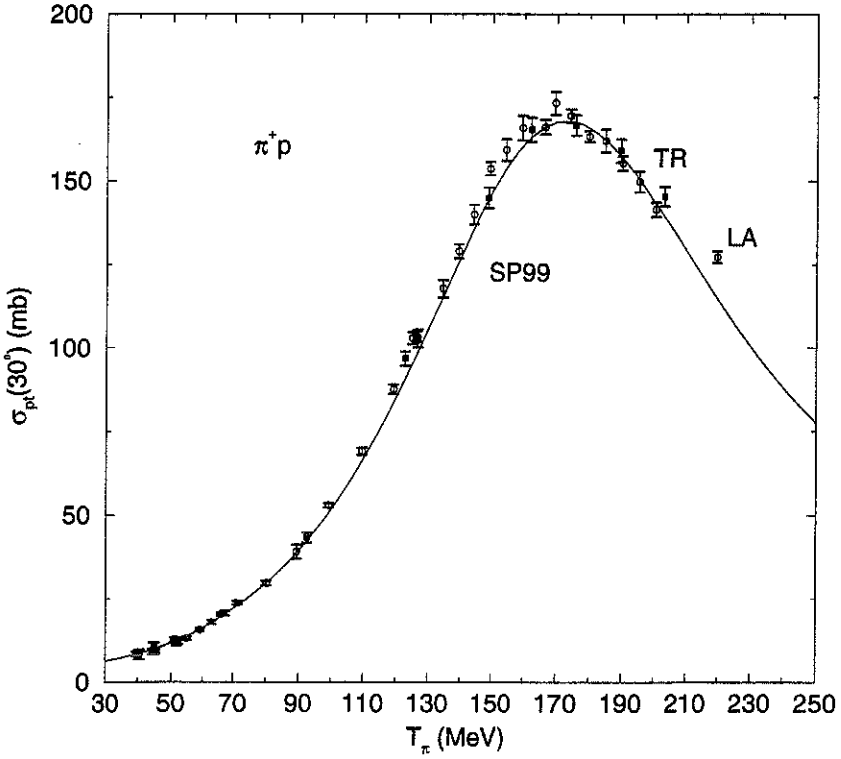

Figure. 1. Partial total cross sections for π^+p interactions, 30°. TRIUMF data- squares, LAMPF data-open circles. Also shown as a solid curve are predictions of SP99, see text.

e.g. too small calculated cross sections near 100-120 MeV for both sets of phase shifts and too large calculated values for KH80 between 50 and 100 MeV. The good consistency between the two experiments is evident here too. Partial total cross sections for the π^+p interaction in this energy range can also be compared with direct integrations of differential cross sections. However, in most cases the differential data are not extensive enough to allow direct integration and one has to perform single energy phase shifts fit in order to be able to perform the integration with the help of the fit parameters. In most cases good agreement is obtained, which is not surprizing when global sets of phase shifts such as SP99 fit the corresponding differential data. In some cases the range of the differential data is too restricted to allow a meaningful calculation of a partial total cross section.

π^-p CROSS SECTIONS

Figure 3 shows ratios of the experimental cross sections to calculated values based on the SP99 and the KH80 phase shifts. The LAMPF results are for 30° and the TRIUMF results are for 20° but the comparison with predictions makes it possible to display them on the same graph. Again the agreement between the two experiments (corrected for the different angles) is very good as is seen from the figure. The predictions of KH80 seem to be too high in the energy range of 110 to 160 MeV. For π^- the partial total cross section includes, by definition, the total cross section for producing uncharged particles, as it measures the cross section for not detecting an outgoing particle following the detection of an incoming particle. Therefore, in addition to the cross section for capture in flight (π^-p $\rightarrow \gamma$ n) it includes the total cross section for the SCX reaction π^-p $\rightarrow \pi^0$ n. We therefore turn attention now to this reaction.

π^-p TOTAL SCX CROSS SECTIONS

Total cross sections for the π^-p SCX reactions can be measured directly by a transmission experiment without recourse to measurements of differential cross sections with gamma ray detectors. The first such measurements were performed by Bugg et al.[9] long

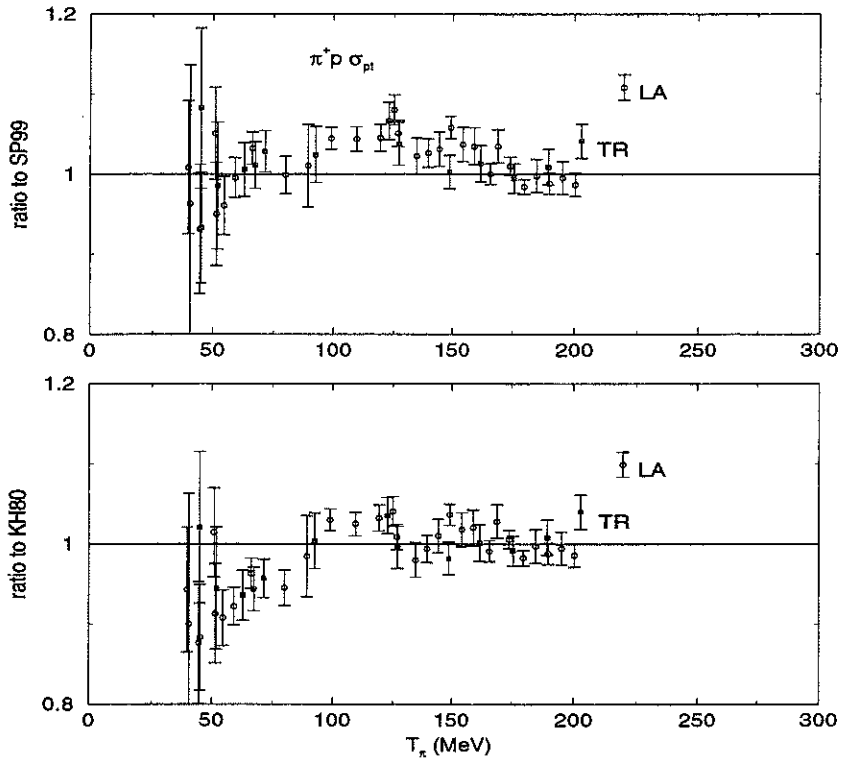

Figure. 2. Ratios of experimental partial total cross sections for π^+p interaction to predictions, see Fig. 1

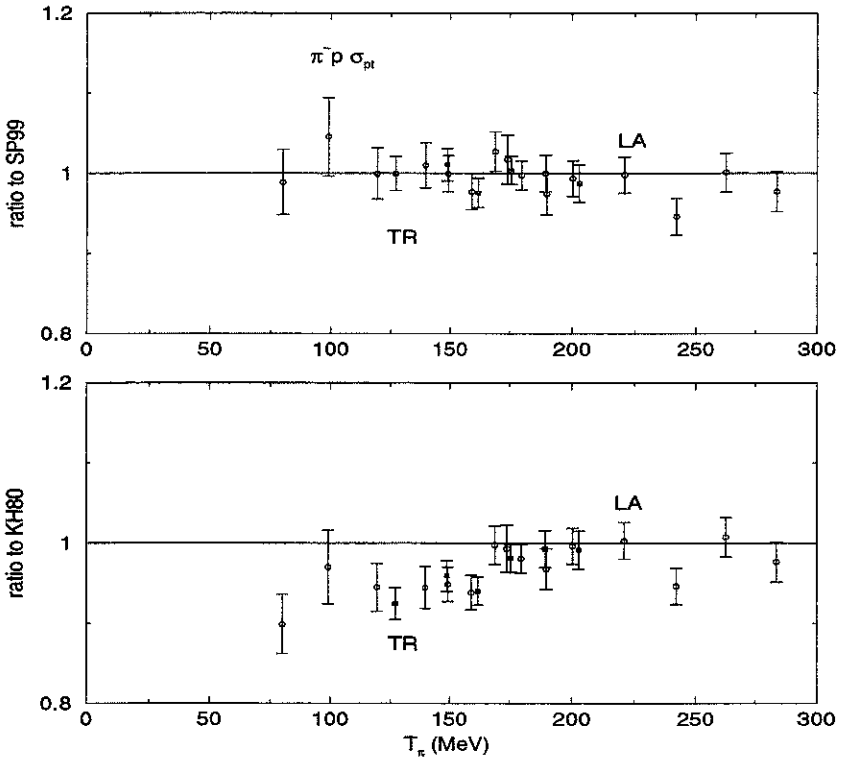

Figure. 3. Ratios of experimental partial total cross sections for π^-p interaction to predictions, see Fig. 1

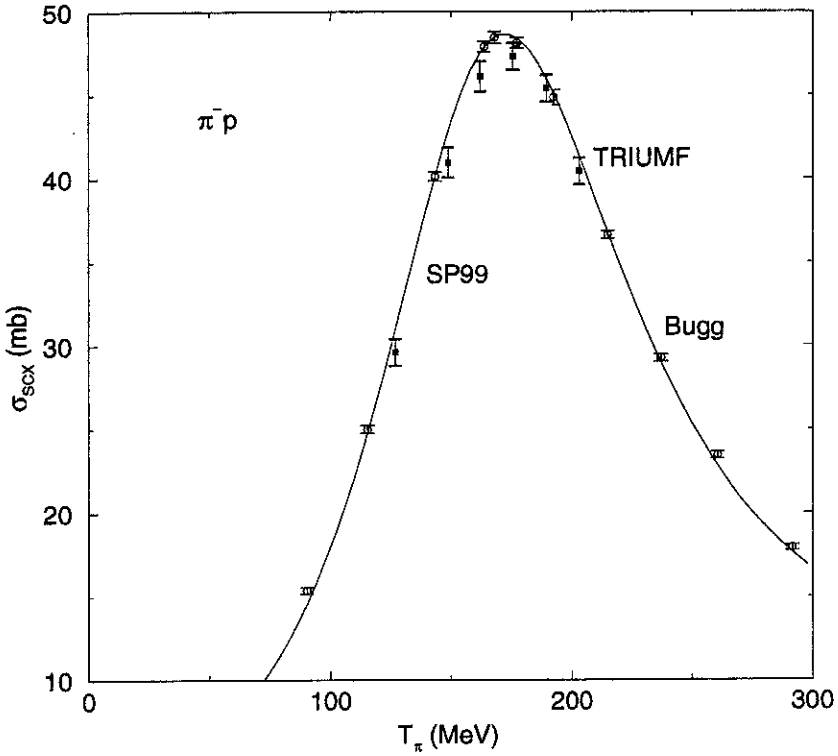

Figure. 4. Total cross sections for the π^-p SCX reaction. Squares for TRIUMF results, open circles for Bugg at al. Also shown as a solid curve are predictions of SP99.

ago and similar measurements were part of the more recent series of transmission measurements at TRIUMF[4]. The results which were summarized in the MENU95 meeting[5] were systematically about 2% lower that those of Bugg et al. with typical errors of ±2%. The TRIUMF experiment used solid targets and the Bugg experiment used liquid hydrogen target. Both recorded only scaler readings.

In view of the very good agreement between the TRIUMF and the LAMPF partial total cross sections we concluded that the energy calibration, corrections due to beam composition and the handling of the CH_2-C subtraction procedure must be correct at the TRIUMF experiments and we re-examined corrections which are peculiar to the SCX measurement. These include detection of neutral particles (neutrons and gammas from π^0 decays) through their interaction with the 4π detector and with the target and structural material. These corrections amount to about 8% of the measured cross sections. Upon very close examination of the various corrections we have concluded that: (i)the calculated gammas detection had to be increased by 0.2%, (ii)the corrections due to the down-stream detector had to be increased by 0.65% because in fact it extended slightly beyond the side detectors[4] and (iii)the corrections due to near-target muons had to be increased by 0.5% because in the SCX experiment we had a slightly larger distance between the last beam-defining detector and the target than was the case in the measurements of the partial total cross sections. We therefore increase systematically our total SCX cross sections by 1.35%, still within the quoted errors of 2%. Figure 4 shows our results and also those of Bugg et al.[9]. The residual discrepancy of about 1% is probably insignificant considering the different techniques used and the different ways of evaluating the corrections due to detection of neutral particles. Figure 5 shows ratios of measured total SCX cross sections to SP99 and KH80 predictions. In addition to our results (TR2) are included total cross sections from two earlier differential TRIUMF experiments (TR0[10] and TR1[11]). Note that all those data were included in the fits which led to SP99 but only the Bugg data were included in the KH80 fits. It is clear from this figure that more accurate data are needed at low energies. It is also clear that there are problems with the KH80 predictions.

Table 1. TRIUMF integral cross sections.

T_π (MeV)	$\pi^+20°$	$\pi^+30°$	π^- SCX	$\pi^-20°$
45.0		10.8 ± 1.0		
52.1		12.4 ± 1.0		
63.1		18.0 ± 0.6		
67.45	21.6 ± 0.7	20.7 ± 0.6		
71.5	24.0 ± 0.6	23.8 ± 0.6		
92.5	45.1 ± 1.2	43.3 ± 1.5		
122.9	102.2 ± 2.0	96.7 ± 2.1		
126.9	108.5 ± 2.4	102.7 ± 2.7	29.6 ± 0.8	41.7 ± 0.9
148.9	161.8 ± 3.0	144.9 ± 3.0	40.9 ± 0.9	59.5 ± 1.2
162.25	178.6 ± 2.0	165.3 ± 3.7	46.1 ± 0.9	64.6 ± 1.2
175.7	187.6 ± 3.3	166.6 ± 3.1	47.3 ± 0.8	68.4 ± 1.2
189.4	183.1 ± 3.4	159.1 ± 3.5	45.4 ± 0.8	65.3 ± 1.5
203.0	164.3 ± 3.3	145.3 ± 3.0	40.4 ± 0.8	58.7 ± 1.4

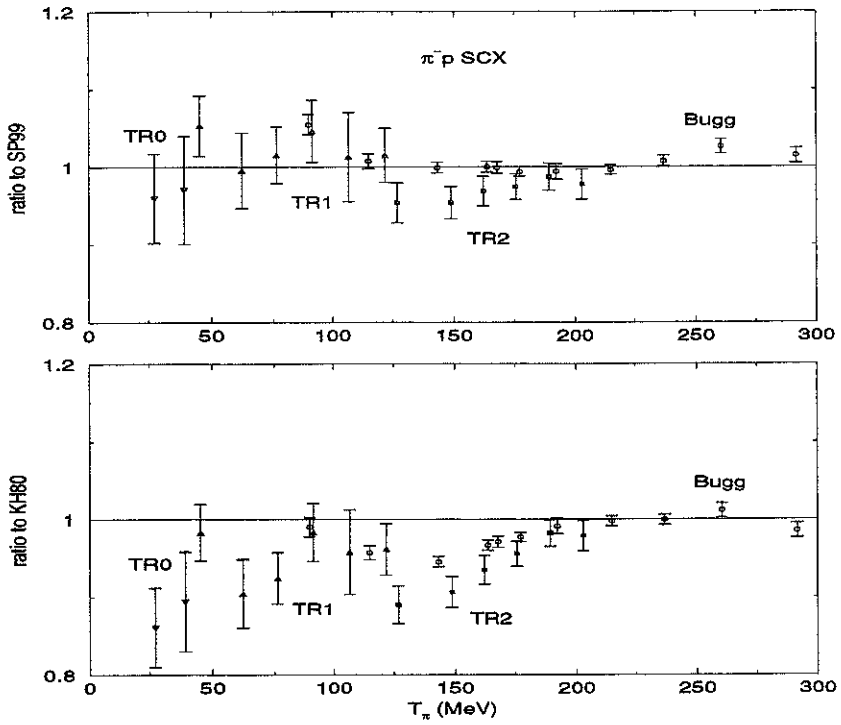

Figure. 5. Ratios of experimental SCX total cross sections for π^+p interaction to predictions. Also included earlier TRIUMF data[10,11].

SUMMARY AND OUTLOOK

Measurements of partial total cross sections provide rather sensitive tool for checking the absolute normalization of differential cross sections. With the publication of the final results of the LAMPF experiment it became possible to make detailed comparisons with the TRIUMF results, and very good agreement is found between the two totally independent experiments. A close examination of the corrections to the total cross sections for the π^-p SCX reaction measured at TRIUMF revealed a 1.35% systematic correction, which now brings those results into good agreement with the older results of Bugg et al.[9]. Table 1 summarizes all the TRIUMF results and it supersedes the SCX results in[5].

Comparisons between the various measured and calculated integral cross sections reveal some problems, particularly with the KH80 phase shifts. There seems to be a need for additional precision measurements of total cross sections for the SCX reaction at energies below 100 MeV, and such measurements between, say, 30 and 200 MeV by a *single* experiment will be useful.

REFERENCES

1. E. Friedman et al., Phys. Lett. **B 231**, 39 (1989).
2. E. Friedman et al., Nucl. Phys. **A 514**, 601 (1990).
3. E. Friedman et al., Phys. Lett. **B 254**, 40 (1991).
4. E. Friedman et al., Phys. Lett. **B 302**, 18 (1993).
5. E. Friedman, πN Newsletter 11, 120 (1995).
6. B.J. Kriss et al., Phys. Rev. **C 59**, 1480 (1999).
7. R.A. Arndt and L.D. Roper, SAID on-line program.
8. R. Koch and E. Pietarinen, Nucl. Phys. **A 336**, 331 (1980).
9. D.V. Bugg et al., Nucl. Phys. **B 26**, 588 (1971).
10. M. Salomon et al., Nucl. Phys. **A 414**, 493 (1984).
11. A. Bagheri et al., Phys. Rev. **C 38**, 885 (1988).

Measurement of π^+p analyzing powers at low energy at PSI

R. Meier[1], R. Bilger[1], B. van den Brandt[2], J. Breitschopf[1], H. Clement[1], J. Comfort[6], M. Cröni[1], H. Denz[1], K. Föhl[5], E. Friedman[7], J. Gräter[1], P. Hautle[2], G. J. Hofman[4] J. A. Konter[2], S. Mango[2], M. Pavan[3], J. Pätzold[1], G. J. Wagner[1]

[1] *Physikalisches Institut, Universität Tübingen, 72076 Tübingen, Germany*
[2] *Paul Scherrer Institut, 5232 Villigen PSI, Switzerland*
[3] *Laboratory for Nuclear Science, MIT, Cambridge MA, USA*
[4] *University of Colorado, Boulder, CO 80309, USA*
[5] *Department of Physics and Astronomy, University of Edinburgh, UK*
[6] *Arizona State University, Tempe, AZ 85287, USA*
[7] *Racah Institute of Physics, The Hebrew University, Jerusalem 91904, Israel*

Abstract

Analyzing powers in π^+p scattering are being measured at PSI using the LEPS spectrometer and a novel active polarized target. The active target provides essential information for background reduction. Up to now, data have been taken in the energy range from 45 to 87 MeV at medium angles, preliminary results are consistent with earlier data at 68.3 MeV.

INTRODUCTION

Over the last 10 years, there have been numerous requests for analyzing power measurements in πp scattering[1]. Experimental data for this observable are an important constraint for the phase shift analysis[2]. Furthermore, measurements of polarization observables are assumed to be able to resolve inconsistencies in the cross section data base, in particular at energies below 100 MeV. Nevertheless, due to experimental difficulties, only one data set for π^+p elastic scattering at 68.3 MeV has been published so far in this energy region[3]. But the data situation for polarization observables at low energies should improve dramatically in the near future as results are expected from three experiments:

- TRIUMF E560 for π^-p elastic scattering[4]. Preliminary results from this experiment with the CHAOS detector are presented by J. Patterson at this conference.
- PSI R99-02 for π^-p single charge exchange[5]. It is proposed to use the Neutral Meson Spectrometer (NMS) for these measurements.
- PSI R97-01 for π^+p elastic scattering. This experiment is the topic of this presentation.

EXPERIMENTAL SETUP

The schematic setup for an analyzing power measurement is shown in Fig. 1.

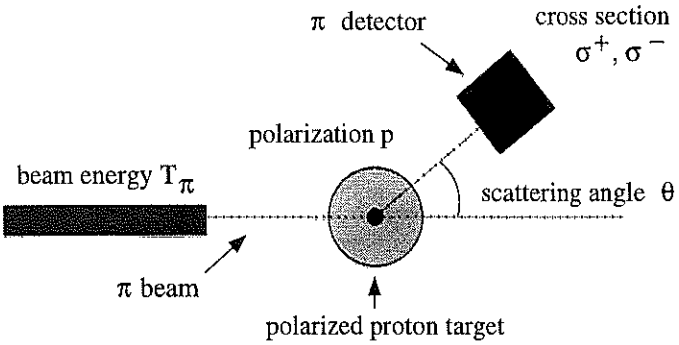

Fig. 1. Setup of an analyzing power measurement.

Incoming pions are scattered from a polarized proton target, the direction of the polarization axis is perpendicular to the scattering plane. The scattered pions are measured in a pion detector which gives the polarization-dependent scattering cross section $\sigma^{\pm}$. When assuming the same magnitude p of the polarization for 'spin up' and 'spin down', the analyzing power is determined by

$$A_y(\Theta, T_\pi) = \frac{1}{p} \times \frac{\sigma^+ - \sigma^-}{\sigma^+ + \sigma^-} \tag{1}$$

As can be seen from the structure of this equation, absolute normalization of the cross sections is not required. Consequently, absolute knowledge of parameters like the solid angle of the detector, the target density, or the beam composition is not required. These quantities are important sources of systematic errors in measurements of absolute differential cross sections.

The experimental problems in analyzing power measurements are quite different. They are caused by the structure of the polarized target. The only available kind of polarized target suitable for use on a pion beam is a dynamically polarized solid state target. The size of the polarized sample in a dynamically polarized target is typically of the order of the beam size. Therefore, the fraction of beam hitting the target sample has to be monitored as it could change over time, with changes of the polarization. This monitoring could be done by placing a beam definition counter in front of the target sample and counting the incoming particles. Unfortunately, due to the cryogenics, heat shields and vacuum volumes surrounding the target and the target magnetic field which is necessary to maintain polarization the use of such a beam definition counter is problematic. An even more severe difficulty is caused by the chemical composition of the target. The polarizable sample is typically an alcohol or ammoniak, containing carbon, oxygen or nitrogen besides the polarized protons. Furthermore, the target sample is immersed in cooling liquid containing helium, and surrounded by a brass or steel target cell. Events from πp elastic scattering must be separated from events due to background reactions on these materials. A very efficient method, the detection of the backscattered proton in coincidence, is not suitable for measurements at low energies and small angles as the backscattered proton does not leave the target. The energy straggling due to the required material in the target region also limits the resolution that can be achieved with the pion detector for a kinematical separation of the various reactions.

A polarized active target helps to overcome these difficulties. It serves as its own beam definition counter, rejecting reactions which take place outside the target sample. Furthermore, the energy deposition in the target gives additional information on the interaction. Active polarized targets have become available only recently, they were developed by the PSI target group[6]. The basic procedure for the production of polarizable scintillator consists in doping standard plastic scintillator with paramagnetic centers. This procedure is still being optimized for better polarizability and higher light output. In the experiment described here polarizations of somewhat over 50% and light output of about 20% of undoped scintillator were achieved.

The experiment used the πE3 beam line at PSI, and the Low Energy Pion Spectrometer LEPS as the pion detector. This magnetic spectrometer consists of a quadrupole triplet and a split dipole. Particles are momentum-analyzed, the momentum is determined from the position in a focal plane drift chamber. Four muon decay cone telescopes at the πE3 beam exit are used for relative beam normalization and beam position monitoring. The polarized active target setup is shown in Fig. 2. The beam hits the target cell which simultaneously serves as mixing chamber of a ^{3}He/^{4}He dilution refrigerator. A vertical magnetic field is generated by superconducting Helmholtz coils located above and below the beam height. The polarization is induced by microwave irradiation and measured with NMR methods. The light produced in the 18*18*5mm^3 target sample is guided to a photomultiplier at room temperature outside the magnetic field.

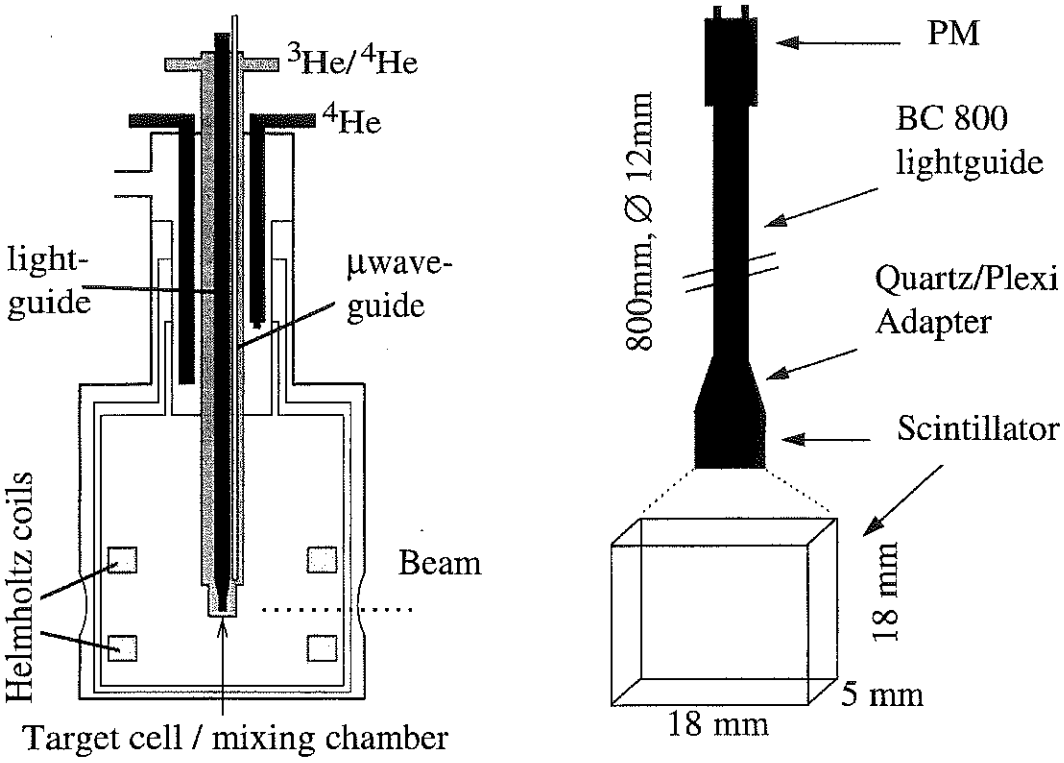

Fig. 2. The polarized active target setup (left) and the light readout system (right).

DATA TAKING

The performance of the active target is illustrated by E_{loss} spectra in Fig. 3.

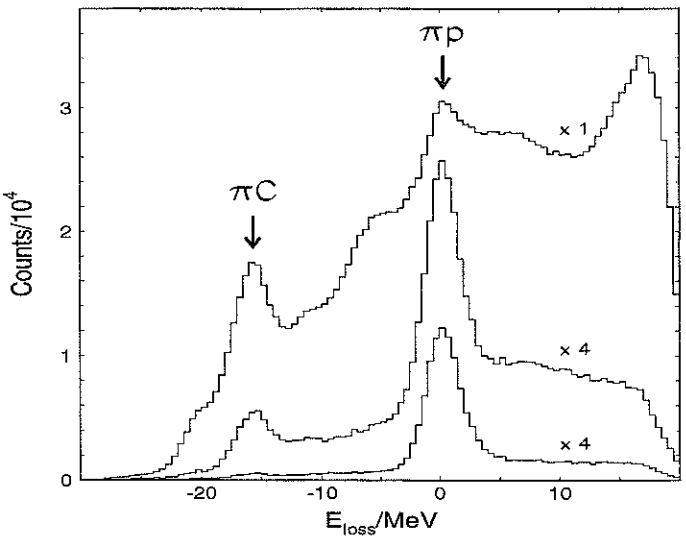

Fig. 3. E_{loss} spectra taken with LEPS and the polarized active target. The upper curve shows the raw LEPS information, for the middle curve a coincident signal in the target is required, for the lower curve a minmum energy deposition in the target is required.

E_{loss} is defined as the difference of the kinetic energy of the scattered pion expected from πp kinematics and the energy measured in the spectrometer. The upper curve is generated by using the LEPS information only. The peaks for πp and πC elastic scattering can be identified, but they are accompanied by a substantial amount of background. For the middle curve, a coincident signal in the active target was required. This requirement

removes a large part of the background. The lower spectrum additionally requires a minimum energy deposition in the active target, now the πp peak dominates. The remaining background is due to Carbon breakup and is measured in separate runs with a Carbon target.

As the determination of the πp yield depends on a cut on the active target ADC value, monitoring of the active target photomultiplier amplification is necessary. We use a light diode pulser (which is itself monitored by a PIN diode) to produce calibration signals in the ADC spectrum. Additionally, the pulse shape for each event is recorded by a 1GHz Flash ADC.

The polarization is changed at least twice for each angular and energy setting to be able to identify changes in the experimental setup. A change of the polarization direction lasts about 8 h. The polarizing field was 2.5 T, for data taking the target was operated in frozen spin mode (with a polarization decay time of 80 h) at a field of 1.2 T.

DATA ANALYSIS

According to Equation 1, several quantities have to be extracted from the data for calculation of the analyzing power:

- The scattering angle Θ_{lab} is given by the spectrometer position and ray tracing of beam particles and scattered particles through the target magnetic field.
- The beam energy T_π is given by the settings of the beam line magnets. We use the calibration established for the experiment by Wieser et al.[3] by time of flight methods. The calibration is tested by the kinematics of πC scattering at various angles and energies using a thin Carbon target.
- The polarization p is determined by NMR methods. Thermal equilibrium (TE) NMR signals are taken at known temperature and magnetic field, i.e. at a known polarization. The polarization of the dynamically polarized material is determined by comparing the size of the dynamical signals and the TE signals. The systematic error of the polarization measurement in this experiment is relative 3.5%.
- The relative cross section $\sigma(p)$ is determined from the πp yields extracted from E_{loss} spectra. The relative normalization is achieved by using scaler values of the muon cone counters at the πE3 beam exit. Chamber and data taking efficiencies are taken into account.

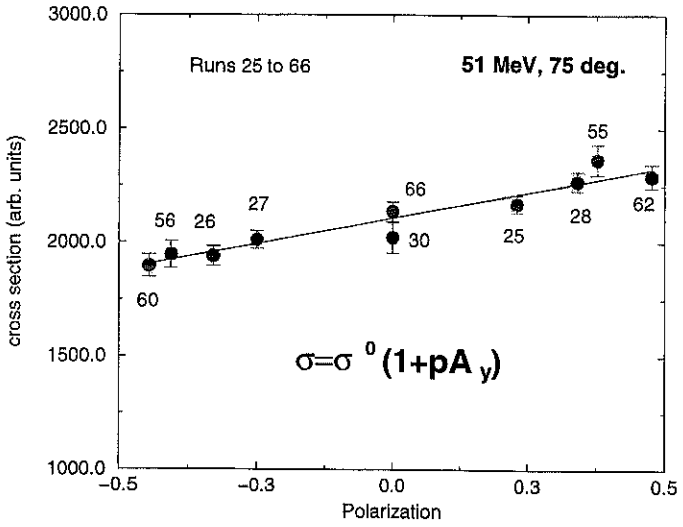

Fig. 4. Straight line fit for the extraction of the analyzing power from a set of relative cross sections at different polarizations.

Finally, we get for each angle and energy a set of relative cross sections at known polarizations. The analyzing power is determined from the parameters of a straight line fit of relative cross section over polarization, an example for this fit is shown in Fig. 4.

PRELIMINARY RESULTS

Data have been taken at 45, 51, 57, 68.3 and 87 MeV, at angles between Θ_{lab} =40° and 120°. The analysis is still in progress. Preliminary results at 87 and 68.3 MeV are shown in Fig. 5 as solid points. The error bars include statistical errors only. The data are in good agreement with the previous measurement by Wieser et al.[3] at 68.3 MeV, shown as open data points. The results of the VPI SP99 and KH80 phase shift solutions are represented by solid and dashed lines.

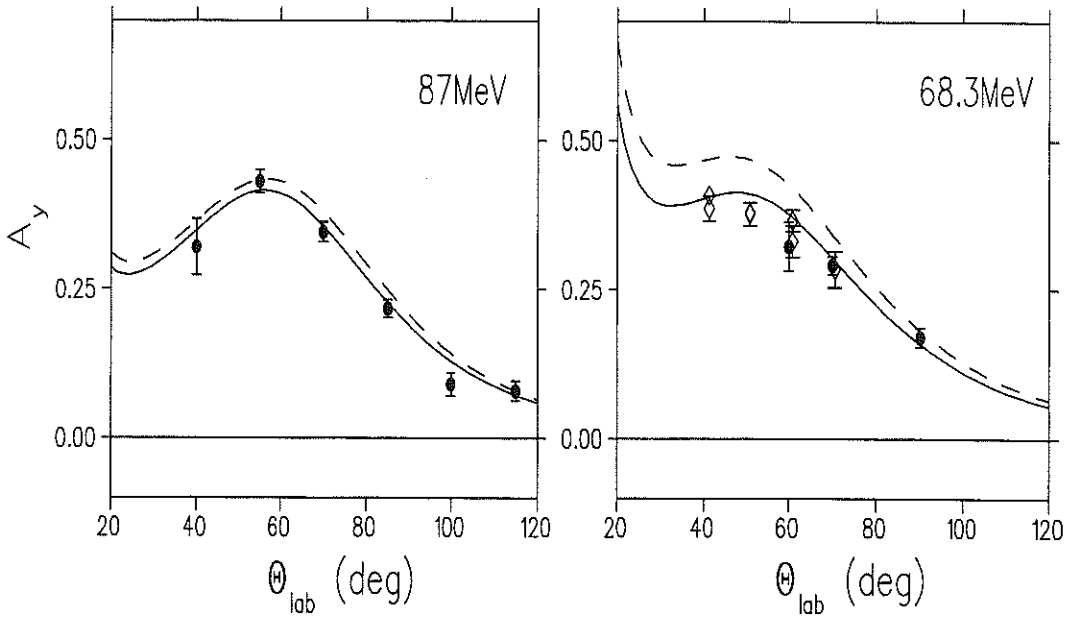

Fig. 5. Preliminary results at 87 and 68.3 MeV are shown as solid data points. Open data points are from Wieser et al.[3]. The lines correspond to the VPI SP99 (solid) and KH80 (dashed) phase shift solutions.

We plan to continue the measurements for π^-p elastic scattering. Here, data at 51 MeV and backward angles are of particular interest as an investigation by Locher and Sainio has shown a strong sensitivity of the analyzing power to the value of the Sigma-term[7].

REFERENCES

1. See for example: G. Höhler, πN Newsletter 2 (1990).
2. M. Sainio, πN Newsletter 13, 144 (1997).
3. R. Wieser et al., Phys. Rev. C 54, 1930 (1996).
4. G. J. Hofman et al., πN Newsletter 13, 157 (1997).
5. J. Comfort et al., PSI research proposal R99-02.1 (1999).
6. B. van den Brandt et al., SPIN 96 Symposium Amsterdam (1996).
7. M. Locher and M. Sainio, Czech J. Phys. B39 (1989).

Nuclear $(\pi, 2\pi)$ reactions: A smoking gun for medium modifications?

M.E. Sevior[1,h],P.A. Amaudruz [e], F. Bonutti [c,d],J.T. Brack [e,j]P. Camerini [c,d], J. Clark [h],L. Felawka [e],E. Fragiacomo [c,d], E.F. Gibson [f],J. Graeter [i],N. Grion [c],G.J. Hofman [a,j], M. Kermani [a],E.L. Mathie [g],V. Mayorov [b], S. McFarland [a], R. Meier [e,i] ,G. Moloney [h], D. Ottewell [e],O. Patarakin [b],K. Raywood [a],R.R. Ristenen [j], R. Rui [c,d],G.R. Smith [e],R. Tacik [g],V. Tikhonov [b] and G. Wagner [i]
(The CHAOS collaboration)
http://www.triumf.ca/chaos/chaos.html

[a] *Physics Department, University of British Columbia, Vancouver, B.C., Canada*
[b] *Kurchatov Institute, Moscow 123182, Russia*
[c] *Istituto Nazionale di Fisica Nucleare, 34127 Trieste, Italy*
[d] *Dipartimento di Fisica dell'Universita' di Trieste, 34127 Trieste, Italy*
[e] *TRIUMF, Vancouver, B.C., Canada V6T 2A3*
[f] *California State University, Sacramento CA 95819, USA*
[g] *University of Regina, Regina, Saskatchewan, Canada S4S 0A2*
[h] *School of Physics, University of Melbourne, Parkville, Vic., 3052, Australia*
[i] *Department of Physics, University of Tuebingen, Germany*
[j] *Department of Physics, University of Colorado, USA*
[1] *email:msevior@physics.unimelb.edu.au*

Abstract

We find that the invariant mass distributions of the $\pi^+\pi^-$ particles from the reaction ^{45}Sc$(\pi^+,\pi^+\pi^-)$X differ substantially from the equivalent reaction on the proton or deuterium over the range of incident pion kinetic energies 240, 260, 280, 300 and 320 MeV respectively. No such change is observed in the $\pi^+\pi^+$ invariant mass distribution from the ^{45}Sc$(\pi^+,\pi^+\pi^+)$X reaction. This is evidence that the isopsin 0 component of $\pi-\pi$ interaction within the nuclear medium is substantially different from that of the vacuum.

INTRODUCTION

Chiral symmetry is the conservation of helicity or handedness. Clearly perfect chiral symmetry is only possible in a system of massless particles, otherwise it is possible to change to helicity of a particle by an appropriate Lorentz boost. The QCD Lagrangian has no terms which depend on the helicity of quarks and no terms that can change the handedness of quarks. Thus if quarks were perfectly massless one might expect QCD to exhibit chiral symmetry.

However even in the absence of an explicit mass term, quarks acquire an effective mass due to their self interactions with the QCD field. Thus the ground state of QCD does not exhibit chiral symmetry. This is an example of spontaneous symmetry breaking, which implies the existence of massless Goldstone bosons. These are identified as the spin 0^- meson octet. The quarks do of course have a non zero mass which in turn gives pions mass too. In fact:

$$M_\pi^2 \propto M_q$$

Which leads to todays estimate of the up and down quark masses. The modern formalism of chiral perturbation theory (ChPT) has been developed from these ideas.

The most accurate prediction from ChPT is for the $\pi-\pi$ scattering lengths (a_0 and a_2) which are the isospin 0 and 2 values respectively. Using the standard, large value of the quark condensate leads to:

$$a_0 = 0.20 \pm 0.01 m_\pi^{-1}$$

$$a_2 = -0.042 \pm 0.002 m_\pi^{-1}$$

Generalized ChPT allows a wider range of the quark condensate. Taking a much smaller value of the condensate, they get:

$$a_0 = 0.26 m_\pi^{-1} and a_2 = -0.022 m_\pi^{-1}$$

which results from a fit to the central value of the K_{e4} measurement of the isopsin 0 $\pi - \pi$ scattering length by Rosselet et al.

The $\pi - \pi$ scattering lengths are a fundamental measurement of the strong interaction and provide a sensitive test of the low energy structure of QCD.

The Nuclear $(\pi, 2\pi)$ reactions.

The experiment reported here is a continuation of a measurement by the CHAOS group of the reactions:

$$\begin{aligned}
\pi^+ + d &\rightarrow X\pi^+\pi^+ \text{ and } \pi^+ + d \rightarrow X\pi^+\pi^- \\
\pi^+ + {}^{12}C &\rightarrow X\pi^+\pi^+ \text{ and } \pi^+ + {}^{12}C \rightarrow X\pi^+\pi^- \\
\pi^+ + {}^{40}Ca &\rightarrow X\pi^+\pi^+ \text{ and } \pi^+ + {}^{40}Ca \rightarrow X\pi^+\pi^- \\
\pi^+ + Pb &\rightarrow X\pi^+\pi^+ \text{ and } \pi^+ + Pb \rightarrow X\pi^+\pi^-.
\end{aligned}$$

This experiment was motivated initially by work by Chanfrey, Aouissat, Schuck and Norenberg (Phys. Lett. B256) which predicted a substantial increase of the yield of $\pi^+\pi^-$ particles at low invariant mass. Their model was based on an medium-induced increase of the isospin 0 component of the $\pi - \pi$ interaction. However subsequent work by the group showed that including the constraints required by chiral symmetry substantially reduces the effect. In contrast the experimental results (as shown in figure 1) from CHAOS[2] do indeed show a substantial increase in the $\pi^+\pi^-$ yield at low invariant mass for the nuclear systems, while the result for deuterium strongly resembles that of the $\pi^- + p \rightarrow n\pi^+\pi^-$ which occurs on the proton.[3]

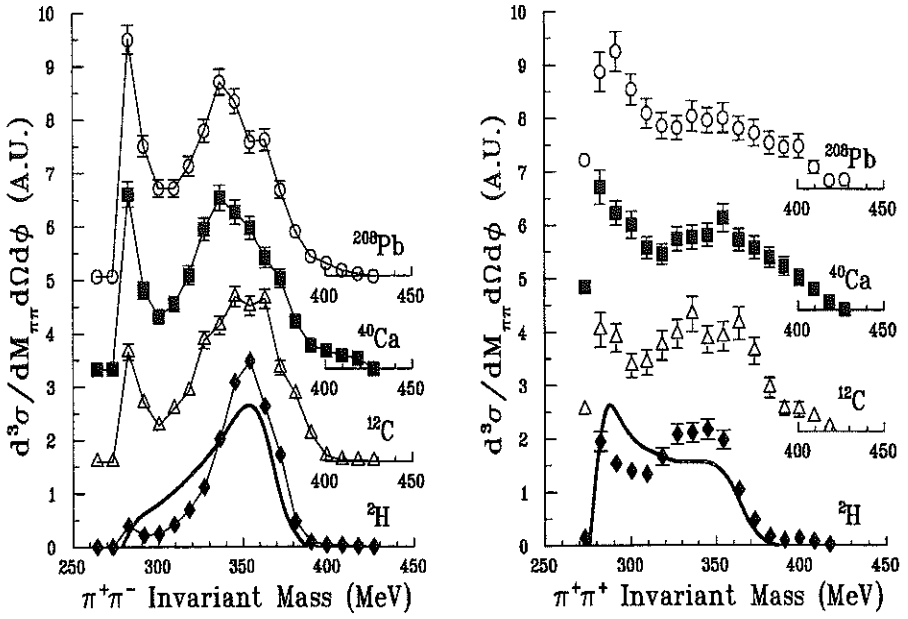

Figure. 1. The original Experiment at $T_\pi = 280$ MeV

It is worth noting here that the distributions shown above are the yields for the reaction within $\pm$ 7 degrees of the incident beam plane. ie. within the CHAOS acceptance. There is an order of magnitude enhancement for the $(\pi^+\pi^-)$ reaction on the heavier targets compared to deuterium, which looks quite like the reaction on Hydrogen. On the other hand the $(\pi^+\pi^+)$ shows nothing like the dramatic change in yield between deuterium and the other nuclei.

Recently Vicente-Vacas and Oset[4] have modelled $(\pi, 2\pi)$ reaction on nuclei. They include fermi-motion and re-scattering effects and find rather good agreement with the CHAOS $(\pi^+\pi^+)$ data but are not able to reproduce the $(\pi^+\pi^-)$ data without introducing an arbitrary and very large final-state interaction in the isospin 0 channel.

Perhaps the most exciting possibility is that the CHAOS data indicate the partial restoration of chiral symmetry within the nuclear medium. This possibility has been explored by Hatsuda, Kunihiro and Shimizu[5] who have investigated the how the isospin 0 $\pi - \pi$ interaction changes as a function of nuclear density in the presence of chiral restoration. They do indeed predict a substantial increase in the $\pi - \pi$ interaction very near threshold. This could manifest itself as a substantial final state interaction between the isospin 0 pions. However Hatsuda et al. have not made specific prediction for the nuclear $(\pi, 2\pi)$ reactions. If partial restoration of chiral symmetry is the explanation of the CHAOS data it would be only the second example of obvious QCD or quark effects observed in nuclear physics. This approach has also been explored within a many body framework by Aouissat et al.[6] who agree that this approach can lead to a substantial increase in low energy strength of the isopsin 0 $\pi - \pi$ interaction.

Experimental details.

In order to provide more experimental information to this very interesting possibility, the CHAOS group has repeated the experiment at a variety of incident pion energies. The idea is that if the increase in yield is due to a final state interaction, the effect should be present at all bombarding energies. On the other hand, if the effect were due to some new in-medium production mechanism, the effect may change as a function of energy. The this end we took data data for the ^{45}Sc$(\pi^+, \pi^-\pi^+)$X and ^{45}Sc$(\pi^+, \pi^+\pi^+)$X reaction incident pion kinetic energies of T_π = 240, 260, 280, 300 and 320 MeV. The experiment was performed on the M11 channel at the TRIUMF Laboratory in Vancouver, Canada and employed the CHAOS detector. The detector is described in detail in reference[7] and a schematic view of the inner regions is shown in figure 2.

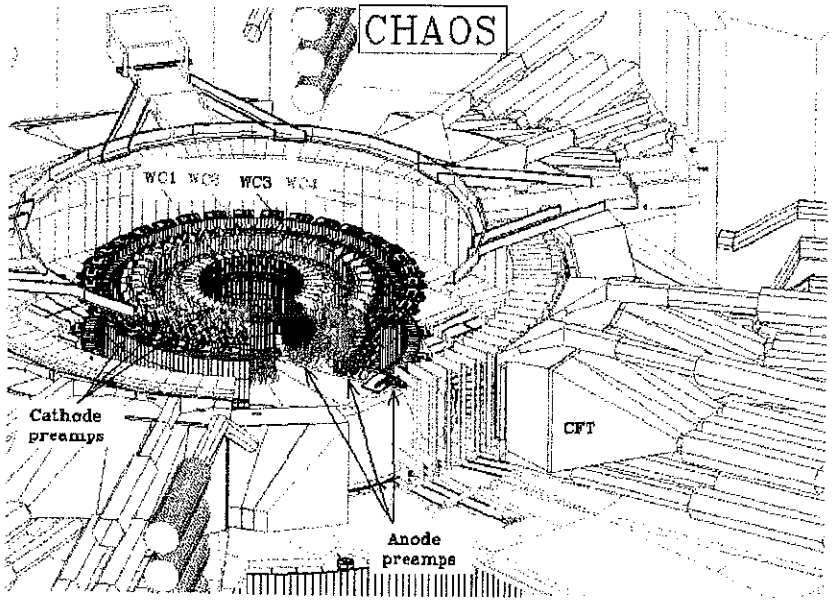

Figure. 2. A schematic view of the inner region of CHAOS showing chambers 1,2,3 and 4 as well as the CHAOS Fast Trigger blocks

Very briefly CHAOS is a magnetic planar detector with 360 degrees coverage in plane

and $\pm$ 7 degree of acceptance out of plane. There are consists of a set of 4 concentric wire chambers, (WC1, WC2, WC3 and WC4) followed by a ring of Scintillation counters and Pb-glass Cherenkov detectors, the CHAOS Fast Trigger blocks (CFT's). These surround a target region located in the center of the detector. The whole setup is placed between the poles of a circular dipole magnet of approximately 1 meter diameter. The incident pion beam is fired through the chambers and onto the target located in the center of the detector. Wire chambers 1 and 2 are very high rate proportional wire chambers. They can be run at rates in excess of 5 Mhz. Chamber 3 is a high magnetic field drift chamber. It must deadened in the region of the incident beam. Chamber is conventional vector drift chamber which must also be deadened in the beam region. The CHAOS detector employs a sophisticated multi-level trigger which enables substantial filtering of events.

The range of energies was limited on the lower side by the dramatic fall in cross section as the energy gets close to threshold and on the end by the maximum energy of pions available from the TRIUMF cyclotron.

The beam intensity varied from 5 Mhz at the lower energies to 0.2 Mhz at 320 MeV. We used a Scandium target since it was of intermediate mass and exists as a single isotope with no particular closed nuclear shells. The original experiment was performed on ^{12}C, ^{40}Ca and ^{208}Pb all of which are closed shell nuclei. While it seemed unlikely that effect was related to specific nuclear properties we deemed it worthwhile to test this possibility in the new experiment. In addition to the experiment on ^{45}Sc we also studied the $(\pi^+, \pi^+\pi^-)$ and $(\pi^+, \pi^+\pi^+)$ reactions on a deuterium by bombarding a CD_2 target at $T_\pi = 280$ MeV. These data provided a useful control on this experiment and were also used as test of the previous measurement.

The first level trigger for the reaction was to require 2 CFT blocks in coincidence ($\approx$3 KHz). The second level trigger uses just wire hits in WC1, WC2 and WC3. Require 2 good tracks, originating in the target, with the requirement $|P_1|^2 + |P_2|^2 \leq$ cutoff. This eliminates most of the quasi-free two-body reactions on the nuclei. This was accomplished with LeCroy Ecline electronics in typically 10 μsecs. After the 2nd level trigger, the data was recorded to tape at a rate of approximately 100 events per second

The off-line analysis performed a full reconstruction of the events using the full drift chamber information. We then cut on $|P_1| + |P_2|$ and cut on the vertex to require that the interaction point be inside target. Next we apply particle identification using the CFT scintillation counters and Cherenkov Detectors and identify $\pi^{45}Sc \rightarrow \pi\pi X$ reactions.

Results

We paid particular attention to e/π discrimination since gamma rays converting to e^+e^- pairs can fake $(\pi, 2\pi)$ reactions and would sit right at the threshold of the $\pi^+\pi^-$ invariant mass spectrum. We achieved 10^{-6} discrimination of e^+e^- faking $\pi^+\pi^-$ events at a cost of 50% Particle Identification efficiency. We expect less than 0.1 e^+e^- events in our $\pi^+\pi^-$ data sample. The preliminary results are presented as the ratio of $\frac{(\pi^+\pi^-)}{(\pi^+\pi^-)}$ corrected for the different CHAOS acceptance for $(\pi^+\pi^-)$ compared with $(\pi^+\pi^+)$

These results are shown in figure 3.

As can be seen the ratio of $\frac{(\pi^+\pi^-)}{(\pi^+\pi^-)}$ for ^{45}Sc is substantially different to that for the reactions on Hydrogen at all bombarding energies. This is manifest as a substantial increase at low $(\pi^+\pi^-)$ invariant mass for Scandium compared with Hydrogen. In addition our control reaction on CD_2 shows as very similar pattern to that for Hydrogen, although the extra phase space available to the reaction on deuterium limits the range with which the data can be compared.

Conclusions

- From the theoretical work so far, it appears that the ideas of Hatsuda et al. are the leading explanation of the existence of a substantial nuclear medium induced Final State Interaction for the $\pi - \pi$ interaction. If true this indicates a different QCD ground state in a nuclear medium than the vacuum and is a genuine QCD effect in nuclear physics.

- The original CHAOS data indicate the presence of a substantial change for the π^+A $\rightarrow \pi^+\pi^-$X reaction, especially at low $\pi - \pi$ invariant mass. This is not present in the $\pi^+\pi^-$ reaction and is consistent with the existence of a large final state $\pi - \pi$ interaction in the isospin 0 channel.

- The new CHAOS data confirm the previous result for ^{40}Ca at 280 MeV and show substantial differences to π^-p $\rightarrow \pi^+\pi^-$n at all energies.

- Our new data supports the possibility that there is a substantial final state interaction in the isospin 0 channel of the $\pi - \pi$ interaction. A very similar result for the $\pi^0\pi^0$ channel has been reported at this conference. There has been a recent experiment at Mainz to measure gamma induced 2 pion production on different nuclear targets. If the the effect observed in pion production reactions is a final state interaction it should also be apparent in the Mainz data. We eagerly await the results of the Mainz experiment.

REFERENCES

1. G. Chanfrey et al. Phys. Lett. **B256** (1991) 325
2. F. Bonutti et al., Phys. Rev. Lett. **77** (1996) 603
3. M. Kermani et al., Phys. Rev. **C58** (1998) 3419
4. M.J. Vicente Vacas and E. Oset, Phys. Rev. **C60** (1999) 064621
5. Hatsuda, Kunihiro and Shimizu Phys. Rev. Lett. **82** (1999) 2840
6. Z. Aouissat et al., Phys. Rev. **C61** (1999) 012202 (R)
7. G.R. Smith et al., Nucl Instr. and Meth. in Phys. Res. **A362** (1995) 541.

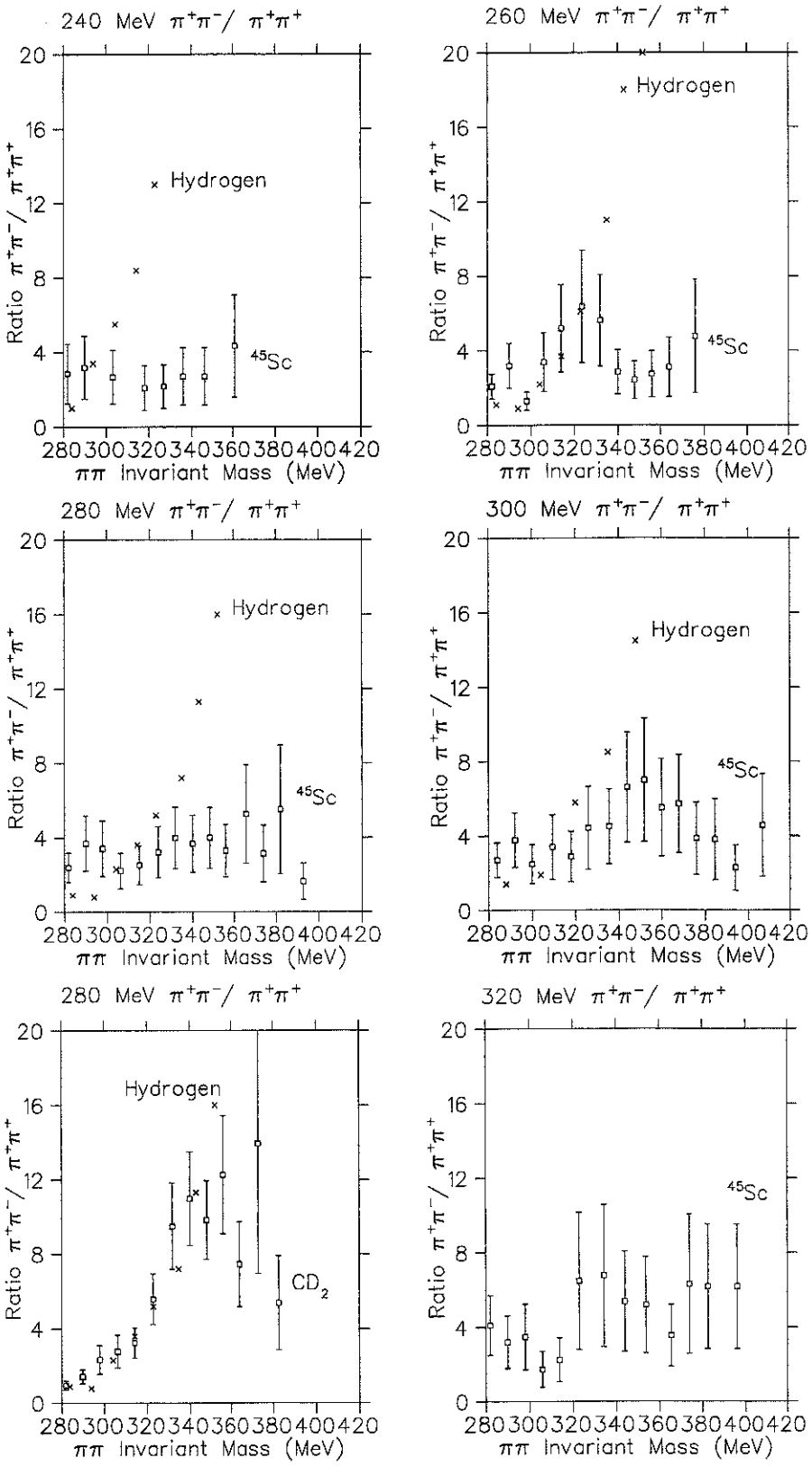

Figure. 3. Preliminary acceptance corrected ratios of $\frac{(\pi^+\pi^-)}{(\pi^+\pi^-)}$ at T_π = 240,260,280,300 and 320 MeV as well as for CD_2 at T_π = 280 MeV. In each figure the crosses represent the ratio of the reaction on Hydrogen and the squares are the results of the present measurement. In the case of 320 MeV, there was no previous Hydrogen data available.

Low-energy $\pi\pi$ scattering in QCD

J. Gasser*
Institut für Theoretische Physik, Universität Bern,
Sidlerstrasse 5, CH-3012 Bern, Schweiz
gasser@itp.unibe.ch

Abstract

This is a brief report on the evaluation of the $\pi\pi$ scattering amplitude in the framework of chiral perturbation theory.

INTRODUCTION

The interplay between theoretical and experimental aspects of elastic $\pi\pi$ scattering is illustrated in the figure. On the theoretical side, Weinberg's calculation[1] of the scattering amplitude at leading order in the low-energy expansion gives for the isospin zero S-wave scattering length the value $a_{l=0}^{I=0} = 0.16$ in units of the charged pion mass. This differs from the experimentally determined value[2] $a_0^0 = 0.26 \pm 0.05$ by two standard deviations. The one-loop calculation[3] enhances the leading order term to $a_0^0 = 0.20 \pm 0.01$ - the correction goes in the right direction, but the result is still on the low side as far as the present experimental value is concerned. To decide about agreement/disagreement between theory and experiment, one should i) evaluate the scattering lengths in the theoretical framework at order p^6, and ii) determine them more precisely experimentally. Let me first comment on the theoretical work.

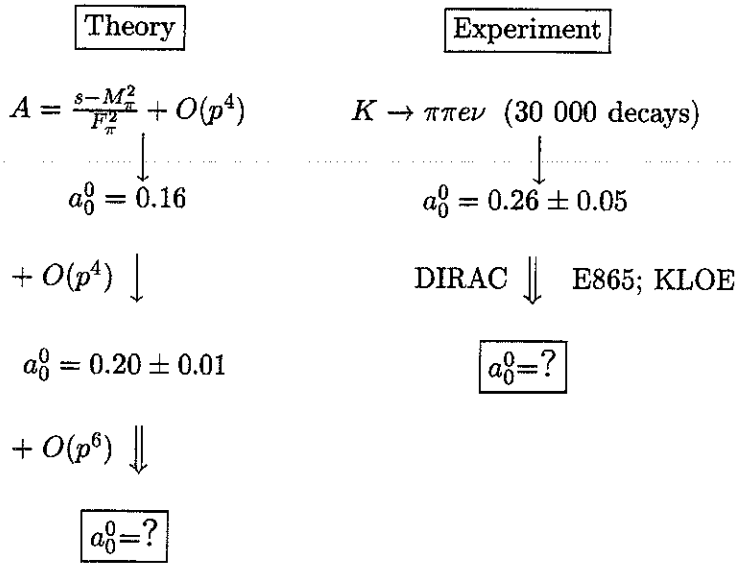

Figure 1. Progress in the determination of the elastic $\pi\pi$ scattering amplitude. References are provided in the text.

THEORETICAL ASPECTS

I consider QCD in the isospin symmetry limit $m_u = m_d \neq 0$. Elastic $\pi\pi$ scattering is then described by a single Lorentz invariant amplitude $A(s,t,u)$, that depends on the standard Mandelstam variables s,t,u. In chiral perturbation theory (ChPT)[4,5], the effective lagrangian that describes this process is given by a string of terms, $\mathcal{L}_{\rm eff} = \mathcal{L}_2 + \hbar\mathcal{L}_4 + \hbar^2\mathcal{L}_6 + \cdots$, where $\mathcal{L}_n$ contains m_1 derivatives of the pion fields and m_2 quark

*Work supported in part by the Swiss National Science Foundation, and by TMR, BBW–Contract No. 97.0131 and EC–Contract No. ERBFMRX–CT980169 (EURODAΦNE).

mass matrices, with $m_1 + 2m_2 = n$ (here, I consider the standard counting rules). The low-energy expansion corresponds to an expansion of the scattering amplitude in powers of $\hbar$,

$$A(s,t,u) = \left\{ \begin{array}{ccccccc} A_2 & + & A_4 & + & A_6 & + & O(p^8) \\ \uparrow & & \uparrow & & \uparrow & & \\ \text{tree} & & \text{1 loop} & & \text{2 loops} & & \end{array} \right. , \tag{1}$$

where A_n is of order p^n. The tree-level result[1] reads

$$A_2 = \frac{s - M_\pi^2}{F_\pi^2} , \tag{2}$$

and the one-loop expression A_4 may be found in[3]. The two-loop contribution A_6 was worked out in[6]. A dispersive evaluation of A_6 has been performed in Ref.[7] in the framework of generalized chiral perturbation theory, see below.

The amplitude $A_2 + A_4 + A_6$ contains several of the low-energy constants (LEC's) that occur in $\mathcal{L}_{\rm eff}$. In $\mathcal{L}_2$, there are two of them, the pion decay constant F in the chiral limit, and the parameter B, which are related to the condensate by $F^2 B = -\langle 0|\bar{u}u|0\rangle$. In the loop expansion, these two parameters can be expressed in terms of the physical pion decay constant $F_\pi \simeq 92.4$ MeV and of the pion mass, $M_\pi = 139.57$ MeV. The $\pi\pi$ scattering amplitude contains, in the two-loop approximation, in addition several LEC's occurring in $\mathcal{L}_4$ and in $\mathcal{L}_6$,

$$\left. \begin{array}{l} \mathcal{L}_2 : F_\pi, M_\pi \\ \mathcal{L}_4 : \bar{l}_1, \bar{l}_2, \bar{l}_3, \bar{l}_4 \\ \mathcal{L}_6 : \bar{r}_1, \ldots, \bar{r}_6 \end{array} \right\} \text{ occur in } \pi\pi \to \pi\pi \text{ (two-loop approximation).} \tag{3}$$

These LEC's are not determined by chiral symmetry - they are, however, in principle calculable in QCD[8].

Once the amplitude is available in algebraic form, it is a trivial matter to evaluate the threshold parameters. To quote an example, the isospin zero S-wave scattering length is of the form

$$a_0^0 = \frac{7M_\pi^2}{32\pi F_\pi^2} \left\{ 1 + c_4 x + c_6 x^2 + O(p^6) \right\} ; \, x = \frac{M_\pi^2}{16\pi^2 F_\pi^2} . \tag{4}$$

The coefficients c_4, c_6 contain the low-energy constants listed in (3). Similar formulae hold for all other threshold parameters - the explicit expressions for the scattering lengths and effective ranges of the S-and P-waves as well as for the D-wave scattering lengths at order p^6 may be found in[6]. It is clear that, before a numerical value for these parameters can be given, one needs an estimate of the low-energy constants. The calculation is under way - it is, however, quite involved: One has to solve numerically the Roy-equations[9] with input from the high-energy absorptive part. Second, one assumes that the couplings that describe the mass dependence of the amplitude may be estimated from resonance exchange. Requiring that the experimental amplitude agrees near threshold with the chiral representation allows one finally to pin down the remaining couplings, as well as the scattering lengths a_0^0 and a_0^2. The remaining threshold parameters may then be obtained from the Wanders sum rules[10]. The first part of the program is completed, and the report will appear soon[11]. The second part, that will allow us to predict the values of all threshold parameters, is under investigation[12]. I illustrate in the following section with a simple example how this program is achieved.

DETERMINATION OF THE LEC'S: A SIMPLE CASE

I consider a single partial wave $f(s)$ and ignore its left hand cut. Further, I assume that it has a chiral representation of the form

$$\mathrm{Re} f^\chi(s) = a^\chi + b^\chi s + \frac{s^2}{\pi} \int_{4M_\pi^2}^\infty \frac{dx}{x^2} \frac{\mathrm{Im} f^\chi(x)}{x - s} , \tag{5}$$

with

$$a^\chi = 1 + c\,,\; b^\chi = c\,, \tag{6}$$

where c is an unknown LEC.

In order to determine c, one may proceed as follows. First, I take it that the physical partial wave $f(s)$ satisfies a once subtracted dispersive representation of the form

$$\mathrm{Re}f(s) = a + \frac{s}{\pi}\int_{4M_\pi^2}^{\infty}\frac{dx}{x}\frac{\mathrm{Im}f(x)}{x-s}\,. \tag{7}$$

If we now assume that

- the absorptive part Imf is known from experiment,
- the chiral representation (5) agrees with the physical amplitude f in the low-energy region,

$$f^\chi = f \text{ at } |s| \leq 4M_\pi^2\;, \tag{8}$$

it follows that c can be evaluated from the sum rule

$$c = \frac{d\mathrm{Re}}{ds}|_{s=0} = \frac{1}{\pi}\int_{4M_\pi^2}^{\infty}\frac{dx}{x^2}\mathrm{Im}f(x)\,. \tag{9}$$

This is not yet the whole story - from the assumption that the chiral amplitude agrees with the physical one in the low-energy region, it also follows that

$$a = a^\chi = 1 + c\,. \tag{10}$$

Therefore, one is able in this case to evaluate the LEC c from the data, *and* to determine the subtraction constant a in the dispersive integral (7).

In the real world, the absorptive part Imf is not known in the whole experimental region. In particular, often low-energy data are sadly missing, and Im f is known only above a certain threshold energy s_0. Nevertheless, if one is able to extrapolate it down to threshold, the above reasoning shows that the low-energy constants a and c can again be determined. In fact, this is the situation encountered in elastic $\pi\pi$ scattering: The phase shifts are known above a certain energy, whereas they would be needed in the low-energy region as well in order to pin down the LEC's and the threshold parameters. The machinery that allows one to extrapolate the data down to threshold in a controlled fashion is provided by the Roy equations, as I will illustrate now.

Let us assume that the data are known above $s = s_0$. We split the dispersive integral (7) accordingly,

$$\begin{aligned}\mathrm{Re}f(s) &= a + \frac{s}{\pi}\int_{4M_\pi^2}^{s_0}\frac{dx}{x}\frac{\mathrm{Im}f(x)}{x-s} + \Psi(s)\;,\\ \Psi(s) &= \frac{s}{\pi}\int_{s_0}^{\infty}\frac{dx}{x}\frac{\mathrm{Im}f(x)}{x-s}\,.\end{aligned} \tag{11}$$

The quantity $\Psi(s)$ is known by assumption. I now further assume that s_0 is in the elastic region (this assumption is not crucial, the procedure can be carried through also in the general case), where one has

$$f = \frac{1}{\sigma}e^{i\delta}\sin\delta\,;\;\; \sigma = \sqrt{1-4M_\pi^2/s}\,. \tag{12}$$

This relation expresses the amplitude f through a single real function δ. Eq. (11) amounts to the singular integral equation

$$\frac{1}{2\sigma}\sin 2\delta(s) = a + \Psi(s) + \frac{s}{\pi}\int_{4M_\pi^2}^{s_0}\frac{dx}{x}\frac{\sin^2\delta(x)}{(x-s)\sigma(x)} \tag{13}$$

for the unknown phase shift δ, to be solved for a given input (a, Ψ) in the low-energy region $s \leq s_0$. This is a simple example of Roy's integral equation, first set up in the coupled channel case for $\pi\pi$ scattering nearly thirty years ago by Roy[9]. The integral equation (13) has been studied recently in great detail in Ref.[13], and I refer the reader to this reference for earlier literature, and for questions concerning uniqueness of the solution. Here I simply note that the solution is unique for the case where the phase shift $\delta(s_0)$ is smaller than $\pi/2$. The subtraction constant a can then be obtained in an iterative manner: First, one solves the Roy equation with input (a, Ψ), with a arbitrary,

$$(a, \Psi) \to \delta \to \mathrm{Im} f \to c \to a^\chi \,. \tag{14}$$

In the second step, one inserts in the input the subtraction constant so obtained, $(a, \Psi) \to (a^\chi, \Psi)$, until the procedure has converged.

This is exactly the method mentioned in the previous section for the case of $\pi\pi$ scattering. The complication that arises there is the fact that one has to consider a coupled system of Roy equations for the $I = 0, 2$ S-waves and for the P-wave[11].

THRESHOLD PARAMETERS FROM EXPERIMENTAL DATA

On the *experimental* side, several attempts are under way to improve our knowledge of the threshold parameters. The most promising ones among them are i) semileptonic K_{l4} decays with improved statistics, E865[14] and KLOE[16], and ii) the measurement of the pionium lifetime - DIRAC[17] - that will allow one to directly determine the combination $|a_0^0 - a_0^2|$ of S-wave scattering lengths. It was one of the aims of the recent workshops in Dubna[18] and Bern[15] to discuss the precise relation between the lifetime of the pionium atom and the $\pi\pi$ scattering lengths - I refer the interested reader to the numerous contributions to these workshops for details. Let me only note that recently, using the effective lagrangian framework proposed by Caswell and Lepage some time ago[19], the width of pionium in its ground state has been determined[20] at leading and next-to-leading order in isospin breaking, and to all orders in the chiral expansion. This result will allow one to evaluate the combination $|a_0^0 - a_0^2|$ with high precision, provided that DIRAC determines the lifetime at the 10% level, as is foreseen[17].

WHY DO WE WISH TO KNOW THE SCATTERING LENGTHS?

Why are we interested in a precise value of the scattering length a_0^0? First, it is one of the few occasions that a quantity in QCD can be predicted rather precisely - which is, of course, by itself worth checking. Second, as has been pointed out in[21], this prediction assumes that the condensate has the standard size in the chiral limit - in particular, it is assumed to be non vanishing. For this reason, the authors of Ref.[21] have reversed the argument and have set up a framework where the condensate is allowed to be small or even vanishing in the chiral limit - the so called generalized chiral perturbation theory. [There is no sign for a small condensate in present lattice calculations[22]. Further interesting investigations of the small condensate scenario have been performed in Refs.[23,24].] Whereas the S-wave scattering lengths cannot be predicted in that framework, one may relate their size to the value of the condensate[21,25,29]. Hence, measuring a_0^0, a_0^2 or a combination thereof may allow one to determine the nature of chiral symmetry breaking by experiment.

Acknowledgments

I wish to thank the organizers for the informative Conference, and for the enjoyable time we have spent in Zuoz.

REFERENCES

1. S. Weinberg, *Phys. Rev. Lett.* **17** (1966) 616.
2. L. Rosselet et al., *Phys. Rev.* **D15** (1977) 574.
3. J. Gasser and H. Leutwyler, *Phys. Lett.* **125B** (1983) 325.
4. S. Weinberg, *Physica* **96A** (1979) 327.

5. J. Gasser and H. Leutwyler, *Ann. Phys. (N.Y.)* **158** (1984) 142; *Nucl. Phys.* **B250** (1985) 465.
6. J. Bijnens et al., *Phys. Lett.* **B374** (1996) 210; *Nucl. Phys.* **B508** (1997) 263; ibid. **B517** (1998) 639 (E).
7. M. Knecht, B. Moussallam, J. Stern, and N.H. Fuchs, *Nucl. Phys.* **B457** (1995) 513; ibid. **B471** (1996) 445.
8. S. Myint and C. Rebbi, *Nucl. Phys.* **B421** (1994) 241; A.R. Levi, V. Lubicz, and C. Rebbi, *Phys. Rev.* **D56** (1997) 1101; *Nucl. Phys. Proc. Suppl.* **53** (1997) 275.
9. S.M. Roy, *Phys. Lett.* **36B** (1971) 353; *Helv. Phys. Acta* **63** (1990) 627.
10. G. Wanders, *Helv. Phys. Acta* **39** (1966) 228.
11. B. Ananthanarayan, G. Colangelo, J. Gasser, and H. Leutwyler, work in progress.
12. G. Colangelo, J. Gasser, and H. Leutwyler, work in progress.
13. J. Gasser and G. Wanders, *Eur. Phys. J.* **C10** (1999) 159.
14. S. Pislak, in[15] p.25; J. Lowe, *Experimental results on semileptonic K decays and form factors*, talk given at the workshop *Physics and Detectors for DAΦNE*, Nov. 16-19, 1999, to appear in the proceedings.
15. J. Gasser, A. Rusetsky, and J. Schacher, Miniproceedings of the Workshop *HadAtom99*, held at the University of Bern, Oct. 14-15, 1999, hep-ph/9911339.
16. P. de Simone, in[15] p.24.
17. B. Adeva et al., Proposal to the SPSLC: *Lifetime measurement of $\pi^+\pi^-$ atoms to test low-energy QCD predictions*, CERN/SPSLC/P 284, December 15, 1994; B. Adeva, *The DIRAC experiment at CERN*, talk given at the workshop *Physics and Detectors for DAΦNE*, Nov. 16-19, 1999, to appear in the proceedings; J. Schacher, in[15] p.6;
18. Proceedings of the International Workshop *Hadronic Atoms and Positronium in the Standard Model*, Dubna, May 26-31, 1998, (M.A. Ivanov et al., eds., Joint Institute for Nuclear Research, Dubna 1998), ISBN 5-85165-514-3.
19. W.E. Caswell and G.P. Lepage, *Phys. Lett.* **167B** (1986) 437.
20. A. Gall, J. Gasser, V.E. Lyubovitskij, and A. Rusetsky, *Phys. Lett.* **B 462** (1999) 335; J. Gasser, V.E. Lyubovitskij, and A. Rusetsky, preprint hep-ph/9910438. See also V.E. Lyubovitskij and A.G. Rusetsky, *Phys. Lett.* **B389** (1996) 181 ; V.E. Lyubovitskij, E.Z. Lipartia, and A.G. Rusetsky, *JETP Lett.* **66** (1997) 743; H. Jallouli and H. Sazdjian, *Phys. Rev.* **D58** (1998) 014011; M.A. Ivanov, V.E. Lyubovitskij, E.Z. Lipartia, and A.G. Rusetsky, *Phys. Rev.* **D58** (1998) 094024; P. Labelle and K. Buckley, preprint hep-ph/9804201; X. Kong and F. Ravndal, preprint hep-ph/9805357, *Phys. Rev.* **D59** (1999) 014031, and preprint hep-ph/9905539; B. R. Holstein, *Phys. Rev.* **D 60** (1999) 114030; D. Eiras and J. Soto, preprint hep-ph/9905543. The earlier literature on the subject may be traced from these references.
21. N.H. Fuchs, H. Sazdjian, and J. Stern, *Phys. Lett.* **B269** (1991) 183; J. Stern, H. Sazdjian, and N.H. Fuchs, *Phys. Rev.* **D47** (1993) 3814; M. Knecht and J. Stern, in Ref.[27] p.169, and references cited therein; J. Stern, in Ref.[28] p.26, and preprint hep-ph/9712438.
22. G. Ecker, *Chiral symmetry*, Proc. of 37. Internationale Universitätswochen für Kern- und Teilchenphysik, Schladming, Feb. 1998, L. Mathelitsch and W. Plessas (eds.), Lecture Notes in Physics, Vol. 521, Springer (Heidelberg, 1999), and hep-ph/9805500; L. Giusti, F. Rapuano, M. Talevi, and A. Vladikas, *Nucl. Phys.* **B538** (1999) 249; V. Gimenez, L. Giusti, F. Rapuano, M. Talevi, and A. Vladikas, *Nucl. Phys. Proc. Suppl.* **73** (1999) 210.
23. M. Knecht and E. de Rafael, *Phys. Lett.* **B424** (1998) 335.
24. I. I. Kogan, A. Kovner, and M. A. Shifman, *Phys. Rev.* **D59** (1999) 016001.
25. M. Knecht, B. Moussallam, J. Stern, and N. Fuchs, *Nucl. Phys.* **B457** (1995) 513; ibid. **B471** (1996) 445.
26. J. Bijnens and Ulf-G. Meißner, Proceedings of the workshop *Chiral Effective Theories* held at the Physikzentrum Bad Honnef, Germany, November 30 to December 4, 1998, hep-ph/9901381.
27. L. Maiani, G. Pancheri, and N. Paver (eds.), *The Second DAΦNE Physics Handbook* (INFN, Frascati, 1995).
28. A.M. Bernstein, D. Drechsel, and T. Walcher (eds.), *Chiral Dynamics: Theory and Experiment*, Proceedings of the Workshop in Mainz, Germany, September 1-5, 1997 (Lecture Notes in Physics, Vol. 513, Springer, Berlin, Heidelberg, 1998).
29. L. Girlanda, in[15] p.28.

Meson Production Experiments with Electromagnetic Beams using CLAS

S.A. Dytman
Department of Physics and Astronomy, University of Pittsburgh, Pittsburgh, PA 15260

Abstract

The CEBAF Large Acceptance Spectrometer (CLAS) started taking production data in February, 1998. It is capable of taking data for many reactions simultaneously with moderate resolution. Spectrometer properties and running conditions are presented. Data has been taken for a variety of conditions with polarized and unpolarized beam and target. Preliminary results of the initial experiments are shown and discussed.

INTRODUCTION

The CEBAF Large Acceptance Spectrometer (CLAS) is presently taking data at a very large rate with essentially all of the initial complement of detectors functioning at design specifications. A primary CLAS goal of interest to this conference is the study of N^* resonances for masses less than about 2.5 GeV. Since these states couple with various strengths to a large number of open inelastic channels, a multi-faceted detector is required. By covering about 80% of 4π solid angle for single particles, many reactions can be studied simultaneously. The measured reactions have common systematic errors, correcting a significant problem in previous N^* analyses. Presently accepted N^* properties are determined almost solely from experiments using pion beams. Thus, the new experiments will be sensitive to N^* states that couple weakly to πN. A more complete description of the apparatus can be found in the published talk of Bernhard Mecking[1]. Another review of CLAS was given by Volker Burkert[2].

The physics of N^*s with CLAS is the study of nonstrange and strange baryons, i.e. N^*, Δ, Λ, and Σ baryons. The first identification of Ξ baryons in CLAS photoproduction events has recently been reported. These states decay to πN, ηN, $\pi\pi N$, ωN, $K\Lambda$, $K\Sigma$, and many other final states. Targets of liquid hydrogen, deuterium, ammonia (NH_3), ^{3}He, ^{4}He, carbon and iron have been run with real and virtual photons using 1.5-5.5 GeV electron beams. By running at a luminosity of $10^{34} cm^{-2} s^{-1}$, data on a large variety of reactions are being accumulated at an instantaneous event rate of about 2.5 kHz. After the first year of data taking, we have approximately equaled the number of events taken before CLAS for reactions accessible with traditional small solid angle spectrometers and greatly exceeded it for more complicated reactions.

PDG lists about 40 N^* states with a variety of quantum numbers and varying degrees of certainty. Presently, a good qualitative understanding of *many* properties of these states using various versions of the Constituent Quark Model (CQM) exists. However, this has not yet been linked to QCD in any formal way and presently does not account for the meson cloud. Although full QCD calculations on the lattice are believed to include all effects correctly, efforts to date have been limited to the quenched (no $g \rightarrow q\bar{q}$) approximation. Recent improvements in numerical techniques and in computing power have been very impressive and significant results are expected.

Limitations in previous data are very clear when extracting resonance properties. The main problem is to turn the experimental observables first into partial wave amplitudes (which carry the strength for each reaction in a particular value of angular momentum and parity), then into the resonant part of the amplitude. Resonances are then found as poles or Breit-Wigner masses and widths. The latter step has more model dependence; a review of that situation can be found in[3]. The new experiments hope to provide significant new information on two general fronts- the spectra of states and their photocoupling amplitudes for $\gamma N \rightarrow N^*$ as a function of Q^2. A significant prediction of the CQM is that many N^* states are yet to be found, the so-called "missing states". For example, the CQM predicts 22 nonstrange L=2 excitations, but only about 10-12 have been identified. There is an additional possibility that hybrid baryons will have a sufficiently different electromagnetic response that they will stand out from the normal baryons. The incident photon causes

a transition from the nucleon ground state (proton and neutron) to the various excited states. The dominant excitation mechanism is often through the s channel (see Fig. 1).

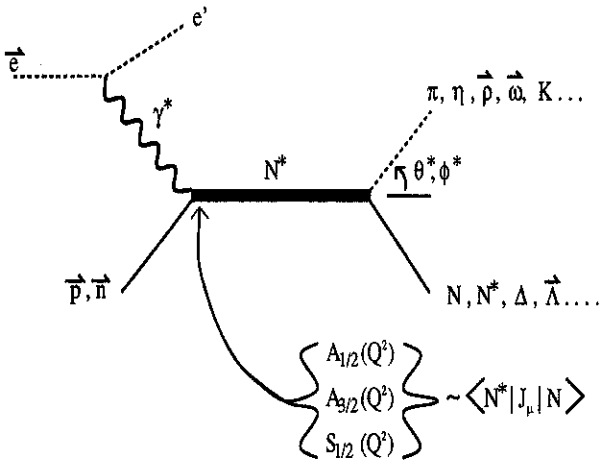

Fig. 1. Excitation of a resonance via s channel. Empirical studies show this to be the dominant reaction mechanism for many final states, but u and t channel processes must be included for a fully correct model. Each event must be kinematically complete. The typical CLAS electroproduction experiment bins events in Q^2 and W (virtual photon mass and invariant mass of the intermediate state) and θ^* and ϕ^* (the decay angles of the meson in the rest frame of the intermediate state.)

The transition strength for $\gamma N \rightarrow N^*$ can be determined in various helicity states using a phenomenological analysis. Since these strengths are defined as matrix elements of the electromagnetic current acting between the N and the N^*, these results can be directly compared with any calculation of the relevant wave functions. Examples from a host of important issues include trying to measure and explain the small size of the quadrupole excitation of the Δ ($P_{33}(1232)$), i.e. the E2/M1 problem, and trying to measure and explain the properties of the Roper ($P_{11}(1440)$) resonance. A large body of data for the delta already exists; nevertheless, CLAS will still greatly add to the electroproduction database. For the Roper, the existing data is of poor quality and a significant improvement is possible in almost all reactions. Interpretation of the existing data has been interesting because the CQM has trouble fitting the mass and the photocoupling is poorly measured. In addition, models suggesting interpretations as a hybrid baryon or a meson-nucleon state rather than a predominantly three quark state have been offered.

Some of the particles in Fig. 1 are displayed as vectors. Polarized beams at Jefferson lab are very common now and there is a polarized target for protons and deuterons (ammonia). A coherent Bremsstrahlung photon beam is being installed and is expected to be tested next year followed by experiments emphasizing vector meson production. With the full coverage of the meson strong decay angles (e.g. $\phi \rightarrow K^+K^-$) and the hyperon weak decay ($\Lambda \rightarrow p\pi^0$), some polarization information about the final state can be determined. Runs with polarized and unpolarized beams and targets have been taken. The events with unpolarized beam and target are the most fully analyzed and only that data will be presented here.

CLAS PROPERTIES

CLAS was built by an international collaboration of physicists from about 30 universities and national labs working with Jefferson lab personnel. Experiments are run by the CLAS collaboration. CLAS has 6 almost identical sectors, each covering about 54° in ϕ. In Fig. 2, we show an event with 2 tracks in opposite sectors. The event has been classified as $ep \rightarrow e'p\eta$ with the final state proton in the upper sector and the electron in the lower sector. The detectors are labelled.

The detectors are conventional in design, but large on a nuclear physics scale. There are a total of 35,148 drift cells that are used to track charged particles through the toroidal field. The drift chambers are divided into 34 layers of hexagonal cells. Although the resolution of each cell is about 200 μm, overall system resolution is presently about a factor of 2 larger. Time of flight resolution for the charged particles detected in the scintillators is about 140 ps for electrons. The electromagnetic calorimeter has energy resolution for photons and electrons of $\sigma_E/E \approx 0.1/\sqrt{E}$. The Cerenkov detector is run in threshold mode, so it will fire only on electrons up to pion momentum of 2.8 GeV/c. Empirical studies

have shown the Cerenkov to have efficiency larger than 99.5% in the area more than 10 cm from the edges.

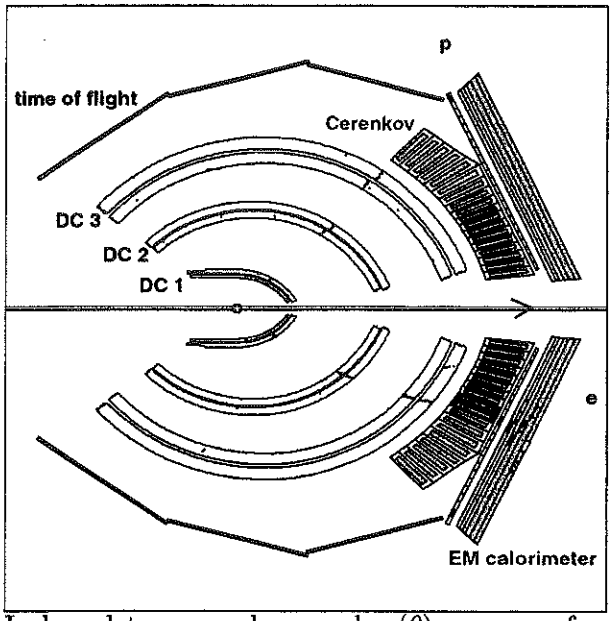

Fig. 2. Single event display of an eta electroproduction event. Various detector systems are labelled. The arcs show locations of the 3 regions of drift chambers; the dots represent drift cells where particles have deposited energy. The electron bends in the magnetic field toward the beam line, has large energy deposition in the calorimeter, and fires a Cerenkov counter. The other track is a proton. Particle identification of charged hadrons is done via time of flight to the scintillators that cover the full CLAS solid angle.

In broad terms, polar angular (θ) coverage for charged hadrons is about 8-140° with moderate resolution. For electrons and photons, the range is about 20-47° due to the sizes of the Cerenkov detector and the electromagnetic calorimeter; in 2 sectors, shower counter coverage is extended to 75°. The momentum resolution is presently about 0.2% in the forward direction and increases to about 2-3% for larger θ. Presently achievable resolution is about a factor of 2 worse than design values. Each event can have charged particle tracks or neutral particles in any sector. Events with 4 charged particles have been completely reconstructed (see Table 2). Electroproduction cross sections must be binned in Q^2, W, θ^*, and ϕ^*; with the full running time allocated, this will provide an average of a few hundred events in each of about a few hundred thousand bins for the reactions with the largest cross sections. Photoproduction reactions have Q^2=0, no phi dependence, and in general better statistics in each bin.

Technical papers covering all CLAS detectors are submitted and some are published[4].

CLAS RUNNING EXPERIENCE

With CLAS, many experiments take data simultaneously. Thus, the normal nuclear physics delineation of experiments by final states is not useful. We label experiments by initial state and a wide range of final states are measured in one detector configuration. For example, the e1 run group covers all experiments with an electron beam and an unpolarized proton or neutron target. That was the first run group to take beam and most of the results shown here are from that run. The beam can be photons or electrons, polarized or unpolarized; the target can be polarized or not. To date, most runs used a liquid hydrogen target- 5 cm long for e1 and 20 cm long for g1 (unpolarized photon beam with an unpolarized hydrogen target). Table 1 lists the run groups which have taken data as of August, 1999. In each case, the trigger particle is listed in bold face. For the electron running, the trigger particle is the electron. For photon beam experiments, a charged particle in coincidence with a tagger signal triggers each event. The loose trigger is a key part of fully utilizing large acceptance. Recent run cycles have produced a few billion events each.

FIRST LOOK AT RESULTS

At this stage of analysis, a few reactions are well understood and reasonably close to publication. However, there are no final results of cross sections presently available. A sampling of distributions will be shown here.

Table 1. Summary of the first 1.5 years of CLAS data-taking. Each run group takes data for many reactions. Polarized beam has become common at the lab. An arrow over a particle shows that it was significantly polarized.

	run group	reaction, trigger particle in bold
Feb-Mar, 98	e1	$ep \to \mathbf{e}'X$
May-June, 98	g1	$\gamma p \to \mathbf{c}X$ (c=charged hadron)
June, 98	g6	$\gamma p \to \mathbf{cc}X$
July, 98	g1	$\vec{\gamma} p \to \mathbf{c}X$
Aug-Dec, 98	eg1	$\vec{e}\vec{p} \to \mathbf{e}'X$
Jan-Apr, 99	e1	$\vec{e}p \to \mathbf{e}'X$
Apr-May, 99	e2	$\vec{e}A \to \mathbf{e}'X$ (A= ^{3,4}He,^{12}C,Fe)
July, 99	g6	$\gamma p \to \mathbf{cc}X, \phi \to f_0\gamma$
Aug, 99	g2	$\gamma d \to \mathbf{c}X$

The acceptance of CLAS is shown in Fig. 3 through the distribution of π^+ seen in a small fraction of the first e1 run. Traditional spectrometers detect particles over a few degrees in θ and ϕ. Here, acceptance falls off at small values of θ due to support structures close to the beam line. The 6 bands of missing events are due to the gaps between sectors filled by the magnet coils and detector supports. These fixed gaps are the major elements in the acceptance calculation. The detailed form of the acceptance depends on the value and sign of the magnetic field. These events were taken with 2.4 GeV beam, normal field (electrons bending toward the beam line), and field value of 60% of full strength (2250 A).

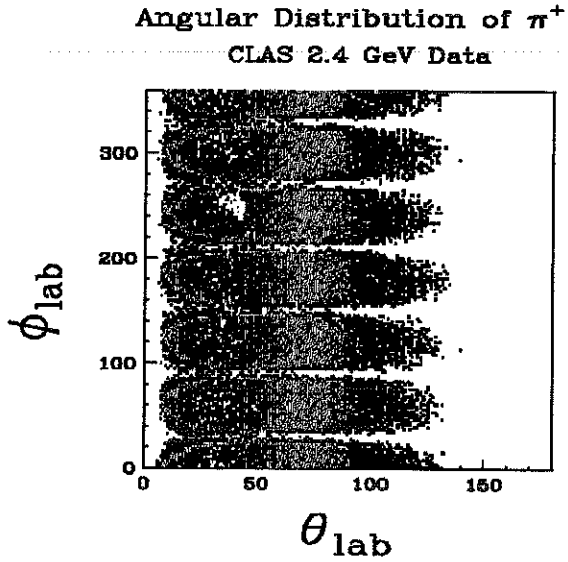

Fig. 3. Preliminary analysis of the distribution of π^+ in the lab from part of the first e1 run.

Fig. 4 provides a broad, preliminary look at the physics to be measured with CLAS. We show W distributions for 4 GeV beam energy and proton target. Final states were identified through missing mass techniques. The Q^2 of these events ranges between 1 and 3 $(\mathrm{GeV/c})^2$. Even though no corrections have been applied and only a simple background subtraction was used, the distributions are quite similar to the final cross sections. The well-known 3 resonance regions are seen, peaked at $W \sim 1.2$, 1.5, and 1.75 GeV. However, the peaks are in different places and have different strengths in the various reactions because each broad peak is a sum of contributions from a few underlying states. The reactions in the upper figures show strength in a variety of resonances; a detailed partial wave analysis will be required to get strengths individual states . Both η and ω distributions have a peak near

Table 2. Reactions identified in CLAS data as of October, 1999. The number of particles detected is also given. Elastic scattering and $\pi^+\pi^-$ production events have been very valuable for calibration and efficiency measurements because they are overdetermined.

$ep \to ep$	1,2		
$ep \to e'p\pi^0$	2	$\gamma p \to p\pi^0$	1
$ep \to e'n\pi^+$	2	$\gamma p \to n\pi^+$	1
$ep \to e'p\eta$	2	$\gamma p \to p\eta$	1
$ep \to e'\Lambda K^+$	2	$\gamma p \to \Lambda K^+$	1
$ep \to e'\Sigma K^+$	2	$\gamma p \to \Sigma K^+$	1
$ep \to e'p\omega$	3	$\gamma p \to p\omega$	2
$ep \to e'p\phi$	3	$\gamma p \to p\phi$	2
$ep \to e'p\pi^+\pi^-$	3,4	$\gamma p \to p\pi^+\pi^-$	2,3
		$\gamma p \to K^+K^+\Xi^-$	2
$ep \to e'p\eta'$	4	$\gamma p \to p\eta'$	3
$ep \to e'p\eta\pi^+\pi^-$	4	$\gamma p \to p\eta\pi^+\pi^-$	2
$ep \to e'\Lambda(1520)K^+$	3	$\gamma p \to \Lambda(1520)K^+$	2
$ep \to e'\Lambda^0K^+\pi^-$	3	$\gamma p \to \Lambda^0K^+\pi^-$	2
$ep \to e'\Lambda^0K^{*0}$	3	$\gamma p \to \Lambda^0K^{*0}$	2

threshold. For η electroproduction, the peak is known to be largely due to excitation of a single resonance, the $S_{11}(1535)$. These events have a largely isotropic angular distribution. Since this is the first data for ω electroproduction that wasn't dominated by diffractive processes, the peak is new. It is probably due to newly discovered coupling of known or new resonances to ωN since the angular distributions have no hint of forward angle peaking close to threshold.

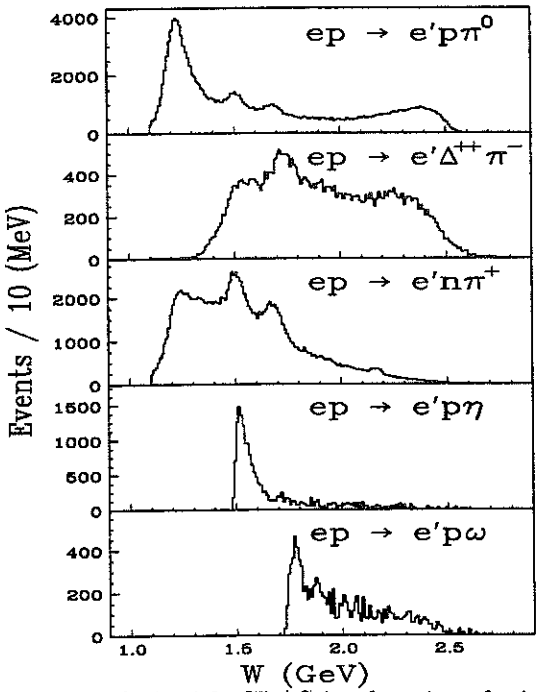

Fig. 4. Preliminary analysis of W distribution for various final states from part of the first e1 run. Although no acceptance correction is applied, the acceptance in this variable is fairly flat. Sideband subtraction in the missing mass spectrum of a neutral particle is sometimes used to isolate final states.

Table 2 lists the reactions that have been identified with CLAS in the g1 and e1 data sets.

Acceptance calculations are in progress and largely understood. The primary contributor to acceptance is the geometric holes shown in Fig. 3. These effects and detector

inefficiencies are accounted for in angular distributions defined in Fig. 1 (θ^* and ϕ^*) by Monte Carlo simulations. Another important effect in experiments with an electron beam is the radiative corrections. An example of preliminary CLAS results, one of the ϕ^* distributions for the $ep \rightarrow e'p\eta$ experiment, is shown in Fig. 5. Previous experiments had very limited ϕ^* coverage; still, the angular distributions at $W \sim 1.5$ GeV over a large range in Q^2 were predominantly isotropic. (This means the interference response functions, R_{LT} and R_{TT} are small, but very poorly measured in previous experiments.) Thus, isotropic results within the $\sim \pm$ 10% errors of previous experiments can be expected. The raw eta yields (data points in the left figure) are decidedly nonisotropic, but the acceptance correction matches its shape to give a cross section that is isotropic. The total correction factor is given as a line in the left plot. The radiative correction is about 15% independent of angle. For these points, the acceptance is about 35-40%; the dips come from situations when either the scattered electron or the proton tend to be in the phi gaps. A quantity proportional to the cross section $d\sigma/d\Omega_{\eta^*}$ is shown in the right plot.

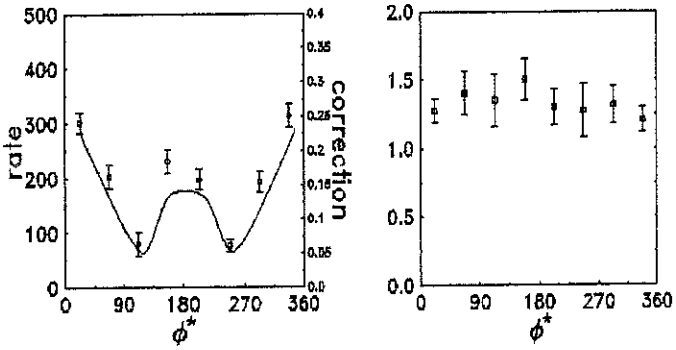

Fig. 5. ϕ^* dependence for eta yield and correction factor (left) and preliminary cross section (right) for $ep \rightarrow e'p\eta$ at Q^2= 0.75 (GeV/c)^2, W= 1.53 GeV, cos(θ^*)= -0.6. Errors shown reflect statistical errors in the data and in the Monte Carlo acceptance calculation. Systematic errors for these points are presently estimated as less than 10%.

SUMMARY

CLAS is now a working device. In standard running mode, data is taken at an instantaneous event rate of 2.5 kHz or about 0.5 Terabyte/day. It presently takes data for 10 months each year. The collaboration has taken data with a variety of targets and with both photon and electron beams. A few run groups have recently accumulated a few billion events each in runs of about 2 months.

At present, a significant number of reactions have been measured with statistical precision equal to or better than previous data. Some reactions are being explored for the first time. Others are being explored in kinematic regions not previously explored. Systematic errors are presently under study.

Use of polarization has become common. At the end of 1998, 2 months were devoted to runs with polarized hydrogen target and polarized electron beam. Those experiments are important for isolating specific spin parity intermediate states and for measuring an important contribution to the GDH Sum Rule at $Q^2 > 0$. A diamond crystal and goniometer are being installed for production of a transverse linearly polarized photon beam in 2000.

ACKNOWLEDGEMENTS

The author is a member of the CLAS collaboration. All results shown have been taken and approved by the collaboration. Special thanks for production of the figures used in this paper go to Stepan Stepanyan, Kui Young Kim, and Richard Thompson.

REFERENCES

1. B.A. Mecking, "First Results from the CEBAF CLAS Spectrometer", in *BARYONS '98, Proceedings of the 8th International Conference on the Structure of Baryons* (World Scientific, Singapore, 1999) pp. 37-48.
2. V. Burkert, to be published in Proceedings of PANIC99.
3. T.P. Vrana, S.A. Dytman, and T.-S. H. Lee,"Baryon Resonance Extraction from πN Data using a Unitary Multichannel Model", accepted for publication, Phys. Repts.
4. J. O'Brien, et al., Nucl. Inst. Meth. **421** 23 (1999), E. Smith, et al., Nucl. Inst. Meth. **432** 265 (1999), M.D. Mestayer, et al., accepted for publication in Nucl. Inst. Meth.

EFFECTIVE FIELD THEORY FOR THE TWO–NUCLEON SYSTEM

Ulf-G. Meißner
FZ Jülich, IKP (Th), D-52425 Jülich, Germany

Abstract

I discuss the dynamics of the two–nucleon system as obtained from a chiral nucleon–nucleon potential. This potential is based on a modified Weinberg power counting and contains chiral one– and two–pion exchange as well as four–nucleon contact interactions. The description of the S–waves is very precise. Higher partial waves are also well reproduced. We also find a good description of most of the deuteron properties.

INTRODUCTION

One of the most important and most intensively studied problems of nuclear physics is deriving the forces between nucleons. While there have been many successful and very precise models (of more or less phenomenological type), only in the last decade the powerful methods of effective field theory (EFT) have been used to study this question. In particular, Weinberg[1] employed power–counting to the irreducible n–nucleon interaction and obtained leading order results by iterating such type of potential in a Lippmann–Schwinger equation. This type of resummation is necessary to deal with the shallow bound states (or large S–wave scattering lengths) present in the two–nucleon system. This is in contrast to conventional chiral perturbation theory in the meson and meson–nucleon sectors, where all interactions can be treated perturbatively. A full numerical study based on Weinberg's approach at next-to-next-to-leading (NNLO) order was performed in ref.[2]. It was concluded that the approach could give qualitative insight but was not precise enough to compete with the accurate modern potentials or even phase shift analysis. In addition, a novel power counting scheme was proposed by Kaplan, Savage and Wise (KSW)[3]. In that approach, only the leading order momentum–independent four–nucleon interaction is iterated and all other effects, in particular the coupling of pions, are treated perturbatively. This is in stark contrast to Weinberg's scheme, were one–pion exchange (OPE) is present already at leading order and is iterated (among other interactions). What I will show in the following is that a suitably modified Weinberg scheme can be turned into a precision tool, which allows to study systematically the interactions between few nucleons. This lends credit to Weinberg's ideas spelled out almost 10 years ago.

CHIRAL EXPANSION OF THE NN POTENTIAL

EFT is, by construction, only useful in a space of momenta below a certain scale. The latter depends on the system one is investigating. In what follows, I will be concerned with the effective potential between nucleons as defined (and somewhat modified) in ref.[1]. In the EFT approach suggested by Weinberg, one has to deal with two different types of interactions. First, there is OPE, two–pion exchange and so on, to describe the long and medium range physics. Second, there are four–nucleon contact interactions to describe the short (and to some extent the medium) range physics. So we have a scale separation, the dividing line being somewhere above twice the pion mass and below the typical scale of chiral symmetry breaking, $\Lambda_\chi \simeq 1\,\mathrm{GeV}$. The problem at hand can be treated exactly by integrating out the pionic degrees of freedom from the Fock space using the projection formalism of Okubo, Fukuda, Sawada and Taketani[4]. The usefulness of this approach when applied to momentum space has been demonstrated in a toy–model calculation, see refs.[5]. Based on this approach, we have set up the following scheme. First, one constructs the irreducible chiral NN potential based on a power counting in harmony with the projection formalism. This is outlined in detail in ref.[6]. To third order in small momenta, this potential is given by the following contributions (LO = leading order, NLO = next-to-leading order):

LO OPE with lowest order insertions and two 4N contact interactions without derivatives.

NLO Vertex and self–energy corrections to the LO interactions, TPE with lowest order insertions and seven 4N contact interactions with two derivatives.

NNLO Vertex and self–energy corrections to OPE as well as TPE with exactly one insertion from the dimension two πN Lagrangian. These terms encode non–trivial information about the pion–nucleon interaction beyond leading order and are thus sensitive to the chiral structure of QCD.

This potential is divergent. All divergences (of quadratic and logarithmic form) can be dealt with by subtracting divergent loop integrals, which leads to an overall renormalization of the axial–vector coupling g_A and seven of the nine coupling constants related to the 4N interactions. The precise prodecure is discussed in detail in ref.[7]. The renormalized potential still has a bad high energy behaviour. Some of the contact interactions (NNLO TPE contributions) grow quadratically (cubically) with increasing momenta. Even the momentum–independent contact interactions necessitate regularization, which is performed on the level of the Lippmann–Schwinger equation. That is done in the following way (with $\vec{p}$ and $\vec{p}\,'$ the initial and final nucleon momenta):

$$V(\vec{p},\vec{p}\,') \to f_R(\vec{p})\, V(\vec{p},\vec{p}\,')\, f_R(\vec{p}\,') \;, \tag{1}$$

where $f_R(\vec{p})$ is a regulator function chosen in harmony with the underlying symmetries. In ref.[7], two different regulator functions are used, the sharp cutoff $f_R^{\rm sharp}(\vec{p}) = \theta(\Lambda^2 - p^2)$, and an exponential form, $f_R^{\rm expon}(\vec{p}) = \exp(-p^{2n}/\Lambda^{2n})$, with $n = 2, 3, \ldots$. The latter form is more suitable for the calculation of some observables. Bound and scattering states can then be obtained by solving the Lippmann–Schwinger equation with the regularized potential.

PARAMETERS, FITTING PROCEDURE AND RESULTS

In this section, I briefly describe how the parameters are pinned down. The parameters related to the pion–nucleon interaction beyond leading order can be fixed by a fit of the chiral perturbation theory pion–nucleon amplitude[8] to the dispersion–theoretical one inside the Mandelstam triangle[9]. In addition, we have nine coupling constants related to four–nucleon contact interactions. These can be uniquely determined by a fit to the S– and P–waves together with the mixing parameter ϵ_1. While both S–waves contain two parameters, the P–waves and ϵ_1 depend one (more precisely, one can form linear combinations of the LECs which appear as these parameters in the considered partial waves). At NLO, the resulting values for the LECs related to the 4N contact terms are sensitive to the energy range used in the fit. At NNLO, the resulting values are more stable, so that we can perform global fits for energies up 100 MeV. For example, such a global fit with $\Lambda = 500$ MeV at NLO and 875 MeV at NNLO leads to a deuteron binding energy of $E_d = -2.17$ and -2.21 MeV at NLO and NNLO, respectively. Therefore, without any fine tuning, we can reproduce the empirical value within 2 percent and 1 permille at NLO and NNLO, in order. The increase of the cut–off value when going from NLO to NNLO is related to the fact that at NNLO, the chiral TPEP includes mass scales above the two–pion mass, which is the scale related to the uncorrelated TPEP appearing at NLO. It is also worth mentioning that the quality of the fits increases visibly as one goes from LO to NLO to NLO (for details, see ref.[7]). This is, of course, expected from the underlying power counting. With that, one can predict these partial waves for energies above 100 MeV. All other partial waves with angular momentum ≥ 2 and the deuteron properties are *predictions*.

Prediction for the S– and P–waves

The resulting S–waves are shown in figs.1,2 in comparison to the Nijmegen phase shift analysis (PSA)[10]. The improvement when going from LO to NLO to NNLO is clealy visible.

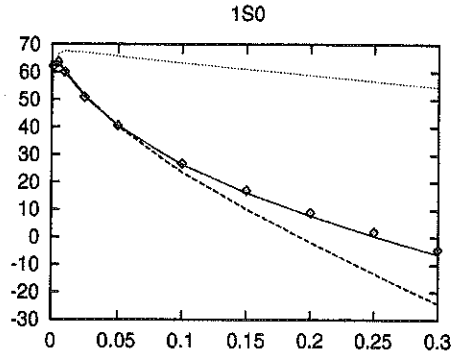

Fig. 1. Predictions for the $^1S_0$ partial wave (in degrees) at LO (dotted curve), NLO (dashed curve) and NNLO (solid curve) in comparison to the Nijmegen PSA (diamonds) for nucleon laboratory energies up to 0.3 GeV.

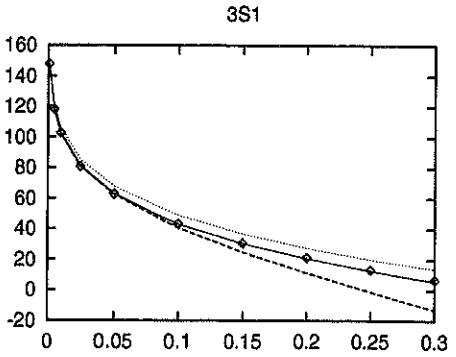

Fig. 2. Predictions for the $^3S_1$ partial wave (in degrees) at LO (dotted curve), NLO (dashed curve) and NNLO (red curve) in comparison to the Nijmegen PSA (diamonds) for nucleon laboratory energies up to 0.3 GeV.

The P–waves are mostly well described, although the NNLO TPEP is a bit too strong in $^3P_1$ and $^3P_2$. Of particular interest is ϵ_1 since it has also been calculated at NLO[3] and NNLO[12] in the KSW approach. Our results (note that we used the so–called Stapp parametrization[13] for the coupled triplet waves) are shown in comparison to the ones of refs.[3,12] in fig.3 as a function of nucleon cms momentum up to 350 MeV. For energies below 150 MeV, the KSW results are comparable to ours, but is obvious from that figure that their approach is tailored to work at low energies. If one wants to go to momenta above 100 MeV, it appears that pion exchange should be treated non–perturbatively.

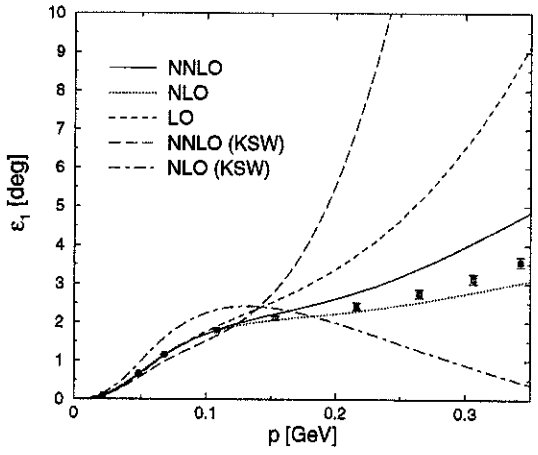

Fig. 3. The $^3S_1 - ^3D_1$ mixing parameter ϵ_1 for our approach and the KSW scheme in comparison to the Nijmegen PSA as a function of the nucleon cms momentum.

I also would like to discuss briefly the so–called effective range expansion. For any partial wave, one can write

$$p \cot\delta(p) = -\frac{1}{a} + \frac{1}{2} r p^2 + v_2 p^4 + v_3 p^6 + v_4 p^8 + \mathcal{O}(p^{10}) \ , \qquad (2)$$

with δ the phase shift, p the nucleon cms momentum, a the scattering length and r the

effective range. It has been stressed in ref.[11] that the shape parameters v_i are a good testing ground for the range of applicability of the underlying EFT. At NNLO, we find e.g. $a = 5.424\,(5.420)\,\mathrm{fm}$, $r = 1.741\ (1.753)\,\mathrm{fm}$, $v_2 = 0.046\ (0.040)\,\mathrm{fm}^3$, $v_3 = 0.67\ (0.67)\,\mathrm{fm}^5$, and $v_4 = -3.9\ (-4.0)\,\mathrm{fm}^7$ for ${}^3S_1$. Similarly, for ${}^1S_0$, we have $a = -23.72\,(-23.74)\,\mathrm{fm}$, $r = 2.68\ (2.67)\,\mathrm{fm}$, $v_2 = -0.61\ (-0.48)\,\mathrm{fm}^3$, $v_3 = 5.1\ (4.0)\,\mathrm{fm}^5$, and $v_4 = -17\ (-29)\,\mathrm{fm}^7$. The numbers in the brackets refer to the np system from the Nijmegen II potential. Note that one can also perform the fit such that the scattering lengths and effective ranges are exactly reproduced. This leads only to modest changes in the values of $v_{2,3}$, e.g. for such a fit in ${}^1S_0$ one has $v_2 = -0.53\,\mathrm{fm}^3$ and $v_3 = 5.0\,\mathrm{fm}^5$. This rather good agreement illustrates again that the long range physics associated with pion exchanges is incorporated correctly and it demonstrates the predictive power of such an EFT approach.

Predictions for higher partial waves

Consider first the D– and F–waves. These are free of parameters and most problematic since the NNLO TPEP can be too strong. In some potential models, TPEP is simply cut at distances of (approximately) less than one fermi. Nevertheless, we find a rather satisfactory description of these partial waves. Of particular interest is ${}^3D_1$ since it is related to the deuteron channel. Also, ${}^1D_2$ is supposedly very sensitive to contributions from the Δ–resonance, which in our approach is subsumed in the LECs related to the dimension two πN interaction. Both these partial waves are well described, see figs.4,5. Even the small ${}^3D_3$ partial wave is very well described up to the opening of the pion production threshold (in the Bonn potential, this partial wave is dominated by correlated TPE). Note, however, that the D–waves are quite sensitive to the choice of the regulator cut–off. However, this cut–off dependence is an artefact of the NNLO approximation. At N^{3}LO, contact terms of the form $\sim \vec{p}^{\,2}\,\vec{p}^{\,\prime 2}$ appear, and one will have exactly one LEC in each D–wave. In ref.[7], we have performed a partial N^{3}LO calculation for ${}^1D_2$ and shown that the resulting phase shift does no longer depend on the cut–off Λ. Of course, that remains to be verified by a complete N^{3}LO calculation including also the modifcations to pion exchanges.

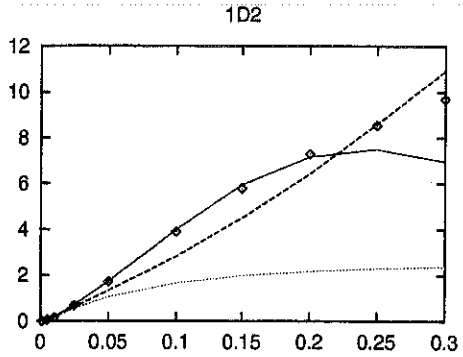

Fig. 4. Predictions for the ${}^1D_2$ partial wave (in degrees) at LO (dotted curve), NLO (dashed curve) and NNLO (solid curve) in comparison to the Nijmegen PSA (blue diamonds) for nucleon laboratory energies up to 0.3 GeV.

The so–called peripheral waves ($l \geq 4$) have already been considered by the Munich group[14]. Their calculation was based on Feynman graphs using dimensional regularization. The potential was constructed perturbatively by proper partial wave projection of the NNLO OPE and TPE. While in most of the peripheral waves OPE is dominant, there are a few exceptions where chiral NNLO TPEP is needed to bring the predictions in agreement with the data or PSA results. Our calculation, which is based on a completely different regularization scheme and treats the potential non–perturbatively, leads to the same results. This is rather gratyfying. One particular example that demonstrates the importance of NNLO TPEP is ${}^3G_5$ as shown in fig.6. The other partial waves in which NNLO TPEP plays a role are ${}^1G_4$, ${}^3H_5$, ${}^3H_6$, and ${}^3I_7$ (for more details, see ref.[7]).

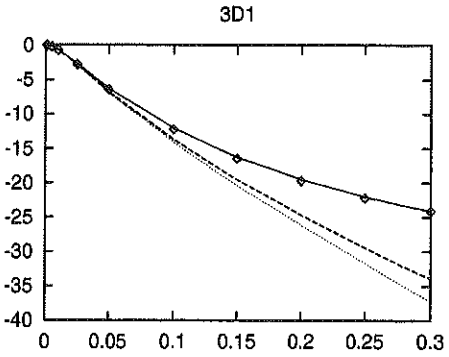

Fig. 5. Predictions for the ${}^3D_1$ partial wave (in degrees) at LO (dotted curve), g NLO (dashed curve) and NNLO (solid curve) in comparison to the Nijmegen PSA (diamonds) for nucleon laboratory energies up to 0.3 GeV.

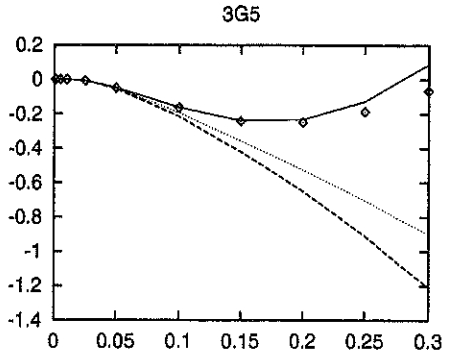

Fig. 6. Predictions for the ${}^3G_5$ partial wave (in degrees) at LO (dotted curve), NLO (dashed curve) and NNLO (solid curve) in comparison to the Nijmegen PSA (diamonds) for nucleon laboratory energies up to 0.3 GeV.

Deuteron properties

It is straightforward to calculate the bound state properties. At NNLO (NLO), we use an exponential regulator with $\Lambda = 1.05\,(0.60)\,\mathrm{GeV}$, which reproduces the deuteron binding energy within an accuracy of about one third of a permille (2.7 percent). No attempt is made to reproduce this number with better precision. In table 1 the deuteron properties are collected and compared to the data and two realistic potential model predictions. We note that deviation of our prediction for the quadrupole moment compared to the

Table 1. Deuteron properties derived from our chiral potential compared to two "realistic" potentials (Nijmegen–93[15] and CD–Bonn[16]) and the data. Here, r_d is the root–mean–square matter radius. An exponential regulator with $\Lambda = 600\,\mathrm{MeV}$ and $\Lambda = 1.05\,\mathrm{GeV}$ at NLO and NNLO, in order, is used.

	NLO	NNLO	Nijm93	CD-Bonn	Exp.
E_d [MeV]	−2.1650	−2.2238	−2.224575	−2.224575	−2.224575(9)
Q_d [fm^2]	0.266	0.262	0.271	0.270	0.2859(3)
η	0.0248	0.0245	0.0252	0.0255	0.0256(4)
r_d [fm]	1.975	1.967	1.968	1.966	1.9671(6)
A_S [fm$^{-1/2}$]	0.866	0.884	0.8845	0.8845	0.8846(16)
P_D[%]	3.62	6.11	5.67	4.83	–

empirical value slightly larger than for the realistic potentials. Still, it remains to be checked whether this problem persists when one includes the meson–exchange currents (compare also the discussion in ref.[17]). The asymptotic D/S ratio, called η, and the strength of the asymptotic wave function, A_S, are well described. The D–state probability,

which is not an observable, is most sensitive to small variations in the cut–off. At NLO, it is comparable and at NNLO somewhat larger than obtained in the CD-Bonn or the Nijmegen-93 potential. This increased value of P_D is related to the strong NNLO TPEP. At N^{3}LO, I expect this to be compensated by dimension four counterterms. It is also worth mentioning that at NNLO, we have two additional very deeply bound states. These have, however, no influence on the low–energy physics and can be projected out. Furthermore, these states are an artefact of the too strong potential and will most probably vanish at N^{3}LO. Altogether, the description of the deuteron as compared to ref.[2] is clearly improved.

COORDINATE SPACE REPRESENTATION

It is also illustrative to consider the coordinate space representation of this potential. I point out that it is intrinsically non–local in momentum as well as in coordinate space. Therefore, it cannot be directly compared to standard local NN potentials. In fig.7, the corresponding potential in the $^1S_0$ partial wave at NLO is shown. Qualitatively, it exhibits all expected features, namely the short–range repulsion, intermediate range attraction and dominance of pion exchange at large separations (as much as this can be seen in a pictorial of a non–local potential). In ref.[7], a more detailed comparison of the chiral potential with the so–called realistic potentials is given.

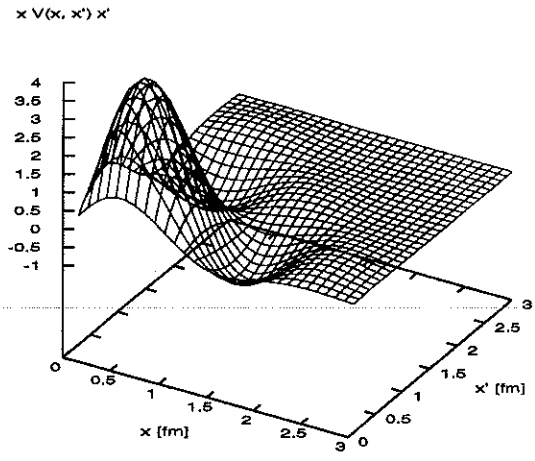

Fig. 7. Coordinate space representation of the potential $xV(x,x')x'$ in the the $^1S_0$ partial wave at NLO.

SUMMARY AND OUTLOOK

In this talk, I have shown some results for the nucleon–nucleon interaction based on effective field theory. The formalism is an extension of the ideas spelled out by Weinberg almost a decade ago. The power counting is performed on the level of the potential. We have worked out the potential to next-to-next-to-leading order in the power counting. At NNLO, it consists of one– and two–pion exchange diagrams with insertions from the dimension one and two pion–nucleon Lagrangian. The corresponding low–energy constants from $\mathcal{L}^{(2)}_{\pi N}$ have been determined from a fit ot the πN amplitudes inside the Mandelstam triangle[9]. In addition, there are two/seven four–nucleon contact interactions with zero/two derivatives. The so–defined potential is divergent. All these divergences can be absorbed by a proper redefinition of the axial–vector coupling g_A and of seven of the nine four–nucleon couplings. This renormalized potential needs to be regularized due to its bad high momentum behaviour, see eq.(1). The regularized potential is used in a Lippmann–Schwinger equation to obtain bound and scattering states by menas of standard Gauss–Legendre quadrature. The corresponding coupling constants can be obtained after proper partial wave decomposition from a fit of the two S– and four P–waves as well as the $^3S_1 - ^3D_1$ mixing parameter ϵ_1 for nucleon lab energies below 100 MeV. The resulting

S–waves are as accurate as obtained from high precision potentials (for energies up to the pion production threshold). The other partial waves are mostly well described. For angular momentum ≥ 2, all phase shifts are parameter free predictions. In particular, the $^3D_1$ wave is well reproduced. In some of the D– and F–waves, the NNLO TPEP is somewhat too strong. This will be cured at N^{3}LO due to the appearance of 4N contact interactions with four derivatives. Their contribution is expected to balance the short distance contribution from the TPEP. This cut–off independence at N^{3}LO has been explicitely demonstrated for $^1D_2$ in ref.[7]. In most peripheral waves ($l \geq 4$), OPE is dominant but there are some exceptions where NNLO TPE is needed to close the gap between the EFT prediction and the data (or PSA). This has been already found before in refs.[14,18] based on completely different approaches. In addition, without any fine tuning we obtain good results for the deuteron, the sole exception being the too low quadrupole moment. However, it is mandatory to calculate the pertinent exchange currents before drawing a conclusion on this issue. In fact, the EFT approach can easily be extended to the coupling of external fields as well as to systems with more than two nucleons. It is my opinion that the chiral Lagrangian approach does more than "... justify approximations (such as assuming the dominance of two–body interactions) that have been used for many years by nuclear physicists..."[19].

ACKNOWLEDGEMENTS

I am grateful to Evgeny Epelbaum and Walter Glöckle for a most enjoyable collaboration and allowing me to present these results before publication. I would like to thank Iain Stewart for supplying me with the results for ϵ_1 in the KSW scheme and Vincent Stoks for providing the range parameters. Last but not least the superbe organization by Christine Kunz and Res Badertscher is warmly acknowledged.

REFERENCES

1. S. Weinberg, Phys. Lett. **B251**, 288 (1990); Nucl. Phys. **B363**, 3 (1991).
2. C. Ordóñez, L. Ray and U. van Kolck, Phys. Rev. **C53** (1996) 2086.
3. D.B. Kaplan, M.J. Savage and M.B. Wise, Nucl. Phys. **B534**, 329 (1998).
4. S. Okubo, Prog. Theor. Phys. **12**, 603 (1954); N. Fukuda, K. Sawada and M. Taketani, Prog. Theor. Phys. **12**, 156 (1954).
5. E. Epelbaoum, W. Glöckle, and Ulf-G. Meißner, Phys. Lett. **B439**, 1 (1998); E. Epelbaoum, W. Glöckle, A. Krüger and Ulf-G. Meißner, Nucl. Phys. **A645**, 413 (1999).
6. E. Epelbaoum, W. Glöckle and Ulf-G. Meißner, Nucl. Phys. **A637**, 107 (1998).
7. E. Epelbaum, W. Glöckle and Ulf-G. Meißner, FZJ-IKP(TH)-1999-19.
8. N. Fettes, Ulf-G. Meißner and S. Steininger, Nucl. Phys. **A640**, 199 (1998).
9. P. Büttiker and Ulf-G. Meißner, `hep-ph/9908247`; Paul Büttiker, *these proceedings.*
10. V.G.J. Stoks et al., Phys. Rev. **C48**, 792 (1993).
11. T.D. Cohen and J.M. Hansen, Phys. Rev. **C59**, 13 (1999).
12. S. Fleming, T. Mehen and I.W. Stewart, `nucl-th/9906056`.
13. H.P. Stapp, T.J. Ypsilantis and N. Metropolis, Phys. Rev. **105**, 301 (1957).
14. N. Kaiser, R. Brockmann and W. Weise, Nucl. Phys. **A625**, 758 (1997).
15. V.G.J. Stoks et al., Phys. Rev. **C49**, 2950 (1994).
16. R. Machleidt, F. Sammarruca and Y. Song, Phys. Rev. **C53**, R1483 (1996).
17. R.B. Wiringa et al., Phys. Rev. **C51**, 38 (1995).
18. M.R. Robilotta and C.A. da Rocha, Nucl. Phys. **A615**, 391 (1997).
19. S. Weinberg, AIP Conference Proceedings **272**, 346 (1993).

SU(3) CHIRAL DYNAMICS WITH COUPLED CHANNELS: ETA AND KAON PRODUCTION

Norbert Kaiser
Physik Department T39, TU München, D-85747 Garching, Germany

Abstract

We identify the next-to-leading order s- and p-wave amplitudes of the SU(3) chiral meson-baryon Lagrangian with a coupled-channel potential which is iterated in a separable Lippmann-Schwinger equation. The nucleon resonance $S_{11}(1535)$ emerges as a quasi-bound state of kaon and Σ-hyperon. Our approach to η- and K-meson photoproduction introduces no new parameters. By adjusting some parameters of the next-to-leading order chiral Lagrangian and a few finite range parameters we are able to describe simultaneously a large amount of low energy data. These include the cross sections for pion- and photon-induced production of η- and K-meson from nucleons.

INTRODUCTION

Over the last few years there has been renewed interest in the photoproduction of eta mesons and kaons from nucleons. At MAMI (Mainz) very precise differential cross sections for the reaction $\gamma p \to \eta p$ have been measured from threshold at 707 MeV up to 800 MeV photon lab energy[1]. The nearly isotropic angular distributions show a clear dominance of the s-wave amplitude E_{0+} in this energy range. The very large total cross sections (up to $17\mu b$) are usually interpreted in terms of the nucleon resonance $S_{11}(1535)$ which has the outstanding feature of a strong ηN decay. At ELSA (Bonn) there is an on-going program to measure strangeness production with photons from proton targets. Total and differential cross sections as well as hyperon recoil polarizations have been measured for the reactions $\gamma p \to K^+\Lambda, K^+\Sigma^0, K^0\Sigma^+$ with improved accuracy from the respective thresholds at 911 and 1046 MeV photon lab energy up to 2.0 GeV[2-4].

Most theoretical models used to describe the abovementioned reactions are based on an effective Lagrangian approach including Born terms and various (meson and baryon) resonance exchanges[5-7] with the coupling constants partly fixed by independent electromagnetic and hadronic data. Whereas resonance models work well for η-production the situation is more difficult for kaon production where several different kaon-hyperon final states are possible. As outlined in ref.[6] resonance models can lead to a notorious overprediction of the $\gamma p \to K^0\Sigma^+$ and $\gamma n \to K^+\Sigma^-$ cross section.

We will use quite a different approach to eta and kaon photoproduction (and the related pion-induced reactions) not introducing any explicit resonance. Our starting point is the SU(3) chiral effective meson-baryon Lagrangian at next-to-leading order. The explicit degrees of freedom are only the baryon and pseudoscalar meson octet with interactions controlled by chiral symmetry and a low energy expansion. The systematic approach to chiral dynamics is chiral perturbation theory, a renormalized perturbative loop-expansion. Its range of applicability can however be very small in cases where strong resonances lie closely above (or even slightly below) the reaction threshold. Prominent examples for this are the isospin $I = 0$, strangeness $S = -1$ resonance $\Lambda(1405)$ in K^--proton scattering, or the $S_{11}(1535)$ nucleon resonance which has an outstandingly large coupling to the ηN-channel and therefore is an essential ingredient in the description of η-photoproduction. In previous work[8] we have shown that the chiral effective Lagrangian is a good starting point to dynamically generate such resonances. The chiral Lagrangian predicts strongly attractive forces in the $\overline{K}N$ isospin 0 and $K\Sigma$ isospin 1/2 s-wave channels. If this strong attraction is iterated to all orders, e.g. via a Lippmann-Schwinger equation in momentum space, quasi-bound meson-baryon states emerge which indeed have all the characteristic properties of the $\Lambda(1405)$ or the $S_{11}(1535)$. The price to be paid in this approach are some additional finite range parameters, which must be fitted to data. However, since one is dealing with a multi-channel problem, it is quite non-trivial to find a satisfactory description of so many available photon- and pion-induced data with just a few free parameters. For both the strong meson-baryon scattering and the meson photoproduction processes we will consider all relevant s- and p-wave multipoles.

COUPLED CHANNEL APPROACH

Let us briefly describe the approach to meson-baryon scattering and its generalization to meson photoproduction (for more details see[9,10]). The indices i and j label the meson-baryon channels (i.e. $\pi N, \eta N, K\Lambda, K\Sigma$) involved. They are coupled through a potential in momentum space

$$V_{ij} = \frac{\sqrt{M_i M_j}}{4\pi f^2 \sqrt{s}} C_{ij} \ , \tag{1}$$

where the relative coupling strengths C_{ij} (explicit expressions are given[9]) are, up to a factor $-f^{-2}$ (with $f = 92.4\,\mathrm{MeV}$), the corresponding s-wave amplitudes calculated from the $SU(3)$ chiral meson-baryon Lagrangian to order q^2. It means they are at most quadratic in the meson center of mass energy $E_i = (s - M_i^2 + m_i^2)/2\sqrt{s}$ and the meson mass m_i. The s-wave potential V_{ij} is iterated to all orders in a separable Lippmann-Schwinger equation of the form

$$T_{ij} = V_{ij} + \sum_n \frac{2}{\pi} \int_0^\infty dl \frac{l^2}{k_n^2 + i0^+ - l^2} \left(\frac{\alpha_n^2 + k_n^2}{\alpha_n^2 + l^2} \right)^2 V_{in} T_{nj} \ , \tag{2}$$

with T_{ij} the resulting T-matrix connecting the in- and outgoing channels j and i. In eq.(2) the index n labels the intermediate meson-baryon states to be summed over and $\vec{l}$ is the relative momentum of the off-shell meson-baryon pair in intermediate channel n. The propagator used in eq.(2) is proportional to a (simple) non-relativistic energy denominator with $k_n = \sqrt{E_n^2 - m_n^2}$ the on-shell relative momentum. The potentials derived from the chiral Lagrangian have zero range since they stem from a contact interaction. To make the dl-integration convergent a "form factor" parameterizing finite range aspects of the potential has to be introduced. This is done via a dipole-like off-shell "form factor" $[(\alpha_n^2 + k_n^2)/(\alpha_n^2 + l^2)]^2$ in eq.(2) with α_n a finite range parameter for each channel n. The cut-offs α_n are fixed in a fit to many data keeping in mind physically reasonable ranges $0.5\,\mathrm{GeV} < \alpha_n < 1.5\,\mathrm{GeV}$.

The separable Lippmann-Schwinger equation for the T-matrix can be solved in closed form by simple matrix inversion $T = (1 - V \cdot G)^{-1} \cdot V$, where G is the diagonal matrix with entries

$$G_n = \frac{k_n^2}{2\alpha_n} - \frac{\alpha_n}{2} - i\, k_n \ , \tag{3}$$

with $k_n = \sqrt{E_n^2 - m_n^2}$ and the appropriate analytic continuation ($i|k_n|$ below threshold $E_n < m_n$). The resulting multi-channel S-matrix $S_{ij} = \delta_{ij} - 2i\sqrt{k_i k_j}\, T_{ij}$ is exactly unitary in the subspace of the kinematically open (two-body) channels and the total (s-wave) cross section for the reaction $(j \to i)$ is calculated via $\sigma_{ij} = 4\pi(k_i/k_j)|T_{ij}|^2$.

The inclusion of the strong p-wave multipoles $p_{1/2}$ and $p_{3/2}$ into the coupled channel scheme is presented in detail in ref.[10]. The construction is completely analogous to the s-wave case.

MESON PHOTOPRODUCTION

We extend the same formalism to s-wave meson photoproduction. The basic assumption is that photoproduction can also be described by a Lippmann-Schwinger equation. In complete analogy to strong interaction we will identify the s-wave photoproduction potential (named B_{0+}) with the electric dipole amplitude E_{0+} calculated to order q^2 from the chiral effective Lagrangian. A welcome feature of such an approach is that it does not introduce any further adjustable parameter. Consequently meson-baryon interactions and meson photoproduction are strongly tied together and the fits of e.g. the finite range parameters α_n are controlled by both sets of data. For the description of the photoproduction reactions $\gamma p \to \eta p$, $K^+\Lambda$, $K^+\Sigma^0$, $K^0\Sigma^+$ we have to know the photoproduction potentials B_{0+} for $\gamma p \to \phi B$, where ϕB refers to the meson-baryon states with total isospin $I = 1/2$ or $I = 3/2$ and isospin projection $I_3 = +1/2$. We label these states by an index which runs from 1 to 6, which refers to $|\pi N)^{(1/2)}$, $|\eta N)^{(1/2)}$, $|K\Lambda)^{(1/2)}$, $|K\Sigma)^{(1/2)}$, $|\pi N)^{(3/2)}$ and

$|K\Sigma)^{(3/2)}$, in that order. The resulting expressions involve as parameters only the axial vector coupling constants $F = 0.49$ and $D = 0.78$ and they read

$$B_{0+}^{(1)} = \frac{eM_N}{8\pi f\sqrt{3s}}(D+F)\,(2X_\pi + Y_\pi)\ , \qquad B_{0+}^{(2)} = \frac{eM_N}{8\pi f\sqrt{3s}}(3F-D)\,Y_\eta\ ,$$
$$B_{0+}^{(3)} = \frac{e\sqrt{M_N M_\Lambda}}{8\pi f\sqrt{3s}}(-D-3F)X_K\ , \qquad B_{0+}^{(4)} = \frac{e\sqrt{M_N M_\Sigma}}{8\pi f\sqrt{3s}}(D-F)(X_K+2Y_K)\ ,$$
$$B_{0+}^{(5)} = \frac{e\sqrt{2}M_N}{8\pi f\sqrt{3s}}(D+F)(Y_\pi - X_\pi)\ , \qquad B_{0+}^{(6)} = \frac{e\sqrt{2M_N M_\Sigma}}{8\pi f\sqrt{3s}}(D-F)(X_K - Y_K)\ . \quad (4)$$

The dimensionless function X_ϕ takes the form

$$X_\phi = \frac{1}{2} - \frac{1}{4M_0}\left(2E_\phi + \frac{m_\phi^2}{E_\phi}\right) + \left(1 + \frac{m_\phi^2}{2M_0E_\phi}\right)\frac{m_\phi^2}{2E_\phi\sqrt{E_\phi^2 - m_\phi^2}}\ln\frac{E_\phi + \sqrt{E_\phi^2 - m_\phi^2}}{m_\phi}\ , \quad (5)$$

and it sums up the contributions of all tree diagrams to the s-wave photoproduction multipole of a positively charged meson. The logarithmic term comes from the meson pole diagram in which the photon couples to the positively charged meson. If the photoproduced meson is neutral the corresponding sum of diagrams leads to a simpler expression,

$$Y_\phi = -\frac{1}{3M_0}\left(2E_\phi + \frac{m_\phi^2}{E_\phi}\right)\ . \quad (6)$$

Infinitely many rescatterings of the photoproduced meson-baryon state due to the strong interaction are summed up via the Lippmann-Schwinger equation. The "full" electric dipole amplitude $E_{0+}^{(i)}$ for channel i is then given by

$$E_{0+}^{(i)} = \sum_j [(1 - V\cdot G)^{-1}]_{ij}\, B_{0+}^{(j)}\ . \quad (7)$$

where V is the matrix of the strong interaction potential and G the diagonal propagator matrix defined in eq.(3). The total (s-wave) photoproduction cross section for the meson-baryon final state i reads $\sigma_{\rm tot}^{(i)} = 4\pi(k_i/k_\gamma)|E_{0+}^{(i)}|^2$ with $k_\gamma = (s - M_N^2)/2\sqrt{s}$ the photon center of mass energy and $s = M_N^2 + 2M_N E_\gamma^{lab}$ in terms of the photon lab energy E_γ^{lab}. The inclusion of the photoproduction p-wave multipoles M_{1+}, M_{1-}, E_{1+} into the coupled channel approach is presented in detail in ref.[10]. Only the well-known baryon anomalous magnetic moments κ_B enter as new parameters in the p-wave photoproduction potentials.

RESULTS

Total Cross Sections for π-induced η- and K-production

Fig.1 shows results for the total cross sections for pion-induced η- and K-production: $\pi^- p \to \eta n, K^0\Lambda, K^0\Sigma^0, K^+\Sigma^-$ and $\pi^+ p \to K^+\Sigma^+$. The data are taken from the compilation[11]. The agreement of the coupled channel calculation including s- and p-wave amplitudes with the existing data is very good, even for energies considerably above threshold (i.e. up to $p_{\pi,lab} \simeq 2$ GeV). The contributions of the s-wave amplitude and the two p-wave amplitudes to the total cross section are shown separately for each reaction channel. With the inclusion of the p-waves one is able to describe the data in the (pure isospin-3/2) channel $\pi^+ p \to K^+\Sigma^+$ up to $p_{\pi,lab} = 1.4$ GeV. In this channel the s-wave contributes very little, and the p-wave contribution is completely dominant. Furthermore, with the inclusion of p-wave amplitudes one can describe the total cross section data for $\pi^- p \to K^+\Sigma^-$ up to $p_{\pi,lab} = 1.8$ GeV whereas the s-wave approximation starts to break down around $p_{\pi,lab} = 1.2$ GeV. Note that the large η-production cross section in $\pi^- p \to \eta n$ near threshold (usually interpreted in terms of the nucleon resonance $S_{11}(1535)$ having a

large branching ratio into ηN) is still dominated by the s-wave amplitude. In the present approach a s-wave quasi-bound $K\Sigma$-state is formed through the coupled channel dynamics. Furthermore, the peak in the $\pi^- p \to K^0\Lambda$ total cross section is generated by a strong s-wave cusp effect at the $K\Sigma$-threshold. Altogether it is highly non-trivial to produce the pattern of relative weights of s- and p-waves as shown in Fig.1. In a coupled channel calculation all reactions get linked together and changes in one channel will immediately affect all the others.

Total and Differential Cross Sections for η- and K-photoproduction

Fig.2 shows the total cross section for η-photoproduction, $\gamma p \to \eta p$, together with the data of[1] (MAMI). This total cross section is dominated by the s-wave multipole E_{0+}, whose value at threshold is $E_{0+,th}^{(\eta p)} = (9.8 + 12.8\,i) \cdot 10^{-3} m_\pi^{-1}$. Again, this large cross section arises from coupled channel dynamics (forming a $K\Sigma$ quasi-bound state) with no explicit $S_{11}(1535)$ introduced. Furthermore, we show in Fig.2 the total cross sections for K^+-photoproduction $\gamma p \to K^+\Lambda, K^+\Sigma^0$ together with the recent ELSA data[3]. In the channel $\gamma p \to K^+\Lambda$ a strong s-wave cusp effect is visible at the $K\Sigma$-threshold. In fact the data show a structure around $E_\gamma = 1.05$ GeV which is consistent with this interpretation. Above $E_\gamma = 1.2$ GeV the p-wave multipole amplitudes ($E_{1+}, M_{1\pm}$) become very important in order to reproduce the energy dependence of the $K^+\Lambda$-data. The same feature applies to the channel $\gamma p \to K^+\Sigma^0$. In both cases there appears in the data an enhancement around $E_\gamma \simeq 1.5$ GeV. It may be due to a nucleon resonance decaying into $K\Lambda$ and $K\Sigma$. The coupled channel calculation can generate only non-resonant background amplitudes in p-waves and is thus not able to describe this enhancement if it is due to a resonance. Finally, we show results for neutral kaon-photoproduction, $\gamma p \to K^0\Sigma^+$, together with the recent ELSA data[4]. In this channel the p-wave multipoles are completely dominant and we find a fair reproduction of the total cross section data from threshold up to about $E_\gamma = 1.4$ GeV. Again, it is highly non-trivial to generate the pattern of s- and p-wave contributions as shown in Fig.2, given all the additional constraints from pion-induced η- and K-production (Fig.1). In Fig.2, we show also some typical examples of angular distributions of differential cross sections for η- and K-photoproduction. In the case $\gamma p \to p\eta$ the MAMI data[1] display an almost isotropic angular distribution. The small deviations from isotropy at the higher energies $E_\gamma \simeq 0.8$ GeV can be explained by the interference term of the large s-wave with the small p-wave multipoles. The angular distributions for $\gamma p \to K^+\Sigma^0$ of the recent ELSA data[3] are reasonably well reproduced from threshold up to $E_\gamma \simeq 1.7$ GeV in our calculation. Similar features apply to the reaction $\gamma p \to K^+\Lambda$ for $E_\gamma \leq 1.4$ GeV, although the measured angular distributions[4] are (within errorbars) close to a straight line whereas the calculated ones have larger curvature. Finally, we show in Fig.2 an angular distribution for $\gamma p \to K^0\Sigma^+$ together with the recent ELSA-data[4]. For photon energies up to $E_\gamma \simeq 1.4$ GeV the overall behavior of these data can be well described. There remain however some problems in the description of the corresponding polarization observables.

REFERENCES

1. B. Krusche *et al.*, *Phys. Rev. Lett.* **74** (1995) 3736.
2. M. Bockhorst *et al.*, (SAPHIR collaboration), *Z. Phys.* **C63** (1994) 37.
3. M.Q. Tran *et al.*, (SAPHIR collaboration), *Phys. Lett.* **B445** (1998) 20.
4. S. Goers *et al.*, (SAPHIR collaboration), *Phys. Lett.* **B464** (1999) 331.
5. H. Tanabe *et al.*, *Phys. Rev.* **C39** (1989) 741; R.A. Adelseck, B. Saghai, *Phys. Rev.* **C42** (1990) 108; **C45** (1992) 2030; L. Tiator *et al.*, *Nucl. Phys.* **A580** (1994) 455.
6. T. Mart, C. Bennhold and C.E. Hyde-Wright, *Phys. Rev.* **C51** (1995) R1074.
7. Ch. Sauermann, B.L. Friman and W. Nörenberg, *Phys. Lett.* **B341** (1995) 261.
8. N. Kaiser, P.B. Siegel and W. Weise, *Nucl. Phys.* **A594** (1995) 325; N. Kaiser, P.B. Siegel and W. Weise, *Phys. Lett.* **B362** (1995) 23.
9. N. Kaiser, T. Waas and W. Weise, *Nucl. Phys.* **A612** (1997) 297 and refs. therein.
10. J. Caro Ramon, N. Kaiser, S. Wetzel and W. Weise, *"Chiral SU(3) Dynamics with Coupled Channels: Inclusion of P-Wave Multipoles"*, submitted to *Nucl. Phys.* **A**.
11. A. Baldini *et al.*, Landolt–Börnstein. Vol. 12a,(Springer, Berlin, 1988).

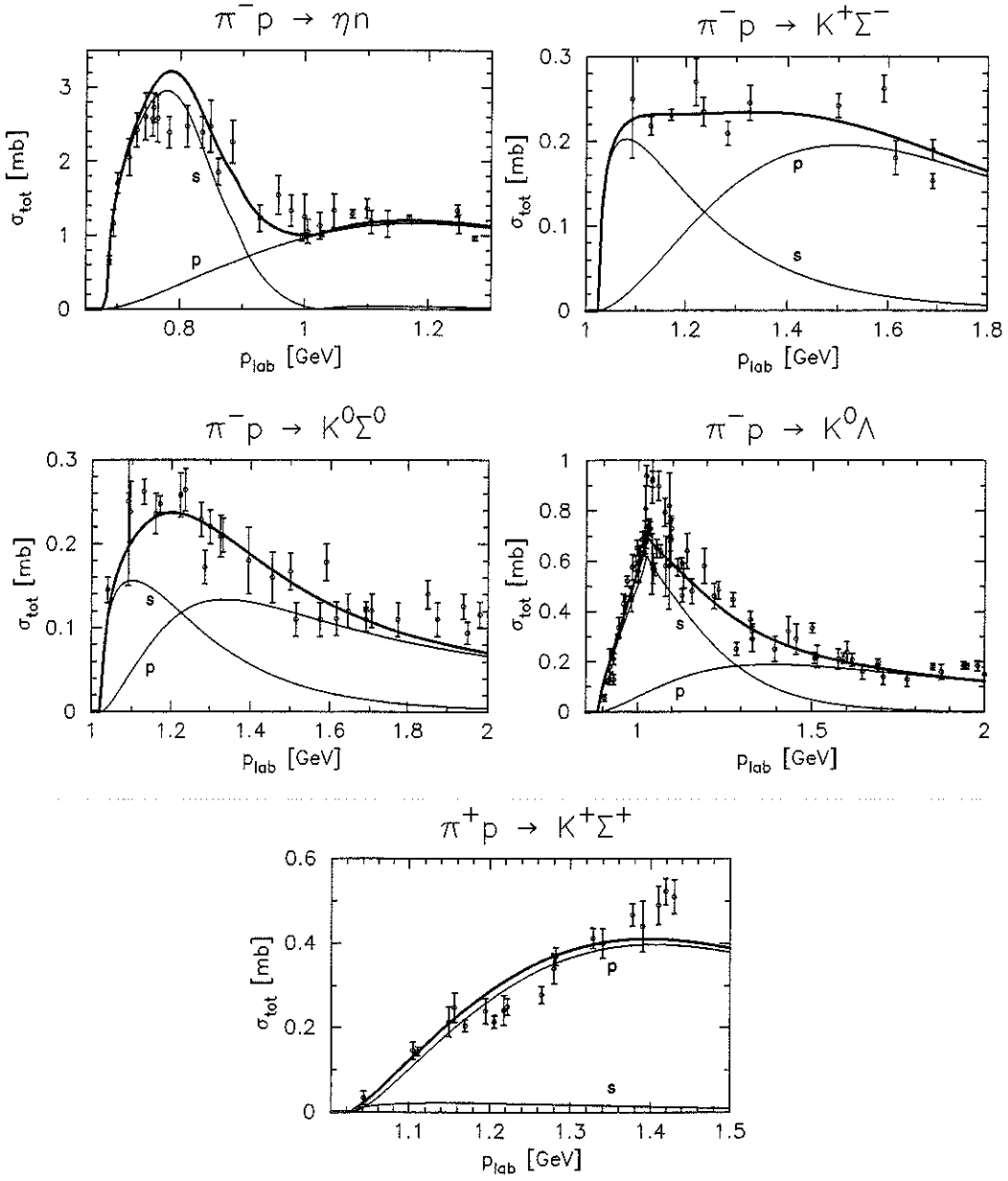

Figure. 1. Total cross sections for pion-induced η- and K-production as a function of the pion laboratory momentum. The s- and p-wave contributions are shown separately. The data are taken from the compilation[11].

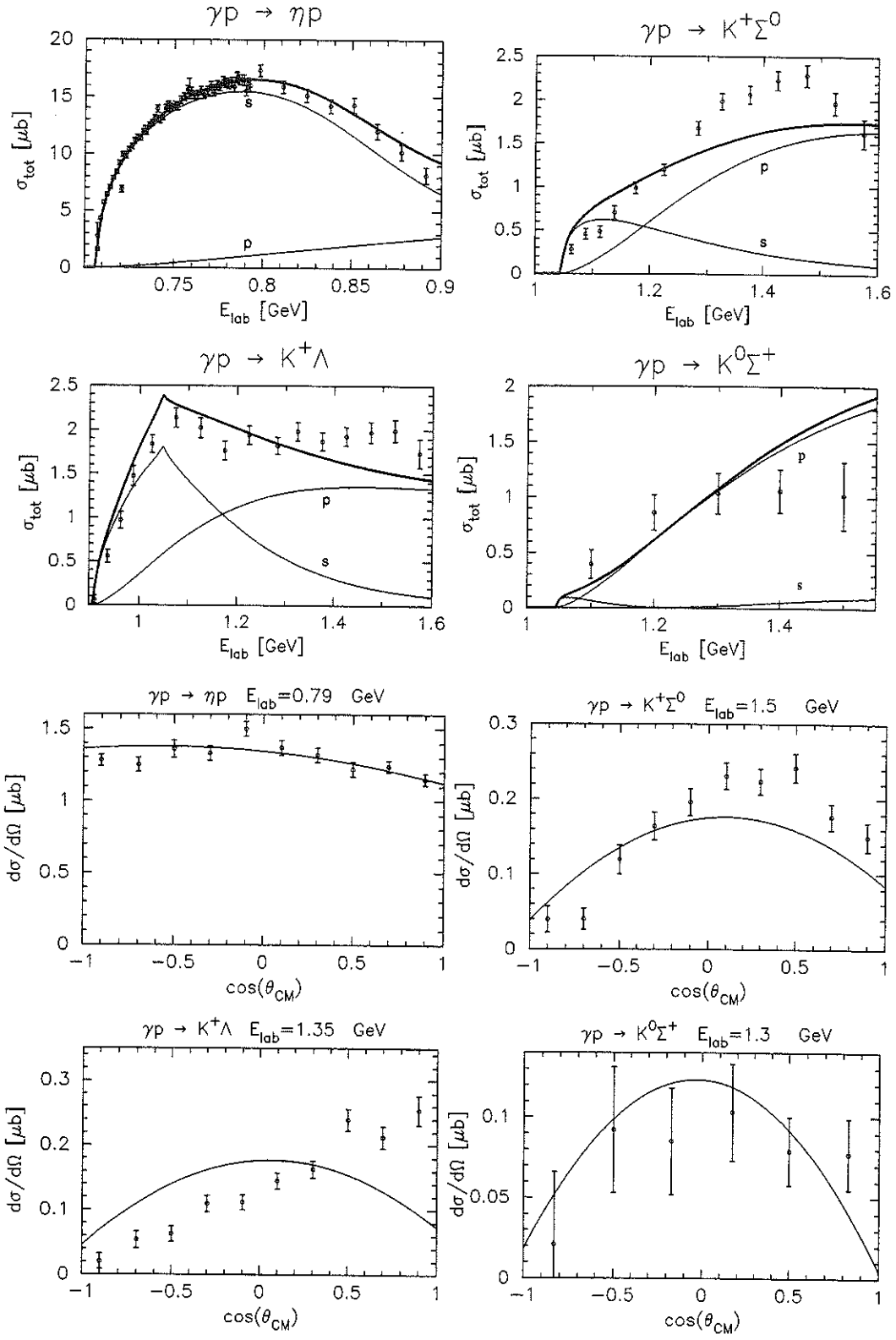

Figure. 2. Total and differential cross sections for η- and K-photoproduction as a function of the photon laboratory energy or the cosine of the cm scattering angle, respectively. The s- and p-wave contributions to the total cross sections are shown separately. The data are taken from refs.[1,3,4].

Hadron Physics with the Crystal Ball

B.M.K. Nefkens and A.B. Starostin [†] for the Crystal Ball Collaboration [‡§]
UCLA, Los Angeles, CA 90095, USA

Abstract

Preliminary results are presented for π^- and K^- interactions on protons leading to neutral final states. Included are the production of π^0, $2\pi^0$, $3\pi^0$, η, γ, and K_s. The data are used for the investigation of the production and decay of nucleon and hyperon resonances in the mass region up to 1700 MeV/c^2. We have also measured $2\pi^0$ production on H, ^{12}C, ^{27}Al, and ^{64}Cu targets by 750 and 408 MeV/c π^- mesons. The shape of the $2\pi^0$ invariant mass spectrum depends strongly on the target nucleus which is indicative of a major medium modification. Finally, we present new upper limits on C, CP, and P forbidden η-meson decays.

The principal objectives of the physics program carried out by the Crystal Ball Collaboration at the AGS are:

- The Structure of the Nucleon.
  This includes the properties of all N^*, Δ^*, Λ^* and Σ^* baryons.
- The Symmetries of Quark Interactions.
  Special attention is given to the role of Chiral Symmetry.
- QCD at Intermediate Energy.
- The Origin of the Quark Masses.
  This includes the study of the medium modifications discovered in meson production on complex nuclei.

INTRODUCTION

The Crystal Ball, CB, is a multiphoton spectrometer. It has excellent energy and angular resolution and it features a near 4π acceptance. It has been outfitted with a liquid H_2 target located in the center. A successful data run at the AGS was completed in late 1998, which was devoted mainly to π^- and K^- interactions on protons to the neutral final states. The maximum beam momentum was 760 MeV/c.

SELECTION OF EARLY RESULTS

Some of the highlights from the long list of reactions that were investigated in the first run of the Crystal Ball at the AGS are given below.

$$\pi^- p \to 3\pi^0 n$$

We applied the special condition that the $3\pi^0$ could not come from an η decay. The invariant mass spectrum of the $3\pi^0$ events is shown in Fig. 1, the beam momentum is 660 MeV/c which is well below the η production threshold. We have found that σ_t $(\pi^- p \to 3\pi^0 n) = (4 \pm 2)$ μb. This value increases moderately with increasing incident beam momentum; at 760 MeV/c we estimate that $\sigma_t < 20$ μb. Older experiments have reported much larger σ_t, ten times and more. We speculate that this was due to inadvertent η production.

[†] On leave from Petersburg Nuclear Physics Institute, Gatchina, Russia, 188350

[‡] The Crystal Ball Collaboration consists of E. Berger, M. Clajus, A. Marušić, S. McDonald, B.M.K. Nefkens, N. Phaisangittisakul, S. Prakhov, M. Pulver, A. Starostin and W.B. Tippens, *UCLA*, D. Isenhower and M. Sadler, *ACU*, C. Allgower and H. Spinka, *ANL*, J. Comfort, K. Craig and T. Ramirez, *ASU*, T. Kycia, *BNL*, J. Peterson, *UCo*, W. Briscoe and A. Shafi, *GWU*, H.M. Staudenmaier, *UKa*, D.M. Manley and J. Olmsted, *KSU*, D. Peaslee, *UMd*, V. Bekrenev, A. Koulbardis, N. Kozlenko, S. Kruglov and I. Lopatin, *PNPI*, G.M. Huber, N. Knecht, G.J. Lolos and Z. Papandreou, *UReg*, I. Slaus and I. Supek, *RBI*, D.Grosnick, D. Koetke, R. Manweiler and S. Stanislaus, *ValU*.

[§] Supported in part by US DOE, NSF, NSERC, Russian Ministry of Sciences and Volkswagen Stiftung.

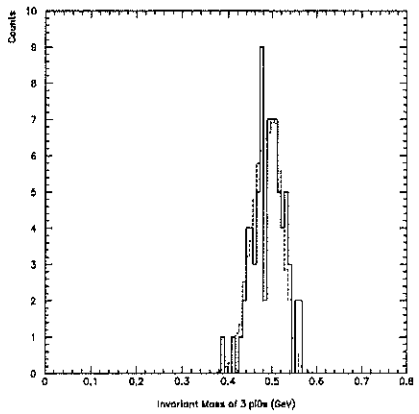

Figure. 1. Invariant mass of $3\pi^0$ events of the reaction $\pi^- p \to 3\pi^0 n$ at $P_{\pi^-} = 660$ MeV/c. The solid line is the data and the dashed line is the Monte Carlo distribution for uniform phase space.

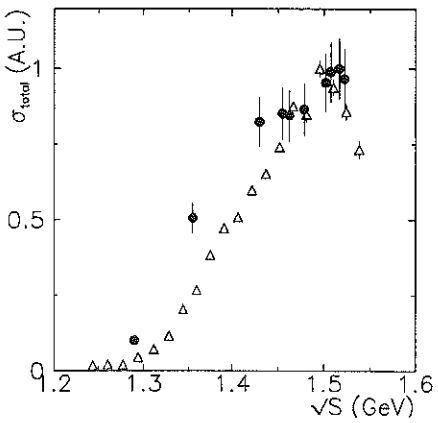

Figure. 2. Excitation function for $\pi^- p \to 2\pi^0 n$ (black dots) compared to the corresponding photoproduction channel (triangles).

Meson production by pions at low and intermediate energy occurs principally by s-channel baryon resonance formation. $3\pi^0$ production occurs via sequential baryon resonance decay. At our energy we have $\pi^- p \to N^* \to P_{11}(1440)\pi^0$ followed by $P_{11} \to 2\pi^0 n$. The expected N^*'s are the $D_{13}(1520)$ and $S_{11}(1535)$. The small value that we measured for the σ_t allows us to conclude that $BR\ \{D_{13}(1520) \to P_{11}(1440)\pi^0\} < 0.5\%$ and $BR\ \{S_{11}(1535) \to P_{11}(1440)\pi^0\} < 0.5\%$.

$$\pi^- p \to 2\pi^0 n$$

The preliminary results for σ_t ($\pi^- p \to 2\pi^0 n$) are given in Fig. 2. The production of the $P_{11}(1440)$, the Roper resonance, by π^- from threshold to 700 MeV/c is much smaller than S_{11} and D_{13} excitation[1]. $2\pi^0$ production is dominated by the P_{11} intermediate state and occurs via two different channels:

i. $P_{11} \to \pi^0\Delta$ followed by $\Delta \to \pi^0 n$. A simple Monte Carlo calculation shows that the resulting $2\pi^0$ invariant mass spectrum has the gross features of a uniform phase–space distribution.

ii. The other channel is $P_{11} \to \sigma\, n$ where the σ, now called $f_0(400-1200)$ in the Review of Particle Physics [1], is a $J = I = 0$ state of two strongly interacting pions. The $2\pi^0$ invariant mass spectrum of this decay should peak at high mass.

The Dalitz plot and the $2\pi^0$ invariant mass projection of $\pi^- p \to 2\pi^0 n$ at 660 MeV/c are shown in Fig. 3. In the Dalitz plot we expect to see the Δ band, surprisingly that is not the case, we find only a local, very strong enhancement that has a πN invariant mass around 1230 MeV/c^2. The $2\pi^0$ invariant mass shows a strong peak at the high energy end and a smaller phase-space like distribution. Note that the $2\pi^0$'s cannot be in a P-wave and that the tail of the $\rho \to \pi^+\pi^-$ decay which plays a role in $\pi^- p \to \pi^+\pi^- n$ is absent.

For comparison we show in Fig. 2 also σ_t ($\gamma p \to 2\pi^0 n$) measured by the TAPS Collaboration [2]. The photoexcitation of baryon resonances is different than the excitation by pions. Above 600 MeV/c the main resonance produced in photon absorption is the D_{13} and very little P_{11} and S_{11}. Thus 2π photoproduction is predominantly $\gamma p \to D_{13}$; the latter can decay via the $\pi^0\Delta$ intermediate state as $\rho \to 2\pi^0$ decay is forbidden by Bose statistics. Thus we expect the Dalitz plot of $2\pi^0$ photoproduction to show a Δ band and the $2\pi^0$ invariant mass spectrum to be like phase space without a peak at the high end. This is observed, see Fig. 4. We want to stress the complementarity of mesoproduction

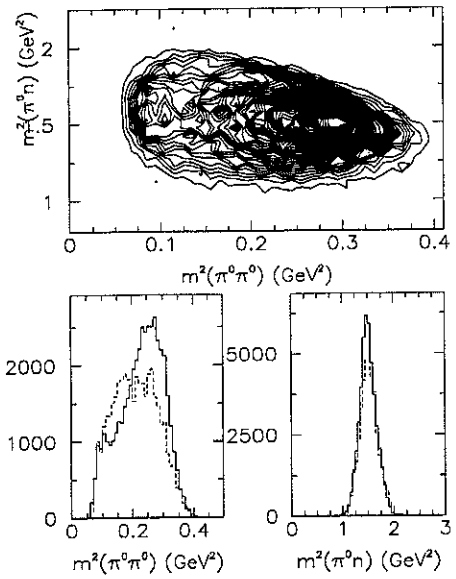

Figure. 3. Dalitz plot (top) for $\pi^- p \to 2\pi^0 n$. $M^2_{2\pi^0}$ projection (left) and $M^2_{\pi^0 n}$ (right). The dashed line in the projections is the phase-space distribution for $\pi^- p \to \pi^0 \Delta \to \pi^0(\pi^0 n)$.

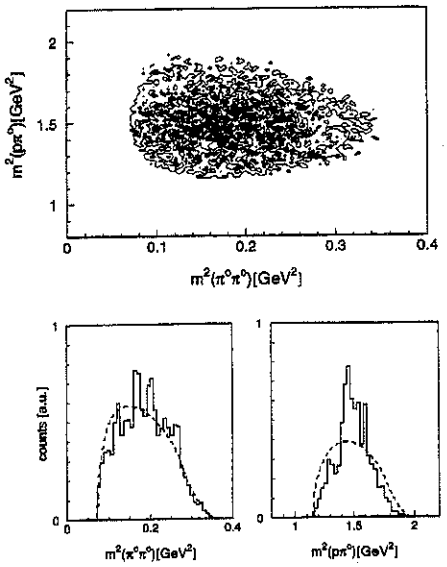

Figure. 4. Dalitz plot (top) for $\gamma p \to p2\pi^0$[2]. $M^2_{2\pi^0}$ projection (left) and $M^2_{p\pi^0}$ (right). The dashed line in the projections is the uniform phase-space distribution.

and photoproduction and the importance of studying both reactions for obtaining the full understanding of the decay of the baryon resonances.

$$\pi^- A \to 2\pi^0 A'$$

Considerable attention has been given in recent months to the properties of the σ di-meson state in nuclear matter [3–8]. The σ, or f_0(400-1200), is an S-wave isoscalar $\pi - \pi$ interaction. The interest in this system is fueled by the search for the onset of chiral restoration, χR, which could occur significantly below the creation of a quark-gluon plasma. There is speculation that χR may happen at modest temperature and/or nuclear density. The quantum numbers of the σ, $I^G(J^{PC}) = 0^+(0^{++})$ are those of the vacuum, making the σ the favorite hadron for finding a large medium modification. The interest in the σ has been piqued even more by a report of the CHAOS group[9] about an anomalous, large, sharp spike in the $\pi^+\pi^-$ invariant mass spectrum near the low-mass limit of $2m_\pi$. This was observed in a $\pi^+\pi^-$ production experiment by incident π^+ of 400 MeV/c on different nuclear targets, it is known as the CHAOS effect, see Fig. 5.

The experimental results of CHAOS have been interpreted by their authors as evidence that nuclear matter strongly modifies the $\pi\pi$ interaction in the $J = I = 0$ channel. The CB is particularly suited for investigations of $\pi^0\pi^0$ production by π^- on nuclear targets.

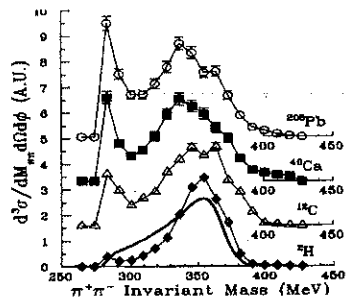

Figure. 5. The $\pi^+\pi^-$ invariant mass distribution for the $\pi^+ A \to \pi^+\pi^- A'$ reaction reported by CHAOS[9]. The vertical scale is arbitrary units. The CHAOS effect is the sharp peak at low mass

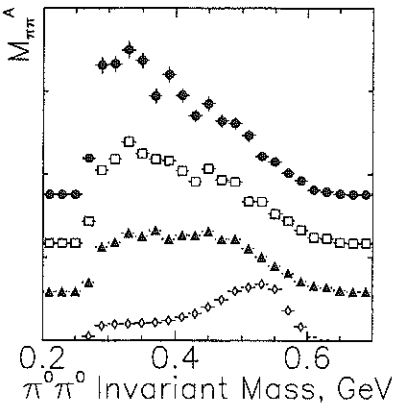

Figure. 6. $2\pi^0$ invariant mass distribution for the $\pi^- A \rightarrow \pi^0\pi^0 A'$ reaction for H (diamonds), ^{12}C (triangles), ^{27}Al (squares), and ^{64}Cu (circles) at $P_{\pi^-} = 750\ MeV/c$.

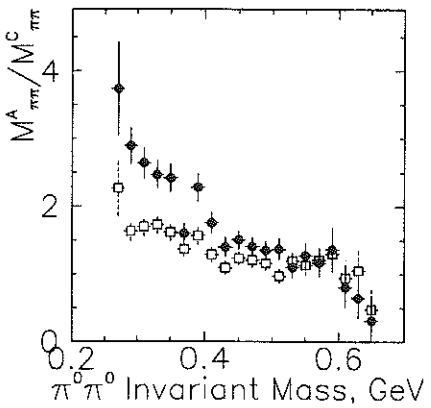

Figure. 7. The ratio of the $2\pi^0$ invariant mass distributions at 750 MeV/c. $M^{Cu}_{\pi\pi}/M^C_{\pi\pi}$ (circles) and $M^{Al}_{\pi\pi}/M^C_{\pi\pi}$ (squares)

The $\pi^0\pi^0$ system has an important advantage over the $\pi^+\pi^-$ case because $\pi^0\pi^0$ cannot be in a P–state. The results for the $\pi^0\pi^0$ invariant mass spectra obtained by 750 MeV/c π^- interactions on H, ^{12}C, ^{27}Al and ^{64}Cu are shown in Fig. 6. We see a major modification of the shape of the $2\pi^0$ spectrum. It peaks for hydrogen at the maximum allowed mass, the peak is lower for increasing A and for the copper target the peak occurs near the low end. The same conclusion holds for the data at 408 MeV/c incident π^-, which is similar to the CHAOS beam momentum. The resolution of the $\pi^0\pi^0$ at low energy is quite good $\sim$ 5 MeV. We see no evidence for the sharp peak reported by CHAOS. We conclude that the CB measurements of $2\pi^0$ do not support the CHAOS effect though we see a dramatic medium modification. It is possible that the CHAOS effect is the result of not including the peculiar CHAOS detector geometry appropriately. To further probe the A dependence of the $\pi^0\pi^0$ spectrum we show the ratio of the yields of the different targets in Fig. 7. There is a forward peaking at 750 and at 408 MeV/c because of the medium modification.

$$K^- p \rightarrow \Lambda\eta$$

The η is readily and uniquely identified via the decay $\eta \rightarrow 2\gamma$ yielding two very energetic photons which have the invariant mass of the η; the missing mass associated with the η corresponds to that of the Λ. The icing on the cake is the detection of the π^0 from the decay $\Lambda \rightarrow \pi^0 n$. This is accomplished readily by selecting 4 neutral cluster events and requiring that the missing mass be that of the neutron. The results on σ_t $(K^- p \rightarrow \Lambda\eta)$ measured with the Crystal Ball using an incident K^- beam on a hydrogen target is shown in Fig. 8. The number of events exceeds quite a bit the previous world data for this reaction. The peak of the cross section occurs at $E = 1672$ MeV/c^2; this is just at the mass of the $\Lambda(1670)$ hyperon, which is a four star S-wave Λ^* resonance. The shape of σ_t is consistent with the models in which η production by π^- is also dominated by an S-wave resonance, the $S_{11}(1535)$. In both cases the magnitude of the η decay channel is larger than expected on the basis of the available phase space.

The angular distribution for $K^- p \rightarrow \Lambda\eta$ at 735 MeV/c is shown in Fig. 9. The slight dip is indicative of a very small D-wave contribution. Interestingly, the shape of the differential cross sections is the same for threshold eta production by K^- and π^-, namely concave or bowl-shaped. This is to be compared to the other η production processes, $\gamma p \rightarrow \eta p$ and $pp \rightarrow pp\eta$ for which the angular distributions are convex. The different shapes are consistent with models in which the $p\gamma$ and pp reactions are dominated by a vector meson intermediary; the π and K induced reactions have a pseudoscalar amplitude.

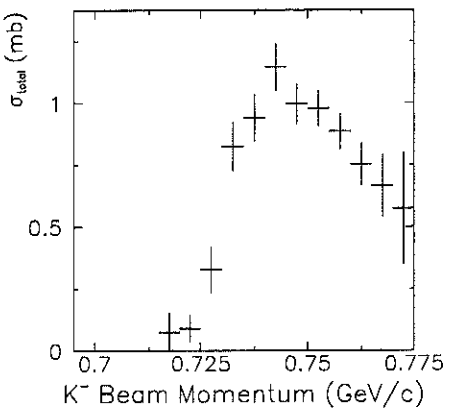

Figure. 8. Total cross section for $K^- p \to \Lambda\eta$ in *mb*.

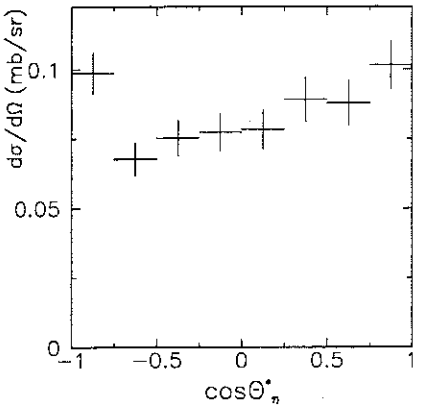

Figure. 9. Angular distribution for $K^- p \to \Lambda\eta$ for $P_K = 735$ MeV/c.

$$K^- \; p \to \Lambda\pi^0$$

The $\Lambda\pi^0$ is a pure $I = 1$ state, it comes only from the decay of Σ^* hyperons. In the energy region of our experiment which is limited by the highest available K^- momentum of 760 MeV/c, there are 6 established Σ^* states plus 4 more "bumps" for a maximum of 10 possible states. The quark models would like to see fewer that 10 Σ^* states in our energy region. It is expected that our new data on the various neutral channels, once they are fully analyzed, will clean up the status of the Σ^* states.

The $\Lambda\pi^0$ final state features 4 photon clusters in the CB which form two π^0's. One of these π^0's has the associated missing mass of the Λ. Because $K^- p \to \Lambda\pi^0$ is a background to our $K^- p \to \Lambda\gamma$ experiment we have measured it. An example of the preliminary result for the $K^- p \to \Lambda\pi^0$ angular distribution obtained at $P_{K^-} = 750$ MeV/c is shown in Fig. 10. Our results are in agreement with earlier, less precise data.

$$K^- \; p \to \bar{K} n$$

K^- charge exchange is a readily measurable reaction with the CB using the decay mode $K_s \to 2\pi^0$. Unlike the two preceding reactions which are isospin unique, charge exchange requires 2 isospin amplitudes: A_0 which has $I = 0$ and A_1 for $I = 1$. Thus, $d\sigma/d\Omega(K^- p \to \bar{K} n) \sim |A_1 - A_0|^2$. An example of the preliminary results for the angular distribution at 750 MeV/c is shown in Fig. 11. There are many other neutral final states in $\pi^-\, p$ and $K^-\, p$ interactions that we are studying with the CB but space limitations does not allow for them to be discussed here.

Search for P-, C- and CP-Forbidden Eta Decays

The Standard Model implies that CP violation in family-conserving interactions is very small. This prediction has scarcely been tested for lack of suitable processes. The best opportunity is found in η decay. We have searched for the P and CP-forbidden decay mode $\eta \to 4\pi^0$ in a sample of 3.0×10^7 η's produced in the reaction $\pi^- p \to \eta n$ near threshold. The phase space for the $4\pi^0$ decay is small, but, this η decay has no known background. The decay is unique. There must be 8 photon clusters that reconstruct to $4\pi^0$'s, which reconstruct to the η while the missing mass of these 8 photons must correspond to the neutron mass. No events in the above sample were found which satisfies these conditions, this gives $BR\ (\eta \to\ 4\pi^0) < 7.0 \times 10^{-7}$ with a 90% confidence level.

Among the three discrete symmetries C, P, and T, which play an important role in nuclear physics because they are conserved in strong interactions, C (particle-antiparticle conjugation) has come under scrutiny because of the baryon-antibaryon asymmetry in the known universe. No evidence has been seen thus far for the existence of galaxies made of antimatter. Big-Bang Cosmology predicts the existence of plenty of antimatter in the

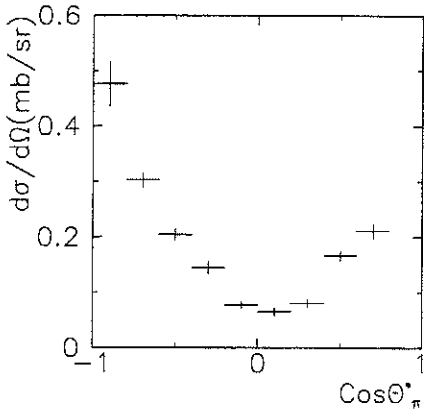

Figure. 10. Angular distribution for $K^-p \to \Lambda\pi^0$ for $P_K = 750$ MeV/c.

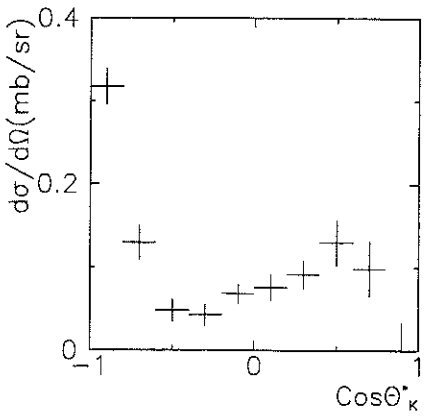

Figure. 11. Angular distribution for $K^-p \to \overline{K^0}n$ for $P_K = 750$ MeV/c.

universe. Investigating C-invariance has not been done very sensitively for lack of suitable tests. In the course of our search for $\eta \to 4\pi^0$ we have made three interesting tests of C-invariance in the strong and/or electromagnetic interactions of hadrons. Firstly, we determined that the $BR\ (\eta \to 3\pi^0\gamma) < 9 \times\ 10^{-5}$. This is the first known search for this η decay channel. To assess the sensitivity of this search, one could compare with the major $3\pi^0$ decay: $BR\ (\eta \to 3\pi^0) = 0.32$. Secondly, we report $BR\ (\eta \to 2\pi^0\gamma) < 3 \times\ 10^{-3}$. This is the first known search for this decay also. The sensitivity can be estimated by comparison with the allowed decay to charged pions, $BR\ (\eta \to \pi^+\pi^-\gamma) = 0.048$. Finally the CB has set a new limit, $BR\ (\eta \to 3\gamma) < 9 \times 10^{-5}$ which is five times better than the existing limit. These tests are consistent with the expectations based on the Standard Model and further limit the window for New Physics.

SUMMARY

Some highlights of the first data run with the Crystal Ball spectrometer are:

$\sigma_t\ (\pi^-p \to 3\pi^0 n) = (4 \pm 2)\ \mu$b at $P_{\pi^-} = 660$ MeV/c and below 20 μb at 760 MeV/c that allows us to conclude what $BR\ \{D_{13}(1520) \to P_{11}(1440)\pi^0\} < 0.5\%$ and $BR\ \{S_{11}(1535) \to P_{11}(1440)\pi^0\} < 0.5\%$ up to 760 MeV/c.

The reaction $\pi^-p \to 2\pi^0 n$ is dominated by P_{11} production from threshold to 750 MeV/c. The $2\pi^0 n$ Dalitz plot is very non–uniform with a large concentration of the $\pi^0 n$ invariant mass at the value of the $\Delta(1232)$ resonance, but there is no Δ band. The $2\pi^0$ invariant mass is strongly peaked toward the maximal possible mass.

New data are obtained on K^-p to $\Lambda\eta$, $\Lambda\pi^0$ and $\overline{K^0}n$.

We have observed a major medium modification, namely, a large shape dependence of the $2\pi^0$ invariant mass on A obtained on complex nuclei at $P_{\pi^-} = 408$ and 750 MeV/c.

New upper limits on forbidden η decays are obtained: $BR\ (\eta \to 4\pi^0) < 7 \times 10^{-7}$ which is a test of $P-$ and $CP-$invariance, while $BR\ (\eta \to 3\pi^0\gamma) < 9 \times\ 10^{-5}$, $BR\ (\eta \to 2\pi^0\gamma) < 3 \times\ 10^{-3}$ and $BR\ (\eta \to 3\gamma) < 9 \times 10^{-5}$ are tests of $C-$invariance.

REFERENCES

1. Review of Particle Physics, Eur. Phys. J. **C3**, 1998.
2. F. Härter, et al., Phys. Lett. **401**, 229 (1997).
3. P. Schuck, W. Norenberg and G. Chanfray, Z. Phys. Rev. **A330**, 119 (1988).
4. M.J. Vicente Vacas and E. Oset, Preprint FTUV-99-50, IFIC-99-52 (1999).
5. T. Hatsuda, T. Kunihiro and H. Shimiru, Phys. Rev. Lett. **82**, 2840 (1999).
6. R. Rapp et al., Phys. Rev. **C59**, 1237 (1999).
7. A. Bhattacharyya, S.K. Ghosh and S.C. Phatak, Phys. Rev. **C60**, 044903 (1999).
8. S. Chiku and T. Hatsuda, Phys. Rev. **D58**, 076001 (1998).
9. F. Bonutti et al., Phys. Rev. Lett. **77**, 603 (1996).

Meson Physics at DAΦNE

G. Pancheri
INFN Laboratori Nazionali di Frascati, P.O. Box 13, I00044 Frascati, Italy

Abstract

An overview of the main physics items to be studied at DAΦNE is presented, including rare K-decays, scalar and pseudoscalar spectroscopy through radiative ϕ-decays and measurement of the hadronic e^+e^- cross-section.

DAΦNE is an electron-positron collider operating in INFN Frascati National Laboratories at a c.m. energy corresponding to the production of the ϕ-meson, i.e. $\sqrt{s} = 1.020\ GeV$. Frascati has a long history in e^+e^- collisions, which were first observed in AdA, Anello di Accumulazione, whose contruction was proposed by B. Touschek and his collaborators in 1960[1]. The successful operation of AdA inspired the construction of a number of electron-positron storage ring projects around the world, one of them in Frascati itself, ADONE, where the multihadronic production was first observed in 1970, and the discovery of the J/Ψ in November 1974 confirmed. After a few years of operation as a synchrotron light facility, in the late 80's ADONE was brought back to operate as an electron-positron storage ring taking data on the time-like form factors of protons and neutrons. DAΦNE is a multi-bunch machine, with up to a maximum of 120 bunches, with single bunch design luminosity of $4 \times 10^{30} cm^{-2} sec-1$. While the presently attained luminosity is below project design, as it is operating with $30 \div 50$ bunches circulating with single bunch luminosity slightly less than 10^{29}, work is in progress to improve it. There are two interaction regions planned at DAΦNE and three experiments to share the two interaction regions. In November 1999 the luminosity at the K-Long Observation Experiment (KLOE) site has reached a maximum value of $4 \times 10^{30}\ cm^{-2}\ sec^{-1}$ and the total integrated luminosity delivered to KLOE has been 8 nb^{-1}. The machine has also been made to operate with collisions in the second interaction region where the atomic physics detector DAΦNE Exotic Atom Research (DEAR) will soon be taking data. Later, in the year 2000, the nuclear physics detector FINUDA, which will study hypernuclei formation and decay, will be installed.

The physics spectrum reacheable at DAΦNE has been investigated in detail in the Second DAΦNE Physics Handbook[2]. We show in Table 1 the number of events expected at DAΦNE at full luminosity in the main channels of interest. We see that the DAΦNE

Table 1. Main ϕ-decay modes and Branching Ratioes at DAΦNE at $L = 5 \times 10^{32} cm^{-2} sec^{-1}$

decay channel	branching ratio	events in 1 y
K^+K^-	49%	1.1×10^{10}
$K_S^0 K_L^0$	34%	7.5×10^9
$\rho\pi + \pi^+\pi^-\pi^0$	16%	3.4×10^9
$\eta + \gamma$	1.3 %	2.8×10^8
$\eta' + \gamma$	1.2×10^{-4}	
$f_0, a_0\ \gamma$	$< 1 \times 10^{-4}$	

physics program can be divided into three main areas of interest with some further subdivision, i.e. :

- K-Physics from $e^+e^- \to \phi \to K_L K_S, K^+K^-$ with studies of

  CP-violation in correlated K-meson pairs

  CP-violation in given K-decays

  low energy QCD phenomena in K-decays, like in $K_{\ell 3}$ and $K_{\ell 4}$.

- Meson Spectroscopy from $e^+e^- \to VM$ with $V = \gamma, \rho, \omega$ and $M = \pi, \eta, \eta', f_0, a_0$.
- Inclusive production $e^+e^- \to X$ with $X = hadrons$ or $X = \gamma + hadrons$.

1 K-physics

1.1 CP-violation in the K-system

The main reason for constructing DAΦNE had been the study of direct CP-violation in K-decays. There are two possible sources of CP-violation in the neutral Kaon system,

1. Kaon-mixing $K^0 \leftrightarrow \bar{K}^0$ characterized by the parameter $\epsilon \approx 10^{-3}$
2. weak decays of Kaons into pairs of pions of definite isospin, characterized by the much smaller parameter ϵ'

Although ϵ and ϵ' are both non-zero in the Standard Model, with ϵ' very small due to near zero cancellations between some strong and weak interaction matrix elements, the question has arisen in the past as to whether there are other sources of CP-violation, outside the SM predictions, and hence the great interest in the measurement of these parameters[3]. During the last year, the experimental value for the ratio ϵ'/ϵ has stabilized around a world average of $(2.12 \pm 0.46) \times 10^{-3}$[4], with theoretical expectations[5–8] oscillating between 10^{-3} and 10^{-4}. For the central values the Rome[5] and Munich[6] groups find values below 10^{-3}. An enhancement is found by the Trieste[7] and Dortmund-Frascati[8] groups leading to central values of order 10^{-3}. Recently, in ref.[9] an enhancement of ϵ'/ϵ has also been observed due to final state interactions.

Can KLOE add anything to the present situation? The special quantum state configuration and experimental setup can give a measurement of the double ratio

$$\Re(\epsilon'/\epsilon) \approx \frac{1}{6}\left(\left|\frac{A(K_L \to \pi^+\pi^)/A(K_S \to \pi^+\pi^-)}{A(K_L \to \pi^0\pi^0)/A(K_S \to \pi^0\pi^0)}\right|^2 - 1\right) \qquad (1)$$

resulting in an independent way to test the reached agreement between the FermiLab and CERN measurements. Eventually other interesting effects will play a role, as in the case of the interferometry[10] measurements, although the precision in this case would not be as good as in the case of the double ratio.

From the theoretical point of view, the present knowledge of the hadronic matrix elements does not reach the precision required to extract information on physics beyond the Standard Model at present machines. What is required is a substantial improvement in the precision of our description of low energy hadronic interactions. Such improvement can in part come from precise measurements of a number of K-decays, as we shall discuss in the next section.

1.2 Hadronic physics and K-decays

The list of interesting physics items includes the rare K-decays. Whereas the very rare ones, with B.R. of the order 10^{-8} or 10^{-9} are not in easy reach, I shall discuss here the more accessible and very interesting $K_{\ell 3}$ and $K_{\ell 4}$ processes[11], i.e. $K^+ \to \pi^0\ell^+\nu$ or $K^0 \to \pi^-\ell^+\nu$ with B.R. of order 10^{-2} and $K \to \pi\pi\ell\nu$ with B.R. of order 10^{-5}, and with $\ell = e, \mu$. $K_{\ell 3}$-decays can be expressed through two form factors, corresponding to the S and P-wave projection of the matrix elements, both of which are predicted by Chiral Perturbation theory (ChPT). A linear expansion of these two form factors is characterized by the two slope parameters λ_+ and λ_0. $K^{+,0}_{e3}$ allows for a determination of λ_+ (terms in λ_0 are proportional to m_ℓ^2 and hence negligible in K_{e3}-decays). Chiral perturbation theory predictions relate the slope parameters to the radius of the $K\pi$ system, and through this to the charged radius of the pion. There is not much controversy here and the expected agreement with ChPT expectations is being confirmed through large statistic experiments like E785[12]. and the expected measurements at DAΦNE .

Next in the KLOE list of interesting K-decays is $K_{\ell 4}$, since it provides one of the cleanest ways to measure the $\pi\pi$ system at threshold and hence the scattering lengths. Other ways to study the $\pi\pi$ system at threshold are provided by $\pi N \to \pi\pi N$ through the One Particle Exchange process and the study of the pionic atoms[13], whereupon the decay width of pionium into neutral pions is proportional to the quantity $|a_0^0 - a_0^2|^2$. Apart from the present measurements of the $K_{\ell 4}$ decays by E865 at BNL, the most extensive measurements of this quantity come from the Rosselet experiment[14], whose data for the $\pi\pi$ phase shift difference $\delta_0^0 - \delta_1^1$ are shown in Fig. 1 in comparison with predictions by ChPT[15] and expectations from Generalized ChPT[16].

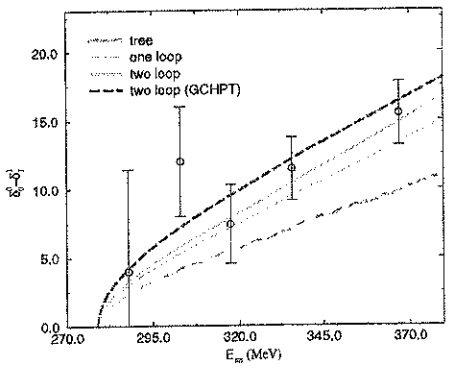

Figure. 1. Comparison between data and theoretical expectations in ChPT.

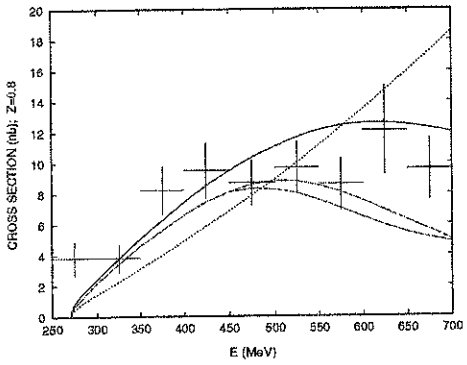

Figure. 2. Data from Crystal Ball[17] and theoretical predictions.

It should be noticed that a complementary source of information on the $\pi\pi$ system at threshold, and thus to the S-wave scattering lengths, comes from the unitarity related process $\gamma\gamma \to \pi^0\pi^0$. Predictions for this cross-section are also given by ChPT and are shown in Fig. 2. The curves correspond to one loop[18] $O(p^4)$ (dashes) and two loop result[19]$O(p^6)$ (full), as well as to a dispersive analysis[20] with $a_0^0 = 0.2$ (band). To measure $\gamma\gamma \to \pi^0\pi^0$ near threshold with a precision better than what is already available, DAΦNE and the KLOE detector are an excellent possibility. There is no immediate program to perform this experiment at DAΦNE , but a feasibility study[21] has shown its capabilities.

2 Meson Spectroscopy through radiative ϕ-decays

With branching ratioes ranging from 10^{-2} to 10^{-5} and beyond, the radiative decays of ϕ into scalar and pseudoscalar mesons offer a very promising field of investigation at DAΦNE in the near future. For what concerns the pseudoscalar mesons, from the simultaneous measurement of the decays $\phi \to \gamma\,\pi^0, \eta, \eta'$ one can get information on the quark content and on the decay constants of these mesons. Neglecting, in first approximation, the gluon contribution, the quark content can be obtained from the ratio[22]

$$\frac{\Gamma(\phi \to \eta'\gamma)}{\Gamma(\phi \to \eta\gamma)} = \left(\frac{m_\phi^2 - m_{\eta'}^2}{m_\phi^2 - m_\eta^2}\right)^3 \left(\frac{y_{\eta'}}{y_\eta}\right)^2 \tag{2}$$

where $y_{\eta,\eta'}$ is the strange quark content. A high precision measurement of these decays, with error smaller than a few percent, may shed light on the mixing angle in the decay constants[23,24] and the energy dependence of the mass mixing angle[25], an interesting possibility given the fact that, in the pseudoscalar nonet, the mass range is a factor 10 in the masses and 100 in the squares.

The radiative ϕ decays include the poorly known decays of the ϕ into the scalar sector, i.e. $\phi \to S\gamma$. There are two well established members of the nonet, $a_0(980)$ and $f_0(975)$ but there are also the following questions to which DAΦNE could provide an answer :

- where is the ninth partner?

Table 2. Radiative ϕ decays into scalar mesons

Structure	B.R. for $\phi \to \gamma f_0(975)$	Structure	Ratio=$\frac{\Gamma(\phi\to\gamma f_0)}{\Gamma(\phi\to\gamma a_0)}$
$qq\bar{q}\bar{q}$	$\mathcal{O}(10^{-4})$	$K\bar{K}$	≈ 1
$s\bar{s}$	$\mathcal{O}(10^{-5})$	$(n\bar{s})(\bar{n}s)$	≈ 1
$K\bar{K}$	*less than* 10^{-5}	$(ns)(\bar{n}s)$	≈ 9
gluon gluon	*less than* 10^{-5}	$(n\bar{n})(s\bar{s})$	structure dependent

- what exactly is the quark content of $a_0(980)$ and $f_0(975)$?
- is the broad $\sigma(400-1200)$ part of this system?
- is there any gluonic content of these states?

Different possibilities exists for the scalar states, discussed in[26], i.e. $q\bar{q}$ or $qq\bar{q}\bar{q}$ states, and the latter in various diquark combinations, $K\bar{K}$ molecule or *gluon gluon* state, as suggested recently by J. Ellis, H. Fujii and D. Kharzeev[27], who find that the mixing between the quark-antiquark and the glueball components is strong, even close to maximal. Table 2 from[28] shows some predictions for the decay rates and ratios of branching ratioes. Presently measured values[29] for the branching ratio $\phi \to f_0\gamma$ seem to exclude[30] the simplest possibility, i.e. the $q\bar{q}$ structure.

The measurement of these radiative decays is affected by large backgrounds from initial and final state radiation. However such backgrounds can also contain interesting information, as we shall try to show in the next section.

3 Inclusive cross-section measurements and $(g-2)_\mu$

The inclusive cross-section $e^+e^- \to hadrons$ is of special importance to particle physics as it probes the structure of the vacuum polarization tensor down to the lowest energies in the hadronic domain. This cross-section is related to the hadronic contribution to the anomalous magnetic moment of the muon $a_\mu = 1/2(g-2)_\mu$ through the well known sum rule,

$$a_\mu^{vac-pol} = \int_{4m_\pi^2}^{\infty} \sigma_{e^+e^-\to hadrons}(s) K(s) \frac{ds}{s} \tag{3}$$

where $K(s)$ is a monoticaly decreasing function of s. A similar relation holds for $\Delta\alpha(5)(M_Z)$, the contribution from the five light quarks to the running of α_{QED}. Because of the present lack of theoretical precision in the low energy hadronic regime, these sum rules provide the most precise way to evaluate the hadronic contribution to the vacuum polarization graph and thus to the comparison between theoretical expectations and the precisions measurement[31,32] of $(g-2)_\mu$[33], provided the error on the measurement of the cross-sections in the above integrals is small enough. It must be emphasized that present possibilities of extracting information from the SM precision measurements at LEP and at BNL[32] are limited by the error which comes from the above integral and the analogous one for $\Delta\alpha(5)(M_Z)$.

A theoretical estimate of a_μ in units of 10^{-11} gives[34]

$$a_\mu^{th} = 116\ 591\ 596 \pm 67 \tag{4}$$

with the result coming from a number of different contributions. The largest part of the error comes from the hadronic part, and the above result includes the analysis[35] from τ-lepton decays. In[36] this error is larger and the overall estimate is

$$a_\mu^{th} = \overbrace{116\ 584\ 705.6 \pm 2.9}^{a_\mu^{QED}} + \overbrace{154 \pm 4}^{a_\mu^{Weak}} + \overbrace{6967 \pm 119}^{a_\mu^{had}}$$

An energy scan around the ρ at DAΦNE could reduce the error to the desirable $10 \div 20\%$ of the electroweak contribution[37]. However, since there are no short term plans for DAΦNE

Table 3. DAΦNE Physics spectrum

$\sqrt{s}$ in MeV	500÷1000	1020	1100÷ 1500
CP/CPT		ϵ'/ϵ	
K-decays precision		up to $10^{-8} \div 10^{-9}$	
η, η' physics		$\phi \to \eta, \eta'\gamma$	
$\pi\pi$ phase-shifts		$\phi \to K\bar{K}$ $K \to e\nu\pi\pi$	
Scalar and Pseudoscalar meson structure		$\phi \to a_0/f_0\gamma$ $\to \eta'\gamma \to (\rho,\omega)\gamma\gamma$	$\rho,\omega(1450)$ $\to (\eta,\eta',\eta^*)\gamma$
Light Vector mesons	VMD and ChPT refined	the $q\bar{q}$ content of ϕ,ω	
Higher Vector Mesons			decay width mass parameters
Scalar Glueballs		$\phi \to a_0/f_0\gamma$	
$\sigma_{total} \to e^+e^-$ and hadronic contribution to $(g-2)_\mu$	presently most of the error (60%) comes from here	5% of the error	15%

to have collisions outside the ϕ peak, an alternative proposal[38] has been put forward and is been examined for its feasibility, i.e. that of triggering on Initial State Bremsstrahlung to tune the energy of the hadronic system and access c.m. energies below the ϕ through the process $e^+e^- \to \gamma + X$. Presently the theoretical and phenomenological effort[39] is concentrated on the determination of the ρ excitation curve and the two pion final state.

As a conclusion, Table 3 shows the physics spectrum which can be studied at DAΦNE in the next 5 year.

Acknowledgments

The authors is grateful to all the members of the EuroDAΦNE Collaboration whose work is reported here, and to the MENU99 organizers for their hospitality. This work was partly supported by the EEC through TMR-CT98-0169.

REFERENCES

1. C. Bernardini, G.F. Corazza, G. Ghigo and B. Touschek, Il Nuovo Cimento **18** 1293 (1960).
2. *The Second DAΦNE Physics Handbook*, eds. L. Maiani, G. Pancheri and N. Paver, INFN-LNF, ISBN 88-86409-02-8 (Frascati, 1995).
3. L. Maiani in [2], Ch. 1, pp. 3-26.
4. KTeV Collaboration, A. Alavi-Harati et al, Phys. Rev. Lett. **83**, 22 (1999); NA48 Collaboration, V. Fanti et al., Phys. Lett. **B465**, 335 (1999).
5. M. Ciuchini, E. Franco, L. Giusti, V. Lubicz, G. Martinelli, hep-ph/9910237; hep-ph/9910236.
6. A. J. Buras, hep-ph/9908395; A. J. Buras, M. Gorbahn, S. Jäger, M. Jamin, M. E. Lautenbacher and L. Silvetrini, hep-ph/9904408.

7. Marco Fabbrichesi, hep-ph/9909224; S. Bertolini, J.O. Eeg, M. Fabbrichesi and E.I. Lashin, Nucl. Phys. **B514** 93 (1998).
8. T. Hambye, P.H. Soldan,hep-ph/9908232; T. Hambye, G.O. Kohler, E.A. Paschos and P.H. Soldan, hep-ph/9906434.
9. E. Pallante and A. Pich, hep-ph/9911233.
10. G. D'Ambrosio, G. Isidori and A. Pugliese, " CP and CPT Measurement at DAΦNE", in [2], Ch. 1, pp. 63-95.
11. J. Bijnens, G. Colangelo, G. Ecker and J. Gasser, in[2], Ch. 7, pp. 315-388.
12. J. Lowe, "Experimental Status of Semileptonic K-decays", to be published in the proceedings of *DA*ΦNE99, Frascati November 1999.
13. J-P. Eggert for the DIRAC Collaboration in these Proceedings.
14. L. Rosselet et al., Phys. Rev. **D15** 574 (1977).
15. J. Bijnens, G. Colangelo, G. Ecker, J. Gasser and M.E. Sainio, Phys. Lett. **B374** 210 (1996); Nucl. Phys. **B508** 263 (1997).
16. M. Knecht, B. Moussallam, J. Stern and N.H. Fuchs, Nucl. Phys. **B457** 513 (1995); Nucl. Phys. **B471** 445 (1996).
17. H. Marsiske et al., Phys. Rev. **D41** 3324 (1990).
18. J.Bijnens and F.Cornet (1988), B.Donoghue, B.Holstein and Lin.
19. S. Bellucci, J. Gasser and M. Sainio, Nucl. Phys. **B423** 80 (1994).
20. D. Morgan and M.R.Pennington, Phys. Lett. **B272** 80 (1994); M.R.Pennington, " What We learn by Measuring $\gamma\gamma \to \pi^0\pi^0$ at DAΦNE ", in [2], Ch. 10, pp. 531-558.
21. G. Alexander et al., Il Nuovo Cimento **A107**, 837 (1994).
22. J. Rosner, Phys. Rev. **D27**, 1101 (1983).
23. H. Leutwyler, Nucl. Phys. B (proc. Suppl) **64**, 223 (1998).
24. T. Feldmann and P. Kroll, Eur. Phys. J. **C5**, 327 (1998).
25. R. Escribano and J.M. Frere, Phys. Let. **B459**, 288 (1999).
26. N. Brown and F. Close, "Scalar Mesons and Kaons in ϕ Radiative Decay and Their Implications for Studies of CP Violation at DAΦNE ", in [2], Ch. 11, pp. 649-662; F.E. Close, N. Isgur and S. Kumano, Nucl. Phys. **B389**, 513 (1993).
27. J. Ellis, H. Fujii and D. Kharzeev, " Scalar Glueball-Quarkonium Mixing and the Structure of QCD Vacuum", hep-ph/9909322.
28. M. Pennington, "Low energy Hadron Dynamics", to be published in the Proceedings of DAFNE99 Workshop on Physics and Detectors at DAΦNE , see also http://wwwsis.lnf.infn.it/conferencetalks.html.
29. M.N. Achasov et al., "New experimental data for the decays $\phi \to \mu^+\mu^-$ and $\phi \to \pi^+\pi^-$ from SND detector", hep-ex/9910070.
30. N.N. Achasov, "On nature of scalar a(0)(980) and f(0)(980) mesons", hep-ph/9910540.
31. J. Bailey et al., Phys. Lett. **B68** 191 (1977); F. Farley and E. Picasso, Ann. Rev. Nucl. Sci. **29** (1979) 243.
32. R. Carey et al. Phys. Rev. Lett. **82** 1632 (1999).
33. T. Kinoshita, Phys. Rev. Lett. **75** 4728 (1995). S. Laporta and E. Remiddi, Phys. Lett. **B379** 283 (1996). Phys. Rev. **D52** 3137 (1996);
34. A. Czarnecki and W. Marciano, Invited Talk at the 5th InternWorksh. on Tau Lepton Physics (Tau '98), September 98, Santander, Spain, hep-ph/9810512 and references therein. A. Czarnecki, B. Krause and W. Marciano, Phys. Rev. Lett. **76** 3267 (1996); Phys. Rev. **D52** R2619 (1995). S. Peris, M. Perrotet and E. de Rafael, Phys. Lett. **B355** 523 (1995)
35. R. Alemany, M. Davier and A. Hocker, Eur. Phys. J.C **2** (1998) 123; M. Davier and A. Hoecker, Phys. Lett. **419** 419 (1998); ibid. Phys. Lett. **B435** 427 (1998).
36. F. Jegerlehner, "Hadronic effects in $(g-2)_\mu$ and $\alpha_{QED}(M_Z)$: Status and perspectives",hep-ph/9901386.
37. P. Franzini, " The Muon Gyromagnetic Ratio and R_H at DAΦNE ", in [2], Ch. 9, pp. 471-476.
38. S. Spagnolo, Lecce PhD Thesis 1998 and EPJ6 (1999) 637.
39. S. Binner, J.H. Kühn, K. Melnikov, Phys. Lett. B459 (1999) 279-287. (3969061)

Search for a Narrow Resonance in the πNN System*

Ralph Bilger
Physikalisches Institut der Universität Tübingen, Auf der Morgenstelle 14, D-72076 Tübingen, Germany
for the
LEPS (Karlsruhe-Moscow-PSI-Tübingen)
TAPS/A2 (Gießen-Göttingen-Jülich-Mainz) and
PROMICE/WASA
(Uppsala-Dubna-Jülich-Lodz-Moscow-Novosibirsk-Osaka-Tübingen-Warsaw)
Collaborations

Abstract

We report on the current status of the search for the hypothetical πNN resonance d' with $I(J^P) = \text{even}(0^-)$ and M = 2.06 GeV in the pionic double charge exchange, the π^0 photoproduction off the deuteron and in the 2π production in pp collisions.

The d' hypothesis

Recently the existence of a narrow, NN-decoupled πNN resonance, called d', has been proposed[1] to explain the peculiar resonance-like behavior of the pionic double charge exchange (DCX) reaction (π^+, π^-) on nuclei at pion energies below the Δ resonance. From the analysis of these DCX data the parameters of d' have been deduced to be $m \approx 2.06$ GeV, $\Gamma_{NN\pi} \approx 0.5$ MeV and $I(J^P) = \text{even}\ (0^-)$. From the small width it was concluded that this resonance is NN-decoupled, hence the isospin should be even. A major critique on this interpretation was that the DCX reaction takes place on nuclei, where subtle, not yet understood medium effects cannot be excluded unambiguously as a possible alternative reason. To meet this critique, we have carried out a series of different and alternative experiments:

1. Extension of our systematic DCX studies to closed-shell and to light nuclei, in particular to non-analog transitions, where conventional mechanisms are expected to give particularly small cross sections.

2. Study of the reaction $\gamma d \to d' \to \pi^0 pn$, the photoproduction on the deuteron, which has the advantage of being a resonance reaction on a simple system[2]. At resonance energy $E_\gamma \approx 200$ MeV we expect a resonance cross section of $\sigma_{d'} \approx 0.1 - 1\,\mu$b. This has to be compared with the corresponding 1π-production cross sections at this energy. The π^0 channel was chosen because the quasifree or incoherent photoproduction of neutral pions, $d(\gamma,\pi^0)np$ has a smaller cross section ($\approx 15\,\mu$b) than the production of charged pions ($\approx 120\,\mu$b - $160\,\mu$b). A further background reaction in the π^0-channel is the coherent π^0-photoproduction with a cross section of $\approx 35\,\mu$b. The total cross section for background reactions in the π^0-channel is therefore $\sigma_{tot}(\gamma,\pi^0) \approx 50\,\mu$b, which is at least a factor of 50 larger than the expected cross section for d'-formation. A high statistics measurement of the π^0 photoproduction thus enables a search for d' in the photoproduction. Based on these considerations first measurements have been carried out with the TAPS-setup at MAMI.

3. Investigation of the 2π production in pp collisions according to $pp \to d'\pi^+ \to pp\pi^-\pi^+$, where the NN-decoupled resonance d' could be produced hadronically in an elementary reaction. The d' contribution there has been estimated[3,4] to be in the order of (3 – 10)% of the conventional 2π cross section at 750 MeV, i.e. about 40 MeV above d' threshold. In case of I=0 the d' should show up only in the invariant-mass spectrum $M_{pp\pi^-}$, whereas in case of I=2 the resonance would appear both in $M_{pp\pi^-}$ and in $M_{pp\pi^+}$. The 2π production has been measured with the PROMICE/WASA detector at the CELSIUS storage ring.

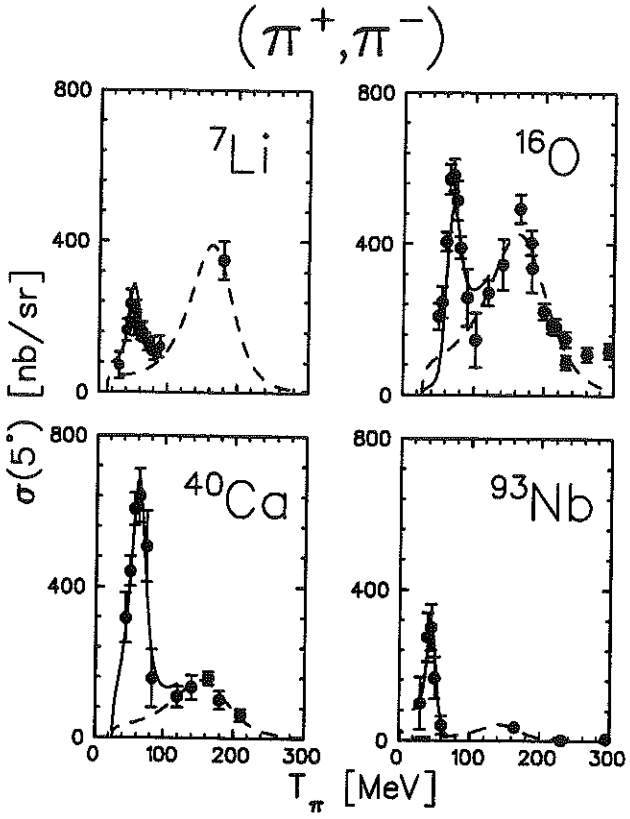

Figure. 1. Energy dependence of the forward angle cross sections for nonanalog GSTs. As examples the transitions on ^{7}Li[5], ^{16}O, ^{40}Ca[6] and ^{93}Nb[7] are shown. The data for $T_\pi \geq 100$ MeV are from LAMPF, the others are from PSI. The dashed lines indicate a phenomenological representation of the $\Delta\Delta$ process, whereas the solid lines show the result, if the d′ formation amplitude is added.

The DCX reaction on nuclei

The DCX measurements have been carried out with the LEPS spectrometer at PSI. Fig. 1 shows our results on ^{7}Li, ^{16}O, ^{40}Ca and ^{93}Nb for the forward angle cross section, together with the LAMPF-data at higher energies. In all cases the broad structure due to the excitation of the Δ-resonance is accompanied by a narrow, very pronounced peak at low energies, which is very well accounted for by the d′ hypothesis. This structure is also observed in our most recent measurements on ^{7}Li, which constitutes the lightest nucleus, where the DCX can proceed to a quasi-binary final state with ^{7}B$_{g.s.}$ being already proton instable. Inasmuch as the α-core can be considered as a spectator, this measurement constitutes already the observation of the d′ signature in a 3N-system.

So far no conventional reaction model can consistently describe the resonance-like structure in the energy excitation functions systematically observed in the DCX reaction at low energies. The most recent conventional calculations, which have been performed for the Ca-isotopes ^{42,44,48}Ca, can reproduce a peak-like structure at low energies[8]. For these cases however, d′ calculations using realistic values for the collision damping (spreading width) show that the expected d′ effect is very small[9]. So far no conventional calculations are available for angular distributions and for the DCX reaction on nuclei like ^{16}O or ^{40}Ca, where data of much higher statistics are available and also the d′ effects are much larger.

To minimize the influence of the nuclear medium DCX reactions on ^{3,4}He, which are the lightest nuclei where DCX is possible, have been studied by the CHAOS collaboration at TRIUMF (see contribution by R. Tacik to this conference).

*supported by the BMBF under contract 06 TÜ 886, by the DAAD (313/5) and by the DFG (Mu 705/3, Graduiertenkolleg and SFB 201

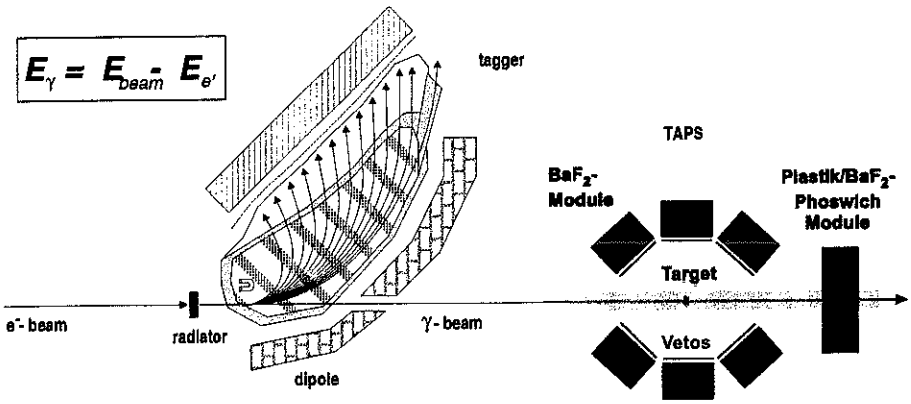

Figure. 2. Setup of the Glasgow tagger and the TAPS detector at the Mainz Microtron MAMI.

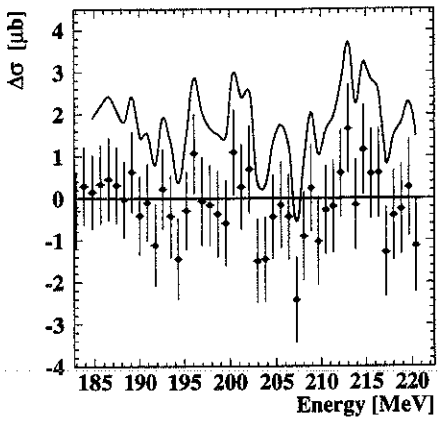

Figure. 3. Preliminary result for the upper limit at 90% C.L. (solid curve) for the production of a narrow resonance in the πNN system in the π^0-photoproduction on the deuteron. The data points show the difference of the measured total cross section and a 4th order polynomial fit to the data as function of energy.

π^0-Photoproduction on the Deuteron

A measurement of coherent and incoherent π^0 photoproduction off the deuteron with tagged photons from π^0 threshold up to the Δ region was performed with the TAPS detector together with the Glasgow tagger at MAMI (see figure 2). This experiment was very successful regarding conventional aspects: Integral and differential cross sections over the full angular range have been obtained, giving coherent and incoherent production cross sections which exhibit very different angle and energy dependences[10]. Considering the search for d′ however, this experiment has to be considered as a feasibility study only, since the integrated luminosity in the experiment was too small.

With the tagger resolution of $\Delta E_\gamma \approx 1\,\mathrm{MeV}$ an upper limit of $2 - 4\,\mu\mathrm{b} \cdot \mathrm{MeV}$ (90% C.L.) for the production of such resonances in this reaction can be deduced (see figure 3). Though these are the first stringent limits for dibaryon resonances in this reaction, they are still above the expected d′ production cross section which has been estimated to be smaller than $1\,\mu b$[2].

2π Production in Proton-Proton-Collisions

In addition to the d′ search, the 2π production in pp collisions has a number of very interesting aspects, in particular close to threshold. One aspect is the possibility to study the $\pi\pi$ interaction in detail. In cases where a bound nuclear system is formed in the exit channel there is the well documented ABC[11] effect, a long-standing problem not yet understood satisfactorily. For the basic reaction, the 2π production in pp collisions with its threshold at $T_p = 600\,\mathrm{MeV}$, there exist no or only low-statistics data in the interesting energy region below $T_p = 800\,\mathrm{MeV}$ — in particular there exist no exclusive measurements.

In order to obtain detailed information about the 2π production process and to search for the d′ resonance outside the nuclear medium exclusive measurements of the reaction $pp \to pp\pi^+\pi^-$ have been carried out at the CELSIUS storage ring of the The Svedberg Laboratory in Uppsala with the WASA/PROMICE setup[12]. Contributions of the d′ production to this reaction via $pp \to d'\pi^+ \to pp\pi^+\pi^-$ should show up as a small peak in the missing mass spectrum MM_{π^+} if the beam energy is above the d' threshold of $T_p \approx 713\,\mathrm{MeV}$.

The data from the 1995 run at $T_p = 750\,\mathrm{MeV}$ do exhibit such a small narrow structure near 2.06 GeV above the continuum of the conventional 2π production process, as expected from the d′ hypothesis[13]. The analysis of control reactions (single pion production) has as of yet not given any evidence for a major detector deficiency as a possible origin of this structure[14]. In order to confirm the observed structure and to clarify its possible nature, further measurements of the 2π production have been carried out. The analysis of these data is still in progress; at present the new data are in agreement with the published ones.

From the measurements at $T_p = 650$, 725 and 750 MeV total cross sections for the reaction $pp \to pp\pi^+\pi^-$ have been extracted (see Fig. 4). The data have been extrapolated

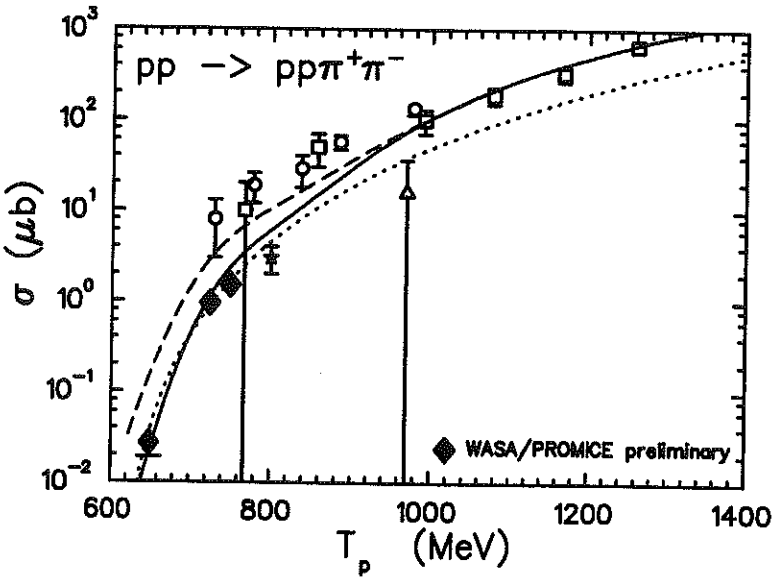

Figure. 4. Energy excitation function of the total cross section for the reaction $pp \to pp\pi^+\pi^-$. Shown are preliminary results of the WASA/PROMICE measurements in comparison with data from[15](○),[16](□),[17](⋆),[18](△) and theoretical calculations from Ref.[19] with (dashed) and without (solid) pp FSI. The dotted curve is an arbitrarily normalized phase space calculation.

to 4π acceptance assuming a pure phase space distribution. The luminosity has been determined with the simultaneously measured pp elastic data normalized to the SAID parametrisation[20]. The resulting total cross sections for 2π production are significantly smaller than the ones of Dakhno et al.[15] from the Leningrad Institute of Nuclear Physics. However, their data are based on quasifree pd bubble chamber measurements, not taking into account important corrections like the Fermi momenta of the involved nucleons in the d target when extracting the $pp \to pp\pi^+\pi^-$ cross sections. The Fermi correction will shift

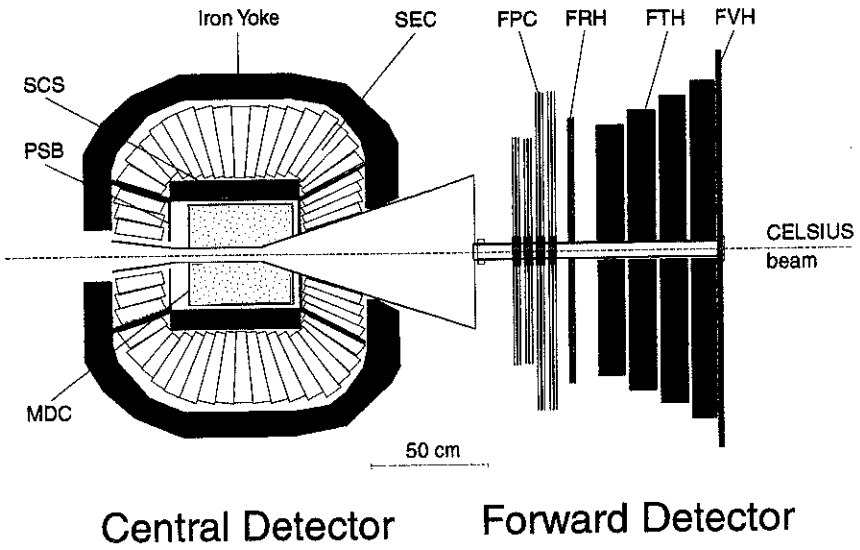

Figure. 5. The WASA detector at the CELSIUS storage ring.

their data points to higher energies by $\approx 50\,\mathrm{MeV}$, considerably reducing the discrepancy with other measurements. The systematic trend of the data is well described by a recent theoretical calculation[19], provided that pp FSI are *not* taken into account. From the knowledge of the total cross section and under the assumption of a d′ contribution of 7%[13] it is possible to estimate a d′ production cross section of $\approx 100\,\mathrm{nb}$ in the reaction $\mathrm{pp} \to \mathrm{pp}\pi^+\pi^-$ at 750 MeV. We note that this value is much smaller than the upper limit deduced recently in an inclusive measurement at ITEP[22].

Summary and Outlook

In this paper a large body of data obtained from experiments devoted to the search for the dibaryon candidate d′ has been presented. Despite these efforts we can not yet draw a conclusion about the existence or non-existence of d′. A statistically significant signal has been found in the DCX reaction on nuclei to discrete final states. This signature is in agreement with a formation of d′. However, such an interpretation is not accepted unequivocally since it suffers from the uncertainty with respect to the influcence of medium effects. Further experiments on light systems have been performed to search for d′. Results from the π^0 photoproduction on deuterium with TAPS at MAMI have been presented, where upper limits for the d′ production cross section in the range of $2-4\,\mu\mathrm{b}\cdot\mathrm{MeV}$ (90% C.L.) could be obtained — still significantly above the predicted production cross section.

Concerning the 2π production in pp collisions a first measurement with the PROMICE/-WASA detector at the CELSIUS storage ring yielded a promising result with an excess of events at 2.06 GeV in the $\mathrm{pp}\pi^-$ invariant mass spectrum. Further measurements with the aim of reproducing and confirming this result have been performed. The analysis is still going on. Because of detector calibration problems the analysis is very complex and time consuming. To overcome these problems and to improve on these experiments, the reaction not only has to be measured in a kinematically complete way (by detecting three of the four particles in the exit channel), but with a maximum of overconstraints. That is, all four particles in the exit channel have to be measured, requiring a detector with an acceptance close to 4π. At CELSIUS the construction of such a detector, the WASA detector, has just been finished with its inauguration having taken place during the recent PANIC'99 conference (see figure 5 and[21]). In addition the upgrade of the TOF detector at COSY at the FZ Jülich with a central calorimeter will provide an alternative possibility to perform kinematically overdetermined measurements to the d′ problem.

REFERENCES

1. R. Bilger, H. Clement, and M. Schepkin, Phys. Rev. Lett. **71**, 42 (1993).
2. R. Bilger et al., Nucl. Phys. **A 596**, 586 (1996).
3. M. Schepkin, O. Zaboronsky, and H. Clement, Z. Phys. **A 345**, 407 (1993).
4. H. Clement et al., Prog. Part. and Nucl. Phys. **36**, 369 (1996).
5. J. Pätzold et al., Phys. Lett. **B 443**, 77 (1998).
6. K. Föhl et al., Phys. Rev. Lett. **79**, 3849 (1997).
7. J. Pätzold et al., Phys. Lett. **B 428**, 18 (1998).
8. M. Nuseirat, M. A. K. Lodhi, M. O. El-Ghossain, W. R. Gibbs, and W. B. Kaufmann, Phys. Rev. **C 58**, 2292 (1998).
9. J. Draeger, Untersuchungen zum pionischen doppelten Ladungsaustausch in Atomkernen, Zulassungsarbeit, Universität Tübingen, Physikalisches Institut, 1999.
10. U. Siodlaczek et al., Contribution to PANIC 1999, to be published in Nucl. Phys. A.
11. A. Abashian, N. E. Booth, and K. M. Crowe, Phys. Rev. Lett. **5**, 258 (1960).
12. H. Calén et al., Nucl. Instr. Methods **A 379**, 57 (1996).
13. W. Brodowski et al., Z. Phys. **A 355**, 5 (1996).
14. A. Betsch et al., Phys. Lett. **B 446**, 179 (1999).
15. L. G. Dakhno et al., Sov. J. Nucl. Phys. **37**, 540 (1983).
16. F. Shimizu et al., Nucl. Phys. **A 386**, 571 (1982).
17. F. H. Cverna et al., Phys. Rev. **C 23**, 1698 (1981).
18. D. V. Bugg et al., Phys. Rev. **133**, B1017 (1964).
19. L. Alvarez-Ruso, E. Oset, and E. Hernandez Nucl. Phys. **A 633**, 519 (1998)
20. R. A. Arndt, C. H. Oh, I. I. Strakovsky, R. L. Workman, and F. Dohrmann, Phys. Rev. **C 56**, 3005 (1997).
21. CERN Courier **39:8**, 8 (1999).
22. B. M. Abramov et al., Eur. Phys. J. **A 1**, 115 (1998).

DCX Experiments and the Search for the d' with the CHAOS Detector at TRIUMF

R. Tacik for The CHAOS Collaboration
TRIUMF, 4004 Wesbrook Mall, Vancouver, B.C. Canada V6T 2A3

Abstract

The CHAOS Collaboration at TRIUMF has carried out several experiments investigating the pionic double charge exchange (DCX) reactions on ^{3}He and ^{4}He. Measurements have been made of inclusive total cross sections, as well as for semi-exclusive channels. The data have been analyzed searching for a signal of the hypothetical d' dibaryon. These analyses indicate that any d' contribution to the DCX reactions is not as large as had been originally predicted.

Introduction

A narrow NN decoupled dibaryon, called the d', has been suggested as the explanation for the peculiar behavior of nuclear pionic double charge exchange (DCX) to discrete final states[1]. For a wide range of nuclear targets, the excitation function of the forward angle DCX cross section shows a resonance-like peak around 50 MeV. In order to minimize possible nuclear structure effects, the CHAOS Collaboration at TRIUMF has investigated the DCX reaction and searched for evidence for the d' using the lightest possible nuclear targets, the ^{3,4}He isotopes. We have performed two inclusive and two semi-exclusive measurements, which are discussed below. All the experiments were performed at TRIUMF on the M11 channel using the CHAOS spectrometer. For a status report on other d' searches, see the contribution of R. Bilger to this conference.

CHAOS consists of a cylindrical dipole magnet which produces a vertical magnetic field. Four concentric cylindrical wire chambers surround the centre of the magnet, where scattering targets can be located. The wire chambers are enclosed by a concentric cylindrical array of scintillation counters and Pb-glass detectors. CHAOS has full 360° angular acceptance in the horizontal plane, and ±7° acceptance out-of-plane. It features good energy resolution, good particle detection capabilities, a flexible and sophisticated multi-level hardware trigger system, and can withstand high incident beam rates. More details can be found in Ref.[2].

E725: The Inclusive ^{4}He(π^+,π^-) Reaction

In this experiment we measured the energy dependence of the ^{4}He (π^+,π^-) total cross sections. The total cross sections were determined by extrapolating the differential distributions $(d^2\sigma/d\Omega dp)$ measured with CHAOS. The well known ^{4}He (π^+,π^+) elastic scattering cross sections[3] were also measured and used for normalization. The liquid ^{4}He target used for the measurements was constructed at the University of Regina and TRIUMF. Data were taken at 70, 80, 90, 100, 115, and 130 MeV.

The main motivation for this experiment comes from the fact that following DCX on ^{4}He, we are left with four identical protons in the final state. These cannot all be in relative $\ell = 0$, and thus calculations based on conventional mechanisms all predict small DCX cross sections near threshold, which increase slowly and smoothly with increasing energy. On the other hand, predictions based on the d' mechanism[4] show a sharp rise in the DCX cross section just above the d' threshold.

Results for this experiment have already been presented at MENU '97, and have been published by Gräter *et al.*[5]. Briefly, there appears to be a 'shoulder' in the data at $\sim$ 90 – 100 MeV, which is not present in conventional calculations based on the sequential single charge exchange (SSCX) mechanism. This shoulder is reproduced if the predicted contribution for d' production is added to the cross section calculated with an on-shell Monte Carlo model of the conventional mechanism. This result supports the d' hypothesis, but does not constitute a proof of its existence.

E719: The Semi-Exclusive ^{4}He$(\pi^+, \pi^- pp)pp$ Reaction

The motivation for this experiment was the same as for E725, but with an emphasis on searching for direct rather than indirect evidence for the d'. If the reaction proceeds via the two step mechanism $\pi^+ {}^4\text{He} \rightarrow d'pp \rightarrow \pi^- pppp$, then a signature of the d' would be a peak in the $\pi^- pp$ invariant mass spectrum.

The are several complications which made this a difficult experiment to perform. Since the protons emerging from the reaction have low energies, we couldn't use a liquid ^{4}He target, and employed instead a helium gas target at STP, filling the inner volume of the first CHAOS wire chamber. Even so, most protons did not reach the outer wire chamber or CHAOS trigger scintillators, and had to be reconstructed from short tracks. In addition, there is a large combinatorial background due to the detection of 'spectator' protons rather that the ones which come from the d' decay.

Measurements were performed at incident π^+ kinetic energies of 105 and 115 MeV. Since the d' contribution to the DCX cross section is predicted to be largest near the d' threshold, one might have expected that it would have been preferable to take data at lower energies. However, simulations showed that the $\pi^- pp$ invariant mass distribution from the conventional nonresonant process looked very similar to the expected spectrum for d' production for energies less than about 30 MeV above the d' threshold.

The invariant mass spectra constructed from the momenta of the detected π^- and protons are shown in Fig. 1[6]. The data points are shown with statistical error bars. The solid line represents the results of an on-shell Monte Carlo model of the conventional SSCX mechanism. The dashed line shows the d' model prediction. Both these curves represent the 'best fit' to the data. The dotted curve represents five-body phase space. To avoid confusion with the other curves, this line has not be fitted to the data. For the 115 MeV data, no d' contribution was required in the best fit, but a d' contribution of 42% was allowed at a 90% confidence level. The 105 MeV data required a 23% d' contribution in the best fit.

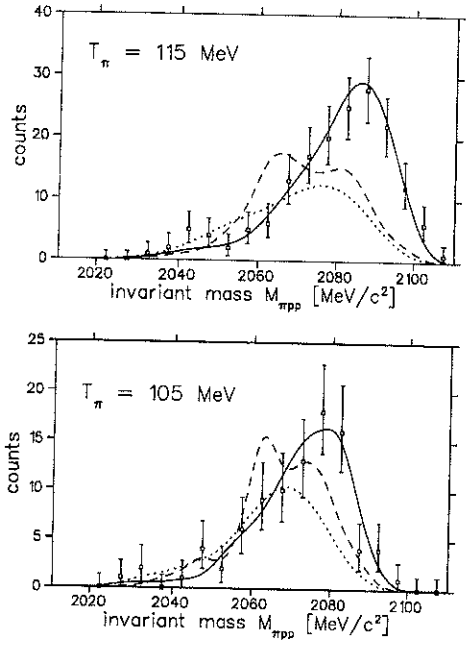

Fig. 1. Invariant mass histograms constructed from the π^- and two protons detected in E719. Solid line: SSCX model; dashed line: d' model; dotted line: phase space. Taken from Ref.[6]

The invariant mass distribution can also be determined using the π^- and the reconstructed momenta of two protons which were *not* detected. The results for this case are shown in Fig. 2[6]. The various line types represent the same models as in Fig. 1. As for Fig. 1., the SSCX model appears to adequately explain the data at both energies. For the

105 MeV data, no d' contribution is required for the best fit, and up to 62% at the 90% confidence level.

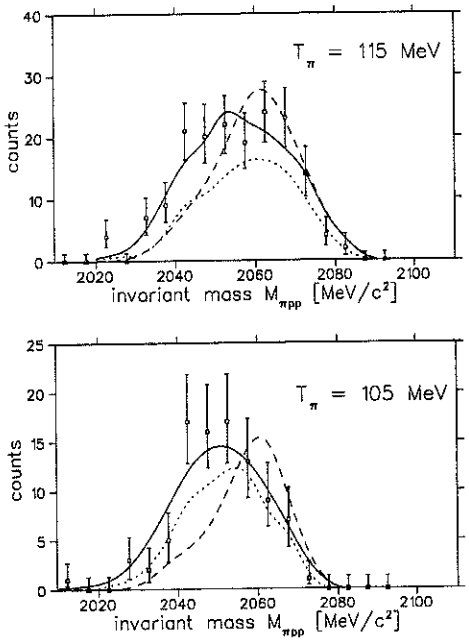

Fig. 2. Invariant mass histograms contructed from the π^- and the two protons which were *not* detected. Curves as in Fig. 1. Taken from Ref.[6]

E785(a): The Semi-Exclusive ^{3}He$(\pi^-, \pi^+ n)nn$ Reaction

As for E719, in this experiment we looked for direct evidence for the d'. If the reaction proceeds via d' production and decay, i.e. $\pi^-{}^3\text{He} \rightarrow d'n \rightarrow \pi^+nnn$, then the intermediate state is a two-body system, and the neutron recoiling against the d' should be monoenergetic at a given angle.

Along with the possibility of obtaining a much cleaner signal for the existence of the d', this experiment has several additional advantages over E719. The combinatorial background, due in this case to the detection of one of the neutrons from d' decay rather than the one from the two-body intermediate state, is lower. A liquid target can be used. Measurements can be performed at incident pion energies close to the d' threshold, where predicted cross sections are large.

A disadvantage comes from the increase in complexity and loss of solid angle coverage due to the operation of an external neutron detector in addition to CHAOS. In this experiment, the outgoing π^+ was detected in CHAOS, and served as a tag for the DCX reaction. Neutrons were detected in coincidence in a time-of-flight (tof) array. The array consisted of two layers. Each layer was composed of seven bars of plastic scintillator. Each bar had dimensions $15 \times 15 \times 105$ cm^3. The front face of the front layer was 350 cm from the centre of CHAOS. Three large plastic scintillator paddles positioned in front of the array were used to veto charged particles.

Measurements were taken at two angular settings of the neutron detector at an incident π^- energy of 75 MeV, and one angular setting at 65 MeV. A schematic diagram of the top view of the experimental arrangement is given in Fig. 3. This figure shows the neutron array in its forward-angle position, where the bulk of the experimental data were taken. Emphasis was placed on forward angles because the angular distribution of neutrons from the analogous $\pi^-{}^3\text{He} \rightarrow dn$ reaction is forward peaked. This known reaction[7], with the deuteron detected in CHAOS and the neutron detected in the tof array, was used to monitor the experiment.

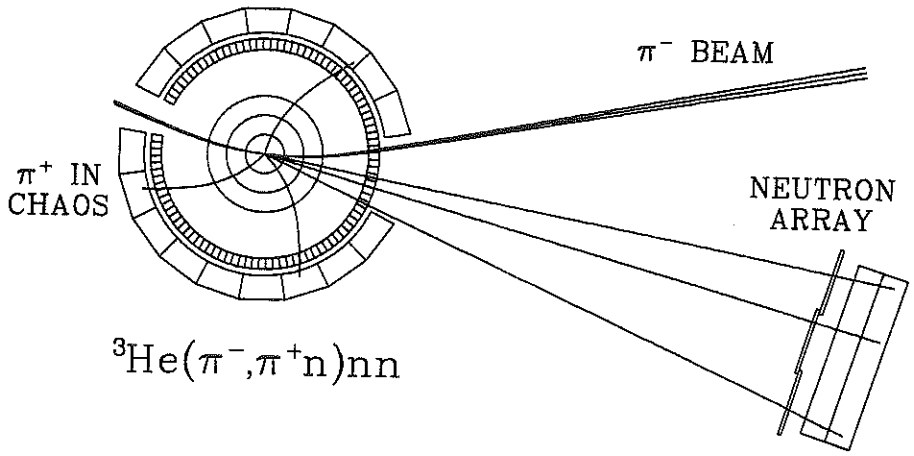

Fig. 3. Schematic scale view of the experimental set-up for E785.

Preliminary results for the neutron tof spectrum measured with $T_{\pi^-} = 75$ MeV at $\theta_n \simeq 11°$ are given in Fig. 4. The data are represented by the solid histograms and are repeated three times to facilitate comparison with model predictions. The model predictions are represented by the dashed histograms, and the curves shown are 'best fit' ones. The upper plot in Fig. 4 shows the comparison with the predictions of a conventional sequential single charge exchange model. The comparison with the d' model, which predicts a sharp peak above a smooth background, is shown in the middle plot. The lower plot shows the comparison with four-body phase space, which assumes that all three nucleons in ^{3}He participate in the DCX reaction. Clearly, the data do not favour the d' model. The best description of the data is provided by a combination of the four-body phase space and SSCX curves.

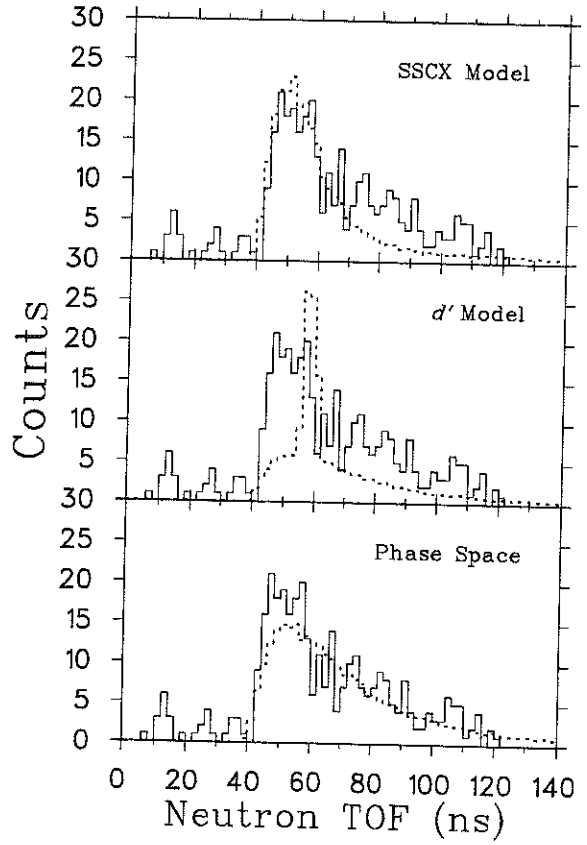

Fig. 4. Neutron time-of-flight distribution measured in E785. The solid histogram represents the data, the dashed histograms represent the predictions of various model calculations.

E785(b): The Inclusive ^{3}He(π^-,π^+) Reaction

Total cross sections for the ^{3}He(π^-,π^+) reaction were measured during a relatively short part of the beam period devoted to measurements of the semi-exclusive ^{3}He(π^-,π^+n) reaction. The same University of Regina/TRIUMF liquid helium target was used as in E725, but modified to condense ^{3}He rather than ^{4}He. The motivation for the measurement was similar and complementary to that for E725. Prior to this experiment, there were no data for DCX on ^{3}He below 120 MeV. As for E725, total cross sections were determined by extrapolating measured $d^2\sigma/d\Omega dp$ differential distributions. Data were obtained at 65, 70, 75, 80, 90, 100, and 120 MeV.

Results are shown in Fig. 5[8]. The solid curve in this figure represents the results of an on-shell Monte Carlo model of the conventional SSCX mechanism. The dashed curve represents the original prediction based on the d' model[4]. The data clearly lie far below the prediction. However, it has been pointed out[8] that the original prediction ignored the possibility of 'collision damping'. That is, rather than decay, $d' \rightarrow NN\pi$, the d', once formed, may disappear via the $d'N \rightarrow NNN$ reaction. Accounting for 'collision damping' reduces the prediction of the d' contribution to the total DCX cross section considerably. The dash-dotted curve in Fig. 5 shows the results of the d' calculation including the estimated effect of this process. The dotted line in Fig. 5 is the incoherent sum of the calculations represented by the solid and dash-dotted curves.

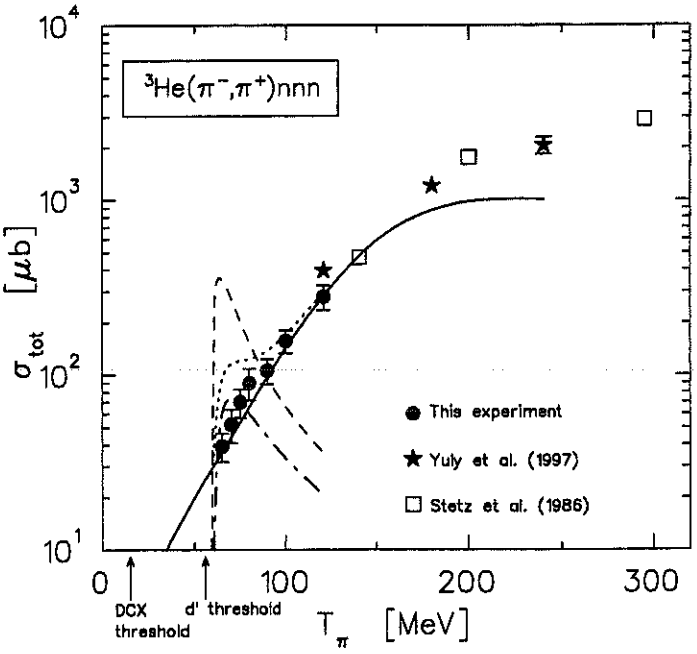

Fig. 5. Total cross section for the ^{3}He(π^-,π^+) reaction. See text for details.

Naturally, the 'collision damping' effect should also affect the predictions for the DCX on ^{4}He, which were measured in E725. The new predictions are shown in Fig. 6[8]. Here, the solid curve represents the results of an on-shell Monte Carlo model of the conventional SSCX mechanism, the dashed curve the d' calculation using a Gaussian ^{4}He wave function[4] without 'collision damping', and the dot-dashed curve the d' calculation for the Gaussian ^{4}He wave function with 'collision damping'. The dotted line is the incoherent sum of the conventional calculation and the d' calculation with 'collision damping'.

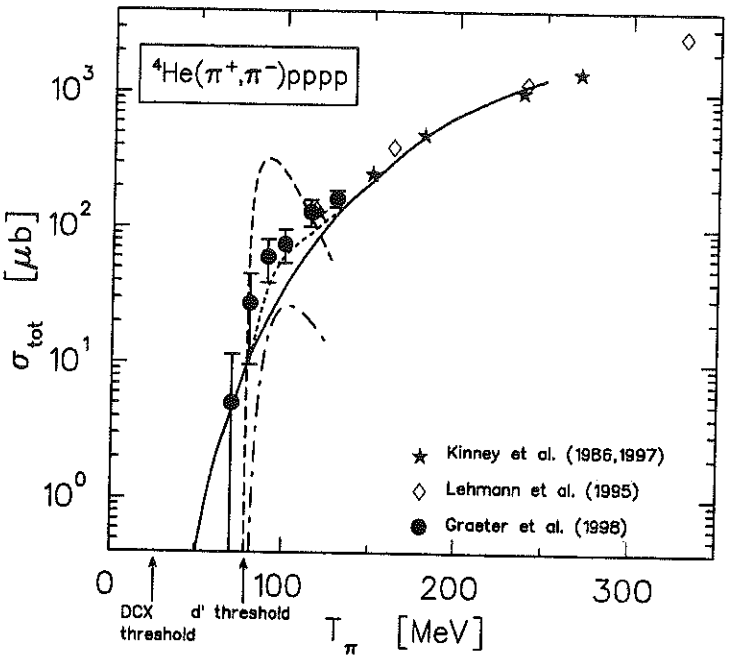

Fig. 6. Total cross section for the ^{4}He(π^+,π^-) reaction. See text for details.

Summary

The measured total cross sections for DCX on ^{4}He show some structure and seemed to support the d' hypothesis. However, the two experiments which should have provided direct evidence for the d', ^{4}He($\pi^+,\pi^- pp$) and ^{3}He($\pi^-,\pi^+ n$), did not reveal as large a signal as had been originally predicted. Nor did the measured total cross sections on ^{3}He. It has now been realized that the original predictions overestimated the d' contribution to DCX because they ignored the possibility of 'collision damping', i.e. $d'N \rightarrow NNN$.

The conventional SSCX model provides a qualitative description of much of the DCX data, but does not describe the ^{4}He(π^+,π^-) total cross sections. Nor does it provide a quantitative description of the pion momentum distributions for either ^{4}He(π^+,π^-) or the ^{3}He(π^-,π^+) reaction. Regardless of the existence of the d', the CHAOS experiments extend the world data base for the DCX reaction at low energies down to the lightest nuclei. It is hoped that the present work will motivate efforts to develop a microscopic theory which will ultimately lead to a good understanding of the underlying reaction mechanism.

REFERENCES

1. R. Bilger *et al.*, Z. Phys. **A343** (92) 491; Phys. Rev. Lett. **71** (93) 42; Phys. Rev. Lett. **72** (94) 2972.
2. G.R. Smith *et al.*, Nucl. Inst. Meth. **A362** (95) 349.
3. B. Brinkmöller and H.G. Schlaile, Phys. Rev. **C48** (93) 1973.
4. H. Clement, M. Schepkin, G.J. Wagner, O. Zaboronsky, Phys. Lett **B337** (94) 43.
5. J. Gräter *et al.*, Phys. Lett. **B420** (98) 37; Phys. Rev. **C58** (98) 1576.
6. J. Clark, PhD Thesis, University of Melbourne; J. Clark *et al.* to be published.
7. P. Weber *et al.*, Nucl. Phys. **A534** (91) 541.
8. J. Gräter *et al.*, accepted for publication in Phys. Lett. **B**.

Meson Production Near Threshold in Nucleon-Nucleon Collisions

T. Johansson
Dept. of Radiation Sciences, Uppsala University, Box 535, S-75121 Uppsala, Sweden

representing the PROMICE/WASA collaboration*

Abstract

The PROMICE/WASA collaboration has studied π and η meson production in nucleon-nucleon collisions near threshold using the CELSIUS ring at the The Svedberg Laboratory, Uppsala. Some of the reaction channels are measured for the first time in any detail. The results are presented together with an outlook.

INTRODUCTION

The study of meson production in light ion collisions has regained interest over recent years. The reason is that, for the first time, high quality data are now available for practically all relevant reaction channels in the threshold region. One objective of these measurements is the study of the reaction mechanism. The interpretation of the data is facilitated by the fact that only the lowest partial waves contribute near threshold. There are also relatively high momentum transfers involved, so that the relevant length scale for π production in N-N reactions is of the order 0.5 fm, which is a region where the two nucleons overlap. There is therefore the prospect of learning something about the short-range part of the N-N interaction in these reactions. In addition, the low relative velocities between the final state particles makes the final state interaction (FSI) important. This is a source for information about low energy meson-nucleon interactions.
Meson production near threshold is a main topic for the experimental programme at the CELSIUS ring at the The Svedberg Laboratory in Uppsala. This paper reviews results obtained by the PROMICE/WASA collaboration at CELSIUS on π and η meson production in proton-nucleon collisions. Results from 2π production are presented by R. Bilger in these proceedings.

THE PROMICE/WASA EXPERIMENT

The Experimental Method

The PROMICE/WASA (PW) experiment was designed to study meson production in the threshold region. It has the capability of measuring both photons and charged particles and a cross section of the set-up in the horizontal plane is shown in Fig. 1. The apparatus has two main constituents, *viz.* a Forward Detector (FD) and a Central Detector (CD). The forward detector has essentially full acceptance for charged particles emitted in an angular range between 4 and 21°. Its main components are a tracker (FPC), used for precise particle track reconstruction, a scintillator hodoscope for triggering and fast pixel determination (FHD), and a scintillator range hodoscope for energy measurements (FRH). The FD is complemented by a hodoscope (FVH) at the rear, to register penetrating particles, and four scintillators near the scattering chamber (FWC) for trigger purposes. The CD is made from two arrays of CsI(Na) crystals arranged in 7×8 matrices (CEC). In front of each array there are scintillators for charged particle identification/rejection (CDE). More details on the PW experimental set-up can be found in Ref.[1]. Additionally, the CELSIUS magnets in the quadrant following the experimental set-up have been used as a spectrometer to detect charged reaction products emitted near zero degrees.
The experiments were performed using a cluster-jet target, giving a typical target density of 10^{14} atoms/cm^2, and a circulating beam of a few times 10^{10} protons. This provides luminosities of the order of 5×10^{30} cm^{2}s^{-1}.

*http://www.tsl.uu.se/wasa

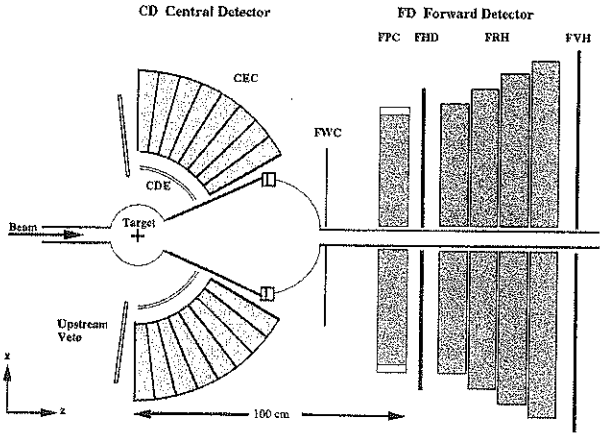

Fig. 1. The PROMICE/WASA experiment.

The $pp \to pp\pi^0$ Reaction

Pion production in $N-N$ collisions near threshold was believed to be well understood for a long time assuming a reaction mechanism with a direct emission term (Born term), together with pion (on-shell) rescattering[2]. It came therefore as a surprise that this theory underpredicted the $pp \to pp\pi^0$ cross section by a factor of five[3] when high quality data became avaliable from IUCF[4,5]. The magnitude of the cross section has subsequently been verified by the PW experiment[6] and which extended the data down to a CM excess energy, Q_{cm} ($Q_{cm} = \sqrt{s} - m_{final}$), of 0.5 MeV. The data are shown in Fig. 2.

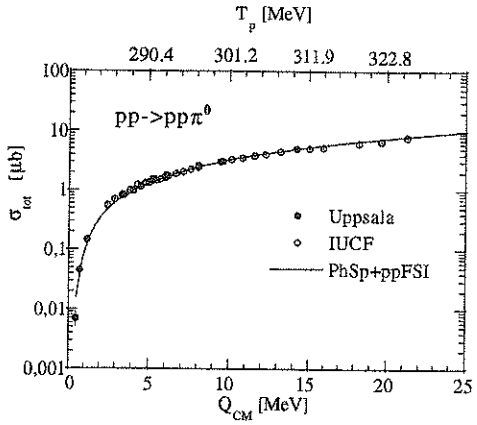

Fig. 2. The near threshold $pp \to pp\pi^0$ cross section plotted as a function of Q_{cm}[4–6]. The equivalent proton energy is shown at the top. The solid line represents a calculation using phase space and pp FSI (arbitrarily normalised).

Two different mechanisms have been proposed to counter this deficiency, *viz.* the inclusion of heavy meson exchanges, *i.e.* short-range physics, and off-shell pion rescattering. Both of them are likely important and more theoretical work is needed for an understanding of this reaction. A review of the theoretical approaches can be found in Ref.[7].

The only surviving production amplitude at threshold corresponds to the transition ${}^3P_0 \to {}^1S_0\, s$, where the standard ${}^{2S+1}L_J$ notation is used for the pp system, with the lower case letter denoting the angular momentum of the meson. Such a transition would lead to isotropic angular distributions but an analysis of a high statistics experiment[8] undertaken at Q_{cm}= 14 MeV (T_p = 310 MeV) shows a clear anisotropy in the π^0-angular distribution as demonstrated in Fig. 2a.

We have used a phenomenological description of the differential distributions for the acceptance corrections and taken the unpolarised matrix element to be of the form

$$|M|^2 = |A|^2 + \left[2\Re\left(A^*B\right)\frac{k^2}{\mu^2} + |B|^2\frac{k^4}{\mu^4}\right]\cos^2\theta_\pi + |C|^2\frac{q^2}{\mu^2} + |D|^2\frac{k^2q^2}{\mu^4}\sin^2\theta_{pp} \qquad (1)$$

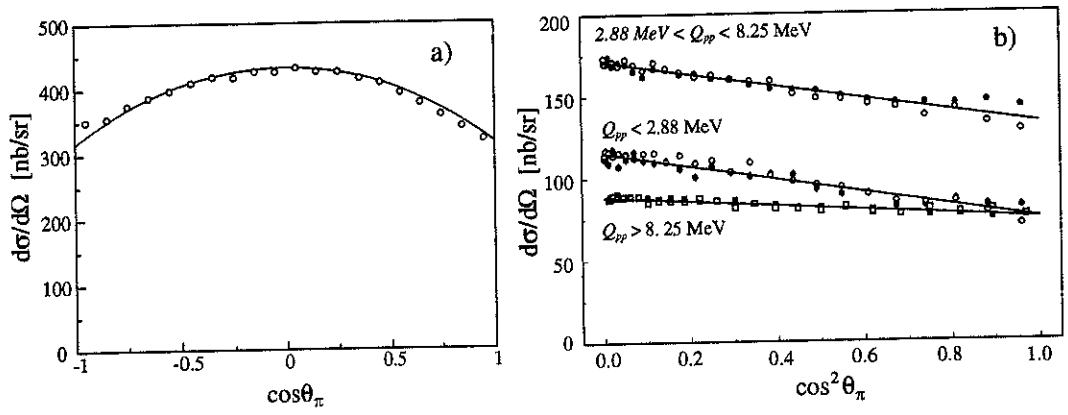

Fig. 3. a) Differential cross section for the $pp \to pp\pi^0$ cross section at $Q_{cm} = 14$ MeV as a function of the cosine of the pion production angle in the overall CM system[8]. The solid line correspond to the the parametrisation of Eq. (1). b) The same data as in (a) as a function of $cos^2\theta_\pi$ in three bins of excitation energy of the final state pp pair, Q_{pp}. The open and closed symbols correspond to data in the two hemispheres.

The momentum of pion in the overall CM system is denoted by k, $2q$ is the relative momentum in the final two-proton system, and μ is the reduced mass in the final state. θ_π is the polar angle of the π^0 in the overall CM system, and θ_{pp} that of the pp relative momentum. The amplitude A corresponds to an admixture of the dominant $^3P_0 \to {}^1S_0\, s$ and the $^3P_2 \to {}^1S_0\, d$ transitions and B to the transition $^3P_2 \to {}^1S_0\, d$. The effect of the proton-proton final state interaction has been taken into account by a multiplicative factor $F_{fsi}(q)$ calculated from the Paris wave function[9]. Agreement with the observed pion angular distribution is only found with $B = (1.2 \pm 0.2)A$, showing that pion d-waves cannot be neglected even this close to threshold. The k^2 dependence of the $s-d$ interference term suggests that the angular asymmetry should increase with decreasing relative proton momenta. This is illustrated in Fig. 3b, where the pion angular distribution is plotted in three intervals of relative proton momenta. The data clearly follow this trend and there is good agreement with the parametrisation of the amplitudes (solid lines). These findings are in agreement with data from RNCP[10]. Work is now in progress within the PW collaboration to analyse differential cross sections with high statistics using data taken at several energies between $Q_{cm} = 14$ MeV and 67 MeV.

η production in pN collisions

In contrast to the pion case, η production near threshold is believed to be dominated by an S-wave resonance, the $N^*(1535)S_{11}$. Theoretical calculations for this process are generally based on the one-boson-exchange model[11] and, although similar in spirit, they differ significantly in their assumptions of the relative importance of different meson exchanges. Therefore data are needed from different channels to clarify the situation. In addition, the presence of the $N^*(1535)$ should influence the observables near threshold, where S-waves dominate, and give rise to a strongly attractive ηN FSI. It has in fact been suggested that this interaction might be strong enough for quasi-bound states to be formed already for the two-nucleon system[12–14].

The total cross section of the $pp \to pp\eta$ reaction, which is a pure isospin-one channel, has been measured by the PW collaboration in a similar fashion to the π^0 experiment[15]. These data are shown in Fig. 4 (open circles) together with data from SATURNE (open diamonds)[16–18] and COSY (open triangles)[19,20]. It is worth mentioning that, unlike the π^0 case, these data do not follow the shape of phase space modified by the pp FSI, demonstrating the importance of the ηN FSI.
To learn more about the η production process one should study the isospin-zero channel.

The pn channel is a mixture of $I = 0$ and $I = 1$, but previous data in this area have been very limited[21,22]. With the PW set-up it was possible, for the first time, to isolate the exclusive pp and pn quasi-free reaction channels by using a deuterium gas-jet target[23–25]. The excitation energy for these reactions could be extracted by exploiting the Fermi momentum of the target nucleon, which affects the CM energy on a event-by-event basis, staying at one fixed beam energy. The resulting quasi-free cross sections for the $pp \to pp\eta$, $pn \to pn\eta$ and $pn \to d\eta$ reactions are shown in Fig. 4. The quasi-free $pp \to pp\eta$ data (open squares) show quite good agreement with the free cross section, giving confidence in the analysis method. The energy dependence of the $pn \to pn\eta$ and $pp \to pp\eta$ cross sections are very similar, but with the former being approximately 6.5 larger. This ratio shows that the $I = 0$ cross section is substantially larger than the $I = 1$ and points to the importance of isovector exchanges in these processes[25]. The fact that the $d\eta$ channel dominates over the $pn\eta$ one for $Q_{cm} < 60$ MeV can be understood from phase space argument.

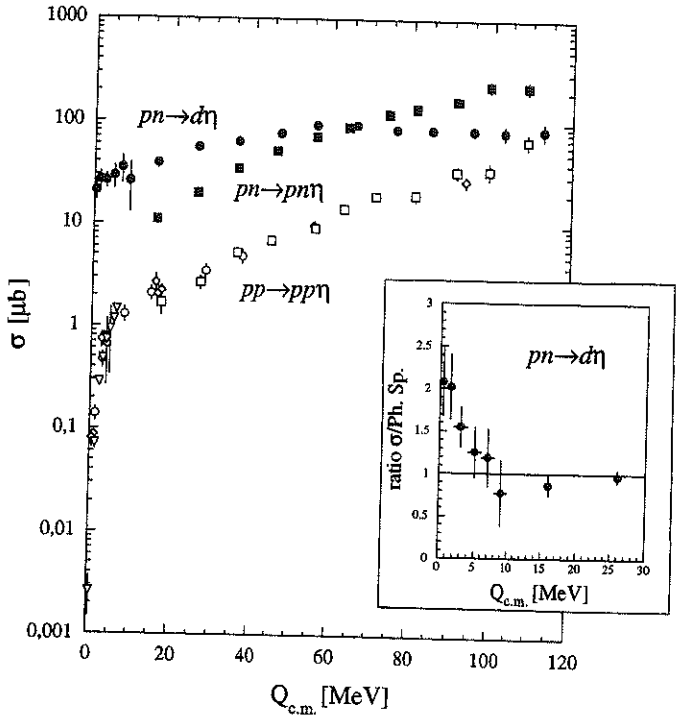

Fig. 4. Total cross sections for the $pp \to pp\eta$ (open symbols)[15–20,23], $pn \to pn\eta$ (solid squares)[25], $pn \to d\eta$ (solid circles)[23,24] reactions. The insert shows the ratio between the measured $pn \to d\eta$ cross section and the two-body phase space in the vicinity of the threshold

It is interesting to investigate the cross section very close to threshold in more detail since this is the region where effects from FSI are the most important. The insert in Fig. 4 shows the ratio between the the experimental $pn \to d\eta$ cross section and the expectation from the two-body phase space. A relative enhancement of the cross section when approaching the threshold is observed, which is typical for a strong and attractive FSI. Whether this reflects presence of a quasi-bound state, or merely a large ηd scattering length remains to be seen.

Differential cross sections have only been been extracted for the $pp \to pp\eta$ reaction at $Q_{cm} = 16$ MeV and 37 MeV[26]. The η angular distribution at $Q_{cm} = 37$ MeV in Fig. 5a shows a negative $\cos^2\theta$ behaviour, indicating the presence of d-waves at this energy. The solid line corresponds to a parametrisation similar to Eq. (1). No significant deviation from isotropy was observed at $Q_{cm} = 16$ MeV. A similar behaviour is observed for the η angular distributions in the $\gamma p \to p\eta$ reaction[27]. Adopting the idea of vector dominance for photoproduction, this point to the importance of ρ-exchange in these processes. The importance of pp FSI is clearly manifested in the η kinetic energy distribution in Fig. 5b. It is strongly shifted towards higher energies with respect to phase space (dashed line). This is a consequence of the strong and attractive FSI between the protons in the $^1S_0$ configuration, which enhances the number of events where the η recoils against protons with low relative momenta.

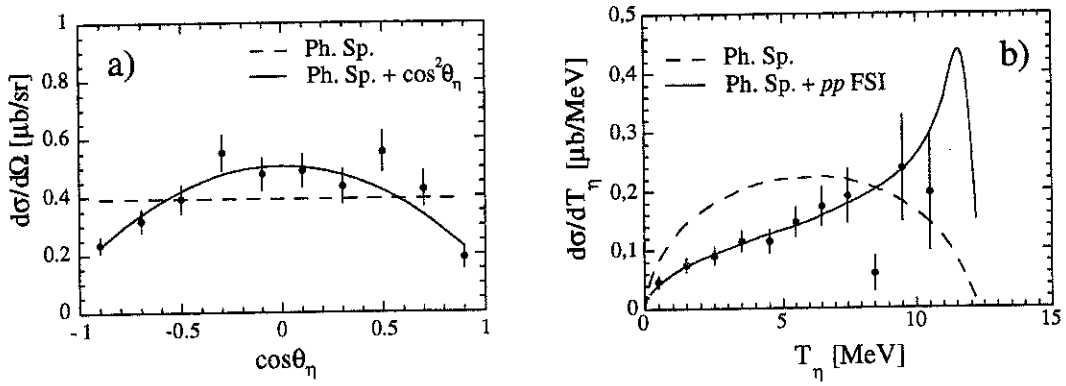

Fig. 5. Differential cross sections for the $pp \to pp\eta$ in the CM system[26]. a) The η angular distribution at $Q_{cm} = 37$ MeV. The dashed curve represents isotropic emission and the solid curve includes a $cos^2\theta$ dependence (see Eq. (1)). b) The η kinetic energy distribution at $Q_{cm} = 16$ MeV. The dashed curve represents phase space distribution whereas the solid line includes the pp FSI.

CONCLUSIONS AND OUTLOOK

Light meson production has been studied in proton-nucleon collisions at the CELSIUS cooler/storage ring by the PROMICE/WASA collaboration. The results include several new findings.

- Non-isotropic meson angular distributions are seen for both the $pp \to pp\pi^0$ and the $pp \to pp\eta$ reactions, showing an early onset of d-waves.
- The excitation functions for the $pn \to pn\eta, d\eta$ reactions have been measured for the first time. The $pn \to pn\eta$ cross section is approximately 6.5 times higher than that for $pp \to pp\eta$, showing the dominance of the isospin zero channel.
- The very near threshold data on the quasi-free $pn \to d\eta$ reaction shows experimental support for a strong and attractive ηN interaction.

To learn more one should measure differential cross sections in detail and the first steps have been taken for the $pp \to pp\pi^0$ and $pp \to pp\eta$ reactions by the PW collaboration. A high acceptance over all the phase space is important for such studies and the PW set-up had limitations in this respect. A new detector system with very high acceptance, WASA 4π, has been designed[28] and is presently being commissioned at the CELSIUS ring. This will allow for unprecedented measurements of differential cross sections as well as rare reactions and meson decays.

REFERENCES

1. H. Calén *et al.*, "Detector setup for a storage ring with an internal target," Nucl. Instr. and Meth. **A379**, 57 (1996).
2. D.S. Koltun and A. Reitan, "Production and absorption of S-wave pions at low energy by two nucleons," Phys. Rev. **141**, 1413 (1966).
3. G.A. Miller and P. Sauer, "Total cross section for $pp \to pp\pi^0$ near threshold," Phys. Rev. **C44**, R1725 (1991).
4. H.O. Meyer *et al.*, "Total cross-section for $p+p \to p+p+\pi^0$ near threshold measured with the Indiana cooler," Phys. Rev. Lett. **65**, 2846 (1990).
5. H.O. Meyer *et al.*, "Total cross-section for $p + p \to p + p + \pi^0$ close to threshold," Nucl. Phys. **A539**, 633 (1992).
6. A. Bondar *et al.*, "The $pp \to pp\pi^0$ reaction near the kinematical threshold," Phys. Lett. **B356**, 8 (1995).
7. T.-S.H. Lee, "Recent development in theories of pion production in nucleon-nucleon collisions," in *Proc. 7th Conf. on Mesons and Light Nuclei '98* (World Scientific, Singapore, 1999) pp. 379–390.

8. J. Złomańczuk *et al.,* "Pionic D-wave effects in $pp \to pp\pi^0$ near threshold," Phys. Lett. **B436**, 251 (1998).
9. M. Lacombe *et al.,* "Parameterization of the deuteron wave function of the Paris N-N potential," Phys. Lett. **101B**, 139 (1981).
10. Y. Maeda *et al.,* "Pion production mechanism from near threshold to Δ-resonance region," in *Proc. 6th Int. Symp. on Meson-Nucleon Physics and the Structure of the Nucleon* (πN Newsletter 13, Vancouver, 1997) pp. 326–329.
11. J.F. Germond and C. Wilkin, "The $pp \to pp\eta$ reaction near threshold," Nucl. Phys. **A518**, 308 (1990);
    J.M. Laget, F. Wellers and J.F. Lecolley, "η meson production in nucleon-nucleon collisions," Phys. Lett. **B257** 258 (1991);
    T. Vetter *et al.,* "η production in nucleon-nucleon collisions," Phys. Lett. **B263**, 153 (1991);
    E. Gedalin, A. Moalem and L. Razdolskaja, "On the $pp \to pp\eta(\eta')$ reactions near threshold," Nucl. Phys. **A650** 471 (1999), and references therein;
    M. Batinic, I. Slaus and A. Svarc, "Near threshold η production in proton-proton collisions," Phys. Scr. **56**, 321 (1997);
    V. Bernard, N. Kaiser and U.-G. Meissner, "Novel approach to pion and eta production in proton-proton collisions near threshold," Eur. Phys. J. **A4**, 259 (1999).
12. T. Ueda, "I=0, J^P=1^- Quasibound state in the $\eta NN - \pi NN$ coupled system," Phys. Rev. Lett. **66**, 297 (1991).
13. S.A. Rakityansky *et al.,* " Quasibound states of η-nucleus systems," Phys. Rev. **C53**, R2043 (1996)
14. A.M. Green, J.A. Niskanen and S. Wycech, "η-deuteron scattering," Phys. Rev. **C54**, 1970 (1996).
15. H. Calén *et al.,* "The $pp \to pp\eta$ reaction near the kinematical threshold," Phys. Lett. **B366**, 39 (1996).
16. A.M. Bergdolt *et al.,* "Total cross section of the $pp \to pp\eta$ reaction near threshold," Phys. Rev. **D48**, R2969 (1993).
17. E. Chiavassa *et al.,* "Measurement of the $pp \to pp\eta$ total cross section between 1.265 and 1.50 GeV," Phys. Lett. **B322**, 270 (1994).
18. F. Hibou *et al.,* "Comparison of η and η' production in the $pp \to pp\eta(\eta')$ reactions near threshold," Phys. Lett. **B438**, 41 (1998).
19. COSY 11 Collaboration, "Production of η mesons at the COSY-11 installation," FZ Jülich Ann. Rep. 1995, p. 39.
20. P. Wüstner, "Die Produktion des η-Mesons am Jülicher Beschleuniger COSY und Entwicklung eines optimierten Datenaufnamesytems'", PhD Thesis, Ruhr-Universtät Bochum, 1998.
21. F. Plouin, P. Fleury and C. Wilkin, "Identification and analysis of the $np \to d\eta$ cross section near threshold," Phys. Rev. Lett. **65**, 690 (1990).
22. E. Chiavassa *et al.,* "η-meson production in pd and pp collisions," Phys. Lett. **B337**, 192 (1994).
23. H. Calén *et al.,* "Measurement of the quasifree $p+n \to d+\eta$ reaction near threshold," Phys. Rev. Lett. **79**, 2642 (1997).
24. H. Calén *et al.,* "Threshold structure of the quasifree $p + n \to d + \eta$ reaction," Phys. Rev. Lett. **80**, 2069 (1998).
25. H. Calén *et al.,* "Measurement of the quasi-free $p + n \to p + n + \eta$ reaction," Phys. Rev. **C80**, 2667 (1998).
26. H. Calén *et al.,* "Higher partial waves in $pp \to pp\eta$ near threshold," Phys. Lett. **B458**, 190 (1999).
27. B. Krusche *et al.,* "Near threshold photoproduction of η mesons off the proton," Phys. Rev. Lett. **74**, 3736 (1995).
28. The Svedberg Laboratory Progress Report 1996-1997, pp. 90–101.

Working group summary: πN sigma term

M. Knecht*
Centre de Physique Théorique, CNRS Luminy, Case 907
F-13288 Marseille Cedex 9, France

Abstract

Several new theoretical and experimental developements concerning the determination of the nucleon sigma term are presented and discussed.

INTRODUCTION

The denomination "sigma term" stands, in a generic way, for the contribution of the quark masses m_q to the mass M_h of a hadronic state $|h(p)>$. According to the Feynman-Hellmann theorem [1], one has the exact result (the notation does not explicitly take into account the spin degrees of freedom)

$$\frac{\partial M_h^2}{\partial m_q} = < h(p)|(\overline{q}q)(0)|h(p) > . \tag{1}$$

In practice, and in the case of the light quark flavours $q = u, d, s$, one tries to perform a chiral expansion of the matrix element of the scalar density appearing on the right-hand side of this formula. In the case of the pion, for instance, one may use soft-pion techniques to obtain the well-known result [2] (here and in what follows, $\mathcal{O}(M^n)$ stands for corrections of order M^n modulo powers of $\ln M$)

$$\frac{\partial M_\pi^2}{\partial m_q} = -\frac{< \overline{q}q >_0}{F_0^2} + \mathcal{O}(m_u, m_d, m_s)\,, q = u, d, \text{ and } \frac{\partial M_\pi^2}{\partial m_s} = 0 + \mathcal{O}(m_u, m_d, m_s), \tag{2}$$

where $< \overline{q}q >_0$ denotes the single flavour light-quark condensate in the $SU(3)_L \times SU(3)_R$ chiral limit, while F_0 stands for the corresponding value of the pion decay constant $F_\pi = 92.4$ MeV.

In the case of the nucleon, the sigma term is defined in an analogous way, as the value at zero momentum transfer $\sigma \equiv \sigma(t = 0)$ of the scalar form factor of the nucleon ($t = (p' - p)^2$, $\hat{m} \equiv (m_u + m_d)/2$),

$$\overline{\mathrm{u}}_N(p')\mathrm{u}_N(p)\sigma(t) = \frac{1}{2M_N} < N(p')|\hat{m}(\overline{u}u + \overline{d}d)(0)|N(p) >, \tag{3}$$

and contains, in principle, information on the quark mass dependence of the nucleon mass M_N. Most theoretical evaluations of the nucleon sigma term consider the isospin symmetric limit $m_u = m_d$, but this is not required by the definition (3).

Another quantity of particular interest in this context is the relative amount of the nucleon mass contributed by the strange quarks of the sea,

$$y \equiv 2\frac{< N(p)|(\overline{s}s)(0)|N(p) >}{< N(p)|(\overline{u}u + \overline{d}d)(0)|N(p) >}. \tag{4}$$

Large-N_c considerations (Zweig rule) would lead one to expect that y is small, not exceeding $\sim 30\%$. The ratio y can be related, *via* the sigma term and the strange to non-strange quark mass ratio, to the nucleon matrix element of the $SU(3)_V$ breaking part of the strong hamiltonian,

$$\sigma(1 - y)\left(\frac{m_s}{\hat{m}} - 1\right) = \frac{1}{2M_N} < N(p')|(m_s - \hat{m})(\overline{u}u + \overline{d}d - 2\overline{s}s)(0)|N(p) > . \tag{5}$$

For the standard scenario of a strong $< \overline{q}q >_0$ condensate, $m_s/\hat{m} \sim 25$, the evaluation of the product $\sigma(1 - y)$ in the chiral expansion gives ~ 26 MeV at order $\mathcal{O}(m_q)$ [3], $\sim 35 \pm 5$ MeV at order $\mathcal{O}(m_q^{3/2})$ [3,4], and $\sim 36 \pm 7$ MeV at order $\mathcal{O}(m_q^2)$ [5].

*Work supported in part by TMR, EC-contract No. ERBFMRX-CT980169 (EURODAPHNE).

THE NUCLEON SIGMA TERM AND πN SCATTERING

Although the nucleon sigma term is a well-defined QCD observable, there is, unfortunately, no direct experimental access to it. A link with the πN cross section (for the notation, we refer the reader to Refs. [6,7]) at the unphysical Cheng-Dashen point, $\Sigma \equiv F_\pi^2 \overline{D}^+(\nu = 0, t = 2M_\pi^2)$, is furnished by a very old low-energy theorem [8],

$$\Sigma = \sigma(1 + \mathcal{O}(m_q^{1/2})). \tag{6}$$

A more refined version of this statement [9] relates Σ and the form factor $\sigma(t)$ at $t = 2M_\pi^2$,

$$\Sigma = \sigma(2M_\pi^2) + \Delta_R, \tag{7}$$

where $\Delta_R = \mathcal{O}(m_q^2)$. The size of the correction Δ_R, as estimated within the framework of Heavy Baryon Chiral Perturbation Theory (HBChPT), is small [10], $\Delta_R < 2$ MeV (an earlier calculation to one-loop in the relativistic approach [11] gave $\Delta_R = 0.35$ MeV).

In order to obtain information on σ itself, one thus needs to pin down the difference $\Delta_\sigma \equiv \sigma(2M_\pi^2) - \sigma(0)$, and to perform an extrapolation of the πN scattering data from the physical region $t \leq 0$ to the Cheng-Dashen point, using the existing experimental information and dispersion relations. The analysis of Refs. [12,13], using a dispersive representation of the scalar form factor of the pion, gives the result $\Delta_\sigma = 15.2 \pm 0.4$ MeV. On the other hand, from the subthreshold expansion

$$\overline{D}^+(\nu = 0, t) = d_{00}^+ + t d_{01}^+ + \cdots \tag{8}$$

one obtains $\Sigma = \Sigma_d + \Delta_D$, with $\Sigma_d = F_\pi^2(d_{00}^+ + 2M_\pi^2 d_{01}^+)$, and Δ_D is the remainder, which contains the contributions from the higher order terms in the expansion (8). In Ref. [13], the value $\Delta_D = 11.9 \pm 0.6$ MeV was obtained, so that the determination of σ boils down to the evaluation of the subthreshold parameters d_{00}^+ and d_{01}^+. Their values can in principle be obtained from experimental data on πN scattering, using forward dispersion relations [6,7]

$$d_{00}^+ = \overline{D}^+(0,0) = \overline{D}^+(M_\pi, 0) + \mathcal{J}_D(0), \;\; d_{11}^+ = \overline{E}^+(0,0) = \overline{E}^+(M_\pi, 0) + \mathcal{J}_E(0), \tag{9}$$

where $\mathcal{J}_D(0)$ and $\mathcal{J}_E(0)$ stand for the corresponding forward dispersive integrals, while the subtraction constants are expressed in terms of the πN coupling constant $g_{\pi N}$ and of the S- and P-wave scattering lengths as follows:

$$\overline{D}^+(M_\pi, 0) = 4\pi(1+x)a_{0+}^+ + \frac{g_{\pi N}^2 x^3}{M_\pi(4 - x^2)}, \;\; \overline{E}^+(M_\pi, 0) = 6\pi(1+x)a_{1+}^+ - \frac{g_{\pi N}^2 x^2}{M_\pi(2-x)^2}. \tag{10}$$

The dispersive integrals $\mathcal{J}_D(0)$ and $\mathcal{J}_E(0)$ are evaluated using πN scattering data, which exist only above a certain energy, and their extrapolation to the low-energy region using dispersive methods. In the analysis of Ref. [7], the two scatering lengths a_{0+}^+ and a_{1+}^+ are kept as free parameters of the extrapolation procedure. In the Karlsruhe analysis, their values were obtained from the iterative extrapolation procedure itself [6]. Using the partial waves of [14,6], the authors of Ref. [7] obtain the following simple representation of d_{00}^+ and d_{01}^+ (with a_{l+}^+, $l = 0, 1$, in units of M_π^{-1-2l}),

$$\begin{aligned} d_{00}^+ &= -1.492 + 14.6(a_{0+}^+ + 0.010) - 0.4(a_{1+}^+ - 0.133), \\ d_{01}^+ &= 1.138 + 0.003(a_{0+}^+ + 0.010) + 20.8(a_{1+}^+ - 0.133). \end{aligned} \tag{11}$$

This leads then to a value $\sigma \sim 45$ MeV, corresponding to $y \sim 0.2$ [12]. Further details of this analysis can be found in Refs. [15,16].

THEORETICAL ASPECTS

In the framework of chiral perturbation theory, the sigma term has an expansion of the form

$$\sigma \sim \sum_{n\geq 1} \sigma_n M_\pi^{n+1}. \tag{12}$$

The first two terms of this expansion were computed in the framework of the non-relativistic HBChPT in Ref. [17],

$$\sigma_1 = -4c_1\,,\ \sigma_2 = -\frac{9g_A^2}{64\pi F_\pi^2}. \tag{13}$$

The determination of the low-energy constant c_1, which appears also in the chiral expansion of the πN scattering amplitude, is crucial for the evaluation of σ. Earlier attempts, which extracted the value of c_1 from fits to the πN amplitude extrapolated to the threshold region using the phase-shifts of Refs. [14,6], obtained rather large values, $\sigma \sim 59$ MeV [18] ($c_1 = -0.94 \pm 0.06$ GeV^{-1}), or even $\sigma \sim 70$ MeV [19] ($c_1 = -1.23 \pm 0.16$ GeV^{-1}), as compared to the result of Ref. [12].

The threshold region in the case of elastic πN might however correspond to energies which are already too highy in order to make these determinations of c_1 stable as far as higher order chiral corrections are concerned. A new determination of c_1, obtained by matching the $\mathcal{O}(q^3)$ HBChPT expansion of the πN amplitude *inside the Mandelstam triangle* with the dispersive extrapolation of the data leads to a smaller value [20,21], $c_1 = -0.81 \pm 0.15$ GeV^{-1}, corresponding to $\sigma \sim 40$ MeV. It remains however to be checked that higher order corrections do not substancially modify this result. Let us mention in this respect that the higher order contribution σ_3 (which contains a non-analytic $\mathcal{O}(M_\pi^4 \ln M_\pi/M_N)$ piece) in the expansion (12) has been computed in the context of the manifestly Lorentz-invariant baryon chiral perturbation theory in Ref. [22], (see also [23]). Once the expression of the πN amplitude is also known with the same accuracy [23], a much better control over the chiral perturbation evaluation of σ should be reached.

Finally, let us also mention that the results quoted above were based on the πN phase-shifts obtained by the Karlsruhe group [6]. Using instead the SP99 phase-shifts of the VPI/GW group, the authors of Ref. [20] obtain a very different result, $c_1 \sim -3$ GeV^{-1}, which leads to $\sigma \sim 200$ MeV. Needless to say that the consequences of this last result ($y \sim 0.8$) would be rather difficult to accept.

EXPERIMENTAL DEVELOPEMENTS

We next turn to the discussion of several new experimental results which have some bearing on the value of the nucleon sigma term. All numerical values quoted below use $M_\pi = 139.57$ MeV and $F_\pi = 92.4$ MeV.

Let us start with the influence of the scattering length a_{0+}^+ on the value of the sub-threshold parameter d_{00}^+, using Eq. (11) and $a_{1+}^+ = 0.133 M_\pi^{-3}$. The first line of Table 1 gives the result obtained from the value of the phase-shift analysis of Ref. [6]. In the second line of Table 1, we show the value reported at this conference [24] and obtained from the data on pionic hydrogen, $10^3 M_\pi \times a_{0+}^+ = 1.6 \pm 1.3$. The analysis of Loiseau *et al.* [25] consists in extracting the combinations of scattering lengths $a_{\pi^- p} \pm a_{\pi^- n}$ from the value of pion deuteron scattering length $a_{\pi^- d}$ obtained from the measurement of the strong interaction width and lifetime of the 1S level of the pionic deuterium atom [26,27]. Assuming charge exchange symmetry ($a_{\pi^+ p} = a_{\pi^- n}$), they find $10^3 M_\pi \times a_{0+}^+ = -2 \pm 1$ (third line of Table 1). Another determination of a_{0+}^+ is also possible using the GMO sum rule (we use here the form presented in [25], with the value of the total cross section dispersive integral $J^- = -1.083(25)$, expressed in mb and $a_{\pi^- p}$, a_{0+}^+ expressed in units of M_π^{-1})

$$g_{\pi N}^2/4\pi = -4.50\, J^- + 103.3\, a_{\pi^- p} - 103.3\, a_{0+}^+. \tag{14}$$

Using the value $a_{\pi^- p} = 0.0883 \pm 0.0008$ obtained by [25] and the determination $g_{\pi N} = 13.51 \pm 12$ from the Uppsala charge exchange np scattering data [28], one obtains $a_{0+}^+ = -0.005 \pm 0.003$. The resulting effect on Σ_d is shown on the fourth line of Table 1.

Table 1. d_{00}^+ for different values of the scattering length a_{0+}^+.

	$a_{0+}^+ \times 10^3 M_\pi$	$F_\pi^2 d_{00}^+$ (MeV)	$\Delta\Sigma_d$ (MeV)
KH[6]	-9.7	-91.0	0
$A_{\pi^- p}$[24]	$+2 \pm 1$	-80 ± 1	$+11$
$A_{\pi^- d}$[25]	-2 ± 1	-84 ± 1	$+7$
$g_{\pi N}$[28]+GMO	-5 ± 3	-87 ± 3	$+4$

Several new determinations of the πN coupling constant $g_{\pi N}$ have also been reported at this meeting, with values which differ from the "canonical" value obtained long ago [6]. Since most of these recent determinations do not result from a complete partial-wave analysis of $\pi - N$ scattering data, we can only compare the effect of variations in the value of $g_{\pi N}$ on the subtraction terms (10). The results are shown in Tables 2 and 3, respectively. Again, we take the value of [6] as reference point, and show the resulting changes for the value $g_{\pi N} = 13.73 \pm 0.07$ from the latest VPI/GW analysis [29]. For comparison, we have also included the determination of [25], using the published data on the $\pi^- d$ atom [27] combined with the GMO sum rule (14), as well as the value determined from the Uppsala charge exchange np scattering data [28]. The repercussion on $\overline{D}^+(M_\pi, 0)$ is negligible in all cases shown in Table 2, whereas in the case of $\overline{E}^+(M_\pi, 0)$, the largest effect comes from the rather low value of $g_{\pi N}$ obtained by the VPI/GW analysis.

Table 2. The subtraction constant $\overline{D}^+(M_\pi, 0)$ of Eq. (10) for different values of the πN coupling constant, and for fixed value of the scattering length $a_{0+}^+ \times 10^3 M_\pi = -9.7$.

	$g_{\pi N}^2/4\pi$	$F_\pi^2 \overline{D}^+(M_\pi, 0)$ (MeV)	$\Delta\Sigma_d$ (MeV)
KH	14.3 ± 0.2	0.53	0
VPI/GW[29]	13.73 ± 0.07	0.16	-0.37
$A_{\pi^- d}$+GMO[25]	14.2 ± 0.2	0.46	-0.07
Uppsala[28]	14.52 ± 0.26	0.67	$+0.14$

Table 3. The subtraction constant $\overline{E}^+(M_\pi, 0)$ of Eq. (10) for different values of the πN coupling constant, and for fixed value of the scattering length $a_{1+}^+ \times 10^3 M_\pi^3 = 133$.

	$g_{\pi N}^2/4\pi$	$F_\pi^2 \overline{E}^+(M_\pi, 0)$ (MeV)	$\Delta\Sigma_d$ (MeV)
KH	14.3 ± 0.2	105	0
VPI/GW[29]	13.73 ± 0.07	108	$+6$
$A_{\pi^- d} + GMO$[25]	14.2 ± 0.2	105	$+1$
Uppsala[28]	14.52 ± 0.26	104	-2

Finally, we have summarized the various results in Table 4, where now the complete results for the determination of the dispersive integrals $\mathcal{J}_D$ and $\mathcal{J}_E$ have beem included where possible, *i.e.* in the case of the KH [6,7] and of the VPI/GW [30,29] analyses (see also Table 1 in [30]). The corresponding values of Σ_d are given in the last column of Table 4. The analysis of the VPI/GW group increases the value of the sigma term by more than 25%, as compared to the value extracted from the KH phase-shift analysis. This would lead to a value of $y \sim 0.5$, which is rather difficult to understand theoretically. It should also be

noticed that this large difference is due for a large part to the value $d_{01}^+ = (1.27 \pm 0.03) M_\pi^{-3}$ (including a shift in the value of the scattering length a_{1+}^+, which by itself accounts for half of the difference between KH and VPI/GW in the d_{01}^+ contribution in Table 4) as quoted by the VPI/GW group and obtained from fixed-t dispersion relation. A similar analysis, but based on so-called interior dispersion relation (see for instance [31] and references therein), yields a much smaller value, $d_{01}^+ = 1.18 M_\pi^{-3}$ [32], which *lowers* the VPI/GW value of Σ_d in Table 4 by 10 MeV. It remains therefore difficult to assess the size of the error bars that should be assigned to the numbers given above. Also, the VPI/GW phase-shifts have sometimes been criticized as far as the implementation of theoretical constraints (analyticity properties) is concerned (see for instance [33]). Furthermore, the issue of having a coherent πN data base remains a crucial aspect of the problem. The VPI/GW partial wave analyses include data posterior to the analyses of the Karlsruhe group, but which are not always mutually consistent (see *e.g.* [16] and references therein). Hopefully, new experiments (see [34]), will help in solving the existing discrepancies.

Table 4. Comparison of the values of the subthreshold parameters d_{00}^+ and d_{01}^+ according to differences in the input discussed in the text.

	$F_\pi^2 d_{00}^+$ (MeV)	$2M_\pi^2 F_\pi^2 d_{01}^+$ (MeV)	Σ_d (MeV)
KH	-89.4	139.2	50
VIP/GW[30]	-77.3	155.2	50 +12+16
$A_{\pi-d} + GMO$[25]	-83	–	50+6
Uppsala[28]	-86	–	50+3.5

Finally, it should be stressed that the above discussion is by no means a substitute for a more elaborate analysis, along the lines of Ref. [7], for instance (see also [31] and [30]). Such a task would have been far beyond the competences of the present author, at least within a reasonable amount of time and of work. Nevertheless, very useful discussions with G. Höhler, M. Pavan, M. Sainio and J. Stahov greatly improved the author's understanding of this delicate subject. The author also thanks R. Badertscher and the organizing committee for this very pleasant and lively meeting in Zuoz.

REFERENCES

1. H. Hellmann, "Einführung in die Quantenchemie", Franz Deuticke, Leipzig and Vienna, 1937.
   R.P. Feynman, Phys. Rev. **56**, 340 (1939).
2. M. Gell-Mann, R.J. Oakes and B. Renner, Phys. Rev. **175**, 2195 (1968).
   S. Glashow and S. Weinberg, Phys. Rev. Lett. **20**, 224 (1968).
   S. Weinberg, in: A Festscrift for I.I. Rabi, ed. L. Motz (New York Academy of Sciences, New York, 1977) p. 185.
3. J. Gasser and H.Leutwyler, "Quark masses", Phys. Rep. **87**, 77 (1982).
4. J. Gasser, "Hadron masses and the sigma commutator in light of chiral perturbation theory", Ann. Phys. (N. Y.) **136**, 62 (1981).
5. B. Borasoy and U.-G. Meißner, "Chiral expansion of baryon masses and σ-terms", Ann. Phys. (N. Y.) **254**, 192 (1997).
6. G. Höhler, "πN Scattering: Methods and Results of Phenomenological Analyses", Landolt-Börnstein, Vol. 9b2, ed. H. Schopper (Springer, Berlin, 1983).
7. J. Gasser, H. Leutwyler, M.P. Locher and M.E. Sainio, "Extracting the pion-nucleon sigma-term from data", Phys. Lett. **B 213**, 85 (1988).
8. T.P Cheng and R. Dashen, Phys. Rev. Lett. **26**, 574 (1971).
9. L.S. Brown, W.J. Pardee and R.D. Peccei, "Adler-Weisberger theorem reexamined", Phys. Rev. D **4**, 2801 (1971).
10. V. Bernard, N. Kayser and U.-G. Meißner, "On the analysis of the pion-nucleon σ-term: The size of the remainder at the Cheng-Dashen point", Phys. Lett. **B 389**, 144 (1996).

11. J. Gasser, M.E. Sainio and A. Švarc, "Nucleons with chiral loops", Nucl. Phys. **B307**, 779 (1988).
12. J. Gasser, H. Leutwyler and M.E. Sainio, "Sigma-term update", Phys. Lett. **B 253**, 252 (1991).
13. J. Gasser, H. Leutwyler and M.E. Sainio, "Form factor of the σ-term", Phys. Lett. **B 253**, 260 (1991).
14. R. Koch and E. Pietarinen, Nucl. Phys. **A336**, 331 (1980).
15. M.E. Sainio, "Pion-nucleon sigma term", in *Chiral dynamics: Theory and Experiment*, A.M. Bernstein and B.R. Holstein eds., Lecture Notes in Physics **492** (Springer, 1995), p. 212.
16. M.E. Sainio, "Low energy pion-nucleon interaction and the sigma-term", πN Newsletter **13**, 144 (1997).
17. V. Bernard, N. Kayser and U.-G. Meißner, "Aspects of pion-nucleon physics", Nucl. Phys. **A615**, 483 (1997).
18. M. Mojžiš, "Elastic πN scattering to $O(p^3)$ in heavy baryon chiral perturbation theory", Eur. Phys. J. C **2**, 181 (1998).
19. N. Fettes, U.-G. Meißner and S. Steininger, "Pion-nucleon scattering in chiral perturbation theory. 1. Isospin symmetric case", Nucl. Phys. **A640**, 199 (1998).
20. P. Büttiker and U.-G. Meißner, "Pion-nucleon scattering inside the Mandelstam triangle", e-print hep-ph/9908247.
21. P. Büttiker, "πN scattering inside the Mandelstam triangle and the sigma term", talk given at this conference.
22. T. Becher and H. Leutwyler, "Baryon chiral perturbation theory in manifestly Lorentz invariant form", Eur. Phys. J. C **9**, 643 (1999).
23. H. Leutwyler, "Effective field theory of the πN interaction", talk given at this conference.
24. H. J. Leisi, "Results from pionic hydrogen", talk given at this conference.
25. B. Loiseau, "How precisely can one determine the πNN coupling constant from the isovector GMO sum rule?", talk given at this conference.
    T.E.O Ericson, B. Loiseau and A. W. Thomas, "Precision determination of the πN scattering lengths and the charged πNN coupling constant", hep-ph/9907433.
26. D. Chatellard *et al.*, "X-ray spectroscopy of the pionic deuterium atom", Nucl. Phys. **A625**, 855 (1997).
27. P. Hauser *et al.*, "New precision measurement of the pionic deuterium s-wave strong interaction parameters", Phys. Rev. C **58**, R1869 (1998).
28. J. Rahm *et al.*, "*np* scattering measurements at 162 MeV and the πNN coupling constant", Phys. Rev. C **57**, 1077 (1998).
29. M.M. Pavan *et al.*, "Determination of the πNN coupling constant in the VPI/GW $\pi N \to \pi N$ partial wave and dispersion relation analysis", contribution to these proceedings.
30. M.M. Pavan *et al.*, "New results for the pion-nucleon sigma term from an updated VPI/GW πN partial-wave and dispersion relation analysis", contribution to these proceedings.
31. G. Höhler, "Determination of the πN sigma term", contribution to these proceedings.
32. J. Stahov, "The subthrehold expansion of the πN invariant amplitude in dispersion theory", talk given at this conference.
33. G. Höhler, "Some results on πN phenomenology", contribution to these proceedings.
34. G. Smith, "CNI experiments with CHAOS", talk given at this conference.

πN scattering inside the Mandelstam Triangle and the Sigma Term

P. Büttiker*
Institut für Kernphysik (Theorie), Forschungszentrum Jülich, D-52425 Jülich, Germany

Abstract

Pion-nucleon scattering has been studied in great detail in heavy baryon chiral perturbation theory to third order. In this frame, the σ-term $\sigma(0)$ seems to be in contradiction to the experimental data the chiral analysis is based on. We show that this is due to an unsuitable chosen fitting procedure in the chiral calculation. Improving the latter, we find $\sigma(0) \approx 40$ MeV, being in reasonable agreement with the underlying data.

INTRODUCTION

A detailed understanding of πN scattering at low energies allows for precise tests of chiral QCD dynamics. This process has been investigated to third order in heavy baryon chiral perturbation theory (HBChPT) by several groups[1–3]. To tree and one-loop order four and five so called low energy constants (LECs), respectively, enter the calculation and most of the quantities of interest, for example the σ-term, depend on these constants. They are not fixed by chiral symmetry, and therefore experimental data must be used to pin them down.
In previous publications, (sub)threshold parameters and the phase shifts of the lowest partial waves, e.g. of the Karlsruhe group (KA84)[4], have been used to fix the LECs. While most of the resulting chiral predictions are in good agreement with the dispersive results of the Karlsruhe group, the chiral value for the σ-term, $\sigma(0) \approx 73$ MeV[3] deviates quiet substantially from the dispersive prediction, $\sigma(0) \approx 44$ MeV[5], although both analysis are based on the data of the Karlsruhe group. It was assumed that one of the reasons for the disagreement is that an order q^3 calculation is not sufficient for determining the σ-term. Of course higher order calculations should improve the predictions. However, this is not the main reason for the deviation: in ChPT, the quantities of interest are expanded in terms of (small) quark masses and small external momenta. This, in turn, means that the most reliable chiral predictions are obtained for s, t and u lying in some region inside the Mandelstam triangle, see Fig. 1. Therefore any matching of HBChPT with "external" information should be done in this region, rather than in one of the physical regions, as it was done before. Since it is an unphysical domain of the Mandelstam plane, there is no direct access by experimental data. However, by using dispersion relations, this problem can be circumvented. This is done in this work[6]. First, using data from phase shift analysis, we reconstruct the pion-nucleon scattering amplitudes inside the Mandelstam triangle. We then use the chiral third order amplitudes constructed in[3] to determine the LECs under consideration by requiring agreement with the dispersive amplitudes inside the Mandelstam triangle, yielding, among others, a more reliable chiral prediction for the σ-term. Obtained the LECs this way, a comparison of chiral results with the experimental data in one of the *physical* sectors can then be regarded as a test for the range of validity in energy of HBChPT.

πN DISPERSION RELATIONS

The first step is to construct the amplitudes inside the Mandelstam triangle. This triangle is bounded by the three lines $s = (M+m)^2, u = (M+m)^2$ and $t = 4M^2$, see Fig. 1. Using unitarity, analyticity, and crossing, one can write down dispersion relations for the invariant amplitudes[7]. While it is clear that unsubtracted dispersion relations are valid for A^- and $B^\pm$, it is still an open question if this holds for A^+, too[8]. To avoid problems related to this question, we prefer to work with a subtracted relation for A^+, $A^+(0,t)$ being the subtraction function,

*Work supported in part by DFG under contract no. ME 864-15/1.

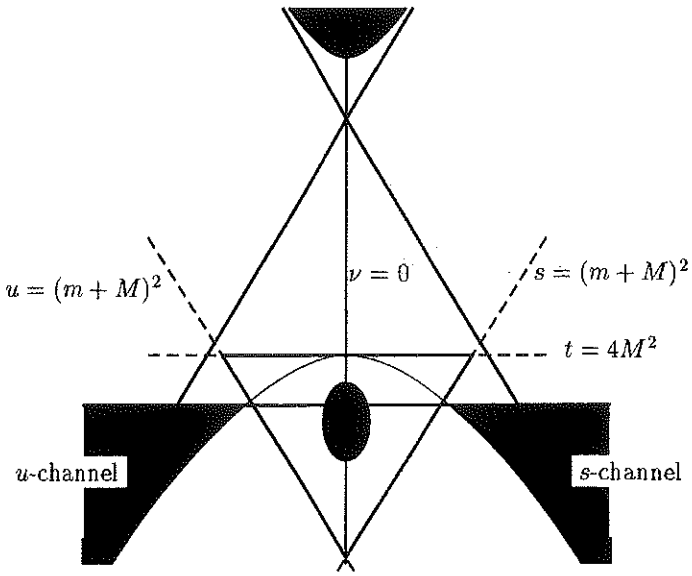

Figure. 1. Mandelstam plane. The Mandelstam triangle is the inside of the thick lines. The shaded region inside the triangle is the region we fitted the chiral amplitude.

$$\begin{aligned}
\text{Re } A^+(\nu,t) &= \text{Re } A^+(0,t) + \frac{2\nu^2}{\pi}\int_{\nu_{\rm thr}}^{\infty} \frac{\text{Im } A^+(\nu',t)}{\nu'(\nu'^2-\nu^2)}\,d\nu' \,, \\
\text{Re } A^-(\nu,t) &= \frac{1}{\pi}\int_{\nu_{\rm thr}}^{\infty} \text{Im } A^-(\nu',t)\left\{\frac{1}{\nu'-\nu}-\frac{1}{\nu'+\nu}\right\}d\nu' \,, \qquad (1) \\
\text{Re } B^\pm(\nu,t) &= \frac{1}{\pi}\int_{\nu_{\rm thr}}^{\infty} \text{Im } B^\pm(\nu',t)\left\{\frac{1}{\nu'-\nu}\mp\frac{1}{\nu'+\nu}\right\}d\nu' + \frac{g^2}{2m}\left(\frac{1}{\nu_B-\nu}\mp\frac{1}{\nu_B+\nu}\right) \,,
\end{aligned}$$

with $\nu = (s-u)/(4m)$, $\nu_{thr} = M + t/(4m)$, $\nu_B = (t-2M^2)/(4m)$, M and m the pion and the nucleon mass, respectively, and

$$f^2 = \frac{g^2}{4\pi}\left(\frac{M}{2m}\right)^2 \approx 0.079. \qquad (2)$$

The only input for the dispersion relations are, apart from masses and the coupling constant, the imaginary parts of the invariant amplitudes and the subtraction function $A^+(0,t)$. The firsts are approximated by a partial wave representation, using the S- to K-waves of KA84. The latter is determined by solving the subtracted dispersion relation for $A^+(0,t)$, approximating the real part of the amplitude in the same way it was done for the imaginary part, and finally averaging the obtained subtraction functions over physical values for ν. We remark that the subtraction function fulfills the Adler consistency condition,

$$A^+(\nu=0, t=M^2, q_1^2=0, q_2^2=M^2) \approx \frac{g^2}{m} \qquad (3)$$

within one percent (see Fig. 2). Since physical pions do not have vanishing four–momenta, one expects a deviation from this relation of the order of $M^2/(4\pi F)^2 \simeq 1.5\%$.

CHIRAL AMPLITUDES INSIDE THE MANDELSTAM TRIANGLE

In heavy baryon chiral perturbation theory, it is common to work with the non-spin-flip and the spin-flip amplitudes $g^\pm(\omega,t)$ and $h^\pm(\omega,t)$ (here as functions of the cm energy ω instead of ν) rather than with the invariant amplitudes,

$$g^\pm(\omega,t) = \frac{C_4 A^\pm(\omega,t) - C_2 B^\pm(\omega,t)}{C_1 C_4 - C_2 C_3} \,, \qquad (4)$$

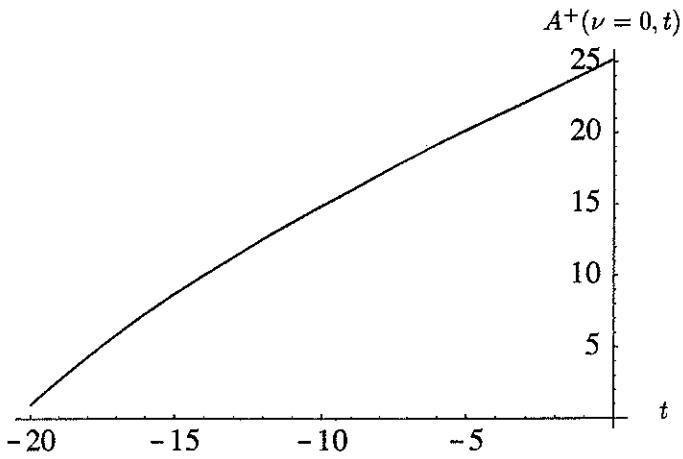

Figure. 2. The subtraction function $A^+(\nu = 0, t)$.

$$h^{\pm}(\omega,t) = \frac{-C_3 A^{\pm}(\omega,t) + C_1 B^{\pm}(\omega,t)}{C_1 C_4 - C_2 C_3}\,, \tag{5}$$

where C_i are functions of ω and t.

As mentioned above, these amplitudes depend on the LECs. An example, the counterterm amplitude g_{ct}^+, is given below,

$$g_{\rm ct}^+ \;=\; \frac{c_2\,\omega}{mF^2}\Big[4\omega^2 - 4M^2 + t\Big] + \frac{1}{F^2}\Big[-4c_1M^2 + 2c_2\omega^2 + c_3(2M^2 - t)\Big]\,, \tag{6}$$

and the σ-term can be written as

$$\sigma(0) \;=\; -4c_1M^2 - \frac{9g_{\pi N}^2 M^3}{64\pi m^2} + \mathcal{O}(M^4), \tag{7}$$

with the LECs c_1, c_2, c_3 and the pion decay constant F. Similar expressions hold for the other amplitudes. It is known that the strict heavy baryon limit tends to modify the analytical structure of the πN amplitudes, but these effects can be dealt with by subtracting from the amplitudes the Born terms. This procedure is not arbitrary since it is common in pion-nucleon physics to work with this kind of amplitudes to avoid the rapid variations in the kinematical variables due to the Born terms.

MATCHING OF THE CHIRAL AND THE DISPERSIVE AMPLITUDES

For the reasons mentioned above, we compare the chiral amplitudes with their dispersive counterparts in some small region inside the Mandelstam triangle. More precisely, we concentrate on two regions. The first one is centered around the point $\nu = t = 0$ whereas

Table 1. The dimension two LECs $c_{1,2,3,4}$ in GeV^{-1} from our determination based on the KA84 phase shifts compared to previous ones using also information from πN scattering in the physical region and the σ–term.

c_i	Our fit	Ref.[1]	Ref.[2]	Ref.[3] (Fit 1)
1	-0.81 ± 0.12	-0.93 ± 0.10	-0.94 ± 0.06	-1.23 ± 0.16
2	8.43 ± 56.9	3.34 ± 0.20	3.20 ± 0.10	3.28 ± 0.23
3	-4.70 ± 1.16	-5.29 ± 0.25	-5.40 ± 0.06	-5.94 ± 0.09
4	3.40 ± 0.04	3.63 ± 0.10	3.47 ± 0.06	3.47 ± 0.05

the second region in centered around $\nu = 0, t = 2M^2/3$. Combining the two fits, we find

the values for the LECs c_1, c_2, c_3 and c_4 as given in Tab. 1. The errors given for our values of the c_i's are purely the ones obtained by the χ^2-fitting routine. Note that our value for c_2 is essentially undetermined. The reason for that is that in the amplitude g^+, which is small, the LECs c_1 and c_3 are weighted with factors of M^2, whereas the term $\sim c_2$ is proportional to ω^2 (to leading order in the $1/m$) and this quantity is suppressed by a factor of 10 compared to M^2 in the region around the center of the Mandelstam triangle.

The value for c_1 is of special interest here, as it determines $\sigma(0)$, see eq. 7. Using our value for c_1, we find $\sigma(0) \approx 40$ MeV. This has to be compared with the dispersion theoretical analysis of[5], of which we believe that it gives the most trustworthy value of the σ-term, $\sigma(0) = (44 \pm 8 \pm 7)$ MeV, and with the earlier chiral predictions $\sigma(0) \approx 50$ MeV[1], 59 MeV[2], and 73 MeV[3], respectively, lending further credit to our procedure of fixing the LECs.

SUMMARY

In HBChPT the quantities of interest are expanded in terms of quark masses and small external momenta, and so the most reliable chiral results are obtained in an unphysical region lying *inside* the Mandelstam triangle. Therefore, any comparison of HBChPT with experimental data should be done in this domain and not in one of the physical regions. Values of the scattering amplitudes for the Mandelstam variables lying inside the Mandelstam triangle can be made available by the use of dispersion relations. By comparing chiral and dispersive πN amplitudes inside this triangle we obtain more reliable chiral predictions for the quantities of interest, closing the gap between the dispersive and the chiral result for the σ-term.

ACKNOWLEDGMENTS

I thank Ulf-G. Meißner for the enjoyable collaboration.

REFERENCES

1. V. Bernard, N. Kaiser and U.-G. Meißner, "Aspects of chiral pion-nucleon physics", Nucl. Phys. **A615** (1997), 483
2. M. Mojžiš, "Elastic Pi N Scattering to $O(p^3)$ in Heavy Baryon Chiral Perturbation Theory" Eur. Phys. J. **C2** (1998) 181
3. N. Fettes, U.-G. Meißner and S. Steininger, "Pion-nucleon scattering in chiral perturbation theory (I): Isospin-symmetric case", Nucl. Phys. **A640** (1998), 199
4. R. Koch, "Improved Pi N Partial Waves Consistent with Analyticity and Unitarity", Z. Phys. **C29** (1985) 597; R. Koch and M. Hutt, "A Partial Wave Dispersion Relation Analysis of Pion-Nucleon Scattering Amplitudes",Z. Phys. **C19** (1983) 119
5. J. Gasser, H. Leutwyler and M.E. Sainio, "Sigma term update," Phys. Lett. **B253** (1991) 252
6. P. Büttiker and U.-G. Meißner, "Pion-nucleon scattering inside the Mandelstam triangle", `hep-ph/9908247`
7. G. Höhler, *Pion-Nucleon scattering* (Springer 1983), Landolt-Börnstein I/9b2, ed. H. Schopper
8. G. Höhler, R. Strauss, "Is a Subtraction Really Necessary in the Isospin Even πN Dispersion Relation?", Z. Physik **232**, 205 (1970); G. Höhler, private communication

New Result for the Pion–Nucleon Sigma Term from an Updated VPI/GW πN Partial–Wave and Dispersion Relation Analysis

M.M. Pavan *
Lab for Nuclear Science, M.I.T., Cambridge, MA 02139
R.A. Arndt †
Dept. of Physics, Virginia Polytechnic and State University, Blacksburg, VA 24061
I.I. Strakovsky and R.L. Workman
Dept. of Physics, The George Washington University, Washington, D.C. 20052

Abstract

A new result for the πN sigma term from an updated πN partial–wave and dispersion relation analysis of the Virginia Polytechnic Institute (now George Washington University) group is discussed. Using a method similar to that of Gasser, Leutwyler, Locher, and Sainio, we obtain Σ =90±8 MeV (preliminary), in disagreement with the canonical result 64±8 MeV, but consistent with expectations based on new information on the πNN coupling constant, pionic atoms, and the Δ resonance width.

Introduction

The pion nucleon sigma term (Σ) continues to be a puzzle some thirty years after initial attempts to determine it. The keen interest in Σ comes from the fact that it vanishes in the massless quark (chiral) limit of QCD, and becomes non-zero only for a non-zero light (up or down) quark mass, so it is a crucial parameter in the understanding of chiral symmetry breaking (see e.g. Refs.[1,2]). The nucleon's strange quark content can be inferred from Σ (see e.g. Ref.[2]), so Σ is also relevant to *quark confinement*, not yet fully understood, since one must understand the mechanism for accommodating strange quarks in an ostensibly light quark object [3]. Thus Σ is a parameter of *fundamental* significance to low energy QCD, making it crucial to obtain its value as precisely as possible. The canonical result for $\Sigma \simeq 64$ MeV [4,5] implies a large nucleon strangeness content [2], and much effort has been spent trying to understand that. This article outlines recent work of the (former) Virginia Polytechnic Institute (VPI), (now George Washington University (GWU)) group to extract the "experimental" value of the sigma term (Σ) from the πN scattering data as part of ongoing πN partial-wave (PWA) and dispersion relation (DR) analyses.

Experimental Σ Term

The "experimental" sigma term Σ is related to the πN isoscalar amplitude $\bar{D}^+$ (bar signifies the pseudovector Born term is subtracted) at the "Cheng-Dashen point" [7]:

$$\Sigma = F_\pi^2 \bar{D}^+(\nu = 0, t = 2m_\pi^2) \tag{1}$$

where F_π=92.4 MeV is the pion decay constant, ν is the crossing energy variable, and t is the four-momentum transfer. Since the Cheng-Dashen point lies outside the physical πN scattering region, the experimental πN amplitudes must be *extrapolated* in order to obtain Σ. The most theoretically well-founded extrapolation approach is based on dispersion relation (DR) analyses of the scattering amplitudes [5]. In the early 80^s, the Karlsruhe-Helsinki group performed extensive investigations into obtaining Σ from πN dispersion relations [5]. The canonical result $\Sigma = 64 \pm 8$ MeV was based on hyperbolic dispersion relation [4] calculations using the groups' πN [8] and $\pi\pi$ [5] phase shifts.

The only recent dispersion theoretic determinations have been by Sainio [6], based on the method of Gasser, Leutwyler, Locher, and Sainio (GLLS)[2]. The method exploits the fact that $\bar{D}^+(t)$ can be expressed as a power series in t [5], the coefficients determined from dispersion relation subtraction constants. The coefficients up to $O(t)$, $\bar{d}_{00}^+$ and $\bar{d}_{01}^+$, are determined from the forward $\bar{C}^+$ and "derivative" $\bar{E}^+$ DRs, respectively. The smaller

*Present address: TRIUMF, Vancouver, B.C. V6T-2A3 ; EMAIL: marcello.pavan@triumf.ca
†Present affiliation: Dept. of Physics, The George Washington University, Washington, D.C. 20052

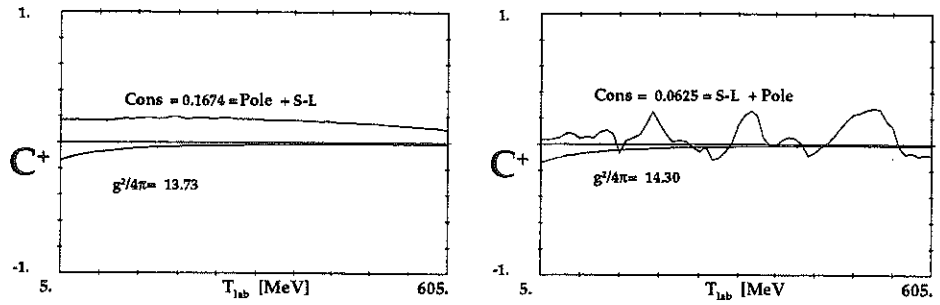

Figure. 1. Left: Subtraction constant ("scattering length + pole") and Born term in the forward C^+ dispersion relation as a function of energy from our πN analysis SM99 ; **Right:** same, for the Karlsruhe KA84 analysis [9]. This DR yields the coefficient $\bar{d}_{00}^+$ in Eqn. 2.

$O(\geq t^2)$ correction $\Delta_D \simeq$12 MeV is determined employing $\pi\pi N\bar{N}$ phase shifts (15 MeV), and Δ isobar exchange (-3 MeV) [2]. Σ is then expressed as:

$$\Sigma = F_\pi^2 \cdot (\bar{d}_{00}^+ + 2m_\pi^2 \cdot \bar{d}_{01}^+) + \Delta_D \equiv \Sigma_d + \Delta_D \qquad (2)$$

In the GLLS approach, the Karlsruhe KH80[8] or KA84[9] πN phases shifts are used as *fixed input* above about T_π=70 MeV, and the D and higher phases are used below the cutoff as well in six forward dispersion relations ($B^\pm, C^\pm, E^\pm$). By fitting the low energy data, $\bar{d}_{00}^+$ and $\bar{d}_{01}^+$ can be determined. Their result [2,6] was $\Sigma_d \simeq$50 MeV, and Δ_D=12 MeV, leading to $\Sigma \sim$ 62 MeV, in agreement with the Karlsruhe results [5,4]. However, since the dispersion relations were constrained to be satisfied, the subtraction constants, which are energy *independent*, must be the *same* at low energies where the data were fit as at high energies where they were *fixed* input. Therefore, Σ_d could not have come out significantly different than the Karlsruhe result. Nonetheless, this analysis provided a very useful *validation* of the method. The technique has been criticized [10] since the E DR is more sensitive to the higher partial waves than the other DRs, so it *could be* rather uncertain due to uncertainty in the higher phases. What the GLLS analyses showed was that this is in fact not the case, and the method can be used reliably to extract Σ_d.

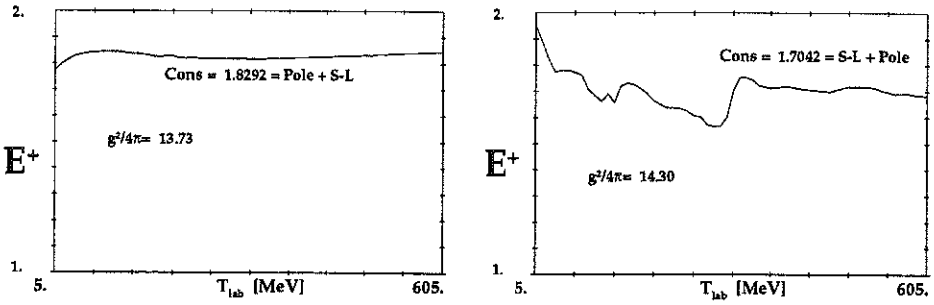

Figure. 2. Left: Subtraction constant in the forward E^+ dispersion relation as a function of energy from our πN analysis SM99 ; **Right:** same, for the Karlsruhe KA84 analysis [9]. This DR yields the coefficient $\bar{d}_{01}^+$ in Eqn. 2.

Since the GLLS analyses simply demonstrated another method to get Σ_d from the KH80 πN analysis, there have been *no* recent DR–based Sigma term analyses independent of the results of the Karlsruhe group [5,4]. Consequently, our group has developed a version of the GLLS technique as part of our own πN partial-wave and dispersion relation analysis. The method will be outlined in the following sections.

VPI/GW Σ Term Analysis Method

The VPI/GW πN partial-wave and dispersion relation analysis is an ongoing project, where new solutions are released when changes to the database and analysis method

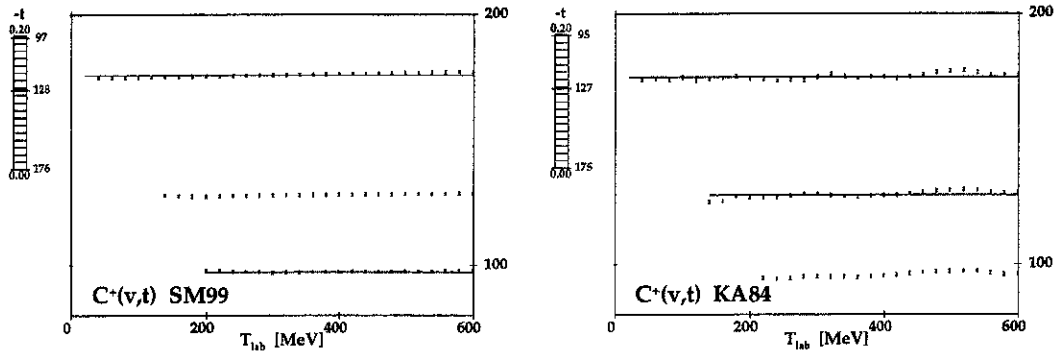

Figure. 3. Left: Subtraction constants in the fixed-t C^+ dispersion relation from our πN analysis SM99 as a function of energy at three values of momentum transfer t ; **Right:** same, for the Karlsruhe KA84 analysis [9]. This DR yields the data points shown in Fig. 4 used to extract the coefficients $\bar{d}^+_{0i}$ (Eqn. 2).

warrant [11]. Analysis details can be found in Ref.[12–14]. Presently, our partial-wave analysis is constrained by the forward $C^{\pm}(\omega)$ and "derivative" $E^{\pm}(\omega)$ dispersion relations, as well as the fixed-t $B_{\pm}(\nu,t)$ ("Hüper" [5]) and $C^{\pm}(\nu,t)$ dispersion relations. These DRs are constrained to be satisfied to within ~1% up to ~800 MeV. As our analysis extends up to 2 GeV, the KH80 [8] phases are used from 2 to 4 GeV in the dispersion integrals. A 4 GeV cutoff is sufficient for adequate convergence in the fixed-t $B_{\pm}$ and C^- DR integrals, however the $E^{\pm}$ and C^+ DR integrals require a parameterization for the high energy parts. After the report at MENU97 [13], we included the high energy parts of the latter DRs using formulas from Ref.[5], resulting in much more satisfactory results.

Pion-nucleon dispersion relations depend on *a priori* unknown constants including the πNN coupling constant f^2 and the subtraction constants (usually chosen to be scattering lengths). Our analysis treats these constants as unknown parameters to be determined by a best fit to data. In practice, for our work-in-progress "SM99"[11], the coupling f^2 and the p-wave scattering volume a^+_{1+} were searched, while the s-wave scattering lengths were taken from the P.S.I. pionic hydrogen results[15]. We also insisted that the GMO sum rule [16] be satisfied.

For every solution, the subthreshold coefficient $\bar{d}^+_{00}$ is calculated using the chosen parameter set and πN phases from :

$$\bar{d}^+_{00} = K_1 \cdot a^+_{0+} + K_2 \cdot f^2 + \int d\nu' K_3(\nu') Im D^+(\nu') \qquad (3)$$

where K_i are kinematical factors, and a^+_{0+} is the isoscalar s-wave scattering length. The expression for $\bar{d}^+_{01}$ is analogous, involving instead the isoscalar p-wave volume a^+_{1+} and the amplitudes E^+, B^+, and C^+. By noting how Σ_d varies for solutions away from the optimum, and fluctuations of the extracted constants with respect to energy, one obtains an indication of the uncertainty. To determine the experimental sigma term Σ, we use Δ_D=12 MeV (see e.g. Ref.[6]), which is insensitive to the πN partial wave input [2,17].

The fixed-t C^+ DR subtraction constants $C^+(\nu = 0, t)$ are equivalent to $D^+(0,t)$. Thus the slope of these constants as a function of t at t=0 is $d^+_{00} + t \cdot d^+_{01}$, so we have another method to determine Σ_d. Note that these subtraction constants are not fixed *a priori* in the DR parameter search procedure (unlike e.g. f^2), so this method of obtaining Σ_d is independent to the GLLS approach and a valuable consistency check.

Results and Discussion

Our solution "SM99" satisfies fixed-t and forward dispersion relations well (up to our ~800 MeV constraint limit), and the data (up to 2 GeV) are fit with χ^2/data point = (2, 2, 2.5) for (π^+,π^-,CEX). Compared to the Karlsruhe KA84 solution[9], these same dispersion relations are better satisfied (see Figs. 1, 2, 3), and the data much better fit

Solution	Σ_d [MeV] =	"a^+_{0+} const.	Born	$\int D^+$	"a^+_{1+}" const.	Born	$\int E^+$
KA84	50 =	-7	+9	-91	+352	-142	-72
SM99	78 =	1.5	+9	-88	+360	-136	-69
difference	28 =	**+9**	**0**	**+3**	**+8**	**+6**	**+3**
Expectation	*21±6=*	*8±3*	0	*5±5*	0	*7±2*	*2±4*

Table 1. Comparison of Σ_d from the Karlsruhe solution KA84 [9] and our recent solution SM99 (values rounded). The change in the C^+ subtraction constant (a^+_{0+}) term, the E^+ Born term, and both integral terms are consistent with *expectations* from pionic atom data [15,18], a lower coupling constant ($f^2 \simeq 0.0755$) [19], and a narrower Δ resonance width. See text for details.

(χ^2/point = (4, 5, 3.5) for KA84). The PWA and DR solutions clearly favour a πNN coupling constant $f^2 = 0.0759 \pm 0.0004$ ($\frac{g^2}{4\pi} = 13.72 \pm 0.07$) *, consistent with our recently published solutions [12]. This value is compatible with most recent determinations[19] and ~5% below the canonical value 0.079 used in the KH80 and KA84 solutions

For the subthreshold coefficients from the GLLS method, we obtain $\bar{d}^+_{00}$= -1.27±0.03 and $\bar{d}^+_{01}$= 1.27±0.03 m_π^{-1}, where the uncertainty is from the energy fluctuations only (see Figs. 1 and 2). This implies $\Sigma_d \simeq$78 MeV (Eqn. 2), which is ~55% larger than the canonical result ≃50 MeV [2,6,5]. As a check of our dispersion relation machinery, we inputed the Karlsruhe KA84 [9] phases and reproduced their f^2 and Σ_d results exactly. Table 1 shows a term by term comparison between SM99 and KA84 to analyze the differences.

Though the difference between the SM99 and KA84 Σ_d values is surprisingly large, one *expects* about 21 MeV of the difference from new information on pionic atoms, a lower coupling constant, and a narrower Δ resonance width. The isoscalar scattering length $a^+_{0+} \simeq -0.008\ m_\pi^{-1}$ for KA84 (and KH80), but analyses of recent PSI pionic hydrogen and deuterium results yields $\simeq -0.0015$ [18] or $\simeq +0.002$ [15]. Our analysis used the latter, while the "expectation" in Table 1 assumes 0.000±0.003. A lower coupling constant around $f^2 = 0.0755 \pm 0.0010$ is favoured by most analyses[19] and this "expectation" contributes +7 MeV in Table 1 from the E^+ Born term. The C^+ Born term does not change due to a well know insensitivity to f^2. And it is well known that the Δ resonance width is too wide in KA84 (overshoots the total cross sections on the left wing), so since ImD^+ is proportional to the sum of the π^+p and π^-p total cross sections via the optical theorem, one expects the D^+ integral contribution to decrease. Due to Δ region dominance of the C DR, the Δ width and f^2 are correlated, and a $\sim$ 5% decrease in f^2 *roughly* corresponds to a same decrease in the integrals, and this expectation is reflected in Table 1. A narrower Δ also would reduce the E^+ DR integral, but possible changes in higher partial waves make predictions less clear. So from rather general considerations, one *expects* a significant increase from the canonical value for Σ_d based on new experimental information.

The result from the tangent of the $\bar{C}^+(0,t)$ subtraction constants at t=0 yields $\bar{d}^+_{00}$= -1.15±0.03 and $\bar{d}^+_{01}$=1.23±0.03, where the uncertainties reflect only the energy fluctuations of the constants (see Fig. 3). This yields Σ_d=80 MeV, consistent with our other determination. Figure 4 shows this result along with the tangent inferred from the forward C^+ and E^+ DR analysis. The consistency is not perfect, and the slight differences in the $\bar{d}^+_{0i}$, which are believed to be understood, are being studied further.

In summary, we have performed a new πN partial wave and dispersion relation analysis, from which we obtain Σ = 91±8 MeV using two different methods, about 27 MeV larger than the canonical result 64±8 MeV from Ref.[4]. At first glance the result is indeed surprising, but a large upward change is in fact *expected* based on new information on $a^+_{0+} \simeq 0.000$ from pionic hydrogen and deuterium [15,18], a lower πNN coupling constant $f^2 \simeq 0.0755$[19], and a narrower Δ resonance width. Further study is planned to explore systematic uncertainties and to resolve small inconsistencies. A new analysis based on the the Karlsruhe methods[8,9] applied to the modern data is urged to check these findings.

*See our companion article on our f^2 determination in these proceedings for details [14].

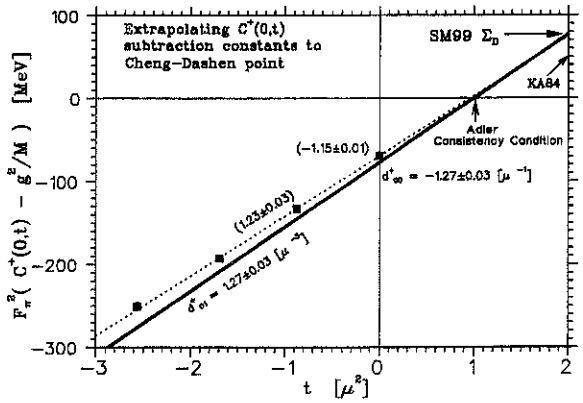

Figure. 4. Tangent at $t = 0$ (dashed line) of the SM99 $\bar{C}^+(0,t)$ subtraction constants (solid squares, which include r.m.s. errors), with tangent inferred from our forward $C+$ and E^+ DR analysis overlayed (solid line). The slight discprepancy is understood and under investigation. Nonetheless, both yield $\Sigma_d \simeq 79$ MeV, and clearly inconsistent with the KA84 result $\simeq 50$ MeV [5,6].

Acknowledgements

We gratefully acknowledge a contract from Jefferson Lab under which this work was done. The Thomas Jefferson National Accelerator Facility (Jefferson Lab) is operated by the Southeastern Universities Research Association (SURA) under DOE contract DE-AC05-84ER40150. MMP thanks A. Badertscher and GWU for their support.

REFERENCES

1. J. Gasser, H. Leutwyler, Phys. Rep. **87** 77 (1982)
2. J. Gasser, H. Leutwyler, M.P. Locher, M.E. Sainio. Phys. Lett. **B213** 85 (1988) ; *ibid* , Phys. Lett. **B253** 252 (1991) ; *ibid* , Phys. Lett. **B253** 260 (1991)
3. R. Jaffe, private communication, 1998.
4. R. Koch, Z. Phys. **C15** 161 (1982)
5. G. Höhler, *Pion Nucleon Scattering*, Landolt-Börnstein, Vol.9 b2, ed. H. Schopper (Springer, Berlin, 1983)
6. M.E. Sainio, *Proceedings of 7th h International Symposium on Meson-Nucleon Physics and the Structure of the Nucleon*, (Universität Karlsruhe, UCLA, 1997) eds. D. Dreschsel, G. Höhler, W. Kluge, H. Leutwyler, B.M.K. Nefkens, H.-M. Staudenmaier, pp. 144–149 ; and references therein.
7. T.P. Cheng and R. Dashen, Phys. Rev. Lett. **26** 594 (1971)
8. R. Koch, E. Pietarinen, Nucl. Phys. **A336** 331 (1980)
9. R. Koch, Z. Phys. **C29** 597 (1984).
10. G. Höhler, private communication ; and remarks made during the meeting.
11. Recent solutions can be accessed via TELNET (or SSH) said.phys.vt.edu (username: *said*) , or at http://said.phys.vt.edu/ .
12. R.A. Arndt, I.I. Strakovsky, R.L. Workman, M.M. Pavan, Phys. Rev. **C52** 2120 (1995) ; R.A. Arndt, R.L. Workman, M.M. Pavan, Phys. Rev. **C49** 2729 (1994).
13. M.M. Pavan and R.A. Arndt, *Proceedings of 7th h International Symposium on Meson-Nucleon Physics and the Structure of the Nucleon*, (Universität Karlsruhe, UCLA, 1997) eds. D. Dreschsel, G. Höhler, W. Kluge, H. Leutwyler, B.M.K. Nefkens, H.-M. Staudenmaier, pp. 165–169 ; and references therein.
14. M.M. Pavan, R.A. Arndt, R.L. Workman, I.I. Strakovsky, these proceedings.
15. H.J. Leisi, private communication, Oberjoch meeting, 1998.
16. M.L. Goldberger and S.B. Treiman, Phys. Rev. **110** 1178 (1958)
17. M. Sainio, private communication.
18. B. Loiseau, et. al., these proceedings.
19. J.J. deSwart, M.C.M. Rentmeester, and R.G.E. Timmermans, *Proceedings of the 7th International Symposium on Meson-Nucleon Physics and the structure of the Nucleon* (Universität Karlsruhe, UCLA, 1997) eds. D. Drechsel, G. Höhler, W. Kluge, H. Leutwyler, B.M.K. Nefkens, and H.-M. Staudenmaier, page 89.

Determinations of the πN Sigma Term

G. Höhler
Institut für Theoretische Teilchenphysik, Universität Karlsruhe
Postfach 6980 D-76128 Karlsruhe, Germany

Abstract

The determination of Σ from analytic continuations based on πN partial wave solutions is discussed.

Introduction

A venerable low-energy theorem due to Brown et al.[1] relates the πN sigma term $\sigma(0)$ to the isoscalar invariant πN scattering amplitude $D^+(\nu,t)$ at the Cheng-Dashen ('CD') point $\nu = 0, t = 2m_\pi^2$:

$$\Sigma \equiv F_\pi^2 \bar{D}^+(0,2m_\pi^2) = \sigma(2m_\pi^2) + \Delta_R; \qquad \sigma(2m_\pi^2) = \sigma(0) + \Delta_\sigma. \tag{1}$$

$F_\pi = 92.4\,MeV$ is the pion decay constant, the bar above D indicates that the PV Born term has been subtracted. $\sigma(t)$ is the scalar nucleon form factor. According to Brown et al. their low energy theorem has at the CD point an error of the order $(m_\pi/m)^4$, whereas the error at other points is of the same order $(m_\pi/m)^2$ as Σ.

The scalar form factor and the σ-term have recently been recalculated from their new version of Chiral Perturbation Theory by Becher and Leutwyler[2], where one can find references to earlier work. In the following, we shall discuss attempts to determine Σ, Eq.(1), from analytic continuations of the amplitude $D^+(\nu,t)$ in the physical region.

The Method of Cheng and Dashen

The authors[1] used a fixed-t dispersion relation at $t = 2m_\pi^2$. The problem of this method is that, in the unphysical region, the Legendre Polynomials P_ℓ are rapidly increasing as t and ℓ are increasing. As a consequence, small partial waves for which only crude estimates can be obtained from data, give substantial contributions at $t = 2m_\pi^2$.

Application of Subthreshold Coefficients

Since 1969 we have calculated from fixed-t dispersion relations and partial wave solutions the coefficients of a *subthreshold expansion of invariant πN amplitudes minus their Born terms.*

$$X(\nu,t) = \sum_{m,n} x_{mn} \nu^{2m} t^n. \tag{2}$$

X denotes either crossing even amplitudes or crossing odd amplitudes divided by $\nu = \omega + t/(4m)$. ω is the total pion energy in the Lab. x_{mn} is written e. g. d^+_{mn} for the amplitude $\bar{D}^+(\nu,t)$.

$$\bar{D}^+(\nu,t) = d^+_{00} + d^+_{01}\, t + d^+_{10}\nu^2 + \ldots \tag{3}$$

For a comparison with the literature, we mention the notation

$$\Sigma = \Sigma_d + \Delta_D; \qquad \Sigma_d = F_\pi^2(d^+_{00} + 2\,m_\pi^2\, d^+_{01}). \tag{4}$$

Σ_d belongs to the linear approximation of $\bar{D}^+(0,t)$ and Δ_D to the effect of the curvature, which leads to the **cusp** at the pseudothreshold $t = 4\,m_\pi^2$.

The dispersion relation for $D^+(\nu,0)$ requires a subtraction, which can be carried out e. g. at $\nu = 0$ or at threshold, where it can be expressed by the S-wave scattering length a^+. The difference is well determined, because it follows from a rapidly converging integral I^+ over σ^+_{tot}. d^+_{00} is related to a^+ by (units m_π^{-1}):

$$d^+_{00} = 14.44\,a^+ + 1.88\,f^2 - I^+; \qquad I^+ = 1.47. \tag{5}$$

The dependence on f^2 is weak. The determinations of a^+ have not yet led to a generally accepted value. With the preliminary result of Ericson et al.[3], which follows from the $\pi^- d$ scattering length determined from the pionic deuterium experiment ($a^+ = -0.0020$) the contribution to Σ reads

$$F_\pi^2 d_{00}^+ = -1.8 + 9.1 - 89.9 = -82.6\, MeV. \tag{6}$$

If we add the result derived from KH80 ($d_{01}^+ = 1.14$), we obtain

$$\Sigma_d = -82.6 + 139.4 \approx 57\, MeV. \tag{7}$$

In d_{01}^+ the integral has a considerable uncertainty because the experimental information on the slope of $d\sigma/dt$ is poor. There is a large discrepancy between the data of Ref.[4], which cover the t-range of interest for the slope but were measured only at a few energies, and the Rutherford data for the whole of the angular range and many energies (see Fig. 6.2.10 in Ref.[5]. The largest experiment of the latter type *was not published*, only a preliminary result is available[6]. If scattering volumes are introduced in Eq.(7), one should use *realistic values of their errors.*

Continuation at fixed $\nu = 0$

In order to determine the curvature and the cusp of the subtraction function $D^+(0,t)$ at $t = 4m_\pi^2$, we have evaluated a fixed-ν dispersion relation at $\nu = 0$. $ImD^+(0,t)$ along the cut from $-\infty$ to $-4m\,m_\pi \approx -0.52\, GeV/c$ cannot be calculated. It is sufficient to use the discrepancy method.

$ImD^+(0,t)$ along the cut from $4m_\pi^2$ to ∞ was expressed in terms of the t-channel partial waves $Imf_+^0(t)$ and $Imf_+^2(t)$, which were calculated in Ref.[7] and by R. Koch from KH80 (Table in Ref.[5]). Contributions from large t are included in the discrepancy.

Furthermore, the real amplitude $D^+(0,t)$ is known from fixed-t dispersion relations in the range $-0.52\, GeV^2 < t \leq 0$. The result of an evaluation with KH80 is given in Ref[5] (p.291): $\Sigma = (63 \pm 6)\, MeV$) (only part of the uncertainty can be given). This result does not yet include the new value for a^+. $\Delta_D \approx 13\, MeV$.

$\tilde{D}^+(0, 2m_\pi^2)$ can be expressed in terms of a rapidly converging sum over t-channel partial waves (Ref.[5],p. 507).

The compatibility with the fixed-ν calculation is not quite satisfactory. The corrections applied by Gasser et al.[8] and further new results for the $\pi\pi$ S-wave should be taken into account in a new calculation.

The subtraction function $C^+(0,t)$ has a simple relation to $f_+^0(t)$ (Ref.[9])

$$C^+(0,t) = \frac{4\pi}{p_-^2}\tilde{f}_+^0(t) - \frac{2}{\pi}\int_{\nu_1}^{\infty} ImC^+(\nu,t)Q_1(z)\frac{d\nu}{\nu}, \tag{8}$$

where $z = m\,\nu/(p_-\,q_-)$, $\nu_1 = m_\pi + t/(4m)$, $p_-^2 = m^2 - t/4$, $q_-^2 = m_\pi^2 - t/4$.

Continuation along 50 hyperbolas

The use of subthreshold coefficients has the disadvantage that good data for an accurate determination of the t-dependence near $t = 0$ are not available. Therefore, R. Koch[10] calculated *analytic continuations along 50 hyperbolas, which pass the CD point.* In the s-channel region, these curves remain as far as possible within the physical range and cover the whole of the angular region. The l.h. cut was evaluated with our $\pi\pi N\bar{N}$ partial waves[5] and the discrepancy method for large t.

Koch's result for Σ was $64 \pm 8\, MeV$. The uncertainty is NOT the error, but it shows the remarkably small deviation of KH80 from Mandelstam's two-variable analyticity. The total uncertainty is larger, but I am sure that nobody can give a reliable estimate.

The Work of Gasser, Leutwyler, Locher and Sainio

These authors wanted to improve the results for Σ_d derived from KH80 and other partial wave solutions by taking into account new meson factory data below 185 MeV/c[8]. A first update did not lead to a significant change of Σ_d, but new calculations of the t-dependence of the scalar form factor led to an important change of the theoretical value for Σ[8,2].

Several further updates were made by M. Sainio. In Ref.[11] he mentioned that calculations with the VPI amplitude SM95 led to a value of Σ_d which is *only slightly higher than the earlier result in contrast to much larger increases reported by the VPI group.*

Continuations using Interior Dispersion Relations

Dispersion relations along hyperbolas in the Mandelstam plane at constant scattering scattering angle (lab.) in the physical region also have the advantage that the nearby part of the l.h. cut can be evaluated from t-channel partial waves[12]. Σ follows from the hyperbola through the CD point. This point belongs to the parameters

$$s = m^2,\ q^2 = -m_\pi^2 \left[1 - \frac{m_\pi^2}{4m^2}\right] = 0.994\, m_\pi^2,\ \theta_{lab} = 90.3°. \tag{9}$$

If the l.h. cut is treated by the discrepancy method[13], the accuracy of the result is poor because of the nearby singularities at $t = 4m_\pi^2$ and $t = 3.98\, m_\pi^2$. J. Stahov has calculated not only the hyperbola through the CD point but also many others in order to get information on the amplitude in regions, which cannot reached by the subthreshold expansion[12], but by predictions from chiral perturbation theory.

Continuation of the s-channel S-wave

Ericson[14] started from the fact that at the CD point the scattering angle in the c.m. frame also is near to 90°. Therefore, it is expected that the S-wave is dominant and the P-wave is strongly suppressed. So he attempted to continue the S-wave from the physical region to the CD point.

However, he did not notice that the continuation leads to a point very near to the 'circle cut' singularity in the s-plane, so *it has an unknown error.* The only reliable way to calculate continuations of s-channel partial waves is the exact partial wave projection of the fixed-t dispersion relation[15].

A continuation of the s-channel S-wave was also attempted in Ref.[16]. The authors introduced for each S- and P-wave a potential with 4 adjustable parameters which were fitted to πN data below $70\, MeV$. They mentioned in their paper that *the unknown model error* is not included, so the method cannot compete with dispersive calculations.

Application of the VPI Method of Arndt et al.

The method and its shortcomings are described in my plenary talk. The determination of Σ_d[17] is closely related to that in our papers in 1971. Because the experimental information on the slope $d\sigma/dt$ at $t = 0$ is poor even nowadays, R. Koch's method[10] is clearly preferable, because *the partial waves are used in the full angular range* and KH80 has analyticity constraints up to the backward direction.

The Extended Tree Model

This model[18,19] attempts to approximate the πN amplitudes by exchanges of nucleons (using a mixture of PS and PV couplings), and of Δ, ρ and an 'effective meson' σ in narrow resonance approximations. The attempt to calculate Σ from the tail of a 'σ meson' resonance ignores the important threshold cusp at $t = 4m_\pi^2$. Since *seven adjustable parameters* are available, it is not surprising that some quantities can be reproduced.

Models for the πN system at low energies can be of interest for the understanding of the dominant contributions in the physical region. However, E. Matsinos[19] writes: 'In

the context of the aim of the present work, the advantages of the method, implemented herin, over the (traditionally used) dispersion relation schemes are important'. I think *that the author strongly overestimates the validity of this model* and is not well informed on dispersion theory.

Conclusions

i) The best method for the determination of Σ from πN scattering data is to use partial wave analyses with sufficiently strong dispersion constraints derived from the Mandelstam hypothesis. Analytic continuations from the s-channel physical region to the CD point should be made *along different paths*, which allow one to express the nearby parts of the l.h. cuts by t-channel partial waves. The works of R. Koch and J. Stahov are good examples.

ii) It will not be possible to give reliable errors for Σ, because the data base contains contradictory data sets.

iii) Since many new data have been published during the last two decades. it is necessary to update the solution KH80.

Thanks

It is a pleasure to thank J. Gasser and H. Leutwyler for numerous informative discussions during a long time which encouraged me to continue my work in this field. I am grateful to T.O.F. Ericson, W.R. Gibbs, U.-G. Meißner, M. Pavan, M. Sainio, and J. Stahov for useful communications and information on new results.

REFERENCES

1. L.S. Brown et al., Phys. Rev. **D4**, 2801 (1971); T.P. Cheng and R. Dashen, Phys. Rev. Lett. **26**, 594 (1971).
2. T. Becher and H. Leutwyler, Eur. J. Ph. **C9**, 643 (1999) and contribution to this symposium.
3. T.E.O. Ericson,B, Loiseau and A.W. Thomas, preprint PANIC-99 and contribution by B. Loiseau to this Symposium.
4. P. Baillon et al., Nucl. Phys. **B105**, 365 (1976).
5. G. Höhler, *Pion-Nucleon Scattering, Landolt-Börnstein, Vol. I/9b2* (Springer 1983).
6. D.J. Bardsley et al., *Topical Conf. on Baryon Resonances*,(1976)
7. E. Pietarinen, Helsinki preprint HU-TFT-17-77 (1977).
8. J. Gasser et al., Phys. Lett. **B213**, 85 (1987), Phys. Lett. **B253**, 252, 260 (1991); Phys. Lett. **B125**, 221, 325 (1983); Ann. Phys. (NY) **158**, 142 (1984).
9. G. Höhler and H.P. Jakob, Z. Phys. **268**, 75 (1974)
10. R. Koch, Z. Physik. **C15**, 161 (1982).
11. M. Sainio, πN Newsletter **10**, 13 (1995).
12. J. Stahov, Thesis (University of Zagreb, 1983) and contribution to this Symposium.
13. W.B. Kaufmann et al., πN Newsletter **13**, 16 (1997).
14. T.O.F. Ericson, Phys. Lett. **B195**, 116 (1987); *International Workshop on Pions in Nuclei*, p.619, (World Scientific Singapore 1991).
15. R. Koch, Nucl. Phys. **A448**, 707 (1986).
16. W.R. Gibbs et al., Phys. Rev. **C57**, 784 (1998).
17. R.A. Arndt et al., submitted to Phys. Rev. C, M.M. Pavan, contributions to this Symposium.
18. P.F.A. Goudsmit et al., Nucl. Phys. **A575**,673 (1994); H.J. Leisi ETHZ-IPP preprint PR-98-11 (1998) and contribution to this Symposium.,
19. E. Matsinos, Phys. Rev. **C56**, 3014 (1997).

WORKING GROUP SUMMARY: ISOSPIN VIOLATION

Ulf-G. Meißner
FZ Jülich, IKP (Th), D-52425 Jülich, Germany

Abstract

I give an introduction to the problem of isospin violation and add some comments to the various topics addressed in the working group.

ISOSPIN VIOLATION: GENERAL ASPECTS

Isospin symmetry was introduced in the thirties by Heisenberg in his studies of the atomic nucleus. Since then, many particles have been found to appear in iso–multiplets, like the nucleons, the pions, the delta isobars, a.s.o. With the advent of QCD, a deeper understanding of isospin symmetry has emerged. In the limit of equal up and down current quark masses and in the absence of electroweak interactions, isospin is an exact symmetry of QCD. The intra–multiplet mass splittings allow to quantify the breaking of this symmetry, which is caused by different mechanisms (for a detailed review, see ref.[1]). First, the light quark masses are everything but equal (still, their absolute masses are much smaller than any other QCD scale and thus this breaking can be treated as a perturbation). Second, the light quarks have different charges and thus react differently to the electromagnetic (em) interactions. The em effects are also small since they are proportional to the fine structure constant $\alpha = e^2/4\pi \approx 1/137$. In the case of the pions, the mass splitting is almost entirely of em origin. This can be traced back to the absence of d–like couplings in SU(2), thus promoting the quark mass difference to a second order effect. For the nucleons, matters are different, strong and em effects are of similar size but different signs. The fact that the neutron is heavier than the proton leads to the conclusion that $m_d > m_u$, consistent with the analysis of the kaon masses. Since we know that isospin is broken - so why bother? First, the picture that has emerged from the hadron masses can not be considered complete, there is still on–going discussion about the size of the violation of Dashen's theorem, the possibility of a vanishing up quark mass to solve the strong CP problem and "strange" results from lattice gauge theory. Also, the analysis of the quark mass dependence of the baryon masses remains to be improved (for a classic, see ref.[2] and a recent study, see ref.[3]). Furthermore, only a few dynamical implications of isospin violation have been verified experimentally and a truely quantitative picture has not yet emerged. In addition, the nucleus as a many–body system offers a novel laboratory to study isospin violation. In addition, with the advent of CW electron accelerators and improved detectors, we now have experimental tools to measure threshold pion photoproduction with an unprecedented accuracy.

THE PION SECTOR

The purely mesonic sector was not touched upon in this working group, but there is one recent result which I would like to discuss. In elastic $\pi\pi$ scattering, the chiral perturbation analysis has been carried out to two loops. It was demonstrated in refs.[4,5] that the em isospin–violating effects are of the same size as the hadronic two–loop corrections. For a precise description of low energy pion reactions, it is thus mandatory to include such effects consistently. A somewhat surprising result was found in case of the scalar and the vector form factor of the pion in ref.[6]. It was shown that the em corrections to the momentum–dependence of both form factors are tiny (due to large cancellations between various contributions), much smaller than the corresponding hadronic two–loop contributions worked out in refs.[7,8]. This result remains to be understood in more detail. It is particularly surprising for the scalar form factor since it is not protected by a conserved current theorem à la Ademello–Gatto. Only the normalization of the scalar form factor exhibits the few percent em corrections anticipated from the study of the $\pi\pi$ scattering lengths. Note, however, that the smallness of the effects of the light quark mass difference for the pion form factors has been known and understood since long[9].

THE PION–NUCLEON SECTOR

The pion–nucleon system plays a particular role in the study of isospin violation. First, the explicit chiral symmetry breaking and isospin breaking operators appear at the same order in the effective Lagrangian which maps out the symmetry breaking part of the QCD Hamiltonian, i.e. the quark mass term (restricted here to the two lightest flavors),

$$\mathcal{H}^{\rm sb}_{\rm QCD} = m_u \bar{u}u + m_d \bar{d}d = \frac{1}{2}(m_u + m_d)(\bar{u}u + \bar{d}d) + \frac{1}{2}(m_u - m_d)(\bar{u}u - \bar{d}d) \ , \qquad (1)$$

so that the strong isospin violation is entirely due to the isovector term whereas the isoscalar term leads to the explicit chiral symmetry breaking. In the presence of nucleons (and in contrast to the pion case), both breakings appear at the same order. This can lead to sizeable isospin violation as first stressed in reactions involving neutral pions by Weinberg[10]. Let me perform some naive dimensional analysis for the general case (say for any given channel in πN scattering that is not suppressed to leading order). Isospin–violation (IV) should be of the size

$$\mathrm{IV} \sim \frac{m_d - m_u}{\Lambda_{\rm hadronic}} \approx \frac{m_d - m_u}{M_\rho} = \mathcal{O}(1\%) \ , \qquad (2)$$

where the mass of the ρ set the scale for the non–Goldstone physcis. In the presence of a close–by and strongly coupled baryonic resonance like the $\Delta(1232)$, IV might be enhanced

$$\mathrm{IV} \sim \frac{m_d - m_u}{m_\Delta - m_N} = \mathcal{O}(2\%) \ . \qquad (3)$$

Of course, such type of arguments can not substitute for full scale calculations. Second, there are two analyses[11,12] which seem to indicate a fair amount of isospin violation (of the order of 6...7%, which is much bigger than the dimensional arguments given above would indicate) in low–energy πN scattering, see Gibbs' talk[13]. This can not be explained in conventional meson–exchange models by standard meson mixing mechanisms. I would also like to mention that in these two analyses the hadronic and the electromagnetic contributions are derived from different models. This might cause some concern about possible uncertainties due to a theoretical mismatch. Clearly, it would be preferable to use here one unique framework. That can, in principle, be supplied by chiral perturbation theory since electromagnetic corrections can be included systematically by a straightforward extension of the power counting. This is most economically, done by counting the electric charge as a small parameter, i.e. on the same footing as the external momenta and meson masses. The heavy baryon chiral perturbation theory machinery to study these questions to complete one–loop (fourth) order has been set up as shown by Müller[14]. It is important to perform such calculations to fourth order since one–loop graphs appear at dimension three *and* four. Furthermore, it is known from many studies that one–loop diagrams with exactly one insertion from the dimension two πN Lagrangian are (often) important. Finally, symmetry breaking (chiral and isospin) in the loops only starts at fourth order. In particular, questions surrounding the πN σ–term or neutral pion scattering off nucleons can now be addressed to sufficient theoretical precision. A first step in this direction for all channels in πN scattering was reported by Fettes[15], but a full scale one–loop calculation including all virtual photon effects still has to be done. Of particular interest is the novel relation between π^0 and $\pi^\pm$ scattering off protons that is extremely sensitive to isospin violation. It should also be stressed that for such tests, it is mandatory to better measure and determine the small isoscalar πN amplitudes. Also, the relations which include the much bigger isovector amplitudes show IV consistent with the dimensional arguments given in eq.(2). I consider the "ordering schemes" discussed by Gibbs and Fettes very useful tools to pin down the strengths and sources of isospin breaking in πN scattering. This also allows to see a priori which type of measurements are necessary to obtain complete information and to what extent various reactions can give redundant information (one example is discussed by Gibbs[13]). Intimately related to this is pion–photoproduction via the final–state theorem, i.e. certain πN scattering phases appear in the imaginary part of the respective

charged or neutral pion photoproduction multipoles. Bernstein[16] stressed that in neutral pion photoproduction off protons, there are two places to look for isospin violation. One is below the $\pi^+ n$ threshold, which might give access to the elusive (but important) $\pi^0 p$ scattering length. At present, it does not appear that the original proposal of measuring the target polarization below the $\pi^+ n$ threshold to high precision is feasible at a machine like e.g. MAMI. The other important effect, which appears to be more easily accessible to an experiment, is the strength of the cusp at the opening of the $\pi^+ n$ threshold, which according to Bernstein's three–channlel S–matrix analysis[16] is quite sensitive to isospin violation. Such a calculation should also be done in the framework of heavy baryon chiral perturbation theory (beyond the charged to neutral pion mass difference effects included so far). Over the last years, there has been a very fruitful interplay between experimenters and theorists particularly in the field of pion photo– and electroproduction and it is of utmost important to further strengthen this. It is a theorists dream that reactions with neutral pions (elastic scattering and photoproduction) will be measured to a high precision. An important point was stressed by Lewis[17]. In a "toy" calculation (i.e. an SU(2) approach to the strange vector form factor of the nucleon, which is clearly related to three flavor QCD), he showed that isospin–breaking effects can simulate a "strange" form factor that intrinsically vanishes in that approach. This nicely demonstrates that to reliably determine small quantities, may they be related to isospin conserving or violating operators, *all* possible effects have to be included. The recent measurements at BATES and JLAB, which seem to indicate small expectation values of the strange vector current in the proton, should therefore be reanalyzed. In this case, isospin violation appears to be a nuisance but can not be ignored.

THE NUCLEON–NUCLEON SECTOR

The only new data with respect to IV were presented by Machner[18]. He analysed recent data from COSY and IUCF for $pp \to \pi^+ d$ and $np \to \pi^0 d$. For exact isospin symmetry (i.e. after removing the Coulomb corrections), the pertinent cross sections should be equal (up to a Clebsch). In the threshold region, one can make a partial wave expansion and finds that the S–wave contribution α_0 shows IV of the order of 10% and no effect is observed in the P–wave terms. To my knowledge, a theoretical understanding of this effect is lacking. Despite a huge amount of efforts over the last years, a model–independent effective field theory description of pion production in proton–proton collisions has not yet been obtained. The energies involved to even produce a pion at rest are too large for the methods employed so far. More progress, however, has been made in the two–nucleon system at low energies. It is well known that IV appears in the NN scattering lengths. In the nuclear jargon, one talks about charge independence breaking (CIB) ($a_{np} \neq (a_{pp} + a_{nn})/2$ after Coulomb subtraction, where a denotes the scattering length) and charge symmetry breaking (CSB) ($a_{pp} \neq a_{nn}$ after Coulomb subtraction). These effects are naturally most pronounced at threshold. Kaplan, Savage and Wise (KSW)[19] have proposed a non–perturbative scheme that allows for power counting on the level of the nucleon–nucleon scattering amplitude. In that framework, IV (CIB and CSB) has recently been investigated[20]. It was shown that isospin violation can be systematically included in the effective field theory approach to the two–nucleon system in the KSW formulation. For that, one has to construct the most general effective Lagrangian containing virtual photons and extend the power counting accordingly. This framework allows one to systematically classify the various contributions to CIB and CSB. In particular, the power counting combined with dimensional analysis allows one to understand the suppression of contributions from a possible charge–dependence in the pion–nucleon coupling constants. Including the pions, the leading CIB breaking effects are the pion mass difference in one–pion exchange together with a four–nucleon contact term. These effects scale as αQ^{-2}, where $Q \approx 1/3$ is the genuine expansion parameter of the KSW scheme. Power counting lets one expect that the much debated contributions from two–pion exchange and $\pi\gamma$ graphs are suppressed by factors of $1/3$ and $(1/3)^2$, respectively. This is in agreement with some, but not all, previous more model–dependent calculations. The leading charge symmetry breaking is simply given by a four–nucleon contact term.

LIGHT NUCLEI

Often, the nucleus can be used as a filter to enhance or suppress certain features of reactions as they appear in free space. Furthermore, measurements on the neutron, which are necessary to get the complete information in the isospin basis (for a discussion on this topic with respect to pion photoproduction, see ref.[21]) can only be done on (preferably polarized) light nuclei. Gibbs[13] has pointed out that a measurement of charge exchange on the proton and the neutron (in forward direction and close to the interference minimum near 45 MeV) could be done in the ^{3}He–triton system. This would be an interesting possibility to get another handle on the elusive neutron and allow one to pin down one of the amplitudes parametrizing IV (according to the ordering scheme mentioned above). For a more detailed discussion concerning the extraction of neutron properties from the deuteron, I refer to the recent summary by Beane[22].

WHERE DO WE STAND AND WHERE TO GO

For sure, isospin symmetry is broken. However, do we precisely know the size of IV from experiment? The answer is yes and no. We have some indicative information but no systematic investigations of all pertinent low energy reactions are available. Also, one might ask the question whether the methodology, which has been used so far to extract numbers on IV, say from low energy πN scattering data, is reliable? If we assume that this is the case, we still have no deeper understanding of the mechanisms triggering IV. To my knowledge, the only machinery to consistently separate strong and electromagnetic IV is based on effective field theory. In that scheme, one can consider various reactions like elastic πN scattering, pion photoproduction or even nucleon Compton scattering to try to get a handle on the symmetry breaking operators $\sim m_d - m_u$. Also, a systematic treatment of isospin violation is mandatory for the determiantion of small quantities like the isoscalar S–wave scattering length or the strange nucleon form factors. Based on that, I have the following wish list for theory and experiment:

THEORY:

- The effective chiral Lagrangian calculations can and need to be improved. In particular, it is most urgent to get a handle on the so–called low–energy constants, which parametrize the effective Lagrangian beyond leading order. Sum rules, models or even the lattice might be useful here.
- A deeper theoretical understanding of certain phenomenological models (like e.g. the extended tree level model of ref.[23]) in connection with the approaches to correct for Coulomb effects would be helpful.
- The dispersion–theoretical approach should be revisited and set up in a way to properly include IV (beyond what has been done so far). For some first steps, see the talk by Oades[24].

EXPERIMENT:

- Clearly, we need more high precision data for the elementary processes, but not only for πN scattering but also for (neutral) pion photo/electroproduction.
- More precise nuclear data are also needed. Embedding the elementary reactions in the nucleus as a filter allows one to get information on the elusive neutron properties. Clearly, this refers to few–nucleon systems where precise theoretical calculations are possible.

Finally, I would like to stress again that a truely quantitative understanding of isospin violation can only be obtained by considering a huge variety of processes. While pion–nucleon scattering is at the heart of these investigations, threshold pion photoproduction or the nucleon form factors also play a vital role in supplying additional information.

ACKNOWLEDGEMENTS

I would like to thank all participants of this working group for their contributions. I am grateful to my collaborators Evgeny Epelbaum, Nadia Fettes, Bastian Kubis, Guido Müller and Sven Steininger for sharing with me their insight into this topic. Last but not least the superbe organization by Christine Kunz and Res Badertscher is warmly acknowledged.

REFERENCES

1. J. Gasser and H. Leutwyler, Phys. Rep. **C87**, 77 (1982).
2. J. Gasser, Ann. Phys. (NY) **136**, 62 (1981).
3. B. Borasoy and Ulf-G. Meißner, Ann. Phys. (NY) **254**, 192 (1997).
4. Ulf-G. Meißner, G. Müller, and S. Steininger, Phys. Lett. **B406**, 154 (1997) 154; (E) *ibid* **B407**, 434 (1997).
5. M. Knecht and R. Urech, Nucl. Phys. **B519**, 329 (1998).
6. B. Kubis and Ulf-G. Meißner, `hep-ph/9908261`.
7. J. Gasser and Ulf-G. Meißner, Nucl. Phys. **B357**, 90 (1991).
8. J. Bijnens, G. Colangelo, and P. Talavera, JHEP **9805**, 014 (1998).
9. J. Gasser and H. Leutwyler, Ann. Phys.(NY) **158**, 142 (1984).
10. S. Weinberg, Trans. N.Y. Acad. of Sci. **38**, 185 (1977).
11. W.R. Gibbs, Li Ai and W.B. Kaufmann, Phys. Rev. Lett. **74**, 3740 (1995).
12. E. Matsinos, Phys. Rev. **C56**, 3014 (1997).
13. W.R. Gibbs, *these proceedings.*
14. G. Müller, *these proceedings.*
15. N. Fettes, *these proceedings.*
16. A.M. Bernstein, *these proceedings.*
17. R. Lewis, *these proceedings.*
18. H. Machner, *these proceedings.*
19. D.B. Kaplan, M.J. Savage and M.B. Wise, Nucl. Phys. **B534**, 329 (1998).
20. E. Epelbaum and Ulf-G. Meißner, Phys. Lett. **B467**, 284 (1999).
21. Ulf-G. Meißner, Nucl. Phys. **A629**, 72c (1998).
22. S.R. Beane, `nucl-th/9909016`.
23. P.F.A. Goudsmit et al., Nucl. Phys. **A575**, 673 (1994).
24. G. Oades, *these proceedings.*

UWThPh-1999-48

Virtual photons to fourth order CHPT with nucleons *

Guido Müller †
Universität Wien , Institut für Theoretische Physik, Boltzmanngasse 5, A–1090 Wien, Austria

Abstract

We discuss the implementation of virtual photons to chiral perutrbation theory with fermions to the fourth order in the chiral counting. This systematic treatment is then applied to the nucleon sigma term and to the famous Weinberg prediction for isospin violation in the scattering of neutral pions and nucleons.

Baryon chiral perturbation theory offers another possibility of investigating isospin violation. As first stressed by Weinberg[1], reactions involving nucleons and neutral pions can lead to gross violations of isospin, e.g. in the scattering length difference $a(\pi^0 p) - a(\pi^0 n)$ he predicted an effect of the order of 30%. This is because chiral symmetry and isospin breaking appear at the same order and the leading isospin symmetric terms involving neutral pions are suppressed due to chiral symmetry. It is, however, known that precise and complete one loop calculations in the baryon sector should be carried out to fourth order since it has also been shown that in many cases one loop graphs with exactly one dimension two insertion are fairly large. Most calculations in baryon CHPT are performed in heavy baryon chiral perturbation theory (HBCHPT)[5,6]. This is based on the observation that a straightforward extension of CHPT with baryons treated fully relativistically leads to a considerable complication in the power counting since only nucleon three–momenta are small compared to typical hadronic scales, as discussed in detail in ref.[7]. However, one has to be careful with strict non–relativistic expansions since in some cases they can conflict structures from analyticity, as discussed e.g. in ref.[8]. Therefore, in ref.[9], a novel scheme was proposed which is based on the relativistic formulation but circumvents the power counting problems (to one loop) by a clever separation of the loop integrals into IR singular and regular parts. In this formulation, all analytic constraints are fulfilled by construction.

The starting point of our approach is to construct the most general chiral invariant Lagrangian built from pions, nucleons and external scalar, pseudoscalar, vector, axial–vector sources *and* virtual photons, parametrized in terms of the vector field $A_\mu(x)$. The Goldstone bosons are collected in a 2×2 matrix-valued field $U(x) = u^2(x)$. The nucleons are described by structureless relativistic spin-$\frac{1}{2}$ particles, the spinors being denoted by $\Psi(x)$ in the relativistic case or by the so–called light component $N(x)$ in the heavy fermion formulation. The effective field theory admits a low energy expansion, i.e. the corresponding effective Lagrangian can be written as

$$\mathcal{L}_{\rm eff} = \mathcal{L}^{(2)}_{\pi\pi} + \mathcal{L}^{(4)}_{\pi\pi} + \mathcal{L}^{(1)}_{\pi N} + \mathcal{L}^{(2)}_{\pi N} + \mathcal{L}^{(3)}_{\pi N} + \mathcal{L}^{(4)}_{\pi N} + \dots \,, \tag{1}$$

where the ellipsis denotes terms of higher order not considered here. For the explicit form of the meson Lagrangian and the dimension one and two pion–nucleon terms, we refer to ref.[11]. More precisely, in the pion–nucleon sector, the inclusion of the virtual photons modifies the leading term of dimension one and leads to new local (contact) terms starting at second order[2]. In particular, since the electric charge related to the virtual photons always appears quadratic, the following pattern for the terms in the electromagnetic effective Lagrangian emerges. At second order, we can only have terms of order e^2, at third

*Work supported in part by TMR, EC-Contract No. ERBFMRX-CT980169 (EURODAΦNE).
†email: gmueller@doppler.thp.univie.ac.at

order e^2q and at fourth order e^2q^2 or e^4 (besides the standard strong terms).The inclusion of the virtual photons proceeds with,

$$Q_\pm = \frac{1}{2}\left(u\,Q\,u^\dagger \pm u^\dagger\,Q\,u\right) \ , \tag{2}$$

which under chiral $\mathrm{SU}(2)_L\times\mathrm{SU}(2)_R$ symmetry transform as any matrix–valued matter field (Q defines the charge matrix).

In particular, to lowest order one finds (in the relativistic and the heavy fermion formulation)

$$\mathcal{L}^{(1)}_{\pi N} = \bar\Psi\left(i\gamma_\mu\cdot\tilde\nabla^\mu - m + \frac{1}{2}g_A\,\gamma^\mu\gamma_5\cdot\tilde u_\mu\right)\Psi \quad = \quad \bar N\left(iv\cdot\tilde\nabla + g_A\,S\cdot\tilde u\right)N + \mathcal{O}(\frac{1}{m}) \ , \tag{3}$$

with

$$\tilde\nabla_\mu = \nabla_\mu - i\,Q_+\,A_\mu \ , \ \ \tilde u_\mu = u_\mu - 2\,Q_-\,A_\mu \ , \tag{4}$$

and[#1]

$$\Psi(x) = \exp\{imv\cdot x\}\,(N(x) + h(x)) \ . \tag{5}$$

Furthermore, v_μ denotes the nucleons' four–velocity, S_μ the covariant spin–vector à la Pauli–Lubanski and g_A the axial–vector coupling constant. These virtual photon effects can only come in via loop diagrams since by definition a virtual photon can not be an asymptotic state.

At second order, local contact terms with finite low–energy constants (LECs) appear. We call these LECs f_i for the heavy baryon approach and f_i' in the relativistic Lagrangian. As stated before, the em Lagrangian is given entirely in terms of squares of $Q_\pm$ (and their traceless companions),

$$\mathcal{L}^{(2)}_{\pi N,\mathrm{em}} = \sum_{i=1}^{3} F_\pi^2\,f_i'\,\bar\Psi\,\mathcal{O}_i^{(2)}\,\Psi = \sum_{i=1}^{3} F_\pi^2\,f_i\,\bar N\,\mathcal{O}_i^{(2)}\,N \ , \tag{6}$$

with the $\mathcal{O}_i^{(2)}$ monomials of dimension two,

$$\mathcal{O}_1^{(2)} = \langle\tilde Q_+^2 - \tilde Q_-^2\rangle \ , \quad \mathcal{O}_2^{(2)} = \langle Q_+\rangle\,\tilde Q_+ \ , \quad \mathcal{O}_3^{(2)} = \langle\tilde Q_+^2 + \tilde Q_-^2\rangle \ . \tag{7}$$

Notice furthermore that only the second term in eq.(6) has an isovector piece and contributes to the neutron–proton mass difference[2]. The factor F_π^2 in eq.(6) ensures that the em LECs have the same dimension as the corresponding strong dimension two LECs. From the third order calculation of the proton–neutron mass difference[2] one deduces the value for f_2, $f_2 = -(0.45\pm0.19)\ \mathrm{GeV}^{-1}$.

The Lagrangian to third order takes the form

$$\mathcal{L}^{(3)}_{\pi N,\mathrm{em}} = \sum_{i=1}^{12} F_\pi^2\,g_i'\,\bar\Psi\,\mathcal{O}_i^{(3)}\,\Psi \ = \sum_{i=1}^{12} F_\pi^2\,g_i\,\bar N\,\mathcal{O}_i^{(3)}\,N \ , \tag{8}$$

with the $\mathcal{O}_i^{(3)}$ monomials in the fields of dimension three[2][3] , in their relativistic form and the heavy baryon counterparts. Again, for the g_i to have the same mass dimension as the d_i of the strong sector defined in ref.[10], we have multiplied them with a factor of F_π^2. Thus the g_i (g_i') scales as [mass^{-2}]. So the complete fourth order pion–nucleon Lagrangian with virtual photons is given by[3]

$$\mathcal{L}^{(4)}_{\pi N,\mathrm{em}} \ = \ \sum_{i=1}^{5} F_\pi^4\,h_i'\,\bar\Psi\,\mathcal{O}_i^{(e^4)}\,\Psi \ + \sum_{i=6}^{90} F_\pi^2\,h_i'\,\bar\Psi\,\mathcal{O}_i^{(e^2p^2)}\,\Psi \tag{9}$$

[#1] We do not spell out the details of how to construct the heavy nucleon EFT from its relativistic counterpart but refer the reader to the extensive review[11].

with the $\mathcal{O}_i^{(4)}$ monomials in the fields of dimension four[3]. To be consistent with the scaling properties of the dimension two and three LECs, the h_i are multiplied with powers of F_π^2 such that the first five LECs take dimension [mass^{-3}] while the others are of dimension [mass^{-1}].

The scalar form factor

The scalar form factor of the nucleon is defined via

$$\langle N(p')|\, m_u \bar{u}u + m_d \bar{d}d \,|N(p)\rangle = \bar{u}(p')u(p)\,\sigma(t)\ , \quad t=(p'-p)^2\ , \tag{10}$$

for a nucleon state $|N(p)\rangle$ of four–momentum p. At $t=0$, which gives the much discussed pion–nucleon σ–term, one can relate this matrix element to the so–called strangeness content of the nucleon. A direct determination of the σ–term is not possible, but rather one extends pion–nucleon scattering data into the unphysical region and determines $\sigma_{\pi N}(t = 2M_\pi^2)$, i.e. at the so–called Cheng–Dashen point. The relation to the σ–term is given by the low–energy theorem of Brown, Peccei and Pardee[13],

$$\sigma_{\pi N}(2M_\pi^2) = \sigma_{\pi N}(0) + \Delta\sigma_{\pi N} + \Delta R \tag{11}$$

where $\Delta\sigma_{\pi N}$ parametrizes the t–dependence of the sigma–term whereas ΔR is a remainder not fixed by chiral symmetry. The most systematic determination of $\Delta\sigma_{\pi N}$ has been given in ref.[14], $\Delta\sigma_{\pi N} = (15 \pm 1)$ MeV. The remainder ΔR has been bounded in ref.[15], $\Delta R < 2$ MeV. It was shown that the third order effects can shift the proton σ–term by about 8% and have a smaller influence on the shift to the Cheng–Dashen (CD) point[2]. In[3] we worked out explicitly the isospin violating corrections to this shift to fourth order. This is motivated by the fact that in the difference most of the counterterm contributions drop out, more precisely, only momentum–dependent contact terms can contribute to the shift. Such terms only appear at fourth order since due to parity one needs two derivatives and any quark mass or em insertion accounts for at least two orders[3]. It can be decomposed as

$$\sigma_{\pi N}^{(4)}(t) = \sigma_{\pi N}^{(4),\mathrm{IC}}(t) + \sigma_{\pi N}^{(4),\mathrm{IV}}(t)\ . \tag{12}$$

The isospin–conserving strong terms have already been evaluated in ref.[15]. Here, we concentrate on the em corrections ~ 1 (in isospin space) and all terms $\sim \tau_3$. We have eye graphs and tadpoles with insertions $\sim f_2, c_5$. These can be evaluated straightforwardly. Because of the tiny coefficients appearing in the evaluation of the loop contributions, these are only fractions of an MeV, $\Delta\sigma_{\pi N}^{4,IV,\mathrm{loop}} = -0.05\,\mathrm{MeV}$ and can thus be completely neglected. For the counterterm contributions, setting all appearing LECs on the values obtained from dimensional analysis as explained[3], one finds a total contribution $\Delta\sigma_{\pi N}^{4,IV,\mathrm{ct}} = \pm 0.01\,\mathrm{MeV}$. For the IC em terms, we find (setting again $f_{1,3} = \pm 1/4\pi$) a completely negligible loop contribution (less than 0.01 MeV) and the counterterms give ± 0.7 MeV for the LECs estimated from dimensional analysis. Note, however, that if the numerical factors $f_{1,3}/(4\pi)$ are somewhat bigger than one, one could easily have a shift of ± 2 MeV, which is a substantial electromagnetic effect.

Neutral pion scattering off nucleons

As pointed out long time ago by Weinberg[1], the difference in the S–wave scattering lengths for neutral pions off nucleons is sensitive to the light quark mass difference,

$$\begin{aligned} a(\pi^0 p) - a(\pi^0 n) &= \frac{1}{4\pi}\frac{1}{1+M_{\pi^+}/m_p}\,\frac{-4B(m_u-m_d)c_5}{F_\pi^2} + \mathcal{O}(q^3) \\ &= \frac{1}{4\pi}\frac{1}{1+M_{\pi^+}/m_p}\,\Delta_2(M_{\pi^0}) + \mathcal{O}(q^3)\ . \end{aligned} \tag{13}$$

It was shown in ref.[2] by an explicit calculation that to third order there are no corrections to this formula. This is based on the fact that the electromagnetic Lagrangian can not contribute at this order since the charge matrix has to appear quadratic and never two additional pions can appear. However, at next order one can of course have loop graphs with one dimension two insertion and additional em counterterms. To obtain the first correction to Weinberg's prediction, eq.(13), one thus has to compute the fourth order corrections[3]. These are due to strong dimension two insertions $\sim c_5$ and em insertions $\sim f_2$. For the difference $a(\pi^0 p) - a(\pi^0 n)$ we only have to consider the operators $\sim \tau^3$[3] Consider first the loop contributions. Since we can not fix the counterterms from data, we are left with a spurious scale dependence which reflects the theoretical uncertainty at this order. For $\lambda = \{0.5, 0.77, 1.0\}$ GeV we find

$$\Delta_2^{\rm str} = \{-7.1, 0.9, 5.7\} \cdot 10^{-2} \ , \quad \Delta_2^{\rm em} = \{11.5, 12.0, 12.3\} \cdot 10^{-2} \ . \tag{14}$$

The counterterms are estimated based on dimensional analysis at the scale $\lambda = M_\rho$ and give a contribution of about $-0.3 \cdot 10^{-2}$. Even if the LECs would be a factor of ten larger than assumed, the counterterm contribution would not exceed $\pm 3\%$. Altogether, the correction to Weinberg's prediction, eq.(13), are in the range of 4 to 18 percent, i.e. fairly small. Finally, we wish to mention that in ref.[16] isospin–violation for neutral pion photoproduction off nucleons was discussed which allows one to eventually measure directly the very small $\pi^0 p$ scattering length by use of the final–state theorem.

Summary

We have developed the whole mechanism to calculate isospin violation effects in the framework of CHPT. In order to get the correct size of isospin violation one has to include all non-isospin symmetric sources like the electromagnetic interaction, the quark mass difference ($\pi_0 - \eta$ mixing), explicit photon loops. In future calculations one has to pin down the two LECs of the second order em Lagrangian $f_{1,3}$ which are not well known and are estimated only by dimensional arguments.

Acknowledgments
I am grateful to Ulf-G. Meißner for enjoyable collaboration.

REFERENCES

1. S. Weinberg, Trans. N.Y. Acad. of Sci. 38 (1977) 185.
2. Ulf-G. Meißner and S. Steininger, Phys. Lett. B419 (1998) 403.
3. Ulf-G. Meißner and G. Müller, Nucl.Phys. B556 (1998) in press.
4. N. Fettes, Ulf-G. Meißner and S. Steininger, hep-ph/9811366, Phys. Lett. B (in press).
5. E. Jenkins and A.V. Manohar, Phys. Lett. B255 (1991) 558.
6. V. Bernard, N. Kaiser, J. Kambor and Ulf-G. Meißner, Nucl. Phys. B388 (1992) 315.
7. J. Gasser, M.E. Sainio and A. Švarc, Nucl. Phys. B307 (1988) 779.
8. V. Bernard, N. Kaiser and Ulf-G. Meißner, Nucl. Phys. A611 (1996) 429.
9. T. Becher and H. Leutwyler, hep-ph/9901384.
10. N. Fettes, Ulf-G. Meißner and S. Steininger, Nucl. Phys. A640 (1998) 199.
11. V. Bernard, N. Kaiser and Ulf-G. Meißner, Int. J. Mod. Phys. E4 (1995) 193.
12. Ulf-G. Meißner, G. Müller and S. Steininger, hep-ph/9809446, Ann. Phys. (NY), in press.
13. L.S. Brown, W.J. Pardee and R.D. Peccei, Phys. Rev. D4 (1971) 2801.
14. J. Gasser. H. Leutwyler and M.E. Sainio, Phys. Lett. B253 (1991) 252.
15. V. Bernard, N. Kaiser and Ulf-G. Meißner, Phys. Lett. B389 (1996) 144.
16. A.M. Bernstein, Phys. Lett. B442 (1998) 20.

Field Theory Approach to Isospin Violation in Low–Energy Pion–Nucleon Scattering

N. Fettes
FZ Jülich, IKP (Theory), D-52425 Jülich, Germany

Abstract

We present an analysis of isospin–breaking effects in threshold pion–nucleon scattering due to the light quark mass difference and the dominant virtual photon effects. We discuss the deviation from various relations, which are exact in the isospin limit. The size of the isospin–violating effects in the relations involving the isovector πN amplitudes is typically of the order of one percent. We also find a new remarkably large effect ($\sim$ 40%) in an isoscalar triangle relation connecting the charged and neutral pion scattering off protons.

INTRODUCTION

Pion–nucleon scattering is one of the prime reactions to test our understanding of the spontaneous and explicit chiral symmetry breaking QCD is supposed to undergo. During the last years, there has been considerable interest in using πN scattering data to extract information about the violation of isospin symmetry of the strong interactions[1,2], some analyses indicating effects as large as 7%[3,4]. Microscopically, there are two competing sources of isospin violation, which are generally of the same size, namely the strong effect due to the light quark mass difference $m_d - m_u \simeq m_u$ and the electromagnetic (em) one caused by virtual photons. To do this in a consistent fashion, one has to develop an effective field theory (EFT) of pions, nucleons and virtual photons. The corresponding effective Lagrangian was developed in refs.[5,6] extending the standard πN EFT (for a review, see ref.[7]). The pertinent power counting of the EFT is based on the observation that besides the pion mass and momenta, the electric charge e should be counted as an additional small parameter, given the fact that $e^2/4\pi \simeq M_\pi^2/(4\pi F_\pi)^2 \simeq 1/100$ (with M_π and F_π the pion mass and decay constant, respectively). We stress again that in the framework we are using, a consistent separation of the electromagnetic and the strong effects is possible and to our knowledge this has not been achieved before.

ISOSPIN SYMMETRIC CASE

The analysis of isospin violation in πN scattering proceeds essentially in three steps. First, one ignores all isospin breaking effects, i.e. one sets $e = 0$ and $m_u = m_d$. Only if within this approximation one is able to describe the low πN partial waves in the threshold region as given by various partial wave analyses, one can be confident to have a sufficiently accurate starting point. In this section, I will show that this is indeed the case.

Since pions form an isotriplet (I=1) and nucleons an isodoublet (I=$\frac{1}{2}$), the pion–nucleon system has total isospin I=$\frac{1}{2}, \frac{3}{2}$. In the isospin symmetric case, the amplitude for the process $\pi^a(q_a)+N(p_1) \to \pi^b(q_b)+N(p_2)$ can be entirely described in terms of two amplitudes: $T_{1/2}, T_{3/2}$ or equivalently the isospin even and odd amplitudes T^+ and T^-:

$$T^{ab}(\omega,t) = \delta^{ab} T^+_{ab}(\omega,t) + i\epsilon^{bac}\tau^c T^-_{ab}(\omega,t) \quad , \tag{1}$$

with $\omega = v \cdot q_a = v \cdot q_b$ the pion cms energy and $t = (q_a - q_b)^2$ the invariant momentum transfer squared.

The amplitudes consist of essentially three pieces, which are the Born and counterterm parts of polynomial type as well as the unitarity corrections due to the pion loops. Analytical expressions for all three pieces up to third order are given in ref.[8].

The amplitude is given in terms of nine combinations of counterterms, the values of which are not fixed by symmetries. In order to determine these low energy constants, we fit them to the six S– and P–wave phase shifts in the low energy region. As input we use the phase shifts of the Karlsruhe (KA85) group[9], from the analysis of Matsinos[10]

(EM98), and the SP98[11]–analysis of the VPI group (fit 1, 2, and 3, in order). Note also that the LEC $\bar{d}_{18}$ is fixed by means of the Goldberger–Treiman discrepancy. The resulting S– and P–wave phase shifts for fit 1 are shown in Fig. 1 .

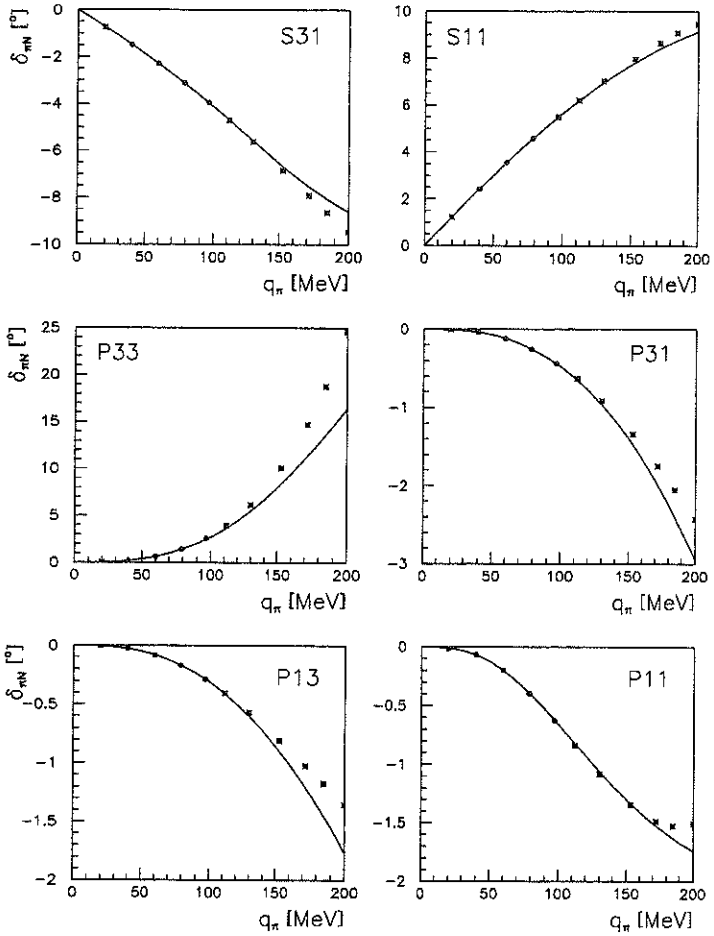

Figure. 1. Fits and predictions for the KA85 phase shifts as a function of the pion laboratory momentum q_π. Fitted in each partial wave are the data between 40 and 97 MeV (filled circles). For higher and lower energies, the phases are predicted.

ISOSPIN SYMMETRY VIOLATING CASE

After having described the large isospin symmetric background of the pion–nucleon scattering amplitude, we will now proceed to add the leading isospin breaking terms encoded in the pion and nucleon mass differences, as well as in the strong interaction vertices which explicitly violate isospin symmetry.

Isospin violation is best quantified in terms of relations which are exactly zero in the isospin limit of equal quark masses and vanishing electromagnetic coupling. With the three pion $(\pi^\pm, \pi^0)$ and two nucleon (p, n) fields, we have ten reaction channels; making use of time reversal invariance, we only have to consider eight reactions. In the case of isospin symmetry, these eight physical channels are entirely described in terms of two amplitudes. One can thus write down six isospin relations (see also ref.[12] for a general analysis)

$$R_1 = 2\,\frac{T_{\pi^+p\to\pi^+p} + T_{\pi^-p\to\pi^-p} - 2\,T_{\pi^0p\to\pi^0p}}{T_{\pi^+p\to\pi^+p} + T_{\pi^-p\to\pi^-p} + 2\,T_{\pi^0p\to\pi^0p}}\,, \tag{2}$$

$$R_2 = 2\,\frac{T_{\pi^+p\to\pi^+p} - T_{\pi^-p\to\pi^-p} - \sqrt{2}\,T_{\pi^-p\to\pi^0n}}{T_{\pi^+p\to\pi^+p} - T_{\pi^-p\to\pi^-p} + \sqrt{2}\,T_{\pi^-p\to\pi^0n}}\,, \tag{3}$$

$$R_3 = 2\frac{T_{\pi^0 p\to\pi^+ n} - T_{\pi^- p\to\pi^0 n}}{T_{\pi^0 p\to\pi^+ n} + T_{\pi^- p\to\pi^0 n}}\ , \tag{4}$$

$$R_4 = 2\frac{T_{\pi^+ p\to\pi^+ p} - T_{\pi^- n\to\pi^- n}}{T_{\pi^+ p\to\pi^+ p} + T_{\pi^- n\to\pi^- n}}\ , \tag{5}$$

$$R_5 = 2\frac{T_{\pi^- p\to\pi^- p} - T_{\pi^+ n\to\pi^+ n}}{T_{\pi^- p\to\pi^- p} + T_{\pi^+ n\to\pi^+ n}}\ , \tag{6}$$

$$R_6 = 2\frac{T_{\pi^0 p\to\pi^0 p} - T_{\pi^0 n\to\pi^0 n}}{T_{\pi^0 p\to\pi^0 p} + T_{\pi^0 n\to\pi^0 n}}\ . \tag{7}$$

To be precise, we consider these ratios formed with the real parts of the amplitudes at threshold, symbolically $T_{\pi^a N\to\pi^b N}$ should read Re $T^{\rm thr}_{\pi^a N\to\pi^b N}$.

The first two of these relations, the so–called triangle relations, are based on the observation that in the isospin conserving case, the elastic scattering channels involving charged pions are trivially linked to the corresponding neutral pion elastic scattering or the corresponding charge–exchange amplitude. Of particular interest is the second ratio, which is often referred to as *the triangle relation*. Only in this case all three channels have been measured. The ratio R_6 parameterizes the large isospin violation effect for π^0 scattering off nucleons first found by Weinberg[13]. Note that as in R_6, the isovector terms drop out completely in R_1 and one can thus also expect a large isospin violation in this ratio. To our knowledge, this is the first time that this particular ratio has been called attention to. From an experimental point of view, it has the advantage of avoiding the almost unmeasurable $n\pi^0$ amplitude appearing in R_6.

In what follows, we will calculate the six ratios R_i to leading one loop accuracy, i.e. to third order in small momenta. For that, we have to consider tree graphs, some with fixed coefficients and some with LECs, and the leading one loop graphs involving lowest order couplings only.

In the presence of isospin violation, one has to generalize the standard form of the πN scattering amplitude to

$$T^{ab}(\omega,t) = \delta^{ab}T^+_{ab}(\omega,t) + \delta^{ab}\tau^3 T^{3+}_{ab}(\omega,t) + i\epsilon^{bac}\tau^c T^-_{ab}(\omega,t) + i\epsilon^{bac}\tau^c\tau^3 T^{3-}_{ab}(\omega,t)\quad , \tag{8}$$

in terms of *two isoscalar* ($T^{+,3+}_{ab}$) and *two isovector* amplitudes ($T^{-,3-}_{ab}$).

We are now in the position to analyze the ratios R_i as defined in Eqs.(2-7). The LECs $c_{1,2,3,4}$ and d_i are taken from fits 1, 2, 3, the strength of the isospin violating vertices c_5 and f_2 is determined from the proton–neutron mass difference[14,6], whereas the difference of the charged and neutral pion masses determines the value of C.

In Table 1, we give the results for the ratios R_i that are not entirely given by isoscalar quantities. Isospin breaking effects are typically of the order of 1% in these relations and are rather independent of the parameter set which is used.

Table 1. Values of the ratios R_i ($i = 2,3,4,5$) for the various parameter sets as given by the fits of[8].

	R_2 [%]	R_3 [%]	R_4 [%]	R_5 [%]
Fit 1	0.9	−0.5	−0.7	1.1
Fit 2	1.1	−0.6	−0.9	1.1
Fit 3	0.9	−0.5	−0.8	1.0

We now turn our attention to the two isoscalar ratios. Let us start with R_6, which was first discussed by Weinberg[13]. For fit 1, we find $R_6 = 19\%$. Interestingly, for the same parameter set (fit 1) the prediction for R_1 is even larger,

$$R_1 = 36.7\% \tag{9}$$

which is again a huge isospin violating effect in an isoscalar quantity.

It is most interesting to separate the hadronic isospin violation encoded in the operator $\sim c_5(m_u - m_d)$ from the virtual photon effects. In order to study this effect, we set all strong interaction vertices to zero, but keep the neutron and proton masses at their physical values. This case is denoted by $c_5(\pi\pi) = 0$ in Table 2. We see that while the em isospin breaking is generally dominant (with the exception of R_6), there is also some sizeable strong isospin breaking.

Table 2. Values of the ratios R_i $(i = 1, 2, 3, 4, 5, 6)$ for the parameters of fit 1 from[8] including the full contribution from the strong isospin breaking ($c_5 \neq 0$) and with the strong isospin violation only contributing to the proton–neutron mass difference ($c_5(\pi\pi) = 0$).

	R_1	R_2	R_3	R_4	R_5	R_6
$c_5 \neq 0$	36.7	0.9	−0.5	−0.7	1.1	19.3
$c_5(\pi\pi) = 0$	45.4	1.6	0.8	−0.7	1.1	0

SUMMARY

We have considered isospin violation in low energy pion–nucleon scattering in the framework of heavy baryon chiral perturbation theory to third order in small momenta. We have taken into account all operators related to strong isospin breaking and the electromagnetic ones which lead to the pion and nucleon mass differences. We have considered a set of six ratios R_i which vanish in the limit of isospin conservation. From these, four involve isovector *and* isoscalar amplitudes ($R_{2,3,4,5}$) and the two others are purely of isoscalar type ($R_{1,6}$). While in the first case, isospin violation is typically of the order of one percent, more sizeable effects are found in R_6 and, as for the first time noted here, in R_1. We also stress again that within the framework presented here, a unique and unambiguous separation of all different isospin violating effects is possible. To access the size of isospin violation encoded in the presently available pion–nucleon scattering data, the extension of this scheme to include Coulomb (hard) and soft photons is mandatory. Once this is done, it will be possible to analyze directly the cross section data without recourse to any model for separating em or hadronic mass effects, thus avoiding any mismatch by combining different approaches or models. Work along such lines is underway.

ACKNOWLEDGMENTS

It is a pleasure to thank Ulf Meißner and Sven Steininger for a very enjoyable collaboration.

REFERENCES

1. S. Weinberg, in *Chiral Dynamics: Theory and Experiment*, A.M. Bernstein and B.R. Holstein (eds.) (Springer Verlag, Berlin, 1995).
2. U. van Kolck, Thesis, University of Texas at Austin (1994), unpublished.
3. W.R. Gibbs, Li Ai and W.B. Kaufmann, Phys. Rev. Lett. **74**, 3740 (1995).
4. E. Matsinos, Phys. Rev. **C58**, 3014 (1997).
5. Ulf-G. Meißner, G. Müller and S. Steininger, Phys. Lett. **B406**, 154 (1997); (E) *ibid* **B407**, 154 (1997).
6. Ulf-G. Meißner and S. Steininger, Phys. Lett. B419, 403 (1998).
7. V. Bernard, N. Kaiser and Ulf-G. Meißner, Int. J. Mod. Phys. **E4**, 193 (1995).
8. N. Fettes, Ulf-G. Meißner and S. Steininger, Nucl. Phys. **A640**, 199 (1998).
9. R. Koch, Nucl. Phys. **A448**, 707 (1986).
10. E. Matsinos, Phys. Rev. **C56**, 3014 (1997); E. Matsinos, private communication.
11. SAID on-line program, R.A. Arndt, R.L. Workman et al., see website http://clsaid.phys.vt.edu/ CAPS/.
12. W.B. Kaufmann and W.R. Gibbs, Ann. Phys. (NY) **214**, 84 (1992).
13. S. Weinberg, Trans. N.Y. Acad. of Sci. **38**, 185 (1977).
14. V. Bernard, N. Kaiser and Ulf-G. Meißner, Nucl. Phys. **A615**, 483 (1997).

Isospin Violation in πN Scattering and the Breakdown of the Fermi-Watson Theorem

A. M. Bernstein
Physics Department and Laboratory for Nuclear Science
M.I.T., Cambridge,Mass.,USA

Abstract

Isospin is expected to be violated in πN scattering as a consequence of the mass difference of the up and down quarks; chiral calculations have been performed at low energies. Two independent empirical analyses of intermediate energy scattering data have concluded that that isospin is not conserved. Here it is demonstrated that isospin violations will produce observable breakdown of the Fermi-Watson theorem (the connection between the phase of the multipole amplitudes in electromagnetic pion production and the πN phase shifts). As a result independent tests of isospin conservation can be performed in electromagnetic meson production which involves charge states that are not accessible in πN scattering experiments.

1 Isospin Violation in πN Scattering

πN scattering is fundamental since the pion is an almost Goldstone Boson reflecting the spontaneously broken chiral symmetry which is present in the QCD Lagrangian in the limit of massless light quarks[1,2]. In this (chiral) limit the πN interaction at low energies, characterized by the s wave scattering length, goes to zero. However,this prediction is modified by the explicit chiral symmetry breaking due to the small masses of the up and down quarks, $m_u \simeq 5MeV, m_d \simeq 9MeV$[3–6]. Since the quark masses are not equal ($m_u/m_d = 0.553 \pm 0.043$[6]), the mass term in the QCD Lagrangian can be written as[1,4]:

$$L_m = m_u \bar{u}u + m_d \bar{d}d = A(m_u + m_d) + B(m_u - m_d) \tag{1}$$

where the B term is isospin violating. Calculations of the have been performed using Chiral Lagrangians[4,8] and Chiral Perturbation Theory(ChPT)[9]. In the low energy region the predictions are that for $\pi^{\pm}N$ scattering and charge exchange the isospin breaking is a few percent effect; for the much smaller $\pi^0 N$ scattering the isospin breaking effect is of order 30%. To date no calculations have been made for higher energies.

There have been two empirical analyses of πN scattering and charge exchange reactions at intermediate energies (pion lab kinetic energies between 30 and 70 MeV) that have concluded that isospin is not conserved. In particular they tested the "triangle relation":

$$D \equiv f(\pi^- p \to \pi^0 n) - \frac{(f(\pi^+ p) - f(\pi^- p))}{\sqrt{2}} \tag{2}$$

where D is the difference between the $\pi^- p \to \pi^0 n$ scattering amplitude as observed experimentally and what would have been obtained from analyzing $\pi^+ p$ and $\pi^- p$ elastic scattering and isospin conservation. Both analyses[10,11] have obtained values of $D \simeq -.012 \pm 0.003 fm$ or $D/f_{exp}(\pi^- p \to \pi^0 n) \simeq 7\%$ This is a significantly larger effect then was predicted at lower energies due to the up, down quark mass differences and electromagnetic effects[3,8,9] calculated in ChPT. Due to this relatively large isospin breaking effect, there was concern about the accuracy of the Coulomb effects used in these analyses. Subsequently new, more accurate Coulomb calculations were performed[12] which do not significantly change the original result[13].

Therefore, to the extent that that the πN scattering and charge exchange data base is accurate, a significant isospin violation has been observed. This is of sufficient importance that further experiments and analyses need to be performed to either verify or alter this conclusion. In the following section a different method, electromagnetic pion production, is shown to be sensitive to this isospin breaking effect. Experiments using this technique are, therefore, both timely and important.

2 Isospin Breaking in Electromagnetic Pion Production

Isospin violation in the πN system will also show up in electromagnetic pion production. To demonstrate how this occurs the derivation of the Fermi-Watson theorem[14] will be sketched; this is the relationship between the phase shifts in πN scattering and the phases of the electromagnetic pion production amplitudes. This theorem is based on time reversal invariance, unitarity, and isospin conservation. When this theorem was derived quarks were not known. It was assumed that isospin violation was caused only by electromagnetic effects and were of order $e^2 = \alpha$ and could be neglected at this order.

To be concrete consider the $\gamma p \to \pi^0 p, \pi^+ n$ reaction. The final state can be characterized either in charge or in isospin space. For the πN system the isospin states are I =1/2 and 3/2. This 3 channel problem is simpler is isospin space (assuming it is a good quantum number). The S matrix for the 3 open channels $(\gamma p, \pi N(2I = 1), \pi N(2I = 3))$ can be written as :

$$\begin{pmatrix} 1 & iM_1 & iM_3 \\ & e^{2i\delta_1} & \\ & & e^{2i\delta_3} \end{pmatrix}, \tag{3}$$

where the multipole amplitudes for the photo-production of the πN channels in the isospin states I =1/2 and 3/2 are written as iM_{2I} , δ_1, and δ_3, represent elastic πN scattering phase shifts in the I = 1/2 and 3/2 states, Although not explicitly written here, the S matrix elements are for a fixed value of W, the total CM energy, and for the quantum numbers l and j, the πN orbital and total angular momenta.

Time reversal invariance requires that the S matrix be symmetric ($S_{ij} = S_{ji}$) and unitary requires that $S^+S = SS^+ = 1$. The form of the 3x3 and 2x2 πN portions of the S matrix have been chosen to be separately unitary and time reversal invariant (for simplicity the redundant matrix elements have not been displayed). The S matrix of Eq.1 is symmetric by construction. Applying the unitary constraint and assuming the weakness of the electromagnetic interaction by dropping terms of order e^2 one obtains:

$$\begin{aligned} M_1 &= e^{i\delta_1} A_1 \\ M_3 &= e^{i\delta_3} A_3 \end{aligned} \tag{4}$$

where $A_{2I=1,3}$ are real functions of the CM energy, and can be identified as the multipole matrix elements M_{2I} (for $\gamma p \to \pi N(I)$) in the absence of final state πN interactions. Eq. 2 is the Fermi-Watson theorem[14]. It shows that the phases of the πN multipoles are simply half of the πN phase shifts in each quantum state characterized by l, j, and I and total energy W. The factor of two can be understood since in πN scattering the pion interacts with the nucleon both on the way in and on the way out, while in electromagnetic pion production the pion interacts only on the way out.

Eqs.1 and 2 can easily be generalized from photo- to electro-pion production. In electroproduction the incident photon is virtual and is characterized by the four momentum transfer q^2. On the other hand, the final πN state is only characterized by its quantum numbers and total energy W but is independent of q^2. Therefore Eq. 2 looks the same for electro-pion production except that $A_{2I=1,3}$ are functions of q^2 as well as l, j and W while δ_1, and δ_3 just depend on l, j and W. The generalization to the isospin violating case presented below generalizes to electroproduction in exactly the same way.

To generalize to the isospin breaking case one can write the S matrix as:

$$\begin{pmatrix} 1 & iM_1 & iM_3 \\ & \cos\psi\, e^{2i\delta_1} & i\sin\psi\, e^{i(\delta_1+\delta_3)} \\ & & \cos\psi\, e^{2i\delta_3} \end{pmatrix} \tag{5}$$

$sin\psi$ represents an isospin violating term where ψ is a real number. For $\psi \to 0$ the isospin violation vanishes. As above the form of the 3x3 and 2x2 πN portions of the S matrix have been chosen to be separately unitary and time reversal invariant. Applying the unitary constraint $S^+S = SS^+ = 1$, and assuming the weakness of the electromagnetic interaction

by dropping terms of order e^2 one obtains:

$$\begin{aligned} M_1 &= e^{i\delta_1}[A_1 \cos\tfrac{\psi}{2} + iA_3 \sin\tfrac{\psi}{2}] \\ M_3 &= e^{i\delta_3}[A_3 \cos\tfrac{\psi}{2} + iA_1 \sin\tfrac{\psi}{2}] \end{aligned} \tag{6}$$

where $A_{2I=1,3}$ are real functions of the CM energy, and can be identified as the multipole matrix elements M_{2I} (for $\gamma p \to \pi N(I)$) in the absence of final state and isospin breaking. This equation shows the violation of the Fermi- Watson theorem due to isospin breaking.As $\psi \to 0$ the isospin violation vanishes and the Fermi-Watson theorem is recovered. Therefore the phases of the πN multipoles should be measured, and not calculated from the πN phase shifts (using the Fermi-Watson theorem) as they now are. To my knowledge only one such measurement of the phases of the photoproduction multipoles has been performed[16] and that did not have the required precision to determine the effects predicted here.

In order to estimate the magnitude of the isospin breaking effect in electromagnetic pion production, the isospin breaking parameter can be obtained from the analyses of πN scattering[10,11]. From the 2x2 πN part of the S matrix (Eq. 3) one can obtain the s wave scattering amplitude $f_{\pi N} = sin\delta e^{i\delta}/q$ (where q is the pion CM momentum) for the $\pi^- p$ system as:

$$\begin{aligned} f(\pi^- p) &= (\tfrac{2}{3}f_1 + \tfrac{1}{3}f_3)cos\psi + \tfrac{\sqrt{2}}{3q}sin\psi e^{i(\delta_1+\delta_3)} \\ f(\pi^- p \to \pi^0 n) &= \tfrac{\sqrt{2}}{3}(f_3 - f_1)cos\psi + \tfrac{1}{6q}sin\psi e^{i(\delta_1+\delta_3)} \\ D \equiv f(\pi^- p \to \pi^0 n) - \tfrac{1}{\sqrt{2}}(f(\pi^+ p) - f(\pi^- p)) &= \tfrac{1}{2q}sin\psi e^{(i\delta_1+\delta_3)} \end{aligned} \tag{7}$$

where f_{2I} are the πN s wave scattering amplitudes in the I = 1/2 and 3/2 states. Note that $D \to 0$ when $\psi \to 0$ as expected. Two independent analyses of πN scattering at medium energies (pion kinetic energies of $\simeq$ 30 to 70 MeV)[10,11] obtained $D \simeq -.012 \pm 0.003 fm$ Here $\psi \simeq -0.010 \pm 0.004$(at a pion kinetic energy of $\simeq 40 MeV$) has been obtained from D using Eq. 7.

To estimate the effect of isospin breaking in electromagnetic pion production the calculated multipoles of the Mainz unitary isobar model, which is isospin conserving, have been used[15]. The isospin violations are then added by taking the differences for the multipoles δM in Eq.6 with ψ equal to the empirical value and zero:

$$\begin{aligned} \delta M_{2I} &= M_{2I}(\psi) - M_{2I}(\psi = 0) \\ \delta M_1 \simeq i\tfrac{\psi}{2}A_3, \delta M_3 &\simeq i\tfrac{\psi}{2}A_1 \end{aligned} \tag{8}$$

where the numerical results presented below were obtained from the first line. For isospin breaking in the s wave at intermediate energies the approximate second and third lines apply. It can be seen that the main effect is in the imaginary part of the s wave multipoles E_{0+} and L_{0+}. To observe this will require experiments which measure the fifth (TL') structure function(requiring polarized electrons and out of plane hadron detection) or the structure functions with polarized targets or recoil nucleons. For photoproduction the simplest such observable is the polarized target asymmetry. All other observables such as unpolarized cross sections will show almost no effect due to isospin breaking.

As an example of an isospin sensitive quantity the polarized target (normal to the reaction plane) asymmetry is presented for the $ep \to e'\pi^+ n$ reaction at $Q^2 = 0.1 GeV^2$ for a center of mass energy W = 1120 MeV (pion lab kinetic energy $\simeq 40 MeV$). This asymmetry is seen to show a significant effect due to isospin breaking, This effect is very similar at the photon point. Other isospin sensitive quantities include $A_{TL}(t)$ for the $ep \to e'\pi^+ n$ reaction and $A_{TL'}$ for the $ep \to e'\pi^0 p$ reaction.

In conclusion we have demonstrated the breakdown of the Fermi- Watson theorem due to isospin breaking effects in the πN System. The equations presented here are based on time reversal invariance and unitarity and are therefore very general. There are some significant, experimentally observable, effects which can be used to make an independent determination of the magnitude of the isospin breaking. This is of particular interest since e.g. the $\gamma^* p \to \pi^+ n, \pi^0 p$ reaction leads to charge states which are not accessible with conventional πN reactions.

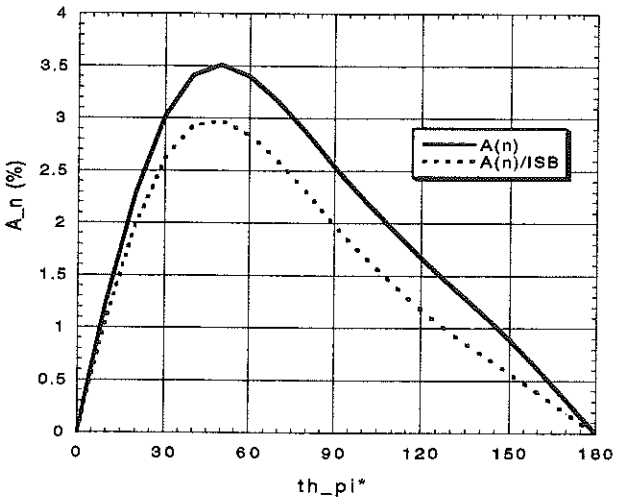

Figure. 1. The polarized target (normal to the reaction plane) asymmetry for the $ep \to e'\pi^+ n$ reaction at $Q^2 = 0.1 GeV^2$ for a center of mass energy W = 1120 MeV (pion lab kinetic energy $\simeq 40 MeV$).

REFERENCES

1. See e.g. Dynamics of the Standard Model, J.F.Donoghue, E.Golowich, and B.R.Holstein, Cambridge University Press (1992).
2. S.Weinberg, Physica A96,327(1979). J.Gasser and H.Leutwyler, Ann. Phys.(N.Y.) 158,142(1984), Nucl.Phys. B250, 465 and 517(1985).
3. S.Weinberg, Phys. Rev. Lett. 17,168(1966)
4. S.Weinberg,Transactions of the N.Y.Academy of Science Series II 38 (I.I.Rabi Festschrift),185(1977),and contribution to the Proceedings of the Workshop on Chiral Dynamics:Theory and Experiment, Springer-Verlag, July 1995, A.M.Bernstein and B. Holstein editors,Springer-Verlag.
5. J.Gasser and H.Leutwyler,Phys. Reports 87,77(1982).
6. H.Leutwyler, Phys.Lett. B378,313(1996) and hep- ph/9602255.
7. H.Leutwyler,contribution to the Proceedings of the Workshop on Chiral Dynamics:Theory and Experiment, Springer-Verlag, July 1995, A.M.Bernstein and B. Holstein editors,Springer-Verlag.
8. U. van Kolck, Ph.D. thesis, University of Texas(1994), unpublished and private communication.
9. U.G. Meissner and S. Steininger, Phys. Lett. B419,403(1998), N.Fettes, U.G. Meissner, and S. Steininger, Nucl. Phys. A640, 199 (1998), N. Fettes, talk in these proceedings.
10. W.R.Gibbs, Li Ali, and W.B.Kaufmann, Phys. Rev. Lett.,74,3740(1995). W.R. Gibbs, paper in these proceedings and private communication.
11. E. Matsinos, Phys. Rev. C56, 3014(1997)
12. A. Gashi, E. Matsinos, G.C. Oades, G. Rasche , W.S. Woolcock hep-ph/9903434, hep-ph/9902224, hep-ph/9902207. G.C. Oades, talk in these proceedings.
13. E.Matsinos, private communication.
14. E.Fermi, Suppl. Nuovo Cimento 2,17(1955). K.M.Watson, Phys.Rev. 95,228(1954).
15. D. Drechsel, O.Hanstein, S.S. Kamalov, and L. Tiator, Nucl. Phys. A645,145(1999). An on line version of the numerical results are available on the internet at http://www.kph.uni-mainz.de/T/maid/
16. V.F.Grushin, in Photoproduction of Pions on Nucleons and Nuclei, Proceedings of the Lebedev Physics Insitute, Academy of Ssciences of the USSR, A.A.Komar, editor, Vol. 186 (Z1988), English Translation by Nova Press, N.Y.(1989).

Isospin Violation and the Proton's Strange Form Factors

Randy Lewis and Nader Mobed
Department of Physics, University of Regina, Regina, SK, Canada S4S 0A2

Abstract

The strange form factors of the proton are basic to an understanding of proton structure, and are presently the focus of many experiments. Before the strangeness effects can be extracted from data, it is necessary to calculate and remove effects due to isospin violation, which exist independently of the strange quark but which contribute nevertheless to the experimentally measured "strange" form factors. A discussion of the isospin violating contributions to vector form factors is given here in the context of heavy baryon chiral perturbation theory.

INTRODUCTION

The interaction between a proton and a neutral weak boson (Z^0) involves form factors which are related to the familiar electromagnetic form factors via the standard electroweak model. For example, the proton's neutral weak vector form factors are

$$G_X^{p,Z}(q^2) = \frac{1}{4}[G_X^p(q^2) - G_X^n(q^2)] - G_X^p(q^2)\sin^2\theta_W - \frac{1}{4}G_X^s(q^2), \quad X = E, M \ , \qquad (1)$$

where $G_{E,M}^p(q^2)$ and $G_{E,M}^n(q^2)$ are the usual electromagnetic form factors of the proton and neutron respectively, and $G_{E,M}^s(q^2)$ are called the proton's strange electric and magnetic form factors. Using Eq. (1), an experimental measurement of $G_X^{p,Z}(q^2)$ leads to a determination of $G_X^s(q^2)$, which provides information about the effects of strange quarks in the proton.

The first measurement of $G_M^{p,Z}(q^2)$ was reported two years ago by the SAMPLE Collaboration[1], and led to

$$G_M^s(0.1\text{GeV}^2) = 0.23 \pm 0.37 \pm 0.15 \pm 0.19 \ . \qquad (2)$$

A linear combination of strange electric and magnetic form factors has been measured by the HAPPEX Collaboration[2]:

$$[G_E^s + 0.39 G_M^s](0.48\text{GeV}^2) = 0.023 \pm 0.034 \pm 0.022 \pm 0.026 \ . \qquad (3)$$

Further efforts are underway by various groups.*

It is important to recall that $G_E^s(q^2)$ and $G_M^s(q^2)$ contain more than just strangeness effects. Even in a world of only two flavours (up and down) $G_{E,M}^s(q^2)$ would be nonzero due to isospin violation. Thus, the true effects of strange quarks can only be extracted from an experimental determination of $G_{E,M}^s(q^2)$ if isospin violating effects can be calculated.

Dmitrašinović and Pollock[4], and also Miller[5], have studied the isospin violating contribution to $G_M^s(q^2)$ within the nonrelativistic constituent quark model. Ma has used a light-cone meson-baryon fluctuation model.[6] More recently, a model-independent study of isospin violating effects (using heavy baryon chiral perturbation theory) has been published[7] and it is this work which will be emphasized below, after a brief review of attempts to calculate the authentic strange quark effects.

THE STRANGENESS CONTRIBUTIONS TO $G_{E,M}^s(q^2)$

Many attempts have been made to calculate the contribution of strange quarks to the "strange" electric and magnetic form factors, $G_{E,M}^s(q^2)$. In principle a lattice QCD calculation could give the definitive answer, and an exploratory calculation has been performed

*See in particular the second SAMPLE measurement, Ref.[3], which appeared after the MENU99 conference. Using a calculation of electroweak corrections as input, they find $G_M^s(0.1\text{GeV}^2) = +0.61 \pm 0.17 \pm 0.21$.

in the quenched theory.[8] The errors due to finite lattice spacing, finite lattice volume and quenching are not yet known, but the existing results, $\langle r_s^2 \rangle_E \equiv 6 \mathrm{d}G_E^s(0)/\mathrm{d}q^2 = -0.06 \to -0.16 \mathrm{fm}^2$ and $G_M^s(0) = -0.36 \pm 0.20$, still provide important inputs to the discussion.

One might consider using chiral perturbation theory to calculate the strangeness contributions to $G_{E,M}^s(q^2)$, but both form factors have a free parameter at their first nonzero order in the chiral expansion, so the magnitude of neither form factor can be predicted from chiral symmetry alone. However, two experimental inputs are sufficient to fix these parameters, and chiral symmetry does determine the q^2-dependence of the form factors at leading chiral order. This tact has been taken by the authors of Ref.[9], who use the SAMPLE and HAPPEX measurements as input.

Beyond lattice QCD and chiral perturbation theory, there are many models and dispersion relation methods which have been employed in the effort to determine the strange quark contributions to $G_{E,M}^s(q^2)$. (The authors of Refs.[8–10] have collected some predictions from the literature.) The various methods lead to differing results. For $G_M^s(0)$, most predictions lie in the range

$$-0.5 \lesssim G_M^s(0) \lesssim +0.05 \ , \tag{4}$$

and it has often been noted that this tendency toward a negative number does not seem to be supported by the experimental data, Refs.[1–3]. Predictions for the magnitude and sign of $\langle r_s^2 \rangle_E$ also span a large range.

A precise experimental measurement would help to distinguish between the various models of strangeness physics, but only after the isospin violating contribution has been calculated and subtracted.

THE ISOSPIN VIOLATING CONTRIBUTIONS TO $G_{E,M}^s(q^2)$

In a world with no strange quark, $G_E^s(q^2)$ and $G_M^s(q^2)$ do not vanish. Instead,

$$G_X^s(q^2) \to G_X^{u,d}(q^2) \text{ as the strange quark decouples, } (X = E, M) \tag{5}$$

where $G_E^{u,d}(q^2)$ and $G_M^{u,d}(q^2)$ are isospin violating quantities. If both the strange and isospin violating components of $G_{E,M}^s(q^2)$ are small, then contributions which are both isospin violating *and* strange are doubly suppressed. The following discussion considers $G_{E,M}^{u,d}(q^2)$ in a strange-free world.

Constituent quark model calculations have led to a vanishing result for $G_M^{u,d}(0)$ and a very mild q^2 dependence: $-0.001 < G_M^{u,d}(-0.25\mathrm{GeV}^2) < 0$[4,5]. There is no symmetry which would force $G_M^{u,d}(0)$ to vanish exactly, but perhaps the constituent quark model is trying to anticipate a "small" result. A light-cone meson-baryon fluctuation model permits a large range, $G_M^{u,d}(0) = 0.006 \to 0.088$.[6]

Heavy baryon chiral perturbation theory (HBChPT) is a natural tool for the study of $G_{E,M}^{u,d}(q^2)$. It is a model-independent approach which employs a systematic expansion in small momenta (q), small pion masses (m_π), small QED coupling (e), large chiral scale ($4\pi F_\pi$) and large nucleon masses (m_N). It is appropriate to use $O(q) \sim O(m_\pi) \sim O(e)$ with $4\pi F_\pi \sim m_N$, and then the HBChPT Lagrangian can be ordered as a single expansion,

$$\mathcal{L}_{\mathrm{HBChPT}} = \mathcal{L}^{(1)} + \mathcal{L}^{(2)} + \mathcal{L}^{(3)} + \mathcal{L}^{(4)} + \mathcal{L}^{(5)} + \dots \ . \tag{6}$$

For the explicit form of the Lagrangian, see Ref.[7] and references therein. For the present discussion, it is simply noted that $\mathcal{L}^{(1)}$ contains parameters g_A, F_π and e; $\mathcal{L}^{(2)}$ contains 11 parameters (7 strong and 4 electromagnetic); $\mathcal{L}^{(3)}$ contains 43 parameters; $\mathcal{L}^{(4)}$ contains hundreds of parameters and $\mathcal{L}^{(5)}$ has even more. Happily, it will be shown that $G_E^{u,d}(q^2)$ is parameter-free at its first nonzero order, and $G_M^{u,d}(q^2)$ is parameter-free at its first and second nonzero orders except for a single additive constant.

The coupling of a vector current (e.g. Z^0) to a nucleon begins at first order in HBChPT, $\mathcal{L}^{(1)}$, but is isospin conserving. To be precise, recall the usual notation,

$$\langle N(\vec{p}+\vec{q})|\bar{f}\gamma_\mu f|N(\vec{p})\rangle \equiv \bar{u}(\vec{p}+\vec{q})\left[\gamma_\mu F_1^f(q^2) + \frac{i\sigma_{\mu\nu}q^\nu}{2m_N}F_2^f(q^2)\right]u(\vec{p}) \ , \tag{7}$$

where f denotes a particular flavour of quark. The Sachs form factors for that flavour are

$$G_E^f(q^2) = F_1^f(q^2) + \frac{q^2}{4m_N^2}F_2^f(q^2) \ , \qquad G_M^f(q^2) = F_1^f(q^2) + F_2^f(q^2) \ . \tag{8}$$

An explicit calculation using $\mathcal{L}^{(1)} + \mathcal{L}^{(2)} + \mathcal{L}^{(3)}$ leads to isospin violating vector form factors which vanish exactly. At first glance this might seem surprising, but it can be readily understood as follows. An isospin violating factor, such as $(m_n - m_p)/m_p$, is suppressed by two HBChPT orders. Moreover, the F_2 term in Eq. (7) has an extra explicit $1/m_N$ suppression factor, so isospin violating F_2 terms cannot appear before $\mathcal{L}^{(4)}$. Meanwhile, F_1 is constrained by Noether's theorem (QCD's flavour symmetries: upness and downness) to be unity plus momentum-dependent corrections, and dimensional analysis therefore requires a large scale, m_N or $4\pi F_\pi$, in the denominator of all corrections. This demonstrates that both $G_E^{u,d}(q^2)$ and $G_M^{u,d}(q^2)$ vanish in HBChPT until the fourth order Lagrangian: $\mathcal{L}^{(4)}$.

A leading order (LO) calculation of $G_E^{u,d}(q^2)$ or $G_M^{u,d}(q^2)$ involves tree-level terms from $\mathcal{L}^{(4)}$ plus one-loop diagrams built from $\mathcal{L}^{(1)} + \mathcal{L}^{(2)}$. Referring to Ref.[7] for details of the calculation and renormalization, the results are

$$G_E^{u,d}(q^2)\Big|_{\rm LO} = -\frac{4\pi g_A^2 m_{\pi^+}}{(4\pi F)^2}(m_n - m_p)\left[1 - \int_0^1 {\rm d}x\, \frac{1-(1-4x^2)q^2/m_{\pi^+}^2}{\sqrt{1-x(1-x)q^2/m_{\pi^+}^2}}\right] , \tag{9}$$

$$G_M^{u,d}(q^2)\Big|_{\rm LO} = {\rm constant} - \frac{16 g_A^2 m_N}{(4\pi F)^2}(m_n - m_p)\int_0^1 {\rm d}x \ln\left(1 - x(1-x)\frac{q^2}{m_{\pi^+}^2}\right) . \tag{10}$$

Notice that the electric form factor contains no unknown parameters, and the magnetic form factor has only a single parameter (an additive constant). The LO results for $G_E^{u,d}(q^2)$ and $G_M^{u,d}(q^2) - G_M^{u,d}(0)$ are plotted in Fig. 1. The contribution of isospin violation to $\langle r_s^2\rangle_E$ is $6{\rm d}G_E^{u,d}(0)/{\rm d}q^2 \approx +0.013{\rm fm}^2$.

Consider next-to-leading order (NLO). Here, one expects tree-level terms from $\mathcal{L}^{(5)}$ plus one- and two-loop diagrams built from lower orders in the Lagrangian. Since small HBChPT expansion parameters without uncontracted Lorentz indices come in pairs (e.g. q^2, m_π^2, e^2), the $\mathcal{L}^{(5)}$ counterterms can contribute to F_1 but not to F_2. Thus $G_M^{u,d}(q^2)$ is independent of these parameters at NLO, although $G_E^{u,d}(q^2)$ is not.

It is also found that no two-loop diagrams contribute to $G_M^{u,d}(q^2)$ at NLO, although in principle they could have. Furthermore, unknown coefficients from $\mathcal{L}^{(3)}$ are also permitted to appear within loops, but none of them actually contribute. This means that the NLO corrections to $G_M^{u,d}(q^2)$ are basic one-loop diagrams. The explicit result is given in Ref.[7]. It needs to be stressed that the NLO contribution is parameter-free; the only new quantities (with respect to LO) are the well-known nucleon magnetic moments.

The LO+NLO result for $G_M^{u,d}(q^2) - G_M^{u,d}(0)$ is shown in Fig. 2. Notice that the NLO corrections serve to soften the q^2-dependence. The NLO correction to $G_M^{u,d}(0)$ is

$$G_M^{u,d}(0)\Big|_{LO+NLO} - G_M^{u,d}(0)\Big|_{LO} = \frac{24\pi g_A^2 m_{\pi^+}}{(4\pi F)^2}(m_n - m_p)\left(\frac{5}{3} - \mu_p - \mu_n\right) \approx 0.013 \ . \tag{11}$$

The value of $G_M^{u,d}(0)$ itself is not determined by chiral symmetry alone, and it receives contributions from physics other than the "pion cloud" of HBChPT (consider, for example,

isospin violation due to vector mesons). The pion cloud contribution to $G_M^{u,d}(0)$ is estimated in Ref.[7] via a physically-motivated cutoff in HBChPT, and is comparable in size to the NLO contribution of Eq. (11).

The full result for the pion cloud contribution to $G_M^{u,d}(q^2)$ is shown in Fig. 2 with error bands to reflect truncation of the HBChPT expansion: the narrow band assumes $|\text{NNLO}| \sim |\text{NLO}| \cdot m_\pi/m_N$ and the wide band assumes $|\text{NNLO}| \sim |\text{NLO}|/2$.

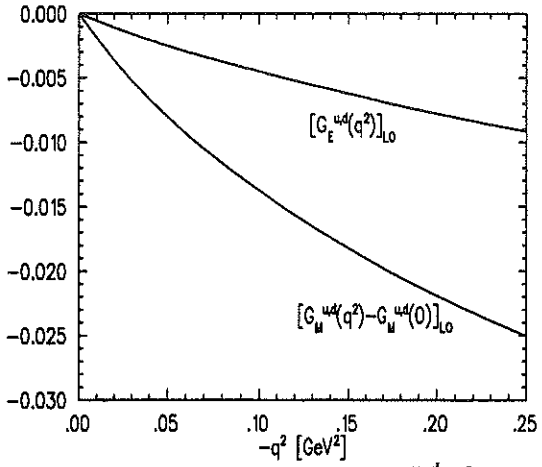

Fig. 1. Parameter-free results for $G_E^{u,d}(q^2)$ and $G_M^{u,d}(q^2) - G_M^{u,d}(0)$ at LO in HBChPT.

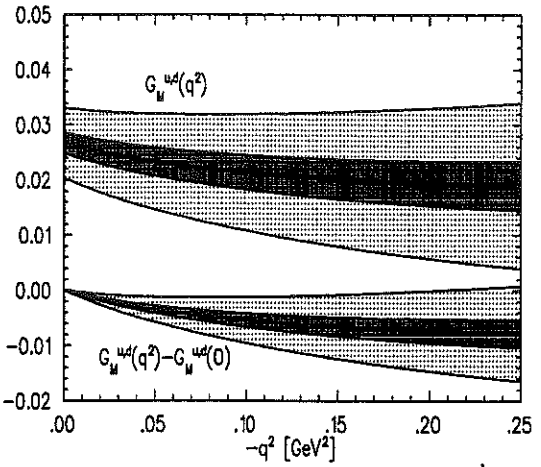

Fig. 2. The pion cloud contribution to $G_M^{u,d}(q^2)$ at LO+NLO, with uncertainties due to truncation of the HBChPT expansion.

CONCLUSIONS

The strange vector form factors of the proton are basic to an understanding of proton structure. The contribution due to strange quarks has proven to be a theoretical challenge. Isospin violation also contributes to the so-called "strangeness" form factors, and this contribution must be calculated and subtracted from experimental data before the strange quark contribution can be identified.

The present work indicates that chiral symmetry is of great value for discussions of the isospin violating effects. Despite the large number of parameters in the Lagrangian, $G_E^{u,d}(q^2)$ is parameter-free at leading order, and $G_M^{u,d}(q^2)$ has only one (q^2-independent) parameter at leading order, and no parameters at next-to-leading order.

The isospin violating effects computed here are large compared to some models of the strange quark effects, but small compared to other models. The experimental results for the full "strangeness" form factors in Eqs. (2) and (3) are not precise enough to indicate their size relative to the isospin violating contributions found in this work. It will be interesting to see what future experiments reveal.

This work was supported in part by the Natural Sciences and Engineering Research Council of Canada.

REFERENCES

1. B. A. Mueller *et al.*, Phys. Rev. Lett. **78**, 3824 (1997).
2. K. A. Aniol *et al.*, Phys. Rev. Lett. **82**, 1096 (1999).
3. D. T. Spayde *et al.*, nucl-ex/9909019 (1999).
4. V. Dmitrašinović and S. J. Pollock, Phys. Rev. C **52**, 1061 (1995).
5. G. A. Miller, Phys. Rev. C **57**, 1492 (1998).
6. B.-Q. Ma, Phys. Lett. B **408**, 387 (1997).
7. R. Lewis and N. Mobed, Phys. Rev. D **59**, 073002 (1999).
8. S. J. Dong, K. F. Liu and A. G. Williams, Phys. Rev. D **58**, 074504 (1998).
9. T. R. Hemmert, U.-G. Meissner and S. Steininger, Phys. Lett. B **437**, 184 (1998); T. R. Hemmert, B. Kubis, U.-G. Meissner, Phys. Rev. C **60**, 045501 (1999).
10. M. Musolf *et al*, Phys. Rep. **239**, 1 (1994); E. J. Beise *et al.*, nucl-ex/9602001 (1996); L. L. Barz *et al.*, Nucl. Phys. A **640**, 259 (1998).

Where is the Isospin Breaking?

W. R. Gibbs
Department of Physics, New Mexico State University, Las Cruces, NM 88003

Abstract

A method is discussed for the isolation of the isospin violation recently observed in the comparison of charge exchange data with predictions from charged pion data.

INTRODUCTION

The comparison of charge exchange data with the predictions from charged pion scattering has revealed an apparent breaking of isospin symmetry[1,2]. While it is always possible that the data are not correct or that the analyses have forgotten some electromagnetic correction, let us assume that this is not the case and that there is some isospin breaking that needs to be understood on the hadronic level.

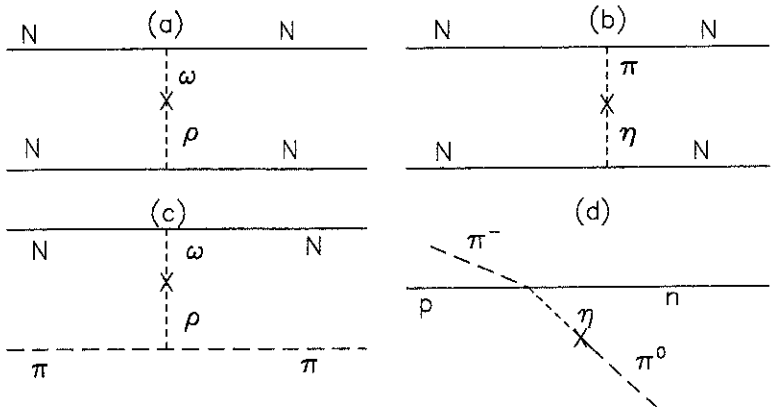

Figure. 1. Diagrams used for isospin mixing arising from meson mixing.

One way to study the source of the breaking is to consider various meson mixing diagrams, starting perhaps with those that have been used in nucleon-nucleon analysis. Figure 1 shows two such graphs and their analogs in the pion-nucleon sector. The $\rho\omega$ graph can be taken directly over[3] and, in fact, gives the same potential for the pion-nucleon as nucleon-nucleon case. When applied to pion-nucleon scattering it gives the right magnitude to explain the breaking seen, but the wrong sign.

EXPANSION OF THE AMPLITUDE IN OPERATORS

A more systematic way to locate the source of the mixing involves expanding an operator representing the general pion-nucleon amplitude in a complete set of isospin operators, θ_i.

$$T = \sum \theta_i a_i$$

For a given reaction, R, the amplitude will be given by the expectation value of this operator.

$$T_R = < \pi^c N^d | T | \pi^a N^b > = \Sigma_i \Theta_{Ri}\ a_i$$

One possible set of operators[4] is given in Table 1. The exact form of these operators is less important than that they are complete. These operators will have the character of scalars, vectors and tensors of higher rank under rotation in isospin space. The scalars will preserve isospin invariance and the vectors correspond to isospin breaking by meson mixing or quark mass differences. The Coulomb interaction can contribute to ranks 0, 1 and 2. The rank 3 operator presumably arises only from second order processes.

Isospin Operators and their Ranks

i	$(\theta_i)^I_0$	I
1	$\sqrt{\frac{1}{6}}1$	0
2	$\sqrt{\frac{1}{6}}\tau_0$	1
3	$\frac{1}{2}t_0$	1
4	$\sqrt{\frac{1}{2}}(\mathbf{t}\otimes\mathbf{t})^2_0$	2
$5,(9),6$	$\frac{1}{2}(\boldsymbol{\tau}\otimes\mathbf{t})^I_0$	$0,(1),2$
$7,(10),8$	$\sqrt{\frac{1}{2}}(\boldsymbol{\tau}\otimes(\mathbf{t}\otimes\mathbf{t})^2)^I_0$	$1,(2),3$

Table 1. A possible set of isospin operators.

πN Amplitudes

Amplitude	Order	Correspondence
a_1	ΔI=0	$\propto 1$
a_2	ΔI=1	np mass difference
a_3	ΔI=1	$\rho-\omega$ mixing
a_4	ΔI=2	pion mass difference
a_5	ΔI=0	$\propto \tau\cdot T$
a_6	ΔI=2	Coulomb
a_7	ΔI=1	$\pi-\eta$ mixing
a_8	ΔI=3	? small

Table 2. Characterization of the coefficients corresponding to the operators.

COMPARISON OF AMPLITUDES AND INTERACTIONS

This expansion can be applied to the amplitudes as a function of angle or to partial wave amplitudes. It can also be applied to the underlying interactions which would cause the breaking. The process of converting these interactions to amplitudes (solving a wave equation, for example) will mix (to a greater or less extent) the amplitudes, but only among the same rank (to first order in isospin breaking). Table 2 gives a rough correspondence of the amplitudes with possible sources of the isospin breaking interaction. It is the $\Delta I = 1$ amplitudes which are the most interesting. These are the ones which could arise from the mixing of $I = 0$ and $I = 1$ mesons or from the differences in quark masses. These two isospin breaking effects cannot contribute to the $\Delta I = 2$ terms. For many of the realizable reactions (on proton targets) the amplitude a_2 does not enter, so perhaps the separation of the a_3 and a_7 amplitudes is the most interesting.

Table 3 gives the matrix elements of these operators that would be needed to expand any amplitude in terms of the fundamental amplitudes. The square root of each element is to be taken with the sign outside of the radical like a table of Clebsch-Gordan coefficients.

A number of useful relations can be obtained with the use of this table. Some of them are:

$$A_{\pi^+p} - A_{\pi^-n} = \sqrt{\frac{2}{3}}a_2 + a_3 - \sqrt{\frac{2}{15}}a_7$$

$$A_{\pi^+n} - A_{\pi^-p} = -\sqrt{\frac{2}{3}}a_2 + a_3 + \sqrt{\frac{2}{15}}a_7$$

$$A_{\pi^0n} - A_{\pi^0p} = \sqrt{\frac{2}{3}}a_2 + 2\sqrt{\frac{2}{15}}a_7$$

Values of $\Theta_{Ri} = (\pi^c N^d|\theta_i|\pi^a N^b)$

Reaction	θ_1	θ_2	θ_3	θ_4	θ_5	θ_6	θ_7	θ_8
$\pi^+p \to \pi^+p$	$\frac{1}{6}$	$\frac{1}{6}$	$\frac{1}{4}$	$\frac{1}{12}$	$-\frac{1}{12}$	$\frac{1}{6}$	$-\frac{1}{30}$	$\frac{1}{20}$
$\pi^+n \to \pi^+n$	$\frac{1}{6}$	$-\frac{1}{6}$	$\frac{1}{4}$	$\frac{1}{12}$	$\frac{1}{12}$	$-\frac{1}{6}$	$\frac{1}{30}$	$-\frac{1}{20}$
$\pi^-p \to \pi^-p$	$\frac{1}{6}$	$\frac{1}{6}$	$-\frac{1}{4}$	$\frac{1}{12}$	$\frac{1}{12}$	$-\frac{1}{6}$	$-\frac{1}{30}$	$\frac{1}{20}$
$\pi^-n \to \pi^-n$	$\frac{1}{6}$	$-\frac{1}{6}$	$-\frac{1}{4}$	$\frac{1}{12}$	$-\frac{1}{12}$	$\frac{1}{6}$	$\frac{1}{30}$	$-\frac{1}{20}$
$\pi^0p \to \pi^0p$	$\frac{1}{6}$	$\frac{1}{6}$	0	$-\frac{1}{3}$	0	0	$\frac{2}{15}$	$-\frac{1}{5}$
$\pi^0n \to \pi^0n$	$\frac{1}{6}$	$-\frac{1}{6}$	0	$-\frac{1}{3}$	0	0	$-\frac{2}{15}$	$\frac{1}{5}$
$\pi^+n \to \pi^0p$	0	0	0	0	$-\frac{1}{6}$	$-\frac{1}{12}$	$-\frac{3}{20}$	$-\frac{1}{10}$
$\pi^0p \to \pi^+n$	0	0	0	0	$-\frac{1}{6}$	$-\frac{1}{12}$	$-\frac{3}{20}$	$-\frac{1}{10}$
$\pi^-p \to \pi^0n$	0	0	0	0	$-\frac{1}{6}$	$-\frac{1}{12}$	$\frac{3}{20}$	$\frac{1}{10}$
$\pi^0n \to \pi^-p$	0	0	0	0	$-\frac{1}{6}$	$-\frac{1}{12}$	$\frac{3}{20}$	$\frac{1}{10}$

Table 3. Coefficients of the amplitudes for the various reactions.

$$A_{\pi^-p\to\pi^0n} - A_{\pi^+n\to\pi^0p} = \sqrt{\frac{3}{5}}a_7$$

For scattering on the deuteron around 50 MeV, where the single scattering approximation gives a reasonable representation of the full multiple scattering amplitude, we may find useful the relation

$$(A_{\pi^+n} + A_{\pi^+p}) - (A_{\pi^-p} + A_{\pi^-n}) = 2a_3.$$

For the triangle rule we have,

$$\sqrt{2}A_{\pi^-p\to\pi^0n} - (A_{\pi^+p} - A_{\pi^-p}) = -a_3 - \sqrt{\frac{3}{2}}a_6 + \sqrt{\frac{3}{10}}a_7.$$

A useful comparison can be made if the scattering of a neutral pion from the nucleon is known[5].

$$A_{\pi^0p} - \frac{A_{\pi^+p} + A_{\pi^-p}}{2} = -\frac{\sqrt{3}}{2}a_4 + \sqrt{\frac{3}{10}}a_7 - \frac{3}{2\sqrt{5}}a_8$$

Neglecting the a_8 coefficient, we see that the same hadronic information is contained in this comparison as in the charge exchange on the neutron and proton, i.e., it is a_7 which is determined in the two cases.

If one were able to measure the cross section for neutral pion scattering from the neutron an appropriate comparison might be

$$A_{\pi^0n} - \frac{A_{\pi^+p} + A_{\pi^-p}}{2} = -\sqrt{\frac{2}{3}}a_2 - \frac{\sqrt{3}}{2}a_4 - \frac{1}{\sqrt{30}}a_7 + \frac{1}{2\sqrt{5}}a_8.$$

In this case the a_2 coefficient now appears because the neutron-proton mass difference is involved.

Thus, we see that the isospin breaking information obtained in various tests is not independent and, in fact, data-to-data predictions can be made.

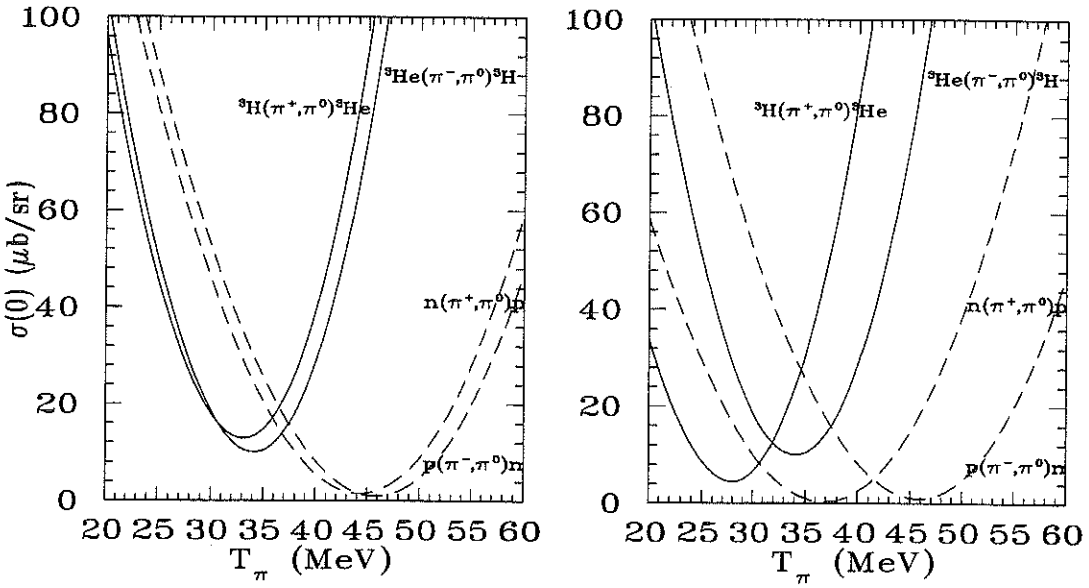

Figure. 2. Pion charge exchange on the ^{3}He-Triton system for no isospin breaking beyond the np mass difference and Coulomb (on the left) and with the addition of an estimate of breaking from the triangle rule (on the right).

It would be very useful to be able to measure charge exchange on the nucleon, both on protons and neutrons, in the forward direction where the cross section passes through a minimum near 45 MeV. The difference in the position of this minimum for the two cases would give information directly on a_7.

A possible solution to the lack of an isolated neutron target is provided by the use of nuclear targets. In order to observe the position of the minimum, analog transitions will need to be measured. Since the only possibility to measure analog transitions in both charge directions is with ^{3}He and ^{3}H, we are led to consider these two targets.

Figure 2 indicates the result to be expected from minimal breaking, as well as that assuming that a_7 is the sole contributer to the breaking seen in the triangle rule. It can be seen that the position of the minimum in energy is predicted to be shifted to lower energies, by the influence of the other nucleons, for both directions of charge exchange. While the precise value of this shift is difficult to predict reliably, the difference between the two minima is very nearly preserved. For this reason, a measurement of both nuclear targets is required. From the spacing between the minima observed in the ^{3}He and ^{3}H cases the spacing of the nucleon case can be inferred.

This work was supported by the U. S. Department of Energy.

REFERENCES

1. W. R. Gibbs, Li Ai and W. B. Kaufmann, Phys. Rev. Lett. 74, 3740(1995); *Sixth International Symposium Meson-Nucleon Physics and the Structure of the Nucleon*, Blaubeuren/Tuebingen, Germany 10-14 July 1995. πN Newsletter No. 11 (ISSN 0942-4148) Vol. II,page 84. MENU97, Vancouver, BC *Pion-nucleon Newsletter* **13**, p. 138; Phys. Rev. C **57**, 784(1998)
2. E. Matsinos, Phys. Rev. **C56**, 3014(1997)
3. B. L. Birbriar and A. B. Gridnov, Phys. Lett. B335, 6(1994)
4. W. B. Kaufmann and W. R. Gibbs, Ann. Phys. (N. Y.) 214, 84(1992)
5. A. M. Bernstein, Proceedings of the Seventh International Symposium on Meson-Nucleon Physics and the Structure of the Nucleon, Vancouver, British Columbia, Canada, July 28 – August 1, 1997. p. 37, and this conference.

Test of Isospin Symmetry in $NN \to d\pi$ Reactions

GEM Collaboration

M. Betigeri [i], J. Bojowald [a], A. Budzanowski [d], A . Chatterjee [i], M. Drochner [b], J. Ernst [g], L. Freindl [d], D. Frekers [h], W. Garske [h], K. Grewer [h], A. Hamacher [a], J. Ilieva [a,e], L. Jarczyk [c], G. Kemmerling [b], K. Kilian [a], S. Kliczewski [d], W. Klimala [a,c], D. Kolev [f], T. Kutsarova [e], J. Lieb [j], H. Machner [a*], A. Magiera [c], H. Nann [a†], L. Pentchev [e], H. S. Plendl [k], D. Protić [a], B. Razen [a], P. von Rossen [a], B. J. Roy [i], R. Siudak [d], J. Smyrski [c], A. Strzałkowski [c], R. Tsenov [f] P. A. Żołnierczuk [a,c], K. Zwoll [b]

a. Institut für Kernphysik, Forschungszentrum Jülich, Jülich, Germany
b. Zentrallabor für Elektronik, Forschungszentrum Jülich, Jülich, Germany
c. Institute of Physics, Jagellonian University, Krakow, Poland
d. Institute of Nuclear Physics, Krakow, Poland
e. Institute of Nuclear Physics and Nuclear Energy, Sofia, Bulgaria
f. Physics Faculty, University of Sofia, Sofia, Bulgaria
g. Institut für Strahlen- und Kernphysik der Universität Bonn, Bonn, Germany
h. Institut für Kernphysik, Universität Münster, Münster, Germany
i. Nuclear Physics Division, BARC, Bombay, India
j. Physics Department, George Mason University, Fairfax, Virginia, USA
j. Physics Department, Florida State University, Tallahassee, Florida, USA

Abstract

We study the excitation functions for the two isospin-related reactions $pp \to d\pi^+$ and $np \to d\pi^+$ close to threshold. A deviation of $11 \pm$ % from isospin symmetry is observed for the s-wave part of the cross section. From the s-wave amplitude of the $pp \to d\pi^+$ reaction at threshold is the isovector πN scattering length calculated. This value together with others from reactions with a real pion yields a new mean value which can be converted into a new πNN coupling constant $\frac{g^2_{\pi NN}}{4\pi} = 13.7 \pm 0.2$.

Isospin symmetry is known to be only an approximate symmetry. In addition to static breaking due to Coulomb effects and mass differences, dynamic effects due to the mass differences between the up and down quark [1] are effective. Up to 1990, the accepted fit to the excitation curve of $pp \to d\pi^+$ reactions was the one given by Spuller and Measday [2]. It is compared in Fig. 1 with Coulomb corrected data, which were published after 1967. Later Hutcheon et al. [3] measured the isospin-related $np \to d\pi^0$ reaction. These cross sections multiplied by the isospin factor 2 are also shown in Fig. 1. They are clearly smaller than the prediction by Spuller and Measday [2]. This discrepancy triggered further measurements of the time–reversed reaction $\pi^+ d \to 2p$ down to 20 MeV pion kinetic energy [4]. A fit performed by Ritchie including the Δ resonance [5] is also shown. The discrepancy between this fit and the previous one is much larger than the $np \to d\pi^0$ data. Furthermore, the whole range $\eta \leq 0.5$ contains only data from the time–reversed reaction. In order to solve this puzzle we have measured differential cross sections covering the full angular range for the $pp \to d\pi^+$ reaction close to threshold. Total cross sections were obtained by fitting Legendre polynomials to the angular distributions. Details of the measurements are given in Ref. [6]. The extracted total cross sections are compared in Fig. 2 with data previously shown in Fig. 1, the isospin corrected $np \to d\pi^0$ data and data from Heimberg et al. [7], which were published shortly after the GEM data. All charged data are Coulomb corrected by applying a Gamow factor. For small values of $\eta = p^{\pi}_{cm}/m_{\pi}$, the data from the neutral reaction are smaller than those from the charged data. In order to be quantitative, s- and p-wave contributions to the cross sections were fitted employing the method discussed in Ref. [8]. By carefully studying the systematic uncertainties, a deviation from isospin symmetry for the s-wave part of the reaction of $11 \pm 4\%$ is found.

*speaker, e-mail: h.machner@fz-juelich.de
†on leave from IUCF, Bloomington, Indiana, USA

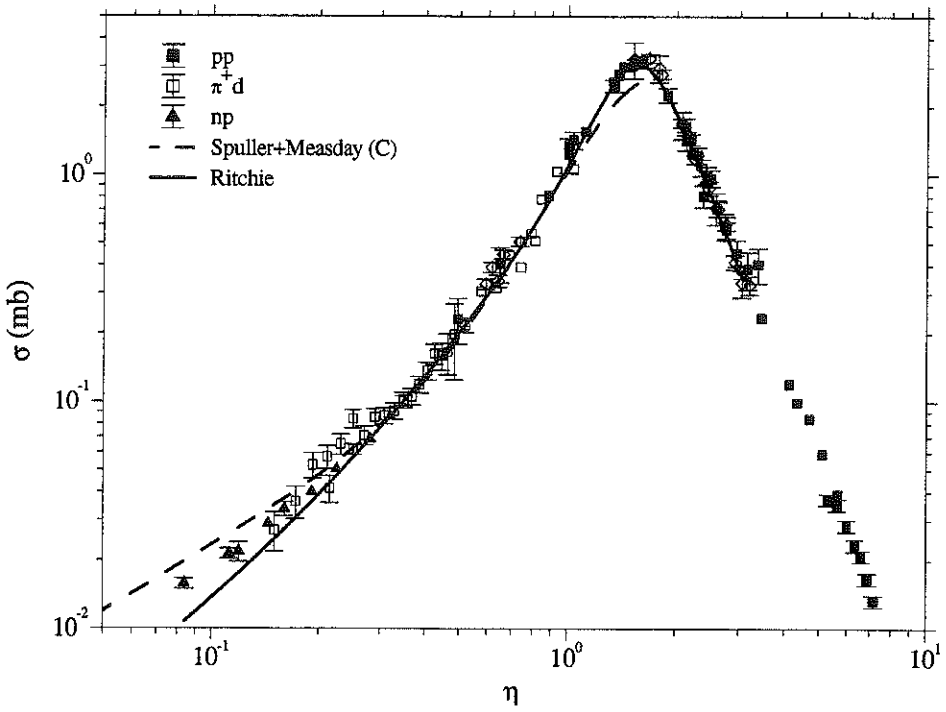

Figure. 1. Total cross sections for the reaction $p + p \rightarrow \pi^+ + d$ as function of the relative pion cm momentum $\eta = p_\pi/(m_\pi c)$. The data have been corrected for Coulomb effects. Data for the $pp \rightarrow \pi^+ d$ reaction are shown as full squares, those from the time–reversed reaction by open squares and the isospin-related reaction as inverted full triangles. Also shown is a fit (fit C from Spuller and Measday) as dashed curve and by Ritchie as solid curve.

From the s-wave cross section at threshold $\alpha_0 = 0.230 \pm 0.019\ mb$, one can extract the $\pi - N$ isovector scattering amplitude by invoking time reversal invariance, charge symmetry and isospin symmetry in pion elastic scattering and pion charge exchange. In addition the ratios

$$P = \frac{w(\pi^- p \rightarrow n\pi^0)}{w(\pi^- p \rightarrow n\gamma)}, \tag{1}$$

$$S = \frac{w(\pi^- d \rightarrow nn)}{w(\pi^- d \rightarrow nn\gamma)}, \tag{2}$$

$$T = \frac{w(\pi^- d \rightarrow nn\gamma)}{w(\pi^- p \rightarrow n\gamma)} \tag{3}$$

have to be applied where w is the transition rate of the corresponding process. This yields:

$$-b_1 = \left[\frac{1}{12\pi m_\pi}\frac{q_n^2}{q_\pi}\frac{P\alpha_0}{ST}\right]^{1/2} = (84.3 \pm 2.3) * 10^{-3} m_\pi^{-1}. \tag{4}$$

This value is compared with other results in Fig. 3. The result labelled pionic H+D is obtained from an analysis [8] of the pionic hydrogen and pionic deuterium atom results [9,10] in terms of two body and three body effects in πNN interactions [11]. The approach denoted potential scattering is from Ref [12], which analyzed elastic pion scattering by adjusting a potential in the Klein-Gordon equation. Radiative pion capture was measured by Kovash et al. [13]. The next four data are from phase shift analysis performed by different groups [14–17] for different data sets. The result from photoproduction is taken

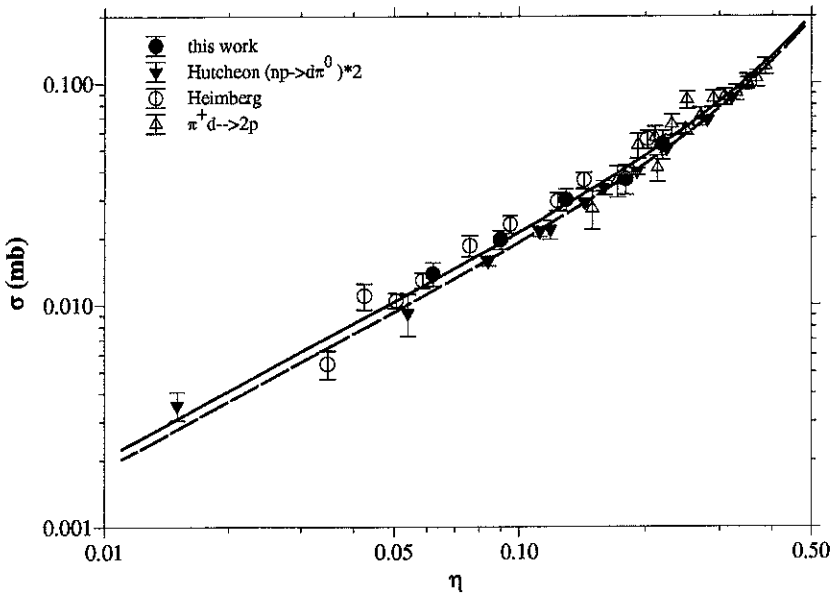

Figure. 2. Near threshold region of the $pp \to d\pi^+$ excitation function. Data are indicated by the different symbols. A fit for the pp reaction is shown as solid curve, the one for the np reaction as dashed curve.

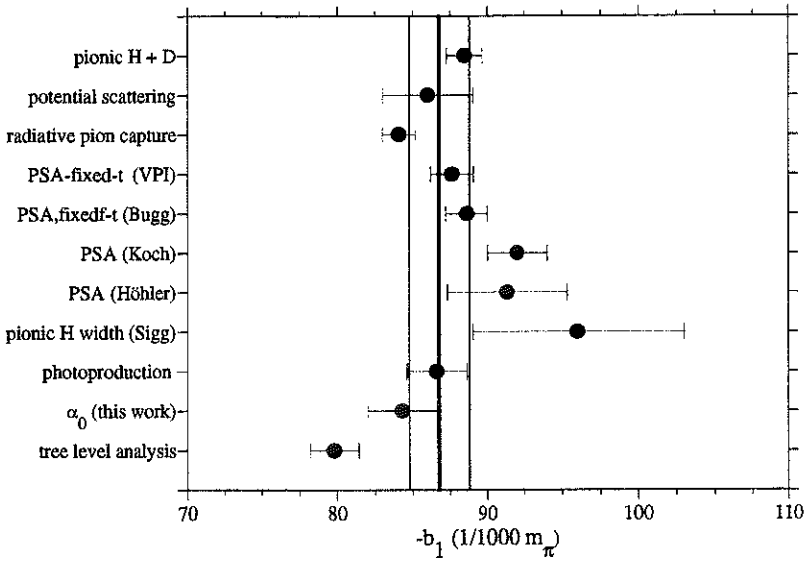

Figure. 3. The π–proton isovector scattering length as deduced from different studies including a real charged pion (see text). Also shown is the mean value with error band.

from Ref. [18]. Matsinos [19] analyzed low–energy pion scattering in terms of a tree–level model. His result for $\pi^+ p$ scattering is $b_0 + b_1 = -0.0769 \pm 0.0026\ /m_\pi$ and for $\pi^- p$ scattering $b_0 - b_1 = -0.0826 \pm 0.0020\ /m_\pi$ and thus yield $-b_1 = -0.0798 \pm 0.0016\ /m_\pi$. This result as well as the one from Ref. [16] are outside the error bar when extracting a mean value. The mean value without these two results is

$$-b_1 = (0.0868 \pm 0.020)/m_\pi. \tag{5}$$

From this value we extract with the help of the GMO sum rule a new value for the πNN coupling constant of

$$f^2_{\pi NN} = 0.0760 \pm 0.0011 \tag{6}$$

or with the help of $f^2_{\pi NN} = (\frac{m_\pi}{2m_N})^2 \frac{g^2_{\pi NN}}{4\pi}$ the more common quantity

$$\frac{g^2_{\pi NN}}{4\pi} = 13.7 \pm 0.2. \tag{7}$$

Related to the reactions studied so far are pion production in

$$pd \rightarrow {}^3H\pi^+ \tag{8}$$

$$pd \rightarrow {}^3He\pi^0 \tag{9}$$

when the additional neutron or proton, respectively is treated as a spectator. We have also started to study these reactions and will have results soon.

We are grateful to the COSY operation crew for their efforts in producing a good beam. Support by BMBF Germany (06 MS 568 I TP4), Internationales Büro des BMBF (X081.24 and 211.6), SCSR Poland (2P302 025 and 2P03B 88 08), and COSY Jülich is gratefully acknowledged.

REFERENCES

1. A. M. Bernstein, Phys. Lett. **B442**, 20 (1998). and references therein
2. J. Spuller and D. F. Measday, Phys. Rev. **D 12**, 3550 (1975).
3. D. A. Hutcheon et al., Phys. Rev. Lett. **64**, 176 (1990), and Nucl. Phys. **A 535**, 618 (1991).
4. B. G. Ritchie et al., Phys. Rev. Lett. **66**, 568 (1991), and Phys. Rev. **C 47**,21 (1993).
5. B. G. Ritchie, Phys. Rev. **C 44**,533 (1991).
6. M. Drochner et al., Phys. Rev. Lett. **77**, 454 (1996), and Nucl. Phys. **A 643**, 55 (1998).
7. P. Heimberg et al., Phys. Rev. Lett. **77**,1012 (1996).
8. H. Machner, Nucl. Phys. **A633**,341 (1988).
9. D. Sigg et al., Phys. Rev. Lett. **75**, 3245 (1995), Nucl. Phys. **A 609**,269 (1996), **A617**, 526(E) (1997).
10. D. Chattelard et al., Phys. Rev. Lett. **74**,4157 (1995), Nucl. Phys. bf A 625, 855 (1997).
11. S. Weinberg, Phys. Lett. **B 295**, 114 (1992).
12. W. R. Gibbs, Li Ai, W. B. Kaufmann, Phys. Rev. **C 57**, 784 (1998).
13. M. A. Kovash et al., πN Newsletter **12**, 51 (1997).
14. R. A. Arndt, I. I. Strakovsky, R. L. Workman, M. Pavan, Phys. Rev. **C 52**, 2120 (1995).
15. F. G. Markopoulou-Kalamara, D. V. Bugg, Phys. Lett. **B318**, 565 (1993).
16. R. Koch, Nucl. Phys. **A 448**, 707 (1986).
17. G. Höhler, Pion-Nucleon Scattering,Landoldt-Börnstein, Vol. I/9b2, ed. H. Schopper, Springer (1983)
18. O. Hanstein, D. Drechsel, L. Tiator, Phys. Lett. **B 399**, 13 (1997).
19. E. Matsinos, Phys. Rev. **C 56**,3014 (1997).

Working Group Summary: Pion-Nucleon Coupling Constant

M.E. Sainio
Helsinki Institute of Physics and
Department of Physics, University of Helsinki
P.O.B. 9, FIN-00014 Helsinki, Finland

Abstract

A brief introduction to different determinations of the πNN coupling constant is given, and some comments on the topics discussed in the working group are made.

INTRODUCTION

Since the birth of the Yukawa theory of the nuclear force in 1935 it was a challenge for the physics community to determine the coupling strength of the Yukawa meson to the nucleon. In 1947 the meson – pion – was finally discovered in cosmic ray emulsion experiments[1] and more systematic work to determine the πNN coupling constant could start. Conventionally[2] the pseudoscalar strength is denoted by g and the pseudovector coupling constant by f such that

$$f^2 = \left(\frac{M_\pi}{2m_p}\right)^2 \frac{g^2}{4\pi}, \tag{1}$$

where M_π is the charged pion mass and m_p is the proton mass. Other conventions concerning the nucleon mass and the factor 4π appear in the literature[3]. Reasonable estimates for the coupling strength were obtained even before the discovery of the pion and without detailed knowledge of the meson mass, e.g., Bethe was able to get an estimate $f^2 = 0.077$ - 0.080 already in 1940[4] on the basis of deuteron properties. The results of various determinations until 1980 are shown in Fig. 1. In the same figure very different techniques to determine f^2 are summarized. In the previous *MENU* symposium de Swart gave a review on the topic[3] and many of the references used in Fig. 1 can be found there. The values of

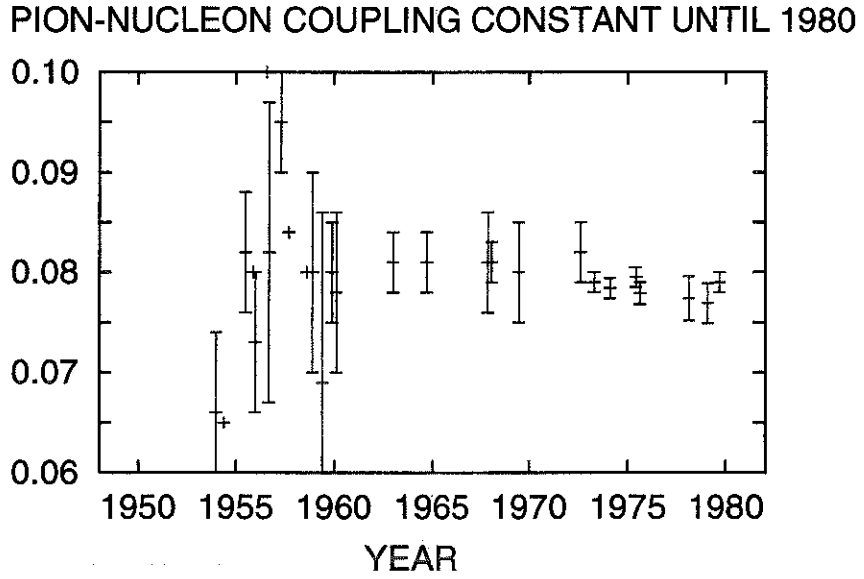

Figure. 1. The values of the pion-nucleon coupling constant f^2 before 1980.

f^2 stabilized for a long time[5–7] and only in the 90's has the discussion of the value of the pion-nucleon coupling constant started again. In[5–7] fixed-t dispersion relations for πN

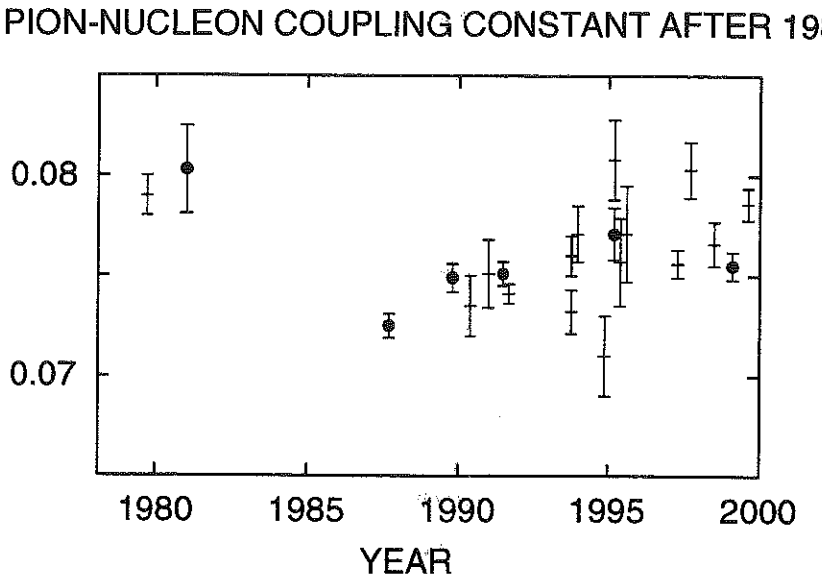

Figure. 2. The values of the pion-nucleon coupling constant f^2 after 1980 until the present. Neutral pion couplings are denoted by the solid dots, the remaining points refer to charged pion couplings or charge independent determinations.

were used. In the determinations displayed in Fig. 1 most of the data date back to the era before the meson factories, LAMPF, SIN and TRIUMF, which, in addition to performing experiments with pions, had programmes to study the NN interaction. In several analyses shown in Fig. 2 NN scattering data have been used to extract the πN coupling strength, i.e. one of the standard methods until the 60's has been adopted again in more refined form. In this activity the Nijmegen group has played an important role[3]. Of course, in Fig. 2 many results from the meson factory πN experiments are included as well in the data bases used to determine f^2.

The central issue in the discussion in the working group has been the scatter of the results of the determinations as shown in Fig. 2. The main questions involve the model dependence of different techniques, the effect of different pieces of data (partly conflicting), the error estimates, the electromagnetic corrections and other isospin violating effects. In the working group contributions were presented by Loiseau[8], Höhler[9] and Pavan[10], and brief commentaries by W.R. Gibbs, M. Birse and D.V. Bugg.

PROBLEMS IN EXTRACTING f^2

The particular issues raised in the discussion include:

- Electromagnetic corrections:
  - πN vs. NN; the different treatment of electromagnetic corrections for these two scattering processes gives a possibility to check the uncertainty due to these effects
  - corrections from Tromborg et al.[11] vs. Oades et al.[12]; the dispersion approach and potential model lead to differences which need checking
  - corrections at high energy; these need to be checked, Tromborg et al. calculated corrections only up to 655 MeV/c
- Lack of transparency of the analyses; the analyses contain large data bases and it is hard to clarify which pieces of information are the crucial ones in determining f^2
- The normalization of the np data is a problem in the (p,n) data analyses

- The determination of the s-wave isoscalar scattering length, a_{0+}^{+}, from the $\pi^- d$ level shift measurement suffers from some model dependence due to electromagnetic and absorption corrections
- Effective theory is not at present suitable for fixing the coupling constant. The problems relate mostly to the convergence of the chiral expansion or to the additional low-energy constants which are not known accurately enough. However, there might be a chance in a precise measurement of the induced pseudoscalar coupling constant, g_P, which would make an accurate determination of the pion-nucleon coupling constant possible[13]
- There is need for a new fixed-t analysis of πN scattering data which extends beyond the present limit of the VPI analysis, 2.1 GeV
- There is need for a new analysis of the forward dispersion relations of the NN system. The amount of NN data has increased considerably since the previous analysis thanks to the meson factories and SATURNE.

The GMO Sum Rule

The Goldberger-Miyazawa-Oehme sum rule (GMO)[14] provides a simple means to estimate the pion-nucleon coupling constant directly from measurable quantities, the πN isovector s-wave scattering length and total cross sections from the threshold to the highest energies. The method still has uncertainties, and will probably never be able to compete with other methods in precision, but the advantage is the possibility to relate the uncertainty in f^2 directly to the experimental errors.

The GMO sum rule is the result of the forward dispersion relation for the $D^-(= A^- + \nu B^-)$ amplitude taken at the physical threshold (the total laboratory energy $\omega = M_\pi$)

$$D^-(M_\pi) = \frac{8\pi f^2}{M_\pi[1-(M_\pi^2/4m_p^2)]} + 4\pi M_\pi J^- = 4\pi(1+x)a_{0+}^-\,, \tag{2}$$

where

$$J^- = \frac{1}{2\pi^2}\int_0^\infty \frac{\sigma^-(k)}{\omega}\,dk \tag{3}$$

and $x = M_\pi/m_p$. The pion-nucleon coupling constant can now be extracted and the result is

$$\begin{aligned} f^2 &= \frac{1}{2}[1-(\frac{x}{2})^2][(1+x)M_\pi a_{0+}^- - M_\pi^2 J^-] \\ &= 0.5712(M_\pi\, a_{0+}^-) - 0.02488(J^-/\mathrm{mb}). \end{aligned} \tag{4}$$

The isovector s-wave scattering length, a_{0+}^-, is accessible through experiment[19]. For the integral J^- several evaluations are displayed in Table 1. As can be seen from Fig. 3 there is potential sensitivity to details of the electromagnetic corrections especially around the Δ-resonance region near 0.3 GeV/c as well as to the treatment of the Δ^{++}, Δ^0 splitting. Making use of the isospin symmetry gives for the scattering length $a_{0+}^- = 0.0962 \pm 0.0071\, M_\pi^{-1}$[19] and taking Koch's value for J^- gives an estimate for the lower limit of the coupling constant f^2 with the result 0.0765. With more conservative errors for J^- the figure 0.0762 is obtained. With the remaining uncertainties in the treatment of various corrections this limit is not in real conflict with the results from other analyses.

Table 1. Values for the J^- integral.

Ref.	J^- (mb)
KH ('83)[2]	-1.058
Koch ('85)[15]	-1.077 ± 0.047
VPI ('92)[16]	-1.072
Gibbs ('98)[17]	-1.051
ELT ('99)[18]	-1.083 ± 0.025

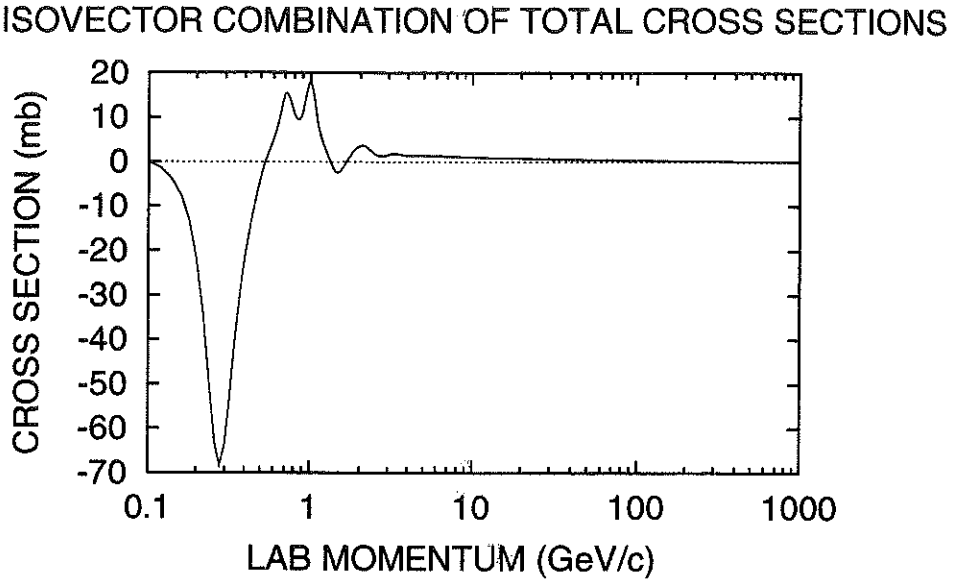

Figure. 3. The isovector combination, $\sigma^- = \frac{1}{2}(\sigma_{\pi^- p} - \sigma_{\pi^+ p})$, of the $\pi^- p$ and $\pi^+ p$ total cross sections[2]. Experimental data extend up to 350 GeV/c.

CONCLUDING REMARKS

The precision of the pion-nucleon experiments has now reached the level where a more careful treatment of the corrections, in particular of electromagnetic origin or due to the u- and d-quark mass difference, is necessary. These theoretical challenges have not yet been met, eventhough the theoretical tool, chiral perturbation theory, has now the capability to answer these questions. Work along these lines is in progress. In the lattice[20] and the QCD sum rule[21] frontiers the present accuracy for g is 20-30 % and it will take a while before this improves significantly.

Table 2 summarizes some recent values for f^2 displayed in Fig. 2. The table demonstrates the current trend, the favoured value for f^2 is slightly smaller than the standard one of Koch and Pietarinen[7]. However, there remains still quite a number of problems which need attention.

The Goldberger-Treiman discrepancy

$$\Delta_{\pi N} = 1 - \frac{m_p\, g_A}{F_\pi\, g}, \tag{5}$$

where F_π and g_A are the pion and neutron decay constants respectively, would be reduced from 4 % to 2 %, if f^2 changes from 0.079 to 0.076. In a recent SU(3) analysis[27] preference for a smaller Goldberger-Treiman discrepancy was found.

In the analysis of np scattering data at backward directions somewhat higher value for the coupling constant has been obtained[28], $f^2 = 0.0803 \pm 0.0014$. Discussion on

Table 2. Values for the pion-nucleon coupling constant f^2 from recent determinations.

Ref.	f^2	Method
KH ('80)[7]	0.079 ± 0.001	πN fixed-t
BM ('95)[22]	0.0757 ± 0.0022	NN data
Gibbs ('98)[17]	0.0756 ± 0.0007	GMO
Machner ('98)[23]	0.0760 ± 0.0011	symmetries
Matsinos ('98)[24]	0.0766 ± 0.0011	model fit
Nijmegen ('99)[25]	0.0756 ± 0.0004	pp PWA
ELT ('99)[18]	0.0786 ± 0.0008	GMO + $\pi^- d$
VPI ('99)[10,26]	0.0760 ± 0.0004	πN fixed-t

the problems in this field continues[29,30]. The spin transfer coefficients in pp scattering are also of interest, the preliminary indications are towards slightly smaller value for the coupling[31]. Machleidt has recently discussed[32] some additional problems with the deuteron properties and low-energy NN analyzing powers which indicate that no coherent picture is yet emerging.

ACKNOWLEDGEMENTS

I thank A.M. Green for useful remarks on the manuscript. Partial support from the EU-TMR programme, contract CT98-0169, is gratefully acknowledged.

REFERENCES

1. C.M.G Lattes, H. Muirhead, G.P.S. Occhialini, and C.F. Powell, "Processes involving charged mesons," Nature **159**, 694 (1947).
2. G. Höhler, *Landolt-Börnstein*, Vol. 9 b2, ed. H. Schopper (Springer, Berlin, 1983).
3. J.J. de Swart, M.C.M. Rentmeester, and R.G.E. Timmermans, "The status of the pion-nucleon coupling constant," in *Proceedings of MENU97* (TRIUMF, Vancouver, 1997) pp. 96–107; nucl-th/9802084.
4. H.A. Bethe, "The meson theory of nuclear forces: Part II. Theory of the deuteron," Phys. Rev. **57**, 390 (1940).
5. J. Hamilton, and W.S Woolcock, "Determination of pion-nucleon parameters and phase shifts by dispersion relations," Rev. Mod. Phys. **35**, 737 (1963).
6. D.V. Bugg, A.A. Carter, and J.R. Carter, "New values of pion-nucleon scattering lengths and f^2," Phys. Lett. **44B**, 278 (1973).
7. R. Koch, and E. Pietarinen, "Low-energy πN partial wave analysis," Nucl. Phys. **A336**, 331 (1980).
8. B. Loiseau, "How precisely can we determine the πNN coupling constant from isovector GMO sum rule?" *these proceedings.*
9. G. Höhler, "Determinations of the πNN coupling constant," *these proceedings.*
10. M. Pavan, "Determination of the πNN coupling constant in the VPI/GW πN $\rightarrow$ πN partial-wave and dispersion relation analysis," *these proceedings.*
11. B. Tromborg, S. Waldenstrøm, and I. Øverbø, "Electromagnetic corrections to πN scattering," Phys. Rev. **D15**, 725 (1977).
12. G.C. Oades, *these proceedings.*
13. V. Bernard, N. Kaiser, U.-G. Meißner, "QCD accurately predicts the induced pseudoscalar coupling constant," Phys. Rev. **D50**, 6899 (1994).
14. M.L. Goldberger, H. Miyazawa, and R. Oehme, "Application of dispersion relations to pion-nucleon scattering," Phys. Rev. **99**, 986 (1955).
15. R. Koch, "Inconsistencies in low-energy pion-nucleon scattering," Karlsruhe preprint TKP 85-5 (1985).
16. R.L. Workman, R.A. Arndt, and M.M. Pavan, "On the Goldberger-Miyazawa-Oehme sum rule," Phys. Rev. Lett. **68**, 1653 (1992); (E) ibid. **68**, 2712 (1992).
17. W.R. Gibbs, Li Ai, and W.B. Kaufmann, "Low-energy pion-nucleon scattering," Phys. Rev. **C57**, 784 (1998).

18. T.E.O. Ericson, B. Loiseau, and A.W. Thomas, "Precision determination of the πN scattering lengths and the charged πNN coupling constant," hep-ph/9907433.
19. D. Sigg et al., "The strong interaction shift and width of the ground state of pionic hydrogen," Nucl. Phys. **A609**, 269 (1996); (E) ibid. **A617**, 526 (1997).
20. K.F. Liu et al., "Valence QCD: Connecting QCD to the quark model," Phys. Rev. **D59**, 112001 (1999).
21. M.C. Birse, and B. Krippa, "Determination of pion-baryon coupling constants from QCD sum rules," Phys. Rev. **C54**, 3240 (1996).
22. D.V. Bugg, and R. Machleidt, "πNN coupling constants from NN elastic scattering data between 210 and 800 MeV," Phys. Rev. **C52**, 1203 (1995).
23. H. Machner, "Symmetries in low energy pion physics and the πNN coupling constant," Acta Phys. Pol. **B29**, 3081 (1998).
24. E. Matsinos, "The low-energy constants of the πN system," hep-ph/9807395.
25. M.C.M Rentmeester, R.G.E. Timmermans, J.L. Friar, and J.J. de Swart, "Chiral two-pion exchange and proton-proton partial-wave analysis," Phys. Rev. Lett. **82**, 4992 (1999).
26. M.M. Pavan, R.A. Arndt, I.I. Strakovsky, and R.L Workman, "Determination of the πNN coupling constant in the VPI/GW πN $\rightarrow$ πN partial-wave and dispersion relation analysis," nucl-th/9910040.
27. J.L. Goity, R. Lewis, M. Schvellinger, and L. Zhang, "The Goldberger-Treiman discrepancy in SU(3)," Jefferson Lab. preprint JLAB-THY-98-51, hep-ph/9901374.
28. J. Rahm et al., "*np* scattering measurements at 162 MeV and the πNN coupling constant," Phys. Rev. **C57**, 1077 (1998).
29. M.C.M. Rentmeester, R.A.M. Klomp, and J.J. de Swart, "Comment on πNN coupling from high precision *np* charge exchange at 162 MeV," Phys. Rev. Lett. **81**, 5253 (1998).
30. T.E.O. Ericson et al., Phys. Rev. Lett. **81**, 5254 (1998).
31. S.W. Wissink, "Spin transfer coefficients for *pp* elastic scattering at 200 MeV: Implications for the πNN coupling constant," Nucl. Phys. **A631**, 411c (1998).
32. R. Machleidt, "How sensitive are various NN observables to changes in the πNN coupling constant?," nucl-th/9909036.

How precisely can we determine the πNN coupling constant from the isovector GMO sum rule?

B. Loiseau
LPNHE/LPTPE, Université P. & M. Curie, 4 Place Jussieu, 75252 Paris, France
T.E.O. Ericson
CERN, CH-1211 Geneva 23, Switzerland, and TSL, Box 533, S-75121 Uppsala, Sweden
A.W. Thomas
CSSM, University of Adelaide, Adelaide 5005, Australia

Abstract

The isovector GMO sum rule for zero energy forward πN scattering is critically studied to obtain the charged πNN coupling constant using the precise π^-p and π^-d scattering lengths deduced recently from pionic atom experiments. This direct determination leads to $g_c^2/4\pi = 14.23 \pm 0.09$ (statistic) ± 0.17 (systematic) or $f_c^2/4\pi = 0.0786(11)$. We obtain also accurate values for the πN scattering lengths

INTRODUCTION: ROBUST FORM OF THE GMO RELATION

The analysis to determine the πNN coupling constant should be clear and easily reproducible. One should do a detailed study for the statistical and systematic errors. The precise determination is an absolute statement, it could be erroneous and it should be improvable. In this perspective the Goldberger-Miyazawa-Oehme (GMO) sum rule[1] might be a good candidate. It is a forward dispersion relation at zero energy for πN scattering. It assumes scattering amplitudes to be analytical functions satisfying crossing symmetry. At first isospin symmetry does not have to be assumed and it reads (for more details see e.g.[2]) with its numerical coefficients: $g_c^2/4\pi = -4.50\ J^- + 103.3\ [(a_{\pi^-p} - a_{\pi^+p})/2]$, where J^- is in mb the weighted integral, $J^- = (1/4\pi^2)\int_0^\infty (dk/\sqrt{k^2+m_\pi^2})[\sigma_{\pi^-p}^{Total}(k) - \sigma_{\pi^+p}^{Total}(k)]$ and $a_{\pi^\pm p}$ are the $\pi^\pm p$ scattering lengths in units of m_π^{-1}. All ingredients are physical observables but so far the lack of precision in $a_{\pi^\pm p}$ (contribution of 2/3 to $g^2/4\pi$) led to applications of the GMO relation as consistency check or constraint[3]. The 1s width of the π^-p atom[4] determines $a_{\pi^-p\to\pi^0n} = -0.128(6)\ m_\pi^{-1}$ and assuming isospin symmetry this gives $a^- = (a_{\pi^-p} - a_{\pi^+p})/2$ and $g_c^2/4\pi = 14.2(4)$ using[5] J^-= -1.077(47) mb. This is not accurate enough although improvements will come[6].

We here report on a possible way to improve the precision on $g_c^2/4\pi$[7]. As a_{π^-p} is precisely known ($0.0883(8)\ m_\pi^{-1}$) from energy shift in pionic hydrogen[8] one can write:

$$g_c^2/4\pi = -4.50\ J^- + 103.3\ a_{\pi^-p} - 103.3\ (\frac{a_{\pi^-p} + a_{\pi^+p}}{2}). \qquad (1)$$

and using the above cited J^- (to be calculated later), $g_c^2 = 4.85(22)+9.12(8)-103.3[(a_{\pi^-p}+a_{\pi^+p})/2]$. This (not our final result) shows that all the action is in the term $1/2(a_{\pi^-p} + a_{\pi^+p})$,which, assuming isospin symmetry, is a^+. If this quantity is positive $g_c^2/4\pi$ is smaller than 14, if it is negative it is larger. One way to determine the small a^+ is to use the accurate π^-d scattering length $a_{\pi^-d} = -0.0261(5)\ m_\pi^{-1}$, from the pionic deuterium 1s energy level[9]. To leading order this is the coherent sum of the π^- scattering lengths from the proton and neutron, which, assuming charge symmetry (viz, $a_{\pi^+p} = a_{\pi^-n}$) is the term required in our 'robust' relation (1) The strong cancellation between the two terms is then done by the physics. In order to match the precision using the width, we only need a theoretical precision in the description of the deuteron scattering length to about 30%.

ZERO-ENERGY π^--DEUTERON SCATTERING AND a^+

In multiple scattering theory of zero-energy s-wave pion scattering from point-like nucleons and in the fixed scattering-center approximation, the leading contribution is[10]:

$a_{\pi^-d}^{static} = S + D$ ... with $S = [(1+m_\pi/M)/(1+m_\pi/M_d)](a_{\pi^-p}+a_{\pi^-n})$, M and M_d being the nucleon and deuteron masses respectively. The double scattering term D is:

$$D = 2\,\frac{(1+m_\pi/M)^2}{(1+m_\pi/M_d)}\,[(\frac{a_{\pi^-p}+a_{\pi^-n}}{2})^2 - 2(\frac{a_{\pi^-p}-a_{\pi^-n}}{2})^2] < 1/r >, \qquad (2)$$

and with our final scattering lengths $D = -0.0256\ m_\pi^{-1}$ quite close to a_{π^-d} experimental.

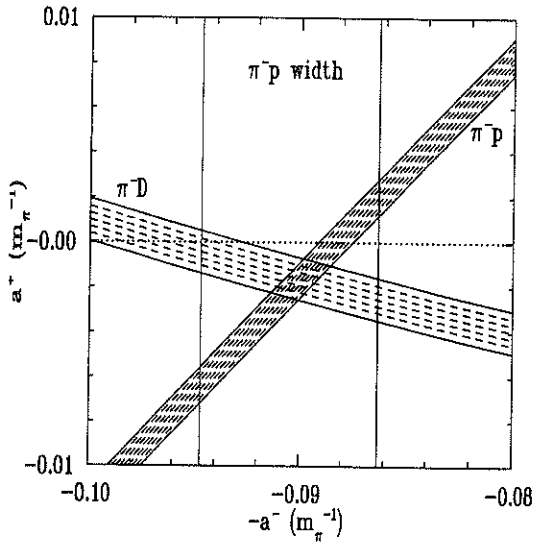

Fig. 1. Our graphical determination of the πN scattering lengths in excellent agreement with the central values of the experimental PSI group[4], $a^+ = -22(43)\cdot 10^{-4} m_\pi^{-1}; a^- = 905(42)\cdot 10^{-4} m_\pi^{-1}$.

We shall here follow the recent theoretical multiple scattering investigation of Baru and Kudryatsev (B-K)[11]. The comparison of typical contributions is listed in Table 1. 1)*Fermi motion*: the nucleons have a momentum distribution which produces an attractive

Table 1. Typical contributions to $a_{\pi d}$ in units of $10^{-4} m_\pi^{-1}$, recall $a_{\pi d}^{exp.} = -261(5)$[9].

Contri -butions	D	Fermi motion 1)	Absorption corr.[16] 2)	s-p interf. 3)	$(\pi^- p, \gamma n)$ double scatt.	Form factor 4)
Present	-256(7)	61(7)	-56(14)	small	-2	17(9)
B-K	-252	50	X	-44	X	29(7)
Contri-butions		Non-static effects 5)	Isospin violation 6)	Higher order 6)	p-wave double scatt. 6)	Virtual pion 6)
Present		10(6)	3.5	4(1)	-3	-7(2)
B-K		10	3.5	6	-3	X

contribution, calculable to leading order from $< p^2 >$ of the nucleon momenta in the deuteron. The uncertainty of 7 comes from the D-state percentage in the deuteron, P_D =4.3% vs. 5.7% for the Machleidt1[12] vs. the Paris[13] wave functions. 2) *Absorption correction*: the absorption reaction π^-d $\rightarrow$nn, using 3-body Faddeev approaches[14–16] produces a repulsive (-20%) contribution (not included in B-K). These studies were done carefully but a modern reinvestigation of this term is highly desirable. 3) *"s-p' interference*: a -15% correction was obtained by B-K. We find that it is a model dependent contribution due nearly entirely to the Born term the contribution of which vanishes exactly. We have then not considered this contribution. 4)*Form factor*: this non-local effect enters mainly via the dominant isovector πN s-wave interaction, closely linked to ρ exchange. It represents only a correction of about -10%. 5) *Non-static effects*: these produce only a rather small correction of about 4%. There are systematic cancellations between single and double scattering as was first demonstrated by Fäldt[17]. It has been numerically investigated by B-K and we have adopted their value, the error of 6 reflects a lack of independent verification. 6) *Isospin violation, higher order terms, p-wave double scattering,virtual pion scattering*: these corrections are all small and controllable. The isospin violation in the

πN interaction comes in part from the $\pi^{\pm} - \pi^0$ mass difference where an additional check comes from the chiral approach[18]. Based on this, we obtain the preliminary, though nearly final, values $(a_{\pi^-p} + a_{\pi^-n})/2 = (-17 \pm 3(\text{statistic}) \pm 9(\text{systematic}))10^{-4} m_{\pi}^{-1}$ and $(a_{\pi^-p} - a_{\pi^-n})/2 = (900 \pm 12)\ 10^{-4} m_{\pi}^{-1}$. Our values represent a substantial improvement in accuracy as seen in Fig. 1. The contribution of the scattering lengths to $g_c^2/4\pi$ has here a precision of about 1%.

TOTAL CROSS SECTION INTEGRAL J^-

The cross section integral contributes only one third to the GMO relation. Total cross sections are inherently accurate and their contribution is calculated with accuracy, but for the high energy region. The possibility of systematic effects in the difference must be considered, particularly since Coulomb corrections have opposite sign for $\pi^{\pm}$p. The only previous evaluation with a detailed discussion of errors is that by Koch[5]. Later evaluations given in Table 2 find values within the errors, but the uncertainties are not stated and analyzed. In view of obtaining a clear picture of the origin of uncertainties we

Table 2. Some values of J^- in mb, Ref.[19] uses 2 different PWA: K-H[20] and their own, VPI.

Ref.	Koch 1985[5]	Workman *et al.* 1992; K-H[19]	Workman *et al.* 1992; VPI[19]	Arndt *et al.* 1995[21]	Gibbs *et al.* 1998[22]	Present work
J^-	-1.077(47)	-1.056	-1.072	-1.05	-1.051	-1.095(31)

have reexamined this problem in spite of the consensus. We limit the discussion to the critical features. The typical shape of the integrands is shown in Fig. 2 up to 2 Gev/c.

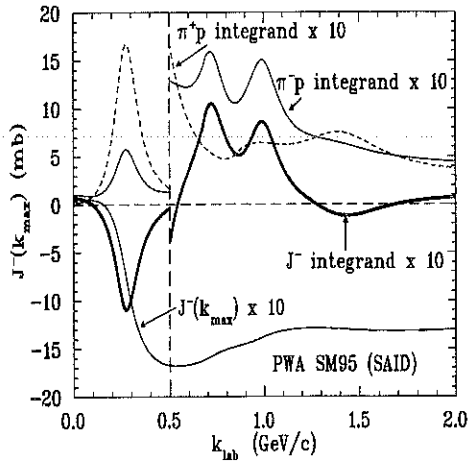

Fig. 2. The J^- separate integrands for $\pi^{\pm}$p as well as their difference as function of k_{lab} together with the cumulative value of the integral $J^-(k_{lab})$ from the region $0 < k < k_{lab}$. The integrands are in units of mb GeV/c.

There are no total cross-section measurements below 160 MeV/c, but the accurately known $a_{\pi^{\pm}p}$ give a strong constraint assuming isospin symmetry. The s- and p-wave contributions nearly cancels. A tiny correction occurs, since isospin is broken by the 3.3 MeV lower threshold for the π^0n channel below the physical π^-p threshold. The main contributions come from the region of the Δ resonance and just above. There are no strong cancellations in the difference between $\pi^{\pm}$p cross sections in that region and the cross sections have been very carefully analyzed. We have first evaluated the hadronic cross sections up to 2 GeV/c based on the VPI phase-shift solution[23]. In doing so Coulomb corrections and penetration factors have been taken into account in the adjustment to experimental data even if the treatment may not be optimal. It also allows for some isospin breaking, since the Δ mass splitting is parameterized[24]. In view of the not so high accuracy we aim for, this should be adequate. Bugg[25,26] has emphasized that in the π^+p scattering the total cross sections are systematically reduced at all energies by the Coulomb repulsion between the particles and, conversely, enhanced in π^-p scattering. One must correct for

this effect, which gives a negative contribution to J^-. Having made no correction for it at higher energies means that we will underestimate the coupling constant somewhat. In the region around 500 MeV/c there are long-standing problems with the experimental total cross section data[24]. This uncertainty, larger than the Coulomb penetrability effects, should be resolved. So we have preferred to use the SM95 PWA solution as the best guide. The real uncertainty in J^- comes from the high energy region and is linked to the relatively slow convergence of the integral.

Table 3. Contributions to J^- in mb according to interval of integration and to the total cross-section input. 'Selected" is for the world data[28] with statistical and systematic errors $\leq 1\%$. Here the first given error is statistical and the second one systematic.

k(GeV/c)	0 to 2	2 to 4.03	4.03 to 240	240 to ∞
Input	SM95[23]	Selected[28]	Selected[28]	Regge(94)[27]
J^-(mb)	(-1.302±0.006)(17)	(0.064±0.002)(7)	(0.133±0.005)(24)	(0.030)
k(GeV/c)	0 to 2	240 to ∞	0 to ∞	0 to ∞
Input	Arndt98)[23]	Regge(98)[28]	SM95+Regge94	Arndt98+Regge98
J^-(mb)	(-1.329±0.006)(17)	(0.018)(3)	(-1.075±0.008)(30)	(-1.114±0.008)(30)

We have evaluated the different contributions (see Table 3) with no other Coulomb and penetration corrections than those introduced by the experimental authors above 2 GeV or by the theoretical analysis below 2 GeV. We find, based on (integration of hadronic cross section) the SM95 and Arndt 12/98 analysis below 2 GeV/c[23], and on the Regge pole PDG94[27] and PDG98[28] extrapolation beyond 240 GeV/c, the values $J^- = (-1.075 \pm 0.008)(30)$ mb and $(-1.114 \pm 0.008)(30)$ mb respectively. We have adopted the mean value $J^- = (-1.095 \pm 0.008)(30)$ mb. In our calculation we have added a systematic uncertainty from Coulomb penetration effect of ± 0.017 from the region less than 2 GeV/c.

RESULTS AND CONCLUSIONS

We have derived first new values for the πN scattering lengths from the π^-d one:

$$a^+ \simeq \frac{a_{\pi^-p} + a_{\pi^-n}}{2} = (-17 \pm 3)(9)) \cdot 10^{-4} m_\pi^{-1}, a^- \simeq \frac{a_{\pi^-p} - a_{\pi^-n}}{2} = 900(12) \cdot 10^{-4} m_\pi^{-1}.$$

Our second conclusion concerns the charged πNN coupling constant using these new accurate values in (1) with $J^- = (-1.095 \pm 0.008)(30)$ and charge symmetry:

$$g_c^2/4\pi = (4.93 \pm 0.04)(14) + (9.12 \pm 0.08) + (0.18 \pm 0.03)(9) = (14.23 \pm 0.09)(17). \quad (3)$$

The uncertainty comes mainly from J^-. This coupling constant which agrees quite well with the text book value, 14.28(18)[20] is intermediate between the low value deduced from the large data banks of NN and πN scattering data[24,29] and the high value from np charge exchange cross sections[30]. It is fully compatible with the latter, differing statistically by only about one standard deviation.

REFERENCES

1. M. L. Goldberger, H. Miyazawa and R. Oehme, *Application of Dispersion Relations to Pion-Nucleon Scattering*, Phys. Rev. **99**, 986 (1955).
2. G. Höhler in *Pion-Nucleon Scattering*, Ed. H. Schopper, Landolt-Börnstein, New Series, Vol. **9b** (Springer, New York 1983); G. Höhler, *Determination of the πNN Coupling Constant*, contribution to this symposium.
3. R. A. Arndt, R. L. Workman and M. M. Pavan, *Pion-nucleon partial-wave analysis with fixed-t dispersion relation constraints*, Phys. Rev. C**49**, 2729 (1994).
4. H.-Ch. Schröder, A. Badertscher, P. F. A. Goudsmit, M. Janousch, H. J. Leisi, *et al.*, *Determination of the πN scattering lengths from Pionic Hydrogen*, Phys. Lett. **B469**, 25 (1999).

5. R. Koch, *Inconsistencies in Low-Energy Pion-Nucleon Scattering*, Karlsruhe preprint 1985 (unpublished) TKP 85-5.
6. D. Gotta, *et al.*, *Measurement of the Ground-State Shift and Width in Pionic Hydrogen to the 1 % Level: A New Proposal at PSI*, contribution to this symposium.
7. T. E. O. Ericson, B. Loiseau and A. W. Thomas, invited contribution to Panic99, Uppsala 1999, *Precision determination of the π N scattering lengths and the charged πNN coupling constant*, Nucl. Phys. **Ac** to appear.
8. D. Chatellard, J.-P. Egger, E. Jeannet, A. Badertscher, M. Bogdan, *et al.*, *X-ray spectroscopy of the pionic deuterium atom* Nucl. Phys. **A625**, 310 (1997).
9. P. Hauser, K. Kirch, L. M. Simons, G. Borchert, D. Gotta, *et al.*, *New precision measurement of the pionic deuterium s-wave strong interaction parameters*, Phys. Rev. **C58**, R1869 (1998).
10. T. E. O. Ericson and W. Weise, *Pions and Nuclei*, Clarendon Press 1988.
11. V. V. Baru and A. E. Kudryatsev, *π N Scattering Lengths from an Analysis of New Data on Pionic Hydrogen and Deuterium Atoms*, Phys. Atom. Nucl. **60**, 1475 (1997) and private communication.
12. R. Machleidt, K. Holinde and Ch. Elster, *The Bonn meson-exchange model for the nucleon-nucleon interaction*, Phys. Rep. **149**, 1 (1987).
13. M. Lacombe, B. Loiseau, R. Vinh Mau, J. Côté, P. Pirés, and R. de Tourreil, *Parameterization of the deuteron wave function of the Paris NN potential*, Phys. Lett. **B101**, 139 (1981).
14. I. R. Afnan and A. W. Thomas, *Faddeev approach to pion production and pion-deuteron scattering*, Phys. Rev. C**10**, 109 (1974).
15. T. Mizutani and D. Koltun, *Coupled Channel Theory of Pion-Deuteron Reaction Applied to Threshold Scattering*, Ann. Phys. (NY) **109**, 1 (1977).
16. A. W. Thomas and R. H. Landau, *Pion-deuteron and pion-nucleus scattering - a review* Physics Reports **58**, 121 (1980).
17. G. Fäldt, *Binding corrections and the pion-deuteron scattering length*, Physica Scripta **16**, 81 (1977).
18. N. Fettes, U.-G. Meissner and S. Steininger, *On the size of isospin violation in low-energy pion-nucleon scattering*, Phys. Lett. **B451**, 233 (1999) and N. Fettes, *Isospin Violation in Pion-Nucleon Scattering*, contribution to this symposium.
19. R. L. Workman, R. A. Arndt and M. M. Pavan, *On the Goldberger-Miyazawa-Oehme Sum Rule*, Phys. Rev. Lett. **68**, 1653 (1992).
20. R. Koch and E. Pietarinen, *Low-Energy πN Partial Wave Analysis*, Nucl. Phys. **A336**, 331 (1980).
21. R. A. Arndt, I. I. Strakovsky, R. Workman and M. M. Pavan, *Updated analysis of πN elastic scattering data to 2.1 GeV: The baryon spectrum* Phys. Rev. **C52**, 2120 (1995).
22. W. R. Gibbs, Li Ai and W. B. Kaufmann, *Low-energy pion-nucleon scattering*, Phys. Rev. **C57**, 784 (1998).
23. R. A. Arndt *et al.*, Scattering Interactive Dial-Up (SAID), VPI, Blacksburg, πN solution SM95 1995 and Arndt 12/98 analysis.
24. M. M. Pavan and R. A. Arndt, *Determination of the π NN Coupling Constant in the VPI/GW $\pi N \rightarrow \pi$ N Partial-Wave and Dispersion Relation Analysis*, contribution to this symposium and private communication.
25. D. V. Bugg and A. A. Carter, *The forward dispersion relation for πN charge exchange* Phys. Lett. **48B**, 67 (1974).
26. D. Bugg, *Summary of the Conference*, contribution to this symposium and private communication.
27. L. Montanet *et al.*, *Review of Particle Properties*, Phys. Rev. D**50**, 1173 (1994) p. 1335.
28. C. Caso *et al.*, *Review of Particle Physics*, Europ. Phys. J. **C3**, 1 (1998) p. 205; http::/pdg.lbl.gov/xsect/contents.html.
29. J. J. De Swart, M. C. M. Rentmeester, R. G. E. Timmermans, *The status of the pion-nucleon coupling constant*, πN Newsletter **13**, 96 (1997).
30. J. Rahm, J. Blomgren, H. Condé, S. Dangtip, K. Elmgren, *et al*, *np scattering measurements at 162 MeV and the πNN coupling constant*, Phys. Rev. **C57**, 1077 (1998).

Determinations of the πNN Coupling Constant

G. Höhler
Institut für Theoretische Teilchenphysik der Universität
Postfach 6980 D-76128 Karlsruhe, Germany

Abstract

Discussion of determinations of the coupling constant from dispersion relations for πN scattering.

Introduction

The pseudoscalar πNN coupling constant g is defined by the numerator of the pole terms of fixed-t dispersion relations for πN scattering (See Ref.[1] for a proof within the framework of QCD). The pole term of the dispersion relation for π^+ photoproduction has also been used, since it is strongly dominant near threshold. However, in the range of inelastic final states, the input for the integrals is much less accurate than for πN scattering.

Accurate determinations of the coupling constant from NN-scattering were the main topic at a workshop in Uppsala in June 1999. To my knowledge, two problems have not yet been studied:

i) the accuracy of g^2 which can be reached from an analysis of the dispersion relation for pp forward scattering[2].

ii) if the much different treatment of the electromagnetic corrections in NN and πN scattering can lead to differences in g^2 of the order of the very small errors given by some authors.

The pseudovector coupling constant f^2 is defined by

$$\frac{g^2}{4\pi} = \frac{4m^2}{m_\pi^2} f^2. \tag{1}$$

The convention is to use the masses of the charged nucleon and pions. If π^0 occurs, the effect of the mass difference has to be taken into account separately.

In the following, we shall discuss only determinations from πN dispersion relations for πN scattering. Determinations from models for πN scattering or fits in small energy intervals have an additional unknown error.

The GMO Sum Rule

The GMO sum rule[3] was derived from the difference between the dispersion relations for the amplitudes $C_\pm$ at $t = 0$, evaluated at threshold. Lower indices refer to $\pi^\pm p$ scattering. We denote crossing even and odd combinations by $C^\pm = D^\pm = (C_- \pm C_+)/2$ and use an analogous notation for the total cross sections $\sigma^\pm$. The data for σ^- suggest strongly the existence of the integral in

$$C^-(m_\pi) = 4\pi \left(1 + \frac{m_\pi}{m}\right) a^- = \frac{8\pi f^2}{m_\pi[1 - (m_\pi^2/4m^2)]} + 4\pi\, m_\pi\, J^-. \tag{2}$$

$$J^- = \frac{1}{2\pi^2} \int_0^\infty \frac{\sigma^-(k)}{\omega}\, dk; \qquad \omega = \sqrt{m_\pi^2 + k^2}. \tag{3}$$

k=pion lab. momentum, a^- = S-wave isovector scattering length.

A recent determination[4] led to $J^- = (-1.083 \pm 0.025)$ mb for the slowly convergent integral. Previous results lie within the errors. If we use this value, the GMO sum rule reads for a^- in units m_π^{-1}

$$f^2 = 0.5712\, a^- + 0.0269 \qquad \text{or} \qquad a^- = 1.751\, f^2 - 0.0471. \tag{4}$$

The same authors also have determined πN S-wave scattering lengths from the pionic deuterium experiment combined with the results from pionic hydrogen[4]. The preliminary

Table 1. S-wave scattering lengths in units m_π^{-1} and f_c^2

a_-	a_+	a^-	a^+	f_c^2	
0.0883	−0.0923	0.0903	−0.0020	0.0786 ± 0.0008	Ericson et al.[4]
0.083	−0.101	0.091	−0.0097	0.079 ± 0.002	KH80

values given in Table 1 follow if charge symmetry ($a_{\pi^+p} = a_{\pi^-n}$) is assumed. f_c^2 belongs to $g_c^2/4\pi = 14.20$. The index c refers to the charged coupling constant. I have calculated a_+ from $2a^+ - a_-$.

A remark on the deviations of the first line from the results given in Ref.[5]: A.W. Thomas is one of the authors of Ref.[4]. In Ref.[5] an earlier article by A.W. Thomas and R.H. Landau(1980) was used.

It is seen that the some results from KH80 are near to the new values. a_+ and a^+ depended on the π^+p data of Bertin et al., which were omitted in all more recent analyses.

The above value for a_+ is in contradiction to $a_+ = -0.077 \pm 0.003$ obtained in Refs.[6,7] from analyses of meson factory data below $T_\pi = 100\,MeV$.

As mentioned above, the GMO sum rule is valid for a^- as defined from $\pi^\pm p$ scattering lengths. *Only if isospin invariance is assumed,* a^- is equal to $-a_0/\sqrt{2}$, where a_0 is the S-wave scattering length for charge-exchange scattering. Then one can also include a^- as determined from inverse pion photoproduction[8,9] and from the line width in pionic hydrogen[5]: $a_0 = (-0.128 \pm 0.006)$ gives $a^- = (0.0905 \pm 0.004)$. So isospin breaking lies within the present errors. An important new information will follow from the final result of the πN charge-exchange experiment at 10 to 40 MeV of D. Isenhower et al. at LAMPF[16]

In the literature one can find a number of papers, in which the authors used *empirical models* for an extrapolation of charge-exchange data to threshold. I think that the results can be ignored, because they disagree with dispersive calculations[11].

It would be of interest to reconsider a question raised by D.V. Bugg and others a long time ago: is it justified to neglect the Coulomb barrier corrections to πN total cross sections above $600\,MeV/c$?

The unsubtracted fixed-t Dispersion Relation for $C^-(\nu, t)$

The GMO sum rule shows that the Born term is about 3 times larger than the dispersion integral. One can use the same ImC^- as in the sum rule for a dispersive calculation of $ReC^-(\omega, t = 0)$ in an energy interval in which the decreasing Born term is large enough. This is related to Ref.[12]. We have started to study the discrepancies with real parts which follow at $t = 0$ (up to a sign) from charge-exchange forward cross sections and from phase shift analyses, where one can also use $t < 0$. A question is, if discrepancies can be reduced by a change of f^2. The calculation will be helpful for a discussion of contradictory meson factory data.

The Hüper Plot

It is known for a long time that the amplitudes $B_\pm$ and B^+ are well suited for a determination of f^2, because the Born term remains comparable with the real part in the region of the higher resonances. I suggested to R. Hüper to make a plot in analogy to the Salzmann-Schnitzer plot for the forward amplitudes $C_\pm$, because it gives more information than a plot for B^+. If a partial wave analysis is compatible with fixed-t analyticity, one obtains a straight line, whose intersection with the ordinate gives the value of f^2(see e. g. Refs.[10]). In the 2nd paper I showed a 'modified Hüper plot' which follows from a rotation of the straight line to a line parallel to the abscissa. This has the advantage that one can choose the scale of the ordinate such that small deviations from fixed-t analyticity and their effect on the uncertainty of f^2 on a level of 1 % can be seen directly. One should note that a best fit in the original plot is not a best fit in the rotated plot.

One problem of the evaluation is that for $t < 0$, $ImB(\nu, t)$ is needed in the unphysical region from threshold ($s = (m + m_\pi)^2$) to the hyperbola for backward scattering. The partial wave expansion converges up to about $t = -0.5\,GeV^2$. But some partial waves, which are negligible in the physical region, give important contributions in the unphysical region, if $\cos\theta$ has large negative values. This enhancement is due to a property of the Legendre Polynomials. For calculations in the unphysical region we have used dispersive methods described in Ref.[11].

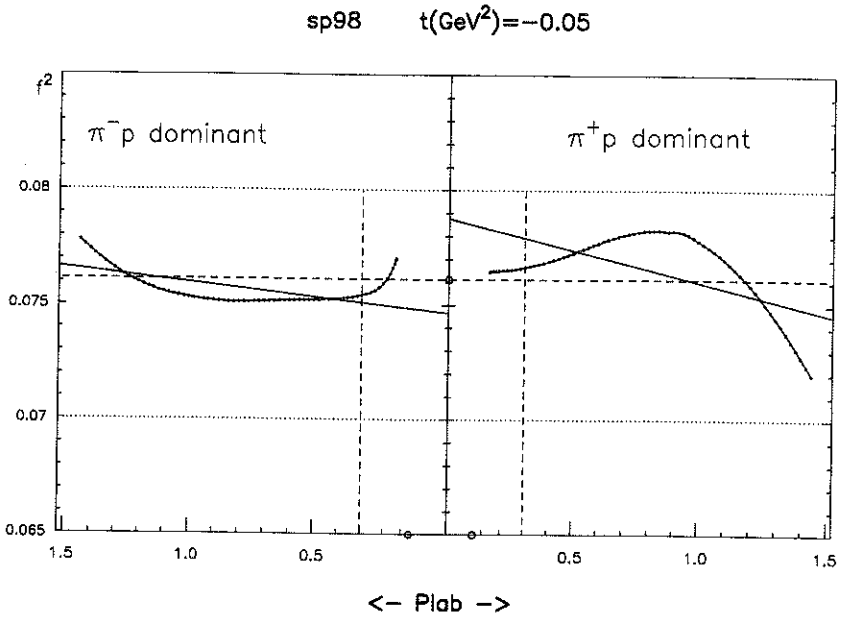

Figure. 1. Modified Hüper plot. Rotated fits made in the original Hüper plot. Over all points: horizontal dashed line, over the left and right hand parts separately: solid lines. Input from KA84: from 2.2 to 6.0 GeV/c. The discrepancies are larger at $t = 0$ and much smaller at $t = -0.1\,GeV^2$.

A second problem is that the input for the imaginary parts at very high energies is not well known. But a correction cannot cancel structures in the plot at low energies, because it will always be slowly variable in this region.

The Salzmann-Schnitzer Plot

A new evaluation of this plot has been made by J. Stahov[12]. The method starts with a combination of once subtracted dispersion relations for the $\pi^{\pm}p$ forward amplitudes C. $ImC_{\pm}(\omega) = plab \cdot \sigma_{\pm}$ follows from a fit to data for hadronic total cross sections (or at low momenta from a partial wave solution). $ReC_{\pm}$ can be determined from experiments in the Coulomb-nuclear interference region. Since most of these data were measured at high energies (up to about $300\,GeV$) and only a few of them at low energies and in the resonance region, most of the real parts were taken from partial wave analyses.

If the input is compatible with fixed-t analyticity, the plot leads to a straight line. The intersection with the ordinate and the slope give a^+ and a^-, respectively. f^2 enters only insofar as the subtracted relation for C^- is valid only if the parameters a^- and f^2 fulfill the GMO sum rule.

If a modified version is introduced by transforming the straight line into a horizontal position, the sensitivity to discrepancies becomes much better. The figures belonging to the solution SM95 in Ref.[12] show strong deviations from fixed-t analyticity and smaller ones in the energy range where the constraint has been approximately enforced.

Interior Dispersion Relations

These dispersion relations are a special case of dispersion relations along hyperbolas studied by Hite and Steiner and others in the early 70's. The hyperbolas pass the

πN threshold and run along a constant value of the scattering angle in the Lab, so they remain in the physical region of the s-channel. Below threshold, they have an intersection with the line for the Born term, which can be used for a determination of f^2[13].

The l.h. cut (also called t-channel cut) starts at $t = 4m_\pi^2$. In addition to the threshold singularity there is a logarithmic singularity at $3.98\,m_\pi^2$. A correct treatment uses an expansion in t-channel partial waves, a procedure applied in all calculations of our group. J. Stahov et al.[15] described a determination of f^2 by a method of this type for KA84 and SM90 for different values of the fixed lab. scattering angle.

Other authors, e. g. in Ref.[14], used the discrepancy function method, which is not suitable in the present case because of the complicated nearby singularities.

Conclusions

1) The most accurate determinations of the πNN coupling constant from results of $\pi N \to \pi N$ scattering experiments follow from dispersive methods, if integrals in unphysical regions and high energy contributions are carefully treated.

2) Since small deviations from analyticity can have large effects, it is useful to work with the *modified plots* described above. These plots give a realistic information on the uncertainties.

3) Parts of the uncertainties can be estimated by calculating f^2 from fixed-t dispersion relations at different values of t.

4) Results derived from partial wave analyses have errors which cannot be treated by statistical methods, because the input includes contradictory data sets. Then a cooperation with experimentalists is more helpful than an application of statistical criteria.

Thanks

I am grateful to A. Badertscher, T.O.E. Ericson and B. Loiseau for discussions and for information on their new results. Discussions with R.A. Arndt, M.M. Pavan, M. Sainio and J. Stahov were useful for this work. I also thank P. Kroll for his detailed comments on points related to the determination of f^2 from NN-scattering. C. Hansch was so kind to write the program for the plot.

REFERENCES

1. R. Oehme, πN Newsletter **7**, 1 (1992)
2. W. Grein and P. Kroll, Nucl. Phys. **A377**, 505 (1982); R. Jakob and P. Kroll, Z. Phys. **A344**, (1992)
3. M.L. Goldberger et al., Phys. Rev. **99**, 986 (1955)
4. T.E.O. Ericson, B.Loiseau, A.W. Thomas, preprint, PANIC-99 and contribution by B. Loiseau to this Symposium.
5. H.-Ch. Schröder et al., ETHZ-IPP PE-99-07 (July 1999), subm. to Phys. Lett. B.
6. N. Fettes and E. Matsinos, Phys. Rev. **C55**, 464 (1997)
7. E. Matsinos. Phys. Rev. **C56**,3014 (1997)
8. M.A. Kovash, TRIUMF E643 collaboration, πN Newsletter **12**, 51 (1997)
9. O. Hanstein et al., πN Newsletter **12**, 56 (1997)
10. G. Höhler, πN Newsletter **3**, 66 (1991) and **6**, 162 (1996)162
11. R. Koch, Z. Physik **C29**, 597 (1985); Nucl. Phys. **A448**, 707 (1986)
12. J. Stahov, πN Newsletter **13**, 174 (1997)
13. G.E. Hite et al., Phys. Rev. **D12**, 2677 (1975)
14. W.B. Kaufmann et al., πN Newsletter **13**, 16 (1997)
15. J. Stahov et al., πN Newsletter **6**, 91 (1992)
16. D. Isenhower, contribution to this Symposium.

Determination of the πNN Coupling Constant in the VPI/GW πN$\rightarrow\pi$N Partial-Wave and Dispersion Relation Analysis

M.M. Pavan *
Lab for Nuclear Science, M.I.T., Cambridge, MA 02139
R.A. Arndt †
Dept. of Physics, Virginia Polytechnic and State University, Blacksburg, VA 24061
I.I. Strakovsky and R.L. Workman
Dept. of Physics, The George Washington University, Washington, D.C. 20052

Abstract

We outline our extraction of the charged pion-nucleon coupling constant from πp elastic scattering data. A partial wave analysis (T_π < 2100 MeV) is performed simultaneously with a fixed-t dispersion relation analysis (T_π < 800 MeV). The coupling constant $g^2/4\pi$ is searched to find the best fit. The result 13.73±0.01±0.07 (first error statistical, second systematic) is found to be insensitive to database changes and Coulomb barrier corrections, and it satisfies important elements of low energy QCD like the Goldberger-Treiman discrepancy, the Dashen-Weinstein sum rule, and chiral perturbation theory pion photoproduction predictions.

Introduction

The pion nucleon coupling constant $g^2/4\pi$ is an important *input* parameter in low energy QCD and nuclear physics, hence one requires its value to be determined as precisely as possible. For example, deviations from the well known Goldberger-Treiman relation [1] has important implications [2] in low energy QCD. The Dashen-Weinstein sum rule [3] connects g^2 to the ratio of the strange and light quark masses, and using the "textbook" value $g^2/4\pi = 14.3$ [4], it has been argued that the large quark condensate assumption of standard chiral perturbation theory may not be valid so that a "generalized" form of the theory may be required [5]. Even from only these two examples, clearly it is of fundamental importance to pin down this important coupling constant.

Our recent partial wave analyses of πN scattering data (with $T_\pi \leq 2100$ MeV (e.g.[6]) include constraints from a simultaneous fixed-t dispersion relation analysis. Our recent work ("SM99"[7]) adds the forward "derivative" $E^\pm$ dispersion relations and the fixed-t $C^\pm$ dispersion relations to our suite of forward $C^\pm$ and fixed-t $B_\pm$ ("Hüper") dispersion relations. The coupling constant g^2 is treated as an *a priori* unknown parameter. The dispersion relation nucleon pole (Born) term is a well defined quantity, and extracting g^2 from the dispersion relations does not involve extrapolations or interpolations.

Bugg, Carter, and Carter [8] employed the $B^+(t)$ dispersion relation and their own partial wave analysis over the energy range (110, 280MeV) to extract the coupling, obtaining $g^2/4\pi$ =14.3±0.2. The analysis was not *constrained* by dispersion relations, so the value comes solely from the data. This value was subsequently used in the Karlsruhe fixed-t dispersion relation analysis of Pietarinen [10] used to constrain the partial wave solution KH80[4], from which the same coupling constant (14.3) was "extracted" using the "Hüper" dispersion relation. It was not tested whether other values of $g^2/4\pi$ gave better fits.

In this article, our approach to extracting the pion nucleon coupling constant from the πN scattering data is outlined, which involves treating it as a free parameter in fixed-t dispersion relations to be determined by χ^2 minimization. We discuss some important systematic checks that were performed, and close with some conclusions.

Dispersion Relations and the Coupling Constant

The multi-energy partial wave analysis part of our analysis procedure has been described in Ref.[11], to which the interested reader is referred. That part of the analysis has *no* explicit dependence on the coupling constant $g^2/4\pi$ and so will not be discussed here.

*Present address: TRIUMF, Vancouver, B.C. V6T-2A3 ; EMAIL: marcello.pavan@triumf.ca
†Present affiliation: Dept. of Physics, The George Washington University, Washington, D.C. 20052

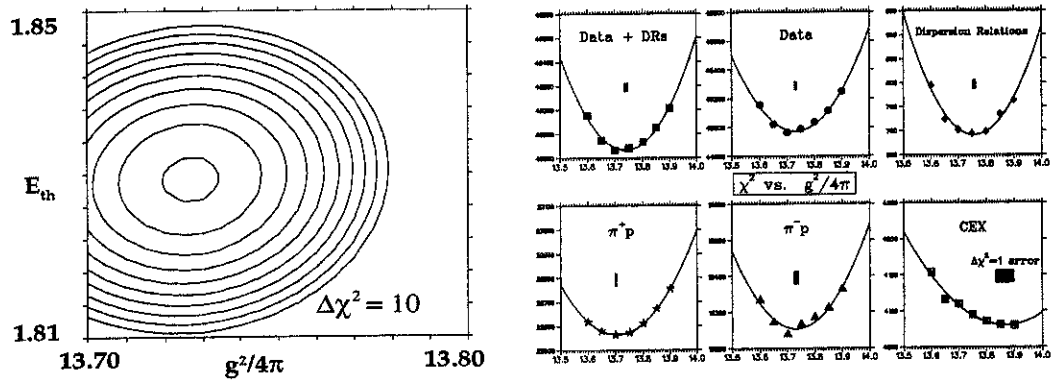

Figure. 1. Left: Total χ^2 contours in the $(E_{th}, g^2/4\pi)$ plane, where E_{th} is the subtraction constant in the forward E^+dispersion relation. The contours were generated from a "grid" of 5x5 solutions of fixed $(E_{th}, g^2/4\pi)$; **Right:** Best-fit χ^2 as a function of $g^2/4\pi$, where all other parameters were fixed to their best fit values. All curves minimize near 13.73. The variation is one indication of the systematic uncertainty in $g^2/4\pi$, while the bars indicate that $\Delta\chi^2$=1 (statistical) uncertainty.

The coupling constant enters into the fixed-t dispersion relations we use as constraints to the partial wave analysis: the forward (t=0) subtracted $C^{\pm}(\omega)$, the derivative subtracted $E^{\pm}(\omega)$, the unsubtracted fixed-t "Hüper" ($B_{\pm}(\nu,t)$) and $C^{+}(\nu,t)$ dispersion relations. These are implemented from $20 < T_\pi < 800$ MeV, and the fixed-t relations over $-0.3 \leq t \leq 0$ GeV^2/c^2. The kinematic range over which the constraints are applied is sufficient for determining the coupling constant since it spans the Δ resonance region which dominates the dispersion integrals, and where the most abundant and precise data sets exist.

A fixed-t dispersion relation relates the real part of the amplitude at some energy to a principal value integral over the imaginary parts at *all* energies, plus a nucleon pole contribution (Born term), and in the case of subtracted relations, an additional energy independent *subtraction constant*. The πNN coupling constant (appearing in the Born term) and the subtraction constants are *a priori* unknown constants, which we treat as *searched parameters* to be determined by minimizing the χ^2 fit to the data *and* dispersion relations. The procedure is as follows: first, the coupling constant and all subtraction constants are fixed, and for each iteration in the analysis, the πN phases are used to determine the principal value integral + Born term + subtraction constant *prediction* for the real part. The real part is then evaluated separately using the phases. The difference "*Re*(from PWA) - *Re*(from DR)" is used to correct the real parts for the next iteration, and to calculate a χ^2 using a prescribed accuracy (adjusted so $\chi^2/pt. \sim 1$) as the "uncertainty". This procedure is iterated until the solution converges to a minimum overall χ^2 (fit to data + dispersion relations). This "best" solution corresponds a *particular set* of dispersion relation parameters. The entire analysis is repeated varying these parameters over a multi-dimensional "grid". Over this grid, the χ^2 versus $g^2/4\pi$ curve is parabolic, and so the parameters for the final solution are determined by fitting quadratics (or bi-quadratics) to these curves and selecting the parameters corresponding to the minimum. This elaborate procedure has the benefit that one is able to define a *statistical* uncertainty for g^2 by the variation which changes the overall χ^2 by 1, and a *systematic* uncertainty from the constancy of g^2 over the applied kinematic range ("extraction error"), and the χ^2 minimum variation from the contributions of the dispersion relations and each scattering channel.

For the coupling constant, two dispersion relations merit special consideration. One is the unsubtracted isoscalar $B^+(\nu,t)$ dispersion relation, which has one unknown parameter, g^2. Bugg, Carter, and Carter [8] used $B^+(\nu,t)$ by inputing in their phase shifts and then "averaging" g^2 over a kinematical range (ν,t) spanning the Δ resonance. This is justified by the dominance of the Δ resonance region in the dispersion integral and the integral's satisfactory convergence with a few GeV cutoff (below which there are abundant data).

The other is the "Hüper" dispersion relation (see Refs.[9] and[4]), which is a clever combination of the invariant B amplitudes such that at fixed t, the relation is linear in

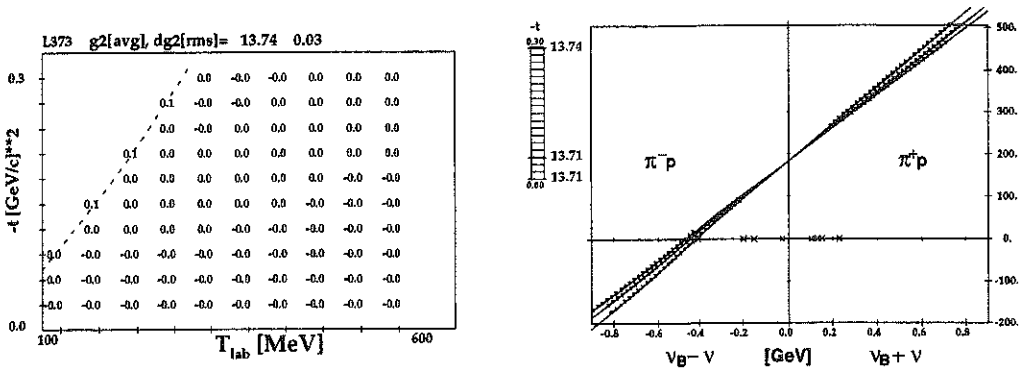

Figure. 2. Left: Results for the B^+ dispersion relation for the solution SM99. At each kinematical point (T_π, t) the deviation from the average coupling constant $g^2/4\pi$ is shown. **Right:** Result for the Hüper dispersion relation at three t values. The y-intercept gives the coupling g^2/M, and the left (right)-hand side of the figure is dominated by $\pi^- p$ ($\pi^+ p$) data.

$\nu_B \pm \nu$ with the intercept equal to g^2/M. Up to several hundred MeV, the dispersion integrals are dominated by the Δ resonance region and suitably convergent with a 4 GeV cutoff when evaluated there. They have the property that due to crossing symmetry, the "left $(\nu_B - \nu)$" ("right $(\nu_B + \nu)$") side is dominated by $\pi^- p$ ($\pi^+ p$) data (see Fig. 2).

Results

Some χ^2 mapping results from our most recent solution (SM99)[7] are shown in Fig. 1. At left are the χ^2 contours of $g^2/4\pi$ versus the forward $E^+(\omega)$ dispersion relation subtraction constant, which are based on 25 (5x5) solutions. Fitting a bi-quadratic to the contours yields $g^2/4\pi = 13.730 \pm 0.009$, where the uncertainty is statistical only ($\Delta\chi^2 = 1$). Similar results are observed when plotting the contours of $g^2/4\pi$ versus the scattering lengths.

The statistical uncertainty from the χ^2 mappings is clearly much smaller than the overall uncertainty. To estimate the systematic uncertainty, the one-dimensional curves of χ^2 versus $g^2/4\pi$ are plotted for each scattering channel, their sum, and the dispersion relation contributions separately (see Fig. 1). One sees that all charge channels minimize near 13.73 (13.70, 13.73, 13.88 for π^+, π^-,and CEX respectively) as well as the dispersion relation contribution (13.76). This spread gives one indication of the systematic uncertainty.

Another indication of the systematic uncertainty in g^2 comes from the fluctuations in its evaluation at various (ν,t) in the $B^+(\nu\, t)$ and Hüper dispersion relations (Fig. 2). The energy and t-dependence is almost negligible ± 0.03 (0.2%) over the full constraint range up to 800 MeV. This "extraction" uncertainty comes from the variations seen in Fig.2.

Systematic Checks

A number of checks were made in order to gauge additional systematic effects. A partial wave analysis solution was generated with *no dispersion relation constraints whatsoever* and the resulting amplitudes used in the dispersion relations to extract $g^2/4\pi$, an approach analogous to that used in Ref.[8]. This was done to see if the dispersion relation constraints were "pulling" g^2 away from a value preferred by the data, but this is *not* the case. The dispersion relation-free solution yields $g^2/4\pi = 13.66 \pm 0.18$ (1.3%) from the $B^+(\nu\, t)$ (see Fig.3), and 13.66 ± 0.07 from the Hüper dispersion relation (not shown). Interestingly, up to ~500 MeV *all* the fixed-t dispersion relations are reasonably well satisfied, indicating that the low/intermediate energy scattering data exhibit the expected analytic properties, so applying dispersion relation constraints "fine tunes" the amplitudes and does not drastically alter them from their unconstrained state.

The dispersion relations must use amplitudes from which all Coulomb contributions have been removed (i.e. "hadronic amplitudes"). Our direct Coulomb and Coulomb phase rotation prescription comes from the Nordita analysis[13] which was used in the KH80 solution[4]. Our simple prescription for the Coulomb barrier correction has been criticized

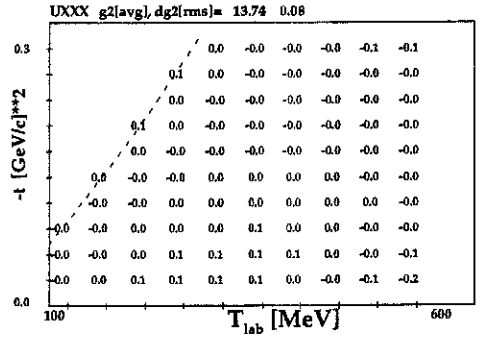

Figure. 3. Results for the B^+ dispersion relation for a solution where NO dispersion relation constraints were used. The result $g^2/4\pi = 13.74 \pm 0.08$ is consistent with the best fit value (Fig. 1).

(see e.g. [14]). To test its effect on the coupling constant extraction, a solution was generated *ignoring it altogether*. The coupling was found to be 13.70, varying from ~13.45 for π^+p to 13.72 for π^-p and 13.67 for charge exchange. Our Coulomb barrier correction is more accurate than ignoring it altogether, so its effect on the systematic uncertainty clearly does not dominate the other aforementioned effects.

The effect of the Coulomb barrier correction on the Hüper dispersion relation was investigated by reintroducing the correction into the hadronic amplitudes before the calculation. The result is shown in Fig. 4. This figure shows that since the plot is dominated by π^+p (π^-p) data on the right (left) hand side, the effect is to "rotate" the line around the intercept, hence leaving the coupling constant relatively unchanged (13.55 *vs.* 13.73). Clearly this insensitivity to the Coulomb correction makes the Hüper dispersion relation valuable for determining the coupling constant.

Another source of systematic uncertainty comes from the elastic pion proton scattering database. We constructed a solution where the total cross section data of Pedroni, et al.[15], were removed, and one where the total cross section data of Carter, et al.[16], the total CEX reaction cross section data of Bugg, et al.[18], and the differential $\pi^\pm p$ differential cross section data of Bussey, et al.[17] were removed. We found only a small change of about ± 0.04. It's clear that the effect of a number of fixed-t dispersion relation constraints and many data sets (differential and total cross sections, and polarization) reduces the sensitivity to any single measurement. We constructed yet another solution where *all* charge exchange data were removed from the database, which resulted in a best fit coupling of 13.65, only 0.6% lower than the nominal value. These results are consistent with our experience of analyzing the $\pi^\pm p$ scattering data over the years, where many new data have entered the database, and many solutions were attempted accepting some and deleting other data sets. Such changes never caused a large change in $g^2/4\pi$.

Concluding Remarks

We have outlined our approach to extracting the pion nucleon coupling constant $g^2/4\pi$ from the πN elastic scattering database using fixed-t dispersion relations. Our most recent preliminary analysis (SM99) yields $g^2/4\pi = 13.73 \pm 0.01 \pm 0.07$, where the first uncertainty is statistical ($\Delta\chi^2 = 1$) and the second is systematic. We have described the checks we made to estimate the latter, and found that the variations in the χ^2 minima for each charge channel and the dispersion relations (Fig.1) dominates.

The result $g^2/4\pi = 13.73$ is consistent with expectations of the Goldberger-Treiman discrepancy ([1],[2]) and with the Dashen-Weinstein sum rule (plus some higher order corrections) [19,3], while they are not consistent with the larger coupling 14.3. Recent measurements of threshold pion photoproduction are also more consistently described in chiral perturbation theory with the smaller coupling than the larger[20]. Along with other recent determinations arriving at a lower coupling constant (see review[21]), we believe that since important aspects of low energy QCD are more consistently described with $g^2/4\pi \simeq 13.7$ than 14.3, it is sensible to adopt a value near 13.7 as the current standard.

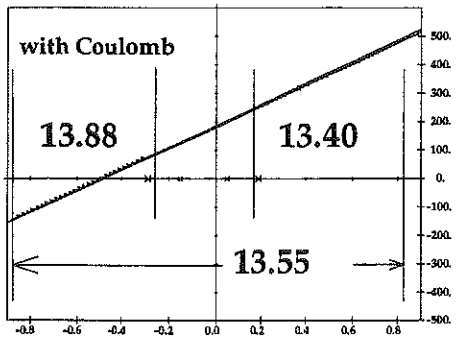

Figure. 4. Hüper dispersion relation at $t = -0.15$ GeV^2/c^2, with the Coulomb barrier correction *reintroduced* into the amplitudes. The amplitudes are enhanced on one side and suppressed on the other, such that the intercept (g^2/M) changes little (13.55 *vs.* 13.73). This "pivoting" around the y-intercept shows that this dispersion relation is *insensitive* to the Coulomb barrier correction.

Acknowledgements

We gratefully acknowledge a contract from Jefferson Lab under which this work was done. The Thomas Jefferson National Accelerator Facility (Jefferson Lab) is operated by the Southeastern Universities Research Association (SURA) under DOE contract DE-AC05-84ER40150. MMP thanks A. Badertscher and GWU for their support.

REFERENCES

1. M.L. Goldberger and S.B. Treiman, Phys. Rev. **110** (1958) 1178.
2. C.A. Dominguez, Riv. Nuovo Cimento. **8** (1985) 1.
3. R. Dashen and M. Weinstein, Phys. Rev. **188** (1969) 2330.
4. R. Koch and E. Pietarinen, Nucl. Phys. **A336** (1980) 331.
5. N.H. Fuchs, H. Sazdjian, and J. Stern, Phys. Lett. **B238** (1990) 380.
6. R. Arndt, I. Strakovsky, R. Workman, and M.M. Pavan, Phys. Rev. C**52** (1995) 2120.
7. R.A. Arndt, I.I. Strakovsky, R.L.Workman, and M.M. Pavan, Los Alamos preprint nucl-th/9807087; and in progress.
8. D.V. Bugg, A.A. Carter, and J.R. Carter, Phys. Lett. **44B** (1973) 278.
9. G. Höhler, in *Pion-Nucleon Scattering*, edited by H. Schopper, Landolt-Börnstein, Vol. I/9b (Springer, New York) 1983.
10. E. Pietarinen, Nucl. Phys. **B107**, (1976) 21.
11. Solution "SM95": see Ref.[6] ; "FA93": R. A. Arndt, R. L. Workman, and M. M. Pavan, Phys. Rev. **C49**, 2729 (1994) ; "SM90" : R.A. Arndt, Z. Li, L.D. Roper, R.L. Workman, and J. Ford, Phys. Rev. D**43** (1991) 2131.
12. Our preliminary solution SM99 can be accessed via TELNET or SSH (username: said@said.phys.vt.edu) , or at: http://said.phys.vt.edu/analysis/pin_analysis.html.
13. B. Tromborg, S. Waldenstrom, and I. Overbo, Phys. Rev. D**3** (1977) 725.
14. D.V. Bugg, in πN Newsletter No.8, Proceedings of the 5^{th} International Symposium on Meson-Nucleon Physics and the Structure of the Nucleon, Vol. 1, Boulder, Colorado, U.S.A. 1993, eds. by G. Höhler, W. Kluge, B.M.K. Nefkens, 1993, page 1.
15. E. Pedroni, et al., Nucl. Phys. A**300** (1978) 321.
16. A.A. Carter, et al., Nucl. Phys. B**26** (1971) 445.
17. P.J. Bussey, et al., Nucl. Phys. B**58** (1973) 363.
18. D.V. Bugg, et al., Nucl. Phys. B**26** (1971) 588.
19. J.L. Goity, et al., Los Alamos preprint hep-ph/9901374.
20. A.M. Bernstein and N. Kaiser, in Proceedings of the Second Chiral Dynamics: Theory and Experiment Workshop, Mainz, Germany 1997, eds. by A.M. Bernstein, D. Drechsel, and T. Walcher, Springer Lecture Notes in Physics, 1998, page 189 ; also H. Ströher, talk given at the above workshop, and private communication.
21. J.J. deSwart, M.C.M. Rentmeester, and R.G.E. Timmermans, in πN Newsletter No. 13, Proceedings of the 7^{th} International Symposium on Meson-Nucleon Physics and the Structure of the Nucleon, Vancouver, Canada 1997, eds. by D. Drechsel, G. Höhler, W. Kluge, H. Leutwyler, B.M.K. Nefkens, and H.-M. Staudenmaier, 1997, page 89.

Report of Working Group on Electromagnetic Corrections

A. Rusetsky
Institute for Theoretical Physics, University of Bern, Sidlerstrasse 5, CH-3012, Bern, Switzerland,
Bogoliubov Laboratory of Theoretical Physics, Joint Institute for Nuclear Research, 141980 Dubna, Russia and
HEPI, Tbilisi State University, 380086 Tbilisi, Georgia

Abstract

The talks delivered by M. Knecht, H. Neufeld, V.E. Lyubovitskij, A. Rusetsky and J. Soto during the session of the working group of electromagnetic corrections to hadronic processes at the Eight International Symposium MENU99, cover a wide range of problems. In particular, those include: construction of the effective Lagrangians that then are used for the evaluation of electromagnetic corrections to the decays of K mesons; evaluation of some of the low-energy constants in these Lagrangians, using sum rules and the large-N_c arguments; complete calculations of electromagnetic corrections to the $\pi\pi$ scattering amplitude at $O(e^2p^2)$; the general theory of electromagnetic bound states in the Standard Model.

The problem of unique disentangling of strong and electromagnetic interactions in hadronic transitions has been a long-standing challenge for theorists. All data obtained in high-energy physics experiments, contain a highly nontrivial interplay of strong and electromagnetic effects, with a huge difference in the interaction ranges. In addition, there are the isospin-breaking effects caused by the difference in quark masses that generally has a non-electromagnetic origin. In the analysis of the experimental data, however, one would prefer to unambiguously subtract all isospin-breaking corrections from the hadronic characteristics in order to obtain the quantities defined in "pure QCD", at equal quark masses – the case where the most of the theoretical predictions are done.

In the context of πN scattering problem, the issue of the electromagnetic corrections has been extensively studied by using the dispersion relations[1], and the potential model[2]. The closely related problem of electromagnetic corrections to the energy-level shift and decay width to the pionic hydrogen and pionic deuterium was analyzed again by using the potential model[3]. Both above approaches are based upon the certain assumptions about the precise mechanism of incorporation of electromagnetic effects in the strong sector, provided that the details of strong interactions are unknown. It remains, however, unclear, how to estimate the systematic error caused by these assumptions or, in other words, how to consistently include within these approaches all isospin-breaking effects which are present in the Standard Model. Given the fact, that the above approaches are used for the partial-wave analysis of πN scattering data and the measurements of $\pi^- p$, $\pi^- d$ atom characteristics that result in the independent determinations of values of the S-wave πN scattering lengths, the consistent treatment of the isospin-breaking effects might be helpful for understanding the discrepancies between the results of different analyses.

Further, the problem of the systematic treatment of electromagnetic corrections is crucial for the analysis of experimental data on the decays of K mesons. In particular, the study of K_{l4} decays that at present time is performed by E865 collaboration at BNL[4], and by KLOE at DAΦNE facility (LNF-INFN)[5], will enable one to measure the parameters of the low-energy $\pi\pi$ interaction and thus provide an extremely valuable information about the nature of strong interactions at low energy. Preliminary results[4] are so far obtained in the negligence of the electromagnetic effects which might significantly affect the amplitudes in the threshold region.

Last but not least, a complete inclusion of electromagnetic corrections is needed in order to fully exploit the high-precision data on hadronic atoms provided by the DIRAC collaboration at CERN ($\pi^+\pi^-$), DEAR collaboration at DAΦNE (K^-p, K^-d) , by the experiments at PSI ($\pi^- p$, $\pi^- d$), KEK ($K^- p$), etc. These experiments, that allow for the direct determination of the hadronic scattering lengths from the measured characteristics of hadronic atoms: level energies and decay widths, contribute significantly to our knowledge of the properties of QCD in the low-energy regime. In particular, the measurement of

the difference of the S-wave $\pi\pi$ scattering lengths $a_0 - a_2$ by the DIRAC experiment will allow one to distinguish between the large/small condensate scenarios of chiral symmetry breaking in QCD: should it turn out that the measured value of $a_0 - a_2$ differs from the prediction of standard ChPT[6], one has to conclude that the symmetry breaking in QCD proceeds differently[7] from the standard picture. Further, the πN scattering length a_{0+}^- that is measured by the experiments on pionic hydrogen and pionic deuterium, can be used as an input to determine the πNN coupling constant, and from the precise knowledge of KN scattering lengths one might extract the new information about e.g. the kaon-sigma term and the strangeness content of the nucleon.

According to the modern point of view, the low-energy interactions of Goldstone bosons (pions, kaons...) in QCD can be consistently described by using the language of effective chiral Lagrangians. The amplitudes of the processes involving these particles below ~ 1 GeV can be systematically expanded in series over the external momenta of Goldstone particles and light quark masses. All nonperturbative QCD dynamics is than contained in the so-called low-energy constants of the effective Lagrangian, and only a finite number of those contribute at a given order in this expansion. These constants should be, in principle, calculable from QCD. However, at the present stage they are considered to be free parameters to be determined from the fit to the experimental data[6–8]. The approach can be generalized to the sector with baryon number equal to 1 or 2[9,10]. Moreover, the approach allows for the systematic inclusion of electromagnetic interactions – albeit at the cost of the increased number of low-energy constants in the effective Lagrangian[11–13]. These new "electromagnetic" low-energy constants describe the high-energy processes corresponding to the direct interaction of quarks with photons, and thus contribute the missing piece to the potential-type models – in the latter, generally, only the long-range part of the electromagnetic interactions, corresponding to the photon exchange between different hadrons, is taken into account. From the size of the effect coming from the "electromagnetic" low-energy constants, along with other missing sources of electromagnetic corrections (see below), one can therefore have a judgment on the systematic error caused by the choice of the potential-type models.

From the above, it seems that the most nontrivial task that one encounters in the systematic treatment of the electromagnetic interactions in the low-energy hadronic processes, is related to the determination of the precise values of the "electromagnetic" low-energy constants in the effective low-energy Lagrangians that, at the present time, are rather poorly known. Different methods have been used to this end so far. The resonance saturation method was used[14] to evaluate these constants in the $O(e^2p^2)$ Lagrangian with Goldsone bosons. Further, in Ref.[15] it was demonstrated that these constants can be expressed as a convolution of a QCD correlation function with the photon propagator, plus a contribution from the QED counterterms. The sum rules were then used to evaluate these constants[15]. Somewhat different approach to the calculation of these constants was used in[16]. The results of these approaches do not all agree. One important lesson, however, can be immediately drawn: since these low-energy constants turn out to be dependent on the QCD scale μ_0 that should be introduced in the QCD Lagrangian after taking into account the electromagnetic corrections[15,16], the naive separation of the isospin-breaking effects into the "electromagnetic" and "strong" parts, the latter corresponding to the difference of quark masses, does not hold in general and can be carried out only in certain observables at a certain chiral order. Generally, both these parts are dependent on QCD scale μ_0 that then cancels in the sum. For this reason, hereafter, we would prefer to speak about the isospin-breaking corrections to the physical observables, rather then consider individual contributions to it.

The session of the working group of electromagnetic corrections at MENU99 symposium was designed to cover all important steps of the treatment of isospin-breaking corrections on the basis of modern effective theories: starting from the construction of the effective Lagrangians containing non-QCD degrees of freedom – photons and leptons, and from the examples of the determination of some of the non-QCD low-energy constants, using sum rules and large N_c arguments, to the actual application of the framework to the calculation of physical quantities: P_{l2} and $P \to \ell^+\ell^-$ decay rates, $\pi\pi$ scattering amplitudes, as well as

observables of $\pi^+\pi^-$ and π^-p hadronic atoms – energy levels and decay characteristics.

A construction of a low-energy effective field theory which allows the full treatment of isospin-breaking effects in semileptonic weak interactions, was discussed in the talk of H. Neufeld[17] (see also[13] for more details). In addition to the pseudoscalars and the photon, also the light leptons were included as dynamical degrees of freedom in an appropriate chiral Lagrangian: only within such a framework, one will have full control over all possible isospin breaking effects in the analysis of new high statistics $K_{\ell 4}$ experiments by the E865 and KLOE collaborations. The same methods are also necessary for the interpretation of forthcoming high precision experiments on other semileptonic decays like $K_{\ell 3}$, etc.

The one-loop functional in the presence of leptonic sources was evaluated by using the superheat kernel technique[18]. At next-to-leading order, the list of low-energy constants has to be enlarged as compared to the case of QCD+photons. If only the terms at most quadratic in lepton fields, and at most linear in Fermi coupling G_F are considered, the number of additional low-energy constants X_i, $i = 1 \cdots 7$ is equal to 7. Further, regarding "pure" lepton or photon bilinears as "trivial", only three from the remaining five low-energy constants will contribute to realistic physical processes. One may therefore conclude that the inclusion of virtual leptons in chiral perturbation theory proceeds at a rather moderate cost.

As an immediate application of the formalism, a full set of electromagnetic corrections to P_{l2} decays were calculated. It was demonstrated that, in some specific combinations of widths of different decay processes, the "new" low-energy constants cancel, thus leading to the predictions at the one-loop order that do not depend on the parameters X_i. A full calculation of the electromagnetic corrections to the K_{l3}, K_{l4} processes is in progress.

As it is evident, the question of actual evaluation of a large number of low-energy constants lies at a heart of the successful application of the effective Lagrangian approach. In the talk by M. Knecht, the evaluation of one of such low-energy constants that contributes to the decays of pseudoscalars into lepton pairs, was given on the basis of sum rules and large N_c arguments (for more details, see[19]). In the large N_c limit, the QCD spectrum consists of a tower of infinitely narrow resonances in each channel. Employing further the so-called Lowest Meson Dominance (LDM) approximation that implies the truncation of the infinite sum over resonances in the sum rules, one can relate the low-energy constants to the known parameters of the low-lying resonances. It was demonstrated that using the value of the particular low-energy constant determined in the LDM approximation leads to the values of ratio of branching ratios $Br(P \to \ell^+\ell^-)/Br(P \to \gamma\gamma)$ for the processes $\pi^0 \to e^+e^-$ and $\eta \to \mu^+\mu^-$ that are consistent with the present experimental data. The predictions for the same value in the process $\eta \to e^+e^-$ were also given.

As another application of the effective theories, in the talk by M. Knecht[20] (see also[21]) a complete calculation of the electromagnetic corrections to the $\pi^0\pi^0 \to \pi^0\pi^0$ and $\pi^+\pi^- \to \pi^0\pi^0$ scattering amplitudes at $O(e^2p^2)$ has been performed. The latter case is particularly interesting since the the results can be directly translated into the corrections to the decay width of the $\pi^+\pi^-$ atom. It turns out that the size of isospin-breaking corrections to the $\pi\pi$ scattering amplitudes is of the same order of magnitude that the two-loop strong corrections and, therefore, can not be neglected.

Bound states of hadrons in chiral effective theories – hadronic atoms – were considered in the talks by J. Soto, V. Lyubovitskij and A. Rusetsky[22–24]. It was demonstrated that, a systematic evaluation of isospin-breaking corrections to the observable characteristics of this sort of bound systems is possible order by order in ChPT. To this end, a nonrelativistic effective Lagrangian approach was used, that provides the necessary bridge between the bound-state characteristics and the scattering S-matrix elements in a most elegant and economical manner: at the end, according to the matching condition of relativistic and nonrelativistic theories, these characteristics are expressed in terms of the scattering matrix elements calculated in the relativistic theory, and to the latter one can apply the conventional machinery of ChPT.

The talk by J. Soto[22] (details – in Ref.[25]) was focused on the foundations of the nonrelativistic effective Lagrangian approach as applied to the $\pi^+\pi^-$ atom decay problem.

Different scales relevant for the problem of interest have been thoroughly discussed and disentangled. It has been demonstrated that, matching the parameters of the nonrelativistic Lagrangian to the relativistic theory, it is possible to evaluate the decay width of the $\pi^+\pi^-$ atom order by order in ChPT.

The nonrelativistic effective Lagrangian approach was applied to the $\pi^+\pi^-$ atom decay problem as well in the talk by V. Lyubovitskij[23] (see[26] for more details). It was demonstrated, however, that employing the different technique for matching of relativistic and nonrelativistic theories, it is possible to obtain the general expression for the decay width of the $\pi^+\pi^-$ atom in the first nonleading order in isospin breaking, without an explicit use of chiral expansion – that is, the result is valid in all orders in ChPT. At order $O(e^2p^2)$ in ChPT, one may use the results of calculations by Knecht and Urech[21] – in this manner, it was demonstrated that the one-loop corrections to the decay width are rather small, including the uncertainty coming from the "strong" and "electromagnetic" low-energy constants. The bulk of total correction is given already by the tree-level diagram that is free from this uncertainty. The results given in the talk by V. Lyubovitskij, finalize the treatment of the $\pi^+\pi^-$ atom decay problem: the width is now known to a sufficient accuracy that allows one to fully exploit the future precision data from DIRAC experiment at CERN.

In the talk by A. Rusetsky[24] the nonrelativistic effective Lagrangian approach was applied to the calculation of the energy of the ground state of the π^-p atom. At this example, one can fully acknowledge the might and flexibility of the nonrelativistic approach: the spin-dependent part of the problem trivializes, and the treatment proceeds very similarly to the case of the $\pi^+\pi^-$ atom. However, the isospin-breaking piece of the relativistic scattering amplitude in the π^-p case already at the tree level (order p^2) contains both "strong" and "electromagnetic" low-energy constants. This part of the isospin-symmetry breaking effect is missing in the potential model[3]. From the explicit expression of the π^-p scattering amplitude at $O(p^2)$, one can immediately identify two distinct sources of isospin-breaking corrections that are not present in the potential model. The terms that depend on the quark masses in the strong part of the π^-p amplitude, contribute to the isospin-breaking piece – this contribution is proportional to charged and neutral pion mass difference. In addition, the direct quark-photon interaction that is encoded in the "electromagnetic" low-energy constants, also contributes to the isospin breaking. Uncertainty introduced by the poor knowledge of these low-energy constants is, unlike the $\pi^+\pi^-$ case, much larger as compared to the estimate based on the potential model – thus, the latter considerably underestimates the systematic error in the analysis of the pionic hydrogen data provided by the experiment at PSI.

To summarize, I shall briefly dwell on the developments that are foreseen in the nearest future.

- A complete treatment of the isospin-breaking corrections to K_{l3} and K_{l4} decays on the basis of modern effective field theories that are now in progress, is of a great importance for the analysis of precision data samples from E865 (BNL) and KLOE (LNF-INFN) experiments.
- For the systematic treatment of the isospin-breaking corrections, the knowledge of the precise values of the low-energy constants that enter the effective Lagrangian, is necessary. In particular, this concerns the values of "electromagnetic" low-energy constants which are poorly known. Activities based on sum rules, resonance saturation models, etc. may provide an extremely useful information in this respect.
- At present, the problem of $\pi^+\pi^-$ atom decay is completely understood, both conceptually and numerically. The expected high-precision data from DIRAC experiment, therefore, can be used to determine the difference of the $\pi\pi$ S-wave scattering lengths $a_0 - a_2$ quite accurately. In the contrary, the issue of the isospin-breaking corrections to the observables of pionic hydrogen (and pionic deuterium) needs to be further investigated. The uncertainty due to the poor knowledge of low-energy constants in the isospin-breaking part of the πN scattering amplitude is large already at tree level, and the evaluation of one-loop contributions are in progress. These studies will be even more important for the future improved experiment at PSI[27] that intends to measure the S-wave πN scatter-

ing lengths, using the data from the pionic hydrogen alone. A detailed investigation of the properties of the kaonic atoms which will be studied by the DEAR collaboration at DAΦNE, is planned.

• The success of the nonrelativistic Lagrangian approach to the hadronic atom problem clearly demonstrates that the formalism of the potential model based on Schrödinger-type equations, can be applied to the evaluation of the isospin-breaking corrections, provided the potential contains a full content of isospin-symmetry breaking effects of the Standard Model. Therefore, it will be extremely important to set up a systematic framework for the derivation of the potentials from the effective field-theoretical Lagrangians – then, the already existing machinery of the potential model can be directly exploited.

Acknowledgments. I would like to thank the organizers of MENU99 symposium for their large effort, that created an atmosphere of intense discussions and learning, and J. Gasser for reading the manuscript. This work was supported in part by the Swiss National Science Foundation, and by TMR, BBW-Contract No. 97.0131 and EC-Contract No. ERBFMRX-CT980169 (EURODAΦNE).

REFERENCES

1. B. Tromborg, S. Waldenstrøm, and I. Øverbø, Ann. Phys. **100**, 1 (1976); B. Tromborg and J. Hamilton, Nucl. Phys. **B76**, 483 (1974).
2. A. Gashi, E. Matsinos, G.C. Oades, G. Rasche, and W.S. Woolcock, Preprints hep-ph/9903434, hep-ph/9902224; G. Rasche and W.S. Woolcock, Helv. Phys. Acta **49**, 435 (1976).
3. D. Sigg, A. Badertscher, P.F.A. Goudsmit, H.J. Leisi, and G.C. Oades, Nucl. Phys. **A609**, 310 (1996).
4. S. Pislak, in Proceedings of HadAtom99 Workshop, Bern, Oct. 14-15 (1999), Preprint hep-ph/9911339.
5. P. de Simone, in Proceedings of HadAtom99 Workshop, Bern, Oct. 14-15 (1999), Preprint hep-ph/9911339.
6. J. Gasser and H. Leutwyler, Phys. Lett. **B125**, 325 (1983); J. Bijnens, G. Colangelo, G. Ecker, J. Gasser, and M.E. Sainio, Phys. Lett. **B374**, 210 (1996).
7. M. Knecht, B. Moussallam, J. Stern, and N.H. Fuchs, Nucl. Phys. **B457**, 513 (1995); ibid. **B471**, 445 (1996).
8. J. Gasser and H. Leutwyler, Nucl. Phys. **B250**, 465 (1985).
9. J. Gasser, M.E. Sainio, and A. Svarč, Nucl. Phys. **B307**, 779 (1988); N. Fettes, U.-G. Meissner, and S. Steininger, Nucl. Phys. **A640**, 199 (1998); T. Becher and H. Leutwyler, Eur. Phys. J. C9 (1999) 643.
10. S. Weinberg, Phys. Lett. **B251**, 288 (1990); Nucl. Phys. **B363**, 3 (1991); D.B. Kaplan, M.J. Savage and M.B. Wise, Phys. Lett **B424**, 390 (1998); Nucl. Phys.**B534**, 329 (1998); E. Epelbaoum, W. Glöckle, A. Kruger, and U.-G. Meißner Nucl. Phys. **A645**, 413 (1999).
11. R. Urech, Nucl. Phys. **B433**, 234 (1995).
12. G. Müller and U.-G. Meißner, Nucl. Phys. **B556**, 265 (1999);
13. M. Knecht, H. Neufeld, H. Rupertsberger, and P. Talavera, Preprint hep-ph/9909284.
14. R. Baur and R. Urech, Nucl. Phys. **B499**, 319 (1997).
15. B. Moussallam, Nucl. Phys. **B504**, 381 (1997).
16. J. Bijnens and J. Prades, Nucl. Phys. **B490**, 239 (1997).
17. H. Neufeld, talk at this conference.
18. H. Neufeld, J. Gasser, and G. Ecker, Phys. Lett. **B438**, 106 (1998).
19. M. Knecht, S. Peris, M. Perrottet, and E. de Rafael, Preprint hep-ph/9908283.
20. M. Knecht, talk at this conference.
21. M. Knecht and R. Urech, Nucl. Phys. **B519**, 329 (1998).
22. J. Soto, talk at this conference.
23. V. Lyubovitskij, talk at this conference.
24. A. Rusetsky, talk at this conference.
25. D. Eiras and J. Soto, Preprint hep-ph/9905543.
26. A. Gall, J. Gasser, V.E. Lyubovitskij, and A. Rusetsky, Phys. Lett. **B462**, 335 (1999); J. Gasser, V.E. Lyubovitskij, and A. Rusetsky, Preprint BUTP-99/20, hep-ph/9910438 (Phys. Lett. **B**, in print).
27. D. Gotta, talk at this conference.

Pionium: an Effective Field Theory Approach

D. Eiras, J. Soto *
Departament d'Estructura i Constituents de la Matèria, Universitat de Barcelona
Diagonal 647, 08028 Barcelona, Catalonia, Spain

Abstract

We summarize the main ideas behind a recent model-independent calculation of the energy levels and decay width of pionium, which heavily relies on modern non-relativistic effective field theory techniques. We compare our results with others which have appeared in the literature.

INTRODUCTION

The pion-pion strong scattering lengths are an important input to fix some parameters of the Chiral Lagrangian (χL), the effective field theory of QCD at energies smaller than the rho mass[1]. These are difficult to obtain from the available scattering data, but turn out to be easily extractable from the decay width of pionium, a $\pi^+\pi^-$ atom[2]. The current DIRAC experiment at CERN[3], which plans to measure the pionium decay width at 10% accuracy, has triggered a lot of theoretical effort in order to pin down this object with the same degree of accuracy[4–12].

We have presented in[12] a model-independent approach to pionium which we briefly summarise here. It basically consist of identifying the relevant energy and momentum scales of the $\pi^+\pi^-$ atom, which are discussed in Section 2, and sequentially integrate them out until we reach the lowest relevant scale, namely the binding energy. This is carried out by introducing a series of non-relativistic effective field theories, which are displayed in Section 3, and requiring them to be equivalent at the desired order of accuracy. We present our results in Section 4 and compare them with the ones existing in the literature.

PHYSICAL SCALES

Pionium is an electromagnetic bound state. As such, it contains at least three dynamical scales: the mass of the charged pions $m \sim 140 MeV$, the typical relative momentum in the bound state $m\alpha/2 \sim 0.5 MeV$, and the binding energy $m\alpha^2/4 \sim 2keV$[13]. In addition pionium decays mainly to two neutral pions through the strong interactions, which brings in an additional energy scale $\Delta m \sim 5 MeV$, the difference between the charged and neutral pion masses, and its associated three momentum $s = \sqrt{2m\Delta m} \sim 40 MeV$. In view of these numerical values two important observations are in order:

i) All the scales are considerably smaller than $m \sim 140$ MeV, which implies that a non-relativistic approach should be appropriated.

ii) All the scales, including m, are considerably smaller than the typical hadronic scale, say the rho mass, and hence all the necessary information is contained in the χL coupled to electromagnetism[14]. Since at these energies not only electromagnetism but also the strong interactions are amenable to a perturbative treatment (in α and in Chiral Perturbation Theory (χPT) respectively), pionium can be addressed in a model independent way.

EFFECTIVE FIELD THEORIES

From a fundamental point of view one would like to describe pionium starting from QCD and QED. However, QCD is a strongly coupled theory at low energies which makes difficult to carry out reliable calculations. The χL provides a low energy representation of QCD, where the high energy information of the later is encoded in a few low energy constants. In the language we shall be using below it means that all energy and momentum scales above, say, the rho mass have been integrated out. The χL has the great advantage that it allows to carry out calculations systematically, either using standard χPT[1] or the so called Generalised Chiral Perturbation Theory (GχPT)[15].

*Work supported by the grants CICYT (Spain), contract AEN98-0431, and the CIRIT (Catalonia), contract 1998SGR 00026

Let us then start with the $SU(2) \times SU(2)$ χL coupled to electromagnetism. After integrating out the scale m for pion pairs near threshold we obtain what may be called a Non-relativistic χL (NRχL). The degrees of freedom of NRχL are photons and non-relativistic charged and neutral pion fields. NRχL is analogous to Non-relativistic QED[13], but contains non-relativistic pseudoscalar fields instead of Pauli spinor fields and includes the effect of the strong interactions. Since $\Delta m \gg m\alpha/2$, $m\alpha^2/4$ we can also integrate out this scale and its associated three momentum s (neutral pions). We obtain a second Non-relativistic χL which may be abbreviated as NRχL$'$. Its degrees of freedom are photons and non-relativistic charged pions. The introduction of NRχL$'$ avoids having to solve eventually a coupled channel problem[9,10]. Finally, integrating out photons of energy or momentum of the order $m\alpha/2$ we obtain what may be called potential NRχL$'$ (pNRχL$'$), in analogy of potential NRQED[16]. At the order we are interested in, pNRχL$'$ contains non-relativistic charged pions interacting through a potential (electromagnetic and strong), and it is totally equivalent to a suitable quantum mechanical Hamiltonian.

We enforce that a given EFT is equivalent to the previous one in a particular kinematical region by requiring that the off-shell Green functions in both EFTs are equal at the desired accuracy. Dimensional Regularisation (DR) is used throughout.

NRχL

The zero charge sector of this lagrangian reads

$$\begin{aligned} L &= \pi_+^\dagger(iD_0 + \frac{\mathbf{D}^2}{2m} + \frac{\mathbf{D}^4}{8m^3})\pi_+ + (+ \leftrightarrow -) + \\ &\quad \pi_0^\dagger(i\partial_0 + \Delta m + \frac{\boldsymbol{\nabla}^2}{2m} + \Delta m\frac{\boldsymbol{\nabla}^2}{2m^2} + \frac{\boldsymbol{\nabla}^4}{8m^3})\pi_0 \\ &\quad + R_{00}\pi_0^\dagger\pi_0^\dagger\pi_0\pi_0 + R_{cc}\pi_+^\dagger\pi_-^\dagger\pi_+\pi_- \\ &\quad + (R_{0c}\pi_0^\dagger\pi_0^\dagger\pi_+\pi_- + h.c.) \\ &\quad + S_{00}(\pi_0^\dagger\pi_0^\dagger\pi_0\boldsymbol{\nabla}^2\pi_0 + h.c.) + \\ &\quad S_{cc}\Big(\pi_+^\dagger\pi_-^\dagger(\pi_+\mathbf{D}^2\pi_- + \pi_-\mathbf{D}^2\pi_+) + h.c.\Big) \\ &\quad + S_{0c}\Big(\pi_0^\dagger\pi_0^\dagger(\pi_+\mathbf{D}^2\pi_- + \pi_-\mathbf{D}^2\pi_+) \\ &\qquad + 2\pi_+^\dagger\pi_-^\dagger\pi_0\boldsymbol{\nabla}^2\pi_0 + h.c.\Big) \\ &\quad + P_{00}\pi_0^\dagger\partial_i\pi_0^\dagger\pi_0\partial_i\pi_0 + \\ &\quad P_{cc}(\pi_+^\dagger D_i\pi_-^\dagger\pi_+ D_i\pi_- + \pi_-^\dagger D_i\pi_+^\dagger\pi_- D_i\pi_+) \end{aligned} \tag{1}$$

The maximum size of each term may be estimated by assigning the scale m^n to any unknown constant of dimension n, Δm to the time derivative and s to space derivatives and remaining dimensionful fields. The matching to the χL can be done order by order in χPT (or in GχPT) and in α treating the isospin violating terms, the external three momenta and the residual energies as perturbations. We refer to[12] for a more detailed discussion on how the parameters above depend on those of the χL.

NRχL$'$

The lagrangian reads

$$\begin{aligned} L' &= \pi_+^\dagger(iD_0 + \frac{\mathbf{D}^2}{2m})\pi_+ + \pi_-^\dagger(iD_0 + \frac{\mathbf{D}^2}{2m})\pi_- \\ &\quad + R'_{cc}\pi_+^\dagger\pi_-^\dagger\pi_+\pi_- + P'\pi_+^\dagger\pi_-^\dagger i\partial_0\pi_+\pi_- \end{aligned} \tag{2}$$

and the new constants are related to the old ones by

$$R'_{cc} = R_{cc} - |R_{0c}|^2 R_{00}\,(\tfrac{ms}{2\pi})^2 + i|R_{0c}|^2\tfrac{ms}{2\pi}$$

$$\times\Big(1-\tfrac{1}{8}\tfrac{s^2}{m^2}-\Big(\tfrac{R_{00}ms}{2\pi}\Big)^2-\tfrac{2S_{0c}(R_{0c}+R_{0c}^*)s^2}{|R_{0c}|^2}\Big)$$

$$P'=i|R_{0c}|^2\tfrac{m^2}{4\pi s} \tag{3}$$

The maximum size of each term may be estimated by assigning $m\alpha^2/4$ to the time derivative (this only holds at lower orders in α[16]) and $m\alpha/2$ to the space derivatives and to the dimensionful fields. The matching to NRχL is done by expanding the external momenta and energies. It produces corrections in powers of $\sqrt{2\Delta m/m}$, $E/\Delta m$ and $\mathbf{p}/s$. Since the neutral pion pair is lighter than the charged one, it also produces imaginary parts in the matching coefficients which give rise to the leading order decay width and to some of its corrections.

pNRχL$'$

The lagrangian reads

$$\begin{aligned}L''&=\pi_+^\dagger(\mathbf{x},t)(i\partial_0+\frac{\boldsymbol{\nabla}^2}{2m})\pi_+(\mathbf{x},t)+(+\leftrightarrow-)\\&+R'_{cc}(\pi_+^\dagger\pi_-^\dagger\pi_+\pi_-)(\mathbf{x},t)+P'(\pi_+^\dagger\pi_-^\dagger)(\mathbf{x},t)i\partial_0(\pi_+\pi_-)(\mathbf{x},t)\\&-\int d^3\mathbf{y}(\pi_+^\dagger\pi_+)(\mathbf{x},t)\Big(V_0(|\mathbf{x}-\mathbf{y}|)+V_1(|\mathbf{x}-\mathbf{y}|)\Big)(\pi_-^\dagger\pi_-)(\mathbf{y},t)\end{aligned} \tag{4}$$

where V_0 is the Coulomb potential and V_1 the correction of the vacuum polarisation due to the electron[6]. The electron mass m_e is of the same order as $m\alpha/2$ and hence it must be integrated out here. In the lagrangian above time derivatives must be counted as $m\alpha^2/4$ and space derivatives, $1/\mathrm{r}$ and dimensionful fields as $m\alpha/2$. This lagrangian is totally equivalent (at the desired order) to the following quantum mechanical Hamiltonian

$$H''=-\frac{\boldsymbol{\nabla}^2}{m}+V_0(|\mathbf{x}|)+V_1(|\mathbf{x}|)-R'_{cc}\delta(\mathbf{x})-P'\frac{1}{2}\{\delta(\mathbf{x}),-\frac{\boldsymbol{\nabla}^2}{m}+V_0(|\mathbf{x}|)\} \tag{5}$$

This Hamiltonian is very singular and requires regularisation. DR and MS has been used.

RESULTS

A second order quantum mechanical perturbation theory calculation leads to

$$\begin{aligned}E_n&=E_n^{(0)}-\frac{|\Psi_n(\mathbf{0})|^2}{2f^2}+\delta_{V_1}E_n^{(1)}\\E_1&=E_1^{(0)}\left(1+1.31\cdot10^{-3}+0.51\cdot10^{-3}\right)\\E_n^{(0)}&=-\frac{m\alpha^2}{4n^2}\end{aligned} \tag{6}$$

and

$$\begin{aligned}\Gamma_n&=\Gamma_n^{(0)}\left(1+\Delta_{\chi PT}+\frac{5\Delta m}{12m}-\frac{m\alpha^2}{16\Delta mn^2}-\frac{m^2\alpha\Delta_n}{4\pi f^2}\right)+\delta_{V_1}\Gamma_n^{(2)}\\\Gamma_1&=\Gamma_1^{(0)}\left(1+\Delta_{\chi PT}+1.37\cdot10^{-2}-1\cdot10^{-4}+1.29\cdot10^{-2}+0.31\cdot10^{-2}\right)\\\Gamma_n^{(0)}&=\frac{9m\sqrt{2m\Delta m}}{64\pi f^4}|\Psi_n(\mathbf{0})|^2\\\Delta_n&=log(\frac{m\alpha}{\sqrt{4\pi}n\mu})+\frac{3}{2}\gamma_E-\frac{1}{2}+\psi(n)-\frac{1}{n}\end{aligned} \tag{7}$$

$\delta_{V_1}E_1^{(1)}$ is given analytically in[12] and $\delta_{V_1}\Gamma_n^{(2)}$ numerically in[6]. We have substituted the leading order values of R_{00} ,R_{0c} , R_{cc} and S_{0c} in the corrections, whereas their relevant contributions beyond leading order are encoded in $\Delta_{\chi PT}$ (see[12] for details). Notice

that $\Delta_{\chi PT}$ must contain a logarithmic dependence in μ which cancels that of Δ_n. This logarithmic dependence would arise from a two loop calculation in the χL coupled to electromagnetism which has not been carried out yet.

Let us briefly comment on the numbers given above. We have placed them in such a way that they always come from the term of the preceeding formula in the same location. For the corrections to the energy levels, notice that the vacuum polarisation contribution is almost as important as the strong vertex. The error of E_1 is dominated by the chiral loop and the $\Delta m/m$ corrections to the strong vertex. For the corrections to the decay width, they are also dominated by the chiral loop and $\Delta m/m$ corrections in $\Delta_{\chi PT}$. A two loop calculation including virtual photons is necessary to obtain $\Delta_{\chi PT}$ with an accuracy of the same order as the remaining numbers. Hence, the uncertainties in the $O(p^4)$, $O(p^2\alpha)$, $O(p^6)$ and $O(p^4\alpha)$ low energy constants of the χL are expected to be the main source of theoretical error in (7). Notice that the correction $m\alpha^2/4\Delta m$ is negligibly small, as expected, but, on the contrary, the correction $m^2\alpha/f^2$ is numerically enhanced, partially due to the logarithm ($\mu = m$ has been taken).

DISCUSSION

Let us finally compare our results with those of similar non-relativistic approaches, which start with the lagrangian (1). The comparison is done before substituting any particular value for the parameters in (1). Part of the corrections $O(\Delta m/m)$ in Γ_n were first calculated in[8] and agree with those coming from the two last terms of R'_{cc} in (3). The remaining corrections $O(\Delta m/m)$ are due to relativistic effects in the neutral pion propagator and correspond to the first correction in the last term of R'_{cc} in (3), which is also in agreement with the results presented later on in[11]. If we neglect $\delta_{V_1}\Gamma_1^{(2)}$ (vacuum polarisation), Γ_1 above coincides with that given in formulas (10) and (11) of[10], upon expanding (11) in $\Delta m/m$ and $m\alpha^2/4\Delta m$ and keeping terms up to next to leading order.

The comparison with the relativistic approaches[5,7] is not straightforward. A brief discussion can be found in[10,18]. The relation between the traditional quantum mechanical approach[4] and the non-relativistic field theoretical approach has been discussed in[9].

We thank A. Andrianov for reading the manuscript.

REFERENCES

1. J.Gasser and H.Leutwyler, *Ann. of Phys.* **158** (1984) 142.
2. L.L. Nemenov, *Yad. Fiz.* **41** (1985) 980.
3. B. Adeva et al.,*CERN-SPSLC*-**95-1**; J. Schacher, hep-ph/9808407.
4. A. Gashi, G. Rasche, G. C. Oades and W. S. Woolcock, *Nucl.Phys.***A628** (1998) 101; G. Rasche and A. Gashi, *Phys.Lett.***B404** (1997) 375.
5. H. Jallouli and H. Sazdjian, *Phys.Rev.* **D58** (1998) 014011; Erratum-ibid. **D58** (1998) 099901.
6. P. Labelle and K. Buckley, hep-ph/9804201.
7. M. A. Ivanov, V. E. Lyubovitskij, E. Z. Lipartia and A. G. Rusetsky,*Phys.Rev.***D58** (1998) 094024.
8. X. Kong and F. Ravndal, hep-ph/9805357.
9. B. R. Holstein, nucl-th/9901041.
10. A. Gall, J. Gasser, V. E. Lyubovitskij and A. Rusetsky, hep-ph/9905309.
11. X. Kong and F. Ravndal, hep-ph/9905539.
12. D. Eiras and J. Soto, hep-ph/9905543.
13. W.E. Caswell and G.P. Lepage, *Phys. Lett.* **B167** (1986) 437.
14. M. Knecht and R. Urech, *Nucl.Phys.* **B519** (1998) 329.
15. M. Knecht, B. Moussallam, J. Stern and N. Fuchs, *Nucl.Phys.* **B457** (1995) 513; **B471** (1996) 445.
16. A. Pineda and J. Soto, *Nucl.Phys.Proc.Suppl.* **64** (1998) 428; *Phys. Lett.* **B420** (1998) 391; *Phys.Rev.* **D59** (1999)016005.
17. H. Sazdjian, talk given at QCD99 (Montpellier) .
18. V. E. Lyubovitskij, these proceedings.

Hadronic Atoms in QCD

J. Gasser
Institute for Theoretical Physics, University of Bern, Sidlerstrasse 5, CH-3012, Bern, Switzerland

V. E. Lyubovitskij*
Bogoliubov Laboratory of Theoretical Physics, Joint Institute for Nuclear Research, 141980 Dubna, Russia and Department of Physics, Tomsk State University, 634050 Tomsk, Russia

A. Rusetsky
Institute for Theoretical Physics, University of Bern, Sidlerstrasse 5, CH-3012, Bern, Switzerland, Bogoliubov Laboratory of Theoretical Physics, Joint Institute for Nuclear Research, 141980 Dubna, Russia and HEPI, Tbilisi State University, 380086 Tbilisi, Georgia

Abstract

We propose a non relativistic effective Lagrangian approach to study hadronic atom observables in the framework of QCD (including photons). We apply our formalism to derive a general expression for the width of the $\pi^+\pi^-$ atom decaying into two neutral pions. It contains all terms at leading and next-to-leading order in isospin breaking. The result allows one to evaluate the combination $a_0 - a_2$ of $\pi\pi$ S-wave scattering lengths from $\pi^+\pi^-$ lifetime measurements, like the one presently performed by the DIRAC experiment at CERN.

The DIRAC collaboration at CERN[1] aims to measure the lifetime of the $\pi^+\pi^-$ atom (pionium) in its ground state at the 10% level. This atom decays predominantly into two neutral pions, $\Gamma = \Gamma_{2\pi^0} + \Gamma_{2\gamma} + \ldots$, with $\Gamma_{2\gamma}/\Gamma_{2\pi^0} \sim 4 \cdot 10^{-3}$[1]. The measurement of $\Gamma_{2\pi^0}$ allows one[2–6] to determine the difference $a_0 - a_2$ of the strong S-wave $\pi\pi$ scattering lengths with isospin $I = 0, 2$. One may then confront the predictions for this quantity obtained in standard ChPT[7,8] with the lifetime measurement, and furthermore analyze the nature of spontaneous chiral symmetry breaking in QCD[9]. In order to perform these investigations, one needs to know the theoretical expression for the width of pionium with a precision that properly matches the accuracy of the lifetime measurement of DIRAC. It is the aim of the present talk to derive a general formula[2] for the $\pi^+\pi^-$ atom decay width in the framework of QCD (including photons) by use of effective field theory techniques. Our result contains all terms at leading and next-to-leading order in the isospin breaking parameters $\alpha \simeq 1/137$ and $(m_u - m_d)^2$. On the other hand, we expect that the contributions from next-to-next-to-leading order are completely negligible, at least for the analysis of DIRAC data, and we therefore discard them here.

In several recent publications[10], the decay of $\pi^+\pi^-$ atoms has been studied in the framework of a non relativistic effective Lagrangian approach - a method originally proposed by Caswell and Lepage[11] to investigate bound states in general. This method has proven to be far more efficient for the treatment of loosely bound systems - such as the $\pi^+\pi^-$ atom - than conventional approaches based on relativistic bound-state equations. It allows one e.g. to go beyond the local approximation used in[12,13]. On the other hand, we are not aware of a systematic investigation of the decay of the $\pi^+\pi^-$ atom in this framework. In particular, the chiral expansion of the width has not been discussed, and a comparison of the corrections found in this framework with the results of[12,13] has never been provided. The main purpose of my talk - based on the papers[2,14] - is to fill this gap.

The formation of the atom and its subsequent decay into two neutral pions is induced by isospin breaking effects in the underlying theory. In the present framework, these are

*Present address: Institute of Theoretical Physics, University of Tübingen, Auf der Morgenstelle 14, D-72076 Tübingen, Germany

the electromagnetic interactions and the mass difference of the up and down quarks. In the following, it is useful to count $\alpha \simeq 1/137$ and $(m_d - m_u)^2$ as small parameters of order δ. More than forty years ago, Deser *et al.*[4] derived the formula for the width of the $\pi^- p$ atom at leading order in isospin symmetry breaking. Later in Refs.[5,6], this result was adapted to the $\pi^+\pi^-$ atom*. In particular, it was shown that - again at leading order in isospin symmetry breaking effects - the width $\Gamma^{\rm LO}_{2\pi^0}$ of pionium is proportional to the square of the difference $a_0 - a_2$,

$$\Gamma^{\rm LO}_{2\pi^0} = \frac{2}{9}\,\alpha^3 p^\star (a_0 - a_2)^2\;; \qquad p^\star = (M^2_{\pi^+} - M^2_{\pi^0} - \frac{1}{4} M^2_{\pi^+}\alpha^2)^{1/2}. \tag{1}$$

At leading order in δ, the momentum $p^\star$ becomes $\sqrt{2M_{\pi^+}(M_{\pi^+} - M_{\pi^0})}$ - this is the expression used in[5,6]. We prefer to use Eq. (1), because in this manner, one disentangles the kinematical corrections - due to the expansion of the square root - from true dynamical ones. In our recent article[2], we derived a general expression for the pionium lifetime, that is valid at leading and next-to-leading order in isospin breaking,

$$\Gamma_{2\pi^0} = \frac{2}{9}\,\alpha^3 p^\star \mathcal{A}^2 (1 + K). \tag{2}$$

The quantities $\mathcal{A}$ and K are expanded in powers of δ. In particular, it has been shown in[2] that†

$$\mathcal{A} \;=\; -\frac{3}{32\pi}\,{\rm Re}A^{+-00}_{\rm thr} + o(\delta), \tag{3}$$

where ${\rm Re}A^{+-00}_{\rm thr}$ is calculated as follows. One evaluates the relativistic scattering amplitude for the process $\pi^+\pi^- \to \pi^0\pi^0$ at order δ near threshold and removes the (divergent) Coulomb phase. The real part of this matrix element develops singularities that behave like $|\mathbf{p}|^{-1}$ and $\ln 2|\mathbf{p}|/M_{\pi^+}$ near threshold ($\mathbf{p}$ denotes the center of mass momentum of the charged pions). The remainder, evaluated at the $\pi^+\pi^-$ threshold $\mathbf{p} = \mathbf{0}$, equals ${\rm Re}A^{+-00}_{\rm thr}$. It contains terms of order δ^0 and δ and is normalized such that, in the isospin symmetry limit, $\mathcal{A} = a_0 - a_2$. Finally, the quantity K starts at order $\alpha \ln \alpha$ - its explicit expression up to and including terms of order δ is given by

$$K = \frac{\Delta_\pi}{9M^2_{\pi^+}}\,(a_0 + 2a_2)^2 - \frac{2\alpha}{3}\,(\ln\alpha - 1)\,(2a_0 + a_2) + o(\delta), \qquad \Delta_\pi = M^2_{\pi^+} - M^2_{\pi^0}. \tag{4}$$

In the derivation of Eqs. (2) - (4), the chiral expansion has not been used. It is the aim of my talk to show how this result can be derived (details will be provided in a forthcoming publication[14]).

We proceed as follows. First, we display the non relativistic effective Lagrangian for pions, as derived from ChPT. Next, we formulate resonance two-channel $\pi\pi$ scattering theory by applying Feshbach's projection technique[15]. This method allows one to explicitly reveal the pole structure of the scattering matrix element and to obtain the equation for the bound-state energy of the $\pi^+\pi^-$ atom. Solving this equation, bound state characteristic of the hadronic atoms are given in terms of the couplings in the non relativistic Lagrangian. At the final stage, unknown couplings in the non relativistic Lagrangian can be expressed in terms of relativistic $\pi\pi$ scattering amplitudes through the matching procedure. Finally, as an illustration of our method, we derive Eqs. (2) - (4).

The non relativistic effective Lagrangian $\mathcal{L} = \mathcal{L}_0 + \mathcal{L}_D + \mathcal{L}_C + \mathcal{L}_S$ - at the order of accuracy we are working here - consists of the free Lagrangian for charged and neutral

*There are a few misprints in Eq. (6) for the pionium decay rate in Ref.[5]. The correct result is displayed in Ref.[6].

†We use throughout the Landau symbols $O(x)$ [$o(x)$] for quantities that vanish like x [faster than x] when x tends to zero. Furthermore, it is understood that this holds modulo logarithmic terms, i.e. we write also $O(x)$ for $x \ln x$.

pions ($\mathcal{L}_0$), the "disconnected" piece ($\mathcal{L}_D$) - providing the correct relativistic relation between the energies and momenta of the pions - the Coulomb interaction piece ($\mathcal{L}_C$), and the "connected" piece ($\mathcal{L}_S$) which contains local four-pion interaction vertices:

$$\begin{aligned}
\mathcal{L}_0 &= \sum_{i=\pm,0} \pi_i^\dagger \Big(i\partial_t - M_{\pi_i} + \frac{\Delta}{2M_{\pi_i}} \Big) \pi_i, \qquad (5)\\
\mathcal{L}_D &= \sum_{i=\pm,0} \pi_i^\dagger \Big(\frac{\Delta^2}{8M_{\pi_i}^3} + \cdots \Big) \pi_i, \quad \mathcal{L}_C = -4\pi\alpha(\pi_-^\dagger\pi_-)\Delta^{-1}(\pi_+^\dagger\pi_+) + \cdots,\\
\mathcal{L}_S &= c_1\pi_+^\dagger\pi_-^\dagger\pi_+\pi_- + c_2[\pi_+^\dagger\pi_-^\dagger(\pi_0)^2 + \text{h.c.}] + c_3\,(\pi_0^\dagger\pi_0)^2\\
&+ c_4[\pi_+^\dagger \overset{\leftrightarrow}{\Delta} \pi_-^\dagger(\pi_0)^2 + \pi_+^\dagger\pi_-^\dagger\pi_0 \overset{\leftrightarrow}{\Delta} \pi_0 + \text{h.c.}] + \cdots,
\end{aligned}$$

where $u \overset{\leftrightarrow}{\Delta} v \equiv u\Delta v + v\Delta u$. The coupling constants c_i are real at $O(\alpha)$ and are determined through matching to the relativistic theory.

We now formulate the two-channel $\pi\pi$ scattering theory. We denote the full Hamiltonian derived from (5) by $H = H_0 + H_C + V$, with $V = H_D + H_S$. The scattering operator T obeys the Lippmann-Schwinger equation $T(z) = (H_C + V) + (H_C + V)G_0(z)T(z)$. The free and the Coulomb Green operators are defined as $G_0(z) = (z - H_0)^{-1}$ and $G(z) = (z - H_0 - H_C)^{-1}$, respectively. The pole structure of the T-matrix is predominantly determined by the static Coulomb interaction H_C, whereas V generates a small shift of the pole positions into the complex z-plane and will be treated perturbatively. To this end, we use the method developed by Feshbach[15] a long time ago. The T-matrix in our theory describes the transitions between charged $|\mathbf{P},\mathbf{p}\rangle_+ = a_+^\dagger(\mathbf{p}_1)a_-^\dagger(\mathbf{p}_2)|0\rangle$ and neutral $|\mathbf{P},\mathbf{p}\rangle_0 = a_0^\dagger(\mathbf{p}_1)a_0^\dagger(\mathbf{p}_2)|0\rangle$ states, where $a_i^\dagger$ denote the creation operators for non relativistic pions. Further, $\mathbf{P} = \mathbf{p}_1 + \mathbf{p}_2$ and $\mathbf{p} = \frac{1}{2}(\mathbf{p}_1 - \mathbf{p}_2)$ are the CM and relative momenta of pion pairs, respectively. We work in the CM system and remove the CM momentum from the matrix elements of any operator R, introducing the notation ${}_A\langle\mathbf{P},\mathbf{q}|R(z)|\mathbf{0},\mathbf{p}\rangle_B = (2\pi)^3\delta^3(\mathbf{P})(\mathbf{q}|\tau_{AB}(z)|\mathbf{p})$, where $A,\ B = +,\ 0$. The operators $\tau_{AB}(z)$ act in the Hilbert space of vectors $|\mathbf{p})$, where the scalar product is defined as the integral over the relative three-momenta of pion pairs.

In order to avoid the complications associated with charged particles in the final states, we consider the elastic scattering process $\pi^0\pi^0 \to \pi^0\pi^0$. In the vicinity of the $\pi^+\pi^-$ threshold, the scattering matrix element develops a pole at[15]

$$z - E_0 - (\Psi_0|\tau_{++}(z)|\Psi_0) = 0, \qquad (6)$$

where $(\mathbf{p}|\Psi_0) = \Psi_0(\mathbf{p})$ stands for the unperturbed Coulomb ground-state wave function, and E_0 is the corresponding ground-state energy. According to the conventional definition, the decay width is $\Gamma = -2\text{Im}z$. The operator $\tau_{AB}(z)$ denotes the "Coulomb-pole removed" transition operator that satisfies the equation

$$\begin{aligned}
\tau_{AB}(z) &= v_{AB} + v_{A+}\hat{g}_{++}(z)\tau_{+B}(z) + \frac{1}{4}v_{A0}g_{00}(z)\tau_{0B}(z),\\
(\mathbf{q}|\hat{g}_{++}(z)|\mathbf{p}) &= (\mathbf{q}|g_{++}(z)|\mathbf{p}) - \frac{\Psi_0(\mathbf{q})\Psi_0(\mathbf{p})}{(z - E_0)}\,. \qquad (7)
\end{aligned}$$

It remains to solve Eq. (6) in the dimensional regularization scheme and with the use of the effective potential technique (see details in[2,14]). We find that the width of the $\pi^+\pi^-$ atom - in terms of the effective couplings c_i - is given by

$$\Gamma_{2\pi^0} = \frac{\alpha^3 M_{\pi^+}^3}{8\pi^2}\rho^{1/2}M_{\pi^0}\Big(1 + \frac{5\rho}{8M_{\pi^0}^2}\Big)(c_2 - 2\rho c_4)^2\Big(1 - \rho c_3^2\frac{M_{\pi^0}^2}{4\pi^2}\Big)\Big(1 - \frac{\alpha M_{\pi^+}^2}{4\pi}\xi c_1\Big) + \cdots, \quad (8)$$

where $\rho = 2M_{\pi^0}(M_{\pi^+} - M_{\pi^0} - M_{\pi^+}\alpha^2/8)$, $\xi = 2\ln\alpha - 3 + \Lambda + \ln(M_{\pi^+}^2/\mu^2)$, $\Lambda = (\mu^2)^{d-3}[(d-3)^{-1} - \Gamma'(1) - \ln 4\pi]$. The ellipsis denotes higher order terms in isospin breaking. The divergent term proportional to Λ stems from a charged pion loop with one Coulomb photon exchange. It is removed by the renormalization procedure in the scattering sector. Next, we consider the matching procedure, which relates the effective couplings c_i to the $\pi\pi$ scattering amplitudes for three channels $\pi^+\pi^- \to \pi^0\pi^0$, $\pi^+\pi^- \to \pi^+\pi^-$ and $\pi^0\pi^0 \to \pi^0\pi^0$ evaluated in the relativistic theory[16]:

$$3M_{\pi^+}^2\, c_1 = 4\pi\,(2a_0 + a_2) + o(\delta), \qquad 3M_{\pi^+}^2\, c_3 = 2\pi\,(a_0 + 2a_2) + o(\delta), \tag{9}$$

$$\mathcal{A} = -\frac{3}{8\pi}M_{\pi^+}^2\left[2c_2 - 4\Delta_\pi\left(c_4 + \frac{c_2c_3^2}{8\pi^2}M_{\pi^0}^2\right) + \frac{\alpha M_{\pi^+}^2}{4\pi}\left(1 - \Lambda - \ln\frac{M_{\pi^+}^2}{\mu^2}\right)c_1c_2\right] + o(\delta) \tag{10}$$

Substituting Eqs. (9), (10) into Eq. (8), we finally arrive at the general formula for the $\pi^+\pi^-$ atom decay width in QCD, given by Eqs. (2) - (4). It is our opinion that these equations finalize the attempts to calculate the width $\Gamma_{2\pi^0}$ at next-to-leading order, relegating the problem to the evaluation of the physical on-mass-shell scattering amplitude for the process $\pi^+\pi^- \to \pi^0\pi^0$ to any desired order in the chiral expansion. Numerical analysis of the $\pi^+\pi^-$ atom lifetime in ChPT at one loop, including a comparison with recent work in literature, was performed recently in Ref.[3].

In conclusion, we have evaluated the width $\Gamma_{2\pi^0}$ of the $\pi^+\pi^-$ atom in its ground state at leading and next-to-leading order in isospin breaking. The non relativistic effective Lagrangian approach of Caswell and Lepage[11] appears to be an extremely suitable tool for this purpose, that allows one to completely solve this problem. Its usefulness may be seen even more clearly for the case of $p\pi^-$, pK^-, $d\pi^-$, dK^- atoms, studied in ongoing or planned experiments (PSI, KEK, DAΦNE), because this approach trivializes the spin-dependent part of the problem.

Acknowledgments. V. E. L. thanks the Organizing Committee of MENU99 Symposium for financial support and University of Bern for hospitality where this work was done. The work was supported in part by the Swiss National Science Foundation, and by TMR, BBW-Contract No. 97.0131 and EC-Contract No. ERBFMRX-CT980169 (EURODAΦNE).

REFERENCES

1. B. Adeva *et al.*, CERN proposal CERN/SPSLC 95-1 (1995).
2. A. Gall, J. Gasser, V.E. Lyubovitskij, A. Rusetsky, Phys. Lett. **B462**, 335 (1999).
3. J. Gasser, V.E. Lyubovitskij, A. Rusetsky, Preprint BUTP-99/20, hep-ph/9910438.
4. S. Deser, M.L. Goldberger, K. Baumann, W. Thirring, Phys. Rev. **96**, 774 (1954).
5. J.L. Uretsky and T.R. Palfrey, Jr., Phys. Rev. **121**, 1798 (1961).
6. S.M. Bilenky, Van Kheu Nguyen, L.L. Nemenov, F.G. Tkebuchava, Sov. J. Nucl. Phys. **10**, 469 (1969).
7. S. Weinberg, Physica **A96**, 327 (1979); J. Gasser, H. Leutwyler, Ann. Phys. (N.Y.) **158**, 142 (1984); Nucl. Phys. **B250**, 465 (1985).
8. J. Gasser, H. Leutwyler, Phys. Lett. **B125**, 325 (1983); J. Bijnens, G. Colangelo, G. Ecker, J. Gasser, M.E. Sainio, Phys. Lett. **B374**, 210 (1996).
9. M. Knecht, B. Moussallam, J. Stern, N.H. Fuchs, Nucl. Phys. **B457**, 513 (1995); ibid. **B471**, 445 (1996).
10. P. Labelle, K. Buckley, preprint hep-ph/9804201; X. Kong, F. Ravndal, Phys. Rev. **D59**, 014031 (1999); preprint hep-ph/9905539; B.R. Holstein, preprint nucl-th/9901041.
11. W.E. Caswell, G.P. Lepage, Phys. Lett. **B167**, 437 (1986).
12. H. Jallouli, H. Sazdjian, Phys. Rev. **D58**, 014011 (1998).
13. V.E. Lyubovitskij, A.G. Rusetsky, Phys. Lett. **B389**, 181 (1996); V.E. Lyubovitskij, E.Z. Lipartia, A.G. Rusetsky, JETP Lett. **66**, 783 (1997); M.A. Ivanov, V.E. Lyubovitskij, E.Z. Lipartia, A.G. Rusetsky, Phys. Rev. **D58**, 094024 (1998).
14. A. Gall, J. Gasser, V.E. Lyubovitskij, A. Rusetsky, in preparation.
15. H. Feshbach, Ann. Phys. **5**, 357 (1958); ibid **19**, 287 (1962).
16. M. Knecht, R. Urech, Nucl. Phys. **B519**, 329 (1998).

Chiral Perturbation Theory with Photons and Leptons

H. Neufeld*
Institut für Theoretische Physik der Universität Wien,
Boltzmanngasse 5, A-1090 Wien, Austria

Abstract

I discuss a low-energy effective field theory which allows the full treatment of isospin-breaking effects in semileptonic weak interactions. In addition to the pseudoscalars and the photon, also the light leptons have to be included as dynamical degrees of freedom in an appropriate chiral Lagrangian. I describe the construction of the local action at next-to-leading order.

INTRODUCTION

In this talk, I would like to report about the status[1] of a research project on isospin-violating effects in the semileptonic decays of pions and kaons which is presently carried out by Marc Knecht, Heinz Rupertsberger, Pere Talavera and myself.

While isospin-breaking generated by a non-vanishing quark mass difference $m_d - m_u$ is fully contained in the pure QCD sector of the effective chiral Lagrangian[2], the analysis of isospin-violation of electromagnetic origin requires an extension of the usual low-energy effective theory. For purely pseudoscalar processes, the suitable theoretical framework for the three-flavour case has been worked out in[3–5] by including virtual photons and the appropriate local terms up to $\mathcal{O}(e^2p^2)$.

The treatment of electromagnetic corrections in semileptonic decays demands still a further extension of chiral perturbation theory. In this case, also the light leptons have to be included as explicit dynamical degrees of freedom. Only within such a framework, one will have full control over all possible isospin breaking effects in the analysis of new high statistics $K_{\ell 4}$ experiments by the E865 and KLOE collaborations at BNL[6] and DAΦNE[7], respectively. The same refined methods are, of course, also necessary for the interpretation of forthcoming high precision experiments on other semileptonic decays like $K_{\ell 3}$, etc.

THE LOWEST ORDER LAGRANGIAN

To lowest order in the chiral expansion, the effective Lagrangian without dynamical photons and leptons (pure QCD) is nothing else than the non-linear sigma model in the presence of external vector, axial-vector, scalar and pseudoscalar sources v_μ, a_μ, $\chi = s + ip$. Following the notation of[8], it takes the form

$$\mathcal{L}_{\text{eff}} = \frac{F^2}{4} \langle u_\mu u^\mu + \chi_+ \rangle, \tag{1}$$

where

$$\begin{aligned} u_\mu &= i[u_R^\dagger(\partial_\mu - ir_\mu)u_R - u_L^\dagger(\partial_\mu - il_\mu)u_L], \\ l_\mu &= v_\mu - a_\mu, \\ r_\mu &= v_\mu + a_\mu, \\ \chi_+ &= u_R^\dagger \chi u_L + u_L^\dagger \chi^\dagger u_R. \end{aligned} \tag{2}$$

Even this Lagrangian allows the treatment of electromagnetic or semileptonic processes as long as the photon or the leptons are occurring only as external fields. One simply takes external sources with the quantum numbers of the photon or the $W^\pm$, respectively.

For the description of dynamical photons and leptons, the extension of the lowest order Lagrangian (1) is rather easy. First of all, the photon field A_μ and the light leptons ℓ, ν_ℓ

*Supported in part by TMR, EC-Contract No. ERBFMRX-CT980169 (EURODAΦNE)

($\ell = e, \mu$) are introduced in u_μ by adding appropriate terms to the external vector and axial-vector sources:

$$\begin{aligned} l_\mu &= v_\mu - a_\mu - eQ_L^{\rm em} A_\mu + \sum_\ell (\bar{\ell}\gamma_\mu \nu_{\ell L} Q_L^{\rm w} + \overline{\nu_{\ell L}}\gamma_\mu \ell Q_L^{\rm w\dagger}), \\ r_\mu &= v_\mu + a_\mu - eQ_R^{\rm em} A_\mu. \end{aligned} \tag{3}$$

The 3×3 matrices $Q_{L,R}^{\rm em}$, $Q_L^{\rm w}$ are additional spurion fields. At the end, one identifies $Q_{L,R}^{\rm em}$ with the quark charge matrix

$$Q^{\rm em} = \begin{bmatrix} 2/3 & 0 & 0 \\ 0 & -1/3 & 0 \\ 0 & 0 & -1/3 \end{bmatrix}, \tag{4}$$

whereas the weak spurion is taken at

$$Q_L^{\rm w} = -2\sqrt{2}\, G_F \begin{bmatrix} 0 & V_{ud} & V_{us} \\ 0 & 0 & 0 \\ 0 & 0 & 0 \end{bmatrix}, \tag{5}$$

where G_F is the Fermi coupling constant and V_{ud}, V_{us} are Kobayashi–Maskawa matrix elements.

Then we have to introduce kinetic terms for the photon and the leptons and also an electromagnetic term of $\mathcal{O}(e^2p^0)$. With these building blocks, our lowest order effective Lagrangian takes the form

$$\begin{aligned} \mathcal{L}_{\rm eff} &= \frac{F^2}{4}\langle u_\mu u^\mu + \chi_+\rangle + e^2F^4 Z \langle Q_L^{\rm em} Q_R^{\rm em}\rangle \\ &\quad - \frac{1}{4}F_{\mu\nu}F^{\mu\nu} + \sum_\ell [\bar{\ell}(i\,\partial\!\!\!/ + e\,A\!\!\!/ - m_\ell)\ell + \overline{\nu_{\ell L}}\, i\,\partial\!\!\!/\,\nu_{\ell L}], \end{aligned} \tag{6}$$

where

$$Q_L^{\rm em,w} := u_L^\dagger Q_L^{\rm em,w} u_L, \qquad Q_R^{\rm em} := u_R^\dagger Q_R^{\rm em} u_R. \tag{7}$$

Finally, we have to define an extended chiral expansion scheme. The electric charge e, the lepton masses m_e, m_μ and fermion bilinears are considered (formally) as quantities of order p in the chiral counting, where p is a typical meson momentum. Note, however, that terms of $\mathcal{O}(e^4)$ will be neglected throughout.

THE NEXT-TO-LEADING ORDER LAGRANGIAN

As we are dealing with a so-called non-renormalizable theory, new local terms are arising at the next-to-leading-order. The associated coupling constants absorb the divergences of the one-loop graphs. Their finite parts are in principle certain functions of the parameters of the standard model. Because of our limited ability in solving the standard model (confinement problem), these low-energy constants have to be regarded as free parameters of our effective theory for the time being.

The list of local counterterms of our extended theory comprises, of course, the well-known Gasser–Leutwyler Lagrangian of $\mathcal{O}(p^4)$[2] and the Urech Lagrangian of $\mathcal{O}(e^2p^2)$[3] with the generalized l_μ and r_μ defined in Eq. (3). In the presence of virtual leptons, we have to introduce an additional "leptonic" Lagrangian[1]

$$\begin{aligned} \mathcal{L}_{\rm lept} &= e^2 \sum_\ell \Big\{ F^2 \Big[X_1 \bar{\ell}\gamma_\mu \nu_{\ell L} \langle u^\mu \{Q_R^{\rm em}, Q_L^{\rm w}\}\rangle \\ &\qquad + X_2 \bar{\ell}\gamma_\mu \nu_{\ell L} \langle u^\mu [Q_R^{\rm em}, Q_L^{\rm w}]\rangle \\ &\qquad + X_3 m_\ell \bar{\ell}\nu_{\ell L} \langle Q_L^{\rm w} Q_R^{\rm em}\rangle \\ &\qquad + iX_4 \bar{\ell}\gamma_\mu \nu_{\ell L} \langle Q_L^{\rm w} \hat{\nabla}^\mu Q_L^{\rm em}\rangle \end{aligned}$$

$$
\begin{aligned}
&+iX_5\bar{\ell}\gamma_\mu\nu_{\ell L}\langle Q_L^{\rm w}\widehat{\nabla}^\mu Q_R^{\rm em}\rangle + h.c.\Big] \\
&+X_6\bar{\ell}(i\not{\partial}+e\not{A})\ell \\
&+X_7 m_\ell\bar{\ell}\ell\Big\}\,. \qquad (8)
\end{aligned}
$$

where

$$
\begin{aligned}
\widehat{\nabla}_\mu Q_L^{\rm em} &= \nabla_\mu Q_L^{\rm em} + \frac{i}{2}[u_\mu, Q_L^{\rm em}] = u(D_\mu Q_L^{\rm em})u^\dagger, \\
\widehat{\nabla}_\mu Q_R^{\rm em} &= \nabla_\mu Q_R^{\rm em} - \frac{i}{2}[u_\mu, Q_R^{\rm em}] = u^\dagger(D_\mu Q_R^{\rm em})u, \qquad (9)
\end{aligned}
$$

with

$$
\begin{aligned}
D_\mu Q_L^{\rm em} &= \partial_\mu Q_L^{\rm em} - i[l_\mu, Q_L^{\rm em}], \\
D_\mu Q_R^{\rm em} &= \partial_\mu Q_R^{\rm em} - i[r_\mu, Q_R^{\rm em}]. \qquad (10)
\end{aligned}
$$

In $\mathcal{L}_{\rm lept}$ we consider only terms quadratic in the lepton fields and at most linear in G_F. The terms with $X_{4,5}$ will not appear in realistic physical processes as the generated amplitudes contain an external (axial-) vector source (see Eqs. (9) and (10)).

In deriving a minimal set of terms in Eq. (8), we have used partial integration, the equations of motion derived from the tree-level Lagrangian (6) and the relations

$$
Q_L^{\rm em}Q_L^{\rm w} = \frac{2}{3}Q_L^{\rm w}, \qquad Q_L^{\rm w}Q_L^{\rm em} = -\frac{1}{3}Q_L^{\rm w}, \qquad \langle Q_L^{\rm w}\rangle = 0. \qquad (11)
$$

Finally, also a photon Lagrangian

$$
\mathcal{L}_\gamma = e^2 X_8 F_{\mu\nu}F^{\mu\nu}, \qquad F_{\mu\nu} = \partial_\mu A_\nu - \partial_\nu A_\mu, \qquad (12)
$$

has to be added. This term cancels the divergences of the photon two-point function generated by the lepton loops.

The "new" low–energy couplings X_i arising here are divergent (except X_1). In the dimensional regularization scheme, they absorb the divergences of the one–loop graphs with internal lepton lines via the renormalization

$$
\begin{aligned}
X_i &= X_i^r(\mu) + \Xi_i\Lambda(\mu), \quad i = 1,\ldots,8, \\
\Lambda(\mu) &= \frac{\mu^{d-4}}{(4\pi)^2}\left\{\frac{1}{d-4} - \frac{1}{2}[\ln(4\pi) + \Gamma'(1) + 1]\right\}. \qquad (13)
\end{aligned}
$$

The coefficients $\Xi_1,\ldots\Xi_7$ can be determined[1] by using super-heat-kernel methods[9,10]:

$$
\begin{aligned}
&\Xi_1 = 0, \quad \Xi_2 = -\frac{3}{4}, \quad \Xi_3 = -3, \quad \Xi_4 = -\frac{3}{2}, \\
&\Xi_5 = \frac{3}{2}, \quad \Xi_6 = -5, \quad \Xi_7 = -1, \quad \Xi_8 = -\frac{4}{3}. \qquad (14)
\end{aligned}
$$

SUMMARY AND OUTLOOK

We have developed the appropriate low-energy effective theory for a complete treatment of isospin violating effects in semileptonic weak processes. The electromagnetic interaction requires the inclusion of the photon field and the light leptons as explicit dynamical degrees of freedom in the chiral Lagrangian. At next-to-leading order, the list of local terms given by Gasser and Leutwyler[2] for the QCD part and by Urech[3] for the electromagnetic interaction of the pseudoscalars has to be enlarged. This is, of course, a consequence of the presence of virtual leptons in our extended theory. Regarding pure lepton or photon bilinears as "trivial", five additional "non-trivial" terms of this type are arising. But two of them will not appear in realistic physical processes. One may therefore conclude that

the main bulk of electromagnetic low-energy constants is already contained in Urech's Lagrangian and the inclusion of virtual leptons in chiral perturbation theory does not substantially aggravate the problem of unknown parameters.

As an illustration of the use of our effective theory, we have calculated[1] the decay rates of $\pi \to \ell\nu_\ell$ and $K \to \ell\nu_\ell$ including the electromagnetic contributions of $\mathcal{O}(e^2p^2)$. An investigation of the $K_{\ell 3}$ decays is presently in progress.

The continuation of our work will follow two principal lines. Firstly, we are now in the position to calculate the electromagnetic contributions to $K_{\ell 3}$ and $K_{\ell 4}$ decays where all constraints imposed by chiral symmetry are taken into account. In spite of our large ignorance of the actual values of the electromagnetic low-energy couplings, it will often be possible to relate the electromagnetic contributions to different processes. For specific combinations of observables one might even find parameter-free predictions. Simple examples of this kind have been given for the $P_{\ell 2}$ decays[1]. In some fortunate cases simple order-of-magnitude estimates for the electromagnetic couplings based on chiral dimensional analysis may even be sufficient.

Secondly, a further major task for the next future is, of course, the determination of the physical values of the electromagnetic low-energy coupling constants in the standard model. In contrast to the QCD low-energy couplings $L_1^r, \cdots L_{10}^r$ which are rather well determined from experimental input and large N_c arguments, only very little is known so far in the electromagnetic sector. First attempts to estimate some of the Urech constants K_i can be found in[11–13]. As far as the constants X_i are concerned, the recent analysis[14] of the counterterms contributing to the decay processes of light neutral pseudoscalars into charged lepton pairs raises hopes that reliable estimates for these constants can be achieved within a large-N_c approach.

REFERENCES

1. M. Knecht, H. Neufeld, H. Rupertsberger, and P. Talavera, "Chiral Perturbation Theory with Virtual Photons and Leptons," hep-ph/9909284.
2. J. Gasser, and H. Leutwyler, "Chiral Perturbation Theory: Expansion in the Mass of the Strange Quark," Nucl. Phys. B **250**, 465 (1985).
3. A. Urech, "Virtual Photons in Chiral Perturbation Theory," Nucl. Phys. B **433**, 234 (1995).
4. H. Neufeld, and H. Rupertsberger, "Isospin Breaking in Chiral Perturbation Theory and the Decays $\eta \to \pi\ell\nu$ and $\tau \to \eta\pi\nu$," Z. Phys. C **68**, 91 (1995).
5. H. Neufeld, and H. Rupertsberger, "The Electromagnetic Interaction in Chiral Perturbation Theory," Z. Phys. C **71**, 131 (1996).
6. M. Zeller, "Kaon Decays," plenary talk at this meeting.
7. G. Pancheri, "Meson Physics at DAPHNE," plenary talk at this meeting.
8. G. Ecker, J. Gasser, A. Pich, and E. de Rafael, "The Role of Resonances in Chiral Perturbation Theory," Nucl Phys. B **321**, 311 (1989).
9. H. Neufeld, J. Gasser, and G. Ecker, "The One-Loop Functional as a Berezinian," Phys. Lett. B **438**, 106 (1998).
10. H. Neufeld, "The Super-Heat-Kernel Expansion and the Renormalization of the Pion–Nucleon Interaction," Eur. Phys. J. C **7**, 355 (1999).
11. R. Baur, and R. Urech, "On the Corrections to Dashen's Theorem," Phys. Rev. D **53**, 6552 (1996).
12. R. Baur, and R. Urech, "Resonance Contributions to the Electromagnetic Low-Energy Constants of Chiral Perturbation Theory," Nucl. Phys. B **499**, 319 (1997).
13. B. Moussallam, "A Sum Rule Approach to the Violation of Dashen's Theorem," Nucl. Phys. B **504**, 381 (1997).
14. M. Knecht, S. Peris, M. Perrottet, and E. de Rafael, "Decay of Pseudoscalars into Lepton Pairs and Large-N_c QCD," hep-ph/9908283.

Electromagnetic Corrections to Low-Energy $\pi\pi$ Scattering

M. Knecht*
Centre de Physique Théorique, CNRS Luminy, Case 907
F-13288 Marseille Cedex 9, France

Abstract

Electromagnetic corrections to the low-energy $\pi^+\pi^- \to \pi^0\pi^0$ scattering amplitude at next-to-leading order in the chiral expansion are reviewed. Their effect on the corresponding scattering lengths are estimated and compared to the two-loop strong interaction contributions.

INTRODUCTION

The Chiral Perturbation Theory (ChPT) analyses, in both the generalized[1,2] and the standard[3,4] frameworks, of two-loop effects in low-energy $\pi\pi$ scattering lead to strong interaction corrections which are rather small as compared to the leading order and one-loop contributions, of the order of 5% in the case of the S wave scattering lengths a_0^0 and a_0^2, for instance. This leads one to expect that higher order corrections to these quantities are well under control and can be safely neglected. However, these calculations were undertaken without taking into account isospin breaking effects, coming either from the mass difference between the u and d quarks, or from the electromagnetic interaction. The smallness of the two-loop corrections naturally raises the question of how they compare to these isospin breaking effects. The quark mass difference induces corrections of the order $\mathcal{O}((m_d - m_u)^2)$, which are expected to be negligible, as already known to be the case for the pion mass difference $M_{\pi^\pm} - M_{\pi^0}$, the latter being in fact dominated by electromagnetic effects due to the virtual photon cloud[5].

In the present contribution, we shall review the status of radiative corrections to the amplitude $\pi^+\pi^- \to \pi^0\pi^0$[6]. The reason why we focus on the latter comes from the fact that it directly appears in the expression of the lifetime of the $\pi^+\pi^-$ dimeson atom[7–10] (see in particular the last of these references), that will be measured by the DIRAC experiment at CERN[11,12].

VIRTUAL PHOTONS IN ChPT: THE GENERAL FRAMEWORK

The general framework for a systematic study of radiative corrections in ChPT has been described in[13,14]. It consists in writing down a low-momentum representation for the generating functional of QCD Green's functions of quark bilinears in the presence of the electromagnetic field,

$$e^{i\mathcal{Z}[v_\mu,a_\mu,s,p,Q_L,Q_R]} = \int \mathcal{D}[\mu]_{QCD}\mathcal{D}[A_\mu]e^{i\int d^4x\mathcal{L}}, \tag{1}$$

with

$$\mathcal{L} = \mathcal{L}^0_{QCD} + \mathcal{L}^0_\gamma + \bar{q}\gamma^\mu[v_\mu + \gamma_5 a_\mu]q - \bar{q}[s - i\gamma_5 p]q + A_\mu[\overline{q_L}\gamma^\mu Q_L q_L + \overline{q_R}\gamma^\mu Q_R q_R]. \tag{2}$$

Here $\mathcal{L}^0_{QCD}$ is the QCD lagrangian with N_f flavours of massless quarks, while $\mathcal{L}^0_\gamma$ is the Maxwell lagrangian of the photon field. The coupling of the latter to the left-handed and right-handed quark fields, $q_{L,R} = \frac{1\mp\gamma_5}{2}q$, occurs via the spurion sources $Q_{L,R}(x)$. Under local $SU(N_F)_L \times SU(N_f)_R$ chiral transformations $(g_L(x), g_R(x))$, they transform as (the transformation properties of the vector (v_μ), axial (a_μ), scalar (s) and pseudoscalar (p) sources can be found in Ref.[15])

$$q_I(x) \to g_I(x)q_I(x)\,,\ Q_I(x) \to g_I(x)Q_I(x)g_I(x)^+\,,\ I = L, R, \tag{3}$$

so that the generating functional $\mathcal{Z}$ remains invariant (up to the usual Wess-Zumino term). Thus, although the electromagnetic interaction represents an explicit breaking of chiral

*Work supported in part by TMR, EC-contract No. ERBFMRX-CT980169 (EURODAPHNE).

symmetry, this breaking occurs in a well defined way, which is precisely the information encoded in the transformation properties of Eq. 3, much in the same way as the transformation properties of the scalar source $s(x)$ conveys the information on how the quark masses break chiral symmetry. At the end of the calculation, the sources $v_\mu(x)$, $a_\mu(x)$ and $p(x)$ are set to zero, $s(x)$ becomes the diagonal quark mass matrix, while the electromagnetic spurions are turned into the diagonal charge matrix of the quarks. Additional symmetries of $\mathcal{Z}$ consist of the discrete transformations like parity and charge conjugation. Finally, $\mathcal{L}$ is invariant under an additional charge conjugation type symmetry, which however affects only the photon field and the electromagnatic spurion sources,

$$Q_{L,R} \to -Q_{L,R}(x)\,,\ A_\mu(x) \to -A_\mu(x)\,. \tag{4}$$

The low-energy representation of $\mathcal{Z}$ is constructed systematically in an expansion in powers of momenta, of quark masses and of the electromagnetic coupling, by computing tree and loop graphs with an effective lagrangian $\mathcal{L}_{\rm eff}$ involving the $N_f \times N_f$ matrix $U(x)$ of pseudoscalar fields, and constrained by the chiral symmetry properties as well as the above discrete symmetries.

At lowest order, in the counting scheme where the electric charge e and the spurions $Q_{L,R}(x)$ count as $\mathcal{O}(\mathrm{p})$, the effective lagrangian is thus simply given by (for the notation, we follow[13,6])

$$\mathcal{L}_{\rm eff}^{(2)} = \frac{F^2}{4}\langle\, d^\mu U^+ d_\mu U + \chi^+ U + U^+\chi\,\rangle - \frac{1}{4}F^{\mu\nu}F_{\mu\nu} + C\,\langle\, Q_R U Q_L U^+\,\rangle\,. \tag{5}$$

The effect of the electromagnetic interaction is contained in the covariant derivative d_μ, defined as $d_\mu U = \partial_\mu U - i(v_\mu + Q_R A_\mu + a_\mu)U + iU(v_\mu + Q_L A_\mu - a_\mu)$, and in the low-energy constant C, which at this order is responsible for the mass difference of the charged and neutral pions,

$$\Delta_\pi \equiv M_{\pi^\pm}^2 - M_{\pi^0}^2 = 2Ce^2/F^2. \tag{6}$$

In fact, for the case of two light flavours ($N_f = 2$), to which we restrict ourselves from now on, this is the only direct effect induced by this counterterm. Of course, this mass splitting will in turn modify the kinematics of the low-energy $\pi\pi$ amplitudes and the corresponding scattering lengths. The details of this lowest order analysis can be found in Ref.[6]. Here, we shall rather consider the structure of the effective theory at next-to-leading order. Besides the counterterms described by the well known low-energy constants l_i[16], there are now, if we restrict ourselves to constant spurion sources, 11 additional counterterms at order $\mathcal{O}(e^2\mathrm{p}^2)$, and three more at order $\mathcal{O}(e^4)$. The latter contribute only to the scattering amplitudes involving charged pions alone. The complete list of these counterterms k_i, $i = 1, ...14$ and of their β-function coefficients can be found in Refs.[6,17].

RADIATIVE CORRECTIONS TO THE ONE LOOP $\pi^+\pi^- \to \pi^0\pi^0$ AMPLITUDE

The computation of the amplitude $\mathcal{A}^{+-;00}(s,t,u)$ for the process $\pi^+\pi^- \to \pi^0\pi^0$, including corrections of order $\mathcal{O}(e^2\mathrm{p}^2)$ and of order $\mathcal{O}(e^4)$, is then a straightforward exercice in quantum field theory. The explicit expressions can be found in Ref.[6] and will not be reproduced here. Let us rather discuss some features of the one-photon exchange graph of Fig. 1, which induces an electromagnetic correction to the strong vertex. This graph contains both the long range Coulomb interaction between the charged pions, and an infrared singularity. The latter is treated in the usual way, the physical, infrared finite, observable being the cross section for $\pi^+\pi^- \to \pi^0\pi^0$ with the emission of soft photons (one soft photon is enough at the order at which we are working here). The Coulomb force leads to a singular behaviour of the amplitude $\mathcal{A}^{+-;00}(s,t,u)$ at threshold (q denotes the momentum of the charged pions in the center of mass frame),

$$Re\mathcal{A}^{+-;00}(s,t,u) = -\frac{4M_{\pi^\pm}^2 - M_{\pi^0}^2}{F_\pi^2}\cdot\frac{e^2}{16}\cdot\frac{M_{\pi^\pm}}{q} + Re\mathcal{A}_{\rm thr}^{+-;00} + O(q)\,, \tag{7}$$

with

$$
\begin{aligned}
Re\mathcal{A}^{+-;00}_{\rm thr} &= 32\pi\left[-\frac{1}{3}(a^0_0)_{\rm str}+\frac{1}{3}(a^2_0)_{\rm str}\right]-\frac{\Delta_\pi}{F^2_\pi}+\frac{e^2M^2_{\pi^0}}{32\pi^2F^2_\pi}\,(30-3\mathcal{K}^{\pm0}_1+\mathcal{K}^{\pm0}_2)\\
&\quad-\frac{\Delta_\pi}{48\pi^2F^4_\pi}\,[M^2_{\pi^0}(1+4\bar{l}_1+3\bar{l}_3-12\bar{l}_4)-6F^2_\pi e^2(10-\mathcal{K}^{\pm0}_1)]\\
&\quad+\frac{\Delta^2_\pi}{480\pi^2F^4_\pi}\,[212-40\bar{l}_1-15\bar{l}_3+180\bar{l}_4]\,, \qquad (8)
\end{aligned}
$$

and $(a^0_0)_{\rm str}$ and $(a^2_0)_{\rm str}$ denote the S wave scattering lengths in the presence of the strong interactions only, but expressed, for convention reasons, in terms of the charged pion mass[16],

$$
\begin{aligned}
(a^0_0)_{\rm str} &= \frac{7M^2_{\pi^\pm}}{32\pi F^2_\pi}\left\{1+\frac{5}{84\pi^2}\,\frac{M^2_{\pi^\pm}}{F^2_\pi}\left[\bar{l}_1+2\bar{l}_2-\frac{3}{8}\bar{l}_3+\frac{21}{10}\bar{l}_4+\frac{21}{8}\right]\right\}\\
(a^2_0)_{\rm str} &= -\frac{M^2_{\pi^\pm}}{16\pi F^2_\pi}\left\{1-\frac{1}{12\pi^2}\,\frac{M^2_{\pi^\pm}}{F^2_\pi}\left[\bar{l}_1+2\bar{l}_2-\frac{3}{8}\bar{l}_3-\frac{3}{2}\bar{l}_4+\frac{3}{8}\right]\right\}, \qquad (9)
\end{aligned}
$$

corresponding to the numerical values (we use $F_\pi = 92.4$ MeV) $(a^0_0)_{\rm str} = 0.20 \pm 0.01$ and $(a^2_0)_{\rm str} = -0.043 \pm 0.004$, respectively[16]. The quantity $Re\mathcal{A}^{+-;00}_{\rm thr}$, which is by itself free of the infrared divergence mentioned above, appears directly in the lifetime of the pionium atom[10], the long range Coulomb interaction being, in that case, absorbed by the bound state dynamics. The contributions of the low-energy constants k_i are contained in the two quantities $\mathcal{K}^{\pm0}_1$ and $\mathcal{K}^{\pm0}_2$. Naive dimensional estimates lead to $(e^2F^2_\pi/M^2_{\pi^0})\,\mathcal{K}^{\pm0}_1 = 1.8\pm0.9$ and $(e^2F^2_\pi/M^2_{\pi^0})\,\mathcal{K}^{\pm0}_2 = 0.5 \pm 2.2$. With these estimates, one obtains[6]

$$
\frac{1}{32\pi}\,ReA^{+-;00}_{\rm thr}-\left[-\frac{1}{3}(a^0_0)_{\rm str}+\frac{1}{3}(a^2_0)_{\rm str}\right] = (-1.2\pm0.7)\times10^{-3}\,, \qquad (10)
$$

whereas the two-loop correction to the same combination of scattering lengths appearing between brackets amounts to $\sim -4\times10^{-3}$. For a more careful evaluation of the contribution of the counterterms k_i to $ReA^{+-;00}_{\rm thr}$, see[18].

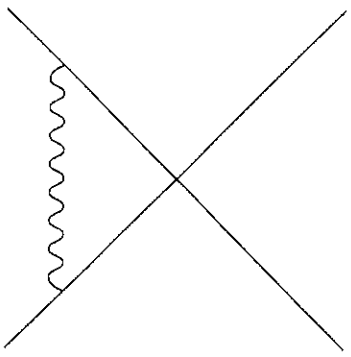

Fig. 1. The one photon exchange electromagnetic correction to the strong vertex.

CONCLUSION

We have evaluated the radiative corrections of order $\mathcal{O}(e^2\mathrm{p}^2)$ and of order $\mathcal{O}(e^4)$ to the amplitude $\mathcal{A}^{+-;00}(s,t,u)$, which is relevant for the description of the pionium lifetime. Similar results for the scattering process involving only neutral pions can be found in Refs.[6,17]. The formalism presented here for the case $N_f = 2$ has also been applied to the study of radiative corrections to the pion form factors[19]. Radiative corrections for the scattering amplitudes involving only charged pions, which would be relevant for the $2p-2s$ level-shift of pionium, for instance, have however not been worked out so far.

Information on the low-energy scattering of pions can only be obtained in an indirect way, either from the pionium lifetime, or from $K_{\ell4}$ decays. This last process, however,

has electromagnetic corrections of its own, which are only partly covered by the present analysis. A systematic framework devoted to the study of radiative correction for the semi-leptonic processes has been presented in Refs.[20,21].

REFERENCES

1. M. Knecht, B. Moussallam, J. Stern and N.H. Fuchs, "The low-energy $\pi\pi$ amplitude to one and two loops", Nucl. Phys. **B457**, 513 (1995).
2. M. Knecht, B. Moussallam, J. Stern and N.H. Fuchs, "Determination of two-loop $\pi\pi$ scattering amplitude parameters", Nucl. Phys. **B471**, 445 (1996).
3. J. Bijnens, G. Colangelo, G. Ecker, J. Gasser and M. Sainio, "Elastic $\pi\pi$ scattering to two loops", Phys. Lett. **B374**, 210 (1996).
4. J. Bijnens, G. Colangelo, G. Ecker, J. Gasser and M. Sainio, "Pion-pion scattering at low energy", Nucl. Phys. **508**, 263 (1997); ibid **B517**, 639 (1998) (erratum).
5. J. Gasser and H. Leutwyler, "Quark masses", Phys. Rep. **87**, 77 (1982).
6. M. Knecht and R. Urech, "Virtual photons in low-energy $\pi\pi$ scattering", Nucl. Phys. **B519**, 329 (1998).
7. H. Jallouli and H. Sazdjian, "Relativistic effects in the pionium lifetime", Phys. Rev. **D58**, 014011 (1998); ibid. **D58**, 099901 (1998) (erratum).
8. M.A. Ivanov, V.E. Lyubovitsky, E.Z. Lipartia and A. Rusetsky, "$\pi^+\pi^-$ atom in chiral perturbation theory", Phys. Rev. **D58**, 0904024 (1998).
9. D. Eiras and J. Soto, "Effective field theory approach to pionium", hep-ph/9905543, and J. Soto, contribution to these proceedings.
10. A. Gall, J. Gasser, V.E. Lyubovitsky and A. Rusetsky, "On the lifetime of the $\pi^+\pi^-$ atom", Phys. Lett. **B462**, 335 (1999).
    V. E. Lyubovitsky, "Hadronic atoms in QCD", contribution to these proceedings.
    A. Rusetsky, "Spectrum and decay of hadronic atoms", contribution to these proceedings.
11. B. Adeva et al., Proposal to the SPSLC, CERN/SPSLC 95-1 (1995).
12. A. Lanaro, "Lifetime measurement of dimeson atoms with the DIRAC experiment", contribution to these proceedings.
13. R. Urech, " Virtual photons in chiral perturbation theory", Nucl. Phys. **B433**, 234 (1995).
14. H. Neufeld and H. Rupertsberger, "Isospin breaking in chiral perturbation theory and the decays $\eta \to \pi\ell\nu$ and $\tau \to \eta\pi\nu$", Z. Phys. **C68**, 91 (1995).
    H. Neufeld and H. Rupertsberger, "The electromagnetic interaction in chiral perturbation theory", Z. Phys. **C71**, 131 (1995).
15. J. Gasser and H. Leutwyler, "Chiral perturbation theory: expansion in the mass of the strange quark", Nucl. Phys. **B250**, 465 (1985).
16. J. Gasser and H. Leutwyler, "Chiral perturbation theory to one loop", Ann. Phys. **158**, 142 (1984).
17. U.-G. Meißner, G. Müller and S. Steininger "Virtual photons in SU(2) chiral perturbation theory and electromagnetic corrections to $\pi\pi$ scattering", Phys. lett. **B406**, 154 (1997); ibid **B407**, 454 (1997) (erratum).
18. J. Gasser, V.E. Lyubovitsky and A. Rusetsky, "Numerical analysis of the $\pi^+\pi^-$ atom lifetime in ChPT", preprint BUTP-99/20 and hep-ph/9910438.
19. B. Kubis and U.-G. Meißner, "Virtual photons in the pion form factors and the energy-momentum tensor", hep-ph/9908261.
20. M. Knecht, H. Neufeld, H. Rupertsberger and P. Talavera, "Chiral perturbation theory with virtual photons and leptons", hep-ph/9909284 and Eur. Phys. J. **C**, to appear.
21. H. Neufeld, "Chiral perturbation theory with photons and leptons", contribution to these proceedings.

Spectrum and Decays of Hadronic Atoms

J. Gasser
Institute for Theoretical Physics, University of Bern, Sidlerstrasse 5, CH-3012, Bern, Switzerland

V. E. Lyubovitskij*
Bogoliubov Laboratory of Theoretical Physics, Joint Institute for Nuclear Research, 141980 Dubna, Russia and
Department of Physics, Tomsk State University, 634050 Tomsk, Russia

and

A. Rusetsky
Institute for Theoretical Physics, University of Bern, Sidlerstrasse 5, CH-3012, Bern, Switzerland,
Bogoliubov Laboratory of Theoretical Physics, Joint Institute for Nuclear Research, 141980 Dubna, Russia and
HEPI, Tbilisi State University, 380086 Tbilisi, Georgia

Abstract

Using non relativistic effective Lagrangian techniques, we analyze the hadronic decay of the $\pi^+\pi^-$ atom and the strong energy-level shift of pionic hydrogen in the ground state. We derive general formulae for the width and level shift, valid at next-to-leading order in isospin breaking. The result is expressed in terms of hadronic threshold amplitudes that include isospin-breaking effects. In order to extract isospin symmetric scattering lengths from the data, we invoke chiral perturbation theory, that allows one to relate the scattering lengths to the threshold amplitudes.

Recent years have seen a growing interest in the study of hadronic atoms. At CERN, the DIRAC collaboration[1] aims to measure the $\pi^+\pi^-$ atom lifetime to 10% accuracy. This would allow one to determine the difference $a_0 - a_2$ of $\pi\pi$ scattering lengths with 5% precision. This measurement provides a crucial test for the large/small condensate scenario in QCD: should it turn out that the quantity $a_0 - a_2$ is different from the value predicted in standard ChPT[2], one has to conclude[3] that spontaneous chiral symmetry breaking in QCD proceeds differently from the widely accepted picture[4]. In the experiment performed at PSI[5], one has measured the strong energy-level shift and the total decay width of the $1s$ state of pionic hydrogen, as well as the $1s$ shift of pionic deuterium. Using the technique described in Ref.[5], these measurements yield[6] isospin symmetric πN scattering lengths to an accuracy which is unique for hadron physics: $a_{0+}^+ = (1.6 \pm 1.3) \times 10^{-3} M_{\pi^+}^{-1}$ and $a_{0+}^- = (86.8 \pm 1.4) \times 10^{-3} M_{\pi^+}^{-1}$. The scattering length a_{0+}^- may be used as an input in the Goldberger-Miyazawa-Oehme[7] sum rule to determine the πNN coupling constant[5,6]. A new experiment on pionic hydrogen[8] has recently been approved. It will allow one to measure the decay $A_{\pi^- p} \to \pi^0 n$ to much higher accuracy and thus enable one, in principle, to determine the πN scattering lengths from data on pionic hydrogen alone. This might vastly reduce the model-dependent uncertainties that come from the analysis of the three-body problem in $A_{\pi^- d}$. Finally, the DEAR collaboration[10] at the DAΦNE facility (Frascati) plans to measure the energy level shift and lifetime of the $1s$ state in $K^- p$ and $K^- d$ atoms - with considerably higher precision than in the previous experiment carried out at KEK[11] for $K^- p$ atoms. It is expected[10] that this will result in a precise determination of the $I = 0, 1$ S-wave scattering lengths - although, of course, one will again be faced with the three-body problem already mentioned. It will be a challenge for theorists to extract from this new information on the $\bar{K}N$ amplitude at threshold a more precise value of e.g. the isoscalar kaon-sigma term and of the strangeness content of the nucleon[12].

*Present address: Institute of Theoretical Physics, University of Tübingen, Auf der Morgenstelle 14, D-72076 Tübingen, Germany

We now turn to *theoretical* investigations of hadronic atoms. At leading order in isospin breaking, the energy-level shift and the decay width of these atoms can be expressed in terms of the strong hadronic scattering lengths through the well-known formulae by Deser *et al.*[13]. More precisely, these formulae relate the ground state level shift - induced by the strong interaction - and its partial decay width into neutral hadrons (e.g., $A_{\pi^+\pi^-} \to \pi^0\pi^0$, $A_{\pi^-p} \to \pi^0 n$) to the corresponding isospin combinations of strong scattering lengths,

$$\Delta E_{\rm str} \sim \Psi_0^2 \,{\rm Re}\, a_{cc}\,, \qquad \Gamma_{c0} \sim ({\rm phase\ space}) \times \Psi_0^2\, |a_{c0}|^2\,. \tag{1}$$

Here, Ψ_0 denotes the value of the Coulomb wave function at the origin, and a_{cc}, a_{c0} stand for the relevant isospin combinations of strong scattering lengths. We have used the notation "c" for "charged" (e.g., $\pi^+\pi^-$, π^-p) and "0" for "neutral" (e.g., $\pi^0\pi^0$, $\pi^0 n$) channels. The accuracy of these leading-order formulae is however not sufficient to fully exploit existing and forthcoming high-precision data on hadronic atoms. Indeed, for that purpose, one has to evaluate isospin-breaking corrections at next-to-leading order. The aim of the present talk is to show how this can be achieved.

Recently, using a non relativistic effective Lagrangian framework, a general expression for the decay width $\Gamma_{A_{2\pi}\to\pi^0\pi^0}$ of the $1s$ state of the $\pi^+\pi^-$ atom was obtained at next-to-leading order in isospin-breaking[14]. We denote the fine-structure constant α and the quark mass difference squared $(m_d - m_u)^2$ by the common symbol δ. Then, the decay width is written in the following form*,

$$\begin{aligned}
\Gamma_{A_{2\pi}\to\pi^0\pi^0} &= \frac{2}{9}\,\alpha^3 p^\star \mathcal{A}_{\pi\pi}^2 (1 + K_{\pi\pi})\,, \qquad \mathcal{A}_{\pi\pi} = a_0 - a_2 + O(\delta)\,, \\
K_{\pi\pi} &= \frac{\Delta M_\pi^2}{9 M_{\pi^+}^2}\,(a_0 + 2a_2)^2 - \frac{2\alpha}{3}\,(\ln\alpha - 1)\,(2a_0 + a_2) + o(\delta)\,.
\end{aligned} \tag{2}$$

Here $p^\star = (M_{\pi^+}^2 - M_{\pi^0}^2 - \frac{1}{4}M_{\pi^+}^2\alpha^2)^{1/2}$, and a_I $(I = 0, 2)$ denote the strong $\pi\pi$ scattering lengths in the channel with total isospin I, and the quantity $\mathcal{A}_{\pi\pi}$ is calculated as follows[14]. One calculates the relativistic amplitude for the process $\pi^+\pi^- \to \pi^0\pi^0$ at $O(\delta)$ in the normalization chosen so that at $O(\delta^0)$ the amplitude at threshold coincides with the difference $a_0 - a_2$ of (dimensionless) S-wave $\pi\pi$ scattering lengths. Due to the presence of virtual photons, the amplitude is multiplied by an overall Coulomb phase that is removed. The real part of the remainder contains terms that diverge like $|\mathbf{p}|^{-1}$ and $\ln 2|\mathbf{p}|/M_{\pi^+}$ at $|\mathbf{p}| \to 0$ ($\mathbf{p}$ denotes the relative 3-momentum of charged pion pairs). The quantity $\mathcal{A}_{\pi\pi}$ is obtained by subtracting these divergent pieces, and by then evaluating the remainder at $\mathbf{p} = 0$. We shall refer to $\mathcal{A}_{\pi\pi}$ as the physical scattering amplitude at threshold.

A few remarks are in order. As it is seen explicitly from Eq. (2), one can directly extract the value of $\mathcal{A}_{\pi\pi}$ from the measurement of the decay width, because the correction $K_{\pi\pi}$ is very small and the error introduced by it is negligible. We emphasize that in derivation of Eq. (2), chiral expansions have not been used. On the other hand, if one further aims to extract strong scattering lengths from data, one may invoke chiral perturbation theory (ChPT) and to relate the quantities $\mathcal{A}_{\pi\pi}$ and $a_0 - a_2$ order by order in the chiral expansion. This requires the evaluation of isospin-breaking corrections to the scattering amplitude.

The corrections to the hadronic atom characteristics, evaluated in this manner contain, in general, contributions which have not been taken into account so far within the potential scattering approach to the same problem[5,15]. An obvious candidate for these contributions is the effect coming from the direct quark-photon coupling that is encoded in the so-called "electromagnetic" low-energy constants (LEC's) in ChPT. A second effect is related to the convention-dependent definition of the isospin-symmetric world against which the isospin-breaking corrections are calculated. We adopt the widely used convention that the masses of the isospin multiplets $(\pi^\pm, \pi^0)$ and (p, n) in this world coincide with the masses of the charged particles in the real world. This definition induces a contribution to the isospin-breaking corrections in the level shifts and decay widths. We shall

*See V.E. Lyubovitskij's talk for the definition of symbols $O(x)$, $o(x)$.

display below both corrections explicitly in the case of the $\pi^- p$ energy-level shift, where these effects emerge already at tree level.

The investigation of the $\pi^- p$ atom is very similar to the procedure used in the description of the $\pi^+\pi^-$ atom[14]. In the following, we restrict ourselves to the case of the strong energy-level shift of the $\pi^- p$ atom in the ground state. Because the proton-neutron mass difference contains terms linear in $m_d - m_u$, we count α and $m_d - m_u$ as quantities of the same order, and denote them by the common symbol δ'. [Since this counting is merely a matter of convenience, our previous results on the $\pi^+\pi^-$ atom remain of course unaltered.] Further, for the energy shift of hadronic atoms, one can no longer neglect the electromagnetic contributions coming from transverse photons as it was done in the case of the width of the $\pi^+\pi^-$ atom. The reason for this can easily be seen from counting powers of α in the energy-level shift. The binding energy of the atom starts at $O(\alpha^2)$ (nonrelativistic value $E_{\rm NR} = -\frac{1}{2}\,\mu_c\alpha^2$, where μ_c denotes the reduced mass of $\pi^- p$ system), and the corresponding QED corrections start at $O(\alpha^4)$. According to Eq. (1), the leading-order strong energy-level shift is $\mathrm{O}(\alpha^3)$, while the next-to-leading order corrections start at $O(\alpha^4)$ and should therefore be treated on the same footing as the QED corrections[†]. QED corrections, however, are not considered here - we focus on the strong energy-level shift alone. For the latter, it is straightforward to obtain a general formula very similar to Eq. (2), that gives the strong energy-level shift including $O(\delta')$ corrections:

$$\Delta E_{\rm str} = -2\alpha^3\mu_c^2\,\mathcal{A}_{\pi N}\,(1 + K_{\pi N})\,, \tag{3}$$

where $K_{\pi N}$ is a quantity of order δ' (modulo logarithms) and can be expressed in terms of the S-wave πN scattering lengths a_{0+}^+ and a_{0+}^-. Since $K_{\pi N}$ is small, the error introduced by the uncertainty in the determination of a_{0+}^+, a_{0+}^- is negligible. The major uncertainty in the energy-level shift comes from the quantity $\mathcal{A}_{\pi N}$ whose definition is very similar to that of $\mathcal{A}_{\pi\pi}$. To evaluate this quantity, one has to calculate the relativistic scattering amplitude for the process $\pi^- p \to \pi^- p$ at $O(\delta')$, subtract all diagrams that are made disconnected by cutting one virtual photon line and remove the Coulomb phase. The real part of the remainder, as for the $\pi^+\pi^-$ case, contains singular pieces that behave like $|\mathbf{p}|^{-1}$ and $\ln|\mathbf{p}|/\mu_c$ that should be again subtracted ($\mathbf{p}$ denotes the relative 3-momentum of the $\pi^- p$ pair in CM). The rest - evaluated at $\mathbf{p} = 0$ - coincides, by definition, with $\mathcal{A}_{\pi N}$. [The normalization of the relativistic amplitude is chosen so that $\mathcal{A}_{\pi N} = a_{0+}^+ + a_{0+}^- + O(\delta')$.]

Further, to analyze the isospin-breaking corrections to the energy-level shift, we relate the physical scattering amplitude at threshold $\mathcal{A}_{\pi N}$ to the scattering lengths a_{0+}^+, a_{0+}^- in ChPT. At $O(p^2)$ in the chiral expansion, where the amplitude is determined by tree diagrams, this relation is remarkably simple. Constructed on the basis of the effective πN Lagrangian[16–18], the amplitude contains the pseudovector Born term $\mathcal{A}_{\pi N}^{\rm pv}$ with physical masses, and a contribution that contains a linear combination of $O(p^2)$ LEC's,

$$\begin{aligned}\mathcal{A}_{\pi N}^{(2)} &= a_{0+}^+ + a_{0+}^- + \epsilon_{\pi N}^{(2)} \\ &= \mathcal{A}_{\pi N}^{\rm pv} + 2\hat{m}B\kappa_1 c_1 + M_{\pi^+}^2(\kappa_2 c_2 + \kappa_3 c_3) + e^2(\sigma_1 f_1 + \sigma_2 f_2)\,,\end{aligned} \tag{4}$$

where the quantity B is related to the quark condensate, and where c_i (f_i) are strong (electromagnetic) LEC's from the $O(p^2)$ Lagrangian of ChPT. Furthermore, κ_i and σ_i denote isospin symmetric coefficients whose explicit expressions are not needed here. From Eq. (4), it is straightforward to visualize both mechanisms of isospin-breaking corrections to the hadronic atom observables, not included in potential approaches. The direct quark-photon coupling is encoded in the coupling constants f_i, whereas the effect of the mass tuning in the hadronic amplitude (described above) is due to the term proportional to

[†]There is one important exception to this rule. Though the vacuum polarization correction starts at $O(\alpha^5)$, it is amplified by a large factor $(\mu_c/m_e)^2$, where m_e denotes the electron mass. Since $\alpha\mu_c/m_e \sim 1$, this contribution is numerically as important as the leading-order strong contribution (see[5]). The graph responsible for this contribution can be, however, easily singled out and the contribution from it merely added to the final result.

$2\hat{m}B$. Indeed, at this order in the chiral expansion, one has $2\hat{m}B = M^2_{\pi^0}$. As we express the strong amplitude in terms of charged masses by convention, we write

$$2\hat{m}B = M^2_{\pi^+} - \Delta_\pi\,; \quad \Delta_\pi = M^2_{\pi^+} - M^2_{\pi^0}\,, \tag{5}$$

and obtain

$$\epsilon^{(2)}_{\pi N} = -\Delta_\pi\,\kappa_1 c_1 + e^2\,(\sigma_1 f_1 + \sigma_2 f_2) + O(\hat{m}\delta') + o(\delta')\,. \tag{6}$$

Estimates for the energy-level shift on the basis of the expression (6) will be presented elsewhere. Here we note that a simple order-of-magnitude estimate for f_1 shows that f_1 induces an uncertainty in the energy-level shift of roughly the same size as the total correction given in Ref.[5].

To summarize, we have applied a non relativistic effective Lagrangian approach to the study of $\pi^+\pi^-$ and π^-p atoms in the ground state. A general expression for the width $\Gamma_{A_{2\pi}\to\pi^0\pi^0}$ and for the strong level shift of pionic hydrogen has been obtained at next-to-leading order in isospin breaking. The sources of the isospin-breaking corrections in these quantities, complementary to ones already considered in the potential scattering theory approach, have been clearly identified.

Acknowledgments. V. E. L. thanks the Organizing Committee of MENU99 Symposium for financial support and the University of Bern, where this work was performed, for hospitality. This work was supported in part by the Swiss National Science Foundation, and by TMR, BBW-Contract No. 97.0131 and EC-Contract No. ERBFMRX-CT980169 (EURODAΦNE).

REFERENCES

1. B. Adeva *et al.*, CERN proposal CERN/SPSLC 95-1 (1995).
2. J. Gasser and H. Leutwyler, Phys. Lett. **B125**, 325 (1983); J. Bijnens, G. Colangelo, G. Ecker, J. Gasser, and M. E. Sainio, Phys. Lett. **B374**, 210 (1996).
3. M. Knecht, B. Moussallam, J. Stern, and N. H. Fuchs, Nucl. Phys. **B457**, 513 (1995); ibid. **B471**, 445 (1996).
4. M.Gell-Mann, R.J. Oakes, and B. Renner, Phys. Rev. **175**, 2195 (1968).
5. D. Sigg, A. Badertscher, P. F. A. Goudsmit, H. J. Leisi, and G. C. Oades, Nucl. Phys. **A609**, 310 (1996); H. J. Leisi, preprint ETHZ-IPP PR-98-11 (1998).
6. H.-Ch. Schröder *et al.*, preprint ETHZ-IPP PR-99-07 (1999), to appear in Phys. Lett. **B**.
7. M.L. Goldberger, H. Miyazawa, and R. Oehme, Phys. Rev. **99**, 986 (1955).
8. D. Gotta, talk at this conference.
9. J. Gasser, H. Leutwyler, M. P. Locher, and M. E. Sainio, Phys. Lett. **B213**, 85 (1988); J. Gasser, H. Leutwyler, and M. E. Sainio, Phys. Lett. **B253**, 252 (1991).
10. The DEAR collaboration (S. Bianco et al.), *The DEAR case*, preprint LNF-98/039(P).
11. M. Iwasaki *et al.*, Phys. Rev. Lett. **78**, 3067 (1997); Nucl. Phys. **A639**, 501 (1998).
12. P.M. Gensini, preprint hep-ph/9804344.
13. S. Deser, M. L. Goldberger, K. Baumann, and W. Thirring, Phys. Rev. **96**, 774 (1954).
14. A. Gall, J. Gasser, V.E. Lyubovitskij, and A. Rusetsky, Phys. Lett. **B462**, 335 (1999); J. Gasser, V.E. Lyubovitskij, A. Rusetsky, preprints BUTP-99/20, hep-ph/9910438 and BUTP-99/24, hep-ph/9910524. See V.E. Lyubovitskij's talk at this conference for earlier literature.
15. U. Moor, G. Rasche, and W. S. Woolcock, Nucl. Phys. **A587**, 747 (1995); A. Gashi, G. C. Oades, G. Rasche, and W. S. Woolcock, Nucl. Phys. **A628**, 101 (1998).
16. J. Gasser, M. E. Sainio, and A. Švarc, Nucl. Phys. **B307**, 779 (1998).
17. U.-G. Meißner and S. Steininger, Phys. Lett. **B419**, 403 (1998).
18. T. Becher and H. Leutwyler, Eur. Phys. J. **C9**, 643 (1999).

Asymmetry in the Anti-Quark Sea of the Proton and Comparison to Meson Models of the Nucleon - Results from Fermilab E866

L. Donald Isenhower
Abilene Christian University, ACU Box 27963, Abilene, TX 79699, USA

for the Fermilab E866(NuSea) Collaboration *

Abstract

The Fermilab dimuon experiment 866/NuSea measured Drell-Yan yields from an 800 GeV/c proton beam incident on liquid hydrogen and deuterium targets. Over 370,000 Drell-Yan muon pairs were recorded to measure the ratio σ_{D2}/σ_{H2}. By assuming charge symmetry and isospin conservation, one is able to use this ratio, along with existing structure functions, to extract the ratio $\bar{d}/\bar{u}$. The E866 measurement has excellent coverage of kinematic variables, especially Bjorken-x. A strong x dependence is observed in the ratio $\bar{d}/\bar{u}$, showing substantial enhancement of $\bar{d}$ with respect to $\bar{u}$ for $x < 0.2$, forcing the nucleon structure function parameterizations to be updated. Such an asymmetry has been compared to various models and should influence future models of the nucleon. It is noted that some pion-nucleon models show promise in predicting such behavior.

Fermilab E866(NuSea) has recently completed a measurement of the ratio of the cross section σ_{D2}/σ_{H2} for Drell-Yan muon pairs[1]. Since the Drell-Yan process involves the annihilation of a quark and an anti-quark, producing a virtual photon that in turn decays into a lepton pair, it is directly sensitive to the anti-quark sea of the nucleon. By assuming charge symmetry and isospin conservation, one is able to use this ratio, along with existing structure functions, to extract the ratio $\bar{d}/\bar{u}$. By measuring ratios, systematic errors are minimized.

Previous to E866 the NA51 experiment at CERN had obtained the result that the ratio $\bar{d}/\bar{u}$ was not equal to one[2], as had been assumed previously for the nucleon. While no known symmetry requires $\bar{u}$ to equal $\bar{d}$, a large $\bar{d}/\bar{u}$ asymmetry was not anticipated. The usual assumption was that the sea of q-$\bar{q}$ pairs is produced from gluon splitting. Since the mass difference of the up and down quark is small compared to the nucleon mass, nearly equal numbers of up and down pairs should result. Thus a large $\bar{d}/\bar{u}$ asymmetry requires a non-perturbative origin for an appreciable fraction of these light anti-quarks. It is this non-perturbative aspect that should be of interest to the pion-nucleon community.

To perform these measurements, E866 used a modified version of the 3-dipole spectrometer[4] employed in previous experiments E605, E772, and E789. The non-interacting beam protons were stopped in an internal beam dump. Immediately after the beam dump was an absorber wall which removed hadrons produced in the target and the dump. The detection system consisted of four tracking stations and a momentum analyzing magnet. Over 370,000 Drell-Yan events were recorded, using three different spectrometer settings optimized for low, intermediate and high mass muon pairs.

Some kinematic quantities commonly used to describe Drell-Yan events are the Feynman-x (x_F) and the dilepton mass (M) which are defined as :

$$x_F = \frac{p_{||}^{\gamma}}{p^{\gamma,max}} \approx \frac{p_{||}^{\gamma}}{\sqrt{s}/2} = x_1 - x_2 \tag{1}$$

and

$$M^2 = Q^2 \approx x_1 x_2 s \tag{2}$$

where $p_{||}^{\gamma}$ is the center of mass longitudinal momentum of the virtual photon, $p^{\gamma,max}$ is its maximum possible value, and s is the total four momentum squared of the initial nucleons. The proton-deuterium cross section is

$$\sigma^{pd} \approx \sigma^{pp} + \sigma^{pn} \tag{3}$$

*We wish to thank the Fermilab Particle Physics, Beams and Computing Divisions for their assistance in performing this experiment. This work was supported in part by the U.S. Department of Energy.

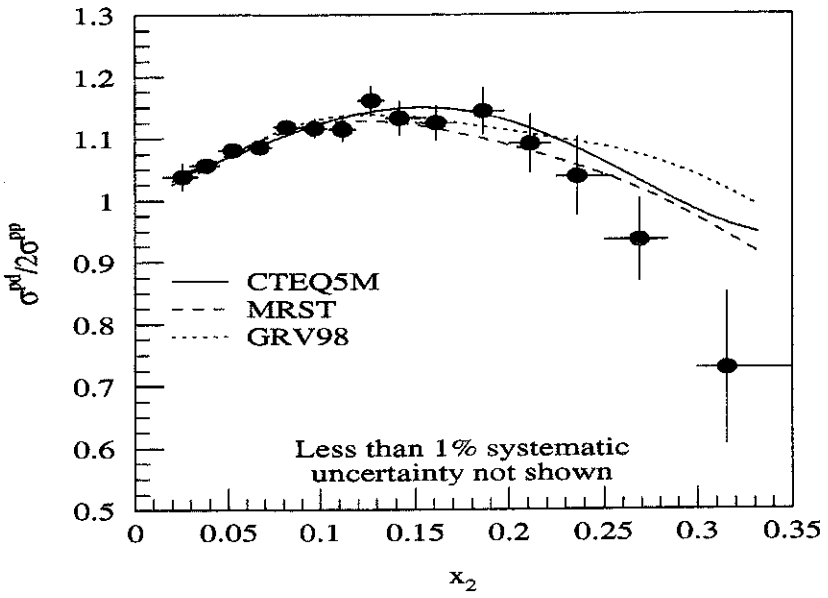

Figure. 1. The Drell-Yan cross section ratio versus x of the target parton. The results from all three mass settings have been combined. The error bars represent the statistical uncertainty. An additional one percent systematic uncertainty is common to all points. The curves are the calculated next-to-leading-order cross section ratios using various parameterizations of the proton. The bottom curve is calculated using CTEQ5M where $\bar{d} - \bar{u}$ has been forced to zero.

which ignores the small nuclear effects inside the deuterium nucleus. Using this approximation, the cross section ratio for DY produced in deuterium and hydrogen targets can be used to determine the ratio of $\bar{d}/\bar{u}$.

The NA51 result was determined at a single point for Bjorken-x, whereas E866 covers a range in the various kinematic variables. The three different magnet settings were used to accept different regions of the invariant mass of the muon pair, resulting in a large coverage of mass and Bjorken-x. Because of this extended coverage, the data from experiment E866 at Fermilab were the first to demonstrate a strong Bjorken-x dependence of the $\bar{d}/\bar{u}$ ratio. The published E866 results[3] used a single mass setting designed to accept high-mass dimuon pairs. Here all three data sets are averaged to provide more accurate measurements of $\bar{d}/\bar{u}$ and $\bar{d} - \bar{u}$[1].

The resulting ratio of the Drell-Yan cross section per nucleon for $p + d$ to that for $p + p$ is shown in Fig. 1 as a function of x_2, the momentum fraction (Bjorken-x) of the target quark in the parton model. (The Bjorken-x of the beam parton is denoted by x_1.) To eliminate contributions from the J/ψ and Υ resonance families, a cut on the muon pair mass, $M_{\mu^+\mu^-}$, was used. The data clearly show that the Drell-Yan cross section per nucleon for $p + d$ exceeds $p + p$ over an appreciable range in x_2.

The ratio $\bar{d}/\bar{u}$ was extracted iteratively by calculating the leading order Drell-Yan cross section ratio using a set of parton distribution functions (PDF) as input and adjusting $\bar{d}/\bar{u}$ until the calculated cross section ratio agreed with the measured value from data. The extracted $\bar{d}/\bar{u}$ ratio is shown in Fig. 2 along with the CTEQ4M[5] parameterization. A qualitative feature of the data, not seen in either CTEQ4M or MRS(R2)[7], is the rapid decrease towards unity of the $\bar{d}/\bar{u}$ ratio beyond $x = 0.2$. At $x = 0.18$, the extracted $\bar{d}/\bar{u}$ ratio is somewhat smaller than the value obtained by NA51. Such a large $\bar{d}/\bar{u}$ asymmetry cannot arise from perturbative effects[6]. Since the publication of the high mass results, the MRS, CTEQ, and GRV calculations have been updated[8–10] (only MRST is shown in Fig. 2).

The possible production mechanisms that can account for the observed excess of $\bar{d}$ quarks in the nucleon can be categorized as either perturbative or nonperturbative. While gluon splitting is a source of quark-antiquark pairs in the nucleon, it can not be the source

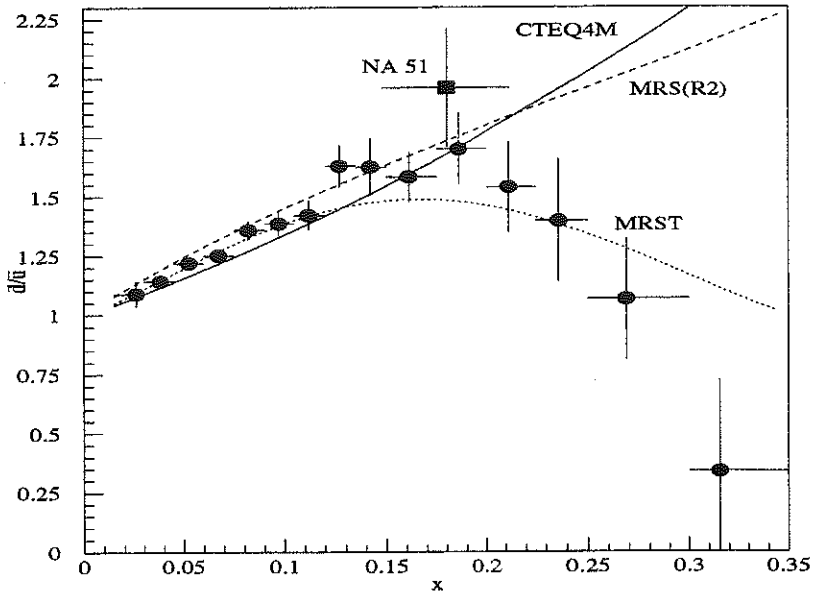

Figure. 2. $\bar{d}(x)/\bar{u}(x)$ versus x. The combined result from all three mass settings is shown along with three parameterizations[5,8,7]. The NA51[2] data point is also shown.

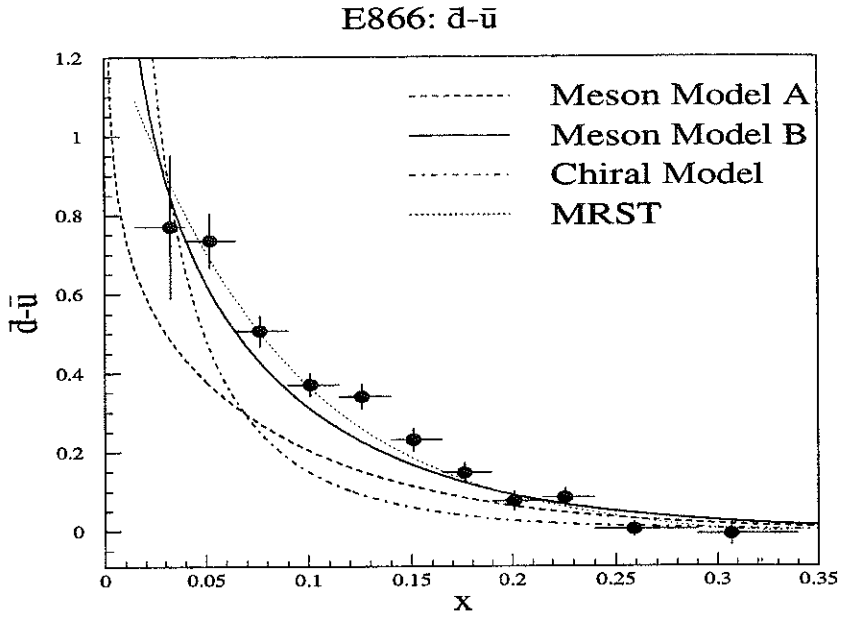

Figure. 3. $\bar{d}(x) - \bar{u}(x)$ versus x. The combined result from all three mass settings is shown along with three parameterizations.

of the large observed flavor asymmetry. Thus, some other non-perturbative processes must be responsible. As these nonperturbative mechanisms are considered, it is important to remember that they act in addition to the perturbative sources, which tends to dilute their effect. In effect the non-perturbative sources must be even stronger to account for the large asymmetries shown here.

The "Sullivan Process" citesullivan is a very natural explanation of the observed asymmetry. It is well known that the ground state of the proton can be written as a linear combination of a bare proton, a pion-nucleon combination, and pion-Delta combination. The domination of the pion-nucleon term over the pion-Delta term yields an excess of $\bar{d}$ quarks coming from the π^+; however, pion models predict a much larger $\bar{d}/\bar{u}$ ratio that observed in E866.

In Fig. 3 the value of $\bar{d}-\bar{u}$ is shown for two different meson models[11]. The two model calculations shown differ in the value for the dipole form factor $\Lambda_{\pi N\Delta}$. Model A has $\Lambda_{\pi N\Delta}$=$\Lambda_{\pi NN} = 1GeV$. Model B has $\Lambda_{\pi N\Delta}$=$0.8\Lambda_{\pi NN}$. From the figure it can be seen that the data prefer a softer $\Lambda_{\pi N\Delta}$[11]. More importantly, one can see that a meson model can do a reasonable job of describing the behavior of $\bar{d}-\bar{u}$ (e.g., see citeprl,nikolaev99,kumano98.

There is no contribution by gluons to first order for $\bar{d}-\bar{u}$ and PQCD first contributes at second order and is quantitatively small. So $\bar{d}-\bar{u}$ is primarily non-perturbative; however, pion models are only sensitive to $\bar{d}^{\pi}/\bar{u}^{\pi}$ and the perturbative processes become dominant at larger x. Also calculations for $\bar{d}/\bar{u}$ must include the contribution to the nucleon sea of the perturbative processes $g \rightarrow u\bar{u}, d\bar{d}$, which generate a symmetric sea. Thus the results of E866 should provide another area where pion-nucleon models can be tested for their ability to explain the structure of the nucleon. It is also important to point out that the valence quark distributions also changed in the new parton distribution parameterizations[8–10], especially for the down valence quark. Since E866, along with other measurements, show us that the nucleon cannot be considered being made up just of valence quarks plus gluons, pion-nucleon models should be checked to see that they can be consistent with the structure of the nucleon sea. Furthermore, the E866 results help demonstrate that to understand the nucleon one must take into account observations over a broad range of energies and types of interactions.

REFERENCES

1. R. S. Towell, Ph.D. Thesis, University of Texas, 1999.
2. The NA51 Collaboration, A. Baldit *et al.*, Phys. Lett. B **332**, 244 (1994).
3. The FNAL E866/NuSea Collaboration, E. A. Hawker *et al.*, Phys. Rev. Lett. **80**, 3715 (1998).
4. G. Moreno *et al.*, Phys. Rev. D **43**, 2815 (1991).
5. H.L. Lai *et al.*, Phys. Rev. D **55**, 1280 (1997).
6. D.A. Ross and C.T. Sachrajda, Nucl. Phys. B **149**, 497 (1979).
7. A. D. Martin, R. G. Roberts, and W. J. Stirling, Phys. Lett. B **387**, 419 (1996).
8. A. D. Martin, R. G. Roberts, W. J. Stirling, and R. S. Thorne, Eur. Phys. J. C **4**, 463 (1998).
9. H.L. Lai *et al.*, hep-ph/9903282.
10. M. Glück, E. Reya, and A. Vogt, Eur. Phys. J. C5, **461** (1998).
11. The FNAL E866/NuSea Collaboration, J. C. Peng *et al.*, Phys. Rev. D **58**, 092004 (1998).
12. J.D. Sullivan, Phys. Rev. D **5**, 1732 (1972).
13. N.N. Nikolaev, W. Schäfer, A. Szczurek, and J. Speth, Phys. Rev. **D60**, 014004-1 (1999).
14. S. Kumano, Phys. Rep. **303**, 183 (1998).

Parton Distributions, Form Factors and Compton Scattering

P. Kroll
Fachbereich Physik, Universität Wuppertal Gaußstrasse 20, D-42097 Wuppertal, Germany

Abstract

The soft physics approach to form factors and Compton scattering at moderately large momentum transfer is reviewed. It will be argued that in that approach the Compton cross section is given by the Klein-Nishina cross section multiplied by a factor describing the structure of the proton in terms of two new form factors. These form factors as well as the ordinary electromagnetic form factors represent moments of skewed parton distributions.

QCD provides three valence Fock state contributions to proton form factors, real (RCS) and virtual (VCS) Compton scattering off protons at large momentum transfer: a soft overlap term with an active quark and two spectators, the asymptotically dominant perturbative contribution where by means of the exchange of two hard gluons the quarks are kept collinear with respect to their parent protons and a third contribution that is intermediate between the soft and the perturbative contribution where only one hard gluon is exchanged and one of the three quarks acts as a spectator. Both the soft and the intermediate terms represent power corrections to the perturbative contribution. Higher Fock state contributions are suppressed. The crucial question is what is the relative strengths of the three contributions at experimentally accessible values of momentum transfer, i.e. at $-t$ of the order of 10 GeV^2? The pQCD followers assume the dominance of the perturbative contribution and neglect the other two contributions while the soft physics community presumes the dominance of the overlap contribution. Which group is right is not yet fully decided although comparison with the pion case[1] seems to favour a strong overlap contribution.

Let me turn now to the soft physics approach to Compton scattering. For Mandelstam variables, s, t and u, that are large on a hadronic scale the handbag diagram shown in Fig. 1 describes RCS and VCS. To see this it is of advantage to choose a symmetric frame of reference where the plus and minus light-cone components of Δ are zero. This implies $t = -\Delta_\perp^2$ as well as a vanishing skewdness parameter $\zeta = -\Delta^+/p^+$. To evaluate the skewed parton distributions (SPD) appearing in the handbag diagram and defined in[2], one may use a Fock state decomposition of the proton and sum over all possible spectator configurations. The crucial assumption is then that the soft hadron wave functions are dominated by virtualities in the range $|k_i^2| \lesssim \Lambda^2$, where Λ is a hadronic scale of the order of 1 GeV, and by intrinsic transverse parton momenta, $k_{\perp i}$, defined with respect to their parent hadron's momentum, that satisfy $k_{\perp i}^2/x_i \lesssim \Lambda^2$. Under this assumption factorisation of the Compton amplitude in a hard photon-parton subprocess amplitude and a soft proton matrix element is achieved[3]. This proton matrix element is described by new form factors specific to Compton scattering.

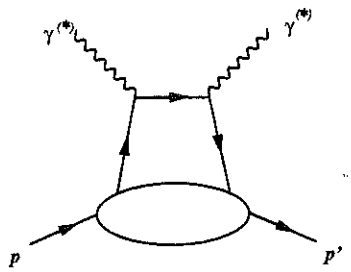

Figure. 1. The handbag diagram for Compton scattering. The momenta of the incoming and outgoing protons (photons) are denoted by p (q) and $p' = p + \Delta$ ($q' = q - \Delta$), respectively.

As a consequence of this result the Compton amplitudes conserving the proton helicity are given by

$$\mathcal{M}_{\mu'+,\mu+} \;=\; 2\pi\alpha_{\rm em}\left[\mathcal{H}_{\mu'+,\mu+}\,(R_V+R_A)\;+\;\mathcal{H}_{\mu'-,\mu-}\,(R_V-R_A)\right]\,. \tag{1}$$

Proton helicity flip is neglected. μ and μ' are the helicities of the incoming and outgoing photon in the photon-proton cms, respectively. The photon-quark subprocess amplitudes, $\mathcal{H}$, are calculated for massless quarks in lowest order QED. The form factors in Eq. (1), R_V and R_A, represent $1/x$-moments of SPDs at zero skewedness parameter. R_V is defined by

$$\begin{aligned}\sum_a e_a^2\int_0^1\frac{\mathrm{d}x}{x}\,p^+\int\frac{\mathrm{d}z^-}{2\pi}\,e^{i\,xp^+z^-}\,\langle p'|\,\overline{\psi}_a(0)\,\gamma^+\,\psi_a(z^-)-\overline{\psi}_a(z^-)\,\gamma^+\,\psi_a(0)\,|p\rangle\\ =R_V(t)\,\bar{u}(p')\,\gamma^+u(p)\;+R_T(t)\,\frac{i}{2m}\bar{u}(p')\sigma^{+\rho}\Delta_\rho u(p)\,,\end{aligned} \tag{2}$$

where the sum runs over quark flavours a (u, d, ...), e_a being the electric charge of quark a in units of the positron charge. R_T being related to proton helicity flips, is neglected in (1). There is an analogous equation for the axial vector proton matrix element, which defines the form factor R_A. Due to time reversal invariance the form factors R_V, R_A etc. are real functions.

As shown in[3] form factors can be represented as generalized Drell-Yan light-cone wave function overlaps. Assuming a plausible Gaussian $k_{\perp i}$-dependence of the soft Fock state wave functions, one can explicitly carry out the momentum integrations in the Drell-Yan formula. For simplicity one may further assume a common transverse size parameter, $\hat{a}$, for all Fock states. This immediately allows one to sum over them, without specifying the x_i-dependence of the wave functions. One then arrives at[3,4]

$$\begin{aligned}F_1(t) &= \sum_a e_a\int\mathrm{d}x\,\exp\left[\frac{1}{2}\hat{a}^2t\frac{1-x}{x}\right]\{q_a(x)-\bar{q}_a(x)\}\,,\\ R_V(t) &= \sum_a e_a^2\int\frac{\mathrm{d}x}{x}\,\exp\left[\frac{1}{2}\hat{a}^2t\frac{1-x}{x}\right]\{q_a(x)+\bar{q}_a(x)\}\,,\end{aligned} \tag{3}$$

and the analogue for R_A with $q_a+\bar{q}_a$ replaced by $\Delta q_a+\Delta\bar{q}_a$. q_a and Δq_a are the usual unpolarized and polarized parton distributions, respectively. The result for F_1 has been derived in Ref.[5] long time ago.

The only parameter appearing in (3) is the effective transverse size parameter $\hat{a}$; it is known to be about 1 GeV^{-1} with an uncertainty of about 20%. Thus, this parameter only allows some fine tuning of the results for the form factors. Evaluating, for instance, the form factors from the parton distributions derived by Glück et al. (GRV)[6] with $\hat{a}=1\,GeV^{-1}$, one already finds good results. Improvements are obtained by treating the lowest three Fock states explicitly with specified x-dependencies[3]. Results for t^2F_1 and t^2R_V obtained that way are displayed in Fig. 2. Both the scaled form factors, as well as t^2R_A, exhibit broad maxima and, hence, mimic dimensional counting rule behaviour in the t-range from about 5 to 15 GeV^2. The position, t_0, of the maximum of t^2F_i, where F_i is one of the soft form factors, is determined by the solution of the implicit equation

$$-t=4\hat{a}^{-2}\left\langle\frac{1-x}{x}\right\rangle^{-1}_{F_i,t}\,. \tag{4}$$

The mean value $\langle\frac{1-x}{x}\rangle$ comes out around 0.5 at $t=t_0$, hence, $t_0\simeq 8\hat{a}^2$. Since both sides of Eq. (4) increase with $-t$ the maximum of the scaled form factor, F_i, is quite broad. For very large momentum transfer the form factors turn gradually into the soft physics asymptotics $\sim 1/t^4$. This is the region where the perturbative contribution ($\sim 1/t^2$) takes the lead.

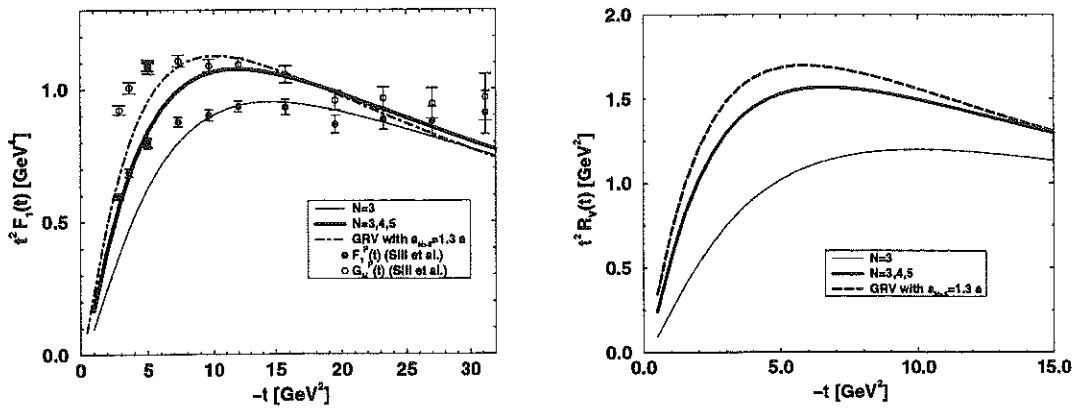

Figure. 2. The Dirac (left) and the vector Compton (right) form factor of the proton as predicted by the soft physics approach[3,7]. Data are taken from[8]. The data on the magnetic form factor, G_M, are shown in order to demonstrate the size of spin-flip effects.

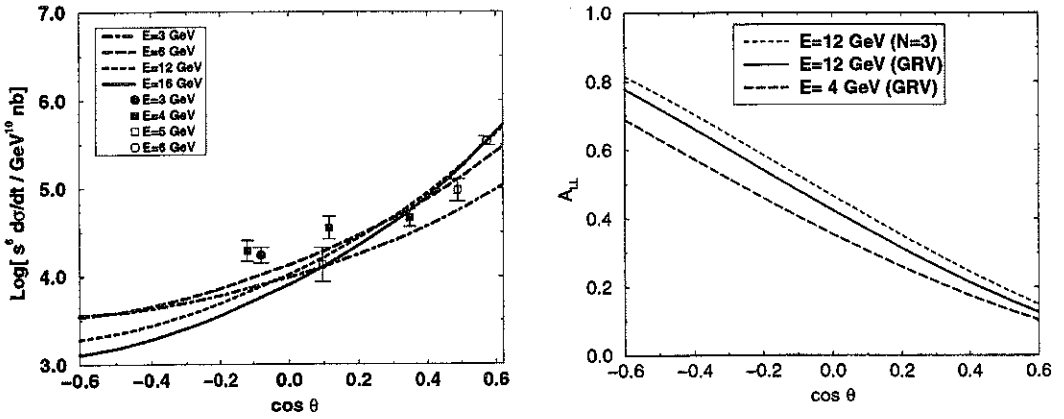

Figure. 3. The Compton cross section, scaled by s^6, (left) and the initial state helicity correlation $A_{\rm LL}$ (right) as predicted by the soft physics approach[3]. Data taken from[9].

The amplitude (1) leads to the RCS cross section

$$\frac{\mathrm{d}\sigma}{\mathrm{d}t} = \frac{\mathrm{d}\hat{\sigma}}{\mathrm{d}t}\left[\frac{1}{2}(R_V^2(t)+R_A^2(t)) - \frac{us}{s^2+u^2}(R_V^2(t)-R_A^2(t))\right]. \tag{5}$$

It is given by the Klein-Nishina cross section

$$\frac{\mathrm{d}\hat{\sigma}}{\mathrm{d}t} = \frac{2\pi\alpha_{\rm em}^2}{s^2}\frac{s^2+u^2}{-us} \tag{6}$$

multiplied by a factor that describes the structure of the proton in terms of two form factors. Evidently, if the form factors scale as $1/t^2$, the Compton cross section would scale as s^{-6} at fixed cm scattering angle θ. In view of the above discussion (see also Fig. 2) one therefore infers that approximate dimensional counting rule behaviour holds in a limited range of energy. The magnitude of the Compton cross section is quite well predicted as is revealed by comparison with the admittedly old data[9] measured at rather low values of s, $-t$ and $-u$ (see Fig. 3).

The soft physics approach also predicts characteristic spin dependencies of the Compton process[10]. Of particular interest is the initial state helicity correlation

$$A_{\rm LL}\frac{\mathrm{d}\sigma}{\mathrm{d}t} = \frac{2\pi\alpha_{\rm em}^2}{s^2}R_V(t)R_A(t)\left(\frac{u}{s}-\frac{s}{u}\right). \tag{7}$$

Approximately, $A_{\rm LL}$ is given by the corresponding subprocess helicity correlation $\hat{A}_{\rm LL} = (s^2 - u^2)/(s^2 + u^2)$ multiplied by the dilution factor $R_A(t)/R_V(t)$. Thus, measurements of both the cross section and the initial state helicity correlation allows one to isolate the two form factors R_V and R_A experimentally[11]. In Fig. 3 predictions for $A_{\rm LL}$ are shown.

Other polarization observables as well as the VCS contribution to the unpolarized $ep \to ep\gamma$ cross section have also been predicted in[10]. In addition to VCS the full $ep \to ep\gamma$ cross section receives substantial contributions from the Bethe-Heitler process, in which the final state photon is radiated by the electron. Dominance of the VCS contribution requires high energies, small values of $|\cos\theta|$ and an out-of-plane experiment, i.e. an azimuthal angle larger than about 60°. For VCS there are characteristic differences to the diquark model[12], the only other available study of VCS. In the soft physics approach all amplitudes are real (if the photon-parton subprocess is calculated to lowest order perturbation theory[3,10]) while in the diquark model there are perturbatively generated phase differences among the VCS amplitudes. So, for instance, the beam asymmetry for $ep \to ep\gamma$

$$A_{\rm L} = \frac{{\rm d}\sigma(+) - {\rm d}\sigma(-)}{{\rm d}\sigma(+) + {\rm d}\sigma(-)}\,, \tag{8}$$

where the labels + and − denote the lepton beam helicity, is zero in the soft physics approachin contrast to the diquark model where a sizeable beam asymmetry is predicted.

In summary, the soft physics approach leads to a simple representation of form factors and to detailed predictions for RCS and VCS. These predictions exhibit interesting features and characteristic spin dependences with marked differences to other approaches. Dimensional counting rule behaviour for form factors, Compton scattering and perhaps for other exlusive observables is mimicked in a limited range of momentum transfer. This tells us that it is premature to infer the dominance of perturbative physics from the observed scaling behaviour, see also[13]. The soft contributions although formally representing power corrections to the asymptotically leading perturbative ones, seem to dominate form factors and Compton scattering for momentum transfers around 10 GeV^2 (see the discussion in[7,14]). However, a severe confrontation of this approach with accurate large momentum transfer data on RCS and VCS is still pending.

REFERENCES

1. R. Jakob and P. Kroll, Phys. Lett. **B315**, 463 (1993), Erratum *ibid.* **B319**, 545 (1993); P. Kroll and M. Raulfs, Phys. Lett. **B387**, 848 (1996); V. Braun and I. Halperin, Phys. Lett. **B328**, 457 (1994); L.S. Kisslinger and S.W. Wang, Nucl. Phys. **B399**, 63 (1993).
2. D. Müller *et al.*, Fortschr. Physik **42**, 101 (1994), hep-ph/9812448; X. Ji, Phys. Rev. Lett. **78**, 610 (1997); Phys. Rev. **D55**, 7114 (1997); A.V. Radyushkin, Phys. Rev. **D56**, 5524 (1997).
3. M. Diehl, T. Feldmann, R. Jakob and P. Kroll, Eur. Phys. J. **C8**, 409 (1999).
4. A.V. Radyushkin, Phys. Rev. **D58**, 114008 (1998).
5. V. Barone *et al.*, Z. Phys. **C5**, 541 (1993).
6. M. Glück, E. Reya and A. Vogt, Z. Phys. **C67**, 433 (1995); Eur. Phys. J. **C5**, 461 (1998); M. Glück, E. Reya, M. Stratmann and W. Vogelsang, Phys. Rev. **D53**, 4775 (1996).
7. J. Bolz and P. Kroll, Z. Phys. **A356**, 327 (1996).
8. A.F. Sill *et al.*, Phys. Rev. **D48**, 29 (1993).
9. M.A. Shupe *et al.*, Phys. Rev. **D19**, 1921 (1979).
10. M. Diehl, T. Feldmann, R. Jakob and P. Kroll, Phys. Lett. **B460**, 204 (1999).
11. A.M. Nathan, hep-ph/9908522.
12. P. Kroll, M. Schürmann and P.A.M. Guichon, Nucl. Phys. **A598**, 435 (1996).
13. B. Kundu, P. Jain, J.P. Ralston and J. Samuelsson, hep-ph/9909239.
14. J. Bolz, R. Jakob, P. Kroll, M. Bergmann and N.G. Stefanis, Z. Phys. **C66**, 267 (1995).

Recent Results from HERMES

W. Lorenzon, for the HERMES collaboration
Randall Laboratory of Physics, University of Michigan, Ann Arbor, Michigan 48109-1120, USA

Abstract

Recent data on the spin structure of the nucleon are presented. Special emphasis is given to the flavor decomposition of the polarized quark distributions in the nucleon from semi-inclusive deep inelastic scattering, and to the spin asymmetries of pairs of hadrons at high transverse momentum p_T, which indicate a positive contribution to the nucleon spin from gluon polarization. Additional data from spin-independent measurements presently underway at HERMES are presented.

INTRODUCTION

Understanding the spin structure of the nucleon in terms of quarks and gluons has been a significant challenge for more than twenty years. In a simple quark parton model the spin of the nucleon can be decomposed schematically as

$$\frac{1}{2} = \frac{1}{2}\Delta\Sigma + \Delta G + L_q + L_G, \tag{1}$$

where $\Delta\Sigma$ denotes the contribution of the quark spins, ΔG the contribution from the gluon spin, and L_q and L_G the contributions of the orbital angular momenta of the quarks and gluons. A decade ago, analysis of data from the EMC experiment[1], based on the quark parton model and assuming $SU(3)_f$ flavor symmetry, led to the conclusion that the quarks contribute only about 12% to the nucleon's spin and that the strange quark sea seems to be negatively polarized. However, in the light of current theoretical understanding, the separation of terms of the right-hand side of Eq. 1 is still not well constrained by even the most recent, high precision inclusive measurements. Many open questions remain: what are the contributions of the other components; what is the contribution of the valence quarks, the sea quarks, in particular the strange quarks, and what is the role of the gluons?

SPIN STRUCTURE STUDIES

Hermes has been designed to address many of these open questions using semi-inclusive spin dependent deep inelastic scattering (DIS), where a hadron is detected in coincidence with the scattered lepton. It is possible in appropriate kinematics that selects hadrons from the current fragmentation region to "identify" the flavor of the struck quark and therefore provide a flavor decomposition of $\Delta\Sigma$. Assuming that the fragmentation process is spin independent, quark polarizations $\Delta q_f(x)/q_f(x)$ can be extracted from a set of measured spin asymmetries on protons and neutrons. Figure 1 shows the results[2] from data taken by the HERMES experiment[3] using the 27.5 GeV beam of longitudinally polarized positrons in the HERA storage ring at DESY, incident on a longitudinally polarized ^{3}He or ^{1}H internal gas target. Since the statistical precision was insufficient for decomposition of all quark polarizations, constraints were imposed on the sea polarization to reduce the number of fit parameters. Two alternatives were chosen for relating the spin distributions of the sea flavors: a flavor independent polarization, where $\Delta u_s/u_s = \Delta d_s/d_s = \Delta s/s$; and a flavor symmetric sea, where $\Delta u_s = \Delta d_s = \Delta s$. The resulting up quark polarizations are positive and the down quark polarizations are negative over the measured range of x. The sea polarization is compatible with zero over the measured range of x. It is also shown that the results are insensitive to the choice of sea assumption.

Whereas the sea quark contribution is found to be close to zero in this semi-inclusive analysis, the strange quark sea is significantly negative in the inclusive analysis. However, neither result represents a direct measurement of Δs, but rather depends on the assumptions of $SU(3)_f$ symmetry for the inclusive case and on the sea symmetry condition for the semi-inclusive case. The newly installed Ring Imaging Cherenkov (RICH) counter offers the possibility of a direct measurement of Δs through kaon identification.

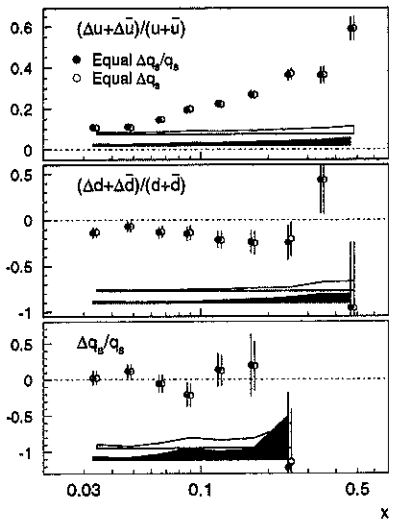

Fig. 1. Flavor decomposition of the quark polarizations as a function of x from HERMES inclusive and semi-inclusive asymmetries. Two assumptions for the sea polarizations are compared as described in the text. The error bars shown are statistical and the bands represent the systematic uncertainties.

How to measure ΔG?

In principle, the polarized gluon polarization ΔG can be extracted from the scaling violation of the polarized structure functions. However, the presently available data on polarized inclusive deep inelastic scattering only poorly constrain $\Delta G(x_G)$, although there is some indication for the integral to be positive[4]. One way to measure ΔG directly is via the isolation of the photon gluon fusion (PGF) process. Two useful experimental signatures of this process are charm production and the productions of jets with high transverse momentum p_T. Both charm production and high-p_T jet production have resulted in direct measurements of the unpolarized structure function G[5–7]. The energies available at present fixed target experiments are however not high enough to produce jets; therefore, high-p_T hadrons must serve in place of jets[8] for HERMES and the COMPASS experiment at CERN[9]. In addition, the RHIC experiments plan to probe the gluon spin by direct photon production[10].

Charm production at HERMES (D^0, D^*, and inelastic J/ψ) can be used as a tag of PGF. However, the presently available statistics on J/ψ and D^0 is only of the order of 20 events for the 1996/97 data set, which was collected on the polarized ^{1}H target. The 1998 charm upgrade to the HERMES detector did increase the acceptance by a factor of four, but no results are available yet from the 1998/99 running period. The other experimental channel available to HERMES is the measurement of the spin asymmetry of pairs of hadrons with high p_T, which has a large negative analyzing power for ΔG.

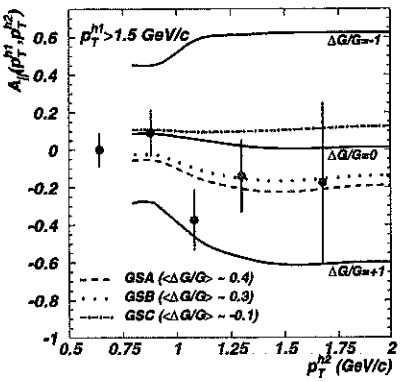

Fig. 2. The measured asymmetry $A_\parallel(p_T^{h^+}, p_T^{h^-})$ for high-p_T hadron production measured at HERMES is compared with Monte Carlo predictions for $\Delta G/G = \pm 1$ (lower/upper solid curves), $\Delta G/G = 0$ (middle solid curve), and the phenomenological LO QCD fits of Ref.[11] (dashed, dotted, and dot-dashed curves).

Such a measurement has been performed[12]. The observed negative asymmetry shown in Fig. 2 is in contrast to the positive asymmetries typically measured in deep inelastic scattering from protons, where scattering from u quarks dominates.

A value of $0.41 \pm 0.18(\text{stat.}) \pm 0.03(\text{syst.})$ for the gluon polarization has been extracted from the observed negative asymmetry. This interpretation is based on a model which takes

into account leading order QCD processes and vector meson dominance contributions to the cross section. Possible higher order QCD processes or contributions from anomalous photon structure have been neglected here, since no spin-dependent analyses of these processes are currently available. If such processes were important, but have no significant spin asymmetry, the extracted value of $\langle \Delta G/G \rangle$ would increase, but still differ from zero by 2.3σ. To alter the conclusion that $\langle \Delta G/G \rangle$ is positive, a significant contribution from a process with a large negative asymmetry would be needed.

UNPOLARIZED DIS STUDIES

HERMES is also studying deep inelastic scattering on various unpolarized nuclei. This was initially done to check the performance of the detector in a more efficient way, because luminosities of a factor of ten or higher can be achieved with unpolarized gases limited only by their impact on the beam lifetime. However, it has also provided a rich physics program[13,14] and most recently, an exciting and unexpected result.

Nuclear Dependence of $R = \sigma_L/\sigma_T$ at low Q^2

HERMES has measured the cross section ratio for deep inelastic positron scattering off ^{14}N and ^{3}He with respect to ^{2}H[15]. In Fig. 3 the ratio for ^{14}N is compared to similar ratios for ^{12}C measured by NMC[16], E665[17], and SLAC[18]. A large difference between the present data and previous data is observed at low x, for $x < 0.06$. In this domain, the HERMES data continues to fall below the NMC and E665 data for decreasing values of x. At high values of x, however, the HERMES data are in good agreement with the SLAC data.

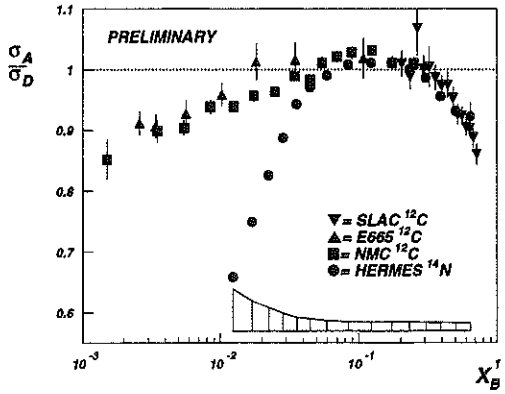

Fig. 3. Ratio of cross sections of inclusive deep inelastic lepton scattering from ^{14}N and ^{2}H versus x. The error bars of the HERMES measurement represent the statistical uncertainties; the systematic uncertainty of the HERMES data is given by the error band. The error bars of the NMC, E665 and SLAC data are the quadratic sum of the statistical and systematic uncertainties.

In deep inelastic charged lepton scattering from an unpolarized target, the ratio of DIS cross sections from a nucleus A and deuterium is given by

$$\frac{\sigma_A}{\sigma_D} = \frac{F_2^A}{F_2^D} \frac{(1+\epsilon R_A)(1+R_D)}{(1+R_A)(1+\epsilon R_D)}, \tag{2}$$

where R_A and R_D represent the ratio σ_L/σ_T for nucleus A and deuterium, ϵ the virtual photon polarization parameter, and F_2^N the unpolarized structure functions. For $\epsilon \to 1$ the cross section ratio equals the ratio of the structure functions F_2^A/F_2^D. For smaller values of ϵ, the cross section ratio is equal to F_2^A/F_2^D only if $R_A = R_D$. A possible difference between R_A and R_D will thus introduce an ϵ-dependence of σ_A/σ_D. Hence measurements of σ_A/σ_D as a function of ϵ can be used to extract experimental information on R_A/R_D, if R_D is known. The resulting values of R_A/R_D are shown in Fig. 4. They show a strong Q^2-dependence of R_A/R_D at low x and Q^2 and represent the first observation of nuclear effects in the ratio of longitudinal to transverse photoabsorption cross sections. There is no inconsistency between the present data and the data reported by previous experiments. Theoretically, a possible A-dependence of R has been suggested by several authors. In Ref.[19], the nucleon Fermi motion is seen to enhance higher-twist effects. It has also been argued that nuclear gluon fields may lead to an enhancement of R[20]. In Ref.[21] it is suggested that nuclear shadowing might be different for the longitudinal and transverse

cross sections.

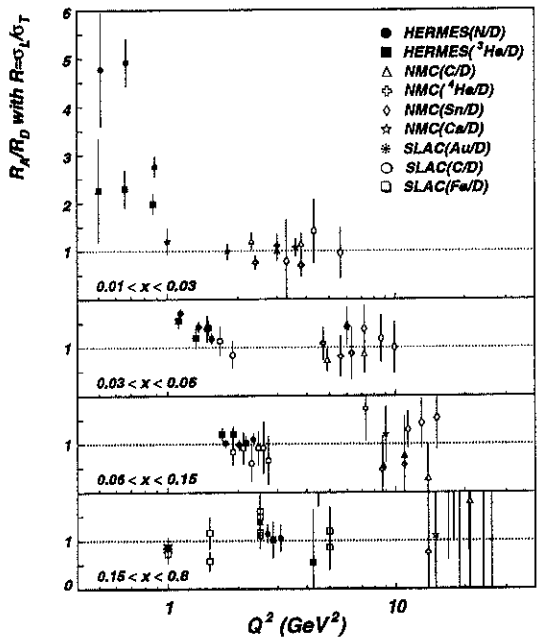

Fig. 4. The ratio R_A/R_D for nucleus A and deuterium as a function of Q^2 for four different x bins. The HERMES data on ^{14}N (^{3}He) are represented by the solid circles (squares). The open triangles (^{12}C) and crosses (^{4}He) have been derived from NMC data using the same technique. The other SLAC and NMC data displayed have been derived from measurements of $\Delta R = R_A - R_D$ taking a parametrization for R_D. The error bars include both statistical and systematic uncertainties.

CONCLUSIONS

The HERMES experiment has finished its forth year of running. Inclusive and semi-inclusive data are collected simultaneously using internal polarized gas targets. HERMES plans to continue running with a longitudinally polarized deuterium target until May 2000. The 1998/99 upgrades to the spectrometer have opened new possibilities. It is expected that by May 2000, HERMES will provide precise knowledge of the valence and sea quark polarizations, and report on the first direct measurement of the strange quark polarization. It is also hoped that the results on $\Delta G/G$ obtained from pairs of hadrons with high-p_T can be improved in precision and confirmed from charm production data. After the luminosity upgrade at HERA, HERMES might switch over to a transverse target program. To that end, a long range plan is being worked out, and will be available shortly.

REFERENCES

1. J. Ashman et al., Phys. Lett. **B206**, 364 (1988); *ibid.*, Nucl. Phys. **B328**, 1 (1989).
2. K. Ackerstaff et al., Phys. Lett. **B**, *in press*; hep-ex/9906035, and references therein.
3. K. Ackerstaff et al., Nucl. Instr. and Meth. **A417**, 230 (1998).
4. R.D. Ball et al., Phys. Lett. **B378**, 255 (1996).
5. S. Aid et al., Nucl. Phys. **B472**, 3 (1996); *ibid.* **B472**, 32 (1996); *ibid.* **B449**, 3 (1995).
6. J. Breitweg at al., Z. Phys. **C76**, 599 (1997); *ibid.* Phys. Lett. **B407**, 402 (1997).
7. D. Allasia at al. Phys. Lett. **B258**, 493 (1991).
8. A. Bravar at el., Phys. Lett. **B421**, 349 (1998).
9. COMPASS proposal, CERN/SPSLC-96-14, March 1996.
10. G. Bunce et al., Part. World **3**, 1 (1992).
11. T. Gehrmann, W.J. Sterling, Phys. Rev. **D53**, 6100 (1996).
12. A. Airapetian et al., hep-ex/9907020, and references therein.
13. K. Ackerstaff et al., Phys. Rev. Lett. **81**, 1164 (1998).
14. K. Ackerstaff et al., Phys. Rev. Lett. **82**, 3025 (1999).
15. A. Airapetian et al., hep-ex/9910071.
16. P. Amaudruz at al., Nucl. Phys. **B441**, 3 (1995).
17. M.R. Adams et al., Z. Phys. **C67**, 403 (1995).
18. J. Gomez et al., Phys. Rev. **D49**, 4348 (1994).
19. J. Milana, Phys. Rev. **C49**, 2820 (1994).
20. T. Gousset and H.J. Pirner, Phys. Lett. **B375**, 349 (1996).
21. N.N. Nikolaev and B.G. Zakharov, Z. Phys. **C49**, 607 (1991).

Recent Results on the Nucleon Structure at HERA

A. Bamberger *
Albert–Ludwigs–Universität Freiburg, Hermann–Herder–Str. 3, D–79104 Freiburg, Germany
on behalf of the H1 and ZEUS Collaboration

Abstract

Recent results from deep inelastic scattering at HERA are presented with the emphasis on structure function measurements. The determination of the structure function F_2 at very low Q^2, the longitudinal structure function F_L, the gluon density xg using different methods, and the structure function for charm F_2^{CHARM} are presented. The description in the framework of next-to-leading-order perturbative QCD proves to be valid down to $Q^2 \sim 1$ GeV^2.

INTRODUCTION

Deep inelastic scattering is an excellent tool to explore the structure of the nucleons[1]. HERA is a unique facility to provide collisions of leptons and hadrons at a center of mass energy of $\sqrt{s}$=300 GeV, a kinematical regime which has never been accessed beforehand. Here the results of the two multi-purpose detectors H1 and ZEUS are summarized including data collected until 1997.

The four momentum transfer $Q^2 = s \cdot x \cdot y$ is proportional to the Bjorken x and the the relative energy transfer y, both bound between zero and unity. Using events at high y the determination of the longitudinal part of the structure function becomes possible. The accurate description of the cross sections in terms of the perturbative QCD for momentum transfer down to 1 GeV^2 turns out to be possible using the next-to-leading-order pertubative QCD (NLO pQCD) calculations. Of special interest is the determination of the gluon density distribution. Two possible ways to access the gluon density are presented here (i) the fit of the structure function with the DGLAP-equations[2] and (ii) the selection of a process where the virtual γ fuses with a gluon, producing a $c\bar{c}$ in the final state, which can be tagged.

DETERMINATION OF F_2

For the reaction $ep \to eX$ the double differential cross section for neutral currents is formulated in terms of the structure functions neglecting the Z^0 exchange:

$$\frac{d^2\sigma^{NC}}{dxdQ^2} = \frac{2\pi\alpha^2}{xQ^4} Y_+ [F_2 - \frac{y^2}{Y_+} F_L]$$

with the kinematical factor $Y_\pm = 1 \pm (1 - y^2)$. The structure function F_2 is interpreted in leading order as the sum of the parton densities. The longitudinal structure function F_L becomes only important at high y. It vanishes at leading order and is therefore a true higher order effect.

Perturbative QCD is used for the description of the Q^2 evolution of the parton densities. This evolution is driven by the gluon emission from the quarks and by the splitting of the gluon into a quark and antiquark pair.

F_2- DETERMINATION AT LOW Q^2

The structure function is found to be monotonically growing with decreasing x for all measured Q^2 values. However the growth becomes smaller with decreasing Q^2. The increase towards low x is caused by the increased gluon density which drives the sea quark density at low x. In Fig. 1 it is shown that this x dependence gets smaller for low $Q^2 \sim$

*Supported by the German Federal Ministry for Education and Science, Research and Technology (BMBF) under contract number 057FR19P.

0.6 GeV^2. Also the prediction of the NLO pQCD fit[3] is shown. At low Q^2=0.9 GeV^2 the description of Regge inspired fit takes over. Here starts a transition region where the description of the cross section changes from the partonic to the hadronic structure.

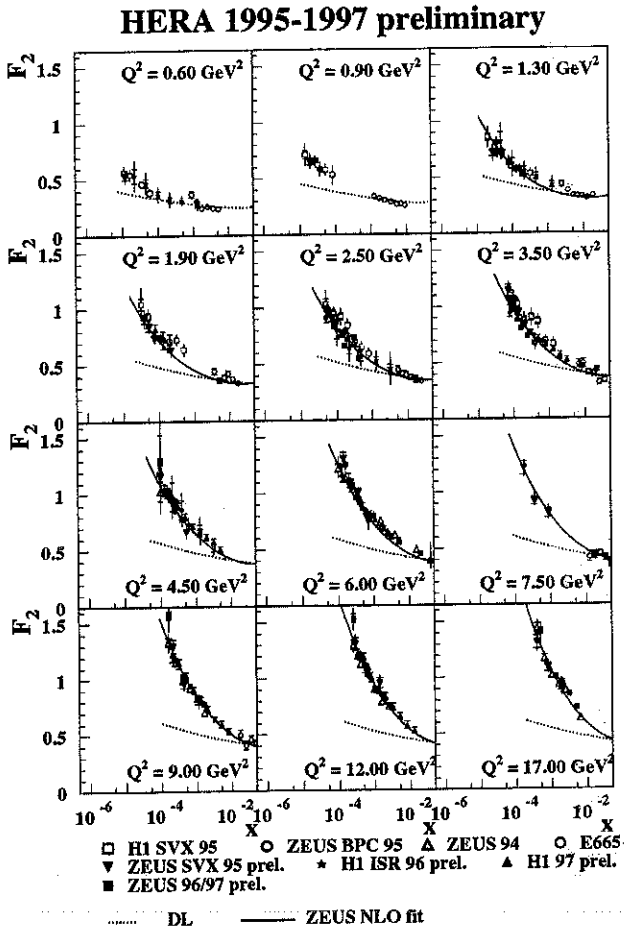

Fig. 1. The ZEUS F_2 data with shifted vertex (SVX95) as a function of x for different Q^2 bins together with earlier ZEUS data (ZEUS94, ZEUS BPC95) data from H1 (SVX95) and fixed target data (E665). The curves shown are (dotted) the Donnachie-Landshoff Regge model and the full line the ZEUS NLO QCD fit.

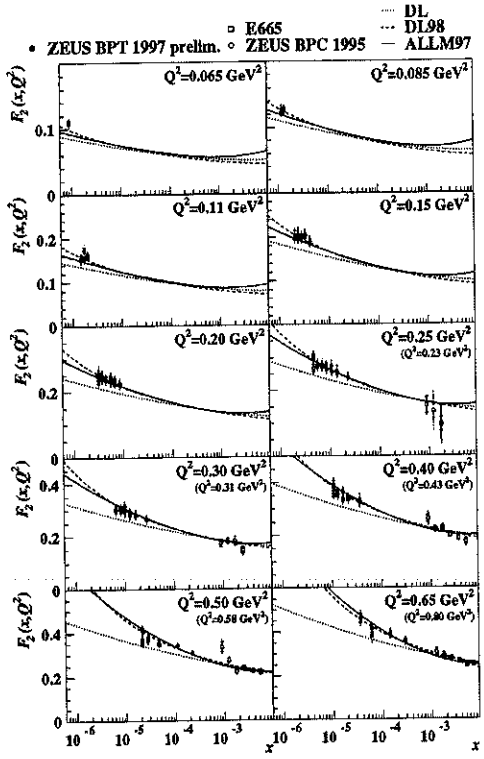

Fig. 2. Measured F_2 vs. x in bins of Q^2. Filled circles denote values measured at ZEUS at very low Q^2 and very low x. Squares are the results from fixed target experiment E665. Shown as lines are Regge inspired fits (DL, DL98 and ALLM97), as well as a ZEUS REGGE 97 fit.

A still lower Q^2 region is investigated by both experiments, H1 and ZEUS, using the shifted vertex method which allows to measure as low as $Q^2 \sim 0.4$ GeV^2. At ZEUS a special beam pipe calorimeter (BPC) is employed extending the momentum transfer range down to 0.1 GeV^2[4]. In Fig. 2 the continuation of the trend at still lower Q^2 than displayed in Fig. 1 is well demonstrated: the parton density flattens. The Regge fits describe the data down to Q^2=0.065 GeV^2.

SCALING VIOLATION AND EXTRACTION OF $xg(x)$

The F_2 data is measured for Q^2 and x ranging over five orders of magnitude. The F_2 data increase monotonically with small x, however less dramatic as Q^2 decreases. This can be understood by gluon emission which reduces the quark momenta to lower values. The overal fit with NLO pQCD gives an excellent agreement including fixed target experiments. Since the DGLAP equation incorporates the gluon density it can be extracted through the fit[3]. The result is shown in Fig. 3 where the error band results from the error propagation of the experimental systematical errors. Here a steep increase of the density towards small x is observed at Q^2=20 GeV^2. At low Q^2 the distribution becomes flat as it is observed for F_2.

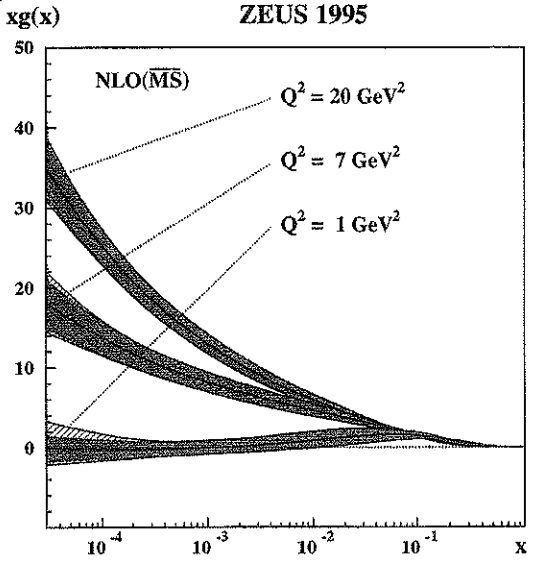

Fig. 3. The gluon density $xg(x)$ obtained by a NLO pQCD fit.

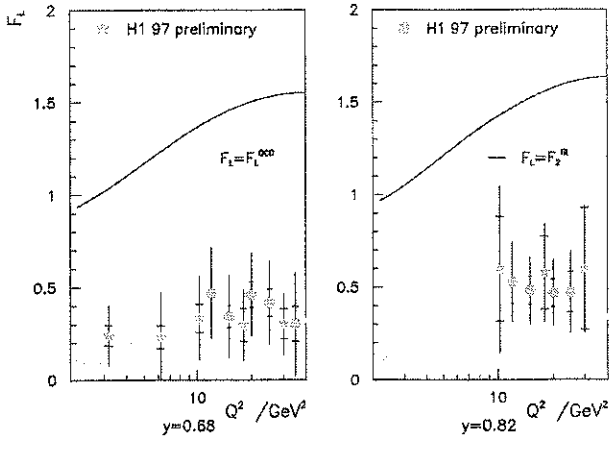

Fig. 4. The determination of F_L by the subtraction method. The hatched band represents the result using QCD fits

LONGITUDINAL STRUCTURE FUNCTION F_L

The measurement at high y allows to study the influence of F_L. Here the energy of the electron is small and the photo production background has to be controlled rather carefully. The H1 collaboration uses the subtraction method as the difference between data and the F_2 extrapolated into the high y region under the assumption of F_L=0[5].

The fit uses only data points with $y < 0.6$ which are independent of F_L. Another method uses the logarithmic scaling violation with y of the cross section. The two methods agree well with each other with the caveat that the same data set is used. The result of the F_L determination is given in Fig. 4 and it is consistent with the expectations from the QCD fits, as shown in hatched band. The values found are well below F_2 also at the high y.

F_2^{CHARM} AND GLUON DENSITY

A test of the NLO pQCD calculations is given by the heavy quark structure functions. Since the heavy quark mass sets another scale it is important to check the consistency of the results. The gluon density can be derived from the boson gluon fusion process. Experimentally, the charm content can be measured by the decay sequence of $D^{*\pm}$. The reconstruction is possible with tracking in the rapidity interval of $|\eta| < 1.5$. The cross section is extrapolated to the full phase space. The F_2^{CHARM} data shows an increase towards small x and its behaviour is consistent with the inclusive F_2 measurement for both experiments H1[6] and ZEUS[7]. The extracted gluon density of the H1 collaboration is shown in Fig. 5[8]. The agreement with the gluon density determined by QCD fits is excellent.

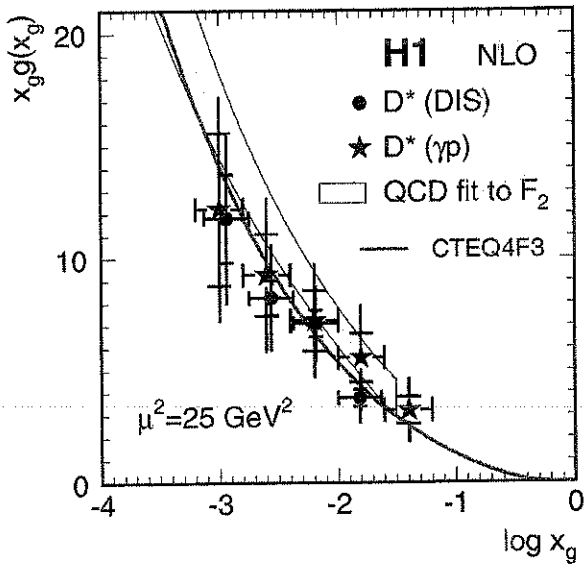

Fig. 5. Gluon Density from Charm

SUMMARY

The investigation of deep–inelastic ep – interaction at HERA by the experiments H1 and ZEUS is extended to very low x and to very low Q^2 with high statistical accuracy. The rise of F_2 with decreasing x persists down to low $Q^2 \sim 1$ GeV^2. Below that the description of the F_2 with Regge based models is appropriate. The scaling violation is well described by NLO pQCD fits. The gluon distribution can be extracted either by these fits or by the F_2^{CHARM} determination. At low x and at high y the cross sections are explained by a sizable F_L part representing a higher order effect. In general NLO pQCD provides a powerful description of the deep inelastic cross sections with an amazing precision.

REFERENCES

1. A. M. Cooper-Sakar, R. Devenish and A. DeRoeck, *Int.J.Mod.Phys.* **A13**, 3385 (1999).
2. G. Parisi, Proc. 11th Rencontre de Morionde (1976); G. Altarelli & G. Parisi, *Nucl Phys.* **B126**, 298 (1977); V. Gribov & L. Lipatov , *Sov. Jour. Nucl. Phys.* **15**, 438

(1972); L. Lipatov, *Sov. Jour. Nucl. Phys.* **20**, 94 (1975); Y. Dokshitzer, *Sov. Jour. JETP* **46**, 641 (1997)
3. ZEUS Collaboration, "ZEUS Results on the Measurement and Phenomenology of F(2) at Low x and Low Q**2", *Eur.Phys.J.* **C7**, 609-630 (1999).
4. ZEUS Collaboration, "Measurement of the Proton Structure Function F_2 at Very Low Q^2 and Very Low x", **Abstract 493**, International Europhysics Conference on High Energy Physics 99, Tampere, Finland, 15 - 21 July 1999.
5. M. Klein, "Precision Measurement of the Inclusive Inelastic ep Scattering Cross Section at Low Q^2", Proceedings fo the 29th International Conference on High Energy Physics, Vancouver 1998 (World Scientific 1999) Vol. 1, pp. 819-825
6. H1 Collaboration, Inclusive D0 and D*+- Production in Deep Inelastic e p Scattering at HERA", *Z.Phys.* **C72**, 593-605 (1996)
7. ZEUS Collaboration, "Measurement of D*+- Production and the Charm Contribution to F(2) in Deep Inelastic Scattering at HERA", DESY 99-101 July 1999, accepted by the *Eur.Phys.J.*
8. H1 Collaboration, "Measurement of D* Meson Cross Sections at HERA and Determination of the Gluon Density in the Proton", *Nucl.Phys.* **B545**, 21-44 (1999).

Pion Absorption on N, Ar and Xe Nuclei Measured with LADS

D. Kotliński, LADS Collaboration
Paul Scherrer Institute, CH-5232 Villigen, Switzerland

Abstract

The pion absorption reaction π^+ on Ar was studied at pion energies of 70, 118, 162, 239 and 330 MeV, and on N and Xe at 239 MeV. Absorption reaction channels with at least two energetic charged particles in the final state have been identified. Partial cross sections split according to the number of protons, neutrons and deuterons in the final state have been determined.

INTRODUCTION

The 4π solid angle Large Acceptance Detector System (LADS) was built at PSI to study multi-nucleon pion absorption at energies around the Δ resonance[1]. A number of papers concerning pion absorption on the light nuclei ^3He and ^4He have been published by our collaboration (see e.g.[2]). In addition to the light target data, measurements with heavier targets, N, Ar and Xe, were also performed

In[3] and[4] we reported first heavy target results which showed the existence of the initial state interaction (ISI) in pion absorption. In the two-step ISI process the pion first scatters quasi-elastically off one nucleon before being absorbed on a nucleon pair.

More recently the heavy target data have been fully analyzed. Here we present the breakup of the absorption cross section into individual channels labelled according to the number of protons, neutrons and deuterons in the final state.

The N and Xe data are presented for a single incident pion energy of 239 MeV, and the Ar data for the five pion energies 70, 118, 162 230 and 330 MeV.

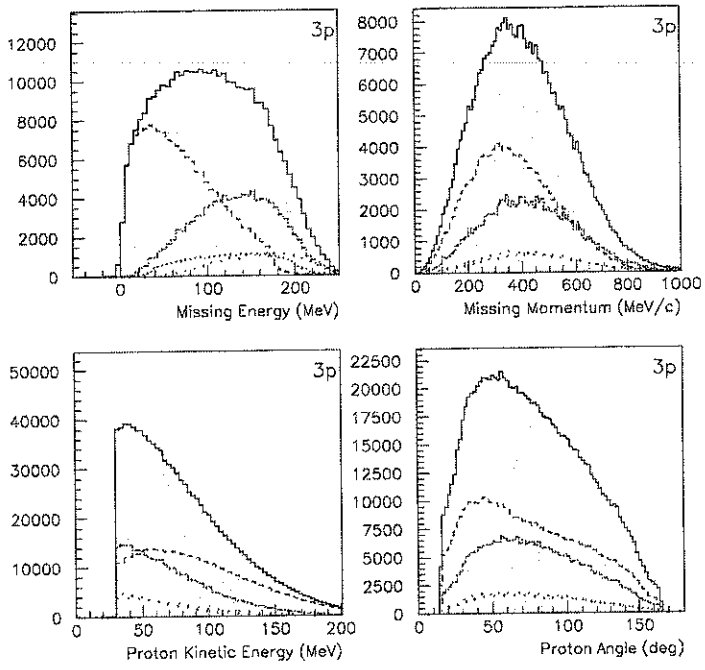

Fig. 1. Data from the Ar(π^+,3p) reaction at T_π = 239 MeV. The shaded area are the experimental data. The solid lines show how these data are reproduced by the Monte Carlo simulations, with other lines representing individual MC components : 3p (dashed), 3p1n (dashed-dotted), 4p (dotted) and 4p1n (wide dotted).

DATA ANALYSIS

Pion absorption events leading to final states with energetic protons, neutrons and deuterons were selected from the N, Ar and Xe target data. Absorption events were identified by requiring no pion in the final state. Charged pions were identified through the

ΔE/E method and neutral pions through high energy (above 10 MeV) gamma rays. In order to discriminate against background only events with at least two well identified tracks (measured with MWPC) were analyzed. This meant that only events with at least two charged particles were taken into account.

The identified absorption events were split according to the number of protons, neutrons and deuterons in the final state. Particles with kinetic energy below 30 MeV were ignored. About 25 final states have been identified. In addition to the expected two particle (2p, 1p1d) and three particle pion absorption (3p, 2p1n) high multiplicity events have been also observed, e.g. 6p, 2p3n or 3p1d1n.

All final states have been simultaneously analyzed with the help of Monte Carlo simulations. This procedure resulted in acceptance corrected cross sections for each of the considered final states. This acceptance correction includes extrapolation of the kinetic energy thresholds from 30 MeV to 0 MeV.

As an example we show the 3 proton final state (3p) following pion absorption on Argon at 239 MeV. Fig. 1 shows the missing energy, missing momentum, proton kinetic energy and proton angular distribution for the 3p final state. The measured distributions are shown with shaded area. The solid line in Fig 1 shows the Monte Carlo prediction for the 3p final state. The simulation takes into account the detector solid angle (incomplete 4π coverage), particle thresholds imposed during the data analysis (30 MeV) and other inefficiencies (e.g. reconstruction and reaction losses). The observed 3p event can originate from a 3p final state, 4p (when one proton escapes undetected), 3p1n (when the neutron is undetected) and others (e.g. 4p1n, 3p2n etc.). The strengths of all Monte Carlo distributions were simultaneously varied to reproduce the observed final states. The difference in the shape of the various distributions is too small to unambiguously determine the strength of each reaction channel. However, since high multiplicity channels are also measured in the experiment, they can be accurately determined with a simultaneous fit. For example, the Monte Carlo 4p component in the measured 3p histogram, cannot vary too much since it has to simultaneously reproduce the measured 4p yield. This is a unique feature of LADS where reaction channels up to high multiplicity were measured. Previous experiments usually could only measure 2 and 3 nucleon final states.

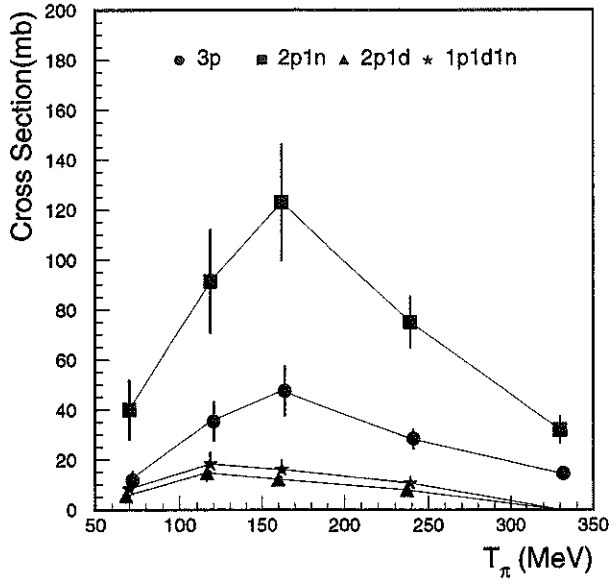

Fig. 2. The measured 3N (three particle channel) cross sections (in mb) for the π^++Ar pion absorption reaction as a function of pion kinetic energy. Cross sections are corrected for all inefficiencies and extrapolated to 0 MeV threshold.

For the Monte Carlo models phase space distributions were used for all channels except 3p and 2p1n where a mixture of ISI, FSI (final state interaction) and phase space was used and 2p which was modeled by the QFA (quasi free two-nucleon absorption) distribution. Phase space distributions describe the data fairly well except for some deuteron channels

which show strong non phase-space components.

The heavy recoil left after the pion absorption process is in general in an excited state. As suggested by the missing mass distribution shown in Fig. 1 this excitation energy can be large. In our Monte Carlo simulations we assumed a flat excitation energy distribution from 0 to some maximum value, which e.g. for Ar at 239 MeV was 170 MeV.

RESULTS

Cross sections determined by the procedure explained above are presented in Figures 2, 3 and 4. The shown cross sections are normalized, acceptance corrected and extrapolated to 0 MeV threshold.

In Fig. 2 the measured cross sections for the three particle (3N) final states are plotted versus the pion beam energy for the Argon target. Here deuterons are treated as a single particle, so e.g. the final state with particle multiplicity three (3N) is obtained by adding 3p, 2p1n, 2p1d and 1p1d1n partial cross sections. Some simple comments can be made:

- All final states show a resonance type behaviour as a function of pion energy,
- Final states with the same number of nucleons peak at roughly the same pion energy,
- The final states which include neutrons are usually much stronger than the final states with protons only,
- Final states which include deuterons are a large part of the total absorption cross section, close to 1/3 at all pion energies.

In order to present the final results in a more compact form we add the cross sections corresponding to the same number of particles in the final state. The ratios of partial cross sections divided by the sum of all partial cross sections for the 2N-6N final states are plotted in Fig. 3 for the Ar target at the five pion energies. In this figure each curve represents the cross section ratio for a given multiplicity (e.g. 3N) plotted as a function of pion energy. One sees a gradual increase of the particle multiplicity with pion energy. The 2N fraction of the absorption cross sections, which dominates at the lowest energy, decreases in importance and becomes negligible at the highest energy while the 3N fraction peaks around 160 MeV. Other multiplicities gain strength with increasing pion energy.

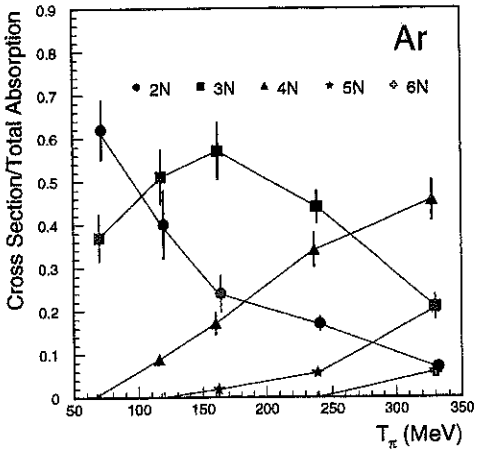

Fig. 3. Comparison of 2N, 3N, 4N, 5N and 6N cross section fractions for the π^++Ar pion reaction as a function of pion kinetic energy. The plot shows cross sections divided by the sum off all measured partial cross sections. The results are corrected for all inefficiencies and extrapolated to 0 MeV threshold.

In Fig. 4 these ratios are plotted as a function of the target mass at one pion energy (239 MeV). To have a better overview data points for the ^3He and ^4He from earlier LADS publications[4,5] have been added. An important feature in this plot is that fractions of the pion absorption cross section going to final states with 2N, 3N, 4N and 5N reach "saturation" values already for Nitrogen. The fractions stay relatively constant for heavier nuclei.

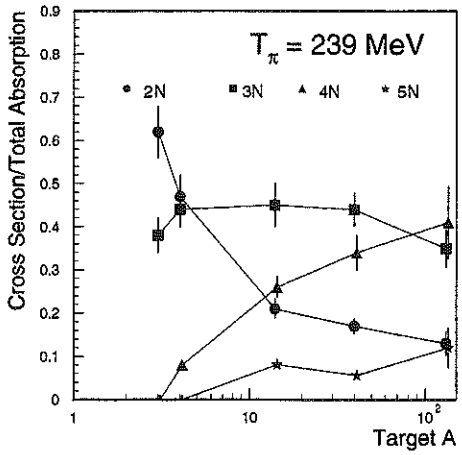

Fig. 4. Comparison of 2N, 3N, 4N and 5N partial cross section fractions at T_π = 239 MeV as a function of target mass. The definition of the plotted quantities is like in Fig. 3. The data for 3He and 4He are taken from Ref.[5,6].

The partial cross sections can be added together. The sum is in all cases within 15% from the previously measured total absorption cross sections. This means that in our analysis we do not miss any large part of the absorption cross section. The channels missed due to the experimental procedure are 1p1n/1d1n and 1p2n/1d2n. These are expected to be small for π^+ induced reactions. In addition, absorption channels with heavier fragments (e.g. alpha particles) are ignored.

In conclusion we have determined the full break-up of the absorption cross section into individual channels. Many high multiplicity final states have been observed. Channels with neutrons are increasingly important with the pion energy (up to 80% for the highest energy). Final states with deuterons populate between 20% and 30% of the absorption cross section at all energies and for all targets.

REFERENCES

1. T. Alteholz *et al.*, Nucl. Instrum. Methods **A373**, 374 (1996).
2. A. Lehmann *et al.*, Phys. Rev. **56** 1872 (1997).
3. D. Androic *et al.*, Phys. Rev. **53** R2591 (1996).
4. D. Kotlinski *et al.*, Euro. Phys. Journal **A1** 435 (1998).
5. A. Lehmann *et al.*, Phys. Rev. **55** 2931 (1997).
6. A.O. Mateos *et al.*, Phys. Rev. **58** 942 (1998).

Charge symmetry breaking in the reaction $np \to d\pi^0$ close to threshold

J. A. Niskanen
Department of Physics, P.O. Box 9,
FIN–00014 University of Helsinki, Finland

Abstract

The charge symmetry breaking forward-backward asymmetry of the cross section in $np \to d\pi^0$ is calculated near threshold. The mixing of the π and η mesons shows up as strongly dominant at these energies. This contrasts elastic np scattering or $np \to d\pi^0$ in the Δ region, where other mechanisms dominate.

1 Introduction

Charge symmetry breaking (CSB) in the nn vs. pp system has been investigated for decades in low-energy NN scattering and mirror nuclei[1,2]. However, the responsible interaction, proportional to the total isospin operator, acts only in isospin one states and cannot change the value of the isospin. In contrast, a CSB force proportional to either $\tau_{10}-\tau_{20}$ or $(\vec{\tau}_1 \times \vec{\tau}_2)_0$ necessarily changes the isospin and acts in the np system, where both isospin zero and one are allowed. These so called class IV forces have three main sources, which are roughly equally important in elastic scattering: i) the np-mass difference, ii) $\rho^0\omega$-meson mixing and iii) the magnetic interaction of the neutron with the proton current. A decade ago their effect was seen experimentally as a difference of the neutron and proton analyzing powers $\Delta A = A_n - A_p$ in polarized np scattering[3].

Class IV forces can also show up in pionic inelasticities. Namely, isospin conserving mechanisms in $NN \to d\pi$ involve only isospin one initial states. This sets strict constraints to the spins and parities of the initial states vs. the angular momentum of the final state pion: for odd l_π only singlet-even initial states are possible and for even l_π only triplet-odd. This separation of initial spins for different parities leads to a symmetric unpolarized cross section. Obviously a class IV force can mix some isospin zero component in the initial state with opposite spin-parity assignments and the cross section is no more exactly symmetric about 90°. This asymmetry in $np \to d\pi^0$ is being measured at TRIUMF[4].

As an interference of opposite parity amplitudes, s- and p-wave pions, the asymmetry should vanish at threshold faster than the cross section. However, there are experimental advantages at threshold allowing smaller relative asymmetries to be detected than at higher energies[4]. Theoretically it is intriguing that at threshold there is less cancellation of possible $\eta\pi$ mixing effects than at higher energies studied in Ref.[5]. This talk presents predictions for the asymmetry in the threshold region where the experiment is performed. A more detailed account can be found in[6].

2 Theory

A standard source of the class IV force, dominant in experiments so far, is the np mass difference in pion exchange. Taking this into account the pion-nucleon coupling becomes

$$H_{\pi NN} = -\frac{f}{\mu}\left[\vec{\sigma}\cdot\nabla\vec{\phi}\cdot\vec{\tau} + \delta\vec{\sigma}\cdot\nabla\phi_0 + \delta\vec{\sigma}\cdot(\vec{p}+\vec{p}')(\vec{\tau}\times\vec{\phi})_0\right] \quad (1)$$

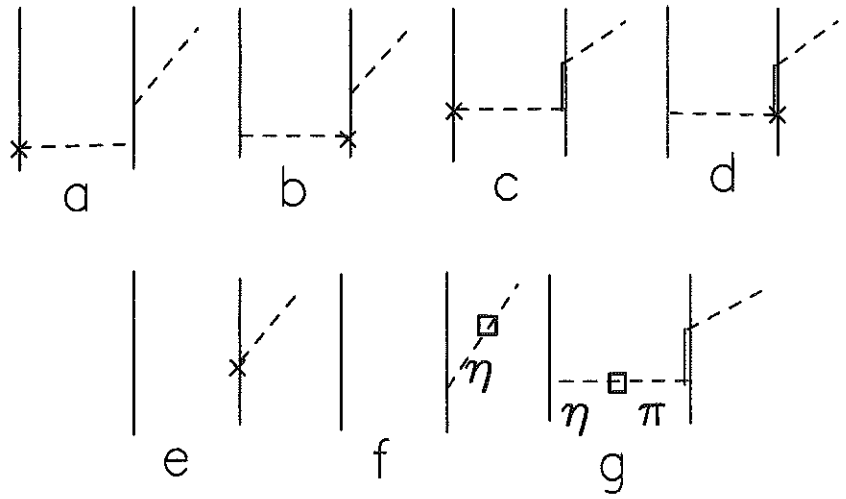

Figure. 1. Isospin breaking mechanisms in $np \to d\pi^0$: isospin mixings in the initial state due to mass difference δ dependent potentials (a–d), CSB production vertices (e and f) and transition potential due to $\eta\pi$ mixing (g). CSB vertices are denoted by a cross or box.

with $\delta = (M_n - M_p)/(M_n + M_p)$. Here the first term is the normal isoscalar interaction giving rise to the standard OPE potential. The initial and final momenta $\vec{p}$ and $\vec{p}'$ operate on nucleons and ∇ on the pion field assumed a plane wave. The latter two terms give rise to a CSB potential of the form (using the usual notations of the literature[5])

$$V_\delta = \delta \frac{f^2}{4\pi} \frac{\mu}{3} \{(\vec{\tau}_1+\vec{\tau}_2)_0 [S_{12} V_T(\mu r)+\vec{\sigma}_1\cdot\vec{\sigma}_2 V_C(\mu r)] - 6(\vec{\tau}_1\times\vec{\tau}_2)_0 (\vec{\sigma}_1\times\vec{\sigma}_2)\cdot\vec{L} V_{LS}(\mu r)\}. \quad (2)$$

The first part conserves the isospin, while the latter term changes both the spin and isospin, i.e. it couples the two possible spins for a given $L = J$ partial wave. This source of isospin breaking in the present reaction is shown in Figs. 1a,b.

In pion physics the coupling of the pion and nucleon to the $\Delta(1232)$ resonance is essential. As above for nucleons, one gets an isovector transition potential from the mass differences (also between different charge states of the Δ, Figs. 1c,d)

$$\begin{aligned} V_\delta^{tr}(\mathrm{OPE}) &= \frac{\delta f f^*}{4\pi} \frac{\mu}{3} \Big\{ T_{10} [S_{12}^{\mathrm{II}} V_T(\mu r) + \vec{S}_1 \cdot \vec{\sigma}_2 V_C(\mu r)] \\ &- 6(\vec{T}_1 \times \vec{\tau}_2)_0 (\vec{S}_1 \times \vec{\sigma}_2) \cdot \vec{L} V_{LS}(\mu r) \Big\} + (1 \leftrightarrow 2). \end{aligned} \quad (3)$$

Here the transition spin (isospin) $\vec{S}$ ($\vec{T}$) changes spin (isospin) $\frac{1}{2}$ particles to those with $\frac{3}{2}$. The mass difference between consecutive charge states of the Δ has been assumed to be the same as for the nucleons. In the tensor operator S_{12}^{II} one spin operator has been replaced by the relevant transition spin operator. Contrary to the case of the NN interaction, now also the first term in (3) can cause a transition from an isospin zero NN state to an intermediate ΔN state which can participate in pion production.

In addition to isospin mixing in the initial np state, the pion coupling (1) gives a possibility for isospin breaking in the final pion producing vertex (Fig. 1e). Namely the middle term is an isoscalar production operator and so there is a finite amplitude of *direct transition* from an initial isospin zero state to the deuteron state plus a pion.

Analogously with the above effective isoscalar meson coupling, also production of first a true off-shell isoscalar pseudoscalar meson (η or η') is possible with its subsequent transformation into a pion, because there is a nonvanishing mixing between the η and π mesons[7] (Fig. 1f). The coupling of pions to nucleons via this is of the form

$$H_{\eta\pi}^{\rm prod} = -\frac{f_\eta}{\mu}\frac{\langle\eta|H|\pi\rangle}{\mu^2-\eta^2}\,\vec{\sigma}\cdot\nabla\phi_0. \tag{4}$$

Using the mixing matrix $\langle\eta|H|\pi\rangle = -5900\,\mathrm{MeV}^2$[7] and the ηNN coupling $G_\eta^2/4\pi = 3.68$[8] with $f_\eta = G_\eta\mu/2M$ it can easily be seen that the strength of this contribution should be about 15 times larger than the isoscalar coupling of the pion from the np mass difference in Eq. (1). So one would expect this to be a very important effect which is further enhanced by the η' meson mixing with the mixing matrix element -5500 MeV^2[7]. (The coupling of the η' to the nucleon is taken to be the same.)

There are great uncertainties in the ηNN and $\eta' NN$ coupling strengths. Much smaller values are also quoted from pion photoproduction[9] and a sensitive probe for this coupling is desirable to clarify the situation. The above value is obtained in a meson exchange NN potential model fit to elastic NN scattering and is consistent with the range 2–7 given in various versions of the Bonn potentials[10]. Another uncertainty is related to a controversy of off-shell $\rho\omega$-meson mixing and is not considered here.

In the NN sector $\eta\pi$ mixing cannot mix isospins, but it can produce an $NN \to \Delta N$ transition potential, which can act also in isospin zero initial states (Fig. 1g). Due to the rather strong effective coupling seen above, also this should have a significant effect in pion production.

Also pion s-wave rescattering from the second nucleon is taken into account in production.

3 Results and conclusion

The quantity of experimental interest here is the integrated forward-backward asymmetry divided by the total reaction cross section

$$A_{fb} \equiv \int_0^{\pi/2}[\sigma(\theta)-\sigma(\pi-\theta)]\sin\theta d\theta \,/\, \int_0^{\pi}\sigma(\theta)\sin\theta d\theta. \tag{5}$$

Here the angle is the CM angle between the detected deuteron and incident neutron directions. The results are shown in Fig. 2. The two dotted curves show the effects due to the np (and the Δ) mass differences, while the larger $\eta\pi$ mixing contributions are given by the dashed curves. The contributions from the production vertices and meson exchange potentials are separated. The total sum is the solid curve. In comparison to meson mixing the mass difference effect is hopelessly small, but if the ηNN coupling is as large as used here its effect could be seen in the experiment.

Preliminary calculations indicate that the ρ and $\rho\omega$-mixing effects as well as the electromagnetic interaction are significantly smaller than $\eta\pi$ mixing at threshold. These are in the same order as the pion effects. An isospin breaking $\eta\pi$-mixing effect may also involve

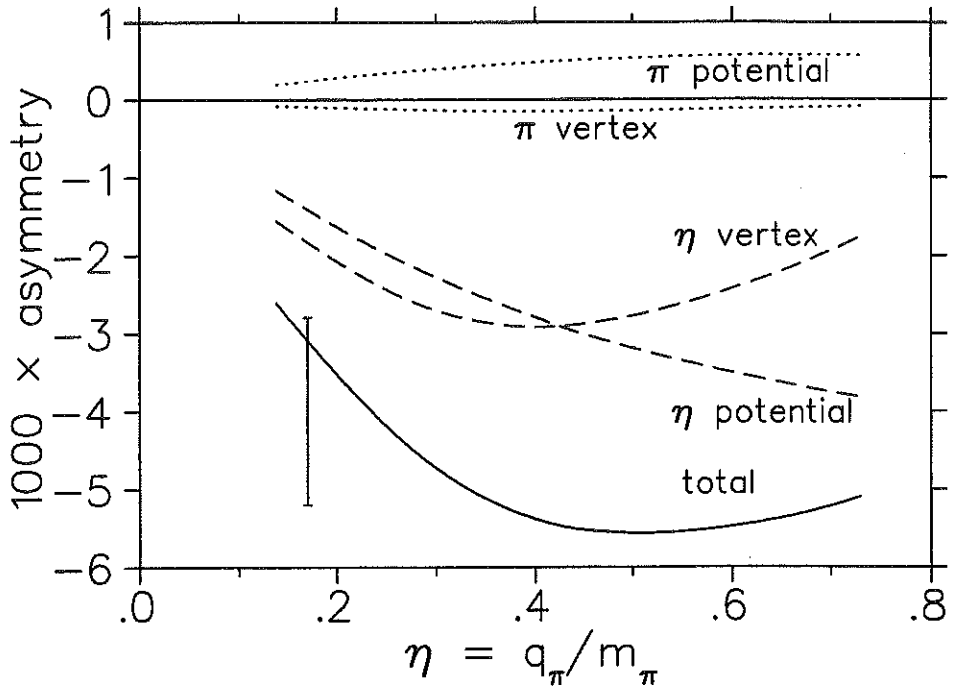

Figure. 2. Contributions dependent on δ (dotted) and $\langle\eta|H|\pi\rangle$ (dashed) to the total integrated forward-backward asymmetry (solid). The "data" point expresses the energy and expected error of the experiment[4].

the s_{11} $N^*(1535)$ resonance, which couples strongly to both the pion and η meson. However, this is very far from the pion threshold region and a simple static estimate indicates it to be small. The isospin conserving reaction is dominated by s-wave πN rescattering at threshold and the possibility a CSB contribution in this[11] is under consideration.

As a summary, it is likely that CSB threshold production is strongly dominated by $\eta\pi$ mixing suggesting CSB measurements as an effective tool to study this phenomenon and constrain the ηNN coupling.

REFERENCES

1. G. A. Miller, B. M. K. Nefkens and I. Slaus, Phys. Rep. **C194**, 1 (1990).
2. G.A. Miller and W.T.H. Van Oers, in *Fundamental Symmetries,* edited by W.C. Haxton and E.M. Henley (World Scientific, Singapore, 1995), p 127.
3. R. Abegg *et al.*, Phys. Rev. **D39**, 2464 (1989); S. E. Vigdor *et al.*, Phys. Rev. **C46**, 410 (1992); J. Zhao *et al.*, Phys. Rev. **C57**, 2126 (1998).
4. TRIUMF experiment E704, spokespersons A. K. Opper and E. Korkmaz.
5. J. A. Niskanen, M. Sebestyen and A. W. Thomas, Phys. Rev. **C38**, 838 (1988).
6. J. A. Niskanen, Few-Body Systems **26**, 241 (1999).
7. S. A. Coon, *et al.*, Phys. Rev. **D34**, 2784 (1986).
8. O. Dumbrajs *et al.*, Nucl. Phys. **B216**, 277 (1983).
9. L. Tiator *et al.*, Nucl. Phys. **A580**, 455 (1994).
10. C. Elster, R. Machleidt and K. Holinde, Phys. Rep. **C149**, 1 (1987); R. Machleidt, Adv. Nucl. Phys. **19**, 189 (1989).
11. U. van Kolck and G. A. Miller, private communication.

Pionic Form Factors of Baryons and Threshold Structure in πNN Amplitude

T. Ueda
Faculty of Science, Ehime University, Matsuyama, Ehime 790-8577, Japan

Abstract

Part I reviews πNN vertex form factor and remarks $\pi\Sigma\Sigma$ and $\pi\Xi\Xi$ vertex form factors based on recent results due to the extension of Ueda-Green NN OBEP to ΛN, $\Lambda\Lambda$,ΞN and ΣN systems in the SU3 nonet meson scheme.

Part II remarks the following. The narrow-width quasi-bound state of $\eta NN - \pi NN$ system near η threshold, predicted by the present author in 1992, corresponds exactly to the experimental signal which has recently been found by WASA group: The enhancement of the cross section for $np \to \eta d$ at the η threshold. Furthermore similar mechanism at π threshold for the πNN system generates a strong and narrow peak in the $I = 0$, $J^P = 0^-$ πNN amplitude and a narrow enhancement in the $I = 1$, $J^P = 0^-$ NN amplitude .

PART I PIONIC FORM FACTORS OF BARYONS

πNN and $\pi N\Delta$ Form Factors and the Π

In early NN OBEP the pionic form factor in πNN vertex was a hard type: The parameter Λ in the monopole parametrization takes about 2-3 GeV much larger than that of the electro-magnetic form factor of about 0.7 GeV[1]. This puzzle was solved by introducing the Π which represents effectively the $I = 1$ and $J^P = 0^-$ part of the correlated three-pion state with mass 730 MeV[2]. It was proved that the one-pion excange potential with the hard pionic form factor is approximately equivalent with the sum of the one-pion exchange potential with a soft pionic form factor such as the electro-magnetic one and the one-Π exchange potential. The soft pionic form factor is interpreted in terms of the contribution of the Π which intermediates between the source nucleon and the emitted (or absorbed) pion.

Another important property about the Π is that the coupling strength of the $\Pi N\Delta$ is weaker than that of ΠNN: It is proved that the ratio of the $\Pi N\Delta$ coupling strength to the ΠNN is less than $\frac{1}{4}$[2]. This explains why the πNN form factor in early NN OBEP was hard, while the $\pi N\Delta$ form factor soft.

Ehime YN and YY OBEP

Very recently the NN OBEP due to Ueda, Riewe and Green[3] has been extended to YN and YY systems and realistic YN and YY OBEP's are presented[4]. This result provides an information on the $\pi\Sigma\Sigma$ and $\pi\Xi\Xi$ vertex form factors. We find puzzles there as are described in later sections, but they are solved by the Π contributions.

So far extensive studies have been made for theoretical YN and YY interactions by Nijmegen, Jülich and Niigata-Kyoto groups. Those aim to make a microscopic description of the YN and YY interactions. However difficulties are in uncertainties in vertex form factors and meson-meson correlations. As a result, none of these attempts is fully consistent with the experimental facts concerning the ΛN scattering and the single and double Λ hypernuclei.

In our Ehime approach YN and YY OBEP's are presented with an SU(3) nonet meson scheme for pseudoscalar, vector and scalar mesons: (π, η, K, η'), $(\rho, \omega, K^*, \phi)$ and $(\delta, S^*, K_0^*(1429)\ f_0(1581))$, respectively. Additionally, the isosinglet scalar meson σ is taken into account which represents the $I = 0, J^P = 0^+$ part of the correlated and uncorrelated 2π exchanges. A part of the σ exchanges between the ΛN and $\Lambda\Lambda$ represents effectively the 2π exchange contributions from the $\Lambda N - \Sigma N$ and $\Lambda\Lambda - \Sigma\Sigma$ channel couplings in the single particle channel approach. On the otherhand the effect of these couplings is explicitly treated in the $\Lambda N - \Sigma N$ coupled particle channel approach.

Our aim is to build an effective model so as to be consistent with related hypernuclei. We allow that the scalar and vector meson exchanges involve effectively correlated and uncorrelated two octet-meson exchanges. The uncertainties arising from this treatment are removed in combined analyses with hypertriton[4].

Single Particle Channel Approach

Our ΛN, $\Lambda\Lambda$ and ΞN OBEP's are consistent with the data on ΛN scattering, hypertriton and double Λ hypernuclei of ${}^{6}_{\Lambda\Lambda}He$, ${}^{10}_{\Lambda\Lambda}Be$ and ${}^{13}_{\Lambda\Lambda}B$. No $\Lambda\Lambda$ bound state is found. Furthermore, by applying the resulting ΞN OBEP to $\Xi^- - {}^{12}C$ atomic states, we find that it reproduces reasonablly the atomic data[5].

The low energy parameters and the binding energies are summarized in Tables 1 and 2.

(1) It is emphasized that the attraction of $\Lambda\Lambda$ is approximately equal with or a little stronger than that of ΛN in the intermediate force range in the ${}^1S_0$ state. It is noted that the attraction of the $\Lambda\Lambda$ force reproduces reasonably the data on the separation energies of ${}^{6}_{\Lambda\Lambda}He$, ${}^{10}_{\Lambda\Lambda}Be$ and ${}^{13}_{\Lambda\Lambda}B$ in balance with the repulsion at short distances[4].

(2) The coupling constants of σ which are most responsible to the attraction take similar values one another as: $g_{\sigma NN} = 1.78$, $g_{\sigma\Lambda\Lambda} = 1.88$, $g_{\sigma\Xi\Xi} = 1.82$.

(3) To reproduce the experimental data for the spectra of $\Xi^- - {}^{12}C$ atomic states, the coupling constant for $\sigma\Xi\Xi$ is approximetely equal to the that of the σNN[3]. Since the σ represents effectively the $I = 0$ and $J^P = 0^+$ part of the two-π exchange, the $\pi\Xi\Xi$ coupling is required to be similarly strong as the πNN coupling. However the SU3 invariance requires that $g_{\pi\Xi\Xi} << g_{\pi NN}$. Thus an additional pionic origin for the enhancement of the $\pi\Xi\Xi$ coupling is required.

Table 1. The scattering lengths a and the effective ranges r in the ${}^1S_0$ and ${}^3S_1$ states for ΛN, $\Lambda\Lambda$ and ΞN scatterings

	ΛN	$\Lambda\Lambda$	$\Xi N(I=0)$	$\Xi N(I=1)$	NN(experiment)
$a({}^1S_0)$ (fm)	-2.71	-3.40	-0.66	-0.27	-23.675 ± 0.095
$r({}^1S_0)$ (fm)	3.21	2.79	7.3	2.0×10	2.69 ± 0.18
$a({}^3S_1)$ (fm)	-1.95		-0.43	-0.56	5.399 ± 0.011
$r({}^3S_1)$ (fm)	3.56		13.5	9.0	1.82 ± 0.05

Coupled Particle Channel Approach

Furthermore the study is developed to ΛN and ΣN coupled channel calculation[6]. In this calculation it is found that a ΛN resonance appears near the ΣN threshold due to a strong channel coupling effect. There is used a hard pionic form factor of about 2 GeV for the $\pi\Sigma\Sigma$ vertex. In view of the fact that the resonance is against the experimental data of the ΛN total cross section, a smaller value for the form factor parameter is preferable such as about 1.5 GeV. Then it is observed that the resonance disappears with 1.5 GeV. Thus an additional pionic origin for the suppression of $\pi\Sigma\Sigma$ coupling is required.

The Π Contribution to the $\pi\Sigma\Sigma$ and $\pi\Xi\Xi$ Vertexes

The two problems encountered in the $\pi\Sigma\Sigma$ and $\pi\Xi\Xi$ vertexes in the previous sections are simultaneously solved by introducing the contribution from the Π which is able to make approximately vanishing contribution to the $\pi\Sigma\Sigma$ vertex, while a sizable contribution to the $\pi\Xi\Xi$ vertex. For this purpose plausible parameter values for Π are found as : $g_{\Pi NN} = 4.82$, $\alpha_\Pi = 0.0$. Noting that the SU(3) invariance gives to octet Π the relation:

$$g_{\Pi NN} = g, \qquad g_{\Pi\Sigma\Sigma} = 2g\alpha, \qquad g_{\Pi\Xi\Xi} = -g(1-2\alpha),$$

Table 2. The hypertriton binding energy, the difference $\Delta B_{\Lambda\Lambda}$ of the double Λ hypernuclei ${}^{6}_{\Lambda\Lambda}He$, ${}^{10}_{\Lambda\Lambda}Be$ and ${}^{13}_{\Lambda\Lambda}B$, and the binding energy of the atomic $\Xi^- - {}^{12}C$ $(1P)$ state

	${}^{3}_{\Lambda}H$	${}^{6}_{\Lambda\Lambda}He$	${}^{10}_{\Lambda\Lambda}Be$	${}^{13}_{\Lambda\Lambda}B$	$\Xi^- - {}^{12}C$ $(1P)$
Theory (MeV)	2.35	3.60	4.14	4.94	0.57
Experiment (MeV)	2.355 ± 0.05	4.7	4.3	4.9	0.57 ± 0.19

then we have:

$$g_{\Pi\Sigma\Sigma} = 0.0 \qquad g_{\Pi\Xi\Xi} = -4.82.$$

The Π with these parameter values makes the vanishing contribution to the $\Pi\Sigma\Sigma$ vertex and so strong contribution to the $\Pi\Xi\Xi$ as to the ΠNN as are required.

REFERENCES

1. T. Ueda and A. E. S. Green, "Realistic $N-N$ One Boson Exchange Potentials", Phys. Rev. **174**, 1304 (1968).
2. T. Ueda, "$\pi NN-$ and Axialvector Form Factors and NN OBE Model", Phys. Rev. Letters, **68**, 142 (1992).
3. T. Ueda, R. E. Riewe and A. E. S. Green, "$N-N$ OBEP Based on Generalized Meson Field Theory", Phys. Rev. **C17**, 1763 (1978).
4. K. Tominaga, T. Ueda, M. Yamaguchi, N. Kijima, D. Okamoto, K. Miyagawa and T. Yamada, "A One-Boson-Exchange Potential for $\Lambda-N$, $\Lambda-\Lambda$ and $\Xi-N$ systems and Hypernuclei", Nucl. Phys. **A642**, 483 (1998).
5. M. Yamaguchi, K. Tominaga, T. Ueda and Y. Yamamoto, "$\Xi N-$ Interaction and Ξ^-Nucleus Potential", presented at 1st Asia Pacific Few-Body Conference, Kashiwa, Japan, August 23-28, 1999.
6. K. Tominaga, "YN and YY Interactions due to OBE Model and Hypernuclei", Ph D Thesis of Ehime University, 1999, unpublished.

PART II THRESHOLD STRUCTURE in πNN AMPLITUDE

ηNN Quasi-Bound State

The possibility of the existence of πNN bound states has been argued by many peaple. Since the strong attractions due to the πN interaction in the P_{33} state and the NN interaction in the ${}^3S_1$ state exist in the system, the bound state has been expected there. However the large centrifugal repulsion in the P_{33} resonance makes the system hard to be bound. Therefore, rather than the bound state, the resonance states exist in the πNN system. The $I=1, J^P=2^+$ and $I=1, J^P=3^-$ resonances are theoretically predicted and this is in agreement with the experimental data [1].

In turn the ηNN system has different property from the πNN system. In that system the important interactions are the $\eta N-\pi N$ interaction in the S_{11} state and the NN interaction in the ${}^3S_1$ state. Namely both interactions are of the S-wave nature giving no centrifugal repulsion and provide much more possibility for the bound ηNN state.

The existence of the $I=0, J^P=1^-$ quasi-bound state in the $\eta NN-\pi NN$ coupled systems is theoretically predicted with the mass of about 2430 MeV and the width 10 - 20 MeV [2]. One solves the three-body equation for the $\eta NN-\pi NN$ coupled systems. There the primary two-body interactions are : (1) The NN interaction in the ${}^3S_1-{}^3D_1$ state and (2) the πN and ηN coupled interaction in the S_{11} state. One finds the remarkable enhancement of the elastic cross section of the ηd scattering near ηd threshold which comes from the pole structure of the $I=0, J^P=1^-$ ηd scattering amplitude on the complex energy plane.

Very recently an experimental signal for this quasi-bound state has been found by the WASA group in Celcius facility. At near threshold in $np \to \eta d$ reaction the group has observed an enhancement with width 10 MeV over the phase space contribution [3]. The prediction of the quasi-bound state corresponds exactly to this experimental signal [2,3,4].

πNN Threshold Dynamics

Consider the threshold of πNN system in $I=0$, $J^P=0^-$ channel. The three-body interactions due to the πN S_{11} and NN ${}^1S_0$ two-body forces are dominating there. Already we have pointed out the following theoretical result. A strong and narrow structure of width

about 5 MeV arises at about 5 MeV of center of mass energy above threshold ($M = 2.025$ GeV) in that channel whose coupling with the NN is forbidden[5].

Concerning this result, we have investigated the analytic structure of the amplitude near the strong structure on the complex energy plane. We have found no pole structure associated with the peak on the real energy axis.

Bilger et al. have reported the signal of the πNN resonance d' with width $\Gamma_{d'} \sim 0.5$ MeV and mass $M_d \sim 2.06$ GeV (40 MeV above threshold) in the $pp \to pp\pi^-\pi^+$ reaction [6]. However the structure predicted by us is different from the d' signal. In view of this situation we would like to suggest the d' search is to be extended to the lower energy region, $M = 2.020 - 2.08$ GeV.

A similar, however less prominant, structure is also appears in the $I = 1, J^P = 0^-$ πNN channel. This was predicted in the absorption parameter of the $I = 1$ $^3P_0$ NN amplitude[7].

Since this πNN channel couples with the NNchannel, the three-body dynamics is much more complex than the $I = 0$ case. The inputs for the three-body equation in the $I = 1$ case are made as follows : the πN P_{11}, P_{33}, S_{11}, S_{31} and NN $^3S_1 - {}^3D_1$, $^1S_0$ and $^3P_2$ two-body forces. In addition to these the backward going pion contribution at the $\pi N\Delta$ vertex, the $\pi N - \rho N$ coupling in the P_{33} state, the OBEP in the $NN - NN$ driving terms and the effect of the off-shell structure in the $\pi N - \rho N$ P_{33} interaction are taken into account. Remind you that the πNN dynamics with these inputs has provided a successfull description of the dibaryon structure in the Δ energy region for the $I = 1, J^P = 2^+$ and $I = 1, J^P = 3^-$ channels[1].

We note that those results both for the $I = 0, J^P = 0^-$ and $I = 1, J^P = 0^-$ channels concern primarily the S wave dynamics of the subsystem in comparison with the P wave ones in the $J^P = 2^+$ and 3^- cases. Therefore it is very significant to confirm the predicted structures in the $I = 0$, $J^P = 0^-$ and $I = 1$, $J^P = 0^-$ channels experimentally, since those are characteristic phenomena due to the hadron degree of freedom. If confirmed experimentally, this indicates that the $S-$wave πNN dynamics is valid in the threshold energy region as well as the $P-$wave πNN dynamics in the Δ energy region. Furthermore, if confirmed, the structures must be distingushed from the phenomena due to the quark degree of freedom.

REFERENCES

1. T. Ueda, "The Pole Structure of the $^1D_2$ and $^3F_3$ $NN-$Amplitudes in the Faddeev πNN Dynamics", Phys. Lett. **B119**, 281 (1982) ; **B141**,157 (1984) ; **B175**, 19 (1986) ; "Elastic and Inelastic Nucleon-Nucleon Scattering in the πNN Dynamics", Nucl. Phys. **A463**, 69c (1987) ; **A573**, 511 (1994).
2. T. Ueda, "$I = 0, J^P = 1^-$ Quasibound State in the $\eta NN - \pi NN$ Coupled System", Phys. Rev. Lett. **66**, 297 (1991).
3. H. Calen, et al,"Threshold Structure of the Quasifree $p + n \to d + \eta$ Reaction", Phys. Rev. Lett. **80**, 2069 (1998) .
4. A.M. Green, J.A. Niskanen and S. Wycech,"η-Deuteron Scattering", Phys. Rev. **C54**, 1970 (1996).
5. T. Ueda, "A Narrow and Strong Structure due to $S-$wave πNN Dynamics near Threshold", Nucl. Phys. **A643**, 83 (1998) ;i.b., "πNN, YN and YY Interactions", πN Newsletter, No.13, 358 (1997).
6. R. Bilger,"Search for a Narrow Resonance in the πNN System", presented at this conference.
7. T. Ueda, K. Tada and K. Kameyama, "A Separable Representation of the NN OBEP and the effect of the $^1S_0$ Potential on the $J^P = 0^-$ πNN System near Pion Threshold", Prog. Theor. Phys. **95**, 115 (1996).

Photo- and electroproduction of kaons in a gauge-invariant framework

H. Haberzettl,* C. Bennhold
Center for Nuclear Studies, Department of Physics, The George Washington University, Washington, DC 20052, U.S.A.

and

T. Mart
Jurusan Fisika, FMIPA, Universitas Indonesia, Depok 16424, Indonesia

Abstract

A previously introduced gauge-invariant formalism for the photoproduction of mesons is extended to electroproduction. The formalism allows for electromagnetic baryon form factors which are fully off-shell. In the case of pseudoscalar coupling, the low-energy limits mandated by chiral symmetry are preserved by utilizing the pseudoscalar analog of the Kroll-Ruderman contact current. Applications to kaon electroproduction are shown.

INTRODUCTION

Gauge-invariance is one of the central issues in dynamical descriptions of how photons interact with hadronic systems (see Ref. [1] and references therein). For meson production from a single nucleon, at the tree level depicted in Fig. 1, the problem can be understood very simply by the fact that the first three s-, u- and t-channel diagrams of Fig. 1 are in general not gauge-invariant by themselves, in particular, if one includes the internal structure of the baryons by utilizing hadronic form factors. Since the precise mechanisms for restoring gauge invariance are not unique at the hadronic level, various recipes for repairing gauge invariance can be found in the literature which, in the diagrammatic language of Fig. 1, amount to adding various contact-type currents to the usual currents represented by the first three diagrams. In Ref. [1], a particular gauge-invariance prescription was put forward which can be applied to any meson production process. It is distinguished from other methods by its flexibility in choosing the functional dependence of the gauge invariance-restoring contact current.

FORMALISM

The gauge-invariance mechanism introduced in Ref. [1] is most easily illustrated by considering the photoproduction process $\gamma p \to n\pi^+$ with pseudoscalar coupling for the πNN vertex at the tree level. Introducing form factors for composite nucleons at the hadronic vertices, the resulting amplitude for the first three diagrams of Fig. 1 is

$$\epsilon \cdot \mathcal{M} = \sum_{j=1}^{4} A_j \overline{u}_{\rm n} \left(\epsilon_\mu M_j^\mu\right) u_{\rm p} - g\overline{u}_{\rm n}\gamma_5 \epsilon_\mu \left[\frac{2p'^\mu}{s-m^2}(\hat{F}-F_s) + \frac{2q^\mu}{t-\mu^2}(\hat{F}-F_t)\right] u_{\rm p} \ , \quad (1)$$

*Email: helmut@gwu.edu

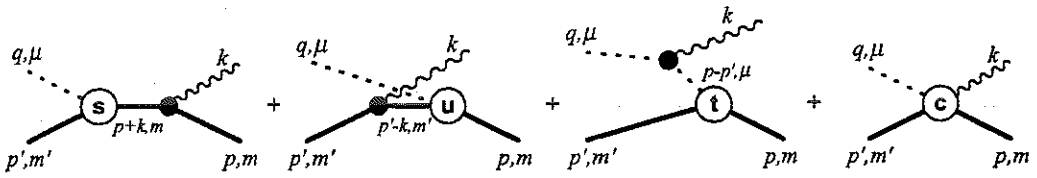

Figure 1. Meson production diagrams (time proceeds from right to left). The last diagram, marked c contains the contact-type currents (see Ref. [1,2]) required to restore gauge-invariance of the entire production current.

where the M_j^μ are the usual gauge-invariant operators [2], with $k_\mu M_j^\mu = 0$, and

$$\begin{aligned} A_1 &= \frac{ge}{s-m^2}(1+\kappa_{\rm p})\,F_s + \frac{ge}{u-m^2}\kappa_{\rm n}F_u \ , \\ A_2 &= \frac{2ge}{(s-m^2)(t-\mu^2)}\hat{F} \ , \\ A_3 &= \frac{ge}{s-m^2}\frac{\kappa_{\rm p}}{m}F_s \ , \\ A_4 &= \frac{ge}{u-m^2}\frac{\kappa_{\rm n}}{m}F_u \ , \end{aligned}$$

describe the coefficient functions depending on the Mandelstam variables s, u, and t; the hadronic vertices F_s, F_u, and F_t correspond to the respective kinematic situations shown in Fig. 1. The right-most term in Eq. (1) violates gauge invariance. Note that the $\hat{F}$ dependencies of this term and A_2 cancel and hence $\hat{F}$ is completely arbitrary in Eq. (1).

Prescriptions to repair gauge invariance amount to introducing an additional contact-type current (cf. Fig. 1) with contributions canceling the gauge-violating term in Eq. (1). Different prescriptions can be understood in terms of different choices for $\hat{F}$ (and possible additional separately transverse current terms). Ohta's formalism [3], for example, amounts to putting $\hat{F} = 1$ which is perhaps the simplest possible choice. In contrast, the gauge-invariant theory of Ref. [1] allows $\hat{F}$ to be taken as any linear combination

$$\hat{F} = a_s F_s + a_u F_u + a_t F_t$$

subject to the condition that $\hat{F} = 1$ if all three hadron legs are on their respective mass shells. We find thus that this formalism allows electric current contributions to be multiplied by a form factor (cf. the A_2 term above), i.e., it does not require that they be treated like bare currents, as in Ohta's approach. Numerical results for kaon photoproduction off the nucleon show that this flexibility afforded by the gauge formalism of Ref. [1] leads to a markedly better description of experimental data [2,4,5]. In Fig. 2 we show an example for the new Bonn SAPHIR data [6].

The gauge-invariance formalism illustrated here by this simple example has now been extended to electroproduction processes. As in the previous photoproduction approach, we describe the baryon structure in terms of hadronic form factors. Moreover, we allow for an arbitrary mixing of pseudoscalar and pseudovector couplings. In the case of pseudoscalar coupling, we repair the low-energy limits mandated by chiral symmetry by adding the pseudoscalar analog of the Kroll-Ruderman term discussed in Ref. [7], which amounts to adding contact-type current terms for both the incoming and the outgoing baryon legs, *viz.*

$$j^\mu_{\rm KR} = \lambda_{\rm PS}\frac{\gamma_5 F_h i\sigma^{\mu\nu}k_\nu \kappa F_2}{4m^2} \ , \qquad (2)$$

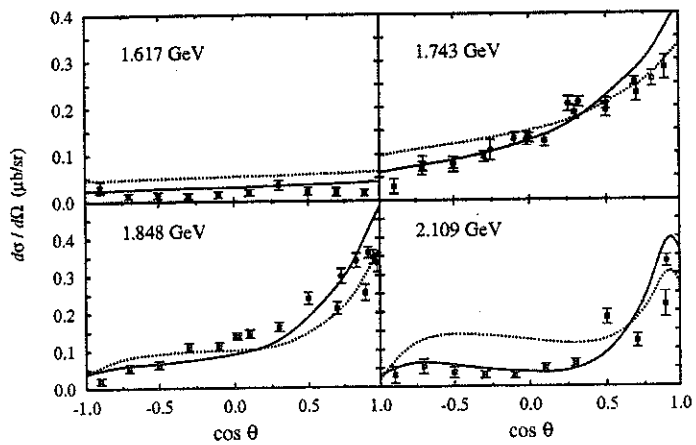

Figure 2. Comparison of results for $p(\gamma, K^+)\Lambda$ obtained with Ohta's [3] (dotted lines) with Haberzettl's [1,2] (solid lines) gauge-invariance prescriptions for the new Bonn SAPHIR data [6].

where λ_{PS} is the strength of the pseudoscalar coupling, and F_h and F_2 are the hadronic form factor (i.e., either F_s or F_u depending on the kinematic situation) and the electromagnetic Pauli form factor, respectively, of the particle.

Furthermore, the full formalism now takes into account the most general off-shell dependence of the electromagnetic currents for spin-1/2 baryons which satisfy the Ward-Takahashi identity. The general off-shell currents Γ^μ for the electromagnetic vertices $\gamma + B \to B'$ (where B and B' may be different baryons, with respective masses m and m') are given by

$$\begin{aligned}
\Gamma^\mu &= \gamma^\mu \delta_{B'B} + \left[\left(\gamma^\mu k^2 - k^\mu \not{k} \right) \frac{F_1^{00} - \delta_{B'B}}{k^2} + i \frac{\sigma^{\mu\nu} k_\nu}{m + m'} F_2^{00} \right] \\
&+ \left[\left(\gamma^\mu k^2 - k^\mu \not{k} \right) \frac{F_1^{01}}{k^2} + i \frac{\sigma^{\mu\nu} k_\nu}{m + m'} F_2^{01} \right] \frac{\not{p} - m}{2m} \\
&+ \frac{\not{p}' - m'}{2m'} \left[\left(\gamma^\mu k^2 - k^\mu \not{k} \right) \frac{F_1^{10}}{k^2} + i \frac{\sigma^{\mu\nu} k_\nu}{m + m'} F_2^{10} \right] \\
&+ \frac{\not{p}' - m'}{2m'} \left[\left(\gamma^\mu k^2 - k^\mu \not{k} \right) \frac{F_1^{11}}{k^2} + i \frac{\sigma^{\mu\nu} k_\nu}{m + m'} F_2^{11} \right] \frac{\not{p} - m}{2m} \,, \qquad (3)
\end{aligned}$$

where $k = p' - p$ is the photon momentum and the F_i^{nm} are the eight independent electromagnetic form factors. For on-shell baryons, the last three terms vanish and F_1^{00} and F_2^{00} reduce to the usual Dirac and Pauli form factors F_1 and F_2, respectively. In most existing treatments of electroproduction processes the last three terms are omitted from the start.

PRELIMINARY NUMERICAL RESULTS

The results reported here for kaon production with real and virtual photons were calculated within the treelevel isobar model described in Ref. [2] which employs pseudoscalar couplings. At present, the numerical implementation of the full off-shell spin-1/2 baryon current, Eq. (3), has not been completed and the results shown here still treat this current in a manner which takes into account its off-shell behavior only approximatively. We would like to point out here that since six of the eight form factors of that current are inaccessible to a direct experimental measurement, a careful study needs to be undertaken as to how various parameterizations of these form factors will affect the description of the experimental data.

We have studied the effect of including the pseudoscalar Kroll-Ruderman analog, Eq. (2), which preserves the chiral-symmetry low-energy limits, and found that in some channels, in particular for $p(\gamma, K^0)\Sigma^+$, the effects may be sizable and lead to a definite improvement of the results when comparing them to the experimental data.

Figure 3 shows an application of the present formalism to the electroproduction process $p(e, e'K^+)\Lambda$. Note that the results shown here are preliminary since the calculation does not yet include a comprehensive investigation of the effects of all off-shell degrees of freedom of the electromagnetic vertices which is currently being undertaken. Moreover, in the present case, we had to include a 'missing resonance' in order to come closer to the experimental data. The importance of this additional state—the best fits determine it to be a D_{13} resonance at 1895 MeV [8]—is particularly evident in Fig. 4 where we show the transverse and logitudinal cross sections for the same reaction.

DISCUSSION

The full details of the formalism briefly outlined here will be published elsewhere [11]. While the full gauge-invariance formalism is quite comprehensive in that it allows for the full off-shell treatment of the currents, at the same time this introduces a number of additional form factors which are not directly measurable. In order to assess the implications of

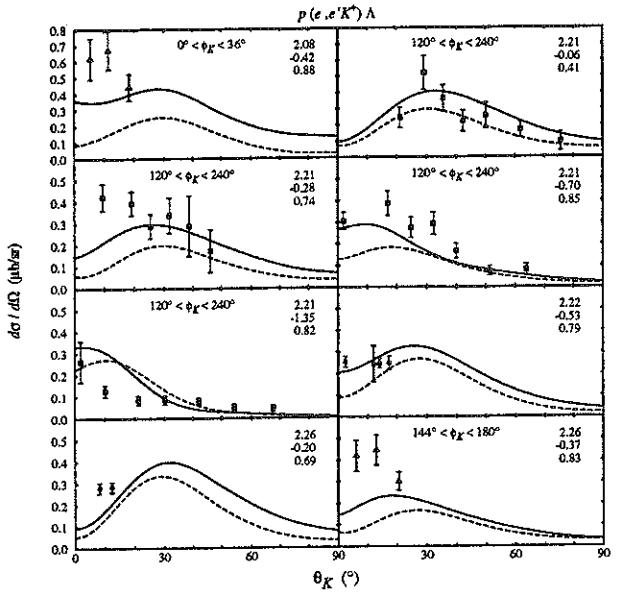

Figure 3. Angular distribution of differential cross sections for $p(e, e'K^+)\Lambda$. The kaon's azimuthal angle ϕ_K is either averaged over the range indicated in the panels or over the range 0–180°. The three numbers in the top right corners of the panels in descending order denote the total c.m. energy W, the square of the virtual photon momentum k^2, and the transversal polarization ϵ of the virtual photon. Solid lines correspond to a fit including a missing $D_{13}(1895)$ resonance (see Ref. [8] for details); dashed lines include only established resonances.

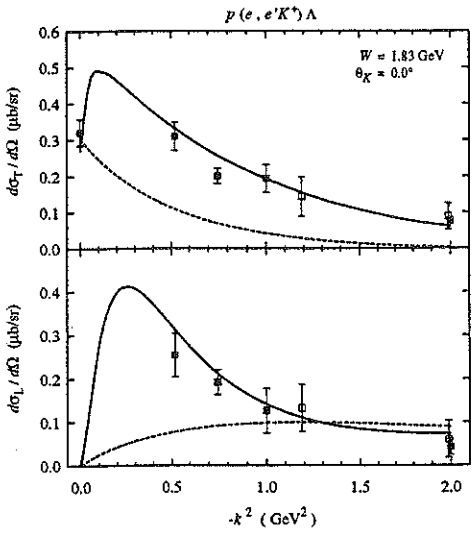

Figure 4. Transverse and longitudinal cross sections for $p(e, e'K^+)\Lambda$. The dotted line shows the result obtained without the $D_{13}(1895)$ resonance discussed in the text. Solid squares show the new JLab data [9], open squares are old data [10]. In the transverse cross section, a photoproduction datum (solid circle) is shown for comparison.

these additional degrees of freedom detailed studies are necessary. Moreover, as the cases reported in Figs. 3 and 4 show, the quality of results pertaining to an individual reaction may depend critically on which mechanisms are included in the calculation. In the end, in order to come to meaningful conclusions, one needs to find ways to constrain all these degrees of freedom as much as possible and it will be necessary to simultaneously describe as many reaction channels as possible in a comprehensive coupled-channels formalism.

ACKNOWLEDGMENT

This work was supported in part by Grant No. DE-FG02-95ER-40907 of the U.S. Department of Energy.

REFERENCES

1. H. Haberzettl, Phys. Rev. C **56**, 2041 (1997).
2. H. Haberzettl, C. Bennhold, T. Mart, and T. Feuster, Phys. Rev. C **58**, R40 (1998).
3. K. Ohta, Phys. Rev. C **40**, 1335 (1989).
4. T. Feuster and U. Mosel, Phys. Rev. C**59**, 460 (1999).
5. B.S. Han, M.K. Cheoun, K.S. Kim, and I.-T. Cheon, **nucl-th/9912011**.
6. SAPHIR Collaboration (M. Q. Tran *et al.*), Phys. Lett. **B445**, 20 (1998).
7. A.M. Bernstein and B.R. Holstein, Comments Nucl. Part. Phys. **20**, 197 (1991).
8. T. Mart, C. Bennhold, Phys. Rev. C **61**, 012201(R) (1999); C. Bennhold, H. Haberzettl, and T. Mart, **nucl-th/9909022**.
9. G. Niculescu *et al.*, Phys. Rev. Lett. **81**, 1805 (1998).
10. P. Brauel *et al.*, Z. Phys. C **3**, 101 (1979).
11. H. Haberzettl, C. Bennhold, and T. Mart, *in preparation.*

Unresolved Problems in the Analysis of Pion Photoproduction around the $\Delta(1232)$

O. Hanstein

Institut für Kernphysik, Universität Mainz, J.-J. Becher-Weg 45, D-55099 Mainz, Germany

Abstract

Several procedures of determining the ratio E2/M1 of the $\Delta(1232)$ are critically reviewed. It is argued that the residues of the resonance poles provide the only information that does not depend on models or other assumptions.

INTRODUCTION

Recently, pion photoproduction experiments at MAMI (Mainz) and LEGS (Brookhaven) have been carried out in order to determine the ratio R_{EM} = E2/M1 of the transition $\gamma N \rightarrow \Delta(1232)$. On the microscopic level, the well known dominance of M1 absorption in this transition is attributed to a spin flip of a constituent quark. The weak E2 quadrupole transition which reveals deviations from spherical symmetry of the quark wave functions of the involved baryons has attracted interest since the sixties. Different microscopic models predict values for R_{EM} in the range of roughly -5 to 0 %. It is hoped that an experimental determination of this number will make it possible to distinguish between several models of the nucleon and its resonances.

Experimental information on the excitation mechanism under consideration is drawn from the multipoles $M_{1+}(3/2)$ and $E_{1+}(3/2)$ of pion photoproduction on the nucleon. The experiments mentioned above included measurements of the beam asymmetry Σ which is particularly sensitive to the small amplitude E_{1+}. Since both π^0 and π^+ production on the proton have been measured, the isospin decomposition can be carried out. The first step of a phenomenological analysis is a partial wave analysis of the experimental data in order to determine the multipoles of interest. In recent years, such analyses have been regularly carried out by the VPI group. In order to impose more rigorous constraints, we applied a technique based on fixed-t dispersion relations in our analysis of the new data.[1] To be more specific, we solved the integral equations for the multipoles which can be derived from the dispersion relations. We followed the method of Omnès which provides a parametrization in a natural way since the particular solutions to the integral equations allow for the addition of solutions to the homogeneous equations each of which can be multiplied by an arbitrary real parameter.

Since the amplitudes $M_{1+}(3/2)$ and $E_{1+}(3/2)$ have appreciable background contributions, the resonance part which is proportional to the electromagnetic excitation strength has to be separated in a sensible way. Common procedures to determine R_{EM} are based on dynamical or Lagrangian models. The coupling constants G_E and G_M of the $\gamma N \Delta$ vertex are fitted to the partial waves. The problems inherent in these and other approaches are discussed in the next paragraph.

APPROACHES

1. In the framework of dynamical models, the $\Delta(1232)$ is explicitly introduced in the πN scattering state. The treatment leads to unitary amplitudes which can be decomposed into a sum of a background, a vertex renormalization part, and a bare resonant multipole the latter of which is interpreted as the contribution due to the electromagnetic excitation process. However, it has been shown that this decomposition is not unique.[2] Given a dynamical model, there exist always unitary transformations which leave the physics described unchanged, but shift the contributions of the bare resonance and the rest into each other so that R_{EM} changes significantly.

2. Lagrangian models that introduce the Δ degree of freedom are not unitary by themselves. Unitarity has to be imposed in a way which is not unique so that a certain model dependence cannot be avoided.

3. The interpretation in terms of the K matrix leads to $R_{EM} = \mathrm{Im}E_{1+}(3/2)/\mathrm{Im}M_{1+}(3/2)$ at the position of the K matrix pole, namely at $W_{\mathrm{R}} = 1232$ MeV. This number is quoted quite often since it can be determined immediately from the multipoles. Nevertheless, it can give no reliable information on the excitation strenght because the imaginary parts also contain background contributions.

4. From a mathematical point of view, the resonance poles of a given T matrix element are unique. We applied the speed plot technique to our solutions for the multipoles as well as to the results of other groups in order to determine the position and the residues of the resonance poles. The pole position was found to agree with the results of corresponding studies of πN scattering. The ratio of the residues turned out to be a complex quantity R^{Δ}_{EM} which is much less model dependent than values of the E2/M1 ratio determined by other methods. On the other hand, we found that the ratio of the residues is quite sensitive to fitted differential cross sections. In our original fit, recent differential cross section data from MAMI were combined with beam asymmetry data from MAMI and LEGS as well as with the target asymmetries measured at ELSA. When we replaced the differential cross sections with data from LEGS and with old data from Bonn, the resonance parameters changed significantly. The corresponding results are compared in Tab. 1.

$\frac{d\sigma}{d\Omega}$ from	$\mathrm{Im}M_{1+}(3/2)$	$\mathrm{Im}E_{1+}(3/2)$	R_{EM}	$A_{\frac{1}{2}}$	$A_{\frac{3}{2}}$	R^{Δ}_{EM}
MAMI	37.66	-0.924	-2.54	-131	-252	-3.5 - i4.6
LEGS	39.35	-1.276	-3.24	-134	-265	-4.6 - i3.8
Bonn (old)	38.31	-0.643	-1.68	-137	-253	-2.9 - i5.0

Table 1. Quantities which characterize the electromagnetic excitation of the $\Delta(1232)$ when fitted to different cross section data. The imaginary parts of the multipoles (unit $10^{-3}/m_{\pi}$) are evaluated at the resonance energy $W_{\mathrm{R}} = 1232$MeV. The helicity matrix elements A_{λ} are given in $10^{-3}/\sqrt{\mathrm{GeV}}$ and the ratios R_{EM} in %.

5. Recently, it has been proposed that the particular solutions to the Omnès equations of the Δ multipoles can be interpreted as the background contributions (see Ref.[3] and references quoted there) so that the additional contributions from solutions to the homogeneous equations can be attributed to electromagnetic resonance excitation. In the simplest case, the particular solution has the form

$$M_l^{\mathrm{part}}(W) = M_l^{\mathrm{pole}}(W) + \frac{1}{\pi}\frac{1}{D(W)}\int_{W_{\mathrm{thr}}}^{\infty} \frac{D(W')h(W')M_l^{\mathrm{pole}}(W')}{W'-W-i\varepsilon}dW' \qquad (1)$$

with $\frac{1}{D(W)} = \exp\left[\frac{W}{\pi}\int_{W_{\mathrm{thr}}}^{\infty}\frac{\phi(W')dW'}{W'(W'-W-i\varepsilon)}\right]$ the Jost function, $\phi(W)$ the phase of the multipole and $h(W) = \exp[i\phi(W)]\sin[\phi(W)]$. In Ref.[3], an analogy is drawn between this solution and the Born term driven contribution of a unitary background with a resonance dominated final state interaction. We have two objections against this interpretation. First of all, in this argument a reference to dynamical models in implicit which is questionable according to point 1. Second, we found that the decomposition is highly dependent on assumptions on the phases of the multipoles at higher energies. The phases of the multipoles enter the solutions via the functions $D(W)$ and $h(W)$ on the whole range of integration. Above 2π threshold where Watson's theorem is no longer valid, an assumption has to be made. Schwela derived two ansatzes based on unitarity with a further assumption which contain the πN scattering phase shift $\delta_l(W)$ and inelasticity $\eta_l(W)$[4]:

$$\phi_1(W) \;=\; \arctan\frac{1-\eta_l(W)\cos 2\delta_l(W)}{\eta_l(W)\sin 2\delta_l(W)}, \qquad (2)$$

$$\phi_2(W) \;=\; \arctan \frac{\eta_l(W)\sin 2\delta_l(W)}{1+\eta_l(W)\cos 2\delta_l(W)}. \tag{3}$$

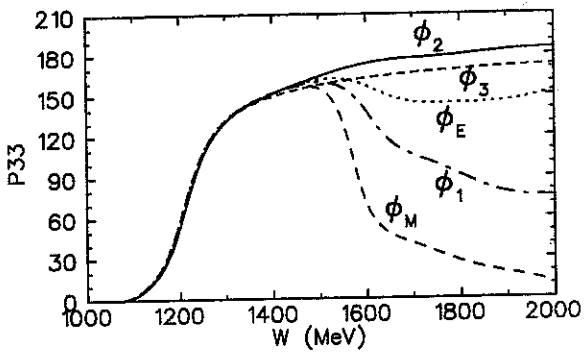

Fig. 1. Different ansatzes for the phases of the P33 multipoles. ϕ_1 and ϕ_2 are the ansatzes derived by Schwela. ϕ_3 is the phase used by Aznauryan. ϕ_E and ϕ_M are the phases of $E_{1+}(3/2)$ and $M_{1+}(3/2)$ respectively according to the solution SM98 by the VPI group.

In Fig. 1, these ansatzes are compared with the phase which has been assumed for both P33 multipoles in Ref.[3] and the multipole phases according to the VPI analysis. We found that the final result for the multipoles is much less dependent on the choice of the phase than the decomposition into particular solution and homogeneous solutions (see Figs. 2 and 3). It should be stressed that, according to our findings, different phases for both multipoles at higher energies are to be preferred. While a phase that approaches π (ϕ_3 in Fig. 3) for $W \to \infty$ leads to the best representation of $E_{1+}(3/2)$ (see Fig. 3), consideration of the solutions at higher energies as well as the result for the phase of $M_{1+}(3/2)$ according to the VPI analysis suggest an ansatz for this phase which decreases above 1600 MeV. From this we conclude that, if the argument of Ref.[3] were correct, one would at least have to ensure that the correct phases have been used in solving the Omnès equations.

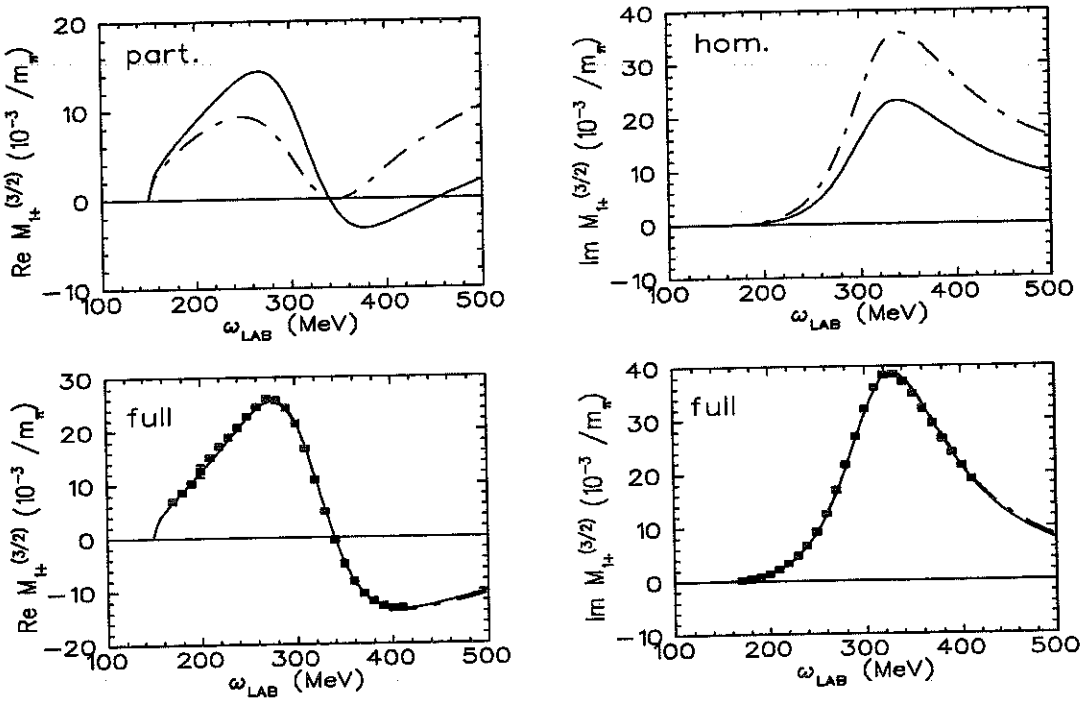

Fig. 2. The decomposition of $M_{1+}(3/2)$ into particular solution and solution to the homogeneous equation according to the ansatzes ϕ_1 (solid lines) and ϕ_3 (dashed-dotted lines). Data points are taken from our local fit (see Ref.[1]).

CONCLUSION

The problem of an experimental determination of the electromagnetic excitation properties of the $\Delta(1232)$ is still unresolved. Although high precision data on pion photoproduction allow for the determination of the relevant multipoles to high accuracy, up to now no unique procedure of extracting the quantities of interest has been established.

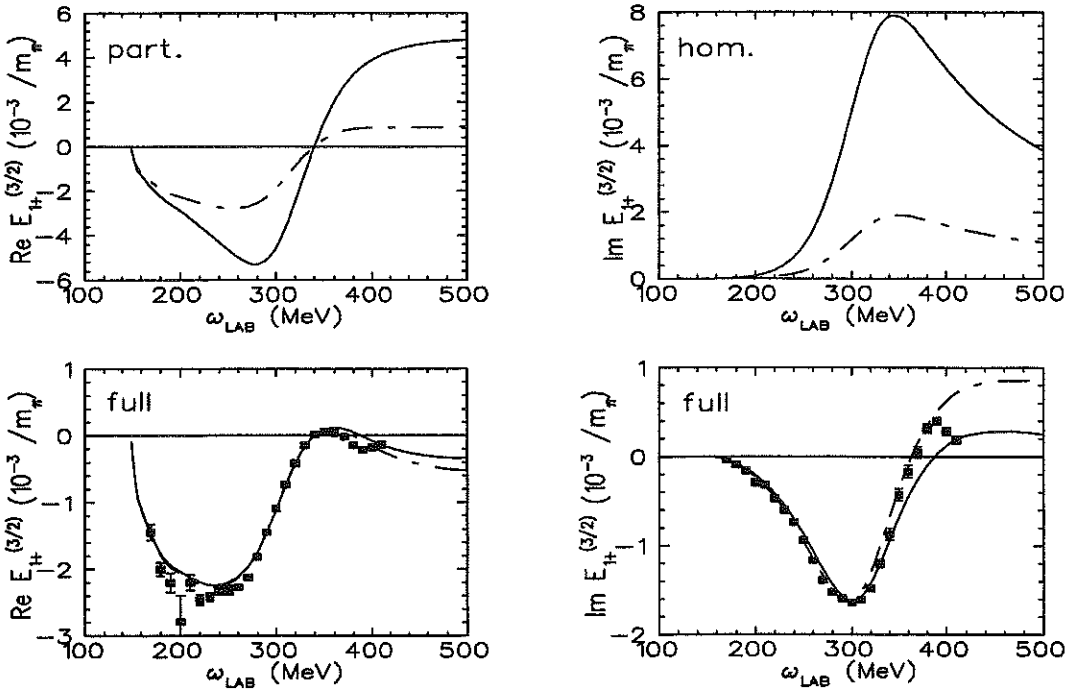

Fig. 3. The decomposition of $E_{1+}(3/2)$ into particular solution and solution to the homogeneous equation according to the ansatzes ϕ_1 and ϕ_3. Symbols as in Fig. 2.

Several methods of determining these parameters from multipoles have been discussed in the literature. They all suffer from one of the following shortcomings:

1. Some of them depend on an underlying model (coupling constants of the $\gamma N\Delta$ vertex) or other additional assumptions (e.g. the contributions of the homogeneous solutions to the Omnès equations).

2. There is no immediate connection between the model independent quantities such as the residues of the K matrix and the T matrix and the predictions of microscopic models.

Since the issue concerns our basic understanding of the structure of the nucleon and its resonances, it deserves further study.

REFERENCES

1. O. Hanstein, D. Drechsel, L. Tiator, "Multipole analysis of pion photoproduction based on fixed t dispersion relations an unitarity," Nucl. Phys. **A 632**, 561 (1998).
2. P. Wilhelm, Th. Wilbois, and H. Arenhövel, "Unitary ambiguity in the extraction of the E2/M1 ratio for the $\gamma N \leftrightarrow \Delta$ transition," Phys. Rev. **C 54**, 1423 (1996).
3. I. G. Aznauryan, "Dispersion relations and the Δ contributions into the amplitudes $M_{1+}^{3/2}, E_{1+}^{3/2}$ from new VPI partial-wave analysis of pion photoproduction", Preprint hep-ph/9904275.
4. D. Schwela and R. Weizel, "Evaluation of Multipoles for Photo- and Electroproduction of Pions," Z. Phys. **221**, 71 (1969).

Kaon Photoproduction in a Confining and Covariant Diquark Model*

R. Alkofer, S. Ahlig, C. Fischer, and M. Oettel
Institute for Theoretical Physics, University of Tübingen
Auf der Morgenstelle 14, D-72076 Tübingen

Abstract

Baryons are modeled as bound states of scalar or axialvector diquarks and a constituent quark which interact through quark exchange. This description results as an approximation to the relativistic Faddeev equation for three quarks. The corresponding effective Bethe-Salpeter equation is solved, and fully four-dimensional wave functions for both octet and decuplet baryons are obtained. Confinement of quarks and diquarks is incorporated by modifying their propagators. Results are given for kaon photoproduction which is one of the applications currently under investigation in this model.

Motivation

In this talk it will be argued that in the study of baryonic structure kaon photoproduction is an especially interesting hadronic reaction. Photo– and electroproduction of pseudoscalar mesons have been studied intensively in isobar resonance models [1,2] and coupled channel calculations of hadronic interactions [3]. These models are capable of describing the wealth of measured data reasonably well. However, by construction they do not allow for an interpretation of the production process in terms of baryon substructure. The aim of the investigation reported here is to clarify whether the notion of diquarks as effective constituents of baryons in meson production close to threshold is helpful in the understanding of subnucleonic physics.

Approaches to the substructure of baryons include nonrelativistic quark models, various sorts of bag models and different types of solitons [4]. Most of these models are designed to work in the low energy region and generally do not match the calculations within perturbative QCD. During this conference impressive reports on the great experimental progress in medium energy physics have been given. This underlines the high demand for models describing baryon physics in this region. Therefore we propose a fully covariant description of baryon structure in the framework of a diquark–quark–model of baryons.

Our motivation to choose such an approach is based on two sources. On the one hand, when starting with the fully relativistic Faddeev equation for bound states of three quarks, diquarks appear as effective degrees of freedom. These diquarks stand for (potentially weakly) correlated quark–quark pairs inside baryons. On the other hand, diquarks as constituents of baryons are naturally obtained when one starts with an NJL–type model of colour octet flavour singlet quark currents [5]. Although in the limit $N_c \to \infty$ baryons emerge as solitons of meson fields [6], it can be shown for the case of three colours that both effects, binding through quark exchange in the diquark-quark picture and through mesonic effects, contribute equally [7].

The four-dimensional Bethe-Salpeter equation: masses and wave functions

As stated above, in a first step we want to reduce the complexity of the full three–body problem of the relativistic Faddeev equation for baryons. This can be achieved by approximating the two–quark irreducible T–matrix by separable contributions that can be viewed as loosely bound diquarks. The three–body problem then becomes an effective two–body one, in which bound states appear as the solution of a homogeneous Bethe–Salpeter equation. The attractive interaction between quark and diquark is hereby provided by quark exchange. This interaction is but the minimal correlation needed to reconstitute the Pauli principle. Due to antisymmetry in the color indices and the related symmetrization of all other quantum numbers the Pauli principle leads to an attractive interaction in contrast to "Pauli repulsion" known in conventional few-fermion systems. All unknown

*Supported by the BMBF (06–TU–888) and by the DFG (We 1254/4-1).

Table 1. Components of the octet baryon wave function with their respective spin and orbital angular momentum. $(\gamma_5 C)$ corresponds to scalar and $(\gamma^\mu C)$, $\mu = 1 \ldots 4$, to axialvector diquark correlations. Note that the partial waves in the first row possess a non-relativistic limit. See [8] for further details.

"non-relat." partial waves	$\begin{pmatrix} \chi \\ 0 \end{pmatrix}(\gamma_5 C)$	$\hat{P}^4 \begin{pmatrix} 0 \\ \chi \end{pmatrix}(\gamma^4 C)$	$\begin{pmatrix} i\sigma^i \chi \\ 0 \end{pmatrix}(\gamma^i C)$	$\begin{pmatrix} i\left(\hat{p}^i(\vec{\sigma}\hat{\vec{p}}) - \frac{\sigma^i}{3}\right)\chi \\ 0 \end{pmatrix}(\gamma^i C)$
spin	1/2	1/2	1/2	3/2
orb.ang.mom.	s	s	s	d
"relat." partial waves	$\begin{pmatrix} 0 \\ \vec{\sigma}\vec{p}\chi \end{pmatrix}(\gamma_5 C)$	$\hat{P}^4 \begin{pmatrix} (\vec{\sigma}\vec{p})\chi \\ 0 \end{pmatrix}(\gamma^4 C)$	$\begin{pmatrix} 0 \\ i\sigma^i(\vec{\sigma}\vec{p})\chi \end{pmatrix}(\gamma^i C)$	$\begin{pmatrix} 0 \\ i\left(p^i - \frac{\sigma^i(\vec{\sigma}\vec{p})}{3}\right)\chi \end{pmatrix}(\gamma^i C)$
spin	1/2	1/2	1/2	3/2
orb.ang.mom.	p	p	p	p

and probably very complicated gluonic interactions between two quarks are effectively treated via the parameterization of the diquark propagator and the diquark–quark–quark vertex function. In Ref. [8] we have formalized this procedure by an effective Lagrangian containing constituent quark, scalar diquark and axialvector diquark fields. This leads to a coupled set of Bethe–Salpeter equations for octet and decuplet baryons.

We avoid unphysical thresholds by an effective parameterization of confinement in the quark and diquark propagators. We solve the four–dimensional equations in ladder approximation and obtain wave functions for the octet and decuplet baryons [8]. The Lorentz invariance of our model has been checked explicitly by choosing different frames.

The implementation of the appropriate Dirac and Lorentz representations of the quark and diquark parts of the wave functions leads to a unique decomposition in the rest frame of the baryon. Besides the well known s-wave and d-wave components of non-relativistic formulations of the baryon octet we additionally obtain non-negligible p-wave contributions which demonstrates again the need for covariantly constructed models. Table 1 summarizes the structure of the octet wave function. Each of the eight components is to be multiplied with a scalar function which is given in terms of an expansion in hyperspherical harmonics and is computed numerically.

In order to obtain the mass spectra for the octet and decuplet baryons we explicitly break SU(3) flavour symmetry by a higher strange quark constituent mass. Using the nucleon and the delta mass as input our calculated mass spectra [8] are in good agreement with the experimental ones, see Table 2. The wave functions for baryons with distinct strangeness content but same spin differ mostly due to flavour Clebsch-Gordan coefficients, the respective invariant functions being very similar. Due to its special role among the other baryons, we investigated the Λ hyperon in more detail and discussed its vertex amplitudes. In our approach, the Λ acquires a small flavour singlet admixture which is absent in $SU(6)$ symmetric non-relativistic quark models.

Table 2. Octet and decuplet masses obtained with two different parameter sets. Set I represents a calculation with weakly confining propagators, Set II with strongly confining propagators, see [8]. All masses are given in GeV.

	m_u	m_s	M_Λ	M_Σ	M_Ξ	M_{Σ^*}	M_{Ξ^*}	M_Ω
Set I	0.5	0.65	1.123	1.134	1.307	1.373	1.545	1.692
Set II	0.5	0.63	1.133	1.140	1.319	1.380	1.516	1.665
Exp.			1.116	1.193	1.315	1.384	1.530	1.672

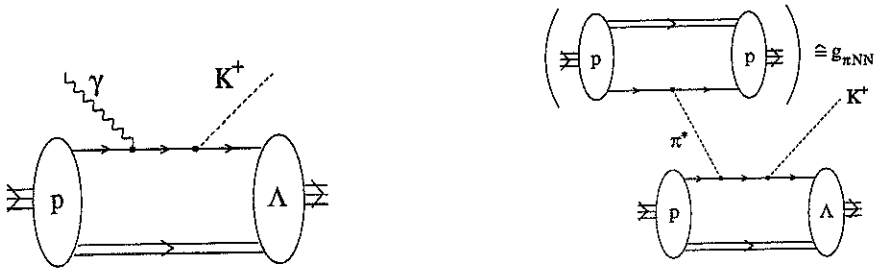

Figure. 1. Typical diagrams to be computed in the diquark spectator picture. Left: kaon photoproduction. Right: strangeness production in proton–proton collisions.

Form Factors

A significant test of our model is the calculation of various form factors [9–11]*. The most important ingredient are the fully four-dimensonal wave functions described above. It turns out that already the electromagnetic form factors of the nucleon provide severe restrictions for the parameters of the model.

For the pion–nucleon form factor at the soft point, $g_{\pi NN}$, we find good agreement with experiment. For spacelike momenta this form factor falls like a monopole with a large cutoff similar to the behaviour in One-Boson-Exchange (OBE) models [11]. Compared with a calculation including only scalar diquarks [9] we find a lower value for the pion–nucleon coupling at the soft point. Serving as a central ingredient for strangeness production processes the kaon–nucleon–lambda form factor $g_{KN\Lambda}$ is a quantity of special interest. Due to flavour algebra the isospin configuration of the Λ singles out the scalar diquark as the only diquark contributing to nucleon–lambda transitions. Since a pseudoscalar kaon does not couple to the scalar diquark we find ourselves in a comfortable position to handle such transitions. We find that the absolute value of the kaon–nucleon–lambda form factor is always smaller than the pion–nucleon form factor [11]. This can be understood from the facts that the axialvector diquark does not contribute and that the kaon decay constant is larger than the pion decay constant.

Kaon Photoproduction

The SAPHIR collaboration has measured the cross section and the asymmetries for the process $p\gamma \to K\Lambda$ with high precision. These measurements continue to prompt corresponding calculations within various models, among these are the isobaric model [1,2], the coupled channel approach [3] and models which describe those processes in terms of the dynamics of the baryon substructure [14].

The reaction $p\gamma \to K\Lambda$ lends itself to a description within the diquark–quark picture. This is for two reasons which greatly simplify the description: first, the scalar diquark is the sole overlap between the wave function of the proton and the lambda, which implies that axialvector diquarks cannot participate in the reaction, and second, the kaon does not couple to the diquark. This leads to the conclusion that the diagram shown in the left half of Fig. 1 and the corresponding crossed diagram are the dominant contributions to kaon photoproduction.

The total cross section for $p\gamma \to K\Lambda$ is shown in the left panel of Fig. 2. For $E < 1.5$ GeV the data are reproduced quite nicely, whereas our results do not fall off fast enough for higher energies. We found that the total cross section depends very little on the details of the baryon wave functions, however, we observed a rather pronounced dependence on the way confinement is parameterized into the propagators. A closer analysis reveals that production processes like $p\gamma \to K\Lambda$ probe the propagators of the constituents in the timelike region, i.e. for timelike momenta of the constituents. This is a highly welcome feature which may be used in conjunction with Dyson–Schwinger studies. This approach is tied to the dynamics of QCD and thus gives access to the nonperturbative quark propagator,

*For a similar calculation of the electromagnetic nucleon form factors within a slightly different diquark model see Ref. [12]

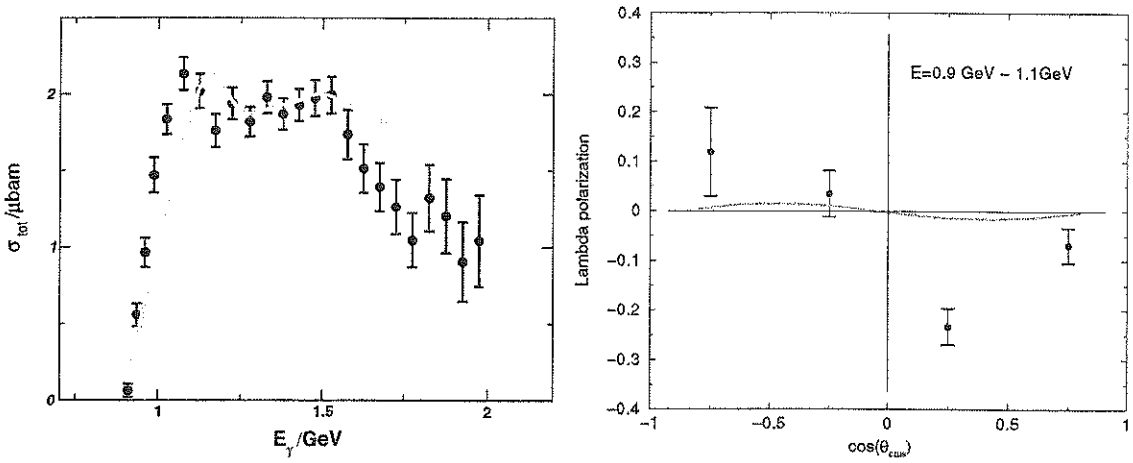

Figure. 2. Total cross section (left panel) and Lambda polarization (right panel) for the reaction $p\gamma \to K\Lambda$. The data are taken from [15] and are shown together with our results.

which enters as a key ingredient in the description of baryons as bound states of quarks and diquarks. Since the Dyson-Schwinger approach gives the propagators for spacelike momenta only, one should take on board the idea, that production processes like $p\gamma \to K\Lambda$ firmly constrain the extrapolation to timelike momenta.

The lambda polarization is shown in the right panel of Fig. 2 for the energy range 0.9 – 1.1 GeV. Our results fall short of the experimental values, however, the change in sign is reproduced. Comparing with, e.g. [1–3] we conclude that apparently none of the current models is able to reproduce the asymmetries to reasonable accuracy.

Acknowledgement: R.A. thanks the organizers for making this conference so pleasant and stimulating. The authors also want to express their gratitude to Hugo Reinhardt and Herbert Weigel for their support of this project.

REFERENCES

1. *see e.g.* H. Haberzettl, *these proceedings*;
   see also: C. Bennhold *et al.*, nucl-th/9901066 and references therein.
2. *see e.g.* L. Tiator, *these proceedings*; L. Tiator *et al.*, Phys. Rev. C **60** (1999) 035210.
3. *see e.g.* N. Kaiser, *these proceedings.*
4. *see e.g.* R. Bhaduri, Models of the Nucleon, Addison-Wesley,New York,1988.
5. R. Alkofer and H. Reinhardt, Chiral Quark Dynamics, Springer Verlag (1995);
   see also: C. J. Burden, R. T. Cahill, and J. Praschifka, Aust. J. Phys. **42** (1989) 147;
   H. Reinhardt, Phys. Lett. **B244** (1990) 316.
6. R. Alkofer, H. Reinhardt, and H. Weigel, Phys. Rep. **265** (1996) 139.
7. U. Zückert, R. Alkofer, H. Weigel, and H. Reinhardt, Phys. Rev. C **55** (1997) 2030.
8. M. Oettel, G. Hellstern, R. Alkofer, and H. Reinhardt, Phys. Rev. C **58** (1998) 2459.
9. G. Hellstern, R. Alkofer, and H. Reinhardt, Nucl. Phys. A 627 (1997) 679.
10. M. Oettel, M. A. Pichowsky and L. von Smekal, nucl-th/9909082.
11. M. Oettel, S. Ahlig, R. Alkofer, and C. Fischer, nucl-th/9910079;
    C. Fischer, Diploma Thesis, University of Tübingen 1999 (in german).
12. J. C. R. Bloch *et al.*, Phys. Rev. C **60** (1999) 062201.
13. K. Kusaka, G. Piller, A. W. Thomas, and A. G. Williams, Phys. Rev. D **55** (1997) 5299.
14. For an investigation of kaon photoproduction in a different diquark model *see e.g.*
    P. Kroll, M. Schürmann, K. Passek, and W. Schweiger, Phys. Rev. D **55** (1997) 4315.
15. SAPHIR coll., Phys. Lett. **B445** (1998) 20.

A Multipole Analysis for Eta Photoproduction

Lothar Tiator
Institut für Kernphysik, Universität Mainz, J.J. Becherweg 45

Abstract

In eta photoproduction new data for total and differential cross sections, target asymmetry and photon asymmetry are analyzed. Using a few reasonable assumptions we perform the first model-independent analysis of the E_{0+}, E_{2-} and M_{2-} eta photoproduction multipoles. Making use of the well-known $A_{3/2}$ helicity amplitude of the $D_{13}(1520)$ state we extract its braching ratio to the ηN channel, $\Gamma_{\eta N}/\Gamma = (0.08 \pm 0.01)\%$. At higher energies the new GRAAL photon asymmetry data show a clear signal of the $F_{15}(1680)$ excitation which permits extracting the $F_{15}(1680) \to \eta N$ branching ratio to be of $(0.15^{+0.35}_{-0.10})\%$.

INTRODUCTION

Over the last several years, eta photoproduction has demonstrated its potential as a new, powerful tool to selectively probe certain resonances that are difficult to explore with pions. It is well known that the low energy behavior of the eta production process is governed by the $S_{11}(1535)$ resonance[1–3]. The recent, precise measurements of total and differential cross sections for eta photoproduction at low energies[4,5] have allowed determining the $S_{11}(1535)$ resonance parameters with unprecedented precision. A well-known example of the power of the (γ,η) reaction is the extraction of the $A^p_{1/2}$ helicity amplitude of the $S_{11}(1535)$ state. Due to the combined cusp-resonance nature of this resonance, analyses based solely on pion photoproduction consistently underestimate this quantity to be around $60 \cdot 10^{-3} GeV^{-1/2}$[6] while extractions from eta photoproduction place the value closer to twice this number[4]. Recent coupled-channel analyses[7,8] that properly include the cusp as well as the resonance phenomena have confirmed a range of values consistent with eta photoproduction.

However, it is because of the overwhelming dominance of the S_{11} that the influence of other resonances in the same energy regime, such as the $D_{13}(1520)$, is difficult to discern. It has been pointed out[2] that polarization observables provide a new doorway to access these non-dominant resonances which relies on using the dominant E_{0+} multipole to interfere with a smaller multipole. Especially the polarized photon asymmetry was shown to be sensitive to the $D_{13}(1520)$.

Recently, polarization data for the target and photon asymmetries in eta photoproduction were measured at ELSA[9] and GRAAL[10], respectively, for the first time. Taken together with the data for the unpolarized cross section from MAMI, we perform in this paper an almost model-independent multipole analysis of the $l = 0$ and 2 eta photoproduction multipoles from threshold to about 900 MeV. This permits a precise determination of the $D_{13}(1520)$ contribution and an extraction of new $D_{13}(1520)$ resonance parameters[11].

MULTIPOLE ANALYSIS

With the following angle-independent quantities

$$a = |E_{0+}|^2 - \mathrm{Re}\left[E^*_{0+}\,(E_{2-} - 3M_{2-})\right], \tag{1}$$

$$b = 2\mathrm{Re}\left[E^*_{0+}\,(3E_{1+} + M_{1+} - M_{1-})\right], \tag{2}$$

$$c = 3\mathrm{Re}\left[E^*_{0+}\,(E_{2-} - 3M_{2-})\right], \tag{3}$$

$$d = \frac{3}{a + c/3}\mathrm{Im}\left[E^*_{0+}\,(E_{1+} - M_{1+})\right], \tag{4}$$

$$e = -\frac{3}{a + c/3}\mathrm{Im}\left[E^*_{0+}\,(E_{2-} + M_{2-})\right], \tag{5}$$

$$f = \frac{3}{a + c/3}\mathrm{Re}\left[E^*_{0+}\,(E_{2-} + M_{2-})\right], \tag{6}$$

we can express the observables in a series of $\cos\theta$ terms that can be fitted to the experimental data at various energies $E_{\gamma,lab}$

$$\frac{d\sigma}{d\Omega} = \frac{q_\eta}{k}\left(a + b\cos\theta + c\cos^2\theta\right), \quad (7)$$

$$T = \sin\theta\,(d + e\cos\theta), \quad (8)$$

$$\Sigma = f\sin^2\theta. \quad (9)$$

It is remarkable that a combined analysis of the three above observables allows a determination of the d–wave contributions to eta photoproduction once the quantities a, c, e and f have been determined from experiment. As was already pointed out in Ref.[4], the total cross section alone determines the magnitude of the S-wave multipole

$$|E_{0+}| = \sqrt{a + \frac{c}{3}} = \sqrt{\frac{1}{4\pi}\frac{k}{q_\eta}\sigma_{total}}. \quad (10)$$

With the knowledge of e and f the helicity 3/2 multipole B_{2-}, defined below, and the phase relative to the S_{11} channel can be determined

$$|B_{2-}| \equiv |E_{2-} + M_{2-}| = \frac{1}{3}\sqrt{(e^2 + f^2)(a + c/3)}, \quad (11)$$

$$\tan(\phi_{E_{0+}} - \phi_{B_{2-}}) = \frac{e}{f}. \quad (12)$$

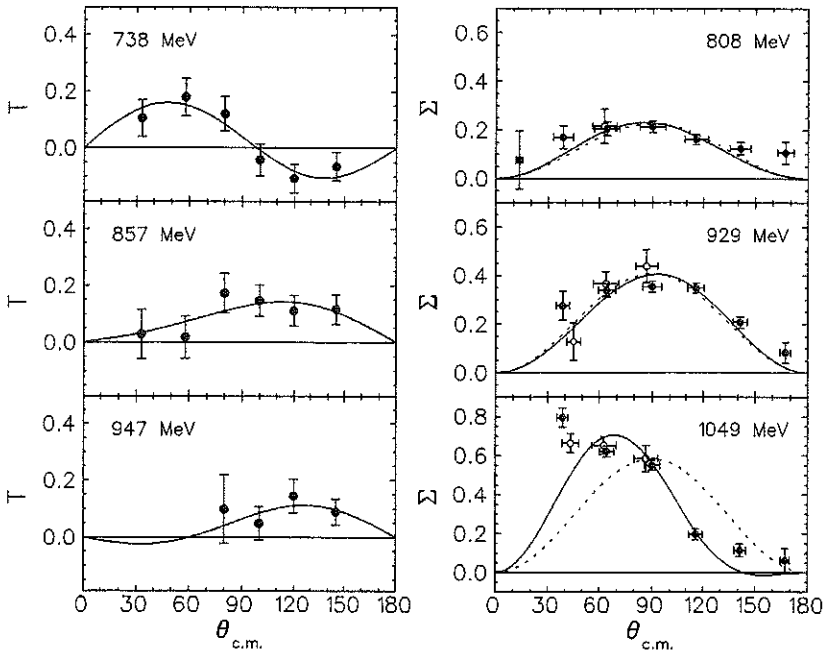

Figure. 1. Target asymmetrie T and photon asymmetry Σ for $p(\gamma,\eta)p$. The full line is the result of our fit to the experimental data of[9,10]. The dotted line is the bestfit for the photon asymmetry if only s, p and d waves are allowed, Eq. (9).

RESULTS

For the angular distributions measured by the TAPS collaboration at Mainz[4] in the energy range between 716 and 790 MeV our results for the coefficients a, b and c are identical to the results of Ref.[4]. As discussed above, the a coefficient can be fitted to a

Breit-Wigner form with an energy-dependent width leading, e.g., to parameters of $M_R = (1549 \pm 8) MeV$, $\Gamma_R = (202 \pm 35) MeV$ and an absolute value of the s-wave multipole at threshold, $|E_{0+}| = 16 \cdot 10^{-3}/m_\pi^+$ (Fit 1, Ref.[4]).

Fig. 1 shows our fit to the target polarization data from Bonn[9] and to the photon asymmetry recently measured at GRAAL[10]. For the target asymmetry all models fail to reproduce the angular shape of the data. In particular, the node found experimentally at low energies with negative T values at backward angles was completely unexpected and as we will demonstrate below leads to strong consequences for the nature of the S_{11} resonance.

For the photon asymmetry Fig. 1 demonstrates that we can achieve an excellent fit with the Ansatz of Eq. (9) up to 900 MeV. However, above 900 MeV the data show the evolution of a forward-backward asymmetry that becomes most pronounced at 1050 MeV. This behavior cannot be fitted any more with the form of Eq. (9) but requires an additional coefficient

$$\Sigma \;=\; \sin^2\theta (f + g\cos\theta)\,. \tag{13}$$

where g is determined solely by multipoles of order 3 and higher. In lowest order we get

$$g \;=\; \frac{15}{a + c/3} \mathrm{Re}\left[E_{0+}^* \left(E_{3-} + M_{3-} + E_{3+} - M_{3+}\right)\right]\,. \tag{14}$$

The obvious need for the coefficient g at higher energies therefore represents a clear signal that partial waves beyond d-waves are required to describe the photon asymmetry data.

Fig. 2 shows the result of our multipole analysis. Most surprising is the relative phase between the s- and d-waves. This phase difference is model-independent. If both the $S_{11}(1535)$ and $D_{13}(1520)$ are parametrized via Breit-Wigner type functions, this phase difference would be rather constant as both resonances are very close in their energy position and, furthermore, have a similar resonance width. From the fact that the S_{11} is a bit higher in energy, the phase difference $\phi_0 - \phi_2$ should be small and negative as is shown in the figure as the dotted line.

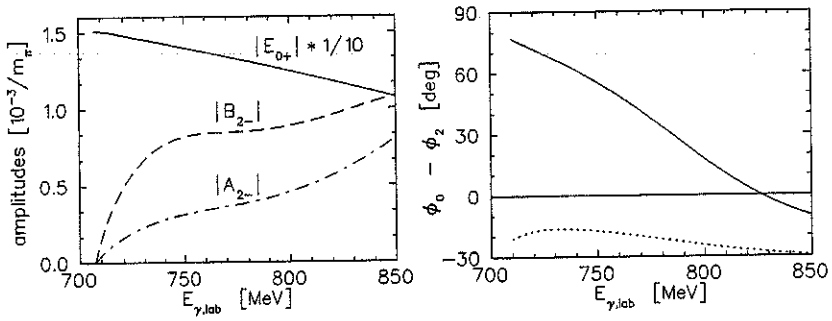

Figure. 2. Result of the multipole analysis for s- and d- waves. On the left the absolute values of the E_{0+}, $A_{2-} = (3M_{2-} - E_{2-})/2$ and $B_{2-} = M_{2-} + E_{2-}$ mulripoles are shown, the s-wave is reduced by a factor of 10 in order to scale. In the figure on the right we compare the phase difference of our fit (solid line) with the difference of two Breit-Wigner forms (dotted line).

From the above analysis we can conclude that this completely unexpected discrepancy is directly connected to the node structure in the target asymmetry. Without a node or with a node but an e-coefficient of opposite sign, the phase difference would be much smaller and closer to an isobar model with BW type of resonances[12]. Other models based either on a coupled-channels approach[8] or on a tree-level effective Lagrangian analysis[13] also cannot reproduce the target asymmetry. It is therefore imperative, this measurement be verified and extended to higher energy as soon as possible.

In Table 1 we show our numerical results for the resonance parameters together with numbers found in the Particle Data Tables[14] and in a recent analysis of Mukhopadhyay

and Mathur[13]. It is very interesting to note that the D_{13} has a branching ratio of only 0.08% in our analysis 1 and nevertheless gives a very pronounced signal in the photon asymmetry of Fig. 1. The photon asymmetry would be practically zero up to $E_\gamma^{lab} \approx 900\,MeV$ without this resonance decay. Also the branching ratio of the F_{15} resonance is still well below 1%. Both resonances could have never been seen in the total cross section, where the S_{11} dominates by 2 orders of magnitude, and even in the angular distribution very high-precision data are required to observe the interferences with the s-wave. It is another very nice success of the constituent quark model with hyperfine quark-gluon interaction (Koniuk and Isgur (1980)[15]) that predicted the ηN branching ratios for the $S_{11}(1535)$, $D_{13}(1520)$ and $F_{15}(1680)$ to 47%, 0.09% and 0.8%, respectively.

Table 1. Resonance properties determined in our analysis. The first entry for each resonance is taken from the Particle Data Tables 1998[14]. Our analyses (case 1 and 2) are based on the average values from PDG for the mass M_R, full width Γ_R and $A_{3/2}$. Only statistical errors are given.

	$b_\eta = \Gamma_\eta/\Gamma_R$ [%]	$A_{1/2}$ $[10^{-3}/\sqrt{GeV}]$	$A_{3/2}/A_{1/2}$	$\xi_{3/2}$ $[10^{-4}/MeV]$	$\xi_{1/2}$ $[10^{-4}/MeV]$
$D_{13}(1520)$	-	-24 ± 9	-6.9 ± 2.6	-	-
case 1	0.08 ± 0.01	-79 ± 9	-2.1 ± 0.2	0.185 ± 0.018	-0.087 ± 0.013
case 2	0.05 ± 0.02	-79 ± 9	-2.1 ± 0.2	0.134 ± 0.018	-0.087 ± 0.013
Ref. [13]	-	-52 ± 10	-2.5 ± 0.5	0.167 ± 0.017	-0.066 ± 0.008
$F_{15}(1680)$	-	-15 ± 6	-8.9 ± 3.6	-	-
case 2	$0.15^{+0.35}_{-0.10}$	-	-	0.16 ± 0.04	-

In comparison with Mukhopadhyay and Mathur, we confirm their finding of a much smaller $A_{3/2}/A_{1/2}$ ratio for the D_{13} resonance compared to much larger values given in the Particle Data Tables and predicted by the quark model.

I would like to thank G. Anton, J.-P. Didelez and D. Rebreyend for very fruitful discussions. This work was supported by the Deutsche Forschungsgemeinschaft (SFB 443).

REFERENCES

1. C. Bennhold and H. Tanabe, Nucl. Phys. **A530** (1991) 625.
2. L. Tiator, C. Bennhold and S.S. Kamalov, Nucl. Phys. **A580** (1994) 455.
3. M. Benmerrouche, N.C. Mukhopadhyay and J.-F. Zhang, Phys. Rev. D **51** (1995) 3237.
4. B. Krusche et al., Phys. Rev. Lett. **74** (1995) 3736.
5. M. Wilhelm, PhD. thesis, Bonn (1993).
6. R. Arndt, I. Strakovsky and R. Workman, Phys. Rev. C **53** (1996) 430.
7. C. Deutsch-Sauermann, B. Friman and W. Nörenberg, Phys. Lett. B **409** (1997) 51.
8. T. Feuster and U. Mosel, Phys. Rev. C **59** (1999) 460.
9. A. Bock et al., Phys. Rev. Lett. **81** (1998) 534.
10. J. Ajaka et al., Phys. Rev. Lett. **81** (1998) 1797.
11. L. Tiator, D. Drechsel, G. Knöchlein and C. Bennhold, Phys. Rev. C **60** (1999) 035210.
12. G. Knöchlein, D. Drechsel and L. Tiator, Z. Phys. A **352** (1995) 327.
13. N.C. Mukhopadhyay and N. Mathur, Phys. Lett. B **444** (1998) 7.
14. Review of Particle Physics: C. Caso et al. (Particle Data Group), European Physical Journal **C3**, 1 (1998).
15. R. Koniuk and N. Isgur, Phys. Rev. D **21** (1980) 1868.

Dynamical Formation of S-Wave Baryon Resonances: How Many Could There Be?

Peter B. Siegel and Steve Guertin
California State Polytechnic University Pomona, Pomona CA 91768

1 Introduction

Baryon resonances have been treated in two different ways: as states consisting of 3 quarks, and as a quasi-bound meson-baryon system. In the quark picture, the baryon resonance is the result of a quark excitation from the ground baryon state. The resonance enters the interaction Lagrangian as a particle which can couple to meson baryon initial and final states.

In the quasi-bound view, the resonance is a result of an attractive interaction between mesons and baryons. If the potential is strong enough, multiple scattering of the mesons and baryons can produce a resonant "quasi-bound" state resulting in a pole in the S-matrix. In practice, the resonance is calculated by iterating the potential to infinite order via a Lippmann-Schwinger or Schroedinger equation, and the resonance is refered to as "dynamically" generated.

¿From the experimental data alone, it is difficult to determine whether a resonance is a 3-quark "s-channel" resonance, or a meson-baryon "t-channel" dynamically formed resonance. In order to uncover the true nature of a baryon resonance, one needs to incorporate as much of the "physics" of the interaction into the analysis as possible. Since it is believed that chiral symmetry is an important symmetry for the meson baryon interaction, we employ this symmetry in the context of the "quasi-bound" picture.

The general approach we have taken is to use a potential which is derived from an effective chiral Lagrangian[1,2]. To test for model dependences, we have examined both a local and separable potential form. The local potential between meson-baryon channel i and meson-baryon channel j is given by:

$$V_{ij} = \frac{C_{ij}}{2f^2}\frac{E_i + E_j}{2}\sqrt{\frac{M_i M_j}{s\omega_i\omega_j}}\frac{\alpha^2 e^{-\alpha r}}{4\pi r} \tag{1}$$

to first order in meson energy E_i. The C_{ij} are determined from the effective Chiral Lagrangian. For the form of the separable potential used, the reader is refered to Refs.[1–3].

The potential model approach has been successful in understanding two baryon resonances: the $\Lambda(1405)$[1,3–6,8–10] and the $N^*(1535)$[2,7,11]. Many properties of both resonances are well described by a potential model derived from an effective chiral Lagrangian. In this paper, we extend this approach to examine other sectors of the meson-baryon interaction. We will determine if any other s-wave resonances could be dynamically formed. We consider the Ξ resonance (strangeness = -2), the $\Sigma(1620)$ resonance (strangeness = -1, I = 1), and the $\Lambda(1670)$ resonance (strangeness = -1, I = 0), and limit the potential to order "q" in meson energy.

2 Strangeness = -2

The C_{ij} in Eq. 1 for the strangeness = -2 sector are:

	$\pi\Xi$	$\bar{K}\Lambda$	$\bar{K}\Sigma$	$\eta\Xi$
$\pi\Xi$	-1	$\sqrt{3/8}$	$-5/4$	0
$\bar{K}\Lambda$	$\sqrt{3/8}$	0	0	$3/4$
$\bar{K}\Sigma$	$-5/4$	0	-1	$\sqrt{3}/4$
$\eta\Xi$	0	$3/4$	$\sqrt{3}/4$	0

Note that there is an attractive potential between the Ξ and π and the Σ and the $\bar{K}$ because of the -1 factors on the diagonal of the matrix above. Since these factors are multiplied by the meson mass, the attraction is further enhanced in the $\bar{K}$-Σ channel. With a common range parameter α we were able to obtain resonances for both the local and separable potentials. For the local potential, a value of α=420 MeV produced a resonance at 1620 MeV, and a value of α=370 MeV procuced a resonance at 1690 MeV. For the separable potential, a value of α=580 MeV gave a resonance at 1620 MeV, and a value of α=520 MeV produced a resonance at 1690 MeV. In all cases, the resonance produced had a strong decay to the π-Ξ channel. One eigenphase went through 90 degrees, while the other one was very small. The particle data table lists Ξ resonances at energies of 1620 and 1690 MeV. Of these two, the resonance at 1620 is believed to have a strong π-Ξ decay. Thus, **we conclude that there is a Ξ s-wave resonance that is dynamically formed that will have a strong π-Ξ decay.** The best candidate for this resonance is the $\Xi(1620)$.

3 Strangeness = -1, Isospin = 1

The C_{ij} couplings for the strangeness = -1, isospin = 1 sector are:

	$\pi\Lambda$	$\pi\Sigma$	$\bar{K}N$	$\eta\Sigma$	K Ξ
$\pi\Lambda$	0	0	$\sqrt{6}/4$	0	$\sqrt{6}/4$
$\pi\Sigma$	0	-1	$1/2$	0	-1/2
$\bar{K}N$	$\sqrt{6}/4$	$1/2$	-1/2	$\sqrt{6}/4$	0
$\eta\Sigma$	0	0	$\sqrt{6}/4$	0	$\sqrt{6}/4$
K Ξ	$\sqrt{6}/4$	-1/2	0	$\sqrt{6}/4$	-1/2

Notice here that in three channels there exists an attractive potential: the π-Σ, the $\bar{K}$-N, and the K^+- Ξ channels. Eventhough C_{ij} is only -1/2, the mass of the kaon will enhance the potential strength. The candidate for this resonance is the $\Sigma(1620)$. We find that a resonance structure can be formed at 1620 MeV using reasonable "range" parameters: α=400 MeV for the local potential and α = 600 MeV for the separable potential.

To evaluate how well the dynamically generated resonance fits the data, we compare the amplitudes determined from the potential model with available scattering amplitude analysis[12,13] from the literature. **We find that the signs of the amplitudes for all reaction channels match the phase shift analysis near the $\Sigma(1620)$ resonance. The amplitudes are also fairly close.** We show a graph of one selected amplitude on the last page.

4 Strangeness = -1, Isospin = 0

The C_{ij} couplings for the strangeness = -1, isospin = 0 sector are:

	$\pi\Sigma$	$\bar{K}N$	$\eta\Lambda$	K Ξ
$\pi\Sigma$	-2	$\sqrt{6}/4$	0	$-\sqrt{6}/4$
$\bar{K}N$	$\sqrt{6}/4$	$-3/2$	$-3\sqrt{2}/4$	0
$\eta\Lambda$	0	$-3\sqrt{2}/4$	0	$3\sqrt{2}/4$
K Ξ	$-\sqrt{6}/4$	0	$3\sqrt{2}/4$	-3/2

In this meson-baryon sector, there is a very strong attractive potential for three of the four channels due to the diagonal C_{ii} values of -2, -3/2, and -3/2. This attraction is responsible for the dynamically formed $\Lambda(1405)$ resonance. We investigate here if the $\Lambda(1670)$ could also be dynamically formed from this attractive potential.

By varying the range parameter, we were able to obtain resonance behavior at 1670 MeV. A range parameter of $\alpha = 350$ MeV for the local potential and $\alpha = 600$ MeV for the separable potential resulted in amplitudes that were close to amplitudes[12,13] obtained from the experimental data: **the signs of the amplitudes for the $KN \to KN$ and $KN \to \pi\Sigma$ match previous phase shift analysis of the data. The amplitudes are also fairly close.**

5 Summary

We have performed a potential model calculation using a potential derived from an effective chiral Lagrangian to examine if any s-wave baryon resonances are dynamically formed as quasi-bound meson-baryon states. In this prelimary investigation we are using only the first term (order "q" in meson energy) of the Lagrangian. There is only one free range parameter. We find that using a reasonable value for the range parameter ($350MeV < \alpha < 600MeV$):

1. An S-wave Ξ resonance is formed as a quasi-bound state at an energy near the $\Xi(1620)$ and $\Xi(1690)$ resonances with a strong decay to the π-Ξ final state.

2. The signs of the s-wave amplitudes (real and imaginary) for the reactions $\bar{K}N \to \bar{K}N$, $\bar{K}N \to \pi\Sigma$ and $\bar{K}N \to \pi\Lambda$ are in agreement with available analysis of the experimental data near the $\Sigma(1620)$ resonance. The magnitude of the amplitudes are also fairly close.

3. The signs of the s-wave amplitudes (real and imaginary) for the reactions $\bar{K}N \to \bar{K}N$ and $\bar{K}N \to \pi\Sigma$ are in agreement with available analysis of the experimental data near the $\Lambda(1670)$ resonance. The magnitude of the amplitudes are also fairly close.

Thus, in addition to the $\Lambda(1405)$ and the $N^*(1535)$ baryon resonances, the $\Xi(1620)$, the $\Sigma(1620)$ and the $\Lambda(1670)$ might also be dynamically formed s-wave quasi-bound meson-baryon resonances. Perhaps more physics can be learned by parameterizing the data using coefficients of an effective chiral Lagrangian and range parameters instead of resonance masses, widths and coupling constants.

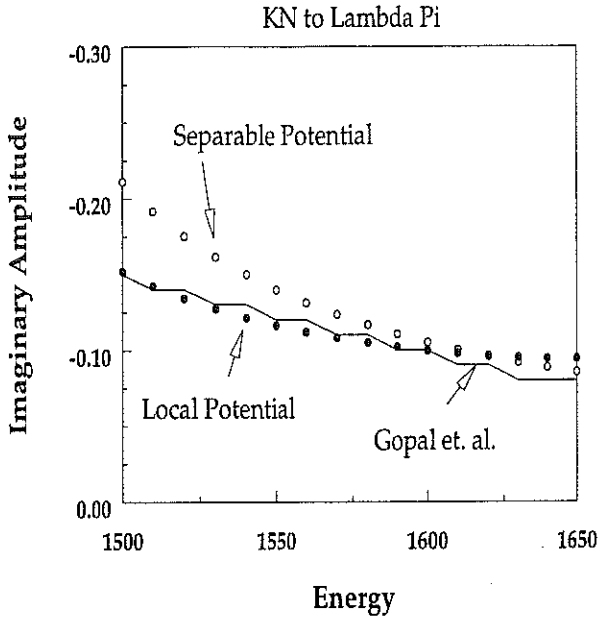

Figure 1. One of the amplitudes calculated, the imaginary part of the $\bar{K}N \to \pi\Lambda$ reaction, showing comparison of the local and separable potential forms with the data of[12].

REFERENCES

1. N. Kaiser, P.B. Siegel and W. Weise, *Nucl. Phys.* **A594** 325-345 (1995).
2. N. Kaiser, P.B. Siegel and W. Weise, *Phys. Lett.* **B362** 23-28 (1995).
3. P.B. Siegel and W. Weise, *Phys. Rev.* **C38** 2221-2229 (1988).
4. R.H. Dalitz, T.-C. Wong and G. Rajesekaran, *Phys. Rev.* **153** 1617 (1967).
5. E.A. Veit, B.K. Jennings, A.W. Thomas and R.C. Barrett, *Phys. Rev.* **D31** 1033 (1985).
6. E. Oset and A. Ramos, "Non perturbative chiral approach to s-wave $\bar{K}N$ interactions", Los Alamos preprint archives nucl-th/9711022 (1997).
7. N. Kaiser, T. Waas and W. Weise, *Nucl. Phys.* **A612** 297-320 (1997).
8. T. Waas, N. Kaiser and W. Weise, *Phys. Lett.***B365** 12 (1996).
9. T. Waas, N. Kaiser and W. Weise, *Phys. Lett.* **B379** 34 (1996).
10. T. Waas and W. Weise, *Nucl. Phys.* **A625** 287 (1997).
11. J. Caro Ramon, N. Kaiser, W. Weise and S. Wetzel, "SU(3) Chiral Dynamics with Coupled Channels: Inclusion of P-waves", submitted to *Nucl. Phys.***A**.
12. G.P. Gopal *et. al.*, *Nucl. Phys.* **B119** 362-400 (1977).
13. M. Alston-Garnjost *et. al. Phys. Rev.* **D**, 182 (1978).

Threshold Behaviour of Meson-Nucleon-$S_{11}(1535)$ Vertexfunctions and Determination of the $S_{11}(1535)$ Mixing Angle

F. Kleefeld*
University of Erlangen–Nürnberg, Institute for Theoretical Physics III, Staudtstr. 7, D-91058 Erlangen, Germany

Abstract

A new method for the determination of the spin-1/2-3/2-mixing angle and the range parameter of the quarkmodel wavefunction of the resonance $S_{11}^-(1535)$ is presented. The method ist based on a quantitative calculation of the total cross section of $pp \to pp\eta$ at threshold. The quantitative on-shell treatment of ISI and FSI is discussed.

INTRODUCTION

Nearly all calculations for the determination of mixing angles between different spin-components of baryon wavefunctions are based on spectroscopic models. Beside their advantages these models also contain some problems which are not dissolved yet.
The goal of the presented work is an independent way of the determination of mixing angles and range parameters in the harmonic oscillator description of nucleonic resonances within the nonrelativistic quark model. Although the approach in a first step is applied to the spin–1/2–3/2–mixing angle θ in the negative parity resonance $S_{11}(1535)$ (the underlying nature of this resonance is at the moment object to various speculations), the approach also can be applied to many other resonances.
The idea of the presented method is as follows: In a first step one has to calculate the total cross section of a process which is dominated by the resonance under consideration in such a way that the only remaining free parameters of the calculation are the mixing angles and the range parameters of the harmonic oscillator wavefunctions of the resonance and the involved ground state nucleons. In a second step the parameters are obtained by adjusting the calculated to the experimentally measured cross section.
One process dominated mainly by the $S_{11}(1535)$ is the reaction $pp \to pp\eta$ at threshold. In order to determine the desired mixing parameters one first has to get a *quantitative* understanding not only of the *short range dynamics* of the process, but also of the *initial and final state interactions* (ISI and FSI) between the in- and outgoing particles. Main investigations along this line have been performed in [1] and references therein.

THE REACTION $pp \to pp\eta$ AT THRESHOLD

The reaction $pp \to pp\eta$ at threshold is described within a relativistic meson-exchange model. The virtual $S_{11}(1535)$ is excited/deexited by the exchange of δ–, σ–, π–, η–, ρ– and ω–mesons, while it is deexcited/excited by the produced η.

Total Cross Section

Using relativistic normalisations for spinors, creation and annihilation operators it is straight forward to write down the expression for the total cross section of $pp \to pp\eta$ ($P_i = p_1 + p_2$, $s = P_i^2$, $\mathcal{F}(s) = 2\sqrt{\lambda(s, m_p^2, m_p^2)}$, $\lambda(x,y,z) = x^2 + y^2 + z^2 - 2(xy + yz + zx)$):

$$\sigma_{pp\to pp\eta}(s) = \frac{1}{2!}\frac{1}{\mathcal{F}(s)}\frac{1}{(2\pi)^5}\int \frac{d^3p_{1'}}{2\,\omega_p(|\vec{p}_{1'}|)}\,\frac{d^3p_{2'}}{2\,\omega_p(|\vec{p}_{2'}|)}\,\frac{d^3p_{3'}}{2\,\omega_\eta(|\vec{p}_{3'}|)}\;\delta^4(p_{1'}+p_{2'}+p_{3'}-P_i)\;\overline{|T_{fi}|^2} \tag{1}$$

The combinatorial factor of 1/2! is due to the two outgoing identical protons. For the relativistic description of $pp \to pp\eta$ the following 5 independent invariants are chosen:

$$s = (p_1+p_2)^2\,,\; s_1 = (p_{1'}+p_{2'})^2\,,\; s_2 = (p_{2'}+p_{3'})^2\,,\; t_1 = (p_1-p_{1'})^2\,,\; t_2 = (p_2-p_{3'})^2 \tag{2}$$

*Email: kleefeld@theorie3.physik.uni-erlangen.de / Publication No. FAU-TP3-99/7

(On–Shell) Watson-Migdal-Approach to ISI and FSI

In order to get a *quantitative* understanding of the ISI and FSI it is crucial to recall the steps which lead to that what the people nowadays call"Watson-Migdal approximation" and what is wrongly implemented in nearly all threshold meson production calculations by now: The system of colliding and produced particles is described by an overall Hamilton operator $H = K + V = K + W + U$, while K is the kinetic energy operator, W is the particle number nonconserving short range interaction potential and U is the particle number conserving interaction potential of long range. For convenience additionally one can define the long range Hamilton operator $h = K + U$. The corresponding eigenstates to the operators H, h and K fulfil the following Schrödinger equations:

$$(E - H)|\psi_\alpha^\pm >= 0 \quad , \quad (E - h)|\chi_\alpha^\pm >= 0 \quad , \quad (E_n - K)|\varphi_n^\pm >= 0 \tag{3}$$

The corresponding Lippmann–Schwinger equations are:

$$\begin{aligned} |\psi_\alpha^\pm > &= |\varphi_\alpha > + \frac{1}{E - H \pm i\varepsilon} V |\varphi_\alpha > = |\chi_\alpha^\pm > + \frac{1}{E - H \pm i\varepsilon} W |\chi_\alpha^\pm > \\ |\chi_\alpha^\pm > &= |\varphi_\alpha > + \frac{1}{E - h \pm i\varepsilon} U |\varphi_\alpha > = |\varphi_\alpha > + \frac{1}{E - K \pm i\varepsilon} T_{el}^\pm(E,K) |\varphi_\alpha > \end{aligned} \tag{4}$$

Defining the free propagator $G_0^\pm(E,K) = (E - K \pm i\varepsilon)^{-1}$ and inserting complete sets of free asymptotic states the T-matrix T_{fi} in Eq. (1) can be separated in a short and long ranged part via ($T_{\beta\alpha} = < \chi_\beta^- |W| \psi_\alpha^+ > = < \psi_\beta^- |W| \chi_\alpha^+ >$):

$$\begin{aligned} T_{\beta\alpha} \simeq < \chi_\beta^- |W| \chi_\alpha^+ > &= < \varphi_\beta | (1 + \sum_n T_{el}^+(E,K) |\varphi_n > G_0^+(E,E_n) < \varphi_n |) W \\ &\quad (1 + \sum_m |\varphi_m > G_0^+(E,E_m) < \varphi_m | T_{el}^+(E,K)) |\varphi_\alpha > \end{aligned} \tag{5}$$

As the in- and outgoing particles in $pp \to pp\eta$ are nearly on-shell one can approximate the free propagator $G_0^\pm(E,K)$ in the following way:

$$G_0^\pm(E,K) = \frac{1}{E - K \pm i\varepsilon} = P \frac{1}{E - K} \mp i\pi\delta(E - K) \approx \mp i\pi\delta(E - K) \tag{6}$$

At this point it is useful to introduce the following relative lab wavenumbers for each pair of particles in the initial and final state ($s_3 = (p_{3'} + p_{1'})^2 = s - s_1 - s_2 + 2m_p^2 + m_\eta^2$):

$$k = \frac{\sqrt{\lambda(s, m_p^2, m_p^2)}}{2(m_p + m_p)} \; , \; \kappa = \frac{\sqrt{\lambda(s_1, m_p^2, m_p^2)}}{2(m_p + m_p)} \; , \; \kappa_1 = \frac{\sqrt{\lambda(s_3, m_p^2, m_\eta^2)}}{2(m_p + m_\eta)} \; , \; \kappa_2 = \frac{\sqrt{\lambda(s_2, m_p^2, m_\eta^2)}}{2(m_p + m_\eta)} \tag{7}$$

and the corresponding wavevectors $\vec{k}$, $\vec{\kappa}$, $\vec{\kappa}_1$, $\vec{\kappa}_2$. Consider now the case, when the only two particles taking part in the ISI and FSI are the two in– and outgoing protons. In this case the subsystem of the two protons interacting via the long range potental U with phaseshifts δ_ℓ (ℓ = orbital angular momentum) can be treated within the framework of standard nonrelativistic scattering theory. By application of the on-shell approximation of Eq. (6) the T-matrix in Eq. (5) can be transformed to ($\vec{k}' = \vec{\kappa}$, $k' = \kappa$):

$$\begin{aligned} T_{fi} \simeq T(\vec{k}', \ell'; \vec{k}, \ell) &= \left(1 + ie^{i\delta_{\ell'}(k')} \sin\delta_{\ell'}(k')\right) < \vec{k}', \ell' |W| \vec{k}, \ell > \left(1 + ie^{i\delta_\ell(k)} \sin\delta_\ell(k)\right) \\ &= \frac{k' \cot\delta_{\ell'}(k')}{k'(\cot\delta_{\ell'}(k') - i)} < \vec{k}', \ell' |W| \vec{k}, \ell > \frac{k \cot\delta_\ell(k)}{k(\cot\delta_\ell(k) - i)} \\ &= \frac{\mathrm{Re} f_{\ell'}(k')}{f_{\ell'}(k')} < \vec{k}', \ell' |W| \vec{k}, \ell > \frac{\mathrm{Re} f_\ell(k)}{f_\ell(k)} = T(\mathrm{FSI})\, \bar{T}_{fi}\, T(\mathrm{ISI}) \end{aligned} \tag{8}$$

Here the Jost functions $f_\ell(k)$ were introduced by $e^{i\delta_\ell(k)} \sin\delta_\ell(k) = -(\mathrm{Im} f_\ell(k))/f_\ell(k)$. It is worth to mention that the ISI– and FSI–factors of Eq. (8) have the correct limit for vanishing ISI or FSI. If there is no ISI or FSI, the phaseshifts will vanish and the corresponding factors will go to 1. The effect of the Watson-Migdal approach is a factorization of T_{fi} into a short ranged T-matrix $\bar{T}_{fi}$ and ISI- and FSI-factors T(ISI) and T(FSI).

The the factor $T(\mathrm{ISI})$ is only a function of s, while the short ranged T-matrix $\bar{T}_{fi}$ close to threshold shows up to be a slowly varying function of the phasespace integration variables and therefore can be set to its threshold value $\bar{T}_{fi}^{\mathrm{thr}}$. Using this observation both factors can be drawn in front of the phasespace integral in Eq. (1) with the result:

$$\begin{aligned}
&\sigma_{pp\to pp\eta}(s) \quad \simeq \\
&\simeq \frac{\left|\bar{T}_{fi}^{\mathrm{thr}}\, T(\mathrm{ISI})\right|^2}{2!\mathcal{F}(s)(2\pi)^5} \int \frac{d^3p_{1'}}{2\,\omega_p(|\vec{p}_{1'}|)}\, \frac{d^3p_{2'}}{2\,\omega_p(|\vec{p}_{2'}|)}\, \frac{d^3p_{3'}}{2\,\omega_\eta(|\vec{p}_{3'}|)}\; \delta^4(p_{1'}+p_{2'}+p_{3'}-P_i)\; |T(\mathrm{FSI})|^2 \\
&= \frac{\left|\bar{T}_{fi}^{\mathrm{thr}}\, T(\mathrm{ISI})\right|^2}{2!\mathcal{F}(s)(2\pi)^5}\, R_3^{FSI}(s) \qquad (9)
\end{aligned}$$

In the last line of Eq. (9) the final state interaction modified phasespace integral $R_3^{FSI}(s)$ for the three body final state $pp\eta$ has been defined. To expand the energy dependence of the total cross section at threshold one usually expresses the cross section in terms of the dimesionless variable $\eta = \sqrt{\lambda(s, m_\eta^2, s_1^{\min})/(4s\, m_\eta^2)}$ instead of the square of the cm-energy s. The quantity η being the maximum momentum of the produced η-meson in the cm-frame vanishes at threshold. It is easy to derive $s_1^{\min} = (2m_p)^2$. Introducing $T_{\mathrm{lab}} = (s-4m_p^2)/(2m_p)$ and $\mu = m_p/m_\eta$ the phaseshifts of the long range potential between the incoming two protons can be expanded at threshold:

$$\delta(T_{\mathrm{lab}}) = \underbrace{\delta(T_{\mathrm{lab}}^{\mathrm{thr}})}_{=:\,\delta^{(0)}} + (T_{\mathrm{lab}} - T_{\mathrm{lab}}^{\mathrm{thr}})\delta'(T_{\mathrm{lab}}^{\mathrm{thr}}) + \ldots = \delta^{(0)} + \underbrace{m_\eta \left(1+\frac{1}{2\mu}\right)^2 \delta'(T_{\mathrm{lab}}^{\mathrm{thr}})}_{=:\,\delta^{(2)}}\, \eta^2 + O(\eta^4) \qquad (10)$$

In terms of these expansion coefficents the factor $T(\mathrm{ISI})$ can be expanded at threshold:

$$T(\mathrm{ISI}) \;=\; 1 + i\, e^{i\delta(k)} \sin\delta(k) \;=\; 1 + i e^{i\delta^{(0)}} \sin\delta^{(0)} + i\, e^{2i\delta^{(0)}} \delta^{(2)} \eta^2 + O(\eta^4) \qquad (11)$$

At the moment there is no clear knowledge of the values of $\delta^{(0)}$ and $\delta^{(2)}$ at the production threshold of $pp \to pp\eta$, but as the incoming relative proton momentum is very large the interaction time is very short, so that one might assume $\delta^{(0)}$ and $\delta^{(2)}$ to be zero which yields $T(\mathrm{ISI}) \approx 1$, while the VPI-values $\delta^{(0)} \approx -60^o$, $\delta^{(2)} \approx 0$ lead to $|T(\mathrm{ISI})| \approx 1/2$.
For the complete determination of $T(\mathrm{FSI})$ one obviously has to solve the Faddeev equations for the outgoing $pp\eta$–system. As this is at the moment out of the scope of this work only the leading terms of the Fadeev expansion are taken into account:

$$T(\mathrm{FSI}) \;\approx\; \frac{\kappa \cot\delta_{1'2'}(\kappa)}{\kappa(\cot\delta_{1'2'}(\kappa) - i)} + \frac{\kappa_1 \cot\delta_{3'1'}(\kappa_1)}{\kappa_1(\cot\delta_{3'1'}(\kappa_1) - i)} + \frac{\kappa_2 \cot\delta_{2'3'}(\kappa_2)}{\kappa_2(\cot\delta_{2'3'}(\kappa_2) - i)} - 2 \qquad (12)$$

The various terms in Eq. (12) which denote the FSI between each pair of particles in the final state can be expanded by effective range expansions. For the outgoing pp–system the s-wave nuclear effective range expansion is given by:

$$\kappa \cot\delta_{1'2'}(\kappa) = -\frac{1}{a} + \frac{r}{2}\kappa^2 + O(\kappa^4) \quad \text{with} \quad a \approx -17.1\ \mathrm{fm}\ ,\ r \approx 0 \ldots 2.84\ \mathrm{fm} \qquad (13)$$

Taking into account only pp-FSI using the shape independent effective range expansion Eq. (13) the FSI-modified phasespace integral can be expanded at threshold ($\bar{a} = a\, m_\eta$):

$$\begin{aligned}
R_3^{FSI}(s) \;&\simeq\; \int \frac{d^3p_{1'}}{2\,\omega_p(|\vec{p}_{1'}|)}\, \frac{d^3p_{2'}}{2\,\omega_p(|\vec{p}_{2'}|)}\, \frac{d^3p_{3'}}{2\,\omega_\eta(|\vec{p}_{3'}|)}\; \delta^4(P_f - P_i) \left| \frac{-\frac{1}{a} + \frac{r}{2}\kappa^2}{-\frac{1}{a} + \frac{r}{2}\kappa^2 - i\kappa} \right|^2 \\
&= \frac{\pi^3}{4}\, m_\eta^2\, \frac{\sqrt{1+2\mu}}{2\mu} \left\{ \frac{\eta^4}{2^2} - \frac{\eta^6}{2^6}[4(2\mu)^{-2} + 7 + 2\bar{a}^2 + 2\bar{a}^2(2\mu)] + O(\eta^8) \right\} \qquad (14)
\end{aligned}$$

It is interesting to observe that even the η^6-term is independent of the effective range r.

Relativistic Meson-Exchange-Amplitudes

For the relativistic meson-exchange model the following compact expression for the ${}^3P_0 \to {}^1S_0 s$ threshold transition amplitude $\bar{T}_{fi}^{\rm thr}$ of $pp \to pp\eta$ is obtained [1,2] ($m_N \simeq m_p$):

$$\begin{aligned}
\bar{T}_{fi}^{\rm thr} &= 2\,m_N\,\sqrt{m_\eta\,(m_\eta+4\,m_N)}\;[\,(X_\delta+X_\sigma)\,(m_N+m_\eta)-(X_\pi+X_\eta)\,(m_N-m_\eta)\,+\\
&+\;(Y_\delta+Y_\sigma-Y_\pi-Y_\eta)\,(m_N+m_\eta)+M_\delta+M_\sigma-M_\pi-M_\eta\,]\,-\\
&-\;X_\rho\,m_N\,[\,4\,(m_\eta-2\,m_N)+K_\rho\,(5m_\eta-4\,m_N)\,]\,+\\
&+\;[\,Y_\rho\,(m_N+m_\eta)+\tilde{M}_\rho\,]\,[\,K_\rho\,(m_\eta-4\,m_N)-8\,m_N\,]\,-\\
&-\;X_\omega\,m_N\,[\,4\,(m_\eta-2\,m_N)+K_\omega\,(5m_\eta-4\,m_N)\,]\,+\\
&+\;[\,Y_\omega\,(m_N+m_\eta)+\tilde{M}_\omega\,]\,[\,K_\omega\,(m_\eta-4\,m_N)-8\,m_N\,]\qquad (K_\rho\approx 6.1, K_\omega\approx 0)
\end{aligned}\tag{15}$$

Here I used the following abbreviations ($\phi \in \{\delta,\sigma,\pi,\eta,\rho,\omega\}$) ($M_{S_{11}} := m_{S_{11}} - i\,\Gamma_{S_{11}}/2$) ($D_\phi(q^2) := (q^2-m_\phi^2)^{-1}$) ($q^2 := -m_p m_\eta$, $p^2 := m_p\,(m_p-2m_\eta)$, $P^2 := (m_p+m_\eta)^2$):

$$\begin{aligned}
&X_\phi := D_\phi(q^2)\;g_{\phi NN}(q^2)\;D_{S_{11}}(p^2)\;g^*_{\phi N S_{11}}(q^2)\;g_{\eta N S_{11}}(m_\eta^2)\\
&Y_\phi := D_\phi(q^2)\;g_{\phi NN}(q^2)\;D^R_{S_{11}}(P^2)\;g^*_{\eta N S^R_{11}}(m_\eta^2)\;g_{\phi N S^L_{11}}(q^2)\\
&M_\phi := X_\phi\,m_{S_{11}}+Y_\phi\,M_{S_{11}}\quad,\quad \tilde{M}_\phi := -X_\phi\,m_{S_{11}}+Y_\phi\,M_{S_{11}}\\
&D^R_{S_{11}}(P^2) := (P^2-M^2_{S_{11}})^{-1}\,,\quad D_{S_{11}}(p^2) := (p^2-m^2_{S_{11}})^{-1}
\end{aligned}\tag{16}$$

Coupling Constants and Vertexfunctions

The meson–nucleon–$S_{11}(1535)$ couplings are in general complex and show a strong non-trivial momentum sensitivity. For that reason it is not enough to evaluate Eq. (16) applying the commonly used on-shell coupling constants combined with standard monopole or dipole formfactors. Hence a model has been developed to estimate the real and imaginary parts of the couplings [1,3]. The real parts of the couplings are derived within the framework of a nonrelativistic quark model, in which the ground state nucleon and the $S_{11}(1535)$ wavefunctions are described by harmonic oscillator solutions. The radial wavefunctions R_p, $R^{(23)}_{S_{11}}$ and $R^{(1,23)}_{S_{11}}$ of the ground state nucleon and the $S_{11}(1535)$ are determined by one unique range parameter b (Here ρ_{23}, $\rho_{1,23}$ are 3–quark–Jacobian coordinates!):

$$R_p \propto e^{-b^2(\rho_{23}^2+\rho_{1,23}^2)/2},\; R^{(23)}_{S_{11}} \propto b\,\rho_{23}\,e^{-b^2(\rho_{23}^2+\rho_{1,23}^2)/2},\; R^{(1,23)}_{S_{11}} \propto b\,\rho_{1,23}\,e^{-b^2(\rho_{23}^2+\rho_{1,23}^2)/2} \tag{17}$$

The imaginary parts of the couplings are calculated close the threshold from relevant lowest order meson loop corrections to the bare couplings.

FIRST RESULTS

Taking into account only π–, η–, ρ– and ω–exchange we observe by reproducing the experimental total cross section of $pp \to pp\eta$ that the following mixing parameters are favourable: $\theta \approx -5^o$, $b^{-1} \approx 0.5$ fm. Because of the uncertainties in the bare meson-nucleon-$S_{11}(1535)$ couplings and the still improvable treatment of ISI and FSI these numbers are by now preliminary. The model gives for the first time a quantitative prediction of the relative phases between the π–, η–, ρ– and ω–exchange amplitudes. An extension of the effective range formalism for ISI and FSI to Coulomb-interactions is on the way.

REFERENCES

1. F. Kleefeld, "Exklusive Schwellenproduktion von π^0–, η– und K^+–Mesonen in Proton–Proton–Stößen", Doctoral Thesis, University of Erlangen (1999).
2. F. Kleefeld, M. Dillig, "Protoninduced Pion-, Eta- and Kaon-Production at Threshold", in *Proc. of* 8^{th} *Int. Conf. on the Structure of Baryons (Baryons 98)* (Bonn, Sept. 22-26, 1998; ©1999 by World Scientific Publishing) pp. 613–616, nucl-th/9811003.
3. F. Kleefeld, M Dillig, "Reinvestigation of $pp \to pp\pi^0$ and $pp \to pp\eta$ at threshold", Acta Phys. Pol. **B29**, 3059 (1998), nucl-th/9806057v2.

Status of the SPES4-π Experiment at Saclay. Exclusive Investigation of the Roper Resonance

G. Alkhazov, A. Kravtsov, and A. Prokofiev
Petersburg Nuclear Physics Institute, 188350 Gatchina, Leningrad District Russia, The SPES4-π Collaboration.

Abstract

Preliminary results of the exclusive study of the p(α, α')X reaction at the α-particle momentum 7 GeV/c are presented. The missing mass spectra show fast changing of the reaction mechanism in the range of the momenta of the scattered α-particles between 6.12 and 6.70 GeV/c. The mechanism of the Δ-resonance excitation in the projectile is confirmed.

INTRODUCTION

The inclusive reaction p(α, α')X was recently studied[1] at the Saturne-II accelerator using the SPES4 spectrometer for measurement of missing mass spectra of the scattered α particles. The results indicated the existence of the strong isoscalar excitation of the target and (or) projectile at the energy close to the energy of the Roper resonance (1440 MeV). Various interpretations of the experiment were proposed[2,3] including, in particular, a radial nucleon excitation which could be used for the nucleon compressibility determination. The latter interpretation of the data includes the existance of a new isoscalar resonance different from the Roper one[4]. The serious problem of this experiment is that both the target and the projectile can be excited and may give contributions to the inclusive spectra. Therefore, it was crucial to separate these different processes and to reduce the physical background connected mainly with the Δ-isobar production. In order to separate the different reaction channels it was necessary to perform the exclusive measurements.

Such measurements were performed during 1995-97 at LNS (CE Saclay) where inelastic p(α, α')X and p$(\vec{\mathrm{d}}, \mathrm{d}')$X reactions were studied in the exclusive experiment with SPES4-π installation[5]. The installation consisted of the SPES4 spectrometer, wide-gap magnet and two spectrometers for registration of the secondary particles. One of them, the Forward Spectrometer (FS) was designed and built at Petersburg Nuclear Physics Institute[6]. Some preliminary results of exclusive investigation of the reaction p(α, α')X at four momentum transfers are presented below.

PHYSICAL MOTIVATION AND PRELIMINARY RESULTS

Theoretical analysis of the reaction p(α, α')X is presented in[2,3,7] where the analysis of the inclusive experiment[1] was carried out. The specific features of the reaction are connected with the limitation caused by the α particle isospin $T = 0$. The isospin conservation law reduces the number of the mechanisms which can contribute to the reaction. In particular the Δ-resonance excitation in the target is forbidden for this reason. Two clear peaks were observed in[1]: a large one, which was associated with Δ excitation in the projectile (DEP), and a small one at higher excitation energy, which was attributed to the Roper excitation in the target. The latter assumption requires the Roper resonance to be excited by the isoscalar exchange, which stimulated to interpret the Roper resonance as a monopole excitation of the nucleon. The main processes which are responsible for the (α, α') reaction are: (a) Δ excitation in the projectile and (b) N* (Roper) excitation in the target. The contribution of any other processes is about 100 times less than (a) or (b). It was shown that such an approximation described rather well the experimental data in the region of Δ resonance excitation. The agreement was worse in the region of the Roper resonance. The better agreement in this region can be obtained if one supposes[4] that here a different resonance is involved, with $M = 1380$ MeV but with the same qantum numbers. This is consistent with the resonance form from $\pi\mathrm{N} \to 2\pi(s)\mathrm{N}$ (of the same quantum numbers as α-p coupling). The real proof of this hypothesis could be obtained in an exclusive investigation of the p(α, α')X reaction in the energy region of Δ and Roper resonances excitation.

The exlusive investigation of the reaction p(α, α')X was carried out at the accelerated α-particle beam by means of the SPES4-π installation including SPES4 and FS spectrometers. The energy of the primary α beam was 4.2 GeV. The scattered α-particles registered by the SPES4 spectrometer had the momenta centered at the values 3.06, 3.15, 3.25 or 3.35 GeV/c. The momentum acceptance of the SPES4 was $\pm 5\%$ and momentum resolution of about 0.8%. The measurements were carried out at four SPES4 momentum settings. The momenta of the positively charged secondaries were measured by the FS.

The spectra of the missing mass obtained at the two highest momenta of the scattered α-particles (p/z = 3.35, 3.25 GeV/c) are presented in Fig. 1. These distributions display only two clean peaks in the missing mass spectra corresponding to the masses of the π^0 and neutrons, connected with the decay of intermediate state into p+π^0 and n+π^+. It supports the DEP mechanism of the reaction. The ratio of the cross sections of the mentioned above reaction channels (for p/c = 3.35 GeV/c) is about 2. This number corresponds to the ratio of the isospin Clebsh-Gordon coefficients for the reaction final states for the Δ-resonance decay. The distribution at p/z = 3.25 GeV also demonstrates opening of the double pion production channel, which leads to broadening of the pion peak. Both distributions were compared with the predictions of[3] and the good coincidence was obtained for the distribution shapes. The exclusive experimental data allow us to calculate directly the invariant mass of the resonance. As it was expected, the value of $M = 1.21 \pm 0.06$ GeV was obtained at the highest momentum (p/z = 3.35 GeV). This is in the good agreement with the mass of Δ resonance (1.232 MeV).

The spectra obtained for two other settings (p/z = 3.15, 3.06 GeV/c) present fast changing of the missing mass distribution shapes (Fig. 2). Reducing of the one-pion peak and increasing of the part of the spectra, which can be interpreted as two-pion production region, demonstrate the change of the reaction mechanism which can be interpreted now as a N* production with a dominant 2π mode decay. Another (third) peak appeared close to the mass of Δ resonance and probably can be connected with the Δ resonance production from the N* decay. The intermediate state mass calculation from the data at p/z = 3.06 GeV/c results in the mass value $M = 1.40 \pm 0.04$ GeV which is close to the Roper resonance mass.

REFERENCES

1. H.P. Morsch et al., Phys.Rev.Lett. **69**, (1992) 1336
2. H.P. Morsch, LNS Saclay preprint LNS/Ph/93-26, Saclay (1993)
3. S. Hirenzaki et al., Phys.Rev. **C53**, 277–284 (1996)
4. H.P. Morsch, P. Zupranski "Mass Distribution of the N*(1/2,1/2)$^+$ Resonance at about 1400 MeV from Alpha-Proton Scattering." Submitted to Phys.Rev.C.
5. Th. Hennino, R. Kunne, Nouvelle de Saturne, **17**, 35–48 (1993)
6. A.N. Prokofiev et al., Few Body System Suppl, **10**, 491–494 (1999)
7. P. Fernandez de Cordoba et al., Nucl. Phys., **A586**, 586–606 (1995)

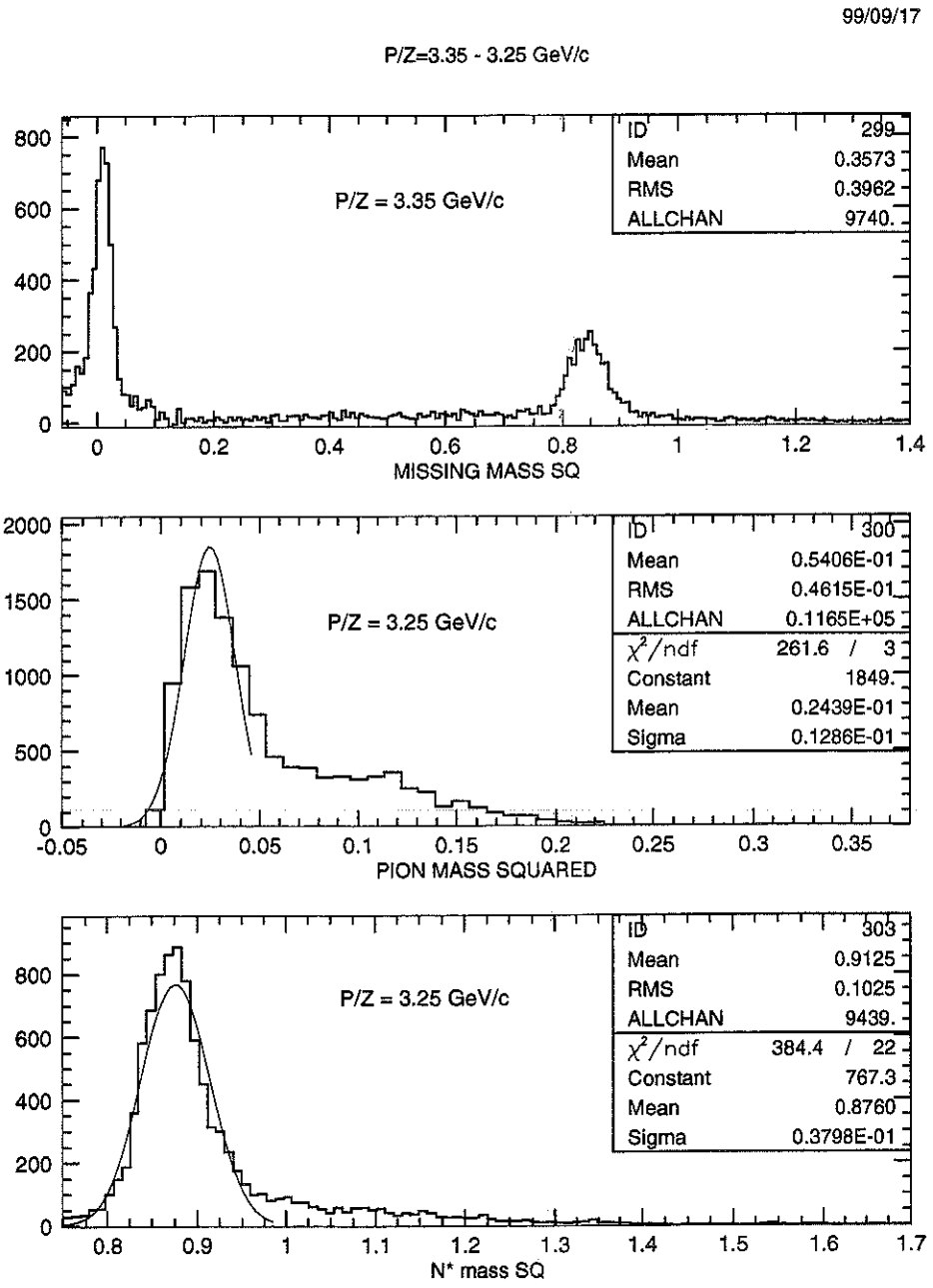

Figure. 1. Squared missing mass spectra from (α, α') reaction for the scattered α-particle momenta $p/z = 3.35$ GeV/c and 3.25 GeV/c.

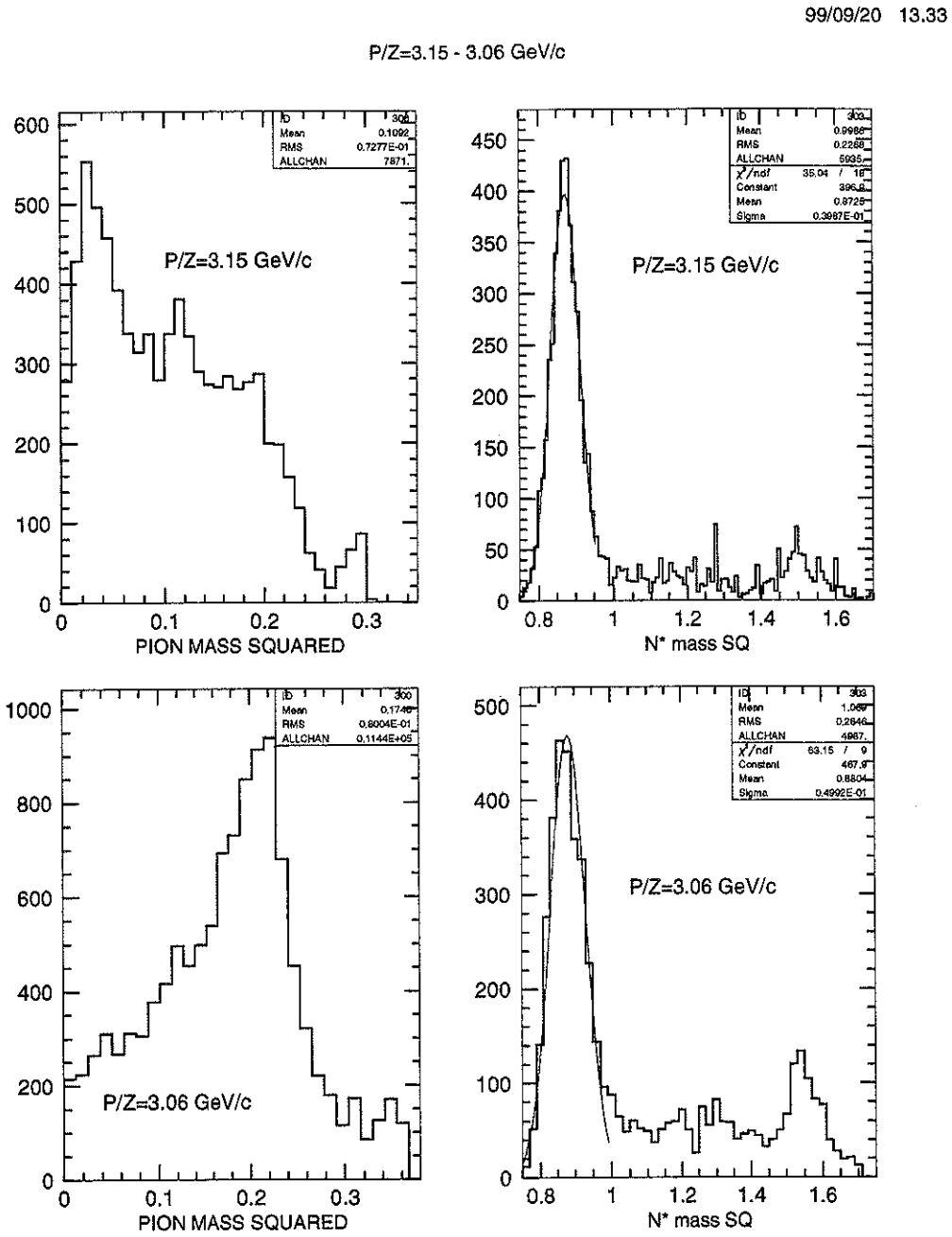

Figure. 2. Same as Fig. 1, for α-particle momenta $p/z = 3.15$ GeV/c and 3.06 GeV/c.

Results from pionic hydrogen

H.J. Leisi
ETH Zurich, Institute for Particle Physics, ETH-Hönggerberg, CH-8093 Zurich, Switzerland

Abstract

The final results from the pionic hydrogen (and deuterium) precision X-ray experiments of the ETH Zurich - Neuchâtel - PSI collaboration are presented.

CONCEPTION OF THE EXPERIMENT

The pionic hydrogen experiment[1,2] and the pionic deuterium experiment[3] have been described in the publications and various contributions to conferences. In this paper, I would like to concentrate on a presentation of the results and their implications. In the introductory section the idea of the pionic hydrogen experiment is outlined by recalling the relations between the measured quantities and the πN scattering amplitudes.

We have measured the $3p-1s$ X-ray transitions. The pionic hydrogen $1s$ ground state decays either by single charge exchange (SCX) into a $\pi^0 n$ or into a γn final state. The observables of the experiment are the transion energy $E^{meas.}_{3p-1s}$ and the transition line width $\Gamma^{meas.}_{3p-1s}$.

The strong-interaction shift is defined as

$$\varepsilon_{1s} = E^{el.magn.}_{3p-1s} - E^{meas.}_{3p-1s} \quad , \tag{1}$$

where $E^{el.magn.}_{3p-1s}$ is the calculated electromagnetic transition energy[4] (the strong-interaction shift of the $3p$ state is negligible). The shift ε_{1s} is mainly due to $\pi^- p$ elastic scattering in the bound state; it is, however, not a purely hadronic quantity. If we switch on the strong-interaction $\pi^- p$ potential, then the π^- wavefunction is slightly changed. As a result, the transition energy also changes. This, together with the mass-splitting effect and its equivalent for the decay channel $\pi^- p \to \gamma n$ are called electromagnetic corrections. In order to establish the relation between ε_{1s} and the $\pi^- p$ elastic scattering amplitude $a_{\pi^- p \to \pi^- p}$, we have investigated the electromagnetic corrections numerically[4]. The result is expressed as a correction $\delta_\varepsilon = (-2.1 \pm 0.5) \times 10^2$ to a Deser-type formula

$$\frac{\varepsilon_{1s}}{E_{1s}} = -4 \frac{a_{\pi - p \to \pi^- p}}{r_B} (1 + \delta_\varepsilon) \quad , \tag{2}$$

where $E_{1s}/r_B = 14.53$ eV/fm.

In order to arrive from $\Gamma^{meas.}_{3p-1s}$ at the total decay width Γ_{1s} of the $1s$ state, one has to consider the Doppler broadening of the (initial) $3p$ state which results from the atom formation process and susequent atomic cascade processes. We define the Doppler correction Δ_{3p} by the equation

$$\frac{\Gamma^{meas.}_{3p-1s}}{\Gamma_{1s}} = 1 + \Delta_{3p} \quad . \tag{3}$$

Based mainly on experimental observations from gaseous hydrogen, we find the correction $\Delta_{3p} = 0.12 \pm 0.05$[5]. In order to obtain from Γ_{1s} the scattering amplitude $a_{\pi^- p \to \pi^0 n}$ for SCX, we use the measured Panofsky ratio ($P = 1.546 \pm 0.009$) and apply a (small) electromagnetic correction[4]. The relation is again expressed by a Deser-type formula:

$$\frac{\Gamma_{1s}}{E_{1s}} = 8 \frac{q}{r_B} \left(1 + \frac{1}{P}\right) [a_{\pi^- p \to \pi^0 n} (1 + \delta_\Gamma)]^2 \quad . \tag{4}$$

Here $\delta_\Gamma = (-1.3 \pm 0.5) \times 10^{-2}$ and $q = 28.04$ MeV/c $= 0.1421$ fm^{-1}.

RESULTS

Isospin-Symmetry Test

At threshold, the most general amplitude for an isospin-symmetric πN interaction is of the form

$$f_{\pi N} = b_0 + b_1 \, \boldsymbol{\tau} \cdot \mathbf{t} \quad , \tag{5}$$

where $1/2\boldsymbol{\tau}$ and $\mathbf{t}$ are the nucleon and pion isospin operators, respectively, b_0 is the isoscalar (s-wave) scattering length and b_1 is the isovector scattering length.

We want to test isospin symmetry of the strong interaction[6]. For this we need a third independent observable, which we take from the $1s$ strong-interaction shift measurement in pionic deuterium[3]. The $1s$ shift is related – by three-body calculations – to the πN, isoscalar and isovector scattering lengths b_0 and b_1. The scattering amplitudes from (2) and (3), expressed in terms of b_0 and b_1, together with the (real part) of the $\pi^- d$ scattering length from the $1s$ shift of pionic deuterium, represent three independent constraints on the two scattering lengths b_0, b_1. These constraints are displayed as three bands in the $b_0 - b_1$ plane of Fig. 1.

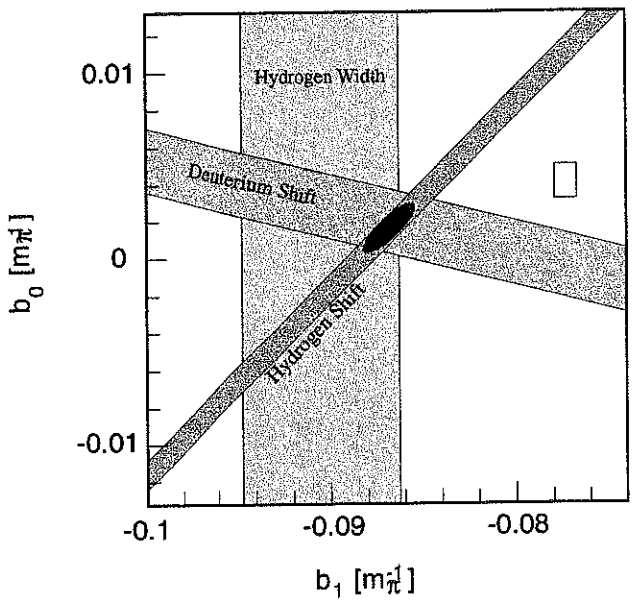

Figure. 1. Constraints on the πN scattering lengths b_0 and b_1 from the pionic hydrogen shift and width measurements and the pionic deuterium shift measurement.

This is an isospin-symmetry test – provided isospin symmetry of the strong interaction was assumed at all steps of the analyses (which was done). Inspection of Fig. 1 shows that the three bands are compatibel and hence *isospin symmetry of the πN interaction at threshold is conserved* (within the present uncertainties).

The Scattering Lengths

From the overlap of the three bands in Fig. 1 (ellipse) we obtain precise values for the isoscalar and isovector (isospin-symmetric) scattering lengths:

$$b_0 = (+1.6 \pm 1.3) \times 10^{-3} \mathrm{m}_\pi^{-1} \quad , \quad b_1 = (-86.8 \pm 1.4) \times 10^{-3} \mathrm{m}_\pi^{-1} \quad . \tag{6}$$

(Note that the two values (6) are correlated; see Fig. 1.) The unique feature of the result (6) is that these scattering lengths are determined directly at threshold – without extrapolations in energy.

Let us confront these values with recent work on *Chiral Perturbation Theory* (ChPT)[7]. The chiral perturbation series at threshold is an expansion in powers of the strong-interaction pion mass M_π; the first-order term corresponds to the current-algebra limit. The individual terms of the series can either be calculated directly, or depend on low-energy constants (LEC's) for which the theory has no predictions.

Table 1 shows the various terms for b_0 and b_1 (up to third order in M_π) from ref.[7], together with the experimental values (6).

	1^{st} *order*	2^{nd} *order*	3^{rd} *order*	*Experiment* $[10^{-3}\mathrm{m}_\pi^{-1}]$
b_0	0	LEC's dependent	8.5	1.6 ± 1.3
b_1	-79.0	0	LEC's dependent	-86.8 ± 1.4

We draw the following conclusions from Table 1:

- The experimental values of the scattering lengths are close to the current-algebra limit – the chiral expansion looks very healthy.
- On the other hand, the 3^{rd} order contribution to b_0 is larger than b_0 itself. This indicates a problem of convergence for b_0.
- The experimental values of the scattering lengths should be used to constrain the LEC's of ChPT.

The πN Coupling Constant

The GMO (Goldberger-Miyazawa-Oehme) sum rule[8] relates the πN coupling constant to the isovector scattering length b_1 and an integral (J) over $\pi^\pm p$ total scattering cross sections (J is dominated by values around the delta resonance). For J we use the average of the two values[9]

$$J_{VPI} = -1.041\,\mathrm{mb} \quad , \quad J_{KH} = -1.056\,\mathrm{mb} \quad . \tag{7}$$

With b_1 from (6) we find the new value of the πN coupling constant (for more details see ref.[10])

$$\frac{f^2}{4\pi} = 0.0757 \pm 0.0010 \quad , \quad g_{\pi NN} = \frac{2m_N}{m_\pi} f = 13.11 \pm 0.09 \quad . \tag{8}$$

Table 2. Our value (8) is compared with πN coupling constants from the VPI dispersion-relation solution[11] and from the analysis of ref.[12] with the extended tree-level model of the πN interaction (ETL-model[13]).

Method	$f^2/4\pi$	Reference
atoms	0.0757 ± 0.0010	[10,2]
VPI	0.0760 ± 0.0005	[11]
ETL	0.0766 ± 0.0011	[12]

All three (selected) values of Table 2 agree perfectly well; they are obtained using totally different methods.

The πN Sigma Term

The sigma term is of prime interest in hadron physics since it is accessible to both, ChPT and QCD lattice calculations.

As a result of our new value of the isoscalar scattering length (6), the πN sigma term is increased by 7 MeV (see refs.[10,2]).

Summary

- From the strong-interaction shifts of the $1s$ states in pionic hydrogen and deuterium and the decay width of pionic hydrogen we find that (within the present uncertainties) the isospin symmetry of the strong πN interaction at threshold is conserved.
- We obtain (directly) precise, πN isospin-symmetric (s-wave) scattering lengths. (The present limitation seems to be the three-body calculations in the $\pi^- d$ system.)
- The scattering lengths are close to the current-algebra limit of ChPT.
- The new πN coupling constant deduced from the isovector scattering length leads to a small Goldberger-Treiman discrepancy[2] which is compatible with standard ChPT (see discussion in ref.[10]).
- With the new isoscalar scattering length the πN sigma term (Σ_d) is increased by 7 MeV[2,10].

An Important Puzzle

The square in Fig. 1 corresponds to the extrapolation to threshold of the ETL-model solution of ref.[12] which is based on the analysis of the low-energy $\pi^{\pm}p$ elastic scattering data ($b_0 = 0.0041 \pm 0.0009\,\mathrm{m}_\pi^{-1}$, $b_1 = -0.0773 \pm 0.0006\,\mathrm{m}_\pi^{-1}$).

What is the reason for the difference between the square and the ellipse in Fig. 1? The ETL-model contains all important pieces of the isospin-symmetric πN interaction at low energies – except possible contributions from higher-order t-channel graphs in which the exchanged meson contains a pion loop (see discussion in ref.[10]). These graphs produce in general a cusp at threshold. In view of the inherent precision of the ETL-model analysis, it would be highly desirabel to have an estimate for the contribution from these graphs in order to test – with *improved precision* – isospin symmetry of the πN interaction at threshold.

REFERENCES

1. D. Sigg et al., "The strong interaction shift and width of the ground state of pionic hydogen," Nucl. Phys. **A609**, 269 (1996).
2. H.-Ch. Schröder et al.,"Determination of the πN scattering lengths from pionic hydrogen," Physics Letters **B**, in print.
3. D. Chatellard et al.,"X-ray spectroscopy of the pionic deuterium atom," Nucl. Phys. **A625**, 855 (1997).
4. D. Sigg et al.,"Electromagnetic corrections to the s-wave scattering lengths in pionic hydrogen," Nucl. Phys. **A609**, 310 (1996).
5. H.-Ch. Schröder et al.,"The pion-nucleon scattering lengths from pionic hydrogen," in preparation.
6. H.J. Leisi et al., *Chiral Dynamics: Theory and Experiment* (Springer, 1994), pp. 241-243.
7. M. Mojzis,"Elastic πN Scattering to $O(p^3)$ in Heavy Baryon Chiral Perturbation Theory," Euro. Phys. J. **C2**, 181 (1998).
8. M.L. Goldberger et al.,"Application of dispersion relations to pion-nucleon scattering," Phys. Rev. **99**, 986 (1955).
9. R.L. Workman et al.,"On the Goldberger-Miyazawa-Oehme sum rule," Phys. Rev. Lett. **68**, 1653 (1992).
10. H.J. Leisi,"Experimental results in pion-nucleon scattering: QCD symmetry tests," in *PSI Proceedings 98-02, December 1998* (ISSN 1019-6447) pp. 33-56.
11. M.M. Pavan and R.A. Arndt, in *Proceedings of the Seventh International Symposium on Meson-Nucleon Physics and the Structure of the Nucleon* (πN Newsletter, No 13, Dec. 1998) pp. 165-169.
12. E. Matsinos,"Isospin violation in the πN system at low energies," Phys. Rev. **C56**, 3014 (1997).
13. P.F.A. Goudsmit et al.,"The extended tree-level model of the pion-nucleon interaction," Nucl. Phys. **A575**, 673 (1994).

Kinetic Energy of $\pi^- p$-Atoms in Liquid and Gaseous Hydrogen

M. Daum, P.-R. Kettle, J. Koglin, V. Markushin, J. Schottmüller
PSI, Paul-Scherrer-Institut, CH-5232 Villigen-PSI, Switzerland

and

A. Badertscher, P.F.A. Goudsmit, M. Janousch, Z.G. Zhao
ETH Zurich, Institute for Particle Physics, ETH-Hönggerberg, CH-8093 Zurich, Switzerland

Abstract

We have measured the Doppler broadening of neutrons from the reaction $\pi^- p \to \pi^0 n$. From the data, we infer that the kinetic energy distribution of $\pi^- p$-atoms in liquid and gaseous hydrogen contains discrete 'high energy' components with energies as high as 200 eV attributed to Coulomb de-excitation. In liquid hydrogen, evidence for Coulomb de-excitation transitions with $\Delta n = 2$ has been found.

INTRODUCTION

Evidence for a substantial fraction of highly energetic ($\gg 1$ eV) $\pi^- p$-atoms in the charge exchange (CEX) reaction $\pi^- p \to \pi^0 + n$, in liquid hydrogen, was found in our previous experiments[1–3]. The effect is observed as a Doppler broadening of the neutron time-of-flight (TOF) peak, which is related to the kinetic energy distribution $f(T_{\pi p})$ of $\pi^- p$-atoms at the instant of the CEX-reaction. Later experiments gave further evidence for such 'high-energy' components in both liquid and gaseous hydrogen[4,5]. A precise knowledge of the kinetic energy distribution of the pionic hydrogen atoms is important for the determination of the strong interaction width of the ground state in pionic hydrogen as derived from the measurements of pionic X-ray transitions[6–9].

The observed Doppler broadening of the TOF-spectra[1–5] can be attributed to Coulomb de-excitation[10]*, $(\pi^- p)_n + p \to (\pi^- p)_{n'} + p$, where the de-excitation energy associated with the transition is shared as kinetic energy between the collision partners. Other cascade processes, such as external Auger effect, are only able to cause a moderate acceleration of the pionic atom (~ 1 eV)[12].

NEW EXPERIMENT

The present experiment was performed at the πE1-channel of PSI; the experimental setup is shown in Fig. 1. The following improvements to the previous experiments[1–4] were made: (i) reduction of the background by introducing several neutron collimators as well as using specially selected low noise photomultiplier (PM) tubes for the neutron counters; (ii) improvement of the time resolution of the neutron counters by placing them in adjustable holders so as to point radially at the target for each of the different neutron flight-paths; (iii) increased counting statistics by enlarging the solid angle of the neutron detector and by using a new beamline setup.

Pions of 117 MeV/c passed the beam counter S1 (see Fig. 1) and a carbon degrader, the thickness of which was optimized for a maximal stop rate in the hydrogen target. The liquid target (LH_2) had a length of 9.3 cm in the direction of the pion beam and a thickness of 0.5 cm in the direction of the neutron flight-path perpendicular to the pion beam. The 40 bar gas target was operated at room temperature and had a length of 21.2 cm in the direction of the pion beam and a diameter of 14 mm. Neutrons from the hydrogen target were detected after a flight-path of variable length (3 – 11 m) in a detector array consisting of 36 scintillator disks coupled directly to PM-tubes. For the measurements in liquid hydrogen, we used PILOT-U scintillators with a thickness of 5 mm, whereas for the measurements in gas, NE102A scintillators with a thickness of 15 mm were used in order to

*It is not excluded that Coulomb de-excitation is part of some new mechanism, e.g. the formation of a resonant state, as was discussed for $n = 2$[11].

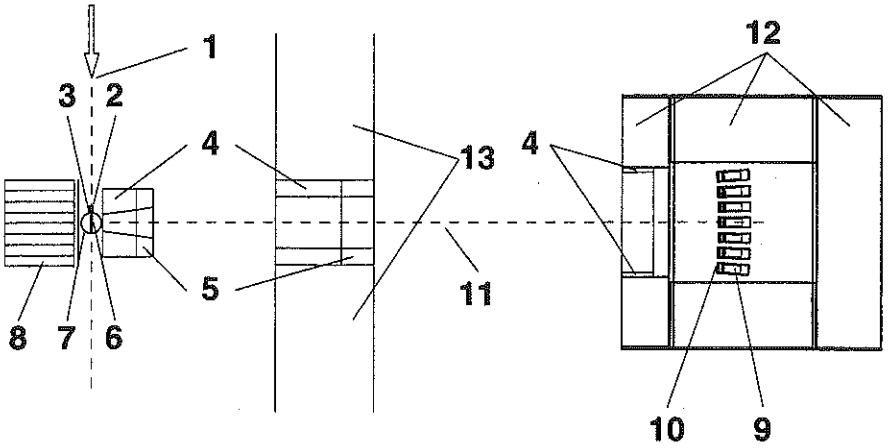

Figure. 1. 1) central pion trajectory; 2) scintillator S1; 3) carbon degrader; 4) CH_2-collimator; 5) lead collimator; 6) hydrogen target; 7) vacuum vessel of the LH_2-target; 8) NaI-crystals (8×8 matrix) for the detection of photons from the π^0-decay; 9) photomultiplier tubes; 10) neutron detection scintillators; 11) central neutron trajectory; 12) CH_2 and lead shielding; 13) concrete shielding.

partially compensate for the lower pion stop density. The neutrons from the CEX-reaction in the target were accepted only if coincident with a suitably delayed π-stop signal and a corresponding π^0-decay signal characterized by a γ-ray detected in the NaI-calorimeter[13].

DATA ANALYSIS

The data are in form of TOF (TDC) and pulse-height distributions (ADC). In a first step of the analysis, which is very similar to that of Ref. [4], a lower and an upper ADC-cut were introduced for each neutron counter separately, in order to suppress noise events from the PMs (lower ADC-cut) and accidental events triggered by photons from the π^0-decays or bremsstrahlung from beam electrons (upper ADC-cut). Both ADC-cuts were optimized for a maximal signal-to-noise ratio for each neutron counter separately. Before summing the spectra of all 36 neutron counters, the centre of each neutron peak was shifted by a few TDC-channels to the same channel number in order to correct for small transit time differences in the PMs and cables as well as small differences in the individual neutron flight-paths.

In a second step, cuts were applied to the summed photon energy from the NaI-calorimeter, accepting only events between 60 and 110 MeV. In this way, photons from bremsstrahlung and from the $\pi^- p \to \gamma n$ reaction were suppressed. These cuts were also optimized for a maximal signal-to-noise ratio. The small remaining background in the TOF-spectra, consisting of a flat component from noise events and accidental peaks from bremsstrahlung and 130 MeV photons from the reaction $\pi^- p \to \gamma n$, was determined and subtracted.

From the resulting TOF-spectra, we have obtained the kinetic energy distribution $f(T_{\pi p})$ using three different methods. **Method A** is based on the TOF-distribution model expected from the Coulomb de-excitation process. The measured spectra were fitted to TOF-distributions generated by a detailed GEANT Monte Carlo programme[14] which accounted for the stopping distribution in the target, geometric effects (intrinsic time resolution) and neutron scattering. The results are described in Refs. [15,16].

In **method B** of the analysis, no assumptions about the energies of the components were made. Here, the data measured in liquid and gaseous hydrogen were fitted using a kinetic energy distribution consisting of 16 energy bins (from T_{i-1} to T_i) corresponding to 16 equidistant time bins (from τ_{i-1} to τ_i). The kinetic energy distribution $f(T_{\pi p})$ was assumed to be constant within each bin. The relationship between the time τ_i and the

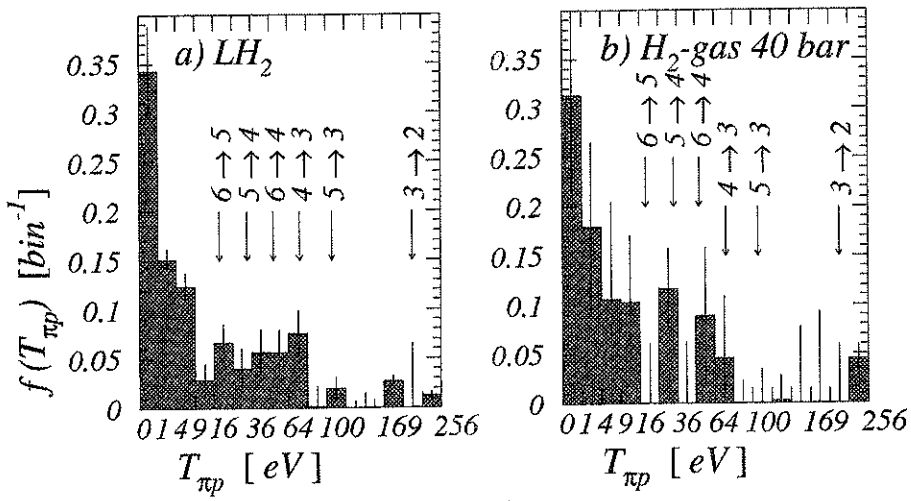

Figure. 2. Model independent kinetic energy distribution $f(T_{\pi p})$ for a) liquid and b) gaseous hydrogen obtained by fitting 16 kinetic energy bins to the measured TOF-spectra. The numbers $n \rightarrow n'$ indicate the positions of the theoretical values of the kinetic energy for the $\pi^- p$-atoms derived for the Coulomb de-excitation process. The errors of the yields are indicated by vertical lines.

energy T_i is given by[15]

$$\tau_i = \frac{l}{v_0^2}\sqrt{\frac{2T_i}{M_{\pi p}}}, \tag{1}$$

with $T_i\,[\mathrm{eV}] = i^2$ $(i = 1, \ldots, 16)$. The resulting kinetic energy distributions are shown in Fig. 2.

In both kinetic energy distributions (Fig. 2), a sharp decrease after the transition 4→3 and indications of discrete peaks due to Coulomb de-excitation can be seen. Moreover, in the kinetic energy distribution for liquid hydrogen, a small peak in the region between 100 eV and 121 eV is visible which could be assigned to the Coulomb de-excitation transition 5→3 corresponding to an energy of 107 eV. In the distribution for gaseous hydrogen, the error bars are larger due to the lower statistics. For the 3→2 transition, the number of events and their uncertainties are consistent with the existence of a peak at 209 eV.

Method C is based on the direct reconstruction of the kinetic energy distribution from the TOF-spectra. The TOF-spectra are deconvoluted with Monte Carlo generated TOF-distributions. Here, neutron scattering, the intrinsic time resolution as well as a distance-independent Gaussian time-jitter corresponding to electronic contributions to the time resolution were taken into account. ¿From these monotonously decreasing, deconvoluted TOF-distributions $F(\tau)$, we have calculated the cumulative energy distributions $W(T_{\pi p})$ which are given by

$$W(T_{\pi p}) = 2\int_0^{\xi\sqrt{T_{\pi p}}} F(\tau)d\tau \; - 2\xi\sqrt{T_{\pi p}}\,F(\xi\sqrt{T_{\pi p}}) \tag{2}$$

with $\xi = \frac{l}{v_0^2}\sqrt{\frac{2}{M_{\pi p}}}$. For the calculation of $W(T_{\pi p})$, only the fast side of the neutron TOF-spectra was used to minimize contributions from scattered neutrons. Finally, the kinetic energy distributions $f(T_{\pi p})$ can be calculated as follows†:

$$f(T_{\pi p}) = \frac{d}{dT_{\pi p}}W(T_{\pi p}). \tag{3}$$

†The kinetic energy distribution could be calculated directly as follows: $f(T_{\pi p}) = -\xi^2\frac{d}{d\tau}F(\tau)$; however, for technical reasons, we have calculated $W(T_{\pi p})$ first.

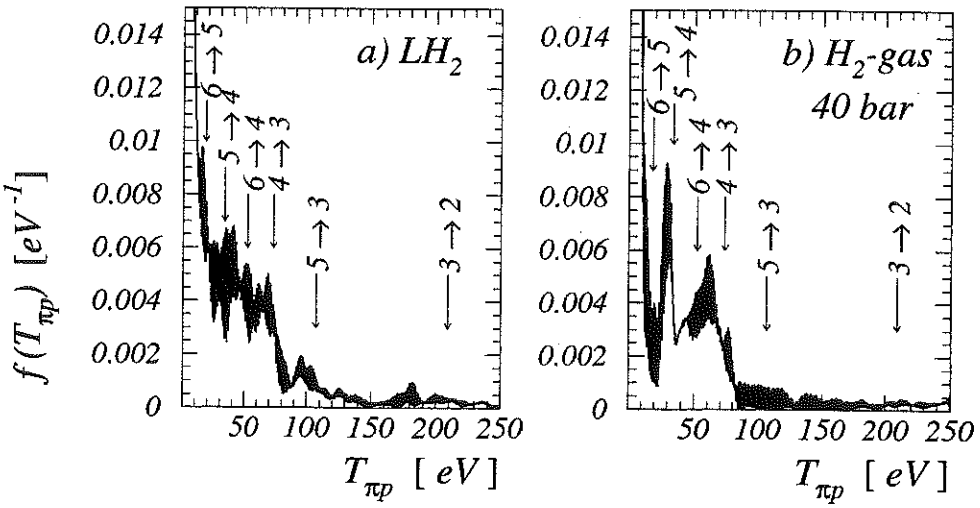

Figure. 3. Kinetic energy distribution $f(T_{\pi p})$ for a) liquid and b) gaseous hydrogen calculated from the deconvoluted TOF-spectra. The numbers $n \to n'$ indicate the positions of the theoretical values of the kinetic energy for the $\pi^- p$-atoms derived for the Coulomb de-excitation process.

The final results shown in Fig. 3 were obtained by averaging the kinetic energy distributions for the three different distances in liquid and for the two distances in gaseous hydrogen, respectively. The shapes of these distributions are consistent with those of Fig. 2.

CONCLUSIONS

In conclusion, the existence of strong 'high-energy' components ($T_{\pi p} \gg 1\,\mathrm{eV}$) in the kinetic energy distribution $f(T_{\pi p})$ of $\pi^- p$-atoms at the instant of the CEX-reaction has been observed for the first time in hydrogen gas up to 209 eV and has been confirmed with improved precision in liquid hydrogen. The results obtained from three different methods of reconstruction of the energy distributions are self-consistent; two of these methods are model-independent. The 'high-energy' components contain about half of the $\pi^- p$-atoms and about four percent have kinetic energies as high as $\simeq 200\,\mathrm{eV}$. The results obtained using a model which does not assume discrete components gives a fit which is completely incompatible with the data. The inclusion of the $\Delta n = 2$ Coulomb de-excitation components in the present analysis gives values which are perfectly consistent with those expected theoretically.

REFERENCES

1. J. F. Crawford et al., Phys. Rev. Lett. **56**, 1043, (1986).
2. J. F. Crawford et al., Phys. Lett. **B213**, 391, (1988).
3. J. F. Crawford et al., Phys. Rev. **D43**, 46, (1991).
4. A. Badertscher et al., Phys. Lett. **B392**, 278, (1997).
5. E. C. Aschenauer et al., Phys. Rev. **A51**, 1965, (1995).
6. D. Chatellard et al., Phys. Rev. Lett. **74**, 4157, (1995).
7. D. Chatellard et al., Nucl. Phys. **A625**, 855, (1997).
8. D. Sigg et al., Phys. Rev. Lett. **75**, 3245, (1995).
9. D. Sigg et al., Nucl. Phys. **A609**, 269, (1996).
10. L. Bracci and G. Fiorentini, Nuovo Cimento **43A**, 9, (1978).
11. P. Froelich and J. Wallenius, Phys. Rev. Lett. **75**, 2108, (1995).
12. L. I. Men'shikov, Muon Catalyzed Fusion **2**, 173, (1988).
13. A. Bay et al., Nucl. Instr. Meth. in Phys. Res. **A271**, 497 (1988).
14. GEANT - Detector Description and Simulation Tool, CERN Program Library.
15. J. Schottmüller et al., Hyperfine Interactions **119**, 95, (1999).
16. J. Schottmüller, Thesis, University of Zürich (1999).

The DEAR Experiment at DAΦNE

presented by C. Petrascu on behalf of the DEAR Collaboration:

W.H. Breunlich, M. Cargnelli, B. Gartner, R. King, J. Marton, J. Zmeskal
Institute for Medium Energy Physics, Austrian Academy of Sciences, Boltzmanngasse 3, A-1090 Vienna, Austria

G. Beer, A.C. Sanderson
Univ. of Victoria, Dept. of Physics and Astronomy, P.O. Box 3055 Victoria, BC V8W 3P6, Canada

S. Bianco, A.M. Bragadireanu*, F.L. Fabbri, C. Guaraldo, M. Iliescu*, B. Lauss†
V. Lucherini, C. Petrascu*
INFN - Laboratori Nazionali di Frascati C.P. 13, Via E. Fermi 40, I-00044 Frascati, Italy

M. Bregant, E. Milotti, E. Zavattini
Univ. degli Studi di Trieste, Dip. di Fisica and INFN Sezione di Trieste, Via A. Valerio 2, I-34127, Trieste, Italy

T. Ishiwatari, M. Iwasaki, D. Tomono, T. Yoneyama
Tokyo Institute of Technology, 2-12-1 Ookayama Meguro, Tokyo 152, Japan

R.S. Hayano
Univ. of Tokyo, Dept. of Physics, 7-3-1 Hongo, Bunkyo, Tokyo 113, Japan

S.N. Nakamura
Inst. of Physical and Chemical Research (RIKEN), 2-1 Hirosawa, Wako, Saitama 351-01, Japan

T. Koike
KEK, High Energy Accelerator Research Organization, Tanashi Campus 3-2-1 Midori, Tanashi, Tokyo 188, Japan

T. Ponta
Inst. of Physics and Nuclear Engineering "Horia Hulubei", Dept. of High Energy Physics, P.O. Box MG-6 R-76900 Magurele, Bucharest, Romania

M. Augsburger, D. Chatellard, P. Knowles, F. Mulhauser, L.A. Schaller, L. Schellenberg, H. Schneuwly
Univ. de Fribourg, Inst. de Physique, Bd. de Perolles, CH-1700 Fribourg, Switzerland

J.-P. Egger
Univ. de Neuchatel, Inst. de Physique, 1 rue A.-L. Breguet, CH-2000 Neuchatel, Switzerland

T.M. Ito, R. Seki**
W.K. Kellogg Radiation Laboratory California Institute of Technology, Pasadena, CA 91125, USA
** *Department of Physics and Astrophysics, California State University, Northridge, CA 91330, USA*

*on leave of absence from Inst. of Physics and Nuclear Engineering "Horia Hulubei", Dept. of High Energy Physics, P.O. Box MG-6 R-76900 Magurele, Bucharest, Romania
†on leave of absence from Institute for Medium Energy Physics, Austrian Academy of Sciences, Boltzmanngasse 3, A-1090 Vienna, Austria

Abstract

This paper gives an overwiew of the DEAR (DAΦNE Exotic Atom Research) experiment, which is fully ready to collect data at the new DAΦNE ϕ-factory at Laboratori Nazionali di Frascati dell'INFN. The objective of the DEAR experiment is to perform a precision measurement of the strong interaction shifts and widths of the K-series lines in kaonic hydrogen and the first observation of the same quantities in kaonic deuterium, with the aim of obtaining a precise determination of the isospin-dependent kaon-nucleon scattering lengths. The final goal is to determine the kaon-nucleon sigma terms, which give a direct measurement of chiral symmetry breaking and are connected to the strangeness content of the proton. The status of the experiment is reported, together with first background results, which are compared with a Monte Carlo calculation.

INTRODUCTION

The low energy kaon-nucleon interaction is still an experimentally largely unexplored field. More than 15 years ago, R.H. Dalitz made the following statement[1]: "The most important experiment to be carried out in low energy K-meson physics today is the definitive determination of the energy level shift in the K^-p and K^-d atoms, because of their direct connection with the physics of the $\bar{K}N$ interaction and their complete independence from all other kinds of measurements which bear on this interaction", statement that can be repeated today.

DEAR (DAΦNE Exotic Atom Research)– one of the first experiments which will collect data at the new ϕ-factory DAΦNE of the Laboratori Nazionali di Frascati dell'INFN, will observe X rays from kaonic hydrogen and kaonic deuterium, using the "K^- beam" from the decay of ϕs produced by DAΦNE, a cryogenic pressurized gaseous target and Charge-Coupled Devices (CCDs) as X ray detectors[2].

The number of events which DEAR can collect in *one week* with kaonic hydrogen at $10^{32}\mathrm{cm}^{-2}\mathrm{s}^{-1}$ luminosity will surpass by an order of magnitude the current world data set.

DEAR SCIENTIFIC PROGRAM

A kaonic atom is formed when a negative kaon entering a target loses its kinetic energy and is captured, replacing the electron, in an excited orbit. Three processes then compete in the deexcitation of the newly formed kaonic atom: dissociation of the surrounding molecules, external Auger transitions and radiative transitions.

When a kaon reaches low-n states with small angular momentum, it is absorbed through a strong interaction with the nucleus. This strong interaction is causing a shift in the energies of the low-lying levels from their purely electromagnetic values, whilst the finite lifetime of the state results in an increase of the observed level width.

The shift ϵ and the width Γ of the $1s$ state of kaonic hydrogen are related in a fairly model-independent way to the real and imaginary parts of the complex S-wave scattering length:

$$\epsilon + \frac{i}{2}\Gamma = 2\alpha^3 \mu_{K^-p}^2 a_{K^-p} = (412\ eV\ fm^{-1}) \cdot a_{K^-p} \qquad (1)$$

where α is the fine structure constant and μ_{K^-p} the reduced mass of the K^-p system. This expression is better known as the Deser-Trueman formula[3]. A similar relation applies for the case of kaonic deuterium and the corresponding scattering length a_{K^-d}:

$$\epsilon + \frac{i}{2}\Gamma = 2\alpha^3 \mu_{K^-d}^2 a_{K^-d} = (601\ eV\ fm^{-1}) \cdot a_{K^-d} \qquad (2)$$

where μ_{K^-d} is the reduced mass of the K^-d system.

These observable scattering lengths (a_{K^-p} and a_{K^-d}) are then related to the isospin dependent scattering lengths (a_0 and a_1). An accurate determination of the K^-N isospin dependent scattering lengths will place strong constraints on the low energy K^-N dynamics, which in turn constrains the SU(3) description of chiral symmetry breaking.

Crucial information about the nature of chiral symmetry breaking, and to what extent chiral symmetry is broken, is provided by the calculation of the meson-nucleon sigma terms[4]. The meson-nucleon sigma term is defined[4] as the expectation value of a double commutator of the chiral symmetry breaking part of the strong-interaction Hamiltonian, H_{SB}:

$$\sigma_N^{ba} = i < p|[Q_b^5, [Q_a^5, H_{SB}]]|p > \tag{3}$$

with the proton state $|p >$ of momentum p, Q_a^5 and Q_b^5 representing the axial-vector charges.

The low energy theorem relates the sigma terms to the meson-nucleon scattering amplitude[4]. A phenomenological procedure starting from the experimental scattering amplitudes is then used to determine the sigma terms and, therefore, to measure chiral symmetry breaking[5]. According to an evaluation based on the uncertainities in the phenomenological procedure[6], the sigma terms can be extracted at a level of 20%, by combining the DEAR precision measurement at threshold with the bulk of most recent analyses of low energy $K^{\pm}N$ scattering data.

The sigma terms are important also as inputs for the determination of the strangeness content of the proton. The strangeness fraction is dependent on both kaon-nucleon and pion-nucleon sigma terms, but is more sensitive to the first one[7].

EXPERIMENTAL SETUP

The scientific program of DEAR will be developed in two stages: with an NTP (Normal Temperature and Pressure) target and with a cryogenic target (hydrogen and deuterium).

The NTP target consists of a pure nitrogen volume at room temperature, equipped with 2 CCD detectors each containing two CCD-05 chips. Its purpose is to observe background, compare to Monte Carlo calculations and to tune the degrader thickness by optimizing the signal for the kaonic nitrogen $7 \rightarrow 6$ transition at ~ 4.5 keV. The yield of the signal being higher than that of kaonic hydrogen faster feedback is possible.

A description of the DEAR NTP setup can be found in[8].

In order to achieve a balance between high kaon stopping density in the target cell and decreasing x-ray yield due to Stark mixing, a pressurized cryogenic gaseous target has been realized for the measurement of kaonic hydrogen.

The initial target conditions will be a hydrogen pressure of 3 bar and a temperature of 25 K, which results in a target density of 3.6×10^{-3} g/cm^3. After the kaon has been slowed down in the target, it is captured by a hydrogen atom and the cascade begins. Some K-series X rays exit the target and interact with the CCD detector. The CCD chips are cooled to a temperature of 160 K to limit dark current noise. The CCDs are then read out by a set of custom electronics and digitized data are transmitted via a fiber-optic link to the two data acquisition computers in the DEAR control room. Compressed data are stored on magnetic-optical disks for further analysis; online diagnostic and analysis programs also exist for the real-time monitoring of the data.

Further details and a description of the DEAR cryogenic setup can be found in[2].

STATUS OF THE EXPERIMENT

At the date of this paper (October, 1999), no e^+e^- collisions were produced in the DEAR interaction region, and, consequently, no ϕ-production occured. Under these conditions only background studies could be performed. The background relevant for the DEAR experiment - low energy (≤ 20 keV) X rays and ionizing particles - was investigated.

Using the fully shielded DEAR NTP setup the following types of beams have been monitored in the period March to July 1999: a) only positron beams; b) only electron beams; c) electron and positron beams at the same time. Background data were then compared with DEAR Monte Carlo simulation.

A DEAR Monte Carlo simulation was performed in the framework of the CERN simulation package GEANT 3, using an improved version of the 3.21 code to simulate the physical processes involved in the DAΦNE interaction region and in the DEAR setup. In

particular, the behaviour of photons, electrons and positrons must be accurate below 10 keV, the standard cut-off of the GEANT package[2].

The observed energy spectra do not show any signal of unwanted structure. This proves the cleanness of the used construction materials. The number of x-ray events (single-pixel hits) and of clusters (multi-pixel events), the latter corresponding to particles hitting the active area of the CCD detector, were observed. At the present status of the accelerator the most important background comes from Touschek scattering[9] with a contribution from beam-gas interaction[10].

All measurements can be well reproduced by the DEAR Monte Carlo simulation using the standard beam parameters for the DEAR interaction region.The quantitative agreement between simulation and measurements is very convincing. Hence one can conclude that, with respect to the expected background and, therefore, to the control of the statistical error, the configuration chosen for the measurement of the strong interaction shifts and widths in kaonic hydrogen and kaonic deuterium will reach the planned challenging level of accuracy.

Once the machine will deliver kaons in the DEAR interaction region with an acceptable luminosity and under good vacuum conditions, kaonic nitrogen lines with the NTP target will be measured. Then the cryogenic target equipped with sixteen CCD-22 chips will be installed. The goal with this setup is a 1% measurement of the shift and a few percent measurement of the width of the K_α line in kaonic hydrogen, followed by the first observation of the shift and width in kaonic deuterium.

SUMMARY

The DEAR experiment will improve the precision in the measurement of the K^-p scattering length by a factor of ten and make the first measurement of the scattering length of kaonic deuterium. In this way the the $\bar{K}N$ isospin dependent scattering lengths will be determined at a percent level precision, revitalizing the field of low-energy kaon-nucleon interaction. These observations will then allow the determination of the kaon-nucleon sigma terms, which will reveal the degree of chiral symmetry breaking and give an indication of the strangeness content of the proton.

At the time of writing this paper, the first stage of the DEAR scientific program is in progress. The NTP nitrogen target is installed at DAΦNE, has performed background measurements and the first kaons are eagerly awaited.

The cryogenic hydrogen target is being tested in the laboratory and is ready for installation in the beginning of 2000.

REFERENCES

1. R.H. Dalitz *et al.*, Proceedings of the *Conference on Hypernuclear and Kaon Physics*, ed. by B. Povh, Max–Plank Institute Report MPI H–1982–V20, p.201 (1982).
2. S. Bianco *et al.*, "The DEAR case", LNF-98/039 (1998), to be published in Rivista del Nuovo Cimento.
3. S. Deser *et al.*, Phys. Rev. **96**, 774 (1954);
   T.L. Trueman, Nucl. Phys. **26**, 57 (1961);
   A. Deloff, Phys. Rev. **C13**, 730 (1976).
4. E. Reya, Rev. Mod. Phys **46**, 545 (1974);
   H. Pagels, Phys. Rep. **16**, 219 (1975).
5. E. Reya, Phys. Rev. **D7**, 3472 (1973).
6. B. Di Claudio *et al.*, Lett. Nuovo Cimento **26**, 555 (1979);
   A.D. Martin and G. Violini, Nuovo Cimento **30**, 105 (1981).
7. R.L.Jaffe and C.L. Korpa, Comments Nucl. Part. Phys. **17**, 163 (1987).
8. C. Petrascu, "Monte Carlo calculation for the new NTP DEAT setup", DEAR Technical Note IR-12 (February 3, 1999).
9. S. Guiducci, in *Proceedings of the 5the EPAC'96 Conference* Eds. S. Myres *et al.*, Institute of Physics Publishing, Bristol and Philadelphia, p.1365 (1996);
10. S. Guiducci and M.A. Iliescu, LNF-97/002 (IR) (1997).

Detection of Pionium with DIRAC

A. Lanaro
CERN, Geneva, Switzerland, and INFN-Laboratori Nazionali di Frascati, Frascati, Italy

on behalf of
"The DIRAC Collaboration"

B. Adeva[o], L. Afanasev[l], M. Benayoun[d], V. Brekhovskikh[n], G. Caragheorgheopol[m],T. Cechak[b], M. Chiba[j], S. Constantinescu[m], A. Doudarev[l], D. Dreossi[f], D. Drijard[a], M. Ferro-Luzzi[a], T. Gallas Torreira[a,o], J. Gerndt[b], R. Giacomich[f], P. Gianotti[e], F. Gomez[o], A. Gorin[n], O. Gortchakov[l], C. Guaraldo[e], M. Hansroul[a], R. Hosek[b], M. Iliescu[e,m], N. Kalinina[l], V. Karpoukhine[l], J. Kluson[b], M. Kobayashi[g], P. Kokkas[p], V. Komarov[l], A. Koulikov[l], A. Kouptsov[l], V. Krouglov[l], L. Krouglova[l], K.-I. Kuroda[k], A. Lanaro[a,e], V. Lapshine[n], R. Lednicky[c], P. Leruste[d], P. Levisandri[e], A. Lopez Aguera[o], V. Lucherini[e], T. Maki[i], I. Manuilov[n], L. Montanet[a], J.-L. Narjoux[d], L. Nemenov[a,l], M. Nikitin[l], T. Nunez Pardo[o], K. Okada[h], V. Olchevskii[l], A. Pazos[o], M. Pentia[m], A. Penzo[f], J.-M. Perreau[a], C. Petrascu[e,m], M. Plo[o], T. Ponta[m], D. Pop[m], A. Riazantsev[n], J.M. Rodriguez[o], A. Rodriguez Fernandez[o], V. Rykaline[n], C. Santamarina[o], J. Schacher[q], A. Sidorov[n], J. Smolik[c], F. Takeutchi[h], A. Tarasov[l], L. Tauscher[p], S. Trousov[l], P. Vazquez[o], S. Vlachos[p], V. Yazkov[l], Y. Yoshimura[g], P. Zrelov[l]

[a] CERN, Geneva, Switzerland
[b] Czech Technical University, Prague, Czech Republic
[c] Prague University, Czech Republic
[d] LPNHE des Universites Paris VI/VII, IN2P3-CNRS, France
[e] INFN - Laboratori Nazionali di Frascati, Frascati, Italy
[f] Trieste University and INFN-Trieste, Italy
[g] KEK, Tsukuba, Japan
[h] Kyoto Sangyou University, Japan
[i] UOEH-Kyushu, Japan
[j] Tokyo Metropolitan University, Japan
[k] Waseda University, Japan
[l] JINR Dubna, Russia
[m] National Institute for Physics and Nuclear Engineering IFIN-HH, Bucharest, Romania
[n] IHEP Protvino, Russia
[o] Santiago de Compostela University, Spain
[p] Basel University, Switzerland
[q] Bern University, Switzerland

Abstract

The aim of the DIRAC experiment at CERN is to provide an accurate determination of S-wave $\pi\pi$ scattering lengths from the measurement of the lifetime of the $\pi^+\pi^-$ atom. The measurement will be done with precision comparable to the level of accuracy of theoretical predictions, formulated in the context of Chiral Perturbation Theory. Therefore, the understanding of chiral symmetry breaking of QCD will be submitted to a stringent test.

INTRODUCTION

The low-energy dynamics of strongly interacting hadrons is under the domain of non-perturbative QCD, or QCD in the confinement region. At present, low energy pion-pion scattering is still an unresolved problem in the context of QCD. However, the approach based on effective chiral Lagrangian has been able to provide accurate predictions on

the dynamics of light hadron interactions [1]. In particular, Chiral Perturbation Theory (CHPT) allows to predict the S-wave $\pi\pi$ scattering lengths at the level of few percent [2]. Available experimental results, on their side, are much less accurate than theoretical predictions, both because of large experimental uncertainty and, in some cases, unresolved model dependency [3].

The DIRAC experiment aims at a model independent measurement of the difference Δ between the isoscalar a_0 and isotensor a_2 S-wave $\pi\pi$ scattering lengths with 5% precision, by measuring the lifetime of the pionium ground state with 10% precision.

PIONIUM

Pionium ($A_{2\pi}$) is a Coulomb weakly-bound system of a π^+ and a π^-, whose lifetime is dominated by the charge-exchange process to two neutral pions. The Bohr radius is 387 fm, the Bohr momentum 0.5 MeV/c, and the binding energy 1.86 keV. The decay probability is proportional to the atom wave function squared at zero pion separation and to the square of $\Delta = a_0 - a_2$. Using the values of scattering lengths predicted by CHPT, the lifetime of the $\pi^+\pi^-$ atom in the ground state is predicted to be 3.25×10^{-15} s [2].

Production of $A_{2\pi}$

In DIRAC, $\pi^+\pi^-$ atoms are formed by the interaction of 24 GeV/c protons with nuclei in thin targets [4]. If two final state pions have a small relative momentum in their system ($q \sim 1 MeV/c$), and are much closer than the Bohr radius, then the $A_{2\pi}$ production probability, due to the high overlap, is large. Such pions originate from short-lived sources (like ρ and ω), but not from long-lived (η, K^0_s), because in the latter case the two-pion separation is larger than the Bohr radius. The production probability for $A_{2\pi}$ can then be calculated using the double inclusive production cross section for $\pi^+\pi^-$ pairs from short-lived sources, excluding Coulomb interaction in the final state [5]. Evidence for $A_{2\pi}$ production was reported in a previous experiment [6].

Fate of $A_{2\pi}$

Pionium travelling in matter can dissociate or break up into a pair of oppositely charged pions with small relative momentum ($q < 3$ MeV/c) and hence with very small angular divergence ($\theta < 0.3$ mrad). This process competes with the charge-exchange reaction or decay, if the target material is dense so that the atomic interaction length is similar to the typical decay length of a few GeV/c dimeson atom (a few tens of microns). In a 100μm Ni foil, for example, the $A_{2\pi}$ breakup probability ($\sim$ 47%) becomes larger than the annihilation probability ($\sim$ 38%). This breakup probability depends on the target nucleus charge Z, the target thickness, the $A_{2\pi}$ momentum, and on the $A_{2\pi}$ lifetime [5,7].

Measurement of the $A_{2\pi}$ lifetime

For a target material of a given thickness, the breakup probability for pionium can be experimentally determined from the measured ratio of the number of dissociated atoms (n_A) to the calculated number of produced $A_{2\pi}$ (N_A). Thus, by comparison with the theoretical value, known at the 1% level, the $A_{2\pi}$ lifetime can be determined.

The number n_A of detected "atomic pairs" is obtained from the experimental distribution of relative momenta q for pairs of oppositely charged pions. It is however necessary to subtract a background contribution, arising mainly from Coulomb-correlated pions pairs in the q region, where the $A_{2\pi}$ signal is prominent ($q < 2$ MeV/c). The low-q background contribution is obtained with an extrapolation procedure using the shape of the accidental pair q-distribution recorded in the region $q > 3$ MeV/c, taking into account e.m. and strong $\pi^+\pi^-$ final state interactions [7].

From the measured ratio n_A/N_A a value for the $A_{2\pi}$ ground state lifetime can be extracted and, hence, a value for $\Delta = |a_0 - a_2|$.

THE EXPERIMENTAL APPARATUS

The DIRAC experimental apparatus (Fig. 1) [4], devoted to the detection of charged pion pairs, was installed and commissioned in 1998 at the ZT8 beam area of the PS East Hall at CERN. After a calibration run at the end of 1998, DIRAC has been collecting data since the summer of 1999.

The primary PS proton beam of 24 GeV/c nominal momentum struck the DIRAC target. The non-interacting beam travels below the secondary particle channel (tilted upwards at 5.7^o with respect to the proton beam), until it is absorbed by a catcher downstream of the setup. Downstream the experimental target, secondary particles travel across the following detectors: three planes of Micro-Strip Gas Chambers (MSGC) and two orthogonal stacks of scintillating fibers (Scintillating Fiber Detector SFD) to provide tracking information upstream of the spectrometer magnet; two planes of vertical scintillator slabs (Ionization Hodoscope IH) to detect the particle energy loss. Downstream the IH, the secondary beam enters a vacuum channel extending through the poles of the spectrometer magnet of 2.3 Tm bending power in the tilted horizontal plane. Downstream the analyzing magnet, the setup splits into two arms (inclined by 5.7^o in the vertical plane, and open by $\pm 19^o$ in the horizontal plane) equipped with a set of identical detectors: 14 drift chamber (DC) planes, one plane of vertical scintillating strips (Vertical Hodoscope VH) and one of horizontal strips (Horizontal Hodoscope HH) for tracking purposes downstream of the magnet; furthermore, a N_2 gas-threshold Cherenkov counter (CH), a Pre-Shower Detector (PS), consisting of Pb converter plates and of vertical scintillator slabs, and a Muon counter (MU), consisting of an array of vertical scintillator elements placed behind a block of iron absorber, with the aim of performing particle identification at the trigger or offline levels.

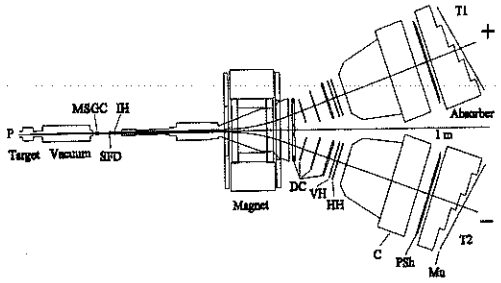

Fig. 1. The DIRAC experimental apparatus.

A multi-level trigger was designed to reduce the secondary particles rate to a level manageable by the data acquisition system, and to yield the most favorable signal-to-noise ratio, by selecting pion pairs with low relative momentum in the pair system (or small opening angle and equal energies in the lab system) and by recording a sufficiently large number of accidental pairs for the offline analysis. An incoming flux of $\sim 10^{11}$ protons/s would produce a rate of secondaries of about 3×10^6/s and 1.5×10^6/s in the upstream and downstream detectors, respectively. At the trigger level this rate is reduced to about 2×10^3/s, with an average event size of about 0.75 Kbytes. With the 95μm thin Ni target, the expected average $A_{2\pi}$ yield in the geometrical and momentum setup acceptance is $\sim 0.7 \times 10^{-3}$/s, equivalent to a total number of $\sim 10^{13}$ protons on target to produce one dimeson atom.

RESULTS FROM FIRST DATA TAKING

A preliminary analysis was performed on a sample of data (Ni target) collected during this summer. The sample consisted of about 10^7 events, corresponding to $\sim$ 1/3 of the statistics, accumulated in a 3-week run period. The data analysis was mostly dedicated

to the calibration of individual detectors and to the tuning of reconstruction algorithms. However, some general features of the apparatus response were investigated, and some results will be presented hereafter.

Figure 2 shows the time difference between hit slabs in the left and right vertical hodoscopes for events with one single track reconstructed in each detector arm. Within a trigger window of 45 ns, one observes the peak of "on-time" hits associated to correlated particles, over the background from accidental hits. The width of the correlated-pair events yields the time resolution of the hodoscope ($\sigma \sim$ 420 ps at the time of measurement, recently improved to $\sim$ 250 ps). The asymmetry on the right of the coincidence peak is due to admixture of protons in the "π^+" sample, thus corresponding to events of the type $\pi^- p$.

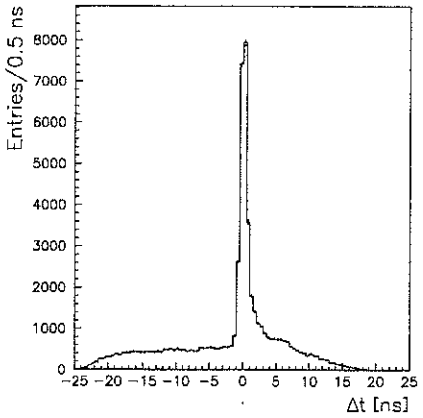

Fig. 2. Time difference between left and right VH scintillator slabs, hit by particles.

Such a contamination sample can be isolated by the time-of-flight measurement along the path from the target to the hodoscope. The discrimination between $\pi^-\pi^+$ and $\pi^- p$ pairs is effective for momenta of positively charged particles below 4.5 GeV/c. This is shown in Fig. 3, where the laboratory momentum of the positive particle in the pair is shown as a function of the arrival-time difference in the vertical hodoscope. The spectrometer single particle momentum acceptance is within the range 1.3 to 7.0 GeV/c.

In Fig. 4, the distribution of the longitudinal component (q_L) of the relative momentum in the pair system is shown for two samples of events: those (Fig. 4a) occurring with time differences close to zero (real coincidence plus admixture of accidental pairs), associated to free pairs with and without final state interaction; and those (Fig. 4b) occurring at time differences far from the peak of correlated pairs (only accidental pairs).

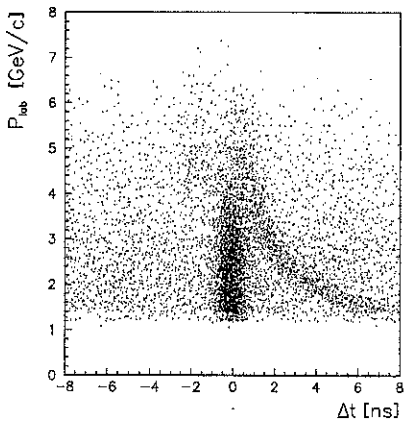

Fig. 3. Momentum of positive particle as a function of time difference between left and right hit slabs of the vertical hodoscopes.

Finally (Fig. 4c), the q_L distribution of correlated pion pairs is obtained from the difference between the distributions of Fig. 4a and 4b, taking into account the relative normalization factor. The distributions in Fig. 4 were obtained from a sample of two-track

events, preselected with momentum of the positive particle less than 4.5 GeV/c, to reject unresolved $\pi^- p$ pairs, and with transverse component (q_T) of the relative momentum below 4 MeV/c, to increase the fraction of low relative momentum pairs. For values of q_L corresponding to correlated pairs ($|q_L| < 10$ MeV/c) the production cross section of Coulomb pairs is enhanced with respect to the cross section of non-Coulomb pairs: Coulomb attraction in the final state is responsible for the peak in the q_L distribution (Fig. 4a and 4c) at small q_L.

A preliminary estimate of the number of pairs associated to $A_{2\pi}$ breakup results in a contribution of about 100 "atomic pairs" in the region $|q_L| < 2$ MeV/c.

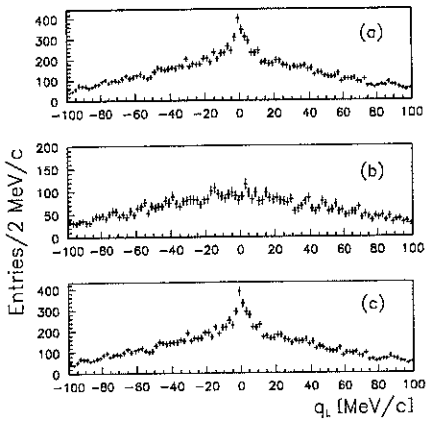

Fig. 4. Distribution of the longitudinal component of the relative momentum for: (a) time-correlated pairs; (b) accidental pairs; (c) spectrum of time-correlated minus accidental pairs.

The reconstruction of Coulomb-correlated $\pi^+\pi^-$ pairs is sensitive to the precision of the setup alignment. Any misalignment of the tracking system in one arm relative to the other arm would generate asymmetrical errors on the reconstructed momenta. This would lead to a systematic shift and additional spread of the Coulomb enhanced peak in the q_L distribution. The mean value of the Coulomb peak is 0.1 MeV/c, well within the accepted tolerances.

When reconstructed momenta of oppositely charged particles are symmetrically overestimated or underestimated then a calibration using detected resonances is adequate. This is done by reconstructing the effective mass of $\pi^- p$ pairs, also detected in the spectrometer. Figure 5 shows the invariant mass distribution of correlated $\pi^- p$ pairs with proton momentum >3 GeV/c.

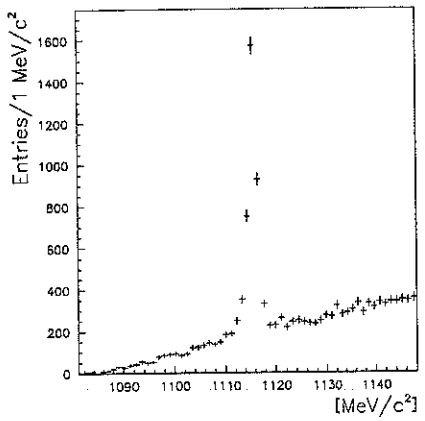

Fig. 5. Invariant mass of reconstructed $\pi^- p$ pairs.

A clear signal at the nominal Λ mass is observed. Such events originate from a few GeV/c Λ, with the decaying proton emitted backward and the pion emitted forward in the Λ system, and both decay particles characterized by small transverse momenta. The experimental mean value and standard deviation of the mass peak are 1115.60 and 0.92 MeV/c^2, respectively. These mass parameter values suggest an excellent calibration of

the momentum scale, with accuracy in momentum reconstruction better than 0.5% in the kinematic range of detected Λ decays, and the absence of errors in the telescope alignment, which otherwise would cause a displacement of the Λ mass peak value.

CONCLUSION

The DIRAC experiment has begun to collect data this year. A preliminary investigation of the apparatus performances demonstrates its full capability to pursue the foreseen experimental program. Improvements to the hardware as well as software tools have already been implemented in the second run period, currently in progress. These will certainly result in better quality of the data and will contribute to the aimed measurement precision of the pionium lifetime.

REFERENCES

1. S.Weinberg, Phys. Rev. **166**, 1569 (1968);
   S.Weinberg, Physica **96A**, 327 (1979);
   H.Leutwyler, in Proceedings of XXVI Conf. on High Energy Physics, **No.272**, Dallas, 1992 (AIP, New York, 1993) p. 185;
   J.Gasser and H.Leutwyler, Phys. Lett. **B125**, 327 (1983);
   J.Gasser and H.Leutwyler, Nucl. Phys. **B250**, 465, 517, 539 (1985);
   J.Stern, H.Sazdjian and N.H.Fuchs, Phys. Rev. **D43**, 3814 (1993);
   M.Knecht et al., Nucl. Phys. **B455**, 513 (1995).
2. J.Bijnens et al.,Phys. Lett. **B374**, 210 (1996);
   D.Eiras, and J.Soto, "Effective Field Theory Approach to Pionium," CERN hep-ph/9905543 v2 (1999) and this Proceedings;
   V. Lyubovitskij, "Hadronic Atoms in QCD," this Proceedings;
   A.Rusetsky, "Isospin Breaking Effects in Bound State Observables," this Proceedings.
3. L.Rosselet et al., Phys. Rev. **D15**, 574 (1977);
   C.D.Froggat and J.L.Petersen, Nucl. Phys. **B129**, 89 (1977);
   W.Ochs, Max Planck Inst. prep. MPI-Ph/Ph 91-35, (1991);
   M.Kermani et al., Phys. Rev. **C58**, 3431 (1998).
4. B.Adeva et al., "Lifetime Measurement of $\pi^+\pi^-$ Atoms to Test Low Energy QCD Predictions," Proposal to the SPSLC, CERN/SPSLC 95-1, SPSLC/P 284, (1994).
5. L.L.Nemenov, Yad. Fiz. **41**, 980 (1985);
   O.E.Gorchakov et al., Yad. Fiz. **59**, 2015 (1996).
6. L.G.Afanasyev et al., Phys. Lett. **B308**, 200 (1993); Phys. Lett. **B338**, 478 (1994); Yad. Fiz. **60**, 1049 (1996).
7. L.G.Afanasyev, JINR E2-91-578, Dubna, (1991);
   L.G.Afanasyev and A.V.Tarasov, JINR E4-93-293 Dubna, (1993).

Measurement of the ground-state shift and width in pionic hydrogen to the 1% level: A new proposal at PSI

D. Gotta
Institut für Kernphysik, Forschungszentrum Jülich, D-52425 Jülich, Germany

Abstract

In the non-perturbative regime of QCD, the pion-nucleon s-wave scattering lengths play a decisive role. They are accessible by measuring the level shift and broadening of the ground-state in pionic hydrogen and deuterium atoms. To pin down the inconsistencies arising from the analysis of the present data, an improvement on the accuracy of the hadronic broadening by almost an order of magnitude is highly desirable, which is the aim of an experiment being set-up at PSI.

In the framework of Chiral Perturbation Theory (ChPT) [1,2], a quantitative description of the low-energy pion-nucleon interaction became possible. The two basic parameters at threshold, the πN isoscalar and isovector s-wave scattering lengths a^+ and a^-, are given in terms of the elastic reactions by

$$a^{\pm} = \frac{1}{2}\,(a_{\pi^-p\to\pi^-p} \pm a_{\pi^+p\to\pi^+p}). \tag{1}$$

Furthermore, from dispersion relation theory a^- is connected to the πN coupling constant $f^2_{\pi N}$ by the Goldberger-Miyazawa-Oehme (GMO) sum rule [3]

$$(1+\frac{m_\pi}{M_N})\frac{a^-}{m_\pi} = \frac{2f^2_{\pi N}}{m^2_\pi-(m^2_\pi/2M_N)^2} + \frac{1}{2\pi^2}\int_0^\infty \frac{\sigma^{tot}_{\pi^-p}(k_\pi)-\sigma^{tot}_{\pi^+p}(k_\pi)}{\omega(k_\pi)}dk_\pi. \tag{2}$$

At present, the integral is known with an accuracy of 1% [4].

From the isospin decomposition follows $a_{\pi^-p\to\pi^-p} = (a^+ + a^-)$ and $a_{\pi^-p\to\pi^0n} = -\sqrt{2}\,a^-$. Hence, a^+ and a^- are directly related to the hadronic shift ϵ_{1s} and level broadening Γ_{1s} of the atomic ground state in the pionic hydrogen [5,6].

$$\frac{\epsilon_{1s}}{E_{1s}} = -\frac{4}{r_B}\,a_{\pi^-p\to\pi^-p}(1+\delta_\epsilon) \tag{3}$$

$$\frac{\Gamma_{1s}}{E_{1s}} = 8\frac{q_0}{r_B}(1+\frac{1}{P})(a_{\pi^-p\to\pi^0n}(1+\delta_\Gamma))^2. \tag{4}$$

E_{1s} is the electromagnetic binding energy of the atomic ground state for a point nucleus, $q_0 = 0.1421 fm^{-1}$ the CMS momentum of the π^0 in the charge exchange reaction $\pi^-p \to \pi^0n$, and r_B the Bohr radius of the πH atom. To obtain the pure hadronic scattering lengths, electromagnetic corrections $\delta_{\epsilon,\Gamma}$ of the order of a few percent must be taken into account [6,7]. A general discussion on the accuracy of electromagnetic corrections is presently going on [8]. A precise value for the branching ratio of charge exchange and radiative capture, the Panofsky ratio P is also required. The experimental value is $P = 1.546 \pm 0.009$ [9].

The shift and width of the 1s ground state of the pionic atom are determined from the spectroscopy of the Lyman X-ray transitions, which are the last deexcitation step of the atomic cascade. For intensity reasons, only the three low-lying transitions $K\alpha$, $K\beta$, and $K\gamma$ were considered. X-ray energies of 2–3 keV and the smallness of ϵ_{1s} and Γ_{1s} required the use of a reflection-type crystal spectrometer. In order to obtain sufficiently high X-ray yields, the cyclotron trap is necessary to stop the pion beam in a gaseous target. As X-ray detectors, only Charge-Coupled Devices (CCDs) fulfill the requirements of both good position resolution and efficient background suppression. The recent experiments for πH [10–12] and πD [13,14] achieved a precision of the order of 1% for ϵ_{1s} and 10% for Γ_{1s} (Table 1). The results for a^+ and a^- are shown in Fig. 1.

Table 1. Transitions from pionic hydrogen and deuterium used for the most recent determinations of ϵ_{1s} and Γ_{1s}. In the second column, the pure electromagnetic energy values are given. A positive /negative) sign for ϵ_{1s} stands for an attractive (repulsiv) interaction. The method of energy calibration (en.c.) and determination of the spectrometer resolution function (res.f.) is indicated.

transition	energy /eV	ϵ_{1s} /eV	Γ_{1s} /eV	p /bar	calibration en.c./resp.f.	ref.
$\pi H(3p-1s)$	2878.808	$+7.108 \pm 0.036$	0.865 ± 0.069	15	Ar $K\alpha/\pi Be(4-3)$	[11,12]
$\pi D(3p-1s)$	3077.95	-2.43 ± 0.10	1.02 ± 0.21	15	Ar $K\alpha/\pi Be(4-3)$	[13]
$\pi D(2p-1s)$	2695.527	-2.469 ± 0.055	1.093 ± 0.129	2.5	Cl $K\alpha/\pi Ne(7-6)$	[14]

In the πD system, the hadronic shift ϵ_{1s} is in leading order proportional to the (small) isoscalar scattering length a^+ because of an almost cancellation of the $\pi^- p$ and $\pi^- n$ contributions. Hence, the analysis faces the problem, that the next to leading order (double scattering) is proportional to the square of the (large) isovector scattering length a^-. These higher order contributions (SS+DS+HC) and in addition absorption corrections (AB) are almost one order of magnitude larger than the isoscalar scattering length a^+ itself.

$$\Re a_{\pi d} \;=\; 4\frac{M_N + m_\pi}{2M_N + m_\pi} a^+ + (SS + DS + HC) + AB \qquad (5)$$

Considerable discrepancies occur in the determination of a^+ from $\epsilon_{1s}^{\pi d}$ (Table 1). Whereas the two experiments are in good agreement [13,14], the values obtained for a^+ in the approaches of [15] and [16] differ by several standard deviations (bands denoted TL'80 and BBLM'98 in Fig. 1). The results of [19] and [20] lie in between these two extreme values. The uncertainty of a^+, applying the corrections of [15], is dominated by the uncertainty of the corrections and not by the accuracy of the experiments, the error of which corresponds to the widths of the bands denoted BBLM'98. Because of such large uncertainties for the multiple-scattering corrections, Coulomb corrections to the Deser formula (3) have been omitted up to now for πD.

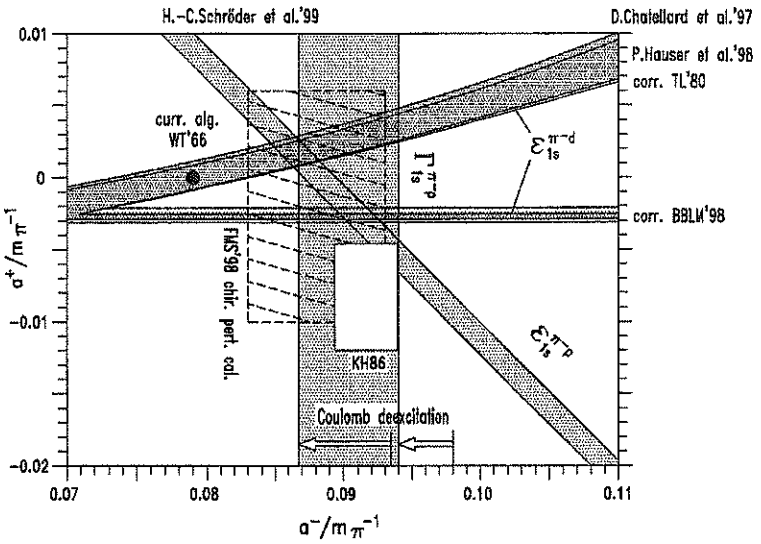

Figure. 1. Isoscalar and isovector πN scattering lengths a^+ and a^-. The bands labeled $\epsilon^{\pi p}$ and $\Gamma^{\pi p}$ show the results from the recent πH experiments [11,12]. The correction for the Doppler broadening due to Coulomb deexcitation is indicated by the two arrows. The value derived from current algebra (WT66) [1] corresponds to the leading order in ChPT, in which a^+ vanishes. The rectangle FMS is the result of an up to third order calculation [17] and the rectangle KH86 is obtained from a phase-shift analysis [18]. The bands labeled $\epsilon^{\pi d}$ were obtained from the results of [13,14] for the 1s level shift in πD according to [15] (TL'80) or [16] (BBLM'98).

In view of the significant discrepancies, even a combined analysis of the πH and πD data will not yield precise values for a^+ and a^- despite the small experimental errors for ϵ_{1s} (see [12]). Also, an identification of strong isospin violation in the πN system, which is expected to amount to 1–2% [21], seems to be difficult. Figure 1 demonstrates, that the accuracy of an unambiguous determination depends practically on the error of Γ_{1s}. In the same way, the accuracy of $f^2_{\pi N}$ determined from the GMO sum rule is mainly determined by Γ_{1s}. The values for $f^2_{\pi N}$, as derived from πN scattering data, phase shift analysis, photo production, radiative capture and the πH atom scatters up to 10% [22], which is regarded to be unsatisfactory for such a basic quantity.

Two major problems exist for a substantial improvement of the accuracy of Γ_{1s}.

- An accurate determination of the resolution function of the crystal spectrometer is essential. Because of the large Auger widths of fluorescence X-rays, the response function had been determined up to now only from pionic X-ray spectra of limited statistics.

- In exotic hydrogen atoms, Auger and X-ray emission compete with Coulomb deexcitation, where the deexciation energy is transferred into kinetic energy during collisions with neighbouring target molecules. This leads to a Doppler broadening of the X-ray lines. At present, the uncertainty of the correction due to Coulomb deexcitation dominates the error of Γ_{1s} as determined from the $\pi H(3p-1s)$ transition[11,12].

The strategy of the experiment being set-up at PSI [23], aiming at an accuracy of 1% for Γ_{1s}, is based on new techniques in the determination of the response function. Besides that, new insights in the atomic cascade will play a decisive role.

- In order to allow for an thorough investigation of the reflection properties of the Bragg crystals, a Electron-Cyclotron-Resonance (ECR) source is being set-up inside the new cyclotron trap [14]. This will allow to produce hydrogen-like electronic atoms, which have natural line widths of a few tens of meV only. The Doppler broadening from the temperature in the ECR source is expected not to exceed 100 meV. In this way, the crystal tests can be performed without time-consuming measurements at the secondary beam lines at PSI. This first step of the experiment will result in an accuracy of 2–3% for Γ_{1s}.

- By measuring the pressure dependence of the line shape of Lyman transitions from muonic hydrogen, the Coulomb deexcitation will be studied without the influence of the strong interaction. Using a cryogenic gas target, measurements in the pressure range of 1–40 bar are planned. Additional information on Coulomb deexcitation comes from time-of-flight measurements of neutrons stemming from the charge-exchange reaction $\pi^- p \to \pi^0 n$ at rest [24]. The structures of the time-of-flight distribution were found to correspond to deexcitation steps in the atomic cascade.

  The results will serve to set-up an improved cascade code, which takes into account the velocity distribution at all stages of the deexcitation [25]. The parameters fixed in that way will be used to model the cascade of pionic hydrogen. Monte-Carlo simulations show, that a knowledge on the 10% level for the Doppler contributions is sufficient to achieve the final goal for an accuracy of 1% for Γ_{1s} [23].

A test measurement has been performed at the $\pi E5$ channel of the PSI in order to investigate count-rate and background conditions. $\pi D(2p-1s)$ and $\pi Ne(7-6)$ transitions were measured by using the new cyclotron trap and a crystal spectrometer equipped with a spherically bent Si 111 crystal [14]. Results from this experiment are included in Fig. 1 ($\epsilon^{\pi D}$ – narrower bands).

By using the new cyclotron trap and a spherically bent Si crystal, the X-ray count rate increased by almost an order of magnitude. A massive concrete shielding improved the peak-to-background ratio by a factor of about 6. It is worthwile to mention that the total measuring time including the detection of the πNe response function amounted to

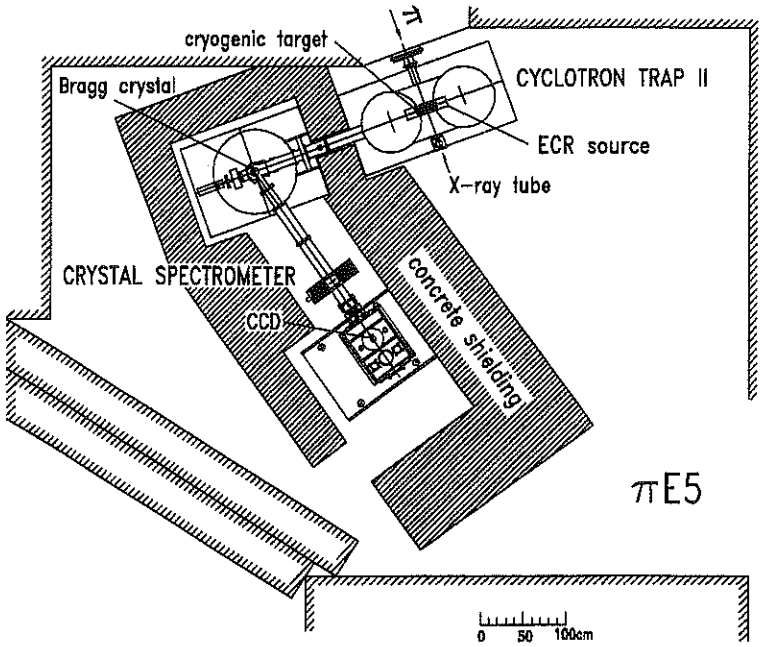

Figure. 2. Set-up of the pionic hydrogen experiment being set-up at PSI.

one day only and yielded a better result than a 9 days measurement during the previous experiments. A new large-area CCD will complete the spectrometer [26]. The set-up of the ECR source and the first measurements at the pion beam are planned for the end of the year 2000.

REFERENCES

1. S. Weinberg, Phys. Rev. Lett. **17**, 616 (1966); Y. Tomozawa, Nuovo Cim. **46 A**,707 (1966)
2. J. Gasser and H. Leutwyler, Ann. Phys. (N.Y.) **158**, 124 (1984)
3. M.L.Goldberger et al., Phys. Rev. **99**, 986 (1955)
4. W.R. Gibbs and Li Ai, nucl-th/9704058
5. S. Deser et al., Phys. Rev. **96**, 774 (1954)
6. G. Rasche and W.S. Woolcock, Nucl. Phys. **A 381**, 405 (1982)
7. D. Sigg et al., Nucl. Phys. **A 609**, 310 (1996)
8. Session on electromagnetic corrections (this workshop)
9. J. Spuller et al., Phys. Lett. **67 B**, 479 (1977)
10. D. Sigg et al., Nucl. Phys. **A 609**, 269 (1996)
11. H.-Ch. Schröder et al., to be published in Phys. Lett. **B**
12. H.J. Leisi (this workshop)
13. D. Chatellard et al., Nucl. Phys. **A 625**, 855 (1997)
14. P. Hauser et al., Phys. Rev. **C 58**, 1869 (1998)
15. A.W.Thomas and R.H.Landau, Phys. Rep. **C 58**, 122 (1980)
16. S.R. Beane et al., Phys. Rev. **C 57**, 424 (1998)
17. N. Fettes, U.-G. Meissner, and S. Steininger, Nucl. Phys. **A 640**, 199 (1998)
18. R. Koch, Nucl. Phys. **A 448**, 707 (1986); see also[13]
19. V.V. Baru and A.E. Kudryavtsev, Phys. of At. Nucl., **60**, 1475 (1997)
20. T.E.O. Ericson and B. Loiseau, Proc. PANIC 99, Uppsala, Sweden, to be published; B. Loiseau (this workshop)
21. Session on isospin breaking (this workshop)
22. G.R. Smith, Proc. MENU'97, Vancouver, Canada, 1997, p.1
23. G.C. Oades et al,.PSI proposal R-98.01
24. M. Daum (this workshop)
25. T. Jensen, V.E. Markushin, priv. comm.
26. D.F. Anagnostopoulos et al., PSI proposal R-97.02

A renormalisation-group approach to two-body scattering

M. C. Birse, J. A. McGovern and K. G. Richardson
Theoretical Physics Group, Department of Physics and Astronomy
University of Manchester, Manchester, M13 9PL, UK

Abstract

Wilson's renormalisation group is applied to nonrelativistic two-body scattering by a short-ranged potential. Two fixed points are identified: a trivial one and one describing systems with a bound state at zero energy. A systematic power-counting to terms in the potential near each of these fixed points. In the case of the nontrivial fixed point, this leads to an expansion which is equivalent to the effective-range expansion.

INTRODUCTION

Recently there has been much interest in the possibility of developing a systematic treatment of low-energy nucleon-nucleon scattering using the techniques of effective field theory[1–3]. Here we approach the problem using Wilson's continuous renormalisation group[4] to examine the low-energy scattering of nonrelativistic particles which interact through short-range forces[5].

The starting point for the renormalisation group (RG) is the imposition of a momentum cut-off, $|\mathbf{k}| < \Lambda$, separating the low-momentum physics which we are interested in from the high-momentum physics which we wish to "integrate out". Provided that there is a separation of scales between these two regimes, we may demand that low-momentum physics should be independent of Λ.

The second step is to rescale the theory, expressing all dimensioned quantities in units of Λ. As the cut-off Λ approaches zero, all physics is integrated out until only Λ itself is left to set the scale. In units of Λ any couplings that survive are just numbers, and these define a "fixed point". Such fixed points correspond to systems with no natural momentum scale. Examples include the trivial case of a zero scattering amplitude and the more interesting one of a bound state at exactly zero energy.

Real systems can then be described in terms of perturbations away from one of these fixed points. For perturbations that scale as definite powers of Λ, we can set up a power-counting scheme: a systematic way to organise the terms in an effective potential or an effective field theory. A fixed point is said to be stable if all perturbations vanish like positive powers of Λ as $\Lambda \to 0$ and unstable if one or more of them grows with a negative power of Λ.

TWO-BODY SCATTERING

We consider s-wave scattering by a potential that consists of contact interactions only. Expanded in powers of energy and momentum this has the form

$$V(k',k,p) = C_{00} + C_{20}(k^2 + k'^2) + C_{02}\,p^2 \cdots, \tag{1}$$

where k and k' denote momenta and energy-dependence is expressed in terms of the on-shell momentum $p = \sqrt{ME}$. Below all thresholds for production of other particles, this potential should be an analytic function of k^2, k'^2 and p^2.

Low-energy scattering is conveniently described in terms of the reactance matrix, K. This is similar to the scattering matrix T, except for the use of standing-wave boundary conditions. It satisfies the Lippmann-Schwinger (LS) equation

$$K(k',k,p) = V(k',k,p) + \frac{M}{2\pi^2}\mathcal{P}\int q^2 dq\,\frac{V(k',q,p)K(q,k,p)}{p^2-q^2}, \tag{2}$$

where $\mathcal{P}$ denotes the principal value.

On-shell, with $k = k' = p$, the K-matrix is related to the phase-shift by

$$\frac{1}{K(p,p,p)} = -\frac{M}{4\pi}p\cot\delta(p), \tag{3}$$

which means it has a simple relation to the effective-range expansion[6],

$$p \cot \delta(p) - \frac{1}{a} + \frac{1}{2} r_e p^2 + \cdots, \tag{4}$$

where a is the scattering length and r_e is the effective range. We shall see that this turns out to be equivalent to an expansion around a nontrivial fixed point of the RG.

RENORMALISATION GROUP

To set up the RG we first impose a momentum cut-off on the intermediate states in the LS equation (2). This can be written

$$K = V(\Lambda) + V(\Lambda) G_0(\Lambda) K, \tag{5}$$

where we have included a sharp cut-off in the free Green's function,

$$G_0 = \frac{M\theta(\Lambda - q)}{p^2 - q^2}. \tag{6}$$

We now demand that $V(k', k, p, \Lambda)$ varies with Λ in order to keep the off-shell K-matrix independent of Λ:

$$\frac{\partial K}{\partial \Lambda} = 0. \tag{7}$$

This is sufficient to ensure that all scattering observables do not depend on Λ. Differentiating the LS equation (5) with respect to Λ and then operating from the right with $(1 + G_0 K)^{-1}$, we get

$$\frac{\partial V}{\partial \Lambda} = \frac{M}{2\pi^2} V(k', \Lambda, p, \Lambda) \frac{\Lambda^2}{\Lambda^2 - p^2} V(\Lambda, k, p, \Lambda). \tag{8}$$

We now introduce dimensionless momentum variables, $\hat{k} = k/\Lambda$ etc., and a rescaled potential,

$$\hat{V}(\hat{k}', \hat{k}, \hat{p}, \Lambda) = \frac{M\Lambda}{2\pi^2} V(\Lambda\hat{k}', \Lambda\hat{k}, \Lambda\hat{p}, \Lambda). \tag{9}$$

From the equation (8) satisfied by V we find that the rescaled potential satisfies the RG equation

$$\Lambda \frac{\partial \hat{V}}{\partial \Lambda} = \hat{k}' \frac{\partial \hat{V}}{\partial \hat{k}'} + \hat{k} \frac{\partial \hat{V}}{\partial \hat{k}} + \hat{p} \frac{\partial \hat{V}}{\partial \hat{p}} + \hat{V} + \hat{V}(\hat{k}', 1, \hat{p}, \Lambda) \frac{1}{1 - \hat{p}^2} \hat{V}(1, \hat{k}, \hat{p}, \Lambda). \tag{10}$$

FIXED POINTS

We are now in a position to look for fixed points: solutions of (10) that are independent of Λ. These provide the possible low-energy limits of theories as $\Lambda \to 0$ and hence the starting points for systematic expansions of the potential.

The trivial fixed point

One obvious solution of (10) is the trivial fixed point,

$$\hat{V}(\hat{k}', \hat{k}, \hat{p}, \Lambda) = 0, \tag{11}$$

which describes a system with no scattering.

For systems described by potentials close to the fixed point we can expand in terms of eigenfunctions, $\hat{V} = \Lambda^\nu \phi(\hat{k}', \hat{k}, \hat{p})$, of the linearised RG equation,

$$\hat{k}' \frac{\partial \phi}{\partial \hat{k}'} + \hat{k} \frac{\partial \phi}{\partial \hat{k}} + \hat{p} \frac{\partial \phi}{\partial \hat{p}} + \phi = \nu\phi. \tag{12}$$

These have the form

$$\hat{V}(\hat{k}', \hat{k}, \hat{p}, \Lambda) = C\Lambda^{\nu}\hat{k}'^{l}\hat{k}^{m}\hat{p}^{n}, \tag{13}$$

with eigenvalues $\nu = l + m + n + 1$, where l, m and n are non-negative even integers. The eigenvalues are all positive and so the fixed point is a stable one: all nearby potentials flow towards it as $\Lambda \to 0$.

These eigenfunctions can be used to expand any potential that lies close to the fixed point. The power counting in this expansion is just the one proposed by Weinberg[1] if we assign an order $d = \nu - 1$ to each term in the potential. This fixed point can be used to describe systems where the scattering at low energies is weak and can be treated perturbatively.

A nontrivial fixed point

The simplest nontrivial fixed point is one that depends on energy only, $\hat{V} = \hat{V}_0(\hat{p})$. It satisfies

$$\hat{p}\frac{\partial \hat{V}_0}{\partial \hat{p}} + \hat{V}_0(\hat{p}) + \frac{\hat{V}_0(\hat{p})^2}{1-\hat{p}^2} = 0. \tag{14}$$

The solution, which must be analytic in $\hat{p}^2$, is

$$\hat{V}_0(\hat{p}) = -\left[1 - \frac{\hat{p}}{2}\ln\frac{1+\hat{p}}{1-\hat{p}}\right]^{-1}. \tag{15}$$

Although the detailed form of this potential is specific to our particular choice of cut-off, the fact that it tends to a constant as $\hat{p} \to 0$ is a generic feature, which is present for any regulator.

The solution to the LS equation for K with this potential is infinite, or rather $1/K = 0$. This corresponds to a system with infinite scattering length, or equivalently a bound state at exactly zero energy.

To study the behaviour near this fixed point we consider small perturbations about it that scale with definite powers of Λ. These satisfy the linearised RG equation

$$\hat{k}'\frac{\partial \phi}{\partial \hat{k}'} + \hat{k}\frac{\partial \phi}{\partial \hat{k}} + \hat{p}\frac{\partial \phi}{\partial \hat{p}} + \phi + \frac{\hat{V}_0(\hat{p})}{1-\hat{p}^2}\left[\phi(\hat{k}', 1, \hat{p}) + \phi(1, \hat{k}, \hat{p})\right] = \nu\phi. \tag{16}$$

Solutions to (16) that depend only on energy ($\hat{p}$) can be found straightforwardly by integrating the equation. They are

$$\phi(\hat{p}) = \hat{p}^{\nu+1}\hat{V}_0(\hat{p})^2. \tag{17}$$

Requiring that these be well-behaved as $\hat{p}^2 \to 0$, we find the RG eigenvalues $\nu = -1, 1, 3, \ldots$. The fixed point is unstable: it has one negative eigenvalue. As a result, only potentials that lie exactly on the "critical surface" flow into the nontrivial fixed point as $\Lambda \to 0$. Any small perturbation away from this surface eventually builds up and drives the potential either to the trivial fixed point at the origin or to infinity.

For perturbations around the nontrivial fixed point, we can assign an order $d = \nu - 1 = -2, 0, 2, \ldots$ to each term in the potential. This power counting for (energy-dependent) perturbations agrees with that found by Kaplan, Savage and Wise[2] using a "power divergence subtraction" scheme and also by van Kolck[3] in a more general subtractive renormalisation scheme.

The on-shell K-matrix for this potential is (to any order in the C's)

$$\frac{1}{K(p,p,p)} = -\frac{M}{2\pi^2}\left(C_{-1} + C_1 p^2 + \cdots\right). \tag{18}$$

This is just the effective-range expansion (4). There is thus a one-to-one correspondence between the perturbations in V and the terms in that expansion. The expansion around the nontrivial fixed point is the relevant one for systems with large scattering lengths, such as s-wave nucleon-nucleon scattering.

SUMMARY

We have applied Wilson's renormalisation group to nonrelativistic two-body scattering and identified two important fixed points[5].

The first is the trivial fixed point. Perturbations around it can be used to describe systems with weak scattering. These perturbations can be organised according to Weinberg's power counting[1].

The second fixed point describes systems with a bound state at exactly zero energy. In this case the relevant power-counting is the one found by Kaplan, Savage and Wise[2] and van Kolck[3]. The expansion around this fixed point is exactly equivalent to the effective-range expansion.

These ideas can be extended in various ways. Three-body systems are also being studied from the point of view of effective field theory[7]. In some cases these display much more complicated behaviour under the RG than the two-body ones discussed above[8].

Various nucleon-nucleon scattering observables as well as deuteron properties have been calculated using the expansion around the nontrivial fixed point[2,9,10]. In this approach, pion-exchange forces treated as perturbations. An alternative approach which is being explored by other groups is to use Weinberg's power counting in the expansion of the potential, but then to iterate that potential to all orders in the LS equation[11–13]. This may provide a way to evade problems of slow convergence when one-pion exchange is included explicitly[14,15].

REFERENCES

1. S. Weinberg, Phys. Lett. **B251**, 288 (1990); Nucl. Phys. **B363**, 3 (1991).
2. D. B. Kaplan, M. J. Savage, and M. B. Wise, Phys. Lett. **B424**, 390 (1998); Nucl. Phys. **B534**, 329 (1998); Phys. Rev. **C59**, 617 (1999).
3. U. van Kolck, Nucl. Phys. **A645**, 273 (1999).
4. K. G. Wilson and J. G. Kogut, Phys. Rep. **12**, 75 (1974); J. Polchinski, Nucl. Phys. **B231**, 269 (1984).
5. M. C. Birse, J. A. McGovern and K. G. Richardson, hep-ph/9807302, Phys. Lett. **B** (in press).
6. J. M. Blatt and J. D. Jackson, Phys. Rev. **76**, 18 (1949); H. A. Bethe, Phys. Rev. **76**, 38 (1949).
7. P. F. Bedaque and U. van Kolck, Phys. Lett. **B428**, 221 (1998); P. F. Bedaque, H.-W. Hammer and U. van Kolck, Phys. Rev. **C58**, R641 (1998).
8. P. F. Bedaque, H.-W. Hammer and U. van Kolck, Phys. Rev. Lett. **82**, 463 (1999); Nucl. Phys. **A646**, 444 (1999); nucl-th/9906032.
9. J.-W. Chen, H. W. Griesshammer, M. J. Savage and R. P. Springer, Nucl. Phys. **A644**, 221 (1998).
10. M. J. Savage, K. A. Scaldeferri and M. B. Wise, Nucl. Phys. **A652**, 273 (1999).
11. C. Ordonez, L. Ray and U. van Kolck, Phys. Rev. **C53**, 2086 (1996).
12. E. Epelbaum, W. Glöckle and U.-G. Meissner, Nucl. Phys. **A637**, 107 (1998); nucl-th/9910064.
13. S. R. Beane, M. Malheiro, D. R. Phillips and U. van Kolck, Nucl. Phys. **A656**, 367 (1999).
14. T. D. Cohen and J. M. Hansen, Phys. Rev. **C59**, 13 (1999).
15. D. B. Kaplan and J. V. Steele, nucl-th/9905027.

Two-loop calculations in HBCPT

J. A. McGovern and M. C. Birse
Theoretical Physics Group, Department of Physics and Astronomy, University of Manchester, Manchester M13 9PL, UK

Abstract

We present two recent two-loop calculations in HBCPT; the fifth-order contribution to the nucleon mass and the lowest-order contribution of the Wess-Zumino-Witten anomalous Lagrangian to forward spin-dependent Compton scattering. In both cases there are checks on the results which confirm the consistency of HBCPT at two-loop level, and in addition the smallness of the mass correction is very encouraging for the convergence of the theory.

INTRODUCTION

Chiral perturbation theory[1] is establishing itself as the principal tool for determining the consistency of data in disparate low energy processes involving pions, nucleons and photons. The purely mesonic theory is now on a very firm footing, and two-loop calculations are becoming commonplace[2]. Including nucleons originally appeared impossible to do consistently, as the existence of the nucleon mass as an extra mass scale destroys the power counting of the relativistic theory[3]. This problem can be circumvented, however, by expanding about the limit in which the nucleon mass is infinitely large, generating a systematic expansion in which M_N occurs only in the denominator. This theory has been extensively tested at one-loop order, proving consistent with—and indeed providing another method of demonstrating—all low-energy theorems (LET's) based on such considerations as Lorentz and gauge invariance and chiral symmetry.

However until now calculations in HBCPT have been almost exclusively one loop, for the excellent reason that two-loop diagrams enter only at fifth order, while the fourth-order Lagrangian is still in the process of been worked out[4]. There are however some processes where the leading contribution is two-loop; an example is the imaginary part of the nucleon electromagnetic form factors, which involves the anomalous $\gamma \to 3\pi$ vertex, with all the pions coupling to the nucleon. This process was considered by Bernard *et al.* in ref.[5]. However since the imaginary part comes from the kinematical regime where the pions are on-shell, this is not a two-loop calculation in the sense of having two internal momenta to integrate over. Here we present two calculations which are two-loop in the full sense.

The two calculations have one thing in common; for different reasons, they can have no contribution from counterterms at the order to which we are working. Thus they must both be finite, and the results are particularly clean. In fact neither requires knowledge of $\mathcal{L}_{\pi N}$ beyond third order, and in fact the final results are entirely free of low energy constants (LEC's) beyond lowest order. The first calculation is the fifth-order piece of the chiral expansion of the nucleon mass, in which the only non-vanishing contribution turns out to come from the expansion of the relativistic one-loop graph in powers of $1/M_N$. The other two-loop calculation is the leading (seventh-order) contribution of the anomalous Wess-Zumino-Witten Lagrangian[6] to forward spin-dependent Compton scattering in the limit that the photon energy goes to zero. To satisfy the LET of Low, Gell-Mann and Goldberger[7] this should vanish. We find that it does so, quite non-trivially, and the result enhances our confidence in the consistency of HBCPT, as well as showing the compatibility of the WZW Lagrangian and HBCPT, and testing the structure of the former in a novel way.

THE NUCLEON MASS

Just about the simplest HBCPT calculation at any order is the nucleon mass shift. Here the chiral expansion is just an expansion in powers of M_π. The even orders can receive counterterm contributions, but the odd orders, corresponding to fractional powers of the quark mass, can only come from loops; the lowest one-loop contribution is of order M_π^3.

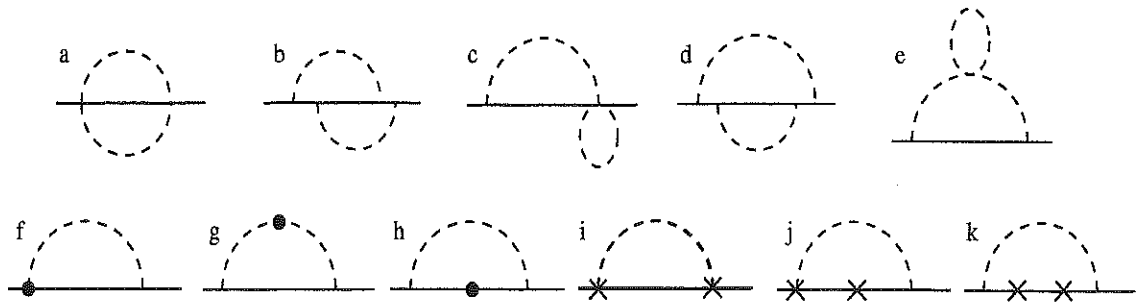

Fig. 1. Contributions to $\Sigma^{(5)}$. Solid dots represent insertions from $\mathcal{L}^{(3)}_{\pi N}$ and $\mathcal{L}^{(4)}_{\pi\pi}$, and crosses from $\mathcal{L}^{(2)}_{\pi N}$ (both include fixed terms from the expansion in $1/m_N$).

So far the counterterms at second and fourth order have not been well determined, so it is of interest to consider the convergence of the odd terms in the series separately.

The heavy-baryon propagator is given by

$$S^{-1} = \omega - \Sigma(\omega, \mathbf{k}), \tag{1}$$

where the nucleon momentum is written as $p = mv + k$, m is the bare mass, and $\omega = v \cdot k$. The mass shift $\delta m = m_N - m$ is the value of ω for which the propagator has a pole at zero three-momentum:

$$\delta m - \Sigma(\delta m, 0) = 0. \tag{2}$$

To order M_π^3, we have $\Sigma(\delta m) = \Sigma(0)$, so[8]

$$\delta m^{(2)} + \delta m^{(3)} = -4c_1 M_\pi^2 - \frac{3g_A^2 M_\pi^3}{32\pi F_\pi^2}, \tag{3}$$

where the second term comes from the one-loop self-energy diagram. Writing as $\Sigma^{(n)}$ the expression for the $O(q^n)$ part of Σ, which can in turn be expanded in powers of ω/M_π, we obtain

$$\delta m^{(5)} = \Sigma^{(5)}(0) + \delta m^{(2)}\Sigma^{(4)'}(0) + \delta m^{(3)}\Sigma^{(3)'}(0) + \tfrac{1}{2}(\delta m^{(2)})^2\Sigma^{(3)''}(0) \tag{4}$$

where primes indicate derivatives with respect to ω.

The set of graphs which contribute to $\Sigma^{(5)}$ are shown in Fig. 1. Those which contribute to the first derivative of $\Sigma^{(4)}$ are like Figs 1f and h, but with second order vertices. The two-loop diagrams 1a, b and d all contain the same single irreducible two-loop integral

$$I = \int \frac{d^d l\, d^d k}{(2\pi)^{2d}} \frac{1}{v \cdot k\,(M^2 - l^2)((M^2 - (k-l)^2)}. \tag{5}$$

This integral can be done by using Feynman parameters, yielding

$$\begin{aligned} I &= -\frac{M^{2d-5}\pi^{\frac{1}{2}}\Gamma(\frac{5}{2} - d)}{(4\pi)^d} \int_0^1 (x - x^2)^{(1-d)/2} dx \\ &= -\frac{M^{2d-5}\, 2^{d-2}\pi\Gamma(\frac{5}{2} - d)\Gamma(\frac{3-d}{2})}{(4\pi)^d \Gamma(2 - \frac{d}{2})}. \end{aligned} \tag{6}$$

which tends to zero as $d \to 4$. Thus only pieces which are the product of two one-loop integrals are left. These contain divergences, which are cancelled by graphs with counterterm insertions, Figs. 1f-h. The full contribution from Eq. 4 is as follows:

$$\delta m^{(5)} = \frac{3g^2 M^5}{32\pi F^2}\left(\frac{2\bar{l}_4 - 3\bar{l}_3}{F^2} - \frac{4(2\bar{d}_{16} - \bar{d}_{18})}{g} + \frac{g^2}{8\pi^2 F^2} + \frac{1}{8m^2}\right). \tag{7}$$

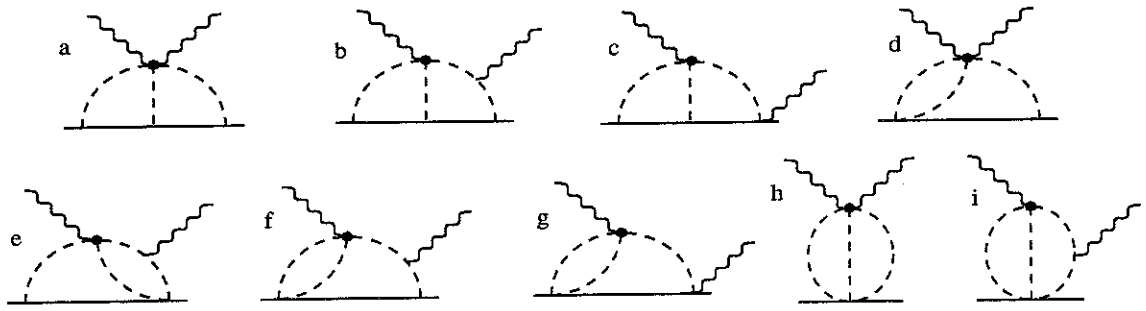

Fig. 2. Diagrams with anomalous vertices (solid dots) which contribute to Compton scattering in the $\epsilon \cdot v = 0$ gauge.

The LEC's $\bar{l}_i$ are from the fourth-order mesonic Lagrangian, and the $\bar{d}_i$ are from the third-order pion-nucleon Lagrangian as given in ref.[9]. They are defined with a renormalisation scale of M_π, hence the absence of chiral logarithms.

This is not however the final result for the fifth-order mass term. It is customary to express results in CPT not in terms of the bare parameters that appear in the Lagrangian, for instance M, g, F and m, but in terms of the physical values M_π, g_A, F_π and m_N; this ensures that the values of lower order results do not change when a higher-order calculation is done. Since the bare and physical parameters are equal to lowest order, we can simply make the substitution in Eq. 7; the error introduced is of seventh order. However, when we do the same for $\delta m^{(3)}$, we generate corrections of fifth order, which must also be included. In this case, since the one-loop graph involves two pion-nucleon couplings, we choose to use the physical pion-nucleon coupling constant $g_{\pi NN}$, rather than g_A/f_π. The fifth order corrections so generated then cancel almost completely with the explicit fifth order terms, leaving as our final result

$$\delta m^{(3)} + \delta m^{(5)} = -\frac{3g_{\pi NN}^2 M_\pi^3}{32\pi m_N^2}\left(1 - \frac{M_\pi^2}{8m_N^2}\right). \tag{8}$$

Further details are given in ref.[10]. Thus in the heavy-baryon limit the contribution of order M_π^5 vanishes, with all corrections being absorbed in the physical pion mass and pion-nucleon coupling constant in the M_π^3 contribution. For finite nucleon mass, the correction is just that obtained if the relativistic one-loop contribution is expanded in powers of M_π/m_N[3]. Since the $1/m_N$ terms in the HBCPT Lagrangian are constructed to respect Lorentz invariance, this agreement is reassuring but certainly not surprising. It is also worth noting that the fifth-order piece is only 0.3% of the third-order piece, which is most encouraging for the convergence of the theory.

COMPTON SCATTERING

Compton scattering from the nucleon has recently been the subject of much work, both experimental and theoretical. For the case of unpolarised protons the experimental amplitude is well determined, and in good agreement with the results of HBCPT. However the situation with regard to scattering from polarised targets is less satisfactory. The usual notation for spin-dependent pieces of the forward scattering amplitude for photons of energy ω, momentum q is

$$\epsilon_2^\mu \Theta_{\mu\nu} \epsilon_1^\nu = ie^2 \omega W^{(1)}(\omega) \boldsymbol{\sigma} \cdot (\boldsymbol{\epsilon}_2 \times \boldsymbol{\epsilon}_1) + \ldots \tag{9}$$

From a theoretical perspective there is particular interest in the low-energy limit of the amplitude: $W^{(1)}(\omega) = 4\pi(f_2(0) + \omega^2\gamma_0) + \ldots$, where γ_0 is the forward spin-polarisability. The LET of Low, Gell-Mann and Goldberger[7] states that $f_2(0) = -e^2\kappa^2/8\pi M_N^2$, where κ is the anomalous magnetic moment. While direct measurements of f_2 at zero energy are not currently feasible, it can be related to the photon absorption cross-section at energies

above the pion production threshold by the Gerasimov-Drell-Hearn sum rule[11]; the cross-sections in turn can be estimated from pion electroproduction data. All analyses so far have shown a significant discrepancy between the sum rule and the LET[12].

In HBCPT the LET is satisfied at third order, with the bare anomalous magnetic moment. At fourth order, there is a non-zero contribution also, which is the correction from the difference between the bare and full anomalous magnetic moment[13]. Here we will look at a subset of two-loop diagrams, those which involve an anomalous photon-pion coupling, as shown in Fig. 2. Since these have a factor of N_c in the amplitude, they can be cleanly distinguished from all the other diagrams which would contribute at the same order. This time, to satisfy the LET, the total contribution to $f_2(0)$ has to be zero.

We have calculated the contributions from all of the diagrams of Fig. 2. The first three are proportional to g_A^3, the rest to g_A. It is relatively straightforward to show that the second set cancel and make no net contribution. The first set do also cancel, but to prove it integration-by-parts identities have to be used to find relationships between various two-loop integrals. The details are given in ref.[14]. This provides a highly non-trivial test of the consistency of HBCPT at the two loop level, and also of the consistency of the WZW and HBCPT Lagrangians.

REFERENCES

1. J. Gasser and H. Leutwyler, Ann. Phys. (N.Y.) **158** 142 (1984); Nucl. Phys. **B250** 465 (1985).
2. For a review see J. Bijnens, hep-ph/9710341.
3. J. Gasser, M. E. Sainio and A. Švarc, Nucl. Phys. **B307** 779 (1988).
4. U-G. Meißner, G. Müller and S. Steininger, hep-ph/9809446.
5. V. Bernard, N. Kaiser and U-G. Meißner, Nucl. Phys. **A611** 429 (1996).
6. E. Witten, Nucl. Phys. **B223** 422 (1983).
7. F. Low, Phys. Rev. **96** 1428 (1954); M. Gell-Mann and M. Goldberger, Phys. Rev. **96** 1433 (1954).
8. V. Bernard, N. Kaiser and U-G. Meißner, Int. J. Mod. Phys. E **4** 193 (1995).
9. N. Fettes, U-G. Meißner and S. Steininger, Nucl. Phys. **A640** 199 (1998).
10. J. A. McGovern and M. C. Birse, Phys. Lett. B **446** 300 (1999).
11. S. B. Gerasimov, Sov. J. Nucl. Phys. **2** 430 (1966); S. D. Drell and A. C. Hearn, Phys. Rev. Lett. **16** 908 (1966).
12. I. Karliner, Phys. Rev. **D 7** 2717 (1973); A. M. Sandorfi, C. S. Whisnant and M. Khandaker, Phys. Rev. **D 50** R6681 (1994); D. Drechsel and G. Krein, Phys. Rev. **D 58** 116009 (1998).
13. X. Ji, C-W. Kao and J. Osborne, hep-ph/9908526; K. B. V. Kumar, J. A. McGovern and M. C. Birse, hep-ph/9909442.
14. J. A. McGovern and M. C. Birse, hep-ph/9908249.

Quark-Hadron Duality, Analyticity and the Structure of Low-Energy Couplings

Alexander V. Vereshagin and Vladimir V. Vereshagin
St-Petersburg State University, St-Petersburg, 198904, Russia

Abstract

Using the Cauchy's form technique developed in our previous paper we consider the elastic pion-nucleon process and derive the corresponding system of bootstrap constraints (sum rules) for triple coupling constants and masses of relevant resonances. With the help of this system we compute the ratio of tensor/vector $\rho N\bar{N}$ coupling constants and show that it coincides with the known experimental value $g_T/g_V \approx 6$. This result gives a strong argument in favor of our method based solely on general postulates of Effective Field Theory and the analyticity requirements.

INTRODUCTION

In our previous publications[1],[2] we have developed the general method allowing one to fix the values of the low-energy coefficients (LEC's) appearing in ChPT series. The method is based solely on the commonly accepted postulates of Effective Field Theory (EFT) plus certain analyticity requirements (maximal analyticity and the polynomial boundedness) which are not guaranteed by the inner structure of EFT. Besides, we use the quark-hadron duality concept allowing us to work in terms of hadron fields.

In our work we rely on the existence of a special parameterization allowing one to rewrite (without loss of generality) the Hamiltonian of EFT in a form containing only those vertices which survive on the mass shell. This simplifies considerably the process of computations. However, the price to be paid for simplicity is that we can work with S-matrix elements only; the generality happens lost if the method is used to study Green's functions.

The maximal analyticity requirement is formulated as follows: the tree-level amplitude of an arbitrary scattering process must be a meromorphic function of the invariant kinematical variables (pair energies and momentum squares). This is by no means a trivial requirement because the presence of unlimited number of derivatives in the EFT Lagrangian results in the expression of a tree-level amplitude which takes a form of the infinite series expansion in powers of kinematical variables. Thus, even on the first – tree-level – step one meets a problem of convergence. This problem is closely related with the expected *analytic structure* of tree-level amplitudes because the divergency of a series expansion mirrors the presence of a singularity of the amplitude in question. Since the loop expansion machinery automatically produces all the *necessary* singularities (namely, those required by the unitarity condition), we conclude that the only way allowing one to prevent the generating of *unnecessary* ones in the process of loop calculations consists of imposing the formulated above condition of maximal analyticity on the structure of tree-level amplitudes or, the same, on the structure of allowed resonance spectrum and corresponding couplings.

The maximal analyticity requirement, by itself, is too general to fix a theory: in particular, it does not make any difference between strong and weak forces. This is the reason for attracting of one more requirement which takes account of the well known feature of strong interactions – the Regge asymptotic behavior of high energy amplitudes at fixed value of the momentum transfer. Mathematically, it is formulated as the polynomial boundedness requirement for the tree-level binary amplitudes, the bounding polynomial degrees being dictated by the values of Regge intercepts (on a given stage we consider only small values of the momentum transfer). It should be also stressed that the polynomial boundedness of a meromorphic function is understood precisely as in complex analysis (the boundedness on the infinite system of closed contours in a complex plane).

At first glance, the imposing of polynomial boundedness restriction on the tree-level amplitude might look a bit strange because the true high energy behavior cannot be computed if one neglects the loop contributions. However, there is another argument in favor of this requirement: the polynomial boundedness of trees at zero values of corresponding

variables (momentum transfers) is a necessary condition providing the generalized renormalizability of EFT (the detailed proof of this statement would require much space; it will be given elsewhere). Thus, in fact, we need only to fix the specific values of the bounding polynomial degrees.Our choice looks preferable from the phenomenological standpoint (see[2]). Below, it is shown that it results also in a correct value of the experimentally known relation

$$\frac{g_T^\rho}{g_V^\rho} \approx 6.$$

As shown in[1] and[2], the set of the above formulated postulates results in a certain (infinite) system of *bootstrap* equations (sum rules - SR) for the spectrum parameters (triple couplings and the resonance masses). In the case of pion-nucleon scattering there are 4 independent invariant amplitudes: $A^\pm$ and $B^\pm$. Using precisely the same method as in[2], one can obtain – among the others – two following bootstrap conditions for the parameters of πN resonances with spin $J = l+1/2$, $(l = 0, 1, \ldots)$ and isospin $I = 1/2,\ 3/2$ and isovector $\pi\pi$ resonances with $J = 1, 3, \ldots$:

$$\sum_{bar}\left[\frac{Y_B^-(-\Sigma) - Y_B^-(0)}{\Sigma} - \frac{Y_B^-(0)}{M^2}\right] + \sum_{mes}\frac{W_B^-(\frac{\Sigma}{4F})}{M^2} = 0\ , \tag{1}$$

$$\sum_{bar}\frac{Y_A^-(-\Sigma)}{M^2} = \sum_{mes}\frac{W_A^-(\frac{\Sigma}{4F})}{\Sigma}\ . \tag{2}$$

Here m, (μ) stands for the nucleon (pion) mass, M – for the mass of relevant resonance (fermion or boson), $p_R = \pm$ – for the baryon resonance parity,

$$Y_X^-(x) \equiv C_I^- G_r F_X^l(-p_R M, x), \qquad (X = A, B;\ \ I = 1/2,\ 3/2),$$

$$\Sigma = M^2 - 2(m^2 + \mu^2), \qquad C_{1/2}^- = +1, \qquad C_{3/2}^- = -1/3,$$

$$W_A^-(x) \equiv -G_1^V P_J(x) + \frac{4m}{4m^2 - M^2} G_2^V P'_{J-1}(x), \qquad W_B^-(x) \equiv -\frac{G_2^V}{F} P'_J(x),$$

$$F_A^l(M, x) \equiv (M+m)P'_{l+1}\left(1 + \frac{x}{2\Phi}\right) + (M-m)\frac{(M+m)^2 - \mu^2}{(M-m)^2 - \mu^2} P_l'\left(1 + \frac{x}{2\Phi}\right),$$

$$F_B^l(M, x) \equiv P'_{l+1}\left(1 + \frac{x}{2\Phi}\right) - \frac{(M+m)^2 - \mu^2}{(M-m)^2 - \mu^2} P_l'\left(1 + \frac{x}{2\Phi}\right),$$

$$F = \frac{\sqrt{(M^2 - 4m^2)(M^2 - 4\mu^2)}}{4}, \qquad \Phi = \frac{M^4 + m^4 + \mu^4 - 2M^2m^2 - 2M^2\mu^2 - 2m^2\mu^2}{4M^2}\ ,$$

$$G_r = (\Phi)^l \left|g_r(l, I, p_r)\right|^2 \frac{l!}{(2l+1)!!}\ .$$

$$G_1^V = (-F)^J g_{\pi\pi} g_{NN}^1 \frac{J!}{(2J+1)!!}, \qquad G_2^V = (-F)^J g_{\pi\pi} g_{NN}^2 \frac{J!}{(2J+1)!!},$$

The (real) coupling constants g_{NN}^1, g_{NN}^2 and $g_{\pi\pi}$ are defined in accordance with the following effective Lagrangians describing the interaction vertices of isovector mesons (of odd spin) with pions and nucleons:

$$L_{VN\bar{N}} = i g_{NN}^1 \bar{N}\vec{\sigma}\partial_{\mu_1\ldots\mu_J} N\vec{V}^{\mu_1\ldots\mu_J} + g_{NN}^2 J\bar{N}\gamma_{\mu_J}\vec{\sigma}\partial_{\mu_1\ldots\mu_{J-1}} N\vec{V}^{\mu_1\ldots\mu_J}\ ,$$

$$L_{V\pi\pi} = \frac{1}{2} g_{\pi\pi} \vec{V}^{\mu_1 \ldots \mu_J} \cdot (\vec{\pi} \times \partial_{\mu_1 \ldots \mu_J} \vec{\pi}) \ .$$

The constants $g_r(l, I, p_r)$ describing the effective πNR-vertices, where R stands for the baryon resonance of the isospin $I = 1/2,\ 3/2$, spin $J = l + 1/2$ and parity $p_r = \pm$, are defined as follows:

$$L^{1/2}_{\pi NR} = g_r(l, 1/2, p_r) \bar{N} \vec{\sigma} \hat{\Gamma}_{p_r} R^{\mu_1 \ldots \mu_l} \partial_{\mu_1 \ldots \mu_l} \vec{\pi} + H.c. \ ,$$

$$L^{3/2}_{\pi NR} = g_r(l, I, p_r) \bar{N} \hat{\Gamma}_{p_r} \hat{\Pi}^{ab}_{3/2} R^{\mu_1 \ldots \mu_l}_b \partial_{\mu_1 \ldots \mu_l} \pi_a + H.c. \ ,$$

where $\hat{\Gamma}_+ = 1$ $(p_r = +1)$, $\hat{\Gamma}_- = i\gamma_5$ $(p_r = -1)$, and

$$\hat{\Pi}^{ab}_{3/2} \equiv \frac{2}{3} \left[\delta^{ab} - \frac{i}{2} \varepsilon^{abc} \sigma_c \right]$$

is the isospin-3/2 projecting operator.

In (1) and (2) the summation is implied over *all* (baryon or meson) resonances with corresponding quantum numbers; *it should be done in order of increasing mass* (see[2]).

The coupling constants g^1_{NN}, g^2_{NN} and $g_{\pi\pi}$ defined above are related to the corresponding constants $G^V_{NN\rho}$, $G^T_{NN\rho}$ and $G_{\pi\pi\rho}$ introduced in[3] as follows

$$g^1_{NN} = \frac{1}{2m} G^T_{NN\rho}, \quad g^2_{NN} = \frac{G^V_{NN\rho} - G^T_{NN\rho}}{2}, \quad g_{\pi\pi} = \frac{1}{2} G_{\pi\pi\rho}.$$

The existing experimental data (see[3] and[4]) give

$$G^T_{NN\rho}/G^V_{NN\rho} \approx 6.1 \ , \qquad \frac{G_{\pi\pi\rho} G^V_{NN\rho}}{4\pi} \approx 2.4 \ , \qquad G_{\pi\pi\rho} \approx 6.0 \ . \tag{3}$$

Both the Eqs. (1) and (2) converge extremely rapidly: in fact, only three baryons – $N(0.94)$, $N(1.44)$ and $\Delta(1.23)$ – and one boson – $\rho(0.77)$ – produce nonnegligible contributions. This allows one to neglect all the terms corresponding to the contributions of heavier hadrons. The resulting sum rules contain the following set of spectrum parameters: 1. Three pion-baryon coupling constants, three baryon and one meson masses (which can be taken from the known data); 2. The effective $\rho\pi\pi$ coupling constant $G_{\pi\pi\rho}$, and two ρNN constants ($G^V_{NN\rho}$ and $G^T_{NN\rho}$) (which we consider as free parameters). Thus we obtain the system of two equations for three parameters. This gives us a possibility to fix the relation

$$G^T_{NN\rho}/G^V_{NN\rho} \approx 6 \ (\pm 15\%)$$

in excellent agreement with the known experimental result (3). If, in addition, we fix the value of $G_{\pi\pi\rho}$ we can determine also the product

$$\frac{G_{\pi\pi\rho} G^V_{NN\rho}}{4\pi} \approx 2.5 \ (\pm 20\%)$$

– again in complete agreement with data.

Thus we conclude that – similarly to the case of πK elastic scattering (see[2]) – the system of bootstrap equations for the bare parameters of pion-nucleon amplitude contains at least two relations strongly supported by the known data. As far as we know, these relations have been never explained before from such a general standpoint as it is done above: we rely only on the concepts of EFT, maximal analyticity and the polynomial boundedness of the Regge type. Each one of these principles is formulated for the bare Hamiltonian, the polynomial boundedness condition being unavoidable if we require the generalized renormalizability of a theory. In fact, the only phenomenological information

needed to fix the particular form of the bootstrap equations is concentrated in the numerical values of integral parts of intercepts. As pointed out in[1], this system – in any case – happens to be homogeneous with respect to the triple coupling constants. This means that, to fix their values, one needs to attract certain additional principles. In[1] and[2] it is shown that the requirement of low-energy Chiral symmetry happens quite sufficient for this purpose because it results in a relation connecting triple pion-pion-resonance coupling constants (and masses of the pion resonances) with the pion decay constant f_π, this relation being inhomogeneous. We would like to stress that there is no necessity in applying the same condition to the case in question (in which it is difficult to give a constructive formulation of the low-energy Chiral symmetry requirement). Instead, one can use as input the known value of the pion-nucleon coupling constant – this removes an ambiguity connected with overall scaling factor which cannot be fixed with the help of the mentioned above postulates.

It is important to stress also that the relation between two different ρNN *bare* coupling constants remains valid after renormalization. The point is that both triple couplings and masses appearing in bootstrap equations belong to the set of *essential* parameters of a theory (see, e.g.,[5]). By construction (we do not consider a problem of anomalies), EFT is a renormalizable theory (in a general sense – see[5]). Next, by the very meaning of a renormalization procedure, one has to keep fixed the numerical values of the essential parameters appearing in the bare Lagrangian – this is a matter of the renormalization prescription. If we call as *symmetry* any kind of relations between the (essential) bare parameters, we can say that the renormalization should respect symmetry requirements. In our case the symmetry requirements happen to be highly nontrivial: they appear in the form of an infinite system of bootstrap conditions connecting among themselves the values of bare Lagrangian parameters. One extremely interesting property of those relations is that they connect the parameters of boson spectrum with those of the baryon one, in other words, they demonstrate certain features of a (very complicated) *supersymmetry*. As well known, supersymmetry strongly restricts the possible divergences, in certain cases it leads to finite theories. The other – no less important feature of the bootstrap conditions is that they are based on the same principles as those used as the basis for string theories. Altogether, the above notes give a hope that the solution of bootstrap equations does exist and the corresponding spectrum parameters can be explained in terms of superstrings. Perhaps, this very circumstance explains the reason for interest to the models of low-energy effective action based on certain properties of a string theory (see, e.g.,[6]).

REFERENCES

1. Vladimir V. Vereshagin, "Tree-level (π, K) amplitude and analyticity", Phys. Rev. **D55**, 5349 (1997).
2. Alexander V. Vereshagin, and Vladimir V. Vereshagin, "Effective theories with maximal analyticity", Phys. Rev. **D59**, 016002 (1999).
3. O. Dumbrajs et al, "Compilation of coupling constants and low-energy parameters", Nucl. Phys. **B216**, 277 (1983).
4. T. Ericson, and W. Weise, *Pions and Nuclei* (Clarendon Press, Oxford, 1988), Ch. 3, pp. 77-82.
5. S. Weinberg, *"The Quantum Theory of Fields"* (Cambridge University Press, Cambridge, 1996), V. 1.
6. J. Alfaro, A. Dobado, and D. Espriu, "Chiral Lagrangians and the QCD strings", Physics Letters, **B460**, 447 (1999).

Very low energy measurements of pion-nucleon charge exchange scattering

L.D. Isenhower, T. Black, B.M. Brooks, A.W. Brown, K. (Smith) Graessle, J.A. Redmon, M.E. Sadler
Abilene Christian University, Abilene, TX 79699

and

J.D. Bowman, D.H. Fitzgerald, J.N. Knudson, H.W. Baer*, P. Heusi, F. Irom
Los Alamos National Laboratory, Los Alamos, NM 87545

and

T. Bergman, W.J. Briscoe, *The George Washington University, Washington, DC 20052, U.S.A.* †

Abstract

We present measurements of the differential cross sections for $\pi^- p \to \pi^o n$ near $0^o, 90^o, and 180^o$ at $T_{\pi^-} = 10.6, 20.6, and 39.4$ MeV ($P_{\pi^-} = 55.4, 78.6,$ and 112.0 MeV/c) from LAMPF Experiment 882. These data include the lowest energies ever measured for this interaction and are the only low-energy data to cover the entire angular region from 0^o to 180^o. The results are compared with the Karlsruhe and GW/VPI partial wave analyses and the potential model of Siegel and Gibbs.

Differential cross sections were obtained for $\pi^- p \to \pi^o n$ using the LAMPF PI0 Spectrometer[1] to detect the 2γ's from the decay of the π^o at very low energies ($T_{\pi^-} = 10.6$, 20.6, and 39.4 MeV). These are the lowest energies ever measured for any πN process that have nearly full angular coverage Such low energy measurements are important in determining the non-linearity of the isospin-1/2 s-wave phase shifts in an effective range expansion. The acceptance extended approximately 30-40^o around the three spectrometer settings used, providing good angular coverage for this interaction. The dominant systematic uncertainties are the knowledge of the beam flux, π^o acceptance, and target corrections caused by the loss of three LH_2 targets during the experiment, forcing the use of solid CH_2 targets for the majority of the data.

Beam normalizations were done by three methods for most of the beam tunes. These measurements gave consistent results at the 1% level. After including effects seen during each run, the typical beam normalizations are on the order of a few percent. It is important to note that each of these results were obtained with three different spectrometer configurations and beam tunes. Thus the groups of points near 0^o, 90^o, and 180^o have independent beam normalizations. Cuts are made on various parameters such as the fiducial area (or number of radiation lengths) and the energy sharing parameter, x, of the two photons to check for consistency. Fiducials were calculated for 1, 2, 4, 6, and 8 radiation lengths, and two values of x were used for these checks.

The differential cross sections are plotted in Figures 1, 2, and 3. Predictions from the Karlsruhe-Helsinki[2] and VP[5] phase shift analyses and the potential model of Siegel and Gibbs[4] are shown for comparison. These results are also given in Table 1; however, due to space limitations, not all of the points shown in the plots are given in the tables. The full results will appear in a longer paper under preparation that will be submitted to Physical Review. Energies are for the beam pions at the center of the target. The angle setting is the angle at which the spectrometer was optimized for the opening angle of the two photons. The binning of the data was done based on the measured $\cos(\theta)$ value (θ is the lab scattering angle). The cross sections are reported at the c.m. $\cos(\theta_{cm})$ values for the average of the actual thrown angles via the Monte Carlo calculations. The quoted errors include errors on the π^o yield (statistics), $N(\pi^-)$, the number of beam particles,

*deceased

†We wish to thank the Los Alamos Meson Physics Facility staff for their assistance in performing this experiment, especially for the operation of the crossed-field separator that made the attainment of very low energy beams possible. This work was supported in part by the U.S. Department of Energy and the National Science Foundation.

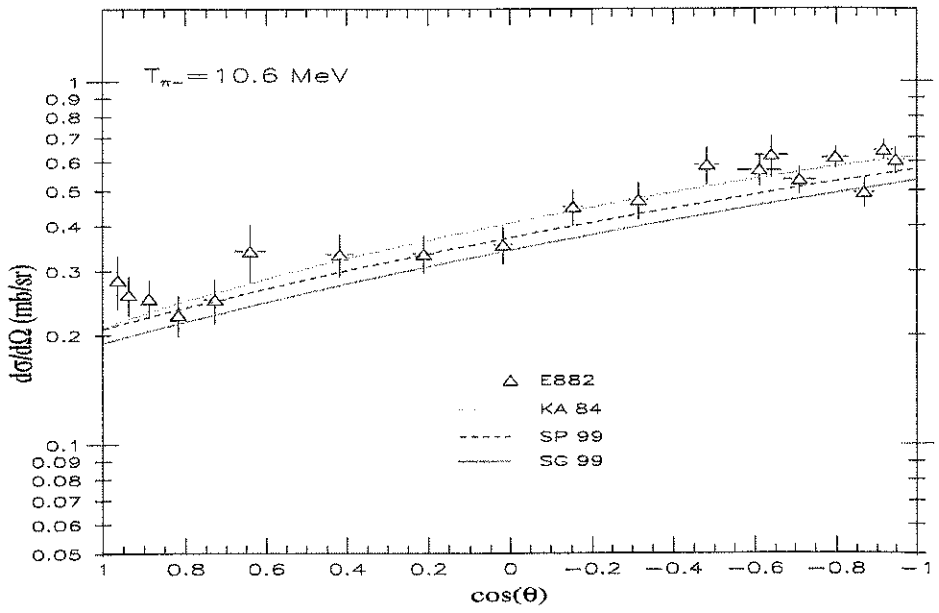

Figure. 1. Differential cross sections for $\pi^- p \to \pi^o n$ at T_{π^-}=10.6 MeV.

N_H, the areal density of hydrogen in the target, f_{abs}, the fraction of photons that make it to the first converter, $\epsilon(\pi^o)$, the π^o detection efficiency, and ϵ_w, the overall wire chamber and tracking efficiency. The π^o acceptance is the dominant systematic error (not shown) and varies from 3-5%.

In general, the data agree well with the existing analyses, especially Ref.[5]. The 0 degree points for the 20.6 MeV data are not plotted due to discrepancies of the results. The data have not been corrected for variations of the absorption of the photons before they reach the first converter plane. For the reported data, the loss of events is an average over the solid angle for all events. For final publication, corrections will be made for each angle bin separately.

The E882 data can be used to explain why the Fitzgerald measurements[6] were somewhat above the theoretical predictions. Their results were high primarily because they only used Carbon target data to subtract the background for the CH_2 target. At very low rates one must use empty target subtraction from the C and CH_2 data to properly normalize the yields. Without empty target subtraction, we obtain cross sections similar to their results at the data point near our 39.4 MeV measurement. For each spectrometer setting this leads to the constant correction seen in the Fitzgerald data (i.e., cross sections at a single spectrometer setting are off by the same value). The relative size of this constant correction is much smaller when the cross sections are larger at larger angles. It is important to note that this offset does not affect the location of the dip in the forward angle cross sections, which was the most important result of the Fitzgerald data.

REFERENCES

1. H. Baer, et al., *Nucl. Inst. and Meth.* **180** (1981) 445.
2. R. Koch and E. Pietarinen, *Nucl. Phys.* **A336** (1980) 331. R. Koch, *Nucl. Phys.* **A448** (1986) 707. G. Höhler, Pion-Nucleon Scattering, Landolt-Börnstein Vol. I/9b, (Springer-Verlag 1983).
3. R. A. Arndt, J. M. Ford and L. D. Roper, *Phys. Rev.* **D32** (1985) 1085.
4. W.R. Gibbs, personal communication, see also P.B. Siegel and W.R. Gibbs, *Phys. Rev.* **C33** (1986) 1407.
5. Provided by I. Strakovsky, GWU [ref: Phys. Rev. **C52**, 2120 (1995),Eprint nucl-th/9505040, Eprint nucl-th/9807087].
6. D.H. Fitzgerald, et al., *Phys. Rev.* **C34** (1986) 619.

Table 1. Results for $T_{\pi^-} = 10.6, 20.6$, and $39.4 MeV$ (center of target) for each of the three angular settings. Angles are the mean thrown angle from Monte Carlo, differential cross sections are given in μb/sr. See text for comment on errors.

energy setting	angle setting	lab angle range [deg.]	c.m. bin mean $\cos(\theta_{cm})$	$\frac{d\sigma}{d\Omega}$ [μb/sr]
10.6	0^o	20-30	0.888	253. ± 30.
10.6	0^o	30-40	0.817	227. ± 29.
10.6	0^o	40-50	0.728	251. ± 46.
10.6	0^o	50-60	0.640	341. ± 63.
10.6	90^o	63-75	0.418	334. ± 44.
10.6	90^o	75-85	0.212	335. ± 40.
10.6	90^o	85-95	0.019	355. ± 41.
10.6	90^o	95-105	-0.153	451. ± 51.
10.6	90^o	105-117	-0.316	471. ± 54.
10.6	180^o	110-120	-0.610	568. ± 56.
10.6	180^o	120-130	-0.712	535. ± 44.
10.6	180^o	130-140	-0.799	616. ± 40.
10.6	180^o	140-150	-0.868	494. ± 44.
10.6	180^o	150-160	-0.918	646. ± 40.
10.6	180^o	160-170	-0.949	606. ± 50.
20.6	90^o	50-63	0.390	230. ± 22.
20.6	90^o	75-85	0.004	338. ± 20.
20.6	90^o	85-95	-0.166	416. ± 23.
20.6	90^o	95-105	-0.325	475. ± 27.
20.6	90^o	105-117	-0.486	551. ± 34.
20.6	180^o	110-120	-0.647	558. ± 36.
20.6	180^o	120-130	-0.745	669. ± 30.
20.6	180^o	130-140	-0.832	759. ± 30.
20.6	180^o	140-150	-0.901	759. ± 30.
20.6	180^o	150-160	-0.948	734. ± 35.
20.6	180^o	160-170	-0.972	732. ± 50.
39.4	0^o	0-6	0.986	9.91 ± 3.5
39.4	0^o	6-12	0.973	14.6 ± 2.3
39.4	0^o	12-18	0.947	15.9 ± 2.0
39.4	0^o	16-24	0.909	24.6 ± 2.1
39.4	90^o	70-78	0.107	339. ± 14.
39.4	90^o	78-86	-0.033	416. ± 15.
39.4	90^o	86-94	-0.170	532. ± 18.
39.4	90^o	94-102	-0.299	671. ± 23.
39.4	90^o	102-110	-0.420	750. ± 29.
39.4	180^o	138-145	-0.861	990. ± 29.
39.4	180^o	145-152	-0.902	1060. ± 30.
39.4	180^o	152-159	-0.936	1128. ± 31.
39.4	180^o	159-166	-0.961	1152. ± 32.
39.4	180^o	166-173	-0.979	1174. ± 34.

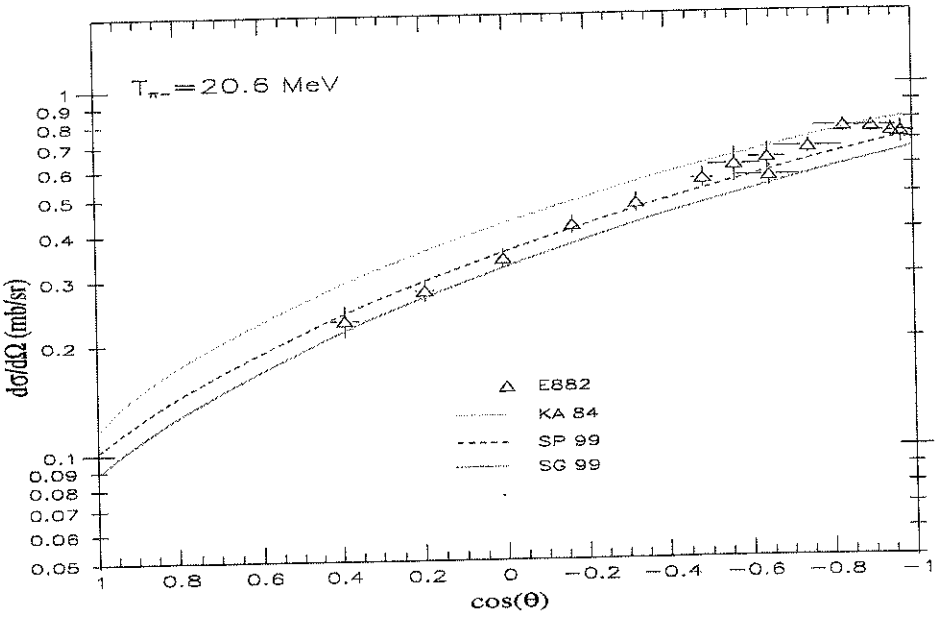

Figure. 2. Differential cross sections for $\pi^- p \to \pi^o n$ at T_{π^-}=20.6 MeV.

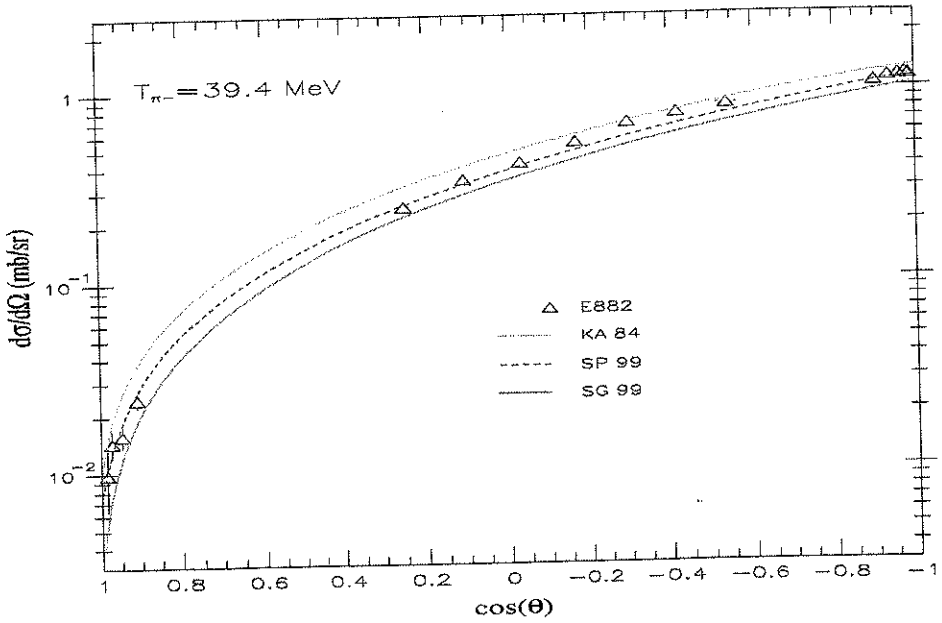

Figure. 3. Differential cross sections for $\pi^- p \to \pi^o n$ at T_{π^-}=39.4 MeV.

Coulomb Corrections to the Low Energy π^+p System

A. Gashi, E. Matsinos and G. Rasche
Institute of Theoretical Physics, Zürich University, CH-8057 Zürich, Switzerland,

G.C.Oades
Institute of Physics and Astronomy, Aarhus University, DK-8000 Aarhus, Denmark

and

W.S. Woolcock
Department of Theoretical Physics, ANU, Canberra, ACT 0200, Australia

Abstract

Electromagnetic corrections to π^+p scattering below 100 MeV are recalculated including magnetic moment and vacuum polarization effects.

I give a brief summary of the continuing work of the Zürich-Aarhus-Canberra group on the problem of Coulomb corrections at low energies. Due to the limited space I will only describe the single channel problem but I will attempt to give sufficient detail so that experimentalists can make use of the table of corrections which will come later. Compared to the report I gave at the last meeting in Vancouver[1] there are several changes. Vacuum polarization effects have now been included as has the electromagnetic spin-flip amplitude and the hadronic interaction is now modified by the same relativistic factor as the electromagnetic amplitudes

The single channel $\pi^+p \to \pi^+p$ f and g scattering amplitudes are written as

$$f(q_c,\cos\theta) = f^{pt} + f^{ext} + f^{rel} + f^{vp} + \sum_{l=0}^{\infty}\left[(l+1)e^{2i\Sigma_{l+}}f_{l+} + le^{2i\Sigma_{l-}}f_{l-}\right]P_l(\cos\theta) \quad (1)$$

$$g(q_c,\cos\theta) = g^{rel} + i\sum_{l=1}^{\infty}\left[e^{2i\Sigma_{l+}}f_{l+} - e^{2i\Sigma_{l-}}f_{l-}\right]P_l^1(\cos\theta) \quad (2)$$

where the partial wave sums represent the nuclear amplitudes, f^{pt} is the point Coulomb amplitude, f^{ext} is the additional modification due to the extended charges of the π and p, f^{rel} and g^{rel} are additional first order relativistic terms and f^{vp} is the vacuum polarization contribution. Explicit expressions for the various terms are

$$f^{pt} = \frac{2\alpha m_c f_c}{t}\exp\left[-i\eta f_c \ln\left(\sin^2\frac{\theta}{2}\right)\right] \quad (3)$$

$$f^{ext} = \frac{2\alpha m_c f_c}{t}\left(F^\pi F_1^p - 1\right) \quad (4)$$

$$f^{rel} = \frac{\alpha}{2W}\left[\frac{W+M_p}{E+M_p}F_1^p + 2\left(W - M_p + \frac{t}{4(E+M_p)}\right)F_2^p\right]F^\pi \quad (5)$$

$$g^{rel} = \frac{i\alpha}{2W\tan(\frac{\theta}{2})}\left[\frac{W+M_p}{E+M_p}F_1^p + 2\left(W + \frac{t}{4(E+M_p)}\right)F_2^p\right]F^\pi \quad (6)$$

where

$$f_c = \frac{W^2 - M_p^2 - \mu_c^2}{2m_c W} \quad (7)$$

$$q_c^2 = \frac{\left[W^2 - (M_p-\mu_c)^2\right]\left[W^2 - (M_p+\mu_c)^2\right]}{4W^2} \quad (8)$$

$$E = \sqrt{M_p^2 + q_c^2} \quad (9)$$

As usual W is the total cm energy, θ is the cm scattering angle and t is given by

$$t = -2q_c^2\,(1-\cos\theta) \tag{10}$$

The vacuum polarization amplitude is given by[2]

$$f^{vp} = -\frac{\alpha\eta f_c}{3\pi q_c}\,(1-\cos\theta)^{-1}\,F\,(\cos\theta) \tag{11}$$

where

$$F\,(\cos\theta) = -\frac{5}{3} + X + \left(1-\frac{1}{2}X\right)(1+X)^{\frac{1}{2}}\ln\left[\frac{(1+X)^{\frac{1}{2}}+1}{(1+X)^{\frac{1}{2}}-1}\right] \tag{12}$$

and

$$X = -\frac{4m_e^2}{t} \tag{13}$$

These expressions are the first terms in an approximation; they are sufficient for most purposes but at very low energies or very close to the forward direction further terms may be needed.They can be found in ref.[2].The Coulomb phases are given by

$$\Sigma_{l\pm} = (\sigma_l - \sigma_0) + \sigma_l^{ext} + \sigma_{l\pm}^{rel} + \sigma_l^{vp} \tag{14}$$

where

$$\sigma_l - \sigma_0 = \sum_{n=1}^{l} \arctan\left(\frac{\eta f_c}{n}\right) \tag{15}$$

$$\sigma_l^{ext} = \alpha m_c f_c q_c \int_{-1}^{+1} dz \frac{1}{t} P_l(z)\,(F_1^p F^\pi - 1) \tag{16}$$

$$\sigma_{l\pm}^{rel} = -\frac{\alpha q_c M_p}{2W}\int_{-1}^{+1} dz P_l(z) F_2^p F^\pi \pm \frac{\alpha q_c}{4W(l\pm\frac{1}{2}+\frac{1}{2})} \tag{17}$$
$$\int_{-1}^{+1} dz\left(P_l'(z)+P_{l\pm1}'(z)\right)\left[\frac{W+M_p}{E+M_p}F_1^p + \left(W+\frac{t}{4(E+M_p)}2F_2^p\right)F^\pi\right]$$

$$\sigma_l^{vp} = -\frac{\alpha\eta f_c}{3\pi}\int_0^1 dy\left(1+\frac{y}{2}\right)(1-y)^{\frac{1}{2}}\frac{1}{y}Q_l(1+\frac{\nu}{y}) \tag{18}$$

with

$$\nu = \frac{2m_e^2}{q_c^2} \tag{19}$$

For the form factors we use the expressions

$$F_1^p = \left(1-\frac{t}{\Lambda_p^2}\right)^{-2} \tag{20}$$

$$F_2^p = \frac{\kappa_p}{2M_p}F_1^p \tag{21}$$

$$F^\pi = \left(1-\frac{t}{\Lambda_\pi^2}\right)^{-2} \tag{22}$$

where κ_p is the anomalous magnetic moment of the proton and where $\Lambda_p = 805$ MeV and $\Lambda_\pi = 1040$ MeV, these values being chosen so as to reproduce the measured charge radii of the proton and the charged pion. Finally

$$f_{l\pm} = \frac{\exp(2i\delta_{l\pm}^n) - 1}{2iq_c} \tag{23}$$

where $\delta^n_{l\pm}$ is the nuclear phase shift. In these expressions M_p is the proton mass, μ_c is the charged pion mass and m_c is the reduced mass. α is the fine structure constant and the Coulomb parameter η is given by

$$\eta = \frac{\alpha m_c}{q_c} \tag{24}$$

The formalism described here is model independent; any description of the single channel system must be of this form no matter whether isospin is conserved or not. Model dependence first comes in when the Coulomb corrections are calculated. These Coulomb corrections are the difference between the nuclear and the hadronic phases i.e.

$$C_{l\pm} = \delta^n_{l\pm} - \delta^h_{l\pm} \tag{25}$$

In our case they are calculated by solving the relativized Schrödinger equation

$$\left(\frac{d^2}{dr^2} - \frac{l(l+1)}{r^2} + q_c^2 - 2m_c f_c V_{l\pm}(r)\right) u_{l\pm} = 0 \tag{26}$$

with

$$V_{l\pm}(r) = V^{em}_{l\pm}(r) + V^h_{l\pm}(r) \tag{27}$$

and

$$V^{em}_{l\pm}(r) = V^{pt}(r) + V^{ext}(r) + V^{rel}_{l\pm}(r) + V^{vp}(r) \tag{28}$$

for that $u_{l\pm}$ which is regular at $r = 0$ and which has asymptotic behaviour as $r \to \infty$

$$\sin\left(q_c r - \eta f_c \ln(2q_c r) - l\frac{\pi}{2} + \sigma_l + \sigma^{ext}_l + \sigma^{rel}_{l\pm} + \sigma^{vp}_l + \delta^n_{l\pm}\right) \tag{29}$$

so as to determine $\delta^n_{l\pm}$. The hadronic phase is determined by solving the similar equation with

$$V_{l\pm}(r) = V^h_{l\pm}(r) \tag{30}$$

for that $u_{l\pm}$ which is regular at $r = 0$ and which has asymptotic behaviour as $r \to \infty$

$$\sin\left(q_c r - l\frac{\pi}{2} + \delta^h_{l\pm}\right) \tag{31}$$

The various terms in $V^{em}_{l\pm}(r)$ are such that each of these potentials reproduce the corresponding terms in f and g. The hadronic potential is determined by an iterative procedure. From some initial set of hadronic phases we find $V^h_{l\pm}(r)$ which reproduce these phases; the Coulomb corrections are then determined and used in a new phase shift analysis to determine a new set of hadronic phases. The whole procedure is iterated until there are no further changes. The corrections determined in this way in a phase shift analysis of π^+p elastic scattering below 100 MeV are shown in table 1. The values in brackets are the corresponding Nordita values[3]. It will be seen that there is qualitative agreement but that there are quantative differences. To judge the significance of these differences typical phase shift errors at 100 MeV are shown in the last row of the table. It will be seen that the differences for $p3/2$ are significant, a fact which needs further investigation

A similar treatment has also been made of the coupled channel π^-p, π^0n problem and details of this more complicated situation will be published shortly.

REFERENCES

1. G.C.Oades,Low Energy Coulomb Corrections, in *Proceedings of the Seventh International Symposium on Meson-Nucleon Physics and the Structure of the Nucleon*, πN Newsletter No. 13 (TRIUMF report TRI-97-1) pp. 367-372. See also the preprints hep-ph/9902207, hep-ph/9902224 and hep-ph/9903434 for details of the earlier stages of the present work.
2. L. Durand III, "Vacuum Polarization Effects in Proton-Proton Scattering," Phys. Rev. **108**, 1597 (1957).
3. B. Tromborg, S. Waldenstrøm and I.Øverbø, "Electromagnetic corrections to πN scattering," Phys. Rev. **D15**, 725 (1977).

Table 1. $\pi^+ p$ Coulomb corrections for the low energy s and p-waves

T_π	C_{0+}	C_{1-}	C_{1+}
5	0.081	0.003	-0.011
10	0.082	0.005	-0.023
20	0.085(93)	0.009(8)	-0.047(64)
40	0.096(95)	0.015(15)	-0.106(157)
60	0.108(95)	0.018(25)	-0.194(297)
80	0.118(97)	0.019(35)	-0.332(464)
100	0.126(101)	0.020(47)	-0.547(724)
$\Delta\delta^h_{l\pm}$	0.17	0.11	0.07

$\pi^- p$ Analyzing Powers From 50 to 140 MeV

J. Patterson
Nuclear Physics Laboratory, Deparment of Physics, University of Colorado, Boulder, Colorado USA 80309-0446

and

The CHAOS Collaboration
TRIUMF, 4004 Wesbrook Mall, Vancouver, B.C. Canada V6T 2A3

Abstract

The $\pi^- p$ elastic scattering analyzing powers were measured using the CHAOS spectrometer at energies below the $\Delta(1232)$ resonance. This work presents π^- data at pion kinetic energies down to 87 MeV. Remaining results are nearing completion.

INTRODUCTION

The primary goal of this experiment is to filter out, by using single energy partial wave analysis (PWA), differential cross section ($d\sigma/d\Omega$) measurements which are inconsistent with the A_y data. At present the low energy ($d\sigma/d\Omega$) data base contains a number of gross inconsistencies between experiments. After which, the new A_y data can be combined with the appropiate $d\sigma/d\Omega$ measurements to perfrom a complete partial wave analysis and extract low energy constants such as the chiral perturbation sigma term and the pion-nucleon coupling strength $f_{\pi NN}$. This type of experiment is not sensitive to many of the systematic normalization errors that occur in absolute differential cross section expriments and, since A_y is an interference between amplitudes, it is sensitive to smaller partial waves.

In order to determine the πN partial wave amplitudes with precision, reliable and precise $d\sigma/d\Omega$ data (which fix the larger amplitudes) must be combined with reliable and precise A_y data (which fix the smaller amplitudes). Analyzing power results in the forward angle (Coulomb-nuclear interference) region for $\pi^+ p$ scattering, and the S-P interference region at backward angles near 50 MeV for $\pi^- p$ scattering are especially useful in this regard. With accurate πN partial wave amplitudes, one can calculate improved values for the πN coupling constant, to extrapolate to threshold where the πN scattering lengths can be obtained, and to extrapolate below threshold as well to obtain a more acurate measure of the πN sigma term. The πN sigma term is an explicit measure of chiral symmetry breaking from which the strange sea quark content of the proton can be deduced.

This experiment was divided into two stages, the first stage being performed with pion beam energies spanning the $\Delta(1232)$ resonance, and the second with beam energies below the resonance, down to 50 MeV. Results of the resonance data were published by Hofman et al,[1], and those measurements utilized both a π^+ and a π^- beam. Unfortunatly, the beam time available to this experiment in the the fall of 1997, was insufficient to pursue the π^+ part of the low energy measurments, and hence only π^- data was taken. The rest of the database is dominated by the Sevior et al. resonance data[2].

As a result, in what turned out to be a very successful run, data were acquired for incident π^- at 51, 57, 67, 87, 98, 117, and 140 MeV. Graphite background data was also collected. The resulting data base span the S-P interference region which is 'centered' at 57 MeV, 180°. Most of the beam time was devoted to the 57 MeV measurement. There the backward angle cross sections are less than 1 μb/sr, more than 3 orders of magnitude less than the corresponding cross sections at 140 MeV. However, it has been shown that the greatest sensitivity to the scattering lengths is right at the S-P interference minimum, so enough time was spent collecting data in this most difficult region to obtain approximatly ± 0.08 uncertainty at the most backward angle, with uncertainties at almost all other angles (and energies) typically ± 0.02 or less.

The CHAOS spectrometer is ideal for analyzing power measurements, especially in coincidence mode. A sophisticated programmable trigger allows us to make vertex and kinematic cuts in hardware. The solid angle, about 10% of 4π is sufficient to investigate

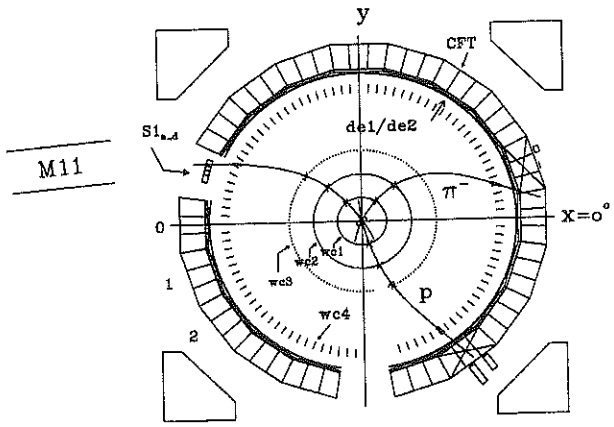

Figure. 1. Typical $\pi^- p$ coincidence event at 140 MeV. The pion beam eneters through S1 and is detected in WC1 and WC2. The rectangular bars behind the energy loss counters represent th amount of energy deposited in the DE1 and DE2 scintillators.

cross sections of the order of μb, and we take data in the full range of scattering angles. Without this feature, the experiment would not have been practical due to the extremely low cross sections involved and subsequent long running times associated with angle-by-angle measurements. Also the 360^o acceptance of CHAOS allowed a novel analysis technique that exploited the self-normalizing features of analyzing power measurements, thus avoiding the systematic errors normally associated with beam counting.

Experimental Technique

The Canadian High Acceptance Orbit Spectrometer (CHAOS)[3], which consists of tracking chambers and particle identification counters in a vertical magnetic field geometry, was used for all the measurements. A deidicated, spin polarized, butanol target was employed in frozen spin mode.

A schematic diagram of the spectrometer, showing a typical $\pi^- p$ coincidence event is shown in Figure 1. The incoming beam is fully reconstructed for every event using the beam momentum and the hits in the proportional chambers WC1 and WC2. The drift chamber WC3 and the vector chamber WC4 are usually deadened in the in and outgoing beam regions. Scintillator blocks DE_1 and DE_2 surrounding the WC4 chamber can be used for particle identification. Beam counting is primarily done using the segmented scintialltor S1, located approximatly 70 cm from the target.

For all incident beam energies, the experiment was run in coincidence mode, meaning that both the scattered pion, and the recoil proton was detected, thus suppressing all πn background reactions (polarized proton target consisted of butanol, C_4H_9OH), except for quasi-elastic scattering processes. Kinematic cuts applied to both the detected pion and recoil protons greatly suppress the quasi-elastic background. For the larger beam energies, the first level trigger (1LT) was set in 'doubles' mode, which means two (one for the pion, another for the proton) of the scintillating blocks surrounding WC4 had to fire. In order to obtain data in the smallest possible scattering angles at the lowest three energies, the 1LT was set in 'singles' mode, meaning any scattered pion could generate a 1LT. This would have led to an overwhelming background of πn scattering, were it not for innovative changes which were made to the second level trigger (2LT). The 2LT was programmed to reconize 'short tracks', i.e. protons which were observed in the correct angular region and with the expected curvature based exclusivley on information from only the inner two wire chambers. Events with (recoil) protons whose trajectories stopped outside of WC2 were not lost; if the protons failed to make it to WC3 their trajectories were determined by WC1/2. Events with protons which made it at least to WC2 were required in the (second level) trigger, which reduced trigger rates to managable levels without having to resort to a 'doubles' 1LT, which would have considerably abbreviated the measured angular distributions at the lowest energies.

The spin polarized target is a slab of butanol, cooled to around 60 mK and operated in frozen spin mode. Polarizations acheived were typically between $75-80\%$. The lengthy polarization procedure consisted of inserting the target in a 2.5 T superconducting solenoid, polarizing using micro-waves and then transfering the target to the CHAOS bore hole. During the transfer an internal magnetic coil provides the holding field but during data taking the CHAOS field (between .85 and 1.6 T depending on beam momentum) is used to maintain target polarization. Polarization decay times were always in excess of 400 hours. Target polarization was measured using standard NMR techniques with a copper coil embedded in the target. The NMR absorbtion signal from the thermal equilibrium polarization at B=2.5 T and T=60 mK is then compared to that obtained after dynamical polarization.

Analysis

The analyzing power can be expressed in terms of the following measurable quantities:

$$A_y = \frac{\frac{d\sigma^\uparrow}{d\Omega} - \frac{d\sigma^\downarrow}{d\Omega}}{P^\downarrow \frac{d\sigma^\uparrow}{d\Omega} + P^\uparrow \frac{d\sigma^\downarrow}{d\Omega}} = \frac{Y^\uparrow/N^\uparrow - Y^\downarrow/N^\downarrow}{P^\downarrow Y^\uparrow/N^\uparrow + P^\uparrow Y^\downarrow/N^\downarrow} \tag{1}$$

In this expression the usual cross section normalization quantities such as solid angle, number of target nuclei, pion decay fraction and detection efficiencies cancel out. This leaves the beam normalization ($N\uparrow\downarrow$), target polarization ($P\uparrow\downarrow$) and background as the only sensitive quantities.

The 360^o acceptance of CHAOS offers a rather unique and powerful way of avoiding systematic errors due to beam normilization. The rotational symmetry inherent to the scattering from a spin 1/2 particle polarized perpendicular to the scattering plane require that

$$A_y(\theta) = -A_y(-\theta) \tag{2}$$

Since CHAOS measures most angles in the 'left' hemisphere simultaneous with this in the 'right' hemisphere equation (1) can be used to introduce a relative normalization parameter ($\alpha = N^\uparrow/N^\downarrow$), which can be computed, thus elimating the need to count the beam, and eliminating the systematic errors typically associated with beam counting.

$$A_y = \frac{Y^\uparrow - \alpha Y^\downarrow}{P^\downarrow Y^\uparrow + \alpha P^\uparrow Y^\downarrow} \tag{3}$$

where α can be computed by minimizing χ^2.

$$\chi^2_\alpha = \sum_i^{n/2} \frac{(A_y(\theta_i) + A_y(-\theta_i))^2}{\delta A_y^2(\theta_i) + \delta A_y^2(-\theta_i)} or \chi^2_\alpha = \sum_i^n \frac{(A_y(\theta_i) - A_{PWA}(\theta_i))^2}{\delta A_y^2(\theta_i)} \tag{4}$$

where n is the total number of data points. The second expression, using some anti-symmetric function A_{PWA} (such as existing phase shift solution) is more convenient. It is important to note that, when the average of the analysing powers at θ and $-\theta$ is calculated, there is *no* dependance on α if the statisical error of the data at the two complementary angles are equal. It should also be noted that the value of α is independant of the anit-symmetric function used to calculate it. Several drastically different functions have been used, *all* giving the same value of α within statical error bars ($\approx 1/2\%$). Thus, α need only be calculated approximately. The error in it's determination is included in the overall statisitcal error of the final data.

Results

The analysis is nearing completion, and the final results are expected to be available within the first few months of the year 2000. In Figure 2, we show results at 139 MeV and 87 MeV. As one can see, for 139 MeV, the SM95 solution (solid) follows the data much more

closely than the KH80 predictions (dashed). At 87 MeV, the SM95 and KH80 solutions are in closer aggrement with each other, but a look at the χ^2/DOF ($\chi^2_{SM95}/DOF = .93$ and $\chi^2_{KH80}/DOF = 2.1$) shows the SM95 does indeed follow the data more acurately than KH80.

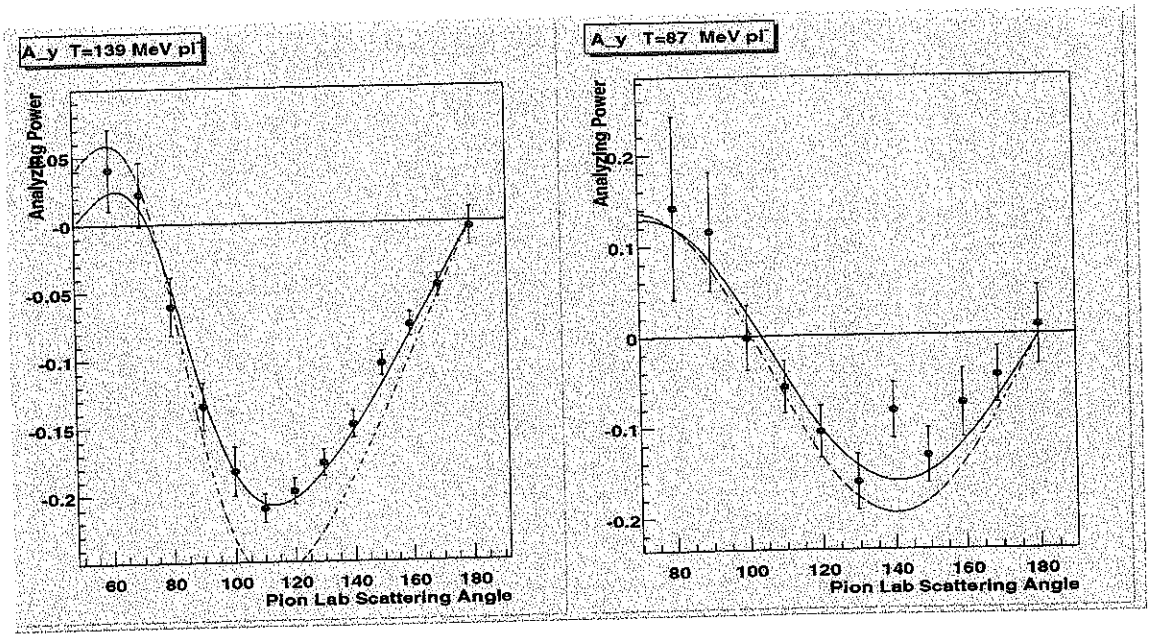

Fig. 2. The new analyzing powers at 139 MeV and 87 MeV π^-. The solid line is the prediction from the SM95 solution, dashed the KH80 solution. Horizontal axis represents the lab scattering angles. Error bars are statistical only.

REFERENCES

1. G.J. Hofman et al., "Analyzing powers for $\pi^{\pm}p$ elastic scattering between 87 and 263 MeV", Phys. Rev. **C 58**(6), 3484 (1998).
2. M.E. Sevior et al., "Analyzing powers in $\pi^{\pm}p$ elastic scattering from $T_\pi = 98$ to 263 MeV", Phys. Rev. **C 40**(6) 2780 (1989)
3. G.R. Smith et al., "The CHAOS spectrometer for pion physics at TRIUMF", Nucl. Instr. Meth. **A 362** 349-360 (1995).

Recent Results from the GW (formally VPI) Data Analysis Center

R.A. Arndt, W.J. Briscoe, I.I. Strakovsky, and R.L. Workman
Center for Nuclear Studies
and
Department of Physics
The George Washington University Virginia Campus
20101 Academic Way, Ashburn, VA 20147, USA

Abstract

We report progress made in our analyses of pion photo- and electro-production, πN and NN elastic scattering, and eta and kaon photoproduction. Electroproduction and the latter two reactions are new additions to the SAID database.

Introduction

The George Washington University Data Analysis Center(formally the Virginia Tech group) has analyzed and maintained databases for a large number of fundamental scattering reactions. We have most recently added kaon and eta photoproduction databases and solutions to the telnet and internet sites. A database for pion electroproduction has also been compiled and preliminary analyses are underway. Because this activity has recently been transferred from Virginia Tech to the Data Analysis Center at The George Washington University, users should expect some new telnet/internet sites[1] to appear, with others disappearing.

In the following, we will mainly concentrate on new results for NN elastic scattering and the electromagnetic reactions. A detailed account of the πN work is being given by a collaborator[2] (Marcello Pavan) in a separate contribution[3] to these proceedings.

Database Changes

Nucleon-Nucleon Scattering

In our last published analysis[4] of NN elastic scattering data, the pp energy range was extended from 1.6 GeV to 2.5 GeV, in T_{Lab}, based mainly on differential cross section measurements from the EDDA collaboration at COSY[5]. Since then our NN database has increased from 27848 (16994 pp and 10854 np) to 31290 (19897 pp and 11393 np) points, most of these being polarization observables measured at SATURN II[6].

Pion-Nucleon Scattering

Data at energies spanning the Delta resonance (80 – 270 MeV) have mainly come from TRIUMF, which has produced analyzing-power data[7]. Very low-energy CXS differential cross sections have been measured at LAMPF[8]. The overall database has increased from 21793 to 22219 points, since our last publication[9].

Pion-Photoproduction

Many of the more recent datasets have been measured at Mainz, below 800 MeV. Preliminary data for the observable Σ have been received from Yerevan and GRAAL, and the first differential cross sections from JLab are now being analyzed. These sets should soon be available for at least preliminary fits. At present, our 'quotable' database has increased from 15563 to 16729 points[10].

Kaon- and Eta-Photoproduction

The kaon- and eta-photoproduction databases have been assembled within the past year. Many more datasets are anticipated from JLab, GRAAL, Mainz, and Bonn in the near future. At present, the kaon (eta)-photoproduction databases contain a sparse 453 (985) points below 2 GeV.

Pion-Electroproduction

This database was also compiled since MENU 97, and continues to be updated as new measurements become available from JLab, Bates, Mainz, and AMPS. The present database contains 22019 points (14341 $\pi^0 p$, 6788 $\pi^+ n$, and 890 $\pi^- p$). About 50% of these have come from DNPL.

Other Reactions

The $\pi^+ d \to pp$ database has increased from 4462 to 4865 points, since our last publication[11], this increase due mainly to IUCF, COSY, and TRIUMF measurements at low energies[12], The πd elastic database has increased slightly with the addition of recent PSI transfer polarization measurements[13].

New Analyses

Nucleon-Nucleon Scattering

We have updated the NN analysis, including the recent SATURN polarization data. Changes to the partial-wave amplitudes were not large. We are now comparing our results with the amplitude-reconstruction results of the Saclay group[14]. New cross section, A_{Y0}, A_{YY}, A_{ZZ}, and A_{ZX} data to 2.5 GeV are expected from COSY, and such measurements (if reasonably precise) could have a significant impact on our partial-wave solutions. Further np polarized quantities, near 200 MeV, are expected from IUCF.

As mentioned in Ref.[4], the extension to 2.5 GeV is interesting as it appears to bridge the gap between the low and high energy regions. At the upper limit of our analysis, a plot of $d\sigma/dt$ versus s appears to join smoothly with the s^{-10} behavior expected from dimensional counting at high energy and fixed c.m. angle.

Pion-Photoproduction

Much of our recent work has concentrated on the first resonance region and problems associated with the E2 and M1 multipole extraction. Issues associated with the data and their influence on these quantities are now fairly well understood. Theoretical problems associated with the resonance-background separation still persist within the community, and are under investigation. Analysis of the preliminary GRAAL, Yerevan, and JLab data presents a greater challenge, as the theoretical problems associated with the second and third resonance regions have received far less attention.

Eta- and Kaon-photoproduction

We expect to soon have much more data in these reactions. At present, there are insufficient data to justify a full multipole analysis similar to that carried out for pion-photoproduction. For eta-photoproduction, we have encoded the Mainz multipole fit[15] to the available cross section, Σ, and T data near threshold. For kaon-photoproduction, we have encoded a simple pole-model fit similar to those of Adelseck, Bennhold and Wright[16]. A second set of fits which simply 'scaled' the photoproduction result, with appropriate kinematics, was also attempted. More sophisticated fits will be attempted once there are sufficient data.

Pion-Electroproduction

Trial fits using a model similar to that used in pion photoproduction, and consistency tests utilizing the recent Mainz fits[17], have been performed thus far. The current data base is dominated by $\pi^0 p$ production experiments, making model-independent isospin decomposition problematic. Given the additional amplitudes and kinematic variables, this database also appears 'sparse' in comparison with pion-photoproduction.

Acknowledgments

This work was supported in part by the U. S. Department of Energy Grant DE–FG02–99ER41110. R.W. and I.S. gratefully acknowledge a contract from Jefferson Lab under which this work was done. The Thomas Jefferson National Accelerator Facility (Jefferson Lab) is operated by the Southeastern Universities Research Association (SURA) under DOE contract DE-AC05-85-84ER40150.

REFERENCES

1. Increased safeguards at many sites have caused problems for users of our telnet facility. In many cases, these can be circumvented by using: ssh -l said said.phys.vt.edu
2. A number of collaborators have also been involved in our analyses. They include: M.M. Pavan (πN), M.W. McNaughton and F. Dohrmann (NN), D.V. Bugg ($\pi d \to pp$), A.M. Green and S. Wycech ($\pi N \to \eta N$), R. Davidson and N.C. Mukhopadhyay ($\gamma N \to \pi N$).
3. M. M. Pavan is scheduled to give an account of our πN analyses, as they pertain to the πNN coupling and σ-term.
4. R. A. Arndt, C. H. Oh, I. I. Strakovsky, R. L. Workman, and F. Dohrmann, Phys. Rev. C **56**, 3005 (1997).
5. D. Albers *et al.*, Phys. Rev. Lett. **78**, 1652 (1997).
6. A compilation of recent SATURNE II measurements is given in: D. Adams *et al.* , "REVIEW OF DATA MEASURED IN THE NUCLEON-NUCLEON PROGRAM AT SATURNE II: np ELASTIC AND QUASIELASTIC SCATTERING BELOW 1.15 GeV", Acta Polytechnica (Prague) **36**, 11 (1996); Recent pp measurements from SATURNE II are compiled in, J. Ball *et al.* , "PROTON-PROTON DATA MEASURED AT SATURNE II", Acta Polytechnica (Prague), to be published.
7. G. J. Hofman *et al.*, Phys. Rev. C **58**, 3484 (1998).
8. L. D. Isenhower *et al.*, these Proceedings.
9. R. A. Arndt, I. I. Strakovsky, R. L. Workman, and M. M. Pavan, Phys. Rev. C **52**, 2120 (1995).
10. R. A. Arndt, I. I. Strakovsky, and R. L. Workman, Phys. Rev. C **56**, 577 (1997).
11. C. H. Oh, R. A. Arndt, I. I. Strakovsky, and R. L. Workman, Phys. Rev. C **56** 635 (1997).
12. P. Heimberg *et al.*, Phys. Rev. Lett. **77**, 1012 (1996), M. Drochner *et al.*, Nucl. Phys. **A643**, 55 (1998), R. G. Pleydon *et al.*, Phys. Rev. C **59**, 3208 (1999).
13. G. Suft *et al.*, Phys. Lett. **B425**, 19 (1998).
14. J. Ball *et al.*, Eur. Phys. J. C **5**, 57 (1998); J. Bystricky, C. Lechanoine-LeLuc, and F. Lehar, Eur. Phys. J. C **4**, 607 (1998).
15. L. Tiator, D. Drechsel, G. Knochlein, and C. Bennhold, Mainz preprint MKPH-T-99-03.
16. R. A. Adelseck, C. Bennhold, and L. E. Wright, Phys. Rev. C **32**, 1681 (1985).
17. D. Drechsel, O. Hanstein, S. S. Kamalov, and L. Tiator, Nucl. Phys. **A645**, 145 (1999).

Finite Contour Dispersion Relations and the Subthreshold Expansion Coefficients of the πN Invariant Amplitudes

G.C. Oades
Institute of Physics and Astronomy, Aarhus University, DK-8000 Aarhus C, Denmark

Abstract

Finite contour dispersion relations are used to calculate the subthreshold expansion coefficients of the πN invariant amplitudes

In[1] finite contour dispersion relations were used to determine the expansion coefficients of the πN invariant amplitudes about the subthreshold point $\nu = 0$, $t = 0$ using the phase shift data available at that time. The method has the advantage of being independent of any model of high energy behaviour and does not require any knowledge of subtraction constants. In our present day situation it enables us to use any set of phase shift data and easily make an extrapolation to $\nu = 0$, $t = 0$ so as to obtain the subthreshold expansion coefficients which can then be used to determine the χPT LEC's or alternatively compared with values obtained by using χPT to extrapolate from the threshold scattering lengths.

For a general crossing symmetric invariant amplitude, a finite contour fixed-t dispersion relation subtracted at $\nu = 0$ can be written in the form

$$Re\overline{X}(\nu,t) = \nu^2 \frac{P}{\pi} \int_{\nu_{th}}^{\nu_1} \frac{Im\overline{X}(\nu',t)}{\nu'^2\left(\nu'^2 - \nu^2\right)} d\nu'^2 + \overline{X}_{FC}(\nu^2,t) \tag{1}$$

where $\overline{X}$ is the Born stripped amplitude obtained by subtracting off the pseudovector nucleon Born term

$$\overline{X}(\nu,t) = X(\nu,t) - X_{pv}(\nu,t) \tag{2}$$

and where X is one of the amplitudes $A^{(+)}, A^{(-)}/\nu, B^{(+)}/\nu, B^{(-)}, D^{(+)}, D^{(-)}/\nu$. The term $\overline{X}_{FC}(\nu^2.t)$ represents the contribution of the finite contour in the complex-ν plane from $\nu = \nu_1$ to $\nu = -\nu_1$ used to close the contour integration. Because of the crossing symmetry it is an even function of ν and so can be expanded about $\nu = 0$ as a power series in ν^2.

If phase shifts are available from threshold up to $\nu = \nu_1$ then $Im\overline{X}(\nu',t)$ can be reconstructed using convergent partial wave series provided t is not too negative ($t \geq -26m_\pi^2$). In the case of $Re\overline{X}(\nu,t)$ the scattering angle is physical for $\nu_L \leq \nu$ where

$$\nu_L = \frac{\sqrt{(4m^2 - t)(4M^2 - t)}}{4M} \tag{3}$$

We see that ν_L coincides with ν_{th} for $t = 0$ but that it moves above ν_{th} for more negative values of t. In the region where the scattering angle is physical $Re\overline{X}(\nu,t)$ can also be constructed from convergent partial wave series and so we can calculate $\overline{X}_{FC}$ from the expression

$$\overline{X}_{FC}(\nu^2,t) = Re\overline{X}(\nu,t) - \nu^2 \frac{P}{\pi} \int_{\nu_{th}}^{\nu_1} \frac{Im\overline{X}(\nu',t)}{\nu'^2\left(\nu'^2 - \nu^2\right)} d\nu'^2 \tag{4}$$

In this way we obtain values of $\overline{X}_{FC}$ for values of ν in the range $\nu_L \leq \nu \leq \nu_U$ where we choose ν_U to lie some way below ν_1. These values are then fitted by a polynomial in ν^2; in practice, if ν_U is chosen to correspond to $p_{lab} = 750MeV/c$, then the values are well fitted by a quadratic in ν^2

$$\overline{X}_{FC}(\nu,t) = z_0(t) + z_1(t)\nu^2 + z_2(t)\nu^4 \tag{5}$$

Making a similar expansion for $\overline{X}(\nu,t)$

$$\overline{X}(\nu,t) = x_0(t) + x_1(t)\nu^2 + x_2(t)\nu^4 \tag{6}$$

we then obtain

$$x_0(t) = z_0(t) \tag{7}$$

$$x_1(t) = z_1(t) + \frac{P}{\pi}\int_{\nu_{th}}^{\nu_1} \frac{Im\overline{X}(\nu',t)}{\nu'^4} d\nu'^2 \tag{8}$$

$$x_2(t) = z_2(t) + \frac{P}{\pi}\int_{\nu_{th}}^{\nu_1} \frac{Im\overline{X}(\nu',t)}{\nu'^6} d\nu'^2 \tag{9}$$

This is repeated for a range of negative t-values and the x_n's are then in turn fitted by a quadratic in t

$$x_0(t) = x_{00} + x_{01}t + x_{02}t^2 \tag{10}$$

$$x_1(t) = x_{10} + x_{11}t + x_{12}t^2 \tag{11}$$

$$x_2(t) = x_{20} + x_{21}t + x_{22}t^2 \tag{12}$$

thus giving the final expansion coefficients of the Born stripped amplitude about $\nu = 0, t = 0$.

These calculations were made for the phase shift sets, KH80[2], SM95[3], SP98[4] and SM99[5]. In the case of KH80 the value 14.28 was used for $\frac{G^2}{4\pi}$[6] while in the other cases the value 13.76[7] was used. Tables 1,2 and 3 give the expansion coefficients for the amplitudes $A^{(+)}, A^{(-)}/\nu, B^{(+)}/\nu, B^{(-)}, D^{(+)}, D^{(-)}/\nu$ calculated from these different sets of input phases. It will be seen that the values are rather stable against changes in the phase shifts. For comparison values calculated by J. Stakov using another method[8] are given for the phase shift set SP98; the agreement with the finite contour values is in general very good. Various heavy baryon chiral perturbation theory predictions of Meissner et al.[9] are also shown. Again there is rather good agreement which is very interesting since no explicit account of the Δ degrees of freedom has been taken into account in their work.

REFERENCES

1. H. Nielsen and G.C. Oades, "Low Energy πN Partial Waves, Expansions of the πN Invariant Amplitudes About $\nu = 0, t = 0$ and the Value of the Current Algebra σ Term ," Nucl. Phys. **B72**, 310 (1974).
2. G. Höhler, F. Kaiser, R. Koch and E. Pietarinen in *Handbook of Pion-Nucleon Scattering*, Physics Data 12-1979 (Fachinformationszentrum, Karlsruhe, 1979).
3. R.A. Arndt, I.I. Strakovsky, R.L. Workman and M.M. Pavan, "Updated analysis of πN elastic scattering data to 2.1 GeV: The baryon spectrum," Phys. Rev. **C52**, 2120 (1995).
4. R.A. Arndt, I.I. Strakovsky, R.L. Workman and M.M. Pavan, Los Alamos preprint nucl-th/980787.
5. I thank Prof. R.A. Arndt for providing details of this preliminary phase shift solution. See the SAID data base.
6. R. Koch and E. Pietarinen, "Low-Energy πN Partial wave Analysis," Nucl. Phys. **A336**, 331 (1980).
7. see ref.[4]
8. J. Stakhov, work based on SP98 presented at this symposium.
9. See V. Bernard, N. Kaiser and U-G. Meissner, "Pion-nucleon scattering in chiral perturbation theory (I): Isospin- symmetric case," Nucl. Phys. **A640**, 199 (1998), N. Fettes, U-G. Meissner and S. Steininger, hep-ph/9803266v2 and P. Büttiker and U-G. Meissner, hep-ph/9908247 presented at this symposium.

Table 1. Expansion coefficients for the A invariant amplitudes

$\overline{A}^+$	KH80	SM95	SP98	SM99	Stahov	HBChPT
a^+_{00}	-1.44±0.19	-1.32±0.11	-1.38±0.11	-1.43±0.11	-1.30±0.01	-1.32
a^+_{01}	0.84±0.26	1.02±0.19	0.99±0.19	1.00±0.19	1.17±0.02	0.97
a^+_{02}	-0.10±0.06	-0.01±0.08	-0.02±0.05	-0.02±0.05	0.02±0.01	
a^+_{10}	4.84±0.20	4.54±0.08	4.58±0.08	4.59±0.08	4.57±0.03	4.49
a^+_{11}	0.02±0.22	0.02±0.10	0.03±0.10	0.04±0.10	0.03±0.01	0.07
a^+_{20}	1.20±0.05	1.16±0.02	1.16±0.02	1.15±0.02	1.20±0.20	
$\frac{\overline{A}^-}{\nu}$						
a^-_{00}	-9.26±0.17	-8.80±0.07	-8.92±0.07	-9.06±0.07	-8.97±0.01	-8.73
a^-_{01}	-0.44±0.21	-0.30±0.09	-0.38±0.09	-0.44±0.09	-0.38±0.01	-0.43
a^-_{02}	0.00±0.05	0.00±0.02	-0.01±0.02	-0.02±0.02	-0.01±0.01	
a^-_{10}	-1.09±0.06	-1.23±0.02	-1.20±0.02	-1.18±0.02	-1.18±0.01	-1.43
a^-_{11}	0.05±0.07	0.00±0.03	0.02±0.03	0.02±0.03	-0.01±0.01	0.0
a^-_{20}	-0.32±0.01	-0.31±0.01	-0.31±0.01	-0.31±0.01	-0.37±0.06	

Table 2. Expansion coefficients for the B invariant amplitudes

$\frac{\overline{B}^+}{\nu}$	KH80	SM95	SP98	SM99	Stahov	HBChPT
b^+_{00}	-3.56±0.10	-3.44±0.04	-3.42±0.04	-3.37±0.04	-3.48±0.02	
b^+_{01}	0.28±0.14	0.22±0.05	0.25±0.05	0.26±0.05	0.19±0.01	0.0
b^+_{02}	0.03±0.04	-0.00±0.01	0.00±0.01	0.01±0.01	-0.01±0.01	0.0
b^+_{10}	-1.04±0.05	-0.96±0.02	-0.96±0.02	-0.97±0.02	-0.96±0.02	0.18
b^+_{11}	0.06±0.06	0.08±0.02	0.08±0.02	0.07±0.02	0.10±0.01	0.0
b^+_{20}	0.31±0.01	-0.30±0.01	-0.30±0.01	-0.30±0.01	-0.31±0.02	0.05
B^-						
b^-_{00}	10.84±0.18	10.26±0.08	10.37±0.08	10.48±0.08	10.45±0.01	9.99
b^-_{01}	0.26±0.22	0.18±0.09	0.26±0.10	0.30±0.10	0.24±0.01	0.20
b^-_{02}	0.00±0.05	0.01±0.02	0.02±0.02	0.03±0.02	0.01±0.01	0.01
b^-_{10}	0.89±0.05	1.07±0.02	1.04±0.02	1.02±0.02	1.01±0.01	1.06
b^-_{11}	-0.10±0.06	-0.04±0.02	-0.06±0.02	-0.06±0.02	-0.03±0.01	0.0
b^-_{20}	0.30±0.01	0.27±0.01	0.27±0.01	0.27±0.01	0.33±0.05	0.18

Table 3. Expansion coefficients for the D invariant amplitudes

$\overline{D}^+$	KH80	SM95	SP98	SM99	Stahov	HBChPT
d^+_{00}	-1.46±0.04	-1.34±0.02	-1.30±0.02	-1.26±0.02	-1.30±0.01	
d^+_{01}	0.99±0.06	1.04±0.02	1.07±0.02	1.08±0.02	1.17±0.02	1.45
d^+_{02}	0.01±0.02	0.02±0.01	0.03±0.01	0.02±0.01	0.02±0.01	0.036
d^+_{10}	1.13±0.04	1.11±0.02	1.11±0.02	1.11±0.02	1.13±0.01	1.19
d^+_{11}	0.14±0.04	0.16±0.02	0.16±0.02	0.16±0.02	0.21±0.01	0.08
d^+_{20}	0.20±0.01	0.20±0.01	0.20±0.01	0.20±0.01	0.23±0.02	0.235
$\frac{D^-}{\nu}$						
d^-_{00}	1.55±0.02	1.45±0.01	1.46±0.01	1.43±0.01	1.47±0.01	1.80
d^-_{01}	-0.07±0.03	-0.08±0.01	-0.06±0.01	-0.08±0.01	-0.14±0.01	-0.29
d^-_{02}	0.01±0.01	0.01±0.01	0.01±0.01	0.01±0.01	0.01±0.01	0.004
d^-_{10}	-0.19±0.01	-0.16±0.01	-0.16±0.01	-0.16±0.01	-0.17±0.01	-0.63
d^-_{11}	-0.05±0.01	-0.03±0.01	-0.04±0.01	-0.04±0.01	-0.04±0.01	0.007
d^-_{20}	-0.04±0.01	-0.04±0.01	-0.04±0.01	-0.04±0.01	-0.04±0.01	0.032

Meson Production Close to Threshold

H. Machner and J. Haidenbauer
Institut für Kernphysik, Forschungszentrum Jülich, D-52525 Jülich, Germany

Abstract

A short overview of experimental results on meson production close to threshold is given with emphasis on the recent data from small emittance beams available at accelerators/storage rings at IUCF Bloomington, CELSIUS Uppsala and COSY Jülich.

INTRODUCTION

The advent of strongly focusing synchrotrons such as the IUCF COOLER in Bloomington, CELSIUS in Uppsala and COSY in Jülich marks a new aera in the study of meson production in the threshold region. Due to their high quality beams experiments could be performed with unprecedented precision and at energies being just a few MeV above the threshold. Indeed a remarkable wealth of data has emerged from the experiments at those sites over the past 10 years or so. In the following we will concentrate only on hadron induced reactions and ignore photon and electron induced reactions although also for these reactions beautiful new data have recently been published. In other words we will concentrate on strong interactions and we will restrict the discussion to only pseudoscalar mesons. First, the vector mesons have much larger widths compared to the pseudoscalar mesons. This makes their detection difficult on top of a large physical background of multi-pion production events. Secondly, there seems to be a general trend that the larger the mass the smaller the cross section, so that the generally heavier vector mesons have small production cross sections, making them much harder to investigate than the lighter mesons. In Fig. 1 we give an overview of total cross sections in pp interactions below 4 GeV beam momentum.

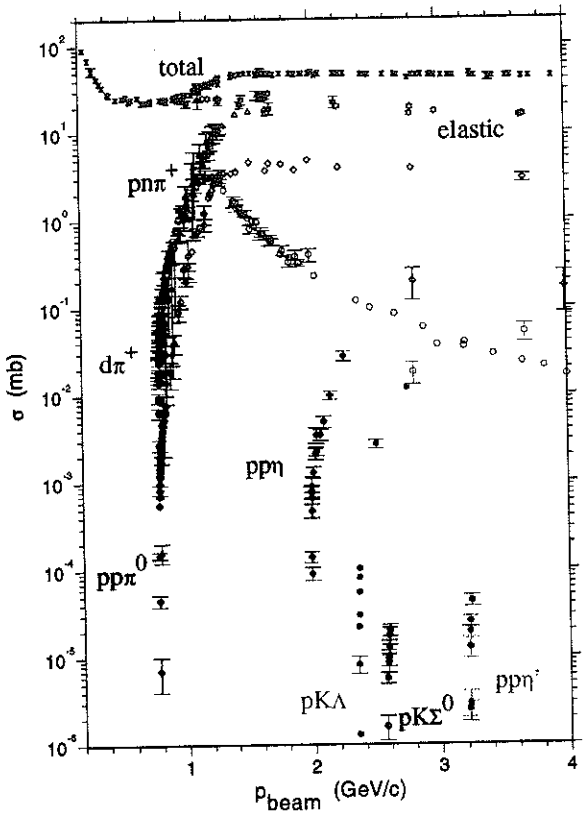

Figure 1. Cross sections for pp interactions as function of the beam momentum. Shown are total and elastic scattering cross sections and the cross sections for light meson production. Open symbols indicate older measurements.

Open symbols denote older data taken from compilations[1,2] and references given in[3]. The full and crossed symbols denote the new data (cf. Ref.[4] for references). The largest cross section is of course the total cross section. Around 800 MeV/c the elastic cross section begins to be smaller than the total cross section because the pion threshold has opened there. The strongest pion-production channel in the threshold region is the $pp \to \pi^+ d$ reaction which accounts for most of the inelasticity in that momentum range. At larger momenta it is the $pp \to pn\pi^+$ reaction which exhausts almost all inelastic cross section. The next threshold that opens is the $pp \to pp\eta$ reaction (multi–pion production is not included in the Figure). It is interesting to note that cross sections have been measured down to 10^{-7} mb which is a fraction of 5×10^{-9} of the total cross section. Later we will show the cross sections again on different scales in order to make different physical effects visible.

PION PRODUCTION

The first threshold which opens in nucleon-nucleon (NN) scattering with increasing beam energy is π^0-production followed very soon by π^+-production. Pion production exhausts all inelasticity in this momentum range (see Fig. 1) and is therefore fundamental for understanding the nucleon–nucleon interaction.

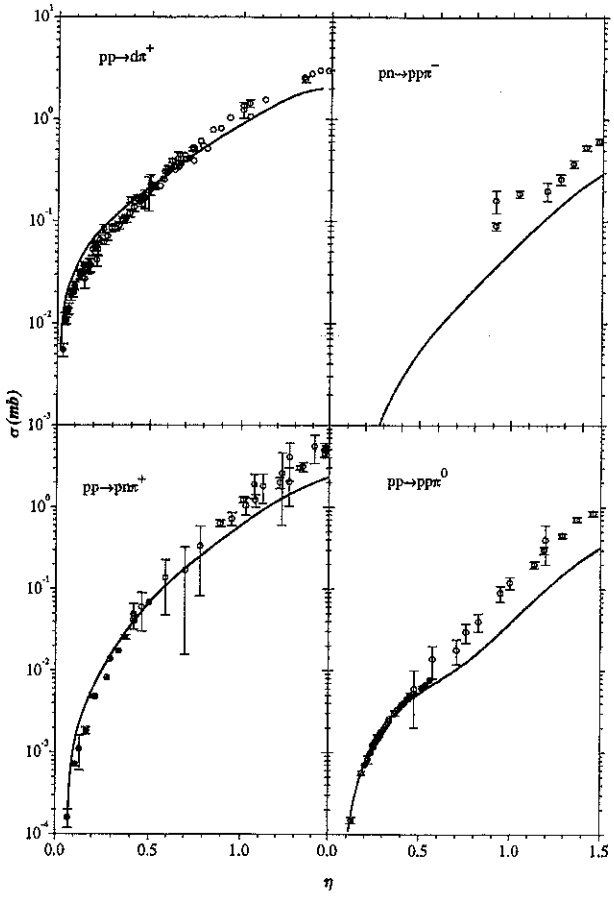

Figure 2. Total cross sections for the $NN \to NN\pi$ in the different charge channels. The meaning of the data symbols is as in previous figures. The data for the reaction $np \to pp\pi^-$ are taken from the compilation in Ref.[7]. The solid curves show the results of the Jülich model[8].

Indeed, the reaction $pp \to pp\pi^0$ was also the first one to be studied with the new facilities[5,6]. The total cross section is presented in Fig. 2 as function of η, i. e. the pion center of mass momentum divided by the pion mass. The new data from IUCF and Uppsala[5,6,9] are shown as solid circles, earlier data from Refs.[1,2] as open circles. The quality of the new data becomes clear when inspecting the error bars which are for the new data usually smaller than the dots. Before the advent of these data, no data below

Table 1. Normalization constant for different reactions (Eq. 1)

reaction	c (mb)
$pp \to pn\pi^+$	0.7
$pp \to pp\pi^0$	0.1
$pp \to pp\eta$	0.2
$pp \to pp\eta'$	0.04
$pp \to p\Lambda K^+$	0.04
$pp \to p\Sigma^0 K^+$	0.003

820 MeV/c existed.

The differential cross sections are found to be in agreement with the assumption of isotropic pion emission[6].

The new data for the reaction $pp \to pp\pi^0$ close to threshold raised a lot of theoretical questions, because the cross sections were much larger than theoretical predictions. New reaction mechanisms seemed to be necessary in order to reproduce the data (cf., e.g. the discussion in Sect. 4.2. in Ref.[4]). On the experimental side it stimulated further research, namely to search in other pion production channels whether these new reaction mechanisms also contribute there. The next reaction of interest is then the $pp \to d\pi^+$ reaction. This is the pion production which - together with its time–reversed reaction - has been studied most intensively. Surprisingly, close to threshold no data existed before the advent of the new accelerators. Total cross sections for the $pp \to d\pi^+$ reaction are also shown in Fig. 2. The new data from COSY and IUCF[10,12] define the sharp rise of the cross sections from the threshold on.

In contrast to the $pp \to pp\pi^0$ reaction, the angular distributions are not isotropic close to threshold[11].

The third pion production reaction is the $pp \to pn\pi^+$ reaction. Its excitation curve as function of the beam momentum close to the threshold is shown in Fig. 2. Again the quality of the new data is impressive when the error bars are compared with the older data. The excitation curve seems to rise less steeply from threshold on than the $pp \to d\pi^+$ reaction. Only for the reaction $pn \to 2p\pi^-$ new data were not available to us but are in these proceedings[13].

COMPARISON OF DIFFERENT MESON PRODUCTION REACTIONS

It is interesting to compare the data on various meson-production reactions close to threshold for a common kinematical variable, namely as a function of the dimensionless cm momentum of the meson, $\eta = p^*_m/m_m$, where p^*_m is the maximum possible meson momentum. Then it becomes evident that all the reactions with three particles in the final state can be reproduced by just a simple power law

$$\sigma(\eta) = c\eta^p. \tag{1}$$

This is demonstrated in Fig. 3 where the data are compared with Eq. 1 using $p = 3.2$ and the normalization constants given in Table 1.

Surprisingly, the η' production and the associated strangeness production have the same cross section on this η scale. Even more surprising is the large constant for η production when compared to π^0 production. When we compare the following pairs of reactions, $pn\pi^+$ and $pp\pi^0$, $pp\eta$ and $pp\eta'$, $p\Lambda K^+$ and $p\Sigma^0 K^+$, we see that in each case the cross section of the first reaction is always much larger than for the second. It is certainly not accidental that for each case it is always the first reaction which can proceed through an intermediate resonance (Δ, $N^*(1535)$ and $N^*(1650)$).

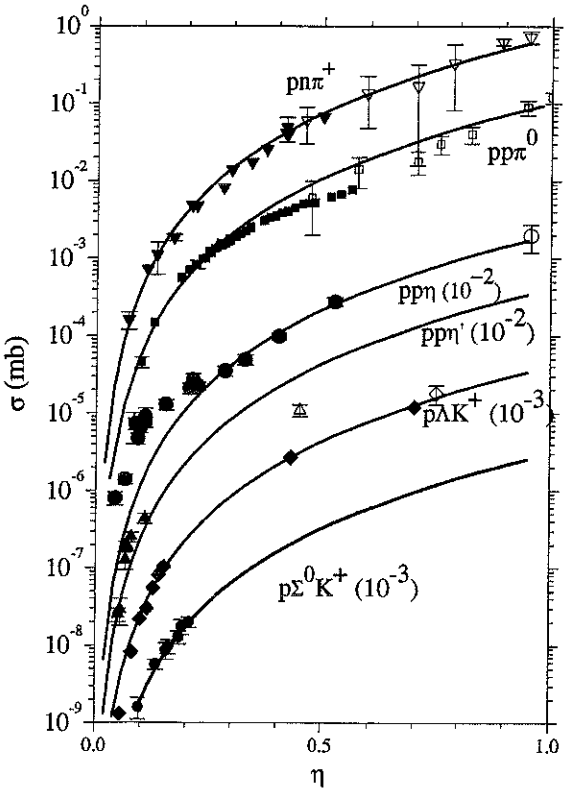

Figure 3. Cross sections for various $pp \to BBm$ reactions with B and m indicating baryons and mesons, respectively are compared with Eq. 1 employing the same exponent $p = 3.2$. The data and the curves have been multiplied by the indicated factors.

Among the reactions considered only the η production data show a significant deviation from the simple power law close to threshold. As a first guess, this enhancement of the cross section may be attributed to the $S_{11}(1535)$ resonance excitation. However, then a similar phenomenon should be also visible in the strangeness channel as was argued earlier. Thus, more probably the observed enhancement close to threshold is a hint for a strong ηN FSI. The common exponent may have its main origin in the common phase space of the three body final state with almost similar FSI between the baryons. The exact values of the constants c depend, of course, on the η interval where the curves were matched to the data. Thus, we want to stress that the values given in Table 1 are not obtained by a χ^2 fit, but by matching the curves to the data "guided by the eye". The numbers are only meant to give an impression on an order-of-magnitude level.

REFERENCES

1. V. Flamino et al., *Compilation of Cross-Sections III: p and $\bar{p}$ Induced Reactions*, CERN-HERA Report 84-1, 1984.
2. A. Baldini, et al., *Landolt–Börnstein New Series I/12b* (Springer Verlag, Heidelberg, 1988).
3. H. Machner, Nucl. Phys. **A 633**, 341 (1998).
4. H. Machner and J. Haidenbauer, J. Phys. **G 25**, R231 (1999).
5. H.O. Meyer et al., Phys. Rev. Lett. **65**, 2846 (1990).
6. H.O. Meyer et al., Nucl. Phys. **A 539**, 633 (1992).
7. Bachman M G et al., Phys. Rev. **C 52**, 495 (1995).
8. Hanhart C et al., Phys. Lett. **B 444**, 25 (1998).
9. A. Bondar et al., Phys. Lett. **B 356**, 8 (1995).
10. M. Drochner et al., Phys. Rev. Lett. **77**, 454 (1996).
11. M. Drochner et al., Nucl. Phys. **A643**, 55 (1998).
12. P. Heimberg et al., Phys. Rev. Lett. **77**, 1012 (1996).
13. T. Johanson, contribution to these proceedings.

The ABC Effect, the $dd \to \alpha X$ Reaction and Charge Symmetry Breaking

A. Gårdestig*
Nuclear Physics Division, Uppsala University, Box 535, S-751 21 Uppsala, Sweden

Abstract

Two-pion production in the $dd \to \alpha X$ reaction is described as two almost independent $NN \to d\pi$ processes, where the two final deuterons fuse to form the α particle. With phenomenological amplitudes as input, the model reproduces all observed features, including the remarkable peak structure in momentum distributions (the ABC effect) and the strongly oscillating deuteron analyzing powers. Be exchanging $NN \to d\pi$ for $np \to d\pi\pi$ the same mechanism explains most of the high energy continuum as due to $dd \to \alpha 4\pi$. With a similar extension the $\gamma\gamma$ production is shown to be very important as background to the charge-symmetry-breaking $dd \to \alpha\pi^0$ reaction.

INTRODUCTION

Consider a general reaction $ab \to AX$, giving several particles in the final state. If we are only able to detect one of them (A) it is still possible to extract information about the undetected particles (X). A common way to do so is to measure and plot laboratory frame momentum distributions. Due to kinematics, the invariant mass of the undetected particles (the missing mass, M_X) is small at the edges of the spectrum and reaches its maximal value in the central region. If the data reveal some kind of structure, i.e., significant deviations from pure phase space behavior, this indicates that something peculiar and interesting is going on.

More physics, when needed, could be obtained from spin measurements. With a polarized deuteron beam or target we obtain the analyzing powers

$$A_y = \frac{\sigma(+) - \sigma(-)}{\sigma(+) + \sigma(-) + \sigma(0)} \text{ and } A_{yy} = \frac{\sigma(+) + \sigma(-) - 2\sigma(0)}{\sigma(+) + \sigma(-) + \sigma(0)},$$

where $(+ - 0)$ are the deuteron transverse spin projections. Measurements of these provide sensitive tests of the interferences between amplitudes.

A striking example of the usefulness of these techniques is the spectacular ABC effect, observed in the $np \to dX$[1], $pd \to {}^3\mathrm{He}X$[2], and $dd \to \alpha X$[3,4] reactions. It is only seen in isospin $I_X = 0$ channels and the features are: sharp peaks slightly above the two-pion threshold and a broad bump at maximal M_X. The phenomenon cannot be a new resonance or particle since the peak positions and widths vary with experimental conditions, and it cannot be due to a strong s-wave $\pi\pi$ interaction since that is contradicted by other experiments and theory. Hence the other particles have to be included in any description and we should look for the solution in the pion production mechanism. Before explaining how this was solved for the $dd \to \alpha X$ reaction, just a few remarks about earlier attempts.

The theoretical interest has mainly focused on the $np \to dX$ reaction because it seemed to be the simplest. Among the various proposals made, the most promising model is the $\Delta\Delta$ model[5]. Although it does a good job at 0° it fails at larger angles. Other models have similar problems. For $pd \to {}^3\mathrm{He}X$ there is only one model, namely the two-step process of[6], but once again the angular distribution is poorly reproduced. Also no absolute normalization was given. No serious model was ever proposed for $dd \to \alpha X$. In summary: there is no really satisfactory model for the ABC effect in any reaction. A detailed review with further references could be found in[7].

MODEL FOR $dd \to \alpha\pi\pi$

Returning to the present, we take a closer look at the two colliding deuterons. Since they are loosely bound we could split them and instead consider two independent $NN \to d\pi$

*Electronic address: grdstg@tsl.uu.se

processes. These reactions are dominated by the Δ resonance and are strongly forward-backward peaked. We thus have two principal configurations of the final deuteron and pion pairs: 1. If the two deuterons are taking off together, they easily form an α particle, and the pions, going in the other direction, will have low relative momentum. This corresponds to the situation at the sharp ABC peaks. 2. If the deuterons are moving in opposite directions it is hard to bind them together and the pion pair, which is also back-to-back, will have a large effective mass. This is then the central bump.

Hence, the ABC structure is a consequence of the strong angular dependence of $NN \to d\pi$ in cooperation with the $dd{:}\alpha$ sticking factor. The latter will suppress the central region compared to the sharp peaks.

These considerations are immediately transformed into the Feynman diagram of Fig. 1. The deuteron split-up and the α-particle formation are modelled by the corresponding wave functions[8], while the $NN \to d\pi$ vertices are parametrized by phenomenological partial wave amplitudes[9]. The dominant partial wave ^1D_2p would give vanishing analyzing powers, which is why all the significant amplitudes were included in the calculations[7].

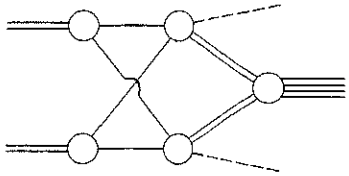

Fig. 1. Feynman diagram for the $dd \to \alpha\pi\pi$ reaction.

The same mechanism could also be applied to $dd \to \alpha 4\pi$, where $NN \to d\pi$ is replaced by $np \to d\pi\pi$. In a simpleminded approach, where the $I = 0$ pion pair is regarded as an s-wave σ meson with varying mass, the 4π spectra could be estimated[10]. The $np \to \sigma d$ amplitude is extracted from data on $np \to d\pi\pi$[1]. Another extension is to $dd \to \alpha\gamma\gamma$, using phenomenological $np \to d\gamma$ partial wave amplitudes as input[11]. This reaction is important as background to the charge-symmetry-breaking (CSB) $dd \to \alpha\pi^0$ reaction. A positive result has been reported for CSB in this reaction only after making severe experimental cuts[12].

RESULTS

The predictions of the angular and energy distributions of $dd \to \alpha\pi\pi$ are compared with data[3] in Figs. 2 and 3. There is a remarkably good quantitative agreement. The calculations are multiplied by scale factors that can be explained as due to distortion in the initial and final states[7]. The deficit at high M_X might be attributed to production of 3π or to simplifications in our model. In this region it is less accurate and also sensitive to the details of the α-particle wave function.

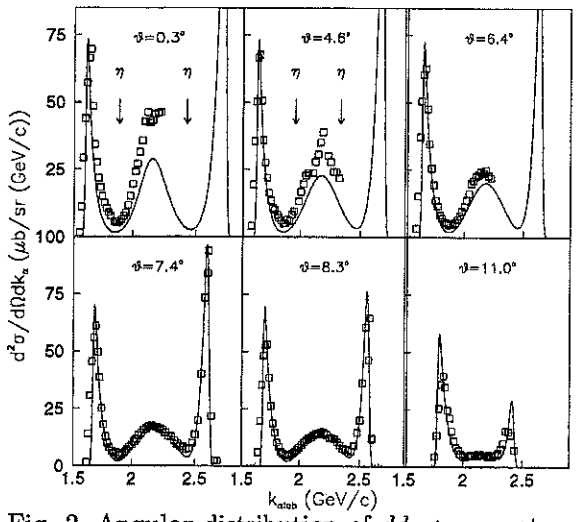

Fig. 2. Angular distribution of $dd \to \alpha\pi\pi$ at 1250 MeV.

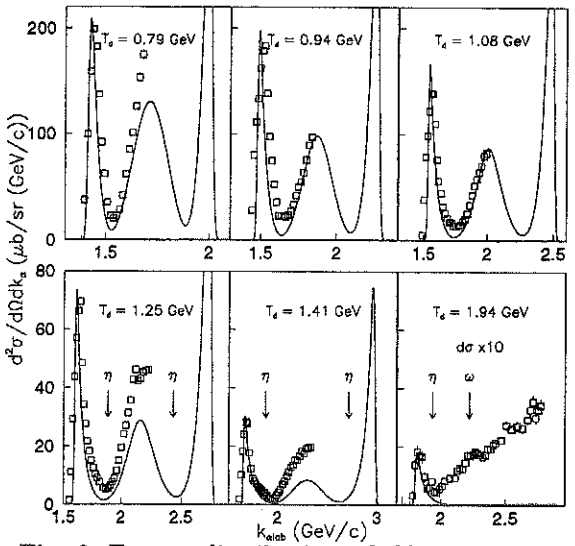

Fig. 3. Energy distribution of $dd \to \alpha\pi\pi$ at $\vartheta_{\alpha\mathrm{lab}} = 0.3°$.

The theoretical missing mass distributions of $dd \to \alpha 4\pi$ are plotted in Fig. 4, with scale factors of 1.3 or less[10]. This difference could be because of the neglect of contributions from $pp \to d\pi\pi$. The main part of these spectra is hence due to 4π production and the

additional structure superposed on this could be the ω meson, although the peak widths are much larger than the stated experimental resolution.

There are also $dd \to \alpha\pi\pi$ data at lower energies[13] showing no deviation from phase space. Here our model underestimates by a factor 20, retaining an ABC-like structure.

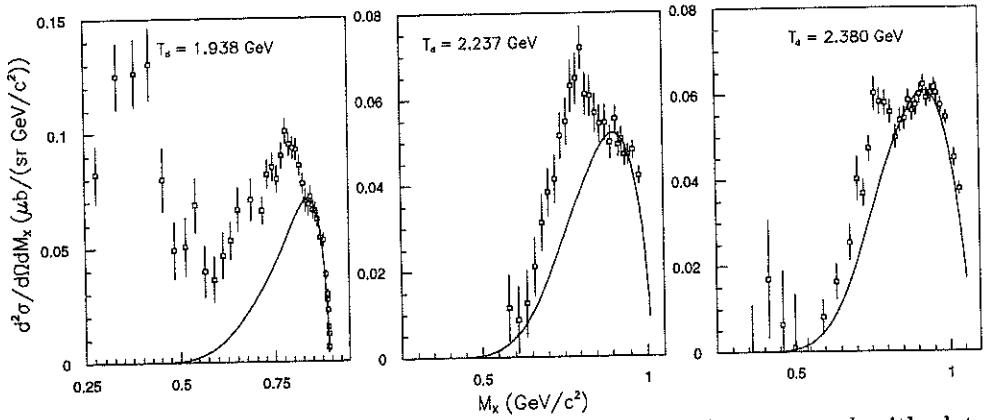

Fig. 4. The missing mass distributions of $dd \to \alpha 4\pi$ compared with data from[3].

As seen in Fig. 5 the tensor and slope of vector analyzing powers closely follows the frequency and magnitude of the oscillations. Remember that it is the non-dominant amplitudes that are responsible for these structures. The differences in the central region could again be related to the uncertainty in our model for high M_X.

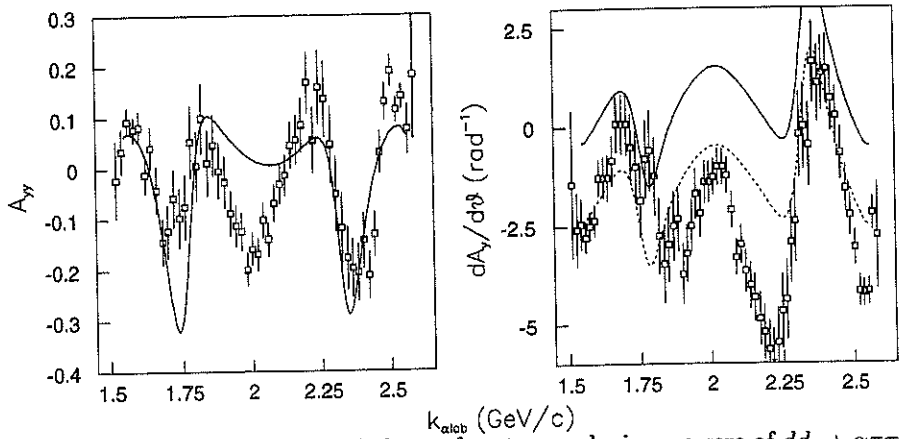

Fig. 5. Predictions of tensor and slope of vector analyzing powers of $dd \to \alpha\pi\pi$ at $T_d \approx 1120$ MeV together with data from Ref.[4]. The A'_y curve has been shifted by -2 rad^{-1} (dotted curve) to facilitate comparison with data.

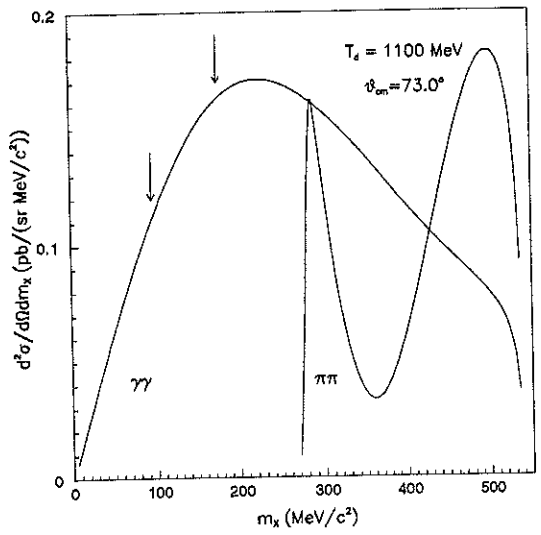

Fig. 6. The missing mass distributions of $dd \to \alpha\gamma\gamma$ and $dd \to \alpha\pi\pi$ at 1100 MeV and $\vartheta_{\alpha cm} = 73°$. The $\pi\pi$ curve has been reduced by a factor 10^4. The experimental cuts in missing mass are indicated.

The calculated missing mass distribution for $dd \to \alpha\gamma\gamma$ at 1100 MeV is seen in Fig. 6. At this energy a π^0 signal of 1 pb/sr has been reported[12], with the experimental cuts in mass indicated in the figure. Integrating the $\gamma\gamma$ spectrum between these limits results in 11.4 pb/sr. This value might be reduced by a factor ≈ 3 because of the other cuts (which could only be properly understood through a Monte Carlo simulation, not at our disposal), which suggests that the π^0 signal might be a misinterpretation.

At 10 MeV over the π^0 threshold in c.m. and at $M_X = m_{\pi^0}$, the integrated $\gamma\gamma$ cross section is 3.6 pb/(MeV/c^2), $A_{yy} \approx 0$, and the photon angular distribution $d\sigma/d\Omega_{\gamma\gamma} \propto (1 + b\sin^2\theta_{\gamma\gamma})^2$, where $b \approx 2$[11]. This would be a good point for new experiments, since $A_{yy}(\pi^0) = -1/2$ at threshold and, of course, π^0 production would give isotropic photons.

CONCLUSIONS

The remarkably good quantitative agreement with the $\pi\pi$ data strongly suggests that the ABC effect (at least in this reaction) is a kinematical enhancement in the production of two independent p-wave pions. Taken together with the successful reproduction of deuteron analyzing powers and the pleasing agreement with the 4π spectra, it seems likely that multi-meson production in the $dd \to \alpha X$ reaction at $0.8 < T_d < 2.4$ GeV is dominated by a single general two-step mechanism. The estimates of $\gamma\gamma$ production could give further support to this suggestion.

We suggest that unpolarized and polarized cross sections as well as two-body angular distributions should be measured at low energies ($T_d < 0.8$ GeV) for $dd \to \alpha\pi\pi$. This would provide the information needed to understand the vanishing of the ABC effect at these energies. A possible way to clarify the situation regarding CSB in $dd \to \alpha\pi^0$ would be the measurement of tensor analyzing power and/or photon angular distribution close to the π^0 threshold.

REFERENCES

1. F. Plouin *et al.*, "Observation of the ABC effect in the reaction $n + p \to d + (mm)^0$ with a 1.88 GeV/c neutron beam," Nucl. Phys. **A302**, 413 (1978).
2. A. Abashian, N.E. Booth, and K.M. Crowe, "Possible anomaly in meson production in $p + d$ collisions," Phys. Rev. Lett. **5**, 258 (1960).
3. J. Banaigs *et al.*, "A study of the inclusive reaction $d + d \to {}^4\mathrm{He} + X$, the ABC effect, and $I = 0$ resonances," Nucl. Phys. **B105**, 52 (1976).
4. R. Wurzinger *et al.*, "Study of the ABC enhancement in the $\vec{d}d \to \alpha X^0$ reaction," Phys. Lett. **445B** 423, (1999).
5. I. Bar-Nir, T. Risser, and M.D. Shuster, "The ABC effect in the reaction $NN \to d\pi\pi$," Nucl. Phys. **B87**, 109 (1975).
6. J.C. Anjos, D. Levy, and A. Santoro, "A Double Nucleon Exchange Model for the ABC Production in the $pn \to d\pi\pi$ Reaction," Nuovo Cimento **33A**, 23 (1976).
7. A. Gårdestig, G. Fäldt, and C. Wilkin, "Structure in two-pion production in the $dd \to \alpha X$ reaction," Phys. Rev. C **59**, 2608 (1999).
8. M. Lacombe *et al.*, "Parametrization of the deuteron wave function of the Paris N-N potential," Phys. Lett. **101B**, 139 (1981); J.L. Forest *et al.*, "Femtometer toroidal structures in nuclei," Phys. Rev. C **54**, 646 (1996).
9. R.A. Arndt *et al.*, "Analysis of the reaction $\pi^+ d \to pp$ to 500 MeV," Phys. Rev. C **48**, 1926 (1993); http://said.phys.vt.edu/said_branch.html/
10. A. Gårdestig, "Multi-pion production in the $dd \to \alpha X$ reaction," (in preparation).
11. D. Dobrokhotov, G. Fäldt, A. Gårdestig, and C. Wilkin, "Has charge symmetry breaking been observed in the $dd \to \alpha\pi^0$ reaction?" Phys. Rev. Lett. (to be published).
12. L. Goldzahl *et al.*, "Première observation de la production de π^0 dans la reaction $d + d \to \alpha + \pi^0$," Nucl. Phys. **A533**, 675 (1991).
13. K.R. Chapman *et al.*, "Observation of the reaction $d + d \to {}^4\mathrm{He} + 2\pi$ at 1.69 GeV/c," Phys. Lett. **21**, 465 (1966); C. Bargholtz *et al.*, "The inclusive reaction $d + d \to {}^4\mathrm{He} + X$ 29 MeV above the $2\pi^0$ threshold," Phys. Lett. **398B**, 264 (1997).

Summary of the Conference

D.V. Bugg
Queen Mary and Westfield College, Mile End Rd., London E1 4NS, UK

Abstract

Many important and interesting sets of new experimental data have been presented on both photoproduction and πN scattering. The very accurate X-ray data from PSI provide an anchor point for the πN S-wave amplitudes at threshold. New values of the πN coupling constant $g_c^2/4\pi$ and the σ commutator are discussed. Some suggestions are made about how to include small but essential, corrections for Coulomb effects and the nucleon pole term into the πN amplitude analysis. The possibility is discussed of hybrids in the mass range 1440-2000 MeV.

1 Introduction

This has been a most enjoyable and informative meeting, with many results which are new to me. It is particularly gratifying to see the high quality of new data. I will try to review presentations, but will not make references to talks appearing in these Proceedings.

The interest of the low energy regime, below 300 MeV, lies in determining the πN couping constant and the σ commutator. In the past, there have been disagreements over data and over theoretical methods. It seems to me that the data-base for the low energy regime up to 300 MeV is fast approaching the point where definitive conclusions may be drawn. We have not quite reached that point. Some experimental results are still 'preliminary'. Nonetheless, I see the end in sight concerning this question, and would like to make some suggestions about how it may be wound up in the most definitive fashion.

At higher masses, there are new data which improve the picture of the S_{11} resonance, $N^*(1535)$ of the Particle Data Group (PDG) [1]. Above this, JLAB promises billions of events once results from CLAS, surveyed by Dytman, have been fully analysed; there is also the prospect of new data on neutral final states from the Crystal Ball experiment at BNL, as reviewed by Nefkens.

My summary will start with the lowest energies and work gradually up in energy.

2 Photoproduction at MAMI

There are excellent data over the $\Delta(1230)$ region measuring M1 and E2 amplitudes. Beck presented experiments measuring the angular distribution for $\gamma p \to \pi^0 p$ in two ways, (i) detecting the recoil proton [2,3] or (ii) both photons from the π^0 (new data). It is a valuable check that results agree well from these two techniques. The angular distribution is dominated by $|M1|^2$. Secondly, they have measured the parameter Σ using a linearly polarised photon beam. This measurement is dominated by $Re(M1 * E2)$. It determines accurately the small $E2$ amplitude, with the result

$$Im(E2)/Im(M1) = -(2.5 \pm 0.2(stat) \pm 0.2(syst))\%. \quad (1)$$

This measurement appears to resolve discrepancies between earlier less accurate determinations. It requires a small D-state admixture in the $\Delta(1232)$, analogous to the D-state contribution to the deuteron. The interpretation is bedevilled by the need to understand 'background', non-resonant contributions, i.e. t-channel exchanges. It would be of interest to hear from theoreticians what they make of this result.

There is a second valuable result from MAMI near threshold. The cross section for $\gamma p \to \pi^0 p$ has been measured across the threshold for $\pi^+ n$. The cusp at this threshold is observed clearly [4]. The data confirm nicely a prediction from Chiral Perturbation Theory. The Low Energy Theorems without Chiral Perturbation Theory predict a threshold cross section of $-2.4 \times 10^{-3}\mu^{-1}$; Chiral perturbation theory changes the prediction to $-1.16 \times 10^{-3}\mu^{-1}$, in close agreement with the observed value of $(-1.31 \pm 0.1) \times 10^{-3}\mu^{-1}$.

3 New πN scattering data

Over the past few years there have been several new πp polarisation measurements. These are valuable because groups appear to be able to agree on normalisations better than for differential cross sections. Data of Sevior et al. from TRIUMF [5] for both $\pi^{\pm}p$ elastic scattering in the mass range 98 to 263 MeV set a standard of $\sim 1.5\%$ in absolute normalisation. These were followed by precise charge exchange polarisation measurements at LAMPF [6], which are shown to be consistent with those of Sevior et al. by the VPI/GWU phase shift analysis.

At low energies, the CHAOS spectrometer has been used to measure polarisations in elastic scattering from 139 MeV down to 87 MeV, and the aim is to cover also 67 and 51 MeV. ¿From the Tübingen group at PSI, competing measurements using a novel active polarised target are reported by Meier in the energy range 99 to 45 MeV. In this energy range, the contribution of $Im(P_{33} * S_{31})$ to $Pd\sigma/d\Omega$ is quite small because P_{33} is far below resonance. The experimental groups have chosen to measure in angular ranges where the sensitivity of P to phase shifts is large. This is the range where P_{33} and S-waves interfere destructively and $d\sigma/d\Omega$ is small; hence the data are really a delicate indirect measurement of $d\sigma/d\Omega$ in regions where it is small. It is essential to be careful about background rejection from events in carbon. The Tübingen results, obtained using a high resolution spectrometer to detect the scattered pion, indeed look very clean.

Sadler showed data from LAMPF on the differential cross section for $\pi^-p \to \pi^0 n$ from 67 to 535 MeV; Isenhower presented data at low energies, 10 to 40 MeV. The low energy data are an important check on charge independence, but require good normalisation.

The Gatchina group [7] has provided precise and extensive $\pi^{\pm}p$ elastic data over the mass range 120 to 600 MeV, including measurements of R and A parameters some years ago. Their data provide a valuable determination of the differences in mass and width between Δ^{++} and Δ^0, as discussed below.

Friedman presented updated results on total cross sections for $\pi^-p \to \pi^0 n$. It is good to see that they now lie within 2% of the earlier data [9]. Furthermore, there is excellent agreement for the energy scale, hence demonstrating that there is agreement within errors on the mass of the Δ.

Before going on to details of how to treat these πN data, I would like to comment on what seems to have become a tradition: namely to compare experimental results with predictions of Höhler and Pietarinen [8], sometimes unfavourably because of disagreements. We need to be conscious that the objective of Höhler and Pietarinen was to apply dispersion relations, particularly at fixed t, over a very large range of both ν and t, up to lab energies of 2 GeV. In this work, mass and width differences of the Δ were ignored as a simplification, although Koch and Pietarinen [10] did make a separate investigation of such effects. It is now generally agreed that the S-wave scattering lengths of Höhler and Pietarinen were a little low; also that differences in mass and width of the Δ between π^-p and π^+p have significant effects. I believe that these two points are responsible for most of the observed discrepancies up to 300 MeV.

Somewhat removed from these πN data are those shown by Sevior on $(\pi, 2\pi)$ reactions from deuterium, ^{12}C, ^{40}Ca and ^{208}Pb. The $\pi^+\pi^+$ mass distribution follows phase space. ¿From deuterium, the $\pi^-\pi^+$ mass distribution has a dip at low mass, because of the Adler zero. However, from nuclei, the low mass region gets filled up and indeed shows a peak from the heaviest nuclei. This is a most intriguing result. The theorists have examined conventional explanations such as Fermi motion and π absorption and cannot explain the result. Does the nucleus somehow filter out high momentum pions? That seems unlikely, since the same should happen for $\pi^+\pi^+$ pairs. An alternative is that the Adler zero disappears in nuclei, because chiral symmetry is increasingly badly broken with increase in atomic number. That would be a spectacularly important result, if true. Further experiments are important, with particular attention to absolute cross sections. It is vital to know whether the low mass $\pi^+\pi^-$ region is enhanced from nuclei or whether the high mass region is attenuated.

I hope this effect does not go the way of the d'. Evidence for this possible narrow dibaryon in $NN\pi$ arose [12] in double charge exchange data from nuclei. Experimental

searches at CELSIUS and COSY have failed to find positive evidence confirming it. Gibbs can explain it in terms of the dip at 50 MeV in πN charge exchange; this makes the nucleus transparent in a narrow range of pion energies around 50 MeV. Gibbs explains the observed peaks, at least for those nuclei where the nuclear physics is under control.

4 Chiral Perturbation Theory

There are now extensive and impressive calculations of the predictions of Chiral Perturbation Theory in low energy πN scattering and photoproduction to many orders. Leutwyler and Gasser reviewed the ideas and results, and I do not feel competent to comment. I will discuss below predictions for the σ-commutator.

A new development is a Chiral Perturbation Theory approach to NN scattering, discussed by Meissner. It is well known that NN scattering is dominated by exchange of π, σ and ρ, with substantial contributions from 3π exchanges, as demonstrated by Grein and Kroll [11]. The short-range exchanges are accomodated by contact terms, fitted empirically. A nice feature is that three-body calculations can be done naturally with this formalism. I have two warnings on points of contact with experiment. Firstly, the $I = 0$ NN phase shifts are not known very precisely from 25 to 150 MeV, though they are much better known from 150 to 500 MeV, the energy range of extensive polarisation experiments are TRIUMF and SIN. Secondly, it is really necessary to build into the calculations production of Δ and the final S-wave πN state; these are known to make large contributions beginning at 300 MeV. Below that, dispersive contributions arising from these inelastic channels are known to be quite significant for $^1D_2$, $^3P_2$, $^3F_3$ and $^3P_1$.

5 X-ray results

One of the crucial advances of the last few years has been the very precise determinations of $\pi^- p$ and $\pi^- d$ scattering lengths, by measuring the strong interaction shifts of X-rays from pionic atoms. These remarkable data [13,14] provide an accurate anchor point for the scattering lengths. Leisi and collaborators [15] have evaluated electromagetic corrections, which change the strong interaction shift ϵ_{1S} in hydrogen by $(2.1 \pm 0.5)\%$, twice the quoted error in ϵ_{1S}. After this correction, results for hydrogen and deuterium are:

$$a(\pi^- p) = \frac{a_3 + 2a_1}{3} = 0.0883 \pm 0.0008 \mu^{-1} \quad (2)$$

$$a(\pi^- d) = -0.0261 \pm 0.0005 \mu^{-1}. \quad (3)$$

To first approximation, the difference between these results measures the scattering length for $\pi^- n$; by charge symmetry, which is likely to be rather accurate, this gives the $\pi^+ p$ scattering length a_3. However, the deuterium result needs correction for double scattering in the deuteron. At present there are slight differences between the PSI group [15] and calculations by Loiseau et al., presented at this meeting. It is important that the experts resolve these discrepancies, even though they are small, since the $\pi^- d$ result may be the best source of information on a_3. My feeling is that it should be possible to reach agreement. However, there are subtleties, and it is important that both groups explain exactly how the calculations are done.

Let me give two examples. Firstly, the elastic scattering amplitude is close to zero and the main contribution to double scattering arises from charge exchange in both scatters. In the intermediate state, it is necessary to allow for the fact that the $\pi^0 n$ channel has larger phase space than $\pi^- p$, because of mass differences. Exactly how is this done, and what is its effect? Secondly, Fermi motion of the nucleons in the deuteron plays a significant role. It is necessary to allow for the fact that the two nucleons have equal and opposite momenta. For the deuteron D-state component, the average Fermi momentum is $\sim$ 150 MeV/c and the scattering from both nucleons lies well up the Δ. Are these effects included and how?

Presently, results for individual scattering lengths are as given in Table 1. The value of $a_1 + 2a_3$ is consistent with zero within the errors. To first order, this is the result expected for massless pions, but it would be interesting to know the perturbation predicted by Chiral

	Loiseau et al	PSI
$a_1 + 2a_3$	$-6 \pm 3 \pm 1.8$	4.8 ± 3.9
a_3	$-92.3 \pm 2.2 \pm 1.2$	$-85.1 \pm 2.8 \pm 1.2$
a_1	$178.6 \pm 1.9 \pm 0.6$	$175.0 \pm 2.1 \pm 0.6$
$a_1 - a_3$	$270.9 \pm 3.9 \pm 1.8$	$260.1 \pm 4.6 \pm 1.8$

Table 1. Scattering lengths in units of $10^{-3}\mu^{-1}$.

Authors	Method	$(a_1 - a_3)$ (μ^{-1})
Bagheri et al.	charge exchange	0.264 ± 0.005
Duclos et al.	charge exchange	0.270 ± 0.014
Spuller et al.	Panofsky ratio	0.263 ± 0.005
Tauscher and Schreider	mesic X-rays	0.258 ± 0.008
Carter et al.	Dispersion relations	0.262 ± 0.004

Table 2. Determinations of the charge exchange scattering length.

Perturbation Theory. The mean value of the charge exchange combination $a_1 - a_3$, obtained assuming charge independence, is $0.265\ \mu^{-1}$. This is in agreement with experimental results shown in Table 2. My conclusion is that there is no significant evidence for violation of charge independence at present, although the errors leave room for a small violation. Leutwyler estimates that isospin breaking should be of order

$$\frac{m_d - m_u}{m_d + m_u} \cdot \frac{M_\pi^2}{M_s^2} = 0.006, \tag{4}$$

i.e. very small. Matsinos [16] has claimed a much larger violation of charge independence. However, his value of a_3, namely $-0.0769 \pm 0.0026\ \mu^{-1}$, is four standard deviations smaller than values in Table 1, because of his selection amongst the low energy $\pi^+ p$ scattering data. My belief is that experiments below 100 MeV agree quite well with phase shift analysis for the *shapes* of angular distributions, but absolute normalisations require substantial adjustment in many cases. It is necessary to reach agreement about which experiments (if any) have the right normalisation.

6 100–300 MeV

The primary objective in the low energy region is to find g^2 and the σ commutator. I wish to examine critically what is required to get the most definitive determinations. The theoretical analysis requires use of dispersion relations. Above 300 MeV, data are little help in determing g^2 and Σ, because the content of the dispersion relations is used up in determining the elasticity parameters. Hence the critical data lie below 300 MeV (and indeed it should be checked that data above 300 MeV are NOT biasing the determinations of g^2 and Σ).

Over the peak of the Δ resonance, phase shifts are determined along the following lines:

$$\sigma_{tot} = |P_{33}|^2 + \textit{small corrections} \tag{5}$$

$$d\sigma/d\Omega = A + B\cos\theta + C\cos^2\theta + \textit{small}\cos^3\theta\ \textit{terms} \tag{6}$$

$$B \rightarrow Re(P_{33}^* S) \rightarrow S \tag{7}$$

$$C/A \rightarrow Re(P_{33}^* P_{1/2}) \rightarrow P_{1/2} \tag{8}$$

$$Pd\sigma/d\Omega = D + E\cos\theta + F\cos^2\theta + \textit{small terms} \tag{9}$$

$$D \rightarrow Im(P_{33}^* S) \rightarrow S \tag{10}$$

$$E \rightarrow Im(P_{33}^{*}P_{1/2}) \rightarrow P_{1/2} \quad (11)$$

$$F \rightarrow Im(P_{33}^{*}D) \rightarrow one\ D-wave\ combination \quad (12)$$

$$\sigma_{CE} \rightarrow |P_{33}-P_{13}|^2 + |S_{31}-S_{11}|^2 \rightarrow P_{13}. \quad (13)$$

For purposes of illustration, I have dropped terms involving squares of small quantities. The S-waves and the small P-waves are well determined near the peak of the Δ resonance by the accurate polarisation data. Sevior et al. remark that their determination is in good agreement with the 1973 values of Carter et al. [17] from differential cross section data; but the polarisation data reduce errors significantly. Polarisation results presented at this meeting seem to agree well with Sevior et al. So it seems that we have a firm and agreed determination of the S and small P waves over the Δ.

I suggest that one should now return to the ancient prescription proposed by Hamilton and Woolcock in 1960–3 [18] and determine the precise s-dependence of the S-waves using fixed-t dispersion relations. This analysis should join up with the anchor point at threshold and establish the s-dependence of the S-wave explicitly from threshold to the resonance. This should resolve discrepancies of normalisation. Of course, the result is inherent in the VPI analysis, which imposes fixed-t dispersion relations up to 600 MeV. Nevertheless, an independent check by Höhler's group would be valuable. The normalisation discrepancies are presently the major outstanding issue.

An important starting point for the whole procedure is to use the accurate total cross section measurements to determine $|P_{33}|$. ¿From the results presented by Friedman, it seems that there is now good agreement between his integrated cross sections, those of Kriss et al. [19], and my old total cross sections. Those of Pedroni et al. [20] are systematically one standard deviation lower below resonance, but my judgement is that all these data are in satisfactory agreement and should all be used. As I remarked in the πN Newsletter [21], I do not agree with the Nijmegen group that total cross sections are ill-defined, since they are well determined experimental quantities; it is necessary only to be realistic in assessing errors on Coulomb corrections and Coulomb-nuclear interference.

Table 3 summarised determinations of differences in mass and width between Δ^0 and Δ^{++} (all after correction for the effects of the Coulomb barrier). I should comment that the earliest value for the width difference, namely 6.4 ± 1.8 MeV, given by Carter et al. [17], was too high; it was corrupted by Berkeley data at 310 MeV subsequently shown to be wrong. The first entry of Table 1 gives the revised value. I would like to point out that this mass difference was quite apparent at the time the actual data were being taken; consequently many experimental checks were made on possible systematic errors.

Authors	$M(\Delta^0)-M(\Delta^{++})$ (MeV)	$\Gamma(\Delta^0)-\Gamma(\Delta^{++})$ (MeV)
Bugg	2.6 ± 0.4	5.1 ± 1.0
Koch(80)	2.3 ± 0.3	2.0 ± 1.5
Gatchina	2.6 ± 0.4	5.1 ± 1.0
Pedroni	2.7 ± 0.3	6.6 ± 1.0

Table 3. Mass and Width differences for the Δ.

Results for the mass difference agree well and are consistent with twice the mass difference between neutron and proton, suggesting that the mass difference arises between down and up quarks. If so, masses of remaining Δ charge states should follow a linear relation with charge. Data of Pedroni et al. on deuterium are consistent with this. They quote $M^{-}-M^{++}+(1/3)(M^0-M^+)=4.6\pm0.2$ MeV, compared with a predicted value of 4.3 MeV.

The heavier Δ^0 has increased phase space for decay, and this accounts for much of the observed differences in width. The phase space is proportional to

$$\rho(p) = p^3/(p^2+1/R^2), \quad (14)$$

where R is the radius of the centrifugal barrier and p the decay momentum in the rest frame of the resonance. There is also an extra decay width for $\Delta^0 \to \gamma n$ of 1.1 MeV. Myhrer and Pilkuhn have shown [22] that these two effects predict $\Gamma(\Delta^0) - \Gamma(\Delta^{++}) = 4.2$ MeV; I have repeated this calculation using the value $1/R^2 = 0.0608$ GeV^2 which I have fitted in meson spectroscopy and find a similar result, 4.4 MeV.

These differences between charge states play a significant role at some energies and angles in fitting data, and I feel it is vital to include them in partial wave analyses. The way to include them is straightforward. The resonance amplitude may be written

$$f = 1/[M^2 - s - M \sum_i \Gamma_i(s)], \tag{15}$$

with separate values of M and Γ_i for each channel. After allowing for the available phase space ρ_i of equn. (14) for P-wave decays, the cross section for $\pi^- p \to \pi^0 n$ is, for example

$$\sigma \propto \frac{\Gamma_{\pi^- p}(s)\Gamma_{\pi^0 n}(s)}{(M^2 - s)^2 + [M \sum_i \Gamma_i(s)]^2}. \tag{16}$$

The s-dependence of Γ may be fitted by a Layson form or some similar empirical formula. The only complications to present analyses are (i) the phase space differences between charge states, (ii) the mass and width differences.

7 The πN coupling constant

There have been many determinations of this imporant parameter, and quite a bit of argument. Competing determinations come from πN scattering, from np charge exchange, from pp Wolfenstein parameters, and from $\bar{p}p \to n\bar{n}$. Loiseau summarised the latest values from PANIC; I assume that convenors of the workshop session will report numerical values.

Most determinations agree now on values $g^2 = 13.45$ to 13.84, significantly lower than evaluations of the 1970's of 14.28 ± 0.18. However, the determination by the Uppsala group from np charge exchange continues to give a high value of $14.52 \pm 0.13(stat) \pm 0.15(syst) \pm 0.17(norm)$. I do not wish to provoke fresh controversy by arguing the merits of various determinations. The crucial experimental difficulty in all the np determinations and for $\bar{p}p$ charge exchange lies in determining the absolute normalisation of cross sections; these determine amplitudes squared, hence g^4. It is important to get a precise value of g_0^2 from pp Wolfenstein parameters, to check charge independence with g_c^2; preliminary results are available from Indiana.

The πN data in the energy range up to 300 MeV should provide a very dependable determination of the charged coupling constant g_c^2 for $\pi^- p \to n$. The nucleon pole term contributes a strong driving term to the $\Delta(1230)$ resonance, which can be measured with great accuracy. The nucleon pole lies between the physical regions for $\pi^+ p$ scattering and $\pi^- p$. Hence g_c^2 is determined by interpolation between these regions, rather than extrapolation, as is the case in nucleon-nucleon scattering.

Pavan reviewed the latest results from the VPI/GWU group. The current value is $g_c^2/4\pi = 13.73$. It is very stable against variations of the data-base; the statistical error is negligible, From different data selections, Pavan estimates an error of $\pm(0.08 - 0.10)$. However, the open question is how stable this value is against *systematic* variations in analysis procedures. This is where attention needs to be focussed. During the meeting, several of us discussed these questions, and a number of well-defined points were agreed where checks and small improvements must be made. I believe these can be made quickly and without great effort, and I am offering a case of wine to Pavan and Arndt if they will eliminate these niggling points of detail before the next conference! I will now discuss these details one by one.

Firstly, the present analysis evaluates Coulomb barrier corrections assuming a point Coulomb source. However, it is well known that the charge form factors of the proton and pion fall exponentially with t, so the Coulomb source really has a Gaussian distribution in r. What effect does this have on phase shifts and g^2? I believe it may be significant. Corrections for a Gaussian source were evaluated by myself [23] and by Tromborg et al.

[24] in the 1970's, so it is only a matter of plugging into the analysis a table of these corrections. Oades presented at the meeting a re-evaluation up to 100 MeV; the difference between his new values and the old ones provides some measure of the uncertainties.

Secondly, in the coupled $\pi^- p - \pi^0 n$ sector, the Coulomb potential acts only within the $\pi^- p$ channel. With these channels as basis states, the Coulomb perturbation is

$$\delta V^C = \begin{pmatrix} -V_C & 0 \\ 0 & 0 \end{pmatrix}.$$

Using the matrix

$$U = \frac{1}{\sqrt{3}} \begin{pmatrix} 2 & -\sqrt{2} \\ -\sqrt{2} & 1 \end{pmatrix}$$

which relates charge and isospin states, one obtains in the isospin basis

$$\delta V = U \delta V^C U^{-1} = -\frac{1}{3} V_C \begin{pmatrix} 2 & -\sqrt{2} \\ -\sqrt{2} & 1 \end{pmatrix}.$$

The off-diagonal term produces an explicit violation of charge independence through an amplitude called f_{13} in the old work of the 1970s [17]. This needs to be included.

Finally, VPI/GMU parametrise phase shifts with an empirical form v. energy. As a matter of internal consistency, this form should contain explicitly the nucleon pole term. Höhler and collaborators have studied partial wave dispersion relations in detail and have compared results with effective range forms. Höhler and Staudenmeier [25] provide very useful illustrations in Fig. 3 of their article in the 1995 Newsletter. They show Chew-Low plots for partial waves P_{33}, P_{31}, P_{13} and an inverse Chew-Low plot for P_{11}. I suggest following these forms in fitting phase shifts at low energies. The virtue of this procedure is that it builds into the phase shift analysis the constraint at the nucleon pole that couplings to P_{33}, P_{13}, P_{31} and P_{11} should be in the ratios 2:-1:-1:-4, as pointed out by Chew and Low [26]. One should also include the important additional contributions from σ and ρ exchange, following Höhler and Staudenmeier.

Values of P_{33} are determined experimentally with great accuracy. However, for the small P-waves at low energies, the constraint should filter large errors and correlations from experimental determinations. The work can be done by using a slightly modified Chew-Low formula as a parametrisation, fitted to the trend of the results of Höhler and Staudenmeier, or alternatively by constraining the analysis to agree closely with this parametrisation (e.g. by a penalty function in χ^2). This should be simple and quick. I believe one can take on trust the σ and ρ exchange terms evaluated by Höehler's group, so it is not necessary at the present point to go through a further iteration of re-evaluating the partial wave dispersion relations. It is likewise desirable to constrain the D and F-waves to contain the correct nucleon pole terms.

These are the essential points requiring attention. Pavan expressed the opinion that they will not have much effect on g^2. Maybe. But let's try it and see; then we can be sure.

8 The GMO Sum Rule

A potentially serious issue [27] concerns Coulomb barrier corrections to the GMO sum rule, which reads [28,29]:

$$a_1 - a_3 = 5.252 f^2 + 2.611 J \tag{17}$$

$$J = \frac{1}{4\pi^2} \int^{\infty} dk \frac{\sigma^-(\nu)}{\nu}. \tag{18}$$

Here k is the lab momentum, ν the total lab energy of the pion and $\sigma^- = \sigma(\pi^- p) - \sigma(\pi^+ p)$. In $\pi^- p$ scattering, the total cross section is systematically decreased at *all* energies by the Coulomb repulsion between the particles. Conversely, in $\pi^+ p$ scattering, the total cross section is systematically enhanced. It is necessary to correct for this effect. Conventionally, the correction is applied, I believe, only over the energy range up to 500 MeV, i.e. over the

energy range where Tromborg's calculations are available. A further correction is needed from 500 MeV to ∞, as outlined in Ref. [27]. The resulting error is quite large compared with the magnitude of the integral J; my belief is that it is several times the error which is currently quoted.

My feeling is that g_c^2 and $a_1 - a_3$ are now rather well determined by the low energy data. It is positively *dangerous* to use the GMO sum rule in fitting the low energy data, since it introduces a potential bias from any errors in the integral of equn. (18) anywhere from zero to infinity! So I recommend it should not be used in the actual phase shift analysis.

9 The σ commutator

The quantity called Σ is F_π^2 times the invariant amplitude $D = A + \nu B$ at the Cheng-Dashen point $\nu = 0$, $t = 2\mu^2$, after subtracting the nucleon pole term. The D amplitude may be extrapolated at fixed t from the physical region to $\nu = 0$, using dispersion relations. In the region of the Mandelstam triangle, in which amplitudes are real, it may be parametrised in terms of a magnitude d_{00}^+ at $t = 0$ and a slope d_{01}^+. Then

$$\Sigma = F_\pi^2(d_{00}^+ + 2\mu^2 d_{01}^+) + \Delta_D, \tag{19}$$

where Δ_D is a curvature correction 11.9 ± 0.6 MeV.

The Berne group has now extended chiral perturbation theory calculations to higher orders, with the following results:

$$\Sigma = 50\ MeV,\ to\ order\ q^2 \tag{20}$$

$$= 59.9\ MeV,\ to\ order\ q^3 \tag{21}$$

$$= 61.4\ MeV,\ to\ order\ q^4 \tag{22}$$

So the theoretical value expected at the Cheng-Dashen point has gone up compared with the earlier value, equn. (20) by ~ 11 MeV. However, the experimental value has likewise gone up. Everyone at the meeting agreed it has risen from the classical value of Höhler, Jakob and Kroll [29], 64 ± 8 MeV, by 8 MeV due to changes in the scattering lengths. Pavan argued for a slightly larger value of 78 ± 8 MeV, because of further effects. So there is still a discrepancy between theory and experiment of 2 standard deviations.

It is sometimes argued that this indicates a stange component in the nucleon of 20% or more. To me that seems unlikely. I have been doing experiments on $\bar{p}p$ annihilation for many years. There, except in special situations, $\bar{s}s$ resonances like $f_2'(1525)$ are not produced strongly. If they were, we would be able to do extensive $s\bar{s}$ spectroscopy via $\bar{p}p$ annihilation. Secondly, Leutwyler pointed out that strange quarks are heavier than up and down quarks by a factor of ~ 20. If there were a large strange content in the nucleon, much of its mass would arise from this source. That seems unlikely and inconsistent with many results from Chiral Perturbation Theory.

Since the discrepancy between theory and experiment is only 2 standard deviations, I suggest we should reverse the usual arguments by *fixing* the value of Σ at the theoretical value and asking what data are responsible for the discrepancy. My guess (only a guess) is that there may be a problem with the high partial waves, D and F, which play a large role in the extrapolation to the Cheng-Dashen point; they may not be determined experimentally so well as is presently believed.

I have a second related suggestion. It has been conventional to determine the D amplitude and its derivative E at $t = 0$ and extrapolate them to $\nu = 0$. However, $t = 0$ is at the edge of the physical region, and uncertainties in D and F waves are largest there, particularly in the derivative. Why not evaluate D and E for a given energy ν near the *centre* of the physical region, where D and F waves make small contributions? If this is done for a series of increasing values of ν, one will obtain, after the extrapolation using the fixed t dispersion relations, the values of D and E at $\nu = 0$ and a series of t values. One can then check these values for consistency and get some estimate of the systematic error. Stahov has followed essentially this idea by using interior dispersion relations, which are evaluated along hyperbolic paths crossing the physical region, as well as the unphysical region. It is noticeable that he gets a somewhat reduced value: $\Sigma = 72 \pm 8$ MeV.

My apologies for going into detail about how to get the best out of the data; but I think we owe it to the experimentalists who have worked so assiduously for so many years.

10 The ηN threshold region

The LAMPF experiments have now identified clearly the cusp at the ηN threshold in data on πN charge exchange. I would just like to remark that it is also *required* by the old data of Binnie et al. [30] on the ηN channel and the newer Crystal Ball data.

In photoproduction, $\gamma p \to \eta n$, Tiator et al. [31] have made precise measurements of polarisation parameters. ¿From interferences with the dominant $E_{0+} \to N^*(1535)$ amplitude, they get precise results for small photoproduction amplitudes P_{11}, D_{13}, D_{15} and F_{15}.

A technical remark is that I think it will be essential in analysing new data from CLAS and Crystal Ball to parametrise the ηN, ωN and ρN thresholds fully [32]. As an example, if a resonance couples to πN and ωN, the required formula for the amplitude is

$$f = \frac{1}{M^2 - s - m(s) - iM[\Gamma_{\pi N} + \Gamma_{\omega N}(s)]} \tag{23}$$

$$\Gamma_{\omega N}(s) \propto p_\omega \textit{ near threshold} \tag{24}$$

$$m(s) = \frac{(M^2 - s)}{\pi} \int_0^\infty \frac{\Gamma_{tot}(s')ds'}{(s' - s)(M^2 - s')}. \tag{25}$$

Here p_ω is the centre of mass momentum of the ω; the term $m(s)$ is a dispersive correction to the mass, making the formula fully analytic. My suspicion is that the reason that so many resonances cluster close to 1690 MeV is connected with the threshold for ωN and ρN. Maybe the apparent degeneracy in masses is simply a consequence of an incomplete parametrisation of the threshold cusps in these channels.

11 Higher Energies

Presently, there is excellent agreement between the πN resonances quoted by the PDG [1] and those expected from the simple quark model in SU(6) multiplets $\{70\}\ 1^-$, $\{56\}\ 2^+$, etc. The only state which does not presently fit nicely into this scheme is D_{35} at 1930 MeV, which is ~ 200 MeV lower than expected. That resonance needs checking, even though it presently has 3-star status.

Isgur et al [33] point out a missing $SU(6)$ representation, the $\{20\}^-$. There are reasons why it may couple weakly to πN. Experiments at JLAB are looking for such new states.

My own feeling is that hybrids $qqqg$ are also to be expected, and one should look for them. A pattern is gradually emerging in meson spectroscopy in which the lightest glueballs, made of two gluons, are believed to lie in the mass range 1500-1700 MeV. One can understand this mass as representing the 'effective' mass of two confined gluons. One then expects hybrids beginning in the mass range ~ 750 MeV above the nucleon and Δ. The lowest excitation of the gluon is expected to be 1^+, hence the expected hybrids are P_{11}, P_{13}, P_{31}, P_{33} and F_{35}. It is likely they will mix with normal qqq states. Hence, one should look for doubling of the number of poles with these quantum numbers; that may not be easy if the hybrids are broad.

An intriguing result from the BES group in Beijing is a large peak in $J/\Psi \to p\bar{p}\pi^0$ for $p\pi^0$ (or $\bar{p}\pi^0$) masses near 1470 MeV. Since J/Ψ decays are a source of gluons, this is a hint that the lowest P_{11} resonance could have a hybrid component mixed into it. So far, however, there is no spin-parity determination of the peak at 1470 MeV. Watch this space!

The Crystal Ball group plans a programme of experiments at BNL on $\pi^- p \to$ neutral final states. I urge them to include polarisation measurements. My own experience is that polarisation information plays a vital *qualitative* role in differentiating between alternative partial wave solutions. Without such information, one is often at the mercy of ambiguities in the analysis. Polarisation data on $K^- p \to K^0 n$ has also been a vital missing link in analysis of Y^* resonances for 20 years.

12 Thanks

On behalf of those who attended the meeting, I would like to thank Andreas Badertscher and Christine Kunz for their excellent organisation in such a pleasant and relaxing environment. I would also like to thank many people for discussions and clarifications during the meeting, and for their help in the difficult task of summarising so many results.

REFERENCES

1. Particle Data Group, Euro. Phys. J. 3 (1998) 1.
2. R. Beck et al., Phys. Rev. Lett. 78 (1997) 606.
3. R. Beck et al., Phys. Rev. C (to be published).
4. M. Fuchs et al., Phys. Lett. B368 (1996) 20; A. Bernstein et al., Phys. Rev. C55 (1997) 1509.
5. M.E. Sevior et al., Phys. Rev. C40 (1989) 2780.
6. C.V. Gaulard et al., Phys. Rev. C60 (1999) 024604.
7. V.V. Abeev and S.P. Kruglov, πN Newsletter 9 (1993) 101.
8. D.V. Bugg et al., Nucl. Phys. B26 (1971) 588.
9. G. Höhler, F. Kaiser, R. Koch and E. Pietarinen, *Handbook of Pion-Nucleon Scattering*, Physics Data 12-11 (1979).
10. R. Koch and E. Pietarinen, Nucl. Phys. A336 (1980) 331.
11. W. Grein and P. Kroll, Nucl. Phys. A338 (1980) 332; ibid A377 (1982) 505.
12. R. Bilger et al., Zeit. Phys. A343 (1992) 491; Phys. Rev. Lett. 71 (1993) 42.
13. D. Sigg et al., Nucl. Phys. A609 (1996) 310.
14. D. Chatellard et al., Phys. Rev. Lett. 74 (1995) 4157; Nucl. Phys. A625 (1997) 855.
15. H. J. Leisi, ETHZ-IPP PR-98-11.
16. E. Matsinos, Nucl. Phys. 56 (1997) 3014.
17. J.R. Carter, D.V. Bugg and A.A. Carter, Nucl. Phys. B58 (1973) 378.
18. J. Hamilton and W.S. Woolcock, Rev. Mod. Phys. 35 (1963) 737; Phys. Rev. 118 (1960) 291.
19. B.J. Kriss et al., Phys. Rev. C59 (1999) 1480.
20. E. Pedroni et al., Nucl. Phys. A300 (1978) 321.
21. D.V. Bugg, πN Newsletter 12 (1997) 14.
22. F. Myrher and H. Pilkuhn, Z. Phys. A276 (1976) 29; H. Pilkuhn, Nucl. Phys. B82 (1974) 365.
23. D.V. Bugg, Nucl. Phys. B58 (1973) 397.
24. B. Tromborg, S. Waldenstrom and I. Overbo, Helv. Phys. Acta, 51 (1978) 584; Phys. Rev. D15 (1977) 725.
25. G. Höhler and H.M. Staudenmeier, πN *Newsletter* 11 (1995) 194, Fig. 3.
26. G.F. Chew and F.E. Low, Phys. Rev. 101 (1956) 1570.
27. D.V. Bugg and A.A. Carter, Phys. Lett. 48B (1974) 67.
28. G. Höhler and R. Strauss, Zeit. Phys. 240 (1970) 377;
29. G. Höhler, H.P. Jakob and P. Kroll, Zeit. Phys. 261 (1973) 401.
30. D.M. Binnie et al., Phys. Rev. D8 (1973) 2789.
31. L. Tiator, G. Knöchlein and C. Bennhold, πN Newsletter 14 (1998) 70.
32. D.V. Bugg, πN Newsletter 8 (1993) 9.
33. R. Koniuk and N. Isgur, Phys. Rev. D21 (1980) 1898; S. Capstick and N. Isgur, Phys. Rev. D34 (1986) 2809.

Corrigendum to

"COMMENT ON THE πNN COUPLING CONSTANT"

πN Newsletter **12** (1997) 16, by T. Ericson, B. Loiseau, J. Blomgren and N. Olsson.

This paper contains an incorrect statement concerning the Nijmegen analysis of NN scattering data on page 17, the middle of the second paragraph:

"As an example, they quote 77 free parameters at 350 MeV." The correct sentence should have been "As an example [2b], they quote 116 free parameters (for the set of ten single energy analyses) up to 350 MeV.", with the reference [2b]: V.G.J. Stoks, R.A.M. Klomp, M.C.M. Rentmeester and J.J. de Swart, Phys. Rev. **C48** (1993) 792 (reference quoted "in preparation" in the Ref. [3], cited in our Newsletter paper). We misinterpreted in the article [2b] the extra 77 parameters needed to go from multienergy analysis (39 parameters) to the analysis of ten single energies (116 parameters) below 350 MeV. We apologize to the Nijmegen group for this incorrect statement on their work, which was made in good faith. This change is of no consequence for the rest of our article and our conclusions.

In addition, we cited an unpublished Comment submitted to Phys. Rev. Letters by the Nijmegen group expecting it to be published shortly thereafter. This material was not available to the general public because of the PRL editorial policy. It has since appeared in modified form in PRL **81** (1998) 5253 followed by our Reply at p. 5254. It is clear from their PRL Comment and our Reply that the positions of the two groups are the same as in 1997 as far as the substance of the physics is concerned. The issues raised have not found a consensus yet. We apologize for having cited their Comment without their permission. We are not aware of other misrepresentations or errors.

List of Participants

Alkofer, Reinhard	Institut für theoretische Physik, Univ. Tübingen, Auf der Morgenstelle 14, D-72076 Tübingen, Germany reinhard.alkofer@uni-tuebingen.de
Badertscher, Andreas	Institute for Particle Physics, ETH Hönggerberg / HPK F27, CH-8093 Zürich, Switzerland badertscher@particle.phys.ethz.ch
Bamberger, Andreas	Fak. f. Physik, Univ. Freiburg, Hermann-Herder Str. 3, D-79104 Freiburg, Germany bamberg@physik.uni-freiburg.de
Becher, Thomas	Institut für theoretische Physik, Univ. Bern, Sidlerstr. 5, CH-3012 Bern, Switzerland becher@itp.unibe.ch
Beck, Reinhard	Institut für Kernphysik, Becherweg 45, D-55099 Mainz, Germany rbeck@kph.uni-mainz.de
Bernard, Veronique	Laboratoire de Physique Theorique, 3 rue de l'Universite, F-67000 Strasbourg, France bernard@lpt1.u-strasbg.fr
Bernstein, Aron M.	Laboratory for Nuclear Science, 26-419, MIT, 77, Massachusetts Ave., USA-Cambridge, MA 2138, USA Bernstein@mitlns.mit.edu
Bertl, Wilhelm	Paul Scherrer Institut, WLGA/D22, CH-5232 Villigen PSI, Switzerland Wilhelm.Bertl@psi.ch
Bilger, Ralph	Physikalisches Institut, Univ. Tübingen, Auf der Morgenstelle 14, D-72076 Tübingen, Germany ralph.bilger@uni-tuebingen.de
Birse, Michael	Dept. of Physics, Univ. of Manchester, Oxford Road, UK-Manchester M13 9PL, United Kingdom mike.birse@man.ac.uk
Briscoe, William	Dept. of Phys., The George Washington Univ., 725 21st Street, NW, USA-Washington, D.C. 20052, USA Briscoe@gwu.edu
Bugg, David	RAL, Chilton, Didcot, Oxon OX11 OQX, UK bugg@v2.rl.ac.uk

Büttiker, Paul	Institut für Kernphysik, Forschungszentrum Jülich, D-52425 Jülich, Germany p.buettiker@fz-juelich.de
Daum, Manfred	Paul Scherrer Institut, WLGA/D31, CH-5232 Villigen PSI, Switzerland manfred.daum@psi.ch
Distler, Michael O.	Institut für Kernphysik, Univ. Mainz, Becherweg 45, D-55099 Mainz, Germany distler@kph.uni-mainz.de
Dytman, Steven	Dept. of Physics and Astronomy, Univ. of Pittsburgh, Pittsburgh, PA 15260, USA dytman@vms.cis.pitt.edu
Egger, Jean-Pierre	Institut de Physique, Univ. de Neuchâtel, Rue Breguet 1, CH-2000 Neuchâtel, Switzerland egger@iph.unine.ch
Fettes, Nadia	Institut für Kernphysik (Theory), Forschungszentrum Jülich, D-52425 Jülich, Germany n.fettes@fz-juelich.de
Friedman, Eli	Racah Inst. Physics, The Hebrew Univ., IL-91904 Jerusalem, Israel elifried@vms.huji.ac.il
Gårdestig, Anders	Division of Nuclear Physics, Uppsala University, Box 535, S-75121 Uppsala, Sweden grdstg@tsl.uu.se
Gasser, Jürg	Univ. Bern, Sidlerstr. 5, CH-3012 Bern, Switzerland gasser@itp.unibe.ch
Gibbs, William	New Mexico State Univ., USA-Las Cruces, New Mexico, 88006, USA gibbs@nmsu.edu
Gibson, Edward	Physcis Dept. 6041, California State University, 6000 J St., USA-Sacramento, CA 95819-6041, USA egibson@csus.edu
Gotta, Detlev	Institut für Kernphysik, Forschungszentrum Jülich, D-52425 Jülich, Germany d.gotta@fz-juelich.de
Gridnev, Anatoli	St. Petersburg Nuclear Physics Institute, GUS-188350 Gatchina, St. Petersburg, Russia gridnev@hep486.pnpi.spb.ru

Haberzettl, Helmut	Dept. of Physics, George Washington University, USA-Washington, DC 20052, USA helmut@gwu.edu
Hanstein, Olaf	Institut für Kernphysik, Univ. Mainz, D-55099 Mainz, Germany hanstein@kph.uni-mainz.de
Hasinoff, Michael	Univ. of British Columbia, 6224 Agricultural Road, CAN-Vancouver V6T 1Z1, Canada hasinoff@physics.ubc.ca
Höhler, Gerhard	Institut für Theoretische Teilchenphysik, Univ. Karlsruhe, Kaiserstr. 12, Postfach 6980, D-76128 Karlsruhe, Germany gerhard.hoehler@phys.uni-karlsruhe.de
Isenhower, Donald	Abilene Christian Univ., ACU Box 27963, USA-Abilene, Texas 79699-7963, USA isenhowe@physics.acu.edu
Jensen, Thomas	Paul Scherrer Institut, WHGA/138, CH-5232 Villigen PSI, Switzerland thomas.jensen@psi.ch
Johansson, Tord	Dept. of Radiation Sciences, Uppsala University, Box 535, S-75121 Uppsala, Sweden tord.johansson@tsl.uu.se
Kaiser, Norbert	Physik Deptartment T39, TU München, James Franckstrasse, D-85747 Garching, Germany nkaiser@physik.tu-muenchen.de
Kleefeld, Frieder	Institute for Theoretical Physics III, Univ. Erlangen-Nürnberg, Staudtstr. 7, D-91058 Erlangen, Germany kleefeld@theorie3.physik.uni-erlangen.de
Kluge, Wolfgang	Univ. Karlsruhe (TH), Postfach 3640, D-76021 Karlsruhe, Germany wolfgang.kluge@phys.uni-karlsruhe.de
Knecht, Marc	Centre de Physique Théorique, CNRS-Luminy, Case 907, F-13288 Marseille, France knecht@cpt.univ-mrs.fr
Kotlinski, Danek	Paul Scherrer Institute, WLGA/D22, CH-5232 Villigen PSI, Switzerland kotlinski@psi.ch

Kroll, Peter	Fachbereich Physik, Univ.Wuppertal, Gaussstrasse 20, D-42097 Wuppertal, Germany kroll@theorie.physik.uni-wuppertal.de
Kruglov, Sergei	Petersburg Nuclear Physics Institute, Leningrad District PNPI, GUS-188350 Gatchina, Russia kruglov@lnpi.spb.su
Kunz, Christine Conference Secretary	Paul Scherrer Institute, WHGA/138, CH-5232 Villigen PSI Switzerland Christine.Kunz@psi.ch
Lanaro, Armando	CERN, CH-1211 Geneva 23, Switzerland Armando.Lanaro@cern.ch
Leisi, Hans Jörg	Institute for Particle Physics, ETH Hönggerberg CH-8093 Zurich, Switzerland h.j.leisi@pop.agri.ch
Leutwyler, Heinrich	Inst. f. theoretische Physik, Univ. Bern, Sidlerstr. 5, CH-3012 Bern, Switzerland leutwyler@itp.unibe.ch
Lewis, Randy	Dept. of Physics, Univ. of Regina, CAN-Regina S4S 0A2, Canada randy.lewis@uregina.ca
Locher, Milan	Paul Scherrer Institut, WHGA/122, CH-5232 Villigen PSI, Switzerland milan.locher@psi.ch
Loiseau, Benoit	Univ. P. & M. Curie, LPTPE, Case 127, Tour 12 - 3eme etage, 4, Place Jussieu, F-75252 Paris Cedex 05, France loiseau@in2p3.fr
Lorenzon, Wolfgang	Phys. Dept., Univ. of Michigan, 2477 Randall Lab., Ann Arbor, MI 48109-1120, USA lorenzon@umich.edu
Lyubovitskij, Valery	Bogoliubov Lab. of Theor. Physics, JINR, RUS-141980 Dubna (Moscow Region), Russia lubovit@thsun1.jinr.ru
Machner, Hartmut	Institut für Kernphysik, FZ Jülich, D-52425 Jülich, Germany h.machner@fz-juelich.de
Markushin, Valeri	Paul Scherr Institut, WHGA/124, CH-5232 Villigen PSI, Switzerland Valeri.Markushin@psi.ch

McGovern, Judith	Dept. of Physics & Astronomy, Univ. of Manchaster, Oxford Road, Manchester M13 9PL, United Kingdom judith.mcgovern@man.ac.uk
Meier, Rudolf	Physikalisches Institut, Univ. Tübingen, Auf der Morgenstelle 14, D-72076 Tübingen, Germany rmeier@pit.physik.uni-tuebingen.de
Meissner, Ulf	IKP (Th), FZ Jülich, D-52425 Jülich, Germany Ulf-G.Meissner@fz-juelich.de
Müller, Guido	Inst. f. theor. Physik, Univ. of Vienna, Boltzmanngasse 9, A-1090 Wien, Austria gmueller@doppler.thp.univie.ac.at
Nefkens, Bernard M.	Dept. of Physics and Astronomy, Univ. of California, 405 Hilgard Ave., Los Angeles, CA 90095-1547, USA nefkens@physics.ucla.edu
Neufeld, Helmut	Institut für Theoretische Physik, Univ. Wien, Boltzmanngasse 5, A-1090 Wien, Austria neufeld@merlin.pap.univie.ac.at
Niskanen, Jouni	Dept. of Physics, Univ. of Helsinki, P.O. Box 9, FIN-00014 University of Helsinki, Finland jouni.niskanen@helsinki.fi
Oades, Geoffrey C.	Institute of Physics and Astronomy, Aarhus University, DK-8000 Aarhus C, Denmark gco@ifa.au.dk
Pancheri, Giulia	Laboratori Nazionali di Frascati, INFN, Via Enrico Fermi 40, I-00044 Frascati (Rome), Italy pancheri@lnf.infn.it
Patterson, Jeffrey	Univ. of Colorado, Campus Box 446, Boulder, CO 80309, USA jeffp@drax.colorado.edu
Pavan, Marcello	M.I.T., 77 Massachusetts Ave., Cambridge, MA 02143, USA marcello.pavan@triumf.ca
Petitjean, Claude	Paul Scherrer Institut, WLGA/D15, CH-5232 Villigen PSI, Switzerland claude.petitjean@psi.ch
Petrascu, Catalina Oana	LNF-INFN, Casella Postale 13, Via E. Fermi 40, I-00044 Frascati (Roma), Italy Petrascu@lnf.infn.it

Prokofiev, Alexander	Petersburg Nuclear Physics Institute, PNPI, High Energy Physics Department, RUS-188350 Gatchina, Russia prokan@hep486.pnpi.spb.ru
Rusetsky, Akaki	Inst. f. theor. Physik, Univ. Bern, Sidlerstr. 5, CH-3012 Bern, Switzerland rusetsky@itp.unibe.ch
Sadler, Michael E.	Abilene Christian Univ., Box 27963, USA-Abilene, TX 79699, USA sadler@physics.acu.edu
Sainio, Mikko	Dept. of Physics, Univ. of Helsinki, P.O. Box 9, FIN-00014 Helsinki, Finland sainio@phcu.helsinki.fi
Sevior, Martin	School of Physics, Univ. of Melbourne, AUS-3052 Parkville, Victoria, Australia msevior@mccubbin.ph.unimelb.edu.au
Siegel, Peter B.	Phys. Dept., California State Polytechnic University of Pomona, 3801 W. Temple Ave., Pomona, CA 91768, USA pbsiegel@csupomona.edu
Silbar, Richard R.	Group T-5, Los Alamos National Laboratory, Whistle Soft Inc., 168 Dos Brazos, Los Alamos, NM 87544, USA silbar@whistlesoft.com
Smith, Greg	TRIUMF, 4004 Wesbrook Mall, CAN-Vancouver, BC V6T 2A3, Canada smith@triumf.ca
Soto, Joan	Dept. d'ECM, Univ. of Barcelona, Diagonal 647, E-08028 Barcelona, Spain soto@ecm.ub.es
Stahov, Jugoslav	Faculty of Chemical Engineering, Univ. Tuzla, Univerzitetska 8, 75000 Tuzla, Bosnia and Herzegovina stahov@bih.net.ba
Staudenmaier, Hans Martin	Fak. für Physik, Physik-Hochhaus 11. Stock, D-76128 Karlsruhe, Germany hans.staudenmaier@physik.uni-karlsruhe.de
Tacik, Roman	Dept. of Physics, University of Regina / TRIUMF, CAN-Regina, Saskatchewan S4S 0A2, Canada tacik@meena.cc.uregina.ca

Tiator, Lothar	Institut für Kernphysik, Universität Mainz, J.-J.Becher-Weg 45, D-55099 Mainz, Germany tiator@kph.uni-mainz.de
Ueda, Tamotsu	Faculty of Science, Ehime University, Bunkyo 2-5, J-790-8577 Matsuyama, Ehime, Japan uedatam@ehimegw.dpc.ehime-u.ac.jp
Vereshagin, Vladimir V.	Theor. Phys. Dept., St.Petersburg State Univ., GUS-198904 St.Petersburg, Russia vvv@av2467.spb.edu
Wagner, Gerhard J.	Physikalisches Institut, Eberhard-Karls-Univ. Tübingen, Auf der Morgenstelle 14, D-72076 Tübingen, Germany wagner@pit.physik.uni-tuebingen.de
Weber, Peter	Institute for Particle Physics, ETH-Hönggerberg / HPK F25, CH-8093 Zürich, Switzerland peter.weber@cern.ch
Zeller, Michael	Phys. Dept., Yale University, P.O. Box 208121, USA-New Haven, CT 06520, USA michael.zeller@yale.edu